

Catalysis for the Conversion of Biomass and Its Derivatives

Max Planck Research Library for the History and Development of Knowledge

Series Editors

Jürgen Renn, Robert Schlögl, Bernard F. Schutz.

Edition Open Access Development Team

Lindy Divarci, Jörg Kantel, Matthias Schemmel and Kai Surendorf.

Scientific Board

Markus Antonietti, Ian Baldwin, Antonio Becchi, Fabio Bevilacqua, William G. Boltz, Jens Braarvik, Horst Bredekamp, Jed Z. Buchwald, Olivier Darrigol, Thomas Duve, Mike Edmunds, Yehuda Elkana, Fynn Ole Engler, Robert K. Englund, Mordechai Feingold, Rivka Feldhay, Gideon Freudenthal, Paolo Galluzzi, Kostas Gavroglu, Mark Geller, Domenico Giulini, Günther Görz, Gerd Graßhoff, James Hough, Manfred Laubichler, Glenn Most, Klaus Müllen, Pier Daniele Napolitani, Alessandro Nova, Hermann Parzinger, Dan Potts, Circe Silva da Silva, Ana Simões, Dieter Stein, Richard Stephenson, Mark Stitt, Noel M. Swerdlow, Liba Taub, Martin Vingron, Scott Walter, Norton Wise, Gerhard Wolf, Rüdiger Wolfrum, Gereon Wolters, Zhang Baichun.

Proceedings 2

**Edition Open Access
2017**

Catalysis for the Conversion of Biomass and Its Derivatives

Malte Behrens and Abhaya K. Datye

**Edition Open Access
2017**

Max Planck Research Library for the History and Development of Knowledge
Proceedings 2

Communicated by:
Robert Schlögl

Edited by:
Malte Behrens and Abhaya K. Datye

Editorial Coordination:
Beatrice Herrmann

Copyedited by:
Beatrice Gabriel

ISBN 978-3-945561-19-5

Published 2017 by Edition Open Access,
Max Planck Institute for the History of Science
Reprint of the 2013 edition

Printed and distributed by

PRO BUSINESS digital printing Deutschland GmbH, Berlin

Edition Open Access

<http://www.edition-open-access.de>

Published under Creative Commons by-nc-sa 3.0 Germany Licence

<http://creativecommons.org/licenses/by-nc-sa/3.0/de/>

The Deutsche Nationalbibliothek lists this publication in the Deutsche
Nationalbibliografie; detailed bibliographic data are available in the Internet at
<http://dnb.d-nb.de>.

The Max Planck Research Library for the History and Development of Knowledge comprises four subseries, *Studies*, *Proceedings*, *Sources* and *Textbooks*. They present research results and the relevant sources in a new format, combining the advantages of traditional publications and the digital medium. The volumes are available both as printed books and as online open access publications. They present original scientific work submitted under the scholarly responsibility of members of the Scientific Board and their academic peers.

The volumes of the four subseries and their electronic counterparts are directed at scholars and students of various disciplines, as well as at a broader public interested in how science shapes our world. They provide rapid access to knowledge at low cost. Moreover, by combining print with digital publication, the four series offer a new way of publishing research in flux and of studying historical topics or current issues in relation to primary materials that are otherwise not easily available.

The initiative is supported, for the time being, by research departments of three Max Planck Institutes, the MPI for the History of Science, the Fritz Haber Institute of the MPG, and the MPI for Gravitational Physics (Albert Einstein Institute). This is in line with the *Berlin Declaration on Open Access to Knowledge in the Sciences and Humanities*, launched by the Max Planck Society in 2003.

Each volume of the *Studies* series is dedicated to a key subject in the history and development of knowledge, bringing together perspectives from different fields and combining source-based empirical research with theoretically guided approaches. The studies are typically working group volumes presenting integrative approaches to problems ranging from the globalization of knowledge to the nature of spatial thinking.

Each volume of the *Proceedings* series presents the results of a scientific meeting on current issues and supports, at the same time, further cooperation on these issues by offering an electronic platform with further resources and the possibility for comments and interactions.

Each volume of the *Sources* series typically presents a primary source—relevant for the history and development of knowledge—in facsimile, transcription, or translation. The original sources are complemented by an introduction and by commentaries reflecting original scholarly work. The sources reproduced in this series may be rare books, manuscripts, documents or data that are not readily accessible in libraries and archives.

Each volume of the *Textbooks* series presents concise and synthetic information on a wide range of current research topics, both introductory and advanced. They use the new publication channel to offer students affordable access to high-level scientific and scholarly overviews. The textbooks are prepared and updated by experts in the relevant fields and supplemented by additional online materials.

On the basis of scholarly expertise the publication of the four series brings together traditional books produced by print-on-demand techniques with modern information technology. Based on and extending the functionalities of the existing open access repository European Cultural Heritage Online (ECHO), this initiative aims at a model for an unprecedented, Web-based scientific working environment integrating access to information with interactive features.

Contents

	Introduction	1
	Opening Remarks	1
	List of Authors, Communicator and Editors	6
1	Raw Material Change in the Chemical Industry and the Role of Biomass	
	<i>Friedrich Seitz</i>	15
1.1	Introduction	15
1.2	Raw Material Alternatives	15
1.3	Existing Businesses with Renewables	17
1.4	Existing Businesses with Renewables: Issues	18
1.5	The Use of Biomass	19
1.6	Outlook/Conclusions	20
1.7	Figures	23
2	The Role of Startup Companies in the Conversion of Biomass to Renewable Fuels and Chemicals	
	<i>Leo E. Manzer</i>	43
2.1	Introduction	43
2.2	Results and Discussion	44
2.3	Conclusion	57
3	Nutrient Cycling in the Bioeconomy: A Life Cycle Perspective	
	<i>Robert Anex</i>	61
3.1	Introduction	61
3.2	Life Cycle Assessment Methodology	62
3.3	Life Cycle Inventory	65
3.4	Impact Assessment	67
3.5	LCA of Biorenewable Chemical Systems	68
3.6	Prospective, Consequential, and Attributional LCA	71
3.7	Resource Constraints on Biorenewable Chemical Production	72
3.8	Conclusion	76

4	Plant Growth: Basic Principles and Issues Relating to the Optimization of Biomass Production and Composition as a Feedstock for Energy	
	<i>Mark Stitt</i>	83
4.1	Introduction: The Contribution of Plants to the Global Carbon Cycle	83
4.2	Is the Glass Half Full or Half Empty?	87
4.3	Low Energy Conversion Efficiency in Photosynthesis	90
4.4	The Use of Photosynthesis to Drive Plant Growth	103
4.5	Vegetative Biomass: What to Do with the Cell Walls?	109
4.6	Response of Photosynthesis and Plant Growth to Rising Atmospheric Carbon Dioxide	112
4.7	Integrated Model of Energy Use Efficiency during Photosynthesis and Growth	113
4.8	What is Needed for Efficient Energy Crops?	116
4.9	Current Energy Crops and Their Shortcomings	116
5	Biomass Chemistry	
	<i>Michael Ladisch, Eduardo Ximenes, Youngmi Kim, Nathan S. Mosier</i>	131
5.1	Introduction	131
5.2	Feedstock Availability	131
5.3	The Role of Petroleum	133
5.4	The Cost of Biomass Feedstocks	134
5.5	Maximum Yield as a Function of Biomass Composition	136
5.6	Location	139
5.7	Metrics for Biochemical vs. Thermochemical Conversion	140
5.8	Biomass Chemistry	142
5.9	Hydrolysis of Polysaccharides in Cellulosic Biomass	147
5.10	Chemistry of Pretreatment	148
5.11	Chemical Degradation and Inhibitor Formation During Pretreatment	149
5.12	Impact of Formed Inhibitors	153
5.13	Conclusions	158
6	Chemical and Biological Deconstruction of Aqueous Phase Processing	
	<i>Charles E. Wyman, Carol J. Wyman</i>	165
6.1	Introduction	165
6.2	Why Cellulosic Biomass?	166

6.3	Conversion Options for Aqueous Phase Processing	168
6.4	Laboratory Methods to Make Reactive Intermediates	171
6.5	Pretreatments and Biological Production of Sugars as Reactive Intermediates Through the Consortium for Applied Fundamentals and Innovation (CAFI)	172
6.6	Thermochemical Processing to Sugars and Other Reactive Intermediates	177
6.7	Conclusions	178
7	Analytical Approaches in the Catalytic Transformation of Biomass: What Needs to be Analyzed and Why?	
	<i>Dmitry Murzin, Bjarne Holmbom</i>	183
7.1	Introduction	183
7.2	Analytical Objectives	185
7.3	Basic Analytical Methods	186
7.4	Analytical Examples	195
7.5	Final Words	206
8	Methods for Biomass Compositional Analysis	
	<i>Amie Sluiter, Justin Sluiter, Edward J. Wolfrum</i>	213
8.1	Introduction	213
8.2	Biomass Composition	214
8.3	Measuring Biomass Composition: Forage and Fiber Analysis	215
8.4	Summative Compositional Analysis of Biomass Feedstocks	217
8.5	Summative Compositional Analysis of Pretreated Biomass Slurries and Liquors	228
8.6	Summative Mass Closure-Calculations, Troubleshooting, and Errors	233
8.7	Uncertainty in the Primary Measurements	235
8.8	Propagation of Uncertainty in Primary Measurements	237
8.9	Room for Improvement in Biomass Compositional Analysis	243
8.10	Rapid Biomass Analysis via NIR	246
8.11	Conclusions	247
	Appendix	251
9	Reaction Engineering Concepts for the Catalytic Conversion of Biorenewable Molecules	
	<i>Robert J. Davis</i>	255
9.1	Introduction	255
9.2	Measurement of Reaction Rates	256
9.3	Kinetics of Chemical Reactions	258

9.4	Deactivation of Catalysts	262
9.5	Reactors Used to Evaluate Catalysts	269
9.6	Mass and Heat Transfer Artifacts	270
9.7	Influence of Reactor Configuration	282
9.8	Conclusions	286
10	Catalytic Strategies and Chemistries Involved in the Conversion of Sugars to Liquid Transportation Fuels	
	<i>Elif I. Gürbüz, James A. Dumesic</i>	293
10.1	Introduction	293
10.2	Thermodynamic Considerations	293
10.3	Formulating Strategies for the Conversion of Sugars to Alkane Fuels: Platform Molecules	300
10.4	The Conversion of Sugars and Polyols to H ₂ and Alkanes	309
10.5	Conversion of Sugars/Polyols to Liquid Fuels via the Formation of Monofunctional Intermediates	329
10.6	Levulinic Acid and γ -Valerolactone Platforms for the Production of Liquid Fuels	337
10.7	Concluding Remarks	346
11	Design of Heterogeneous Catalysts for the Conversion of Biorenewable Feedstocks	
	<i>Brent H. Shanks</i>	361
11.1	Introduction	361
11.2	Adsorption of Carbohydrates and Their Derivatives on Solid Surfaces	364
11.3	Selective Bond Cleavage	371
11.4	Aqueous Phase Considerations	378
11.5	Novel Catalytic Materials for Biomass Conversion	384
11.6	Hydrothermally Stable Catalytic Materials	392
11.7	Impurity Tolerant Catalysts	396
11.8	Novel Reaction Systems	400
11.9	Summary	402
12	Tailor-Made Fuels and Chemicals from Biomass	
	<i>Thorsten vom Stein, Jürgen Klankermayer, Walter Leitner</i>	411
12.1	Introduction	411
12.2	Conceptual Approach to Tailor-Made Fuels via Combined Product and Process Design	412
12.3	From Intermediates to Products	414

12.4	From Lignocellulosic Raw Materials to Carbohydrate Feedstock and Platform Molecules.....	425
12.5	Conclusion and Outlook.....	428
13	Solution-Based Deconstruction of (Ligno)-Cellulose	
	<i>Roberto Rinaldi, Jennifer Reece</i>	435
13.1	Introduction.....	435
13.2	Understanding Cellulosic Recalcitrance.....	435
13.3	Cellulose in Solution.....	438
13.4	Homogeneous Hydrolysis of Cellulose.....	451
13.5	Final remarks.....	457

Introduction

Opening Remarks

Fossil fuels such as coal, oil and natural gas currently provide over 75% of the world's energy supply needed to satisfy the great appetite for affordable and freely available energy of individuals and industries worldwide. Unfortunately, the growing global demand for fossil fuel resources comes at a time of rapidly diminishing reserves of non-renewable resources, causing widening concerns about a possible future scarcity of energy and the threat of rising oil prices. Furthermore, questions regarding the developing energy scenario cannot be separated from the discussion of evident changes in global climatic conditions by the increased combustion of fossil energy carriers and the large subsequent contribution to global CO₂ emissions.

In addition to the transportation sector and the energy-producing industries, another important user of fossil resources is the chemical industry, which relies extensively on petroleum for the production of valuable chemical intermediates in a wide variety of applications from polymeric materials to solvents and compounds for pharmaceuticals. There is a demand for renewable carbon-based feedstocks for chemical applications that are independent of fossil sources

The search for renewable alternatives for energy and chemicals is clearly a major societal need in every developed or developing country. Biomass, being a globally distributed resource, can serve as a valuable source for both energy and organic carbon. Due to its renewable nature, it is the only sustainable source of specific functional compounds for the chemical industry. A further advantage of the production of fuels from biomass is the potential to lower greenhouse gas emissions because the CO₂ released during energy conversion is recycled by the subsequent growth of biomass. The selective conversion of renewable biomass resources into tailor-made products is thus an important and attractive new area of research involving the fields of chemistry, biology and engineering.

Molecular manufacturing, i.e., the building of materials from the bottom up while retaining an atom-by-atom precision, has captured the fascination of researchers and the general public alike. However, achieving the same precision on a large scale remains a key challenge. Catalytic technology can carry out such molecular transformations in a precise manner to yield products—fuels, chemicals and other materials to serve the needs of society—in large-scale systems. It

relies on a chain of knowledge spanning such areas as the atomistic level of an elementary surface reaction, the materials science of catalytic particles and bench scale test reactors, and the chemical engineering world of reactors in industrial plants. Indeed, the success of the petrochemical industry can be attributed in part to an understanding of conversion processes and chemical mechanisms at a fundamental level such as metal-catalyzed hydrogenolysis, hydrogenation and oxidation reactions. Whereas a petrochemical refinery has reached its present state of efficiency by continuous improvement over the past 50 years, the “biorefinery” and the understanding and knowledge-based manipulation of the involved chemical reactions is still in its infancy. By utilizing new chemical, biological and mechanical technologies, such an envisaged biorefinery provides a means of transitioning to a more energy-efficient and environmentally sustainable chemical and energy economy. In an integrated biorefinery, the production of high-value chemicals will be coupled with the production of high-volume and low-value transportation fuels, leading to a profitable mix and supporting sustainable operations to meet rising energy demands. The biorefinery of the future will be analogous to the petrochemical refinery of the present: a highly integrated system of processes that are optimized for energy efficiency and resource utilization. New catalysts and catalytic processes must be developed to provide the flexibility needed for the biorefinery to adjust and optimize its performance to accommodate changes in feedstocks and market demands.

The development of the necessary technology has been identified as the greatest challenge to bridge the gap between the concept and the realization of a bio-based chemical industry. In the summer of 2010 a workshop to address the challenges in this growing area of research was organized in order to bring together leading academic and industrial experts in the fields of catalytic conversion, biomass growth, life cycle analysis and industrial applications. The workshop on “Molecular Engineering for the Conversion of Biomass-Derived Reactants to Fuels, Chemicals and Materials” was organized by the Fritz Haber Institute of the Max Planck Society and the Partnership for International Research and Education (PIRE) at Kloster Seeon in Bavaria, Germany (photo by Edward L. Kunkes).¹

¹More information can be found on <https://pire.unm.edu/>. The partner institutions, collaborators and principal investigators of this PIRE program are: University of New Mexico (Abhaya K. Datye, PI), University of Virginia (Robert J. Davis, co-PI and Matthew Neurock, co-PI), University of Wisconsin-Madison (James A. Dumesic, co-PI), Iowa State University (Brent Shanks, co-PI), Fritz-Haber-Institute der Max-Planck-Gesellschaft (Malte Behrens, Matthias Scheffler, collaborators, and Robert Schlögl, host Germany), Max Planck Institute of Colloids and Interfaces (Markus Antonietti, collaborator), Haldor Topsøe A/S (Stig Helveg, collaborator), Technical University of Denmark (Jens K. Nørskov, collaborator and Ib Chorkendorff, host Denmark), Twente University (Leon Leferts, collaborator), Åbo Akademi University (Dmitry Murzin, host Finland), Eindhoven University of Technology (Hans Niemantsverdriet, host Netherlands), Utrecht University (Harry Bitter, Krijn de Jong and Bert Weckhuysen, collaborators).



The objective of this international partnership is to enhance the collaboration between institutions in the United States and the European Union to elucidate the key factors controlling catalytic conversions of biomass-derived reactants, thereby providing a fundamental foundation for the design, development and operation of a biorefinery. The focus of this workshop was primarily pedagogical, assisting students and researchers in the field to clearly formulate some of the challenges and discuss possible paths to achieving a bio-based economy. The lectures presented at the workshop are compiled in this volume for a broader dissemination to the scientific community and interested laypersons.

This volume comprises 13 chapters and starts with the perspectives from industry and start-up companies, which are delivered by Friedrich Seitz and Leo Manzer, respectively. Before taking a deeper look into biomass chemistry, some relevant non-chemical aspects are treated, that define the boundary conditions of a large-scale use of biomass. Robert Anex reports on a life cycle perspective and Mark Stitt discusses aspects of plant growth for biomass production. The following chapter by Michael Ladisch, Eduardo Ximenes, Youngmi Kim and Nathan S. Mosier covers the fundamentals of biomass chemistry. Charles E. Wyman and Carol J. Wyman further focus on its aqueous phase processing. Analytical approaches for biomass conversion reactions are introduced by Dmitry Murzin and Bjarne Holmbom, and Amie Sluiter, Justin Sluiter and Edward J. Wolfrum in the following two chapters. The field of catalytic conversion of biomass is

then introduced by Robert J. Davis, and Elif I. Gürbüz and James A. Dumesic, who report on reaction engineering concepts and catalytic strategies, respectively. The development of suitable heterogeneous catalysts and the related challenges are covered in Brent H. Shank's chapter, while Thorsten vom Stein, Walter Leitner and Jürgen Klankermayer focus on the application of homogeneous catalysts for the conversion of biomass. Finally, the important deconstruction reactions of lingo-cellulose are treated in the chapter by Roberto Rinaldi and Jennifer Reece. In the second part of this introduction, short biographical sketches of the authors, the editors and their affiliations are listed to complement the scientific content of this book.

All lectures present introductory material designed to root the subject back into the respective disciplinary foundations as well as state-of-the-art results illuminating current knowledge. While a remote observer may be fascinated by the detail of understanding gained in some aspects of the treatment of the complex and non-uniform material called "biomass," the experts feel that the current understanding of catalysis, mainly devoted to increase the functionality of feedstock molecules for desired chemical reactivity, is still unsuitable to efficiently deal with the transformation of biomass. Here, the over-functionalized bio-molecule needs de-functionalization, being in strong competition with polymerization once it is activated by catalytic or stoichiometric reactions. A new paradigm of catalysis is needed that focuses on the selective activation of large reaction networks under conditions more favorable to precise kinetic control than those provided by present-day tools.

Also, the dimension of the challenge to develop test-tube chemistry into processes suitable to operate under economical constraints given by today's energy market became obvious. The discussions vividly reflected concerns about the large-scale viability of biomass as a resource for transportation fuels and highlighted the responsibility of science to also consider non-scientific aspects when developing new technologies that might interfere with fundamental requirements of human life such as biodiversity, food production or clean water resources.

The decision to make the teaching material of this course available in the present form was made because we believe that this emerging field of energy science requires input from many disciplines that are traditionally not in close contact with each other. The present text may thus be regarded as an annotated introduction into basic concepts and considerations relevant for biomass conversion research. The text is intended to familiarize researchers with questions and concepts of relevant neighboring fields without providing complete textbook reference or literature coverage. The book may be used as an introduction to those areas of knowledge and challenges required to master biomass transformation on a scale relevant for future energy applications.

We acknowledge the support of the PIRE program from the U.S. National Science Foundation Office of International Science and Education (OISE). Additional funding was provided by the Max Planck Society through a grant to the Fritz Haber Institute in Berlin. Besides the contributions from the authors of these lectures, we note that the students and post-docs participating in this workshop actively contributed to its content through their questions and discussion. In a novel format to stimulate exchange among participants, scientists from different teams and areas of research were selected and randomly assigned to groups of three. The tasks of these groups were to reflect on the lectures and formulate questions to each of the speakers. The discussions after dinner were primarily devoted to questions from students and post-docs. By the end of the workshop, every participant had asked a question or contributed to the discussion. The content of these after-dinner discussions is also incorporated in the lectures reproduced in this volume. The open-access format offered by the Max Planck Library for the History and Development of Knowledge allows us to make the contents freely accessible through the World Wide Web. We also express our gratitude to Beatrice Herrmann, Kai Surendorf and Antje Ota for their invaluable technical assistance. Without their expertise and continuous efforts the print-on-demand version and the online production of this book would not have been possible. We thank Beatrice Gabriel for the thorough and fast copy-editing of the manuscripts and Dorothea Damm for her help with organizational issues. Jürgen Renn is acknowledged for his continuous support of the project. The cover picture was designed by Sylvia Reiche.

Abhaya Datye, Malte Behrens and Robert Schlögl

List of Authors, Communicator and Editors

Robert Anex is Professor of Biological Systems Engineering at the University of Wisconsin, Madison. He received his Ph.D. in environmental engineering from the University of California, Davis in 1995, after which he held faculty positions at Iowa State University and the University of Oklahoma. Prior to joining academia Dr. Anex was senior engineer at Systems Control Technology, Inc., in California (1983–1991). He is a member of the editorial board of the *International Journal of Life Cycle Assessment* and is associate editor for the *Journal of Industrial Ecology*. His research focuses primarily on systems analysis and optimization of biological systems.

R. Anex (anex@wisc.edu), Biological Systems Engineering, University of Wisconsin, Madison, WI, USA

Malte Behrens received his Ph.D. in Chemistry at Kiel University in 2006. He then joined the Department of Inorganic Chemistry at the Fritz-Haber-Institut der Max-Planck-Gesellschaft to do his Habilitation with Robert Schlögl. His research interest is the development of nanochemically-optimized catalytic materials for energy storage applications.

M. Behrens (behrens@fhi-berlin.mpg.de), Department of Inorganic Chemistry, Fritz-Haber-Institut der Max-Planck-Gesellschaft, Berlin, Germany

Abhaya K. Datye is Distinguished Regents Professor of Chemical & Nuclear Engineering at the University of New Mexico, Director of the graduate interdisciplinary program in Nanoscience and Microsystems Engineering and also the Director of the Center for Microengineered Materials, a strategic research center at UNM. He received his B.Tech. degree (1975) from the Indian Institute of Technology, Mumbai, India, his M.S. (1980) from the University of Cincinnati, Cincinnati, OH, USA and his Ph.D. (1984) from the University of Michigan, Ann Arbor, MI, USA, all in chemical engineering. His research interests are in heterogeneous catalysis, materials characterization and nanomaterials synthesis. His research group has pioneered the development of electron microscopy tools for the study of catalysts.

A. Datye (datye@unm.edu), Department of Chemical and Nuclear Engineering, University of New Mexico, Albuquerque, NM, USA.

Robert J. Davis obtained his Ph.D. in Chemical Engineering from Stanford University in 1989. He subsequently worked as a postdoctoral research fellow in the Chemistry Department at the University of Namur in Belgium. He joined the faculty in Chemical Engineering at the University of Virginia in 1990 and

is currently the Earnest Jackson Oglesby Professor. Davis served as the Chair of Chemical Engineering at UVa from 2002 to 2011. His research interests are in the field of heterogeneous catalysis, with a focus on fundamental structure-activity relationships.

R. J. Davis (rjd4f@virginia.edu), Department of Chemical Engineering, University of Virginia, Charlottesville, VA, USA

James A. Dumesic earned his B.S. degree from the University of Wisconsin-Madison and his M.S. and Ph.D. degrees from Stanford University, under the supervision of Professor Michel Boudart. Dumesic joined the Department of Chemical Engineering in 1976, and he currently holds the Steenbock Chair in the College of Engineering and is Michel Boudart Professor of Chemical and Biological Engineering. Dumesic has used spectroscopic, microcalorimetric, and reaction kinetics techniques to study the surface and dynamic properties of heterogeneous catalysts. Dumesic pioneered the field of microkinetic analysis in which diverse information from experimental and theoretical studies is combined to elucidate the essential surface chemistry that controls catalyst performance. He has recently studied how aqueous-phase reforming of biomass-derived carbohydrates can be tailored to selectively produce H₂ or be directed to produce liquid alkanes. Most recently, he has been studying the use of levulinic acid and γ -valerolactone as biomass-derived platform chemicals for the production of fuels and chemicals.

J. A. Dumesic (dumesic@engr.wisc.edu), Department of Chemical and Biological Engineering, University of Wisconsin-Madison, Madison, WI, USA

Elif I. Gürbüz received her B.S. degree in chemical engineering from Middle East Technical University (2007) in Turkey and is currently completing her Ph.D. in chemical engineering at the University of Wisconsin-Madison (2012) under the direction of Professor James A. Dumesic. During graduate school, she studied the conversion of lignocellulose-derived carbohydrates to platform chemicals through successive oxygen removal reactions and upgrading of these platform molecules to obtain fuel and chemical grade products utilizing heterogeneous catalysis. Upon completion of her Ph.D., she will become a postdoctoral fellow under the guidance of Professor Enrique Iglesia at the University of California, Berkeley.

Elif I. Gürbüz, Department of Chemical and Biological Engineering, University of Wisconsin-Madison, Madison, WI, USA

Bjarne Holmbom received his Ph.D. in Chemical Engineering at Åbo Akademi University in 1978. He was visiting scientist at Paprican in Montreal 1979–1980.

He was appointed to full professor in Forest Products Chemistry at Åbo Akademi in 1985. In 1985–1986 he was visiting professor at North Carolina State University in Raleigh, N.C. He was Academy Professor at the Academy of Finland 1998–2003. In 2005 he received the Finnish Science Award and in 2008 the Marcus Wallenberg Prize. He retired in 2009. His research has been focused on wood and paper chemistry, environmental chemistry and related analytical techniques. *B. Holmbom, Wood and Paper Chemistry, Åbo Akademi University, Turku, Finland*

Youngmi Kim received her Ph.D. in 2005 in Agricultural and Biological Engineering from Purdue University. Her B.S. (1999) and M.S. (2001) are from Inha University, Inchon, South Korea, both in Biological Engineering. Upon completing her Ph.D., Youngmi Kim joined Dr. Ladisch's team in the Laboratory of Renewable Resources Engineering (LORRE) as a bioprocess research engineer and has been working in the cellulosic ethanol field since 2005. Dr. Kim specializes in pretreatment and hydrolysis technologies for converting cellulosic biomass to fuels and chemicals, bioseparation technologies, process design and simulation of cellulosic biorefinery processes.

Y. Kim, Department of Agricultural & Biological Engineering, West Lafayette, IN, USA

Jürgen Klankermayer obtained his Ph.D. under the supervision of Henri Brunner at the University of Regensburg in 2002. He conducted research as postdoctoral fellow with François Mathey and Duncan Carmichael at École Polytechnique in Paris and with John M. Brown at the University of Oxford. In 2009, he was appointed as Junior Professor in the Cluster of Excellence “Tailor-Made Fuels from Biomass” at RWTH Aachen University. His research interests focus on the molecular understanding of mechanisms in catalysis using NMR spectroscopy, with application of the knowledge mainly towards catalyst design for asymmetric catalysis, novel hydrogenation processes, and selective biomass conversion.

J. Klankermayer, Institut für Technische und Makromolekulare Chemie, RWTH Aachen University, Aachen, Germany

Michael R. Ladisch is Director of the Laboratory of Renewable Resources Engineering (LORRE), and Distinguished Professor of Agricultural and Biological Engineering, with a joint appointment in the Weldon School of Biomedical Engineering. His B.S. (1973) is from Drexel University, and his M.S. (1974) and Ph.D. (1977) from Purdue University, all in Chemical Engineering. He is con-

tinuing his activities with Mascoma Corporation where he has been Chief Technology Officer since 2007. Dr. Ladisch has 35 years of research experience in biofuels, renewable resources, and biotechnology.

M. R. Ladisch (ladisch@purdue.edu), Department of Agricultural & Biological Engineering, Purdue University, West Lafayette, IN, USA

Walter Leitner holds the Chair of Technische Chemie und Petrolchemie at RWTH Aachen University. He is also External Scientific Member of the Max-Planck-Institut für Kohlenforschung and Scientific Director of CAT, the joint Catalytic Center of RWTH Aachen and the Bayer Company. He currently serves as the Chairman of the German Catalysis Society (GeCatS) and as the Scientific Editor of the Journal *Green Chemistry* published by the Royal Society of Chemistry. His research interests are the molecular and reaction engineering principles of catalysis as related to Sustainable and Green Chemistry. The research on selective biomass conversion in his group is strongly embedded in the interdisciplinary Cluster of Excellence “Tailor-Made Fuels from Biomass” at RWTH Aachen.

W. Leitner (leitner@itmc.rwth-aachen.de), Institut für Technische Chemie und Makromolekulare Chemie (ITMC), RWTH Aachen University, Aachen, Germany

Leo E. Manzer received his Ph.D. from the University of Western Ontario in 1973 and immediately joined the DuPont Company in Wilmington, Delaware, USA. He had a successful 32 year career where he was the Founder and Director of the Corporate Catalysis Center and rose to the rank of DuPont Fellow. Following retirement in 2005 he founded Catalytic Insights, LLC and holds the position of CEO. He is actively involved with venture capital firms in assessing startup companies and serves on the Scientific Advisory Board of numerous companies involved in the field of renewable fuels and chemicals.

Leo E. Manzer (Leo@CatalyticInsights.com), Catalytic Insights, LLC, Wilmington, DE, USA

Nathan S. Mosier is an Associate Professor in Agricultural and Biological Engineering at Purdue University. His research addresses fundamental topics in bioprocessing with current projects in enzyme mimicking catalysts for transforming renewable resources to fuels and chemicals, cellulose pretreatment for biofuel and biochemical production, enzyme-based processing technology, fermentation process modeling, metabolomics and transcriptomics of fermentation, and bio-process simulation. His B.S. (1997) in BioSystems Engineering is from the University of Nebraska, Lincoln, his M.S. (2000) and Ph.D. (2003) in Agricultural

and Biological Engineering is from Purdue University. Dr. Mosier was also a NSF-IGERT Ph.D. fellow in the Innovation Realization Laboratory at the Krannert School of Management.

N.S. Mosier, Department of Agricultural & Biological Engineering, Purdue University, West Lafayette, IN, USA

Dmitry Murzin was born in 1963, graduated from Moscow University of Chemical Technology and received his Ph.D. in 1989 in Chemistry at the Karpov Institute of Physical Chemistry in Moscow with Mikhail Temkin. He defended his Doctor of Science thesis (Habilitation) in 1999 at the same institution. After being associated with BASF from 1995 to 2000, he took the Chair of Chemical Technology at the Åbo Akademi University, Finland. Dmitry Murzin's research focus is in heterogeneous catalysis and catalytic reaction engineering in particular related to biomass valorization.

D. Murzin (dmurzin@abo.fi), Industrial Chemistry and Reaction Engineering, Åbo Akademi University, Turku, Finland

Jennifer Reece was born in 1984 in Conroe, Texas, United States and received her B.A. from Grinnell College in 2006. Her doctorate in chemistry was received from Purdue University in 2010 under the supervision of Dr. Hilkkka I. Kenttämä. During her time there, she worked with C3Bio, an Energy Frontier Research Center funded by the U.S. Department of Energy, towards the direct conversion of plant lignocellulosic biomass to biofuels. Later in 2010 she took a postdoctoral research position at the Max-Planck-Institut für Kohlenforschung in Mülheim an der Ruhr, Germany, investigating mass spectrometric techniques for the analysis of lignin products obtained by novel catalytic strategies developed by Roberto Rinaldi. Currently, she is a postdoctoral fellow with the Colorado Diversity Initiative at Colorado University at Boulder with Dr. Veronica Bierbaum.

J. Reece, Department of Chemistry and Biochemistry, Colorado University at Boulder, Boulder, CO, USA

Roberto Rinaldi studied Chemistry at the State University of Campinas (UNICAMP), Brazil, where he received his doctorate under the supervision of Prof. Ulf Schuchardt in 2006. The award "Outstanding Ph.D. work 2007," sponsored by Evonik-Degussa and the Brazilian Catalysis Society, was given for his work on transition metal free alumina-catalyzed epoxidation. In 2007, he took a postdoctoral position at the Brazilian Synchrotron Laboratory in Campinas, where he worked on the characterization of HTS and LTS-catalysts by XPS. By the end of 2007, he moved to the Max-Planck-Institut für Kohlenforschung, Mülheim an

der Ruhr, Germany to work in the group of Prof. Ferdi Schüth, where he has been developing new strategies to circumvent the recalcitrance of cellulose using ionic liquids. Currently, he is leading a research group on catalysis for lignin, cellulose and coal at the Max-Planck-Institut für Kohlenforschung with funds provided by the Alexander von Humboldt Foundation through the Sofja Kovalevskaja Award 2010.

R. Rinaldi (rinaldi@kofo.mpg.de), Max-Planck-Institut für Kohlenforschung, Mülheim an der Ruhr, Germany

Robert Schlögl was born in 1954 and received his Ph.D. in Chemistry at Ludwig Maximilians University in Munich in 1982. He did his Habilitation with Gerhardt Ertl at the Fritz-Haber-Institut der Max-Planck-Gesellschaft (FHI) in Berlin and went to Frankfurt University for a Full Professorship. Since 1994 he is back in Berlin as the Director of the Department of Inorganic Chemistry at the FHI and since 2011 he is also the Founding Director of the Max Planck Institute for Chemical Energy Conversion in Mülheim. Robert Schlögl's research focuses primarily on the investigation of heterogeneous catalysts, with the aim to combine scientific and technical applicability.

R. Schlögl, Department of Inorganic Chemistry, Fritz-Haber-Institut der Max-Planck-Gesellschaft, Berlin, Germany

Friedrich Seitz was born in 1955 and received his Ph.D. in Chemistry at the Technical University Munich in 1984. Following a postdoc period at the Massachusetts Institute of Technology, he started work at BASF's Polymer Research in 1986. After several positions within the company in Ludwigshafen and Hong Kong, he became President of the Competence Center for Process Research and Chemical Engineering in 2010. Research in this division focuses on process development, catalysis, synthesis, and the development of new technologies.

F. Seitz (monika.lueck@basf.com), BASF SE, Ludwigshafen, Germany

Brent H. Shanks is the Mike and Jean Steffenson Professor of Chemical and Biological Engineering at Iowa State University and Director of the National Science Foundation Engineering Research Center for Biorenewable Chemicals (CBiRC). He received his B.S. degree from Iowa State University in 1983 and his M.S. and Ph.D. degrees from the California Institute of Technology in 1985 and 1988, respectively. From 1988 to 1999 he worked as a Research Engineer and Department Manager in the Catalyst Department at the Shell Chemical Company technology center in Houston, Texas. He joined the faculty at Iowa State University in 1999 where his work has primarily involved the research and development of novel

heterogeneous catalyst systems for efficiently converting biological-based feedstocks to chemicals and fuels.

B.H. Shanks (bshanks@iastate.edu), NSF Engineering Research Center for Biorenewable Chemicals (CBiRC), Iowa State University, Ames, IA, USA

Amie Sluiter began research in the biofuels field in 1996 at the National Renewable Energy Laboratory. She is an author on 11 Laboratory Analytical Procedures (LAPs). She has taught full biomass compositional analysis procedures to both internal and external colleagues. Amie is responsible for the creation and maintenance of many of NREL's rapid near-infrared (NIR) spectroscopic analysis methods. These methods provide predictions for the composition of feedstock and process intermediates at a significant time and cost reduction compared with traditional wet chemical analyses.

A. Sluiter, National Renewable Energy Laboratory NREL, Golden, CO, USA

Justin Sluiter is a biomass composition specialist with 16 years of experience working in the Biofuels Program at the National Renewable Energy Laboratory. Justin is an author on the majority of NREL's Laboratory Analytical Procedures (LAPs), which are worldwide recognized standards for summative compositional analysis of biomass and biomass derived products. He has performed numerous compositional analysis training classes for external partners, from academia to industry. Justin enjoys working on LAP method optimization for new feedstocks and diverse instrumentation.

J. Sluiter, National Renewable Energy Laboratory NREL, Golden, CO, USA

Mark Stitt studied Natural Sciences at Cambridge University/England and received his Ph.D. degree in 1978. He pursued his academic career in Germany and did his Habilitation in biochemistry of plants at the University of Göttingen in 1984. From 1986 he held the Fiebiger Professorship for Plant Biochemistry of the University of Bayreuth and changed to a full Professorship for Botany at Heidelberg University in 1991. Since 2000 he is Director and Scientific Member at the Max Planck Institute of Molecular Plant Physiology and Honorary Professor at the Universities of Potsdam (since 2002) and of Umeo/Sweden (since 2008). His research interests are physiological processes involved in orchestrating photosynthetic carbon metabolism, growth, and storage. His group studies systems biology with forward and reverse genetic tools to look at metabolite production and allocation.

M. Stitt (mstitt@mpimp-golm.mpg.de), Max-Planck-Institut für Molekulare Pflanzenphysiologie, Department 2: System Regulation, Potsdam, Germany

Thorsten vom Stein received his M.S. degree with distinction from RWTH Aachen University in 2010 and is currently a Ph.D. student in the group of Professor Walter Leitner. In his diploma thesis he developed a one-step fractionation system for lignocellulose, which was awarded with the Hochschulpreis der Stiftung Nachwachsende Rohstoffe in 2011. The focus of his Ph.D. thesis, which is supported by the Max-Buchner Fellowship of DECHEMA, is on the development of new homogeneous catalysts for the selective depolymerization of lignin. *T. vom Stein, Institut für Technische und Makromolekulare Chemie, RWTH Aachen University, Aachen, Germany.*

Edward J. Wolfrum serves as the Manager of the Biomass Analysis Section at the National Renewable Analysis Laboratory. This section consists of more than a dozen scientists and technicians who provide analytical chemistry support to both internal and external clients. His research interests include applied spectroscopy and chemometrics, focusing specifically on developing rapid methods for biomass composition determination based on near-infrared spectroscopy. *E.J. Wolfrum (Ed.Wolfrum@nrel.gov), National Renewable Energy Laboratory NREL, Golden, CO, USA*

Charles E. Wyman had devoted most of his career to advancing technologies for aqueous conversion of cellulosic biomass to ethanol and other products through leadership positions in academia, national laboratories, and industry. He is currently Ford Motor Company Chair in Environmental Engineering at the University of California at Riverside and also cofounder, Chief Development Officer, and chair of the Scientific Advisory Board for Mascoma Corporation, a startup biofuels company. Wyman has a B.S. degree in chemical engineering from the University of Massachusetts, M.A. and Ph.D. degrees in chemical engineering from Princeton University, and an M.B.A from the University of Denver. *C.E. Wyman c/o Carol J. Wyman (charles.wyman@ucr.edu), Bourns College of Engineering, Chemical/Environmental Engineering, University of California, Riverside, CA, USA*

Eduardo Ximenes is a Research Scientist in the Laboratory of Renewable Resources Engineering at Purdue University where he leads efforts in Microbiology and protein biochemistry. He also has a special graduate faculty appointment at Purdue University. His B.S. (1991) and M.S. (1994) are from the University of Brasilia, Brazil, and his Ph.D. (1999) is from the University of Georgia, all in Biology. In addition, Dr. Ximenes has 15 years of experience in the study of fungal

fermentations for the production and development of enzymes, characteristics of enzyme formulations from various microbial sources, and genetic engineering of fungal and bacterial hosts.

E. Ximenes, Agricultural & Biological Engineering, Purdue University, West Lafayette, IN, USA

Chapter 1

Raw Material Change in the Chemical Industry and the Role of Biomass

Friedrich Seitz

1.1 Introduction

Today's global economy is highly dependent on fossil fuels with oil being the most important feedstock. The scenario of depleting oil reserves therefore threatens the basis of most of our businesses and has a potentially huge impact on our daily life. At the same time conversion of fossil fuels into carbon dioxide is considered a big threat for our climate. These are the main reasons for the proposal to replace fossil fuels with renewable biomass and close global carbon cycles. This article takes a closer look at the probable consequences of this raw material change specifically for the chemical industry: what is the status, what are issues and what are the opportunities? It might also inspire young researchers to tackle some really important challenges that will arise in the future.

1.2 Raw Material Alternatives

In the beginning of industrialization coal was the most important raw material for the chemical industry, e.g., for the production of dyes. It was soon replaced by oil and later also by natural gas since easier logistics and lower prices made these more attractive. Today, supply with sustainable and affordable energy is one of the main challenges of mankind and this might trigger a third big change in the raw material supply for the chemical industry as well. If prices for fossil fuels rise significantly and permanently, for example due to limited availability or political initiatives to reduce greenhouse gas emissions [1], biomass could become the most attractive feedstock for the chemical industry in the future. However, there should be an awareness of alternative scenarios, e.g., using fossils only for chemicals but not for energy, or the usage of carbon dioxide for chemicals.

The energy industry and the transportation sector are by far the most important consumers of fossil fuels: about 10 billion tons (calculated as oil equivalents) are used for this purpose with roughly 4 billion tons of this being crude oil (Figure

1.1¹, [2]). Only 3% of all fossil fuels are used in the chemical industry. However, compared to the energy industry, the chemical industry is much more restricted in terms of feedstock. Whereas energy can generally be converted from a big variety of sources, most chemicals depend on the carbon content of the corresponding raw material (Figure 1.2). On the one hand, carbon dioxide (and carbonates) is the only large carbon-containing feedstock that is irrelevant for the energy industry. On the other hand, a lot of energy is required for its chemical use due to thermodynamical reasons [3, 4]. If the required energy comes from fossil fuels it is more reasonable to use the fossil fuels directly for chemical production as this leads to an overall lower consumption. However, when non-fossil-based energy is available, carbon dioxide can be a very attractive and sustainable carbon source for chemicals.

Green plants can convert carbon dioxide into biomass using the energy of the sun. Biomass then contains enough energy for both energy production and chemical use; when converted back to carbon dioxide no additional greenhouse gas is produced.

But let us first have a look at today's chemical industry which is mainly based on fossil fuels. More than 70% of all chemicals in Germany are based on crude oil; the rest breaks up into equal portions of natural gas and renewables. Coal as a chemical feedstock is negligible in Germany (Figure 1.3, [5, 6]). The most important process to convert a distillation fraction of crude oil called *naphtha* into the first members of chemical value-added chains is steam cracking (Figure 1.4). At high temperatures and with the dilution of steam, the alkanes of *naphtha* crack into lower olefins like ethylene and propylene and also form aromatics, namely benzene and toluene. Other processes for the production of olefins and aromatics are fluid catalytic cracking (FCC) and reforming. Both processes are carried out in refineries and deliver the mentioned chemicals only as a by-product. However, due to their enormous size they are an important source. Ethane as a component of natural gas is converted by steam cracking into ethylene; in this case virtually no higher olefins or aromatics are formed. Methane, being the main component of natural gas, is converted into synthesis gas (*syngas*), e.g., by steam reforming. Synthesis gas is a mixture of carbon monoxide and hydrogen and predominantly converted into methanol and ammonia. Another source for synthesis gas is the gasification of coal. The old calcium carbide process for transforming coal into acetylene is currently experiencing a revival for polyvinyl chloride production in China. Coke production for the steel industry delivers benzene (*hydrogenated coke-based benzene*, HCBB) as a by-product.

The previously described conventional entries into chemical value-added chains are endangered by the finite nature of fossil fuel supply. For example,

¹All figures are shown at the end of this chapter.

if the availability of oil declines significantly, the olefins and aromatics demand cannot be satisfied. Rather new technologies, like *methanol-to-olefins* (MTO) or *methanol-to-propylene* (MTP), could help by delivering olefins from synthesis gas (via methanol); interestingly, synthesis gas is also available from biomass. No industrially relevant alternative process for aromatics is in use today.

The conventional reserves, i.e., known deposits that can be obtained with today's technologies at competitive costs, might run short in about 40 years for oil and 60 years for gas at the current level of energy use [7, 8]. Non-conventional resources, i.e., assumed deposits that might be available with so far unknown technologies, could be significantly larger (e.g., methane hydrates in the oceans) (Figure 1.5). The enhancements in raw material production technologies and the discovery of new deposits have led to a nearly constant static range for oil and other feedstock in the past (Figure 1.6, [7, 8]). A prominent recent example for a technological breakthrough is shale gas production in the USA. In any case, there will be enough coal for a very long time.

At first glance biomass appears to be infinite compared to fossil fuels. About 160 billion tons of biomass are growing every year, two thirds of which grow ashore. Global stocks are in the same order of magnitude as fossil resources (Figure 1.7, [9]). However, a closer examination shows that only a small part of that biomass can be made available for energy purposes. Optimistic scenarios suggest that 30 to 70% of the worldwide energy demand could be satisfied with biomass in 2050 (Figure 1.8, [2, 10]).

Another issue with fossil fuels is the geographically uneven distribution. About 70% of all known conventional reserves of oil and gas are concentrated in a rather small area of the planet. This leads to a high dependence of the rest of the world on the countries of this area (Figure 1.9, [7, 8]). Biomass in comparison can be potentially produced in many different regions of the world in a reasonable manner (Figure 1.10, [10]).

1.3 Existing Businesses with Renewables

After having gained an idea of the current chemical feedstock use and the supply situation, let us have a look into the current use of renewables in the chemical industry. Roughly half of these renewables are fats and oils. Sugar and starch as well as cellulose also play a significant role (Figure 1.11, [5]). The three most important oils are palm oil, soybean oil and rapeseed oil of which 73% are used for food (Figures 1.12 and 1.13, [5]). The chemical industry transforms another 11% into biofuels and only a minor part into other (oleo)chemicals [11]. Figure 1.14 shows a repertory of chemical value-added chains based on fats and oils. A lot of the derived chemicals end up in personal care products, cosmetics, sur-

factants or lubricants. A chemically interesting example is the production of sebacic acid, e.g., for nylon 6,10, from castor oil. Saponification gives ricinoleic acid which is isomerized and then oxidatively cleaved (Figure 1.15). However, much more important is the transesterification of palm or rapeseed oil to fatty acid methyl esters (FAME), so-called “biodiesel first generation” (Figure 1.16). Sodium methoxide acts as a catalyst in the reaction with (usually non-bio-based) methanol; a by-product of this reaction is glycerol. If the oils are hydrogenated instead, so-called “biodiesel second generation” is obtained; it is more similar to conventional diesel.

The production of glycerol with “biodiesel first generation” has led to a significant price decline for glycerol (Figure 1.17, [12]). Therefore, glycerol has been considered an interesting renewable raw material for many chemicals (Figure 1.18, [13]). For example, BASF developed a very efficient hydrogenation process for mono propylene glycol (Figure 1.19). Due to past subsidization, large over-capacities for biodiesel production have been installed worldwide, but their profitability has often not been sustainable (Figure 1.20). Sucrose, as well as starch-derived glucose, is a suitable feedstock for many important chemicals (Figure 1.21). In most cases fermentation is the first step to convert sugars into useful chemicals; chemical transformations are still much less important. The main challenge is the high degree of functionalization of sugars compared to the target chemical products. Highly efficient methods for defunctionalization have only been a niche business in chemical research in the past. Some interesting examples are shown in Figures 1.22 and 1.23: citric acid, itaconic acid and (iso)butanol are produced by fermentation, and isosorbide is chemically accessible. The most important fermentation of carbohydrates to chemicals is the bioethanol production for motor fuels. 98% of all ethanol worldwide is produced by fermentation. Countries with sugar cane cultivation like Brazil have a competitive advantage since they do not have to convert starch from corn or wheat into sugar as a first step (Figure 1.24). Ethanol may not only be a fuel but also a raw material for other downstream chemicals (Figure 1.25). For example, a BASF process (development stage) for the production of acetic acid is shown (Figure 1.26): the oxidation with oxygen works with high selectivity at high conversion. Although the global bioethanol production is bigger than the biodiesel production, it is still negligible compared to global gasoline consumption (less than 5%; see Figure 1.27).

1.4 Existing Businesses with Renewables: Issues

As long as there are fossil fuels available at a reasonable price, the most important reason to produce bio-based fuels, e.g., bioethanol or biodiesel for mobility

applications, is the reduction of greenhouse gas emissions. However, today's bio-fuels are by far not carbon-neutral: not only the fuel for agricultural machinery is relevant, especially fertilizer and the processing to make the actual biofuel lead to significant greenhouse gas emissions. In the end, there are savings of roughly one to two thirds compared to the emissions with fossil fuels. The picture becomes much worse when areas of unspoiled nature are converted into agricultural land for biofuel production (Figure 1.28). The deforestation leads to significant carbon dioxide emissions and an increase in methane and nitrous oxide emissions [14–16]. The worst examples are the sugar cane and soybean productions in South America and the palm oil production in South East Asia. For example, Indonesia has become the world's third-largest emitter of greenhouse gases due to the deforestation necessary for the production of palm oil [17].

Obviously, general ethical issues are raised when food plants are used for anything else but nutrition. This problem became apparent to everybody when biofuel production led to an increase in food prices and subsequent disturbances in third-world countries with people suffering from malnourishment. An example for such a mechanism is the establishment of a floor price for palm oil in the beginning of 2007: when palm oil prices drop below a certain price compared to crude oil, biodiesel production begins and keeps palm oil prices high (Figure 1.29).

1.5 The Use of Biomass

A reasonable way to avoid the aforementioned issues with the use of renewables is the utilization of the main components of plants, *biomass*, and the avoidance of the usage of small edible fractions. Biomass mainly consists of cellulose, hemicelluloses and lignin (Figure 1.30). Cellulose is based on sugars with six carbons, hemicelluloses consist of sugars with five carbons, lignin is a condensed polyaromatic structure that represents the starting material for geological lignite and hard coal formation. The easiest way to feed biomass into chemical value-added chains is to gasify it into synthesis gas and use processes like MTO to obtain ethylene and propylene or *Fischer-Tropsch* (FT) to produce “biodiesel third generation.” However, this procedure destroys a lot of valuable chemical bonds and adds unwanted oxygen. In order to get the desired products, bonds have to be rebuilt and oxygen has to be removed in the form of water (Figure 1.31). Overall, a lot of—unnecessary—energy is required, which makes these processes less economically favorable. A generally more attractive way is the so-called structural use of renewables: the synthesis work of nature is conserved in the chemical products (Figure 1.32 [18]). A good example for structural use is the aforementioned synthesis of mono propylene glycol from glycerol by selective defunctionaliza-

tion: a hypothetical process via synthesis gas has significantly more steps and is much more energy intensive and thus economically and ecologically unattractive (Figure 1.33).

In order to enable the structural use of biomass, a biorefinery that separates the main components cellulose, hemicelluloses and lignin is required. In analogy to a petroleum refinery, a biorefinery is defined as “a facility that integrates biomass conversion processes and equipment to produce fuels, power and chemicals from biomass.”[19]

A common concept is the separation of cellulose and subsequent enzymatic hydrolysis and fermentation to *cellulosic* bioethanol as fuel (Figure 1.34); the competition with food production could be minimized since agricultural waste and non-food sources could be used. The analogous fermentation of xylose from hemicelluloses is still under development. Xylose could also be the starting point for several interesting value-added chains (Figure 1.35); the current production of furfuryl alcohol and xylitol (sweetener) are examples (Figure 1.36).

1.6 Outlook/Conclusions

The energy industry is the most important driver for the use of renewables. Finite resources of fossil fuels, uneven geographical distribution and climate issues related with fossils are the most important drivers for the use of renewables. The current chemical use (including fuels) of renewables is basically limited to minor components of plants that are also important for nutrition. Therefore, lignocellulosic biomass will become the most important renewable feedstock in the future. Biorefineries are required to feed biomass into value-added chains for fuels and chemicals. Structural use should be given preference over gasification approaches for the production of chemicals. Some potentially very useful “dream reactions” as examples for structural use are shown in Figures 1.37 and 1.38.

Bibliography

- [1] IPCC (International Panel on Climate Change). *Climate Change*. 2007.
- [2] IEA (International Energy Agency). *Key World Energy Statistics*. 2009.
- [3] M. Aresta and A. Dibenedetto. Utilisation of CO₂ as a Chemical Feedstock: Opportunities and Challenges. *Dalton Transactions* (2007):2975–2992.
- [4] T. Sakakura, J.-C. Choi, and H. Yasuda. Transformation of Carbon Dioxide. *Chemical Reviews* 107 (2007):2365–2387.
- [5] FNR (Fachagentur Nachwachsende Rohstoffe). *Nachwachsende Rohstoffe in der Industrie*. 2010.
- [6] VCI (Verband der chemischen Industrie). *Chemie Report*. 2010.
- [7] BGR (Bundesanstalt fuer Geowissenschaften und Rohstoffe). *Energierohstoffe*. 2009.
- [8] BP (British Petroleum). *Statistical Review of World Energy*. 2009.
- [9] H. Schöne and M. Rüsçh. Biogene Kraftstoffe: Potentiale und Grenzen. *Chemie Ingenieur Technik* Vol. 81 (2009):901–908.
- [10] IFEU (Institut für Energie- und Umweltforschung Heidelberg GmbH). *Nachwachsende Rohstoffe für die Chemische Industrie: Optionen und Potentiale für die Zukunft*. 2006.
- [11] T. Mielke. *Global Outlook for Oilseeds & Products for the next 10 Years*. Tech. rep. Oilworld, June 30, 2008.
- [12] Europe Spot. *Europe Spot Refined FD NWE; prices averaged per year*.
- [13] M. Pagliaro, R. Ciriminna, H. Kimura, M. Rossi, and C. Della Pina. Von Glycerin zu höherwertigen Produkten. *Angewandte Chemie International Edition* Vol. 119 (2007):4516–4522.
- [14] IFEU (Institut für Energie- und Umweltforschung Heidelberg GmbH). *Greenhouse Gas Balances for the German Biofuels Legislation*. 2007.
- [15] EPA (Environmental Protection Agency). *Lifecycle Analysis of Greenhouse Gas Emissions from Renewable Fuels*. 2009.

- [16] concawe, EUCAR (European Council for Automotive R&D), and JRC (Joint Research Centre of European Commission). *Well-to-Wheels Analysis of Future Automotive Fuels and Powertrains in the European Context*. 2007.
- [17] World Bank and DFID (Department for International Development). *Executive Summary: Indonesia and Climate Change*. 2007.
- [18] A. Corma, S. Iborra, and A. Velty. *Chemical Reviews* 107 (2007):2411.
- [19] NREL (National Renewable Energy Laboratory). URL: www.nrel.gov/biomass/biorefinery.html.

1.7 Figures

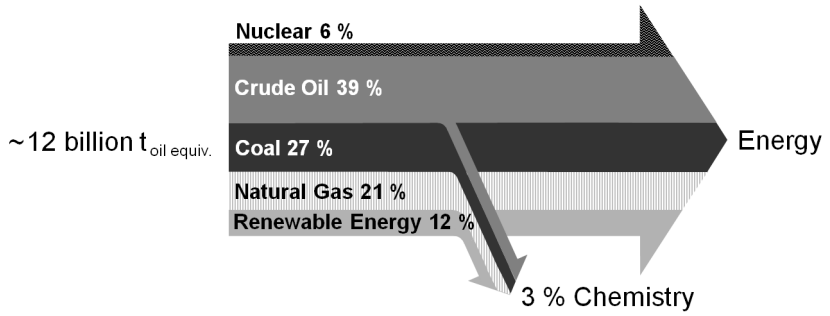


Figure 1.1: Global Energy Demand

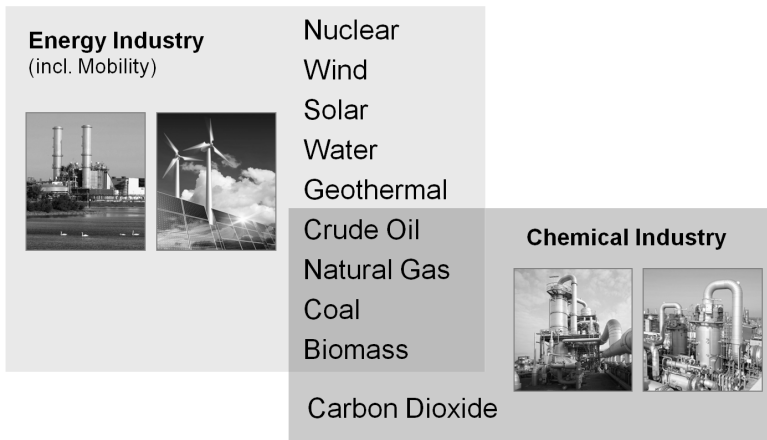


Figure 1.2: Energy versus Chemical Industry

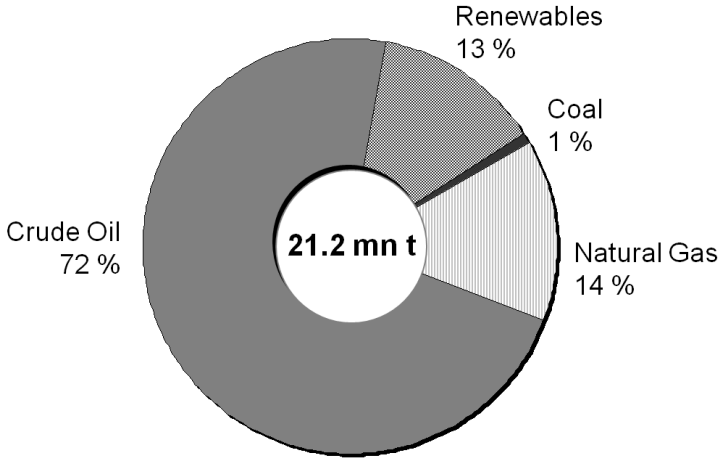


Figure 1.3: Feedstock Usage in German Chemical Industry

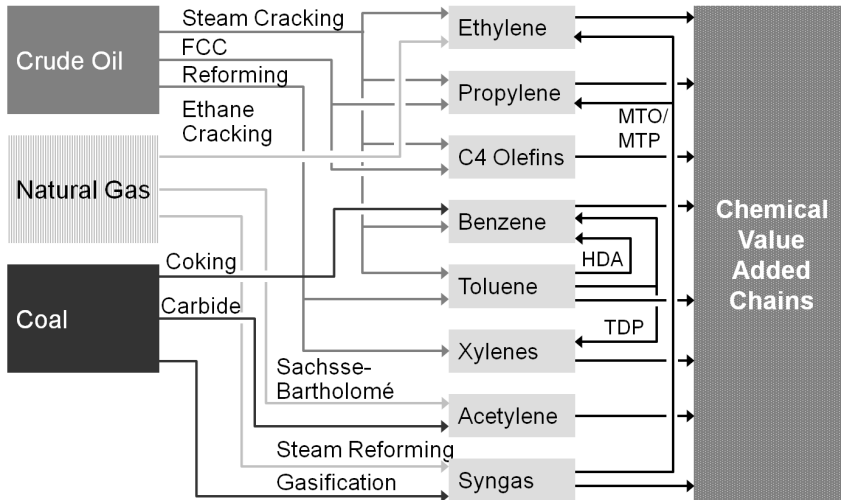


Figure 1.4: Chemical Value-Added Chains: Fossils

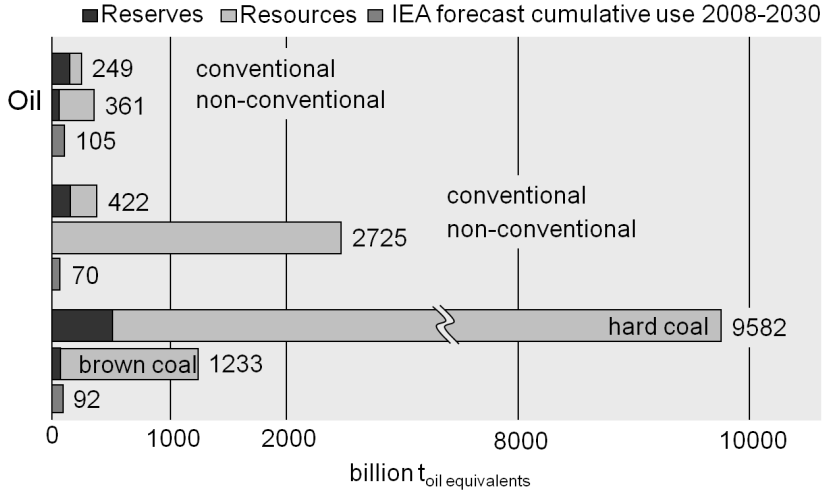


Figure 1.5: Limited Reserves & Resources for Fossil Fuels

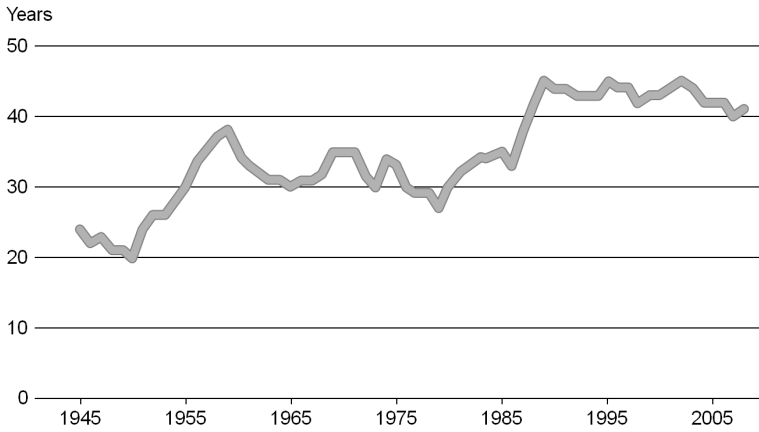


Figure 1.6: Static Range of Oil

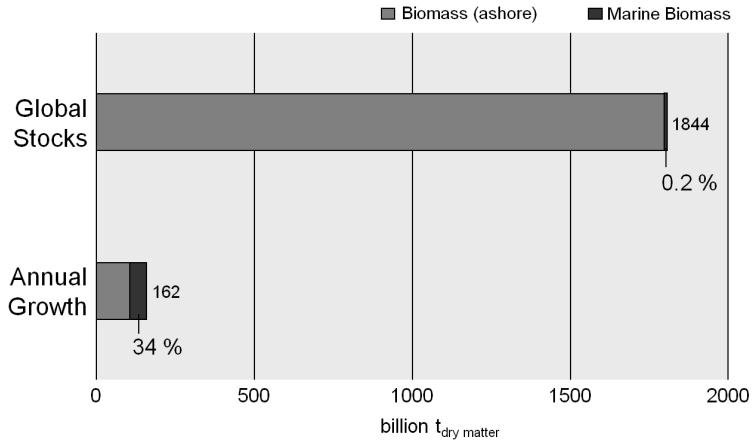


Figure 1.7: “Unlimited” Reserves of Biomass

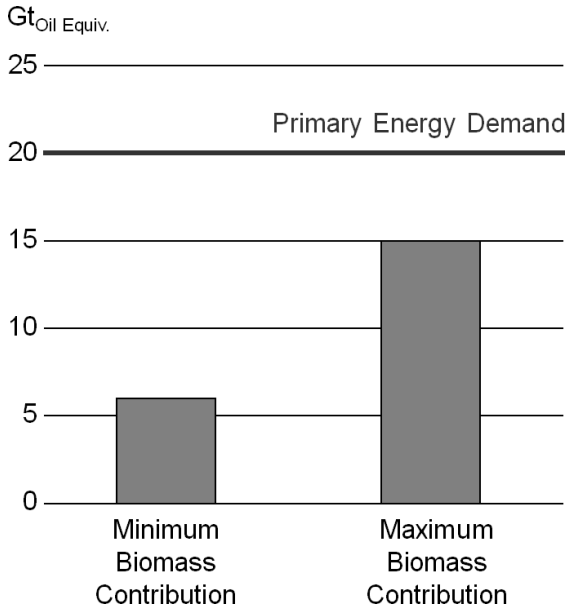


Figure 1.8: Future Scenario for Energy 2050

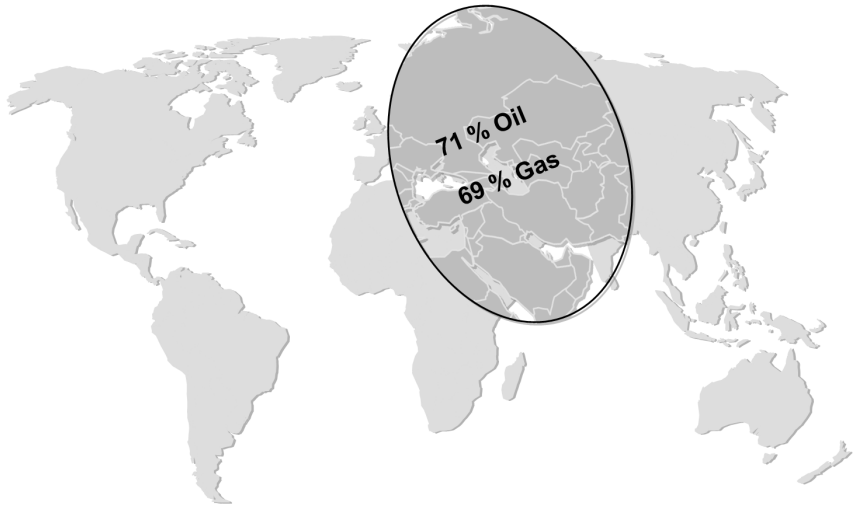


Figure 1.9: “Strategic Ellipse” of Conventional Reserves

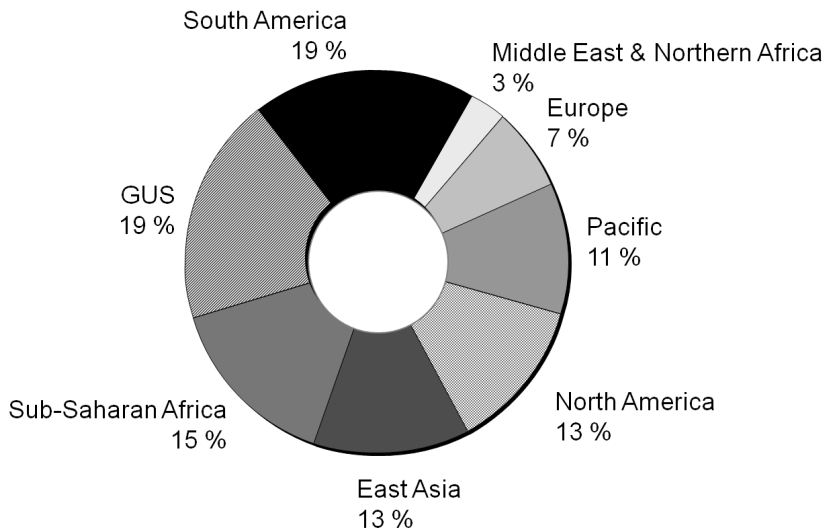


Figure 1.10: Biomass Potential by Region 2050

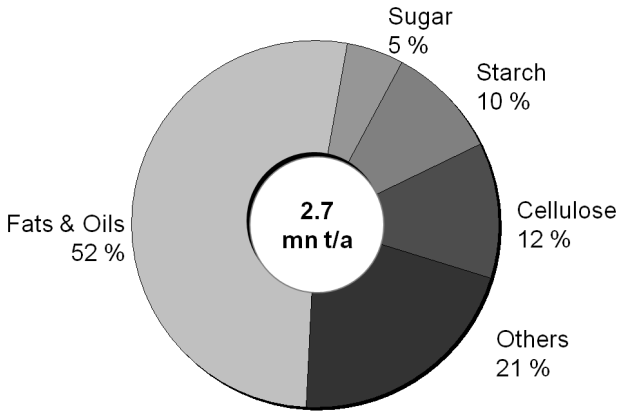


Figure 1.11: Renewable Feedstock Usage in German Chemical Industry. Others: 21%

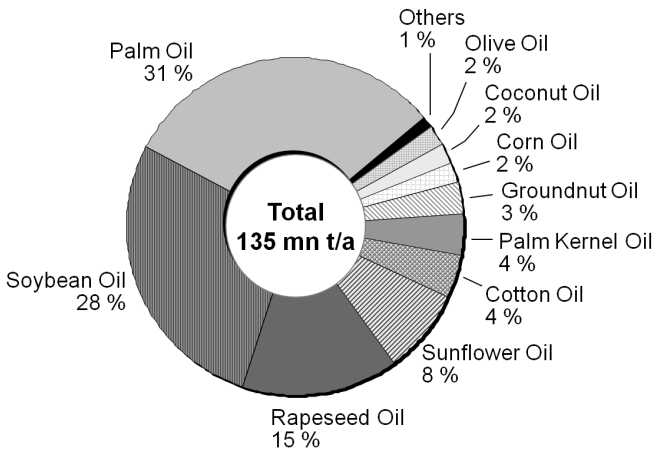


Figure 1.12: Global Market Size for Oils

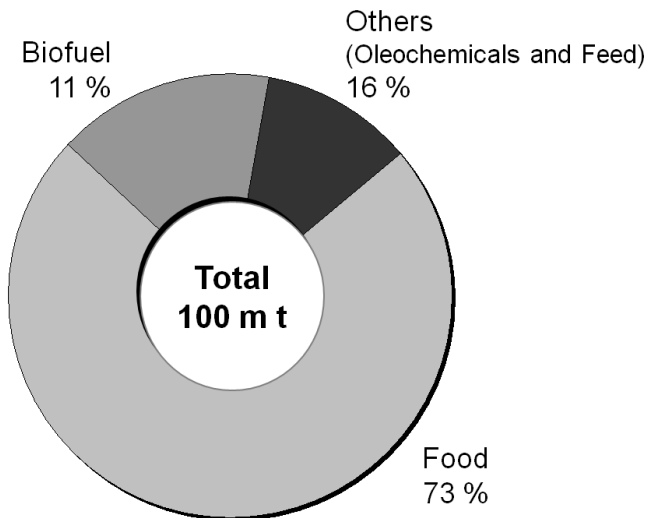


Figure 1.13: Three Major Oils by Application

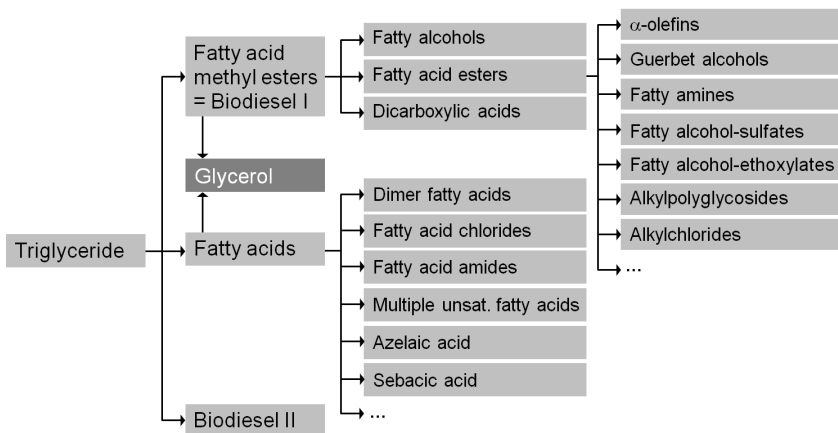


Figure 1.14: Chemical Value-Added Chains: Fats & Oils

Established Process from Castor Oil:

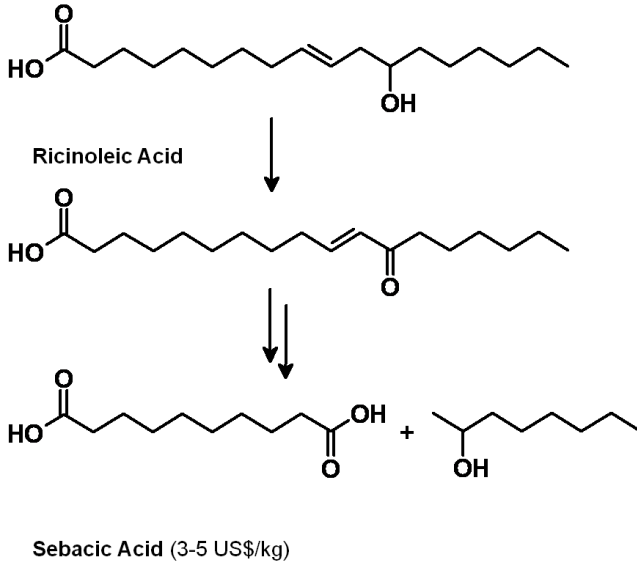


Figure 1.15: Sebacic Acid from Castor Oil

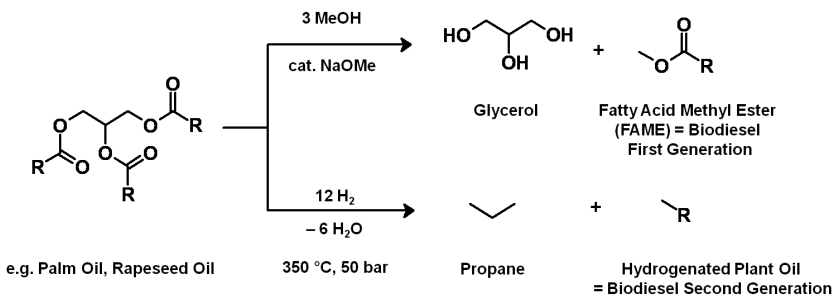


Figure 1.16: Biodiesel First and Second Generation

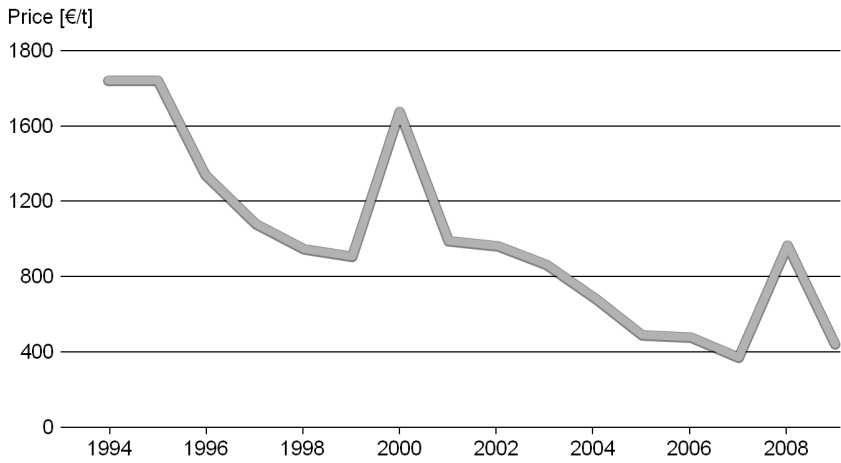


Figure 1.17: Glycerol Price Decline

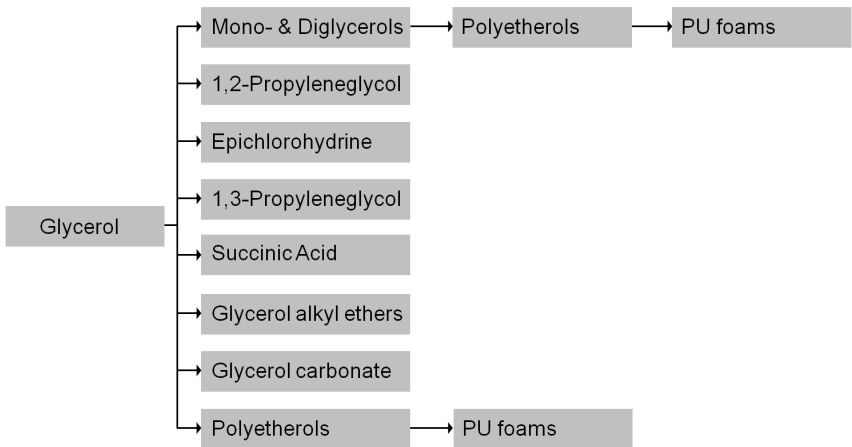


Figure 1.18: Chemical Value-Added Chains: Glycerol

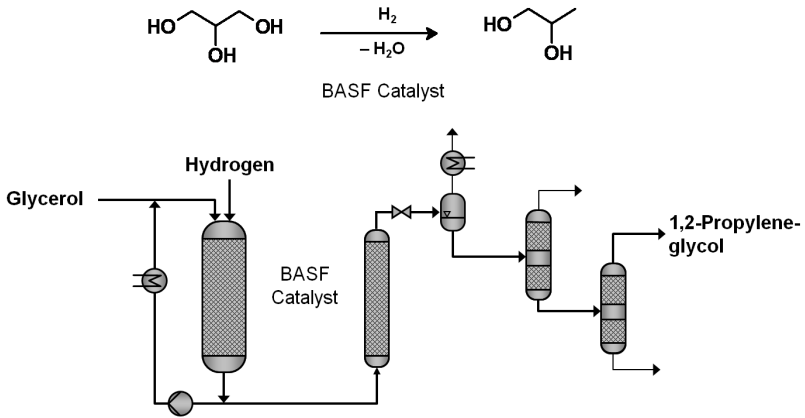


Figure 1.19: 1,2-Propylene-Glycol from Glycerol

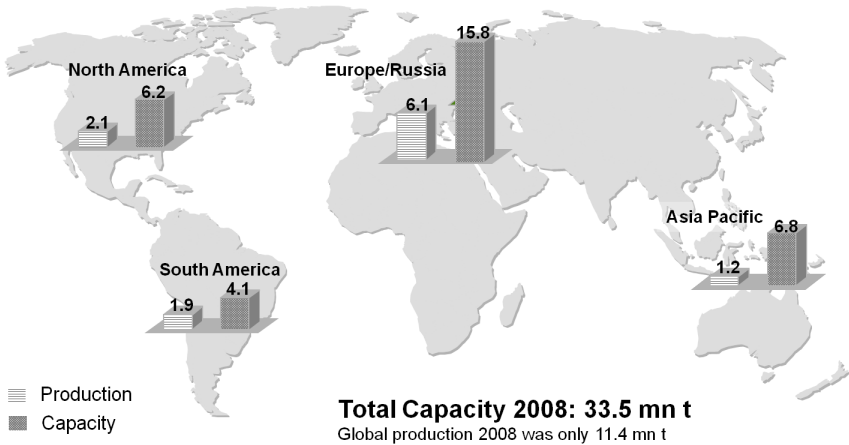


Figure 1.20: Biodiesel First Generation: Production and Capacities

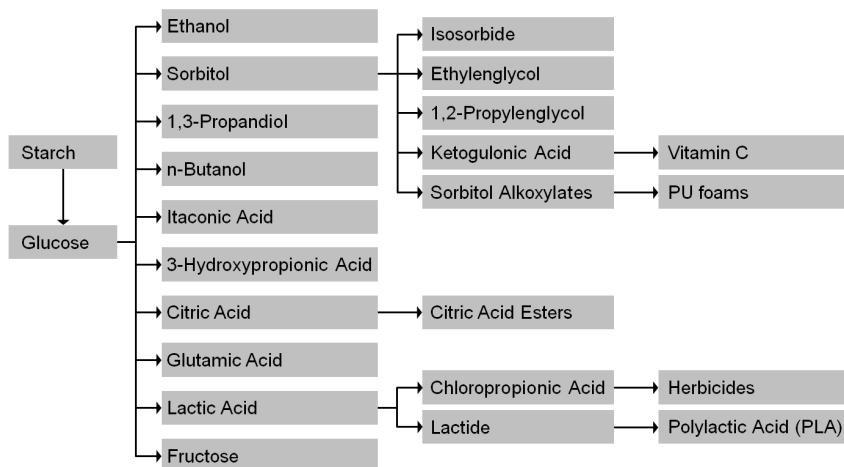


Figure 1.21: Chemical Value-Added Chains: Starch/Glucose

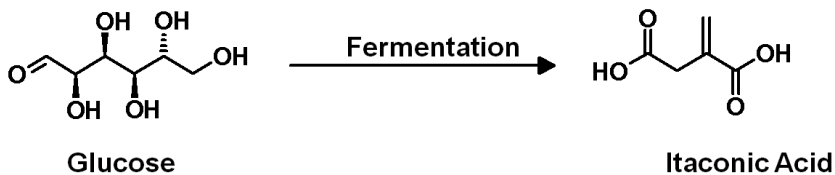
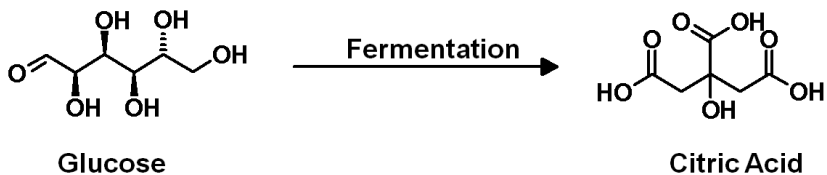


Figure 1.22: Examples of the Use of Glucose

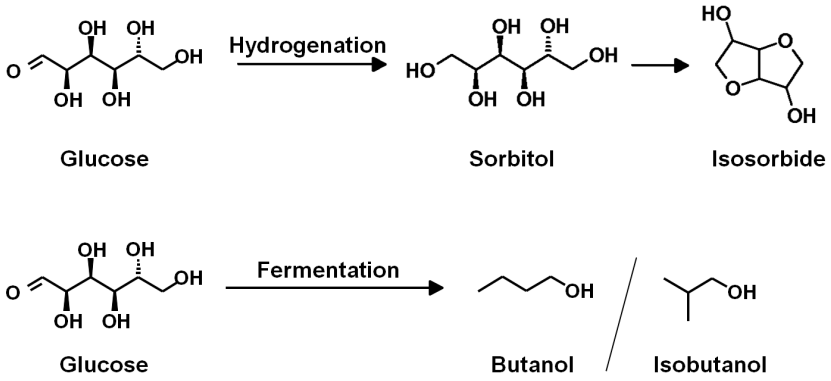


Figure 1.23: Examples of the Use of Glucose

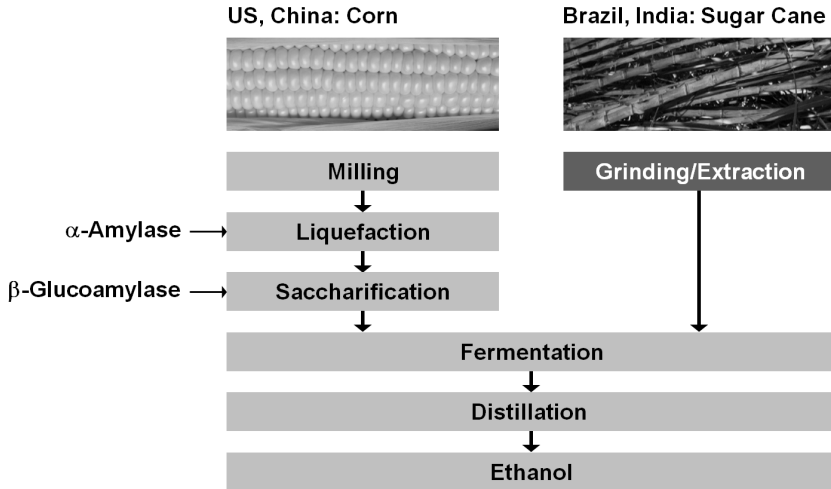


Figure 1.24: Bioethanol from Starch or Sugar

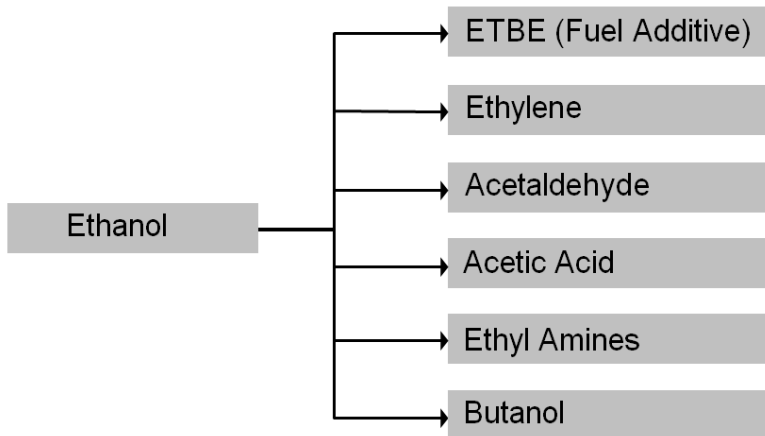


Figure 1.25: Chemical Value-Added Chains: Ethanol

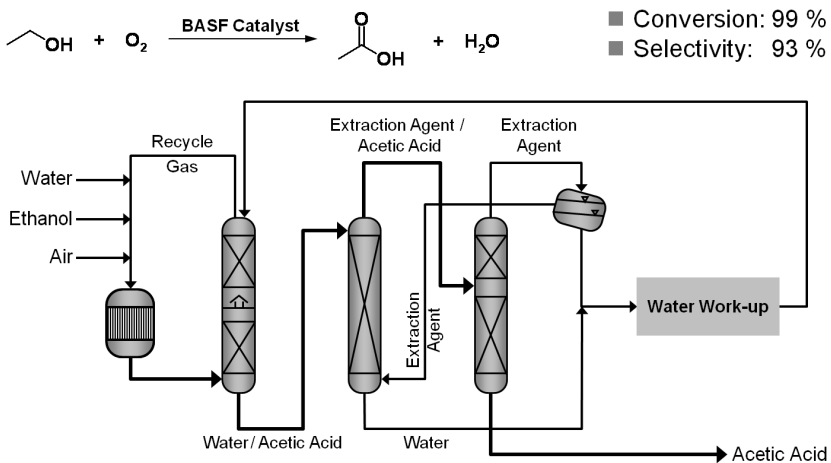


Figure 1.26: Acetic Acid from Ethanol

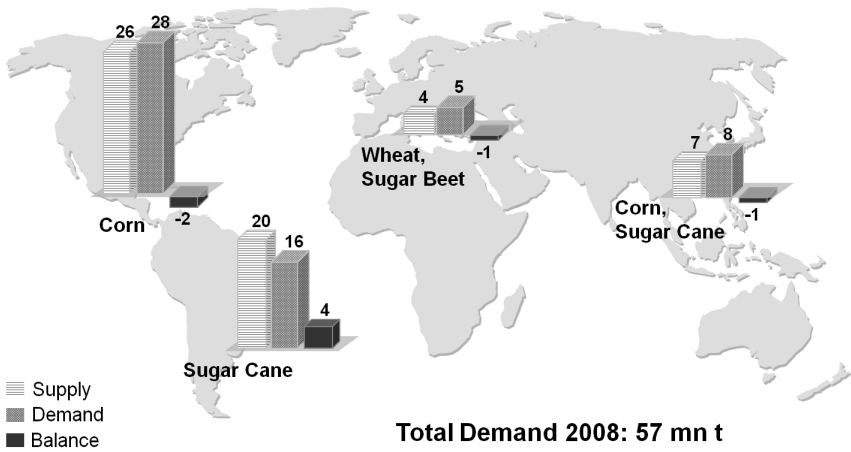


Figure 1.27: Ethanol: Supply and Demand

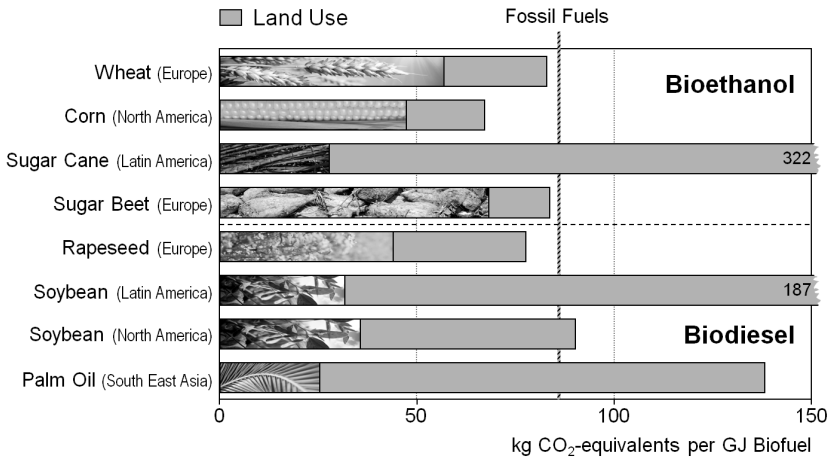


Figure 1.28: Greenhouse Gas Emissions of Biofuels

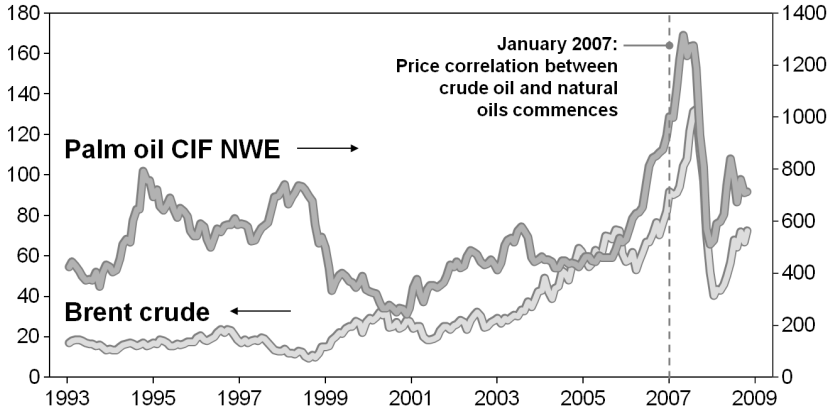


Figure 1.29: Example: Coupling of Food and Energy Prices (in U.S.\$)

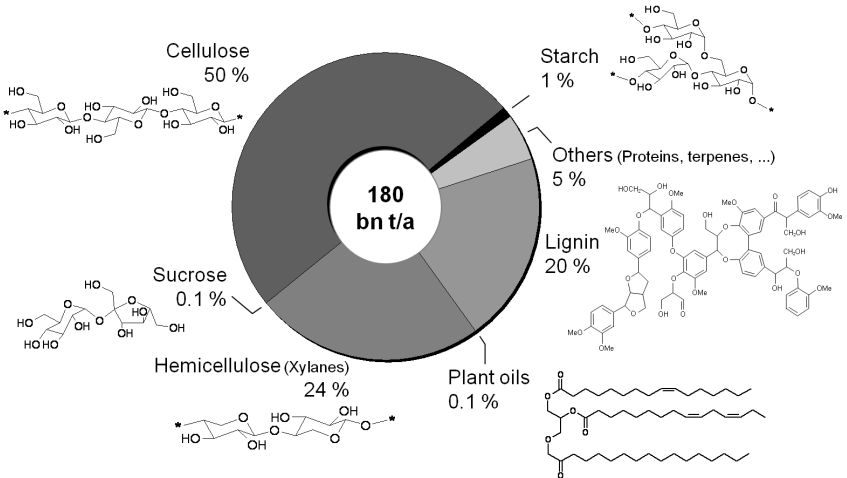


Figure 1.30: Composition of Biomass

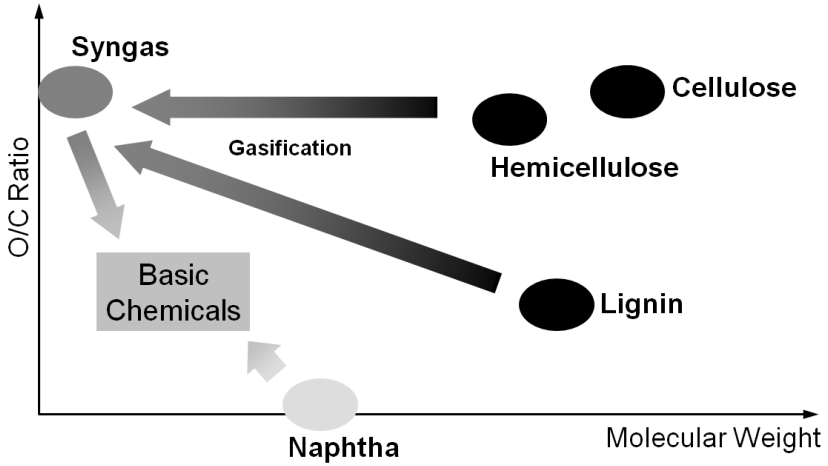


Figure 1.31: Chemical Modification: Gasification

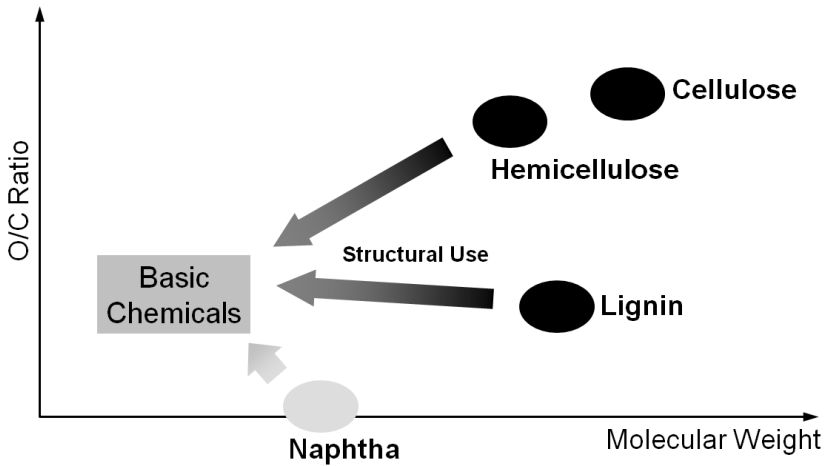


Figure 1.32: Chemical Modification: Structural Use

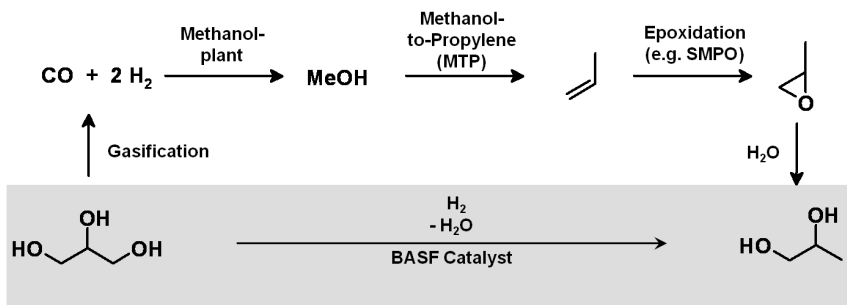


Figure 1.33: Example: Structural Use versus Gasification

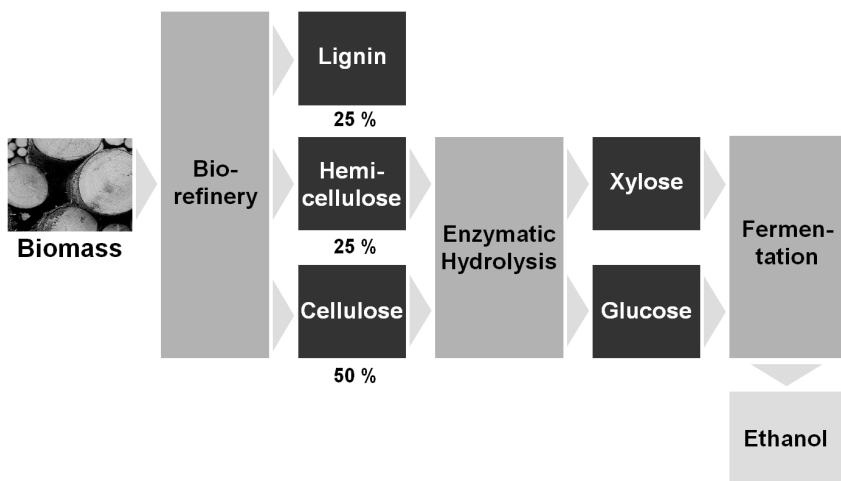


Figure 1.34: Concept of a Biorefinery

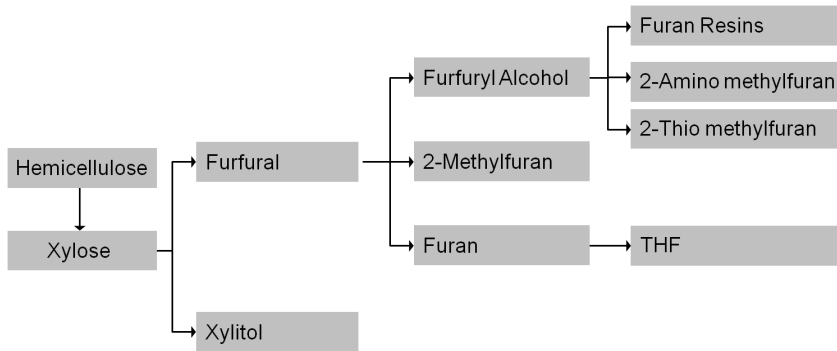


Figure 1.35: Chemical value-added Chains: Xylose

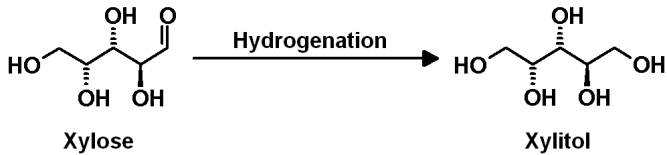
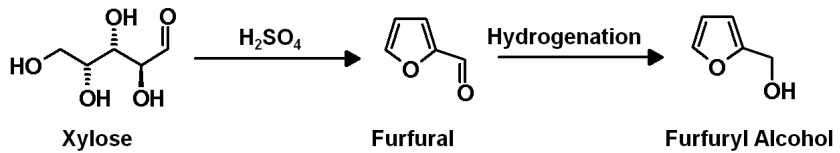


Figure 1.36: Examples of the Use of Xylose

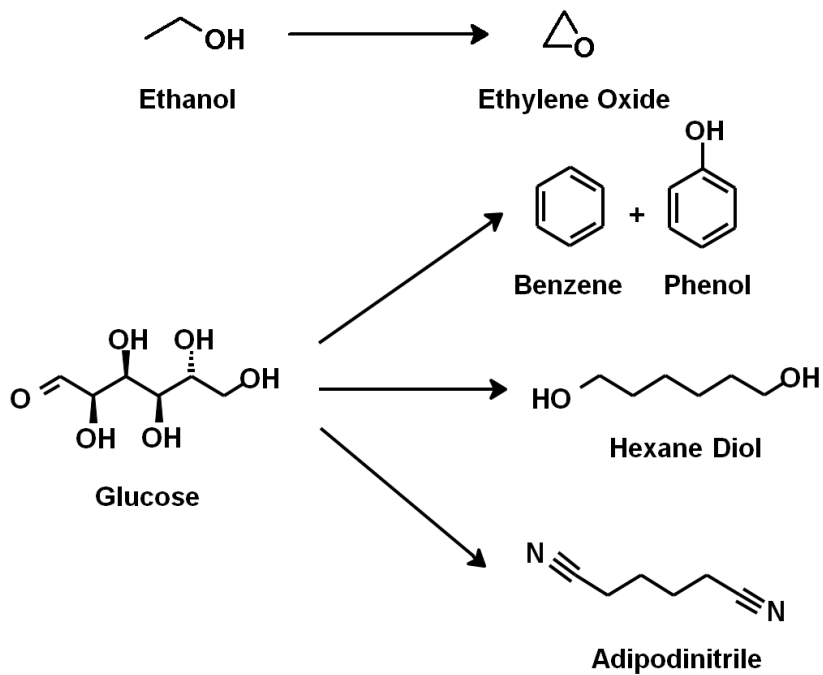


Figure 1.37: Dream Reactions

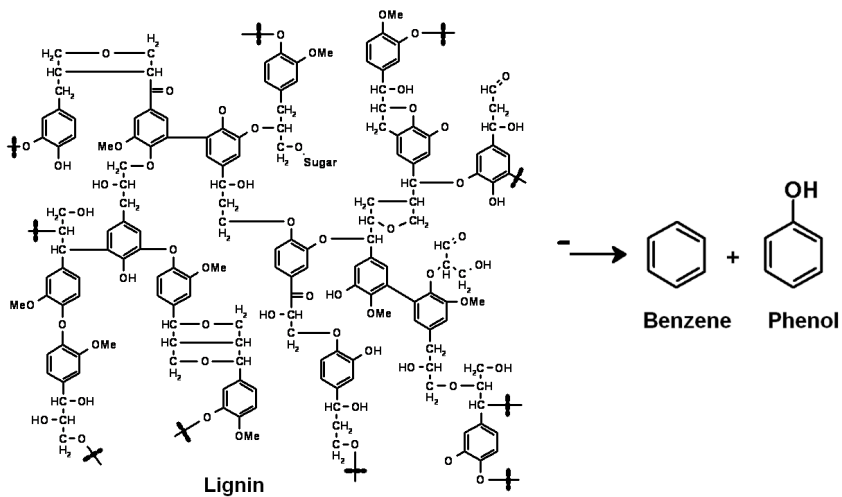
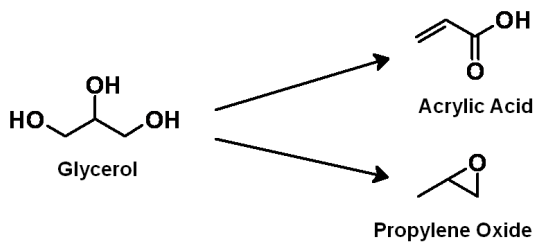


Figure 1.38: Dream Reactions

Chapter 2

The Role of Startup Companies in the Conversion of Biomass to Renewable Fuels and Chemicals

Leo E. Manzer

2.1 Introduction

Rising fuel prices and the location of much of the petroleum reserves has led the United States and other countries to aggressively pursue the development of new technology for the conversion of renewable feedstocks such as wood, agricultural crops, municipal water, and animal residue to renewable fuels and chemicals. The challenges are enormous. It has taken decades to develop technology for the conversion of crude oil and gas into transportation fuels and chemicals that are abundant in our society. The transformation of petroleum to fuels and chemicals typically involves the cracking of carbon-carbon bonds using heterogeneous acid catalysts and hydrotreatment. However, renewable feedstocks require a new collection and distribution system and the conversion of wet, highly functional carbohydrates into products that will ideally be compatible with existing refinery operations. As a result, new catalysis and biology is being developed to convert these oxygenated feedstocks to useful products.

While governments have spent billions of dollars on research, development and piloting to encourage and assist in the commercialization of new processes, much innovation has come from small companies whose technology was often discovered in university research laboratories. These companies were founded with the financial assistance of venture capitalists and will hopefully be successful and develop into large and profitable enterprises. However, there is no intention to diminish the large R&D efforts by many companies such as Shell, BP, DuPont, Dow and others. This paper will highlight only a few of the small startup companies that are moving ahead rapidly as examples of the exciting new developments taking place in the renewable fuels and chemicals area.

2.2 Results and Discussion

Each year, Biofuels Digest polls a large number of readers and comes up with a list of the Top 50 companies that are active in the renewable fuels and chemicals area. A few of the Top 50 Bioenergy Companies for the 2010–2011 survey are shown in Table 2.1. Several of these will be discussed in this chapter. It is interesting to note the distribution of companies and their main focus. The feedstocks are diverse, the products are diverse and over 70% of the ranked companies are in the United States.

Ranking	Company	Ranking	Company
1	Amyris	11	Virent
2	Solazyme	12	Mascoma
3	POET	13	Ceres
4	LS9	14	Cobalt Technologies
5	Gevo	15	UOP
6	DuPont Danisco	16	Enerchem
7	Novozymes	17	BP Biofuels
8	Coskata	18	Genencor
9	Codexis	19	Petrobras
10	Sapphire Energy	20	Abengoa
31	LanzaTech	47	KiOR

Table 2.1: A Partial Ranking of the Top Bioenergy Companies by Biofuels Digest (2010–2011) [1]. The complete ranking comprises 37 US and 13 non-US companies, 15 work in the field of cellulosic ethanol development, 5 with algae, 16 on renewable drop-in hydrocarbon fuels and 13 on renewable chemicals.

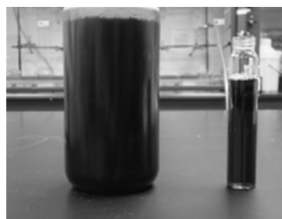
2.2.1 Renewable Fuels

The eventual transition from petroleum-based transportation fuels to renewable fuels provides a huge 200 billion gallon per year (1 trillion lbs) opportunity for new catalysis and process research. The renewable gasoline market is entirely dominated by ethanol, which is obtained by the fermentation of cornstarch as a necessary first step. New fuels and technology based on the use of non-food feedstocks are being developed and will hopefully be commercialized. It is recognized that the use of food feedstocks is not desirable in the long run but it is also important to recognize that the technical challenges for the conversion of

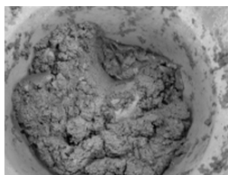
carbohydrates are significant even with pure sugars such as glucose. Once that technology is developed new methods will be required to use real sugar solutions derived from lignocellulosic feedstocks. The nature of these feedstocks is illustrated in Figure 2.1. It is readily apparent that the real feedstocks which will contain biomass residues, tars, oligomers, inorganic metals from nutrient solutions, and sulfur, nitrogen and protein from fermentation derived feedstocks will pose significant challenges to maintained high conversion, selectivity and lifetime of new catalyst systems.



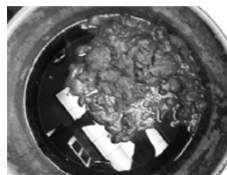
Simulated liquor from dilute-acid pretreated corn stover



Actual liquor from dilute-acid pretreated corn stover



~25% solids dilute-acid pretreated corn stover slurry (recently mixed drum)



~25% solids dilute-acid pretreated corn stover slurry (drum unmixed ~ 1yr)

Figure 2.1: Photos of Solutions Derived from Lignocellulosic Biomass and Pure Sugar (Photographs by courtesy of Dr. Edward J. Wolfrum, NREL)

Ethanol is widely used as an additive for gasoline. However, it has many limitations such as low energy density and cannot be transported in existing pipelines. Bio-butanol is an attractive alternative to ethanol. A number of companies are actively working on organisms that will convert sugars to butanol. The benefits of butanol over ethanol as a fuel are shown in Table 2.2. Butanol offers better safety, improved fuel economy, can be blended with gasoline in high concentrations and used without vehicle modifications. Another important advantage is that butanol can be transported in existing pipelines.

Property Comparison	EtOH	BuOH	Gasoline
Energy Content (BTU/gal)	78M	110M	115M
Reid V.P. @ 100°F (psi)	2.0	0.33	4.5
Motor Octane	92	94	96
Air-to-Fuel Ratio	9	11	12–15

Table 2.2: Comparison of ethanol, butanol and gasoline as fuels

Company	Biofuel
Butamax (BP/DuPont)	iso-butanol
	n-butanol
	2-butanol
Gevo	iso-butanol
Metabolic Explorer	n-butanol
Cobalt Biofuels	n-butanol
Green Biologics Ltd.	n-butanol
Tetravitae Bioscience	n-butanol (ABE)
Butalco	n-butanol

Table 2.3: Non-limiting list of biofuel companies

A non-limiting list of companies that are active in this field is shown in Table 2.3. Large companies like BP and DuPont are moving rapidly to introduce butanol. Smaller startup companies like Gevo and Cobalt Biofuels have received significant venture capital funding and are making great progress with demonstrations in large pilot plants. Gevo Inc. was founded in 2005 with technology discovered at the California Institute of Technology. With some initial funding from Khosla Ventures, the company rapidly grew and after an IPO in February 2011, it currently has a valuation of nearly \$500 million.

Gevo's business model is to develop fermentation processes that can be retro-fit into existing ethanol plants with a limited amount of capital. Since 2009, Gevo is collaborating with ICM, one of the leading providers of ethanol production technology. They have successfully retrofit an existing ethanol plant at St. Joseph, Missouri, with an organism capable of making isobutanol and are currently in the process of retrofitting two additional ethanol plants to make isobutanol. The startup of the first plant is due in 2012. The current capacity is about 1 million gallons per year. They claim to be able to convert current ethanol plants to

butanol production at relatively low cost. Of the three butanols, isobutanol is particularly attractive since it can be readily dehydrated to isobutylene, a valuable feedstock that is used in large volumes today. A biobased source of isobutylene provides an immediate opportunity to substitute a renewable product into existing investments. Some of the very large markets targeted by Gevo are shown in Figure 2.2. These cover a wide range of renewable chemicals and renewable fuels such as jet fuel, high-octane gasoline, solvents, renewable terephthalic acid for PET bottles and butyl rubbers.

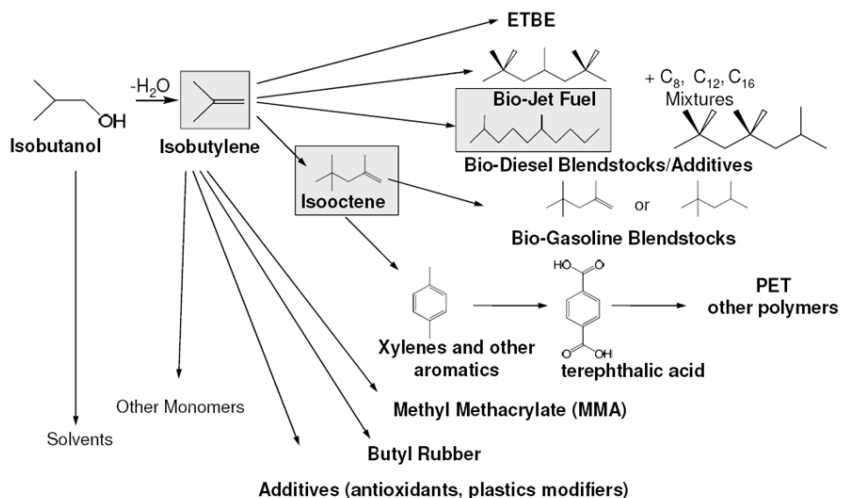


Figure 2.2: Some Derivatives Available from Bio-Isobutanol

Amyris, Inc. is another successful startup that was founded with technology developed at UC Berkeley. Once again, with initial venture capital funding it grew rapidly and after an IPO in September 2010 the current valuation is over \$ one billion. Their product platform is based on sugar fermentation to the isoprene trimer, β -farnesene (Figure 2.3). An attractive feature of their process is that the hydrocarbon product is insoluble in the fermentation broth and readily separates to provide the unsaturated C-15 molecule. After hydrogenation, it yields an attractive diesel fuel. In addition, the unsaturation provides a route to a variety of monomers, polymers and specialty chemicals.

Another bio-company, which converts sugar to hydrocarbon products that readily separate from the fermentation broth, is LS9, Inc. Founded in 2005, it has developed a biological process for the fermentation of sugars to linear hydrocar-

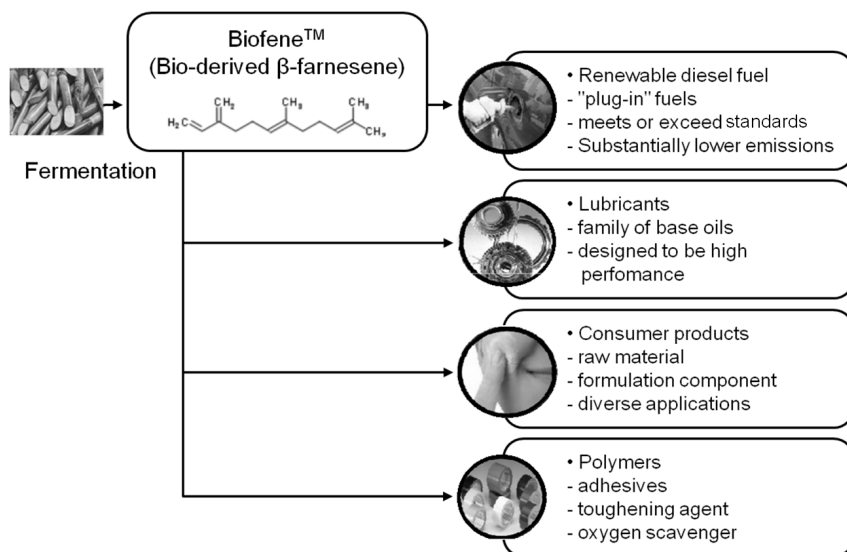


Figure 2.3: Family of Products Derived from Amyris Biofene™

bons as shown in Figure 2.4. By genetically altering the organism that naturally produces lipids, the company is able to make a variety of linear hydrocarbons that may be functionalized to alcohols, olefins, ketones and aldehydes. When this text was published, LS9, Inc. was still a private company.

LanzaTech Inc. is a startup company that was founded in 2005 in New Zealand. LanzaTech's commercial plants effectively convert a variety of nonfood, low value gas feedstocks into bioethanol and other platform chemicals. Using proprietary technology they are able to ferment CO-rich streams into ethanol and other products like 2,3-Butanediol (Figure 2.5). The initial focus is on the conversion of waste streams from steel mills and gasifiers. They have been operating a pilot plant at a steel mill in New Zealand and have just announced the construction of a 100,000 gallon per year demo plant in collaboration with Bao Steel in China. The startup is expected in the first half of 2012. Following a successful scale up of their demo facility, commercial plants are planned for China, South Korea and India.

Next generation fuels, beyond ethanol and butanol derived from sugars, will be hydrocarbon fuels from lignocellulosic feedstocks. Direct gasification of biomass to synthesis gas is technically feasible but presents a number of challenges

such as the removal of tars and inorganics, which are severe poisons to downstream *Fischer-Tropsch* or higher alcohol synthesis catalysts [2].

All unit operations in a single cell catalyst

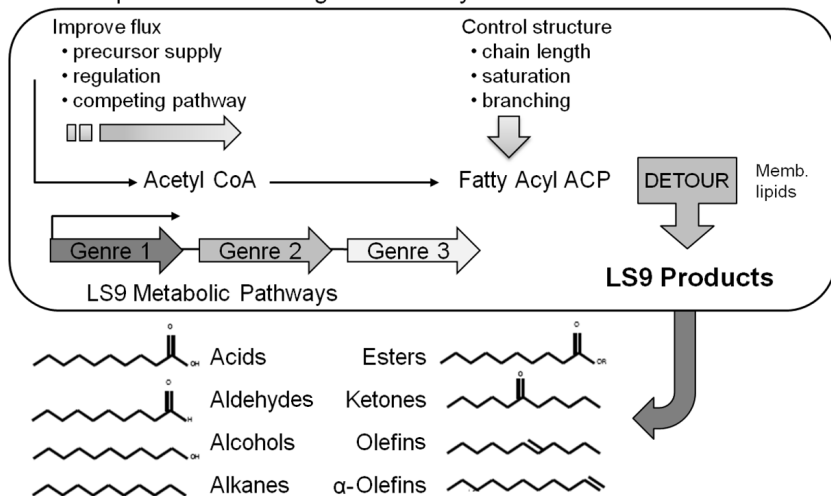
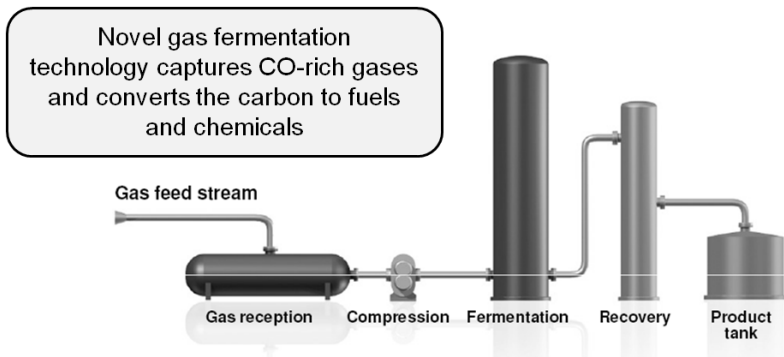


Figure 2.4: Potential Biobased Products Produced by LS9, Inc.

An excellent overview of potential processes to convert lignocellulosic feedstocks to advanced biofuels may be found in a report from a U.S. Department of Energy (DOE) workshop in 2007 [3]. Biomass gasification potentially provides an excellent method of converting lignocellulosic feedstock into synthesis gas. New gasifiers are under development around the world since the variable composition of biomass is significantly different from natural gas or coal, the traditional sources of syngas. The inorganic content of some biomass can contain high levels of silica and other oxides as well as sulfur, nitrogen and phosphorus compounds, which are poisons for the downstream syngas conversion units. Not all startups are successful, unfortunately. Range Fuels, a privately held company in Colorado, received a loan guarantee from the DOE and raised over \$100 million to build a demo plant in Georgia to gasify wood chips to syngas followed by an alcohol synthesis catalyst that would make primarily methanol and ethanol. Unfortunately, this plant did not work as expected. It was shut down and the staff of Range Fuels dismissed [4].

Other processes of significant interest include:

1. Conversion of municipal solid waste to ethanol or butanol using concentrated sulfuric acid (Bluefire Ethanol, Inc.)
2. Gasification of biomass to syngas followed by the fermentation of the syngas directly to ethanol (Coskata, Inc.)
3. Fermentation of sugars to 1,4-Butanediol (Genomatica, Inc.)
4. Conversion of sugars to ethers of hydroxymethylfurfural (HMF) (Avantium – Netherlands)
5. Hydrogenation of fats and oils to long chain linear alkanes for diesel fuel (Neste, Petrobras, ConocoPhillips, UOP, and others)



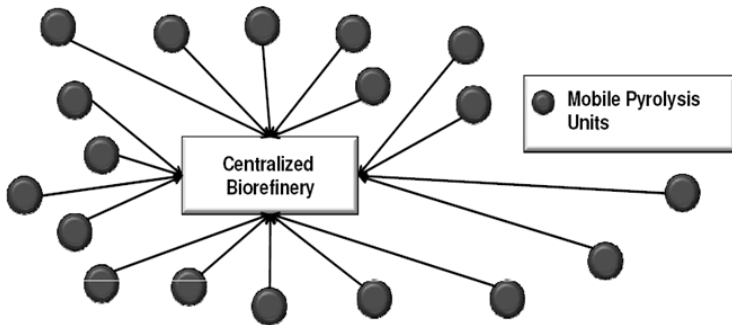
- **Innovative:** Microbe uses gases as its sole source of energy
- **Proprietary:** LanzaTech has filled 58 patents, including two proprietary microbe patents
- **Not just about ethanol**
- **Integrative:** Direct production of fuels and chemicals (2,3-Butanediol, Isoprene, Propanol, Butanol, MEK); multi step production of chemicals and chemical intermediates (olefins)
- **Thermo Chemical Opportunities:** 2,3-Butandiol produced through the LanzaTech Process can be used to make true „Drop in“ hydrocarbon fuels (gasoline, diesel, jet fuel)

Figure 2.5: The LanzaTech Process for Converting CO-rich Streams to Ethanol and 2,3-Butanediol

All of these new processes ultimately will require a large source of biomass to make a significant contribution to society's need for transportation fuels. A 2005 report from the U.S. Department of Agriculture (USDA) [5] suggested that

the U.S. had about 1.366 billion tons of agricultural and forest residue available but that this amount of biomass would satisfy only about 30% of the U.S. transportation fuel needs. Biomass has a high water content which is why economical transportation distances are usually considered about 50 miles or less. Much of the biomass considered in the USDA report is located at a significant distance from any potential biorefinery so it must be converted into a form that may be transported economically. One concept under consideration by many companies is field densification, or partial dehydration of the lignocellulosic material. A preferred process called *fast pyrolysis* involves heating the biomass very quickly (~ 1000 °C/sec) to a temperature of about 400 °C. During this heating step volatile gases are produced, along with a solid char (from the lignin) and a wet oil called *pyrolysis oil*. The oil tends to be very acidic and corrosive, highly colored, immiscible with hydrocarbon fuels and contains about 20–30% residual water. It also is relatively unstable and its composition changes with time. The char and the volatile gases may be burned to provide the heat needed for the process.

Remote Pyrolysis with Central Biorefinery



- Fast pyrolysis is “field densification” of biomass
- Rapid heating of biomass ($1000^{\circ}\text{C}/\text{sec}$) to $\sim 450^{\circ}\text{C}$
- Bio-Oil precursor to green diesel and gasoline
- No commercial units in mass production!
- There are issues to be solved!

Figure 2.6: A Concept for the Collection of Remote Biomass

A number of companies are working on modular fast pyrolysis units that will fit on the bed of a truck and can be moved from site to site as needed (Figure 2.6). Stabilizing and upgrading of the pyrolysis oil prior to shipment is one of the many challenges to commercial use. Ideally, this treatment will significantly deoxygenate the pyrolysis oil so that it becomes less water soluble and phase separates from the water. UOP and Ensyn have formed a Joint Venture called Envergent Inc. with the purpose of developing technology to hydrogenate the pyrolysis oil to a useful hydrocarbon fuel (Figure 2.7). Their current process uses a circulating solids reactor with sand as the heat transfer media.



Envergent
TECHNOLOGIES
A Honeywell Company

- Announced September 2008
- Pyrolysis Oil technology for fuel oil substitution & electricity generation now available
- JV becomes channel for UOP R&D results on upgrading pyrolysis oil to transport fuels



UOP
A Honeywell Company

- Core competence in engineering and technology scale-up
- Co-inventor of Fluidised Catalytic Cracking (FCC) technology
- Modular process unit supplier
- Leader in fundamental catalyst and process development (Upgrading)



ENSYN

- ~20 years of commercial fast pyrolysis operating experience in food industry
- Developers of innovative RTP fast pyrolysis process
- 8 commercial RTP units designed for food application
- Now applying technology to fuel oil and energy

2nd Gen Renewable Energy Company – Global Reach

Figure 2.7: Envergent, a Joint Venture between UOP and Ensyn

Woody biomass is brought in contact with the hot sand at about 510 °C for two seconds to produce pyrolysis oil (Figure 2.8). KiOR Inc. is another startup company based in Texas. A significant difference in their process compared to others is that a catalyst is used during the pyrolysis step. The effect is very significant since the catalyst allows the biomass to be pyrolyzed at a lower temperature while at the same time reducing the oxygen content of the pyrolysis oil. The *Biomass Catalytic Cracking* process (BCC) (Figure 2.9) produces oil with a *Total Acid Number* (TAN) much lower than that of non-catalytic processes. As a result, a hydrocarbon phase separates and can be readily processed. Dynamo-tive is another fast pyrolysis company that has several commercial plants making pyrolysis oil for energy use. It is developing a two-stage hydrogenation process

that first stabilizes the oil by reducing the water and oxygen content and then hydrotreats the first product to give a gasoline/diesel fuel.

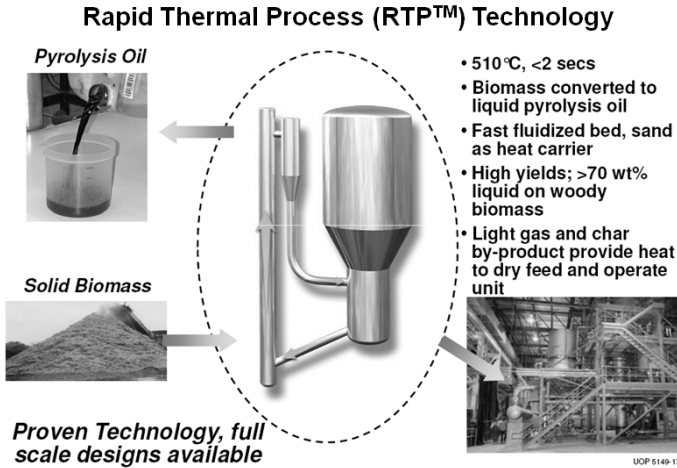


Figure 2.8: Envergent’s Process for the Production of Pyrolysis Oil

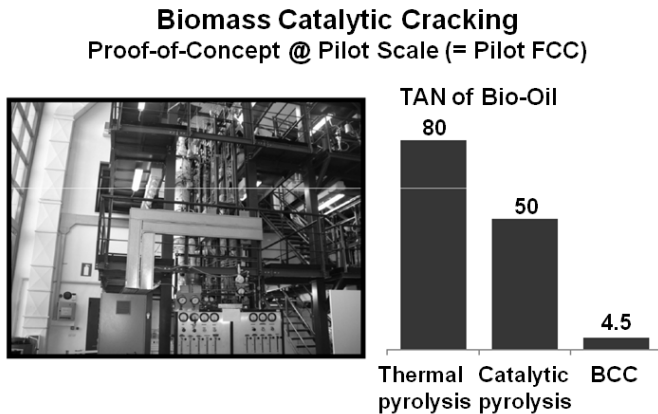


Figure 2.9: KiOR’s catalytic pyrolysis technology

2.2.2 Renewable Chemicals

Chemicals are higher value products than fuels. For this reason a number of companies are working on biological and thermochemical routes to renewable chemicals. In some cases, the products are direct drop-in molecules while in other cases new products are obtained. An important and commonly cited report was prepared by PNNL and NREL [6]. After considerable study, they proposed twelve molecules, shown in Table 2.4, that would be attractive building blocks for future renewable chemicals. This report has stimulated a very significant amount of research within the academic and industrial communities.

1,4 diacids (succinic, fumaric and malic)	itaconic acid
2,5-furandicarboxylic acid	levulinic acid
3-hydroxypropionic acid	3-hydroxybutyrolactone
aspartic acid	glycerol
glucaric acid	sorbitol
glutamic acid	xylitol/arabinitol

Table 2.4: Top 12 Sugar-Derived Building Blocks

One molecule that is receiving considerable attention is succinic acid. A number of small and large companies (BioAmber, Myriant, DSM, BASF and others) have announced plans to commercialize bio-based succinic acid and its derivatives. BioAmber Inc. commissioned the world's first commercial plant in France in January 2010 with an initial capacity of 2,200 MT per year. Succinic acid is a particularly attractive molecule as it is produced today from maleic acid via butane oxidation. A biobased source of succinic acid and its derivatives would be drop-in replacements for the petroleum-derived compound. The markets for products derived from bio-based succinic acid (polymers, plastics, solvents, adhesives, and coatings) (Figure 2.10) are significant so it is not surprising that it has attracted the attention of so many companies.

Levulinic acid has been of interest for many years as a bifunctional keto-acid but it has never been made on a commercial scale [7]. Biofine Renewables, LLC has developed a thermochemical process that produces levulinic acid, furfural, formic acid and char from a wide variety of biomass feedstocks and is operating a fully integrated pilot plant. The process uses two reactors to initially break down the biomass into small components such as hydroxymethylfurfural which are then further converted to levulinic acid. The conditions are extreme, with high temperatures and pressures but a yield of about 50% levulinic acid is achieved. With the ketone and acid group functionality, levulinic acid can be converted

to a wide variety of compounds such as N-alkylpyrrolidones, monomers for the preparation of thermally stable polymers, ionic liquids and nylon intermediates (Figure 2.11).

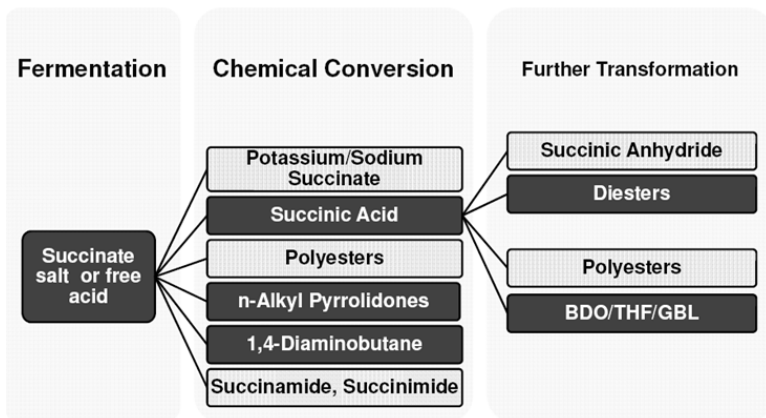


Figure 2.10: BioAmber Inc. production platform

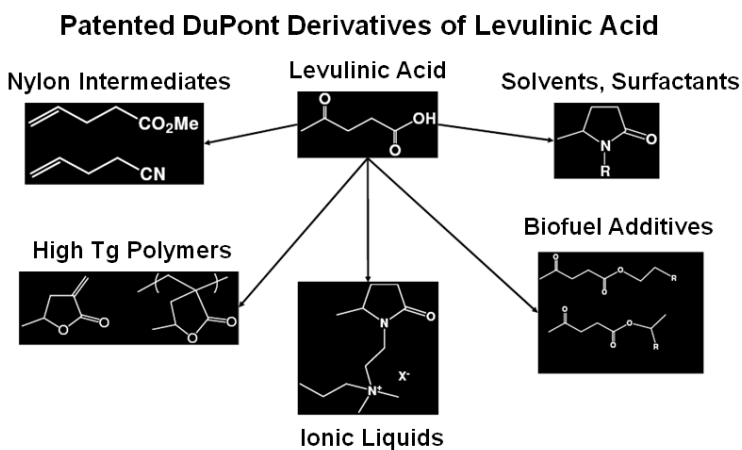


Figure 2.11: Selected Derivatives of Levulinic Acid

While many of these materials are exciting new renewable based chemicals, none have reached commercial production due to the fact that a low cost, high volume source of levulinic acid is not yet available. Some other derivatives of levulinic acid have reached advanced stages of development and are moving to advanced production levels. One example is the startup company Segetis, Inc. It initially received venture capital funding to develop a novel class of ketals formed by the reaction of diols with the ketone group of levulinic acid. Using glycerol and levulinic acid, two of the DOE “Top 12” molecules, new ketal products are produced which have excellent functionality and can potentially replace existing petroleum based solvents, surfactants and plasticizers (Figure 2.12).

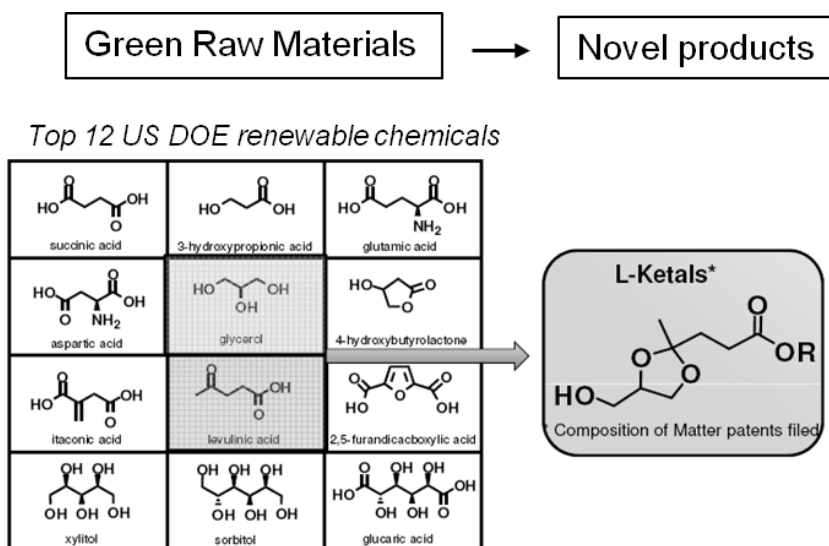


Figure 2.12: Segetis Ketals are Derived from Diols and Levulinic Acid. Levulinic Ketal esters can be readily extended with alcohols, esters, and amines using standard catalysts and reaction conditions to produce a wide range of bio-based ester technologies.

Furandicarboxylic acid (FDCA) is another one of the DOE “Top 12” molecules. It may be prepared by oxidation of hydroxymethylfurfural, HMF (Figure 2.13), which is a difficult molecule to obtain due to its high reactivity. Avantium is pursuing the use of HMF-ethers as renewable diesel compositions. An advantage of forming the HMF-ether is that it is much more stable and easier to work with than HMF. Polymers of FDCA [8], are potential replacements for tereph-

thalic acid esters (Figure 2.14). However, there has never been a viable process for its manufacture. The HMF ethers can provide an excellent feedstock to FDCA by oxidation. Avantium has collaborated with Nature Works to explore the commercial potential of FDCA polyesters.

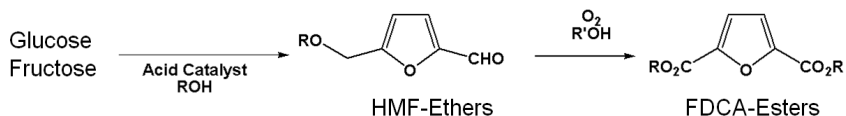


Figure 2.13: Reaction scheme of C6 sugars to FDCA-esters

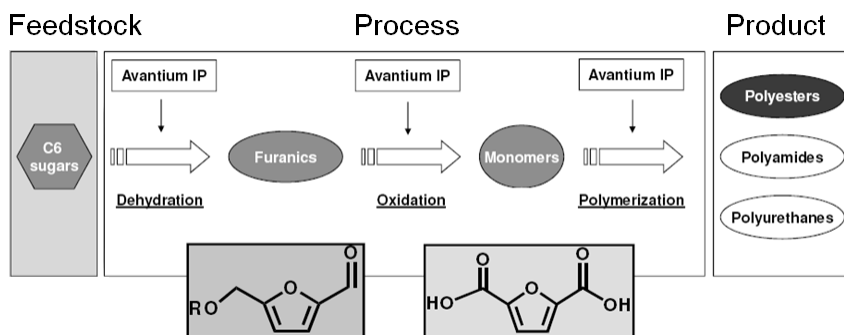


Figure 2.14: Scheme of the Avantium process from C6 sugars to polymers

2.3 Conclusion

The intent of this chapter was to provide examples of the creativity and innovation being developed mostly by new startup companies. These companies are playing a key role in the development of renewable fuels and chemicals. Not all will be successful, larger oil and chemical companies will acquire some, and some will grow into new companies. With luck, perseverance and significant funding the world's needs for fuels and chemicals will someday be based on renewable feedstock. In the 2+ years since this presentation, companies like Amyris, Gevo, KiOR and others have run into scale-up problems and delays resulting in significant decreases in their stock price and valuation since their initial IPO. Hopefully these problems will be overcome and they will be successful but only time will tell.

Acknowledgments

I wish to thank many individuals (too numerous to name) in a number of start-up companies for providing me with the information discussed in this text and allowing it to be publically disclosed.

Bibliography

- [1] URL: <http://www.biofuelsdigest.com/bdigest/2010/12/07/the-50-hottest-companies-in-bioenergy-for-2010-11/>.
- [2] S. Phillips, A. Aden, J. Jechura, and D. Dayton. *Thermochemical Ethanol via Indirect Gasification and Mixed Alcohol Synthesis of Lignocellulosic Biomass*. Tech. rep. NREL/TP-510-41168. NREL, Apr. 2007.
- [3] G.W. Huber. *Breaking the Chemical and Engineering Barriers to Lignocellulosic Biofuels: Next Generation Hydrocarbon Biorefineries*, National Science Foundation. Chemical, Bioengineering, Environmental, and Transport Systems Division. Washington, DC: NSF, 2008.
- [4] The Range Fuels Fiasco. *Wall Street Journal* (2010, February 10th).
- [5] USDA. *Biomass as a Feedstock for a Bioenergy and Bioproducts Industry: The Technical Feasibility of a Billion-Ton Annual Supply*. Tech. rep. U.S. Department of Agriculture, Apr. 2005.
- [6] T. Werpy and G. Petersen. *Top Value Added Chemicals From Biomass*. Tech. rep. Pacific Northwest National Laboratory (PNNL) and the National Renewable Energy Laboratory (NREL), Aug. 2004.
- [7] S. Ritter. Biorefinery Gets Ready to Deliver the Goods. *Chemical & Engineering News* 84 (Aug. 2006):47.
- [8] A. Gandi and M.N. Belgacem. Furans in Polymer Chemistry. *Progress in Polymer Science* 22 (1997):1203–1379.

Chapter 3

Nutrient Cycling in the Bioeconomy: A Life Cycle Perspective

Robert Anex

3.1 Introduction

Concerns about declining reserves of petroleum resources in the face of increasing demand, and the political and environmental costs of petroleum have led to increased interest in fuels and chemicals derived from renewable sources. Biorenewable chemicals, or chemicals derived from biomass, are seen to be promising economically and in addition their production can potentially create markets for agricultural commodities, reduce reliance on imported resources, and mitigate the impacts of fossil resource use on climate and the environment. Relative to bioenergy and biofuels, biorenewable chemicals are seen to be a more economically and environmentally advantageous way to use limited biomass resources [1, 2]. As a result, multiple authors have predicted significant substitution of petroleum-based commodity chemicals by biorenewable chemicals within the next decade and the U.S. Department of Energy has the goal to replace 25% of industrial organic chemicals with biorenewable chemicals by 2025 [3, 4].

Although there have been a few notable commercial successes, most biorenewable chemicals today exist only in development laboratories and business plans. The combination of keen business and governmental interest with very limited commercial-scale production data has led to significant uncertainty and vigorous debate about the preferred technology pathways for future biorenewable chemical production and their likely economic and environmental impacts [5–8]. Important topics in the debate about the best pathways to biorenewable chemicals have included the question whether there is a need to replace existing platform chemicals directly or only functionally [9], and the relative advantages of conversion through heterogeneous catalysis versus biocatalysis, or a combination of the two [1, 10].

Assessing the economic viability and environmental impact of biorenewable chemicals that are in the early stages of development can be very difficult due to the lack of process data [11]. However, because the factors that motivate the pursuit of biorenewable fuels and chemicals include the promise of higher ener-

gy efficiency and environmental improvement relative to their petroleum-derived counterparts, such assessment is important to prevent large investments in possibly undesirable technologies. The tool that has been most commonly used to assess the impact and energy efficiency of biorenewable fuels and chemicals is Life Cycle Assessment (LCA).

In recent years, LCA has been recognized as a useful decision-making framework for reducing the environmental impacts of technology. The essence of LCA is the identification and evaluation of relevant environmental implications of a product, process, or system across its entire life span—from creation to disposal as waste or recovery for re-use. By considering the entire life cycle, LCA can avoid “problem shifting” between life cycle stages and receptors. Although LCA techniques are still evolving, LCA has been used to guide public and private sector decisions for several decades [12, 13], and standard procedures for conducting LCAs have been developed by the U.S. Environmental Protection Agency, SETAC, and the International Standards Organization [14–18].

Life cycle assessment has been used to assess the few commercial or near-commercial biorenewable chemicals, such as poly-lactide (PLA), 1,3-propanediol (PDO), polyhydroxyalkanoates (PHA), and bio-polyethylene [19–22], as well as biorefinery systems that produce both fuels and chemicals [23]. However, in the earliest stages of development, when data about the relative environmental merits of candidate conversion pathways is most valuable, very little information is available. At this stage of development, when choosing between multiple potential pathways can yield the greatest benefits, it is difficult to identify required unit processes, much less conversion efficiencies, likely side products, and waste streams. It is equally difficult to predict how future resource constraints may change the cost of vital process inputs and the value of products.

This chapter continues with an overview of the LCA methodology, followed by ways that LCA can be adapted to make it more useful for screening biorenewable chemicals prior to their full development and commercialization. The chapter proceeds with an examination of influences of resource sufficiency and market fluctuations on the early assessment of biorenewable chemical candidate products, and concludes with final thoughts about assessing biorenewable products during early development.

3.2 Life Cycle Assessment Methodology

The standard procedure for LCA is outlined in ISO 14040:2006 and ISO 14044:2006 which describe the application LCA and define the key stages of analysis as shown in Figure 3.1. The key stages are: setting the goal and scope; creating an inventory of all life cycle uses of resources and environmental interventions

closure to the public. That is, LCAs that analyze two or more product systems, inviting comparisons and judgments.

At the heart of LCA is the idea of a *functional unit*. The “function” is what is to be accomplished by the product, process, or service under study. The functional unit defines the magnitude of service, the duration of service and the expected level of quality of the service provided by the product under study. For example, holding a specific quantity and type of liquid is the function of a drink container. The functional unit in this case encompasses the service of containing a specific amount of liquid, the time over which the service is to be provided, the degree of sterility that can be achieved, and other services such as labeling space on the bottle. The container could be a plastic bottle, a glass bottle, or a multi-layer aseptic carton.

When making comparisons between different products that have the same use, it is critical to have a consistent framework for keeping track of flows of material, energy and waste. The functional unit is the focus of LCA framework that provides this consistency and also differentiates LCA and other analysis methods such as environmental impact assessment and risk assessment. In the case of a shopping bag used to carry groceries from a store, while paper and plastic bags have the same volume, fewer groceries are generally placed in plastic bags than in paper bags. Practices vary from place to place, but the number of plastic bags needed to hold the volume of groceries usually held by a paper bag range from 1.2–3 [24]. This ratio of material, defined by the choice of functional unit, will scale all subsequent aspects of the LCA and profoundly impact the study result and conclusions [25]. For example, a 750 ml glass wine bottle weighs around 400 grams while the same size in PET weighs 54 grams, one-eighth of the weight. The lower weight and volume of the PET container translates into lower energy use and emissions during transport, but PET is more permeable to oxygen than glass, so the contents will likely have a shorter shelf life and result in more spoilage.

LCA goal and scope definition also requires the identification of the reference flow associated with the functional unit. The reference flow is the set of flows associated with the functional unit and defines all other flows in the product system. Other steps in setting goal and scope include definition of the initial system boundaries, criteria for inclusion of inputs and outputs, impact assessment methodology and data quality requirements. The selection of inputs and modeling of the system shall be consistent with the goal of the study; and the system should be modeled in such a manner that inputs and outputs at the system boundaries are elementary flows. In practice, inputs and outputs are defined by a cut-off rule, based on a factor such as mass, energy or environmental impact. A mass-based cut-off rule, for example, would eliminate from the inventory a material

contributing less than a specified percentage of mass input to the product under study.

Assessing and documenting the quality of data are important to the integrity of the LCA. Data quality is described on the bases of data age, geographical coverage, source, collection method, technology coverage, precision, uncertainty, completeness and representativeness [26]. However, when incorporated into a life cycle inventory, no differentiation is made between data of lower or higher quality. For example, data derived from a single personal communication are incorporated in the same way as detailed data based on measurements across an entire industry which are described by a complete set of statistical measures of uncertainty. Various data quality scoring systems have been developed, and a typical example is the data quality scoring of EcoInvent [27] which rank data in each data quality category with a score from 1 to 5 (with a score of 1 representing the highest data quality). These scores are a subjective choice of the LCA practitioner and can vary widely. The quality of inventory data used to evaluate a biorenewable chemical during the early stages of development will vary widely depending on how the data were derived. Quantitative estimates of data uncertainty should be developed whenever possible so that inventory uncertainty can be estimated.

3.3 Life Cycle Inventory

The life cycle inventory (LCI) process entails estimating and recording the resource use, environmental flows, products and intermediate materials for all unit processes within the boundaries of the product system. Figure 3.2 depicts the cradle-to-grave product system. Each stage of the product system contains a set of unit processes, each of which will have input and output flows from the environment in the form of materials, energy and wastes as well as intermediate flows of products among other unit processes.

A principal complication of the LCI is that few industrial processes yield a single output. Most processes yield multiple products or recycle back intermediate and discarded products for use as feed streams. For example, commercial fermentation processes often capture carbon dioxide as a product along with the fermentation product. Waste-to-energy plants provide a service of managing waste but also produce electricity and sometimes heat. Such processes are referred to as multi-functional and their multiple products are called “co-products.” A complication arises when the product system under study uses only one of the “co-products,” but the inventory data represent the full multi-functional process. Under such circumstances the objective is to separate the process into a series of

mono-functional processes so that the inventory data can be distributed or “allocated” among the co-products.

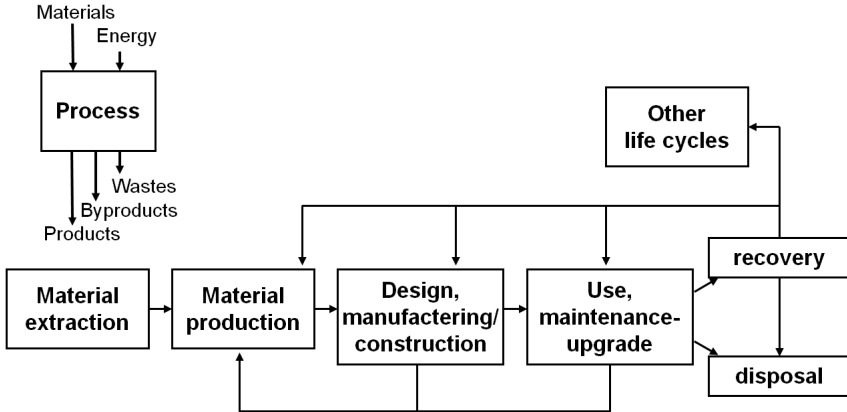


Figure 3.2: The cradle-to-grave product system includes recovery and recycling back into the original system or into other product systems (other life cycles). Recycled and recovered materials are co-products of the system, and thus result in a multi-functional process that often requires allocation of inventory flows among the products.

Biorenewable processing systems are usually multi-functional processes. For example, as shown in Figure 3.3, the corn dry-grind ethanol process with grain produces ethanol from the starch fraction of the corn grain, but also valuable products from the non-starch grain fraction, along with byproducts of the fermentation process in the form of distillers' solubles, carbon dioxide, and distillers' dry grains with solubles (DDGS) or alternately distillers' dry grains (DDG) or distillers' wet grains (DWG). Although ethanol is the principal product, there are several captured product streams. The DDGS stream is used as a protein-rich animal feed and the revenues it provides to the ethanol operation are essential to the economic viability of the process. The way in which these co-product streams are handled in analysis is one of the most significant differences among LCAs of corn grain ethanol [28].

There are several ways to address the problem of multifunctional processes. The ISO standards [14] suggest the following hierarchy of steps (1) Wherever possible allocation should be avoided by (a) dividing the unit process to be allocated into two or more sub-processes and collecting the input and output data

related to these sub-processes (i.e., subdivide the process) or (b) expanding the product system to include the additional functions related to the co-products and then subtracting the equivalent product from main product inventory (i.e., system expansion). (2) Where allocation cannot be avoided, the inputs and outputs of the system should be partitioned between its different products or functions in a way which reflects the underlying physical relationships (i.e., physical allocation). Allocation can be performed on the basis of mass, energy, or economic relationships among the products or functions of the system. Kodera [29] examined allocation practice in the literature of bioethanol LCA and found that of the studies examined, four types of allocation were used: 27 avoided allocation; 12 used mass allocation, 9 energy allocations and 11 market value allocations.

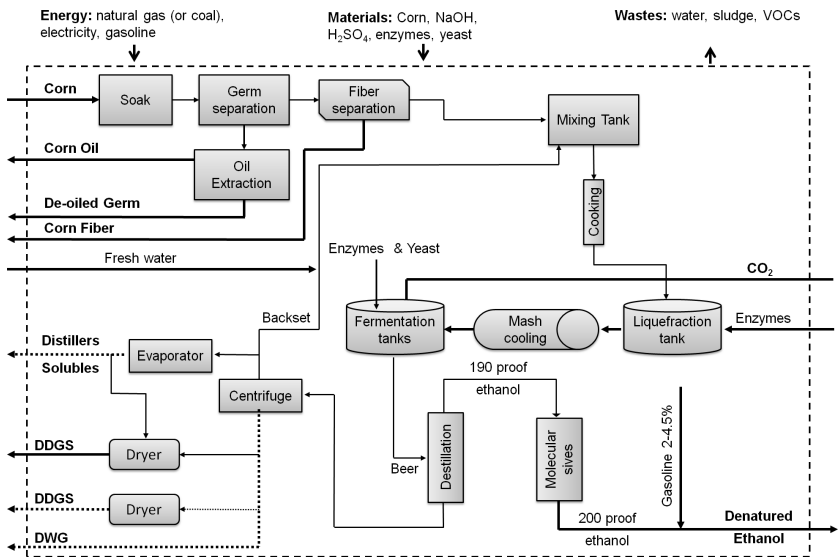


Figure 3.3: The corn ethanol dry-grind process with fractionation produces multiple valuable products.

3.4 Impact Assessment

The last of the major stages of LCA is Life Cycle Impact Assessment (LCIA). The LCIA is carried out in a two-step process:

1. *Classification* is the process of assigning each component of the LCI inventory to one or more impact categories. For example, impact categories include human toxicity, acidification, eutrophication, and climate change.
2. *Characterization* is the process of translating inventory data into a common metric to allow aggregation. The process generally uses equivalency factors that translate LCI data into impact descriptors. For example, climate change is denominated in units of CO₂-equivalents and the IPCC models have provided conversion factors that allow one to convert other GHGs into these units. For example, the *global warming potential* of 1 kg of methane over 100 years is 25 kg CO₂-equivalents and that of nitrous oxide is 298 kg CO₂-equivalents. Likewise, acidification is denominated in units of SO₂-equivalents, and human toxicity in units of benzene-equivalents.

LCIA is sometimes defined to have a third step, *valuation*, which involves weighting and combining the impact data derived during characterization. This step is no longer recommended under ISO standards of practice.

It is important to note that LCIA has not typically provided information about economically-relevant end-points. LCA impact assessment has evolved, but was originally developed not to tell us what sort of environmental or health impacts will occur in a specific place and time, but rather to provide information about what the impacts might potentially be. This type of LCIA is an assessment of mid-points rather than end-points. Stopping at mid-points allows LCI data to be aggregated across space and time to provide a concise measure of the environmental performance of the product system, but in doing so it gives up precision and can tell us little about actual impacts that may be relevant to our own local conditions and decisions. There has been considerable effort in recent years to move life cycle impact assessment toward measures of impact that combine mid-point and end-point (i.e., damage) indicators, particularly related to human toxicity and ecotoxicity [30]. Recent efforts in this direction include the IMPACT 2002 method [31] and the ReCiPe database of characterization factors in 20 categories [32].

3.5 LCA of Biorenewable Chemical Systems

Compared with the number of LCAs that have been performed for biofuels and for conventional chemicals, the number of LCA studies of biorenewable chemicals is rather limited. In addition, the majority of LCAs of biorenewable chemicals tend to focus on a few energy-related impact categories such as fossil fuel displacement and greenhouse gas emissions [20, 33]. In many cases this is because the production processes are still conceptual or commercial-scale production data are not available.

The need to be able to differentiate between candidate biorenewable chemical pathways early in the development process when data are scarce is a challenge for LCA. Indeed, the perceived need for data from existing production processes or well-defined processes in the final stages of the development process has led some to reject LCA as inadequate [34, 35]. However, the limitations are not as severe as they may appear.

In the production of biorenewable chemicals, as with petrochemicals, there are some steps that are common to many production processes. For example, the primary feedstock for most biochemical conversion pathways will be a simple sugar such as glucose. For all processes that utilize sugar from a particular source, such as sucrose from sugar cane or glucose derived from corn starch, the life cycle inventory will be the same. A thorough life cycle inventory for the biorenewable feedstock is a good start to the overall study because from an environmental perspective, biomass production is often the dominant step in the life cycle of a biorenewable chemical [36].

If the biorenewable chemical product under study is a functional replacement for an existing petrochemical product, the inventory during the use and end-of-life stages will be very similar to its petrochemical counterpart, although adjustments may be required to account for different amounts of material used per functional unit or different end-of-life impacts. In cases where the biorenewable chemical is a direct replacement for a petrochemical, the inventories will be the same from the point in the life cycle where the replacement is made through to the end-of-life.

If the goal of the LCA is to compare a biorenewable chemical with a similar petrochemical in a limited number of categories, a relatively rough estimation of the production process inventory data may be sufficient. Because production of feedstock tends to dominate biorenewable chemical inventories, the combination of rough estimates of production data with more complete feedstock, product use and end-of-life inventories will in many cases allow the rejection or acceptance of the hypothesis that the biorenewable chemical is superior in certain environmental categories. The strength of such a conclusion can be tested using sensitivity analysis to ensure that the higher quality data available dominate the inventory. However, if one is trying to differentiate between multiple, candidate biorenewable pathways, among which the principal difference is the chemical production process, more accurate production inventory data will be required.

The synthesis of any type of chemical is a complex and diverse procedure and production data are often scarce or incomplete, even for petrochemicals that have been produced in large quantities for many years. Detailed inventories of chemical synthesis processes are expensive and time consuming, so relatively few chemical inventories exist. A variety of models have been developed for the purpose of estimating the mass and energy flows in the production of chemicals

and to fill in gaps in life cycle inventories. For example, Ciba AG (now BASF Schweiz AG after a 2010 takeover by BASF) developed for internal use an LCI database library called ECOSYS, compiled from both internal process data and external data including tools for estimating missing data [37]. Similarly, LCI estimation methods drawing on similar chemical processes and process models have been developed for in-house use by GlaxoSmithKline [38].

Process-based inventory estimation approaches, however, require a very large amount of data that often is not available during early stages of pathway development. One alternative that has been developed uses molecular structure-based models and extant LCAs of chemicals. The basis of these methods is the idea that the molecular structure of a chemical provides a wealth of information about the energy and resource requirements of its production. Molecular weight, composition, functional groups, chiral centers and similar descriptors are correlated with the specific reaction steps of the chemical synthesis and can thus provide the basis to estimate mass and energy flows during production. Wernet et al. [39, 40] developed models using inventories for around 100 organic chemicals and molecular structure information to train neural networks and in linear regressions in order to estimate life cycle inventories and environmental indicators. They were able to predict a range of output parameters of inventories not included in the training sets with between 10% and 30% relative error. The models developed by Wernet et al. [39, 40] did not, however, include chemical products that included biosynthesis steps in their production due to a paucity of quality data and the diversity of processes and reactions in these pathways.

For many biorenewable chemicals, during the early stages of development only rudimentary process flow sheets and partial mass and energy balances will be available. This level of life cycle uncertainty must simply be tolerated in the effort to screen candidate processes. However, another attribute that may be useful for differentiating between pathways is the environmental risk that is inherent in the intermediate and final products. Even when mass flow rates of products and wastes cannot be estimated with accuracy, pathways that involve less hazardous materials may be preferred. Properties such as toxicity, ecotoxicity, mutagenicity, and biodegradability can be estimated fairly accurately based on chemical structure [41–43]. Likely biodegradation breakdown products and side products can also be predicted using models such as the UM-BBD Pathway Predication System developed at the University of Minnesota [44]. These measures of hazard combined when available with engineering judgment regarding expected quantities and chance of release, can be used along with life cycle assessment data to differentiate between candidate pathways at the earliest stages of development. For such an assessment, it is important to take into account as much quantitative and qualitative information as is available—an approach that is applicable at

early stages of process development and takes into account costs, environmental impacts and human health hazards has been proposed by H. Sugiyama [45].

3.6 Prospective, Consequential, and Attributional LCA

As previously mentioned, most LCAs are performed for existing products that are produced and marketed in relatively constant quantities. In this sort of LCA, the inventory and impact assessments are “snapshots” of production of a product such as a chemical at a given time. Although there are variations among plants or processes, inventory data are averages of those available for the relevant product. For example, inventory data for electricity production represent the average of the generation plants feeding the relevant electricity distribution grid. LCAs performed in this manner are termed *attributional* because they describe the environmental attributes of existing products or services in an average sense.

Attributional LCA is essentially an environmental accounting method that has clear parallels to the methods of managerial cost accounting used to manage production operations in most commercial firms. Attributional LCA meets the same sorts of needs as managerial accounting tools, providing at a reasonable cost a rapid measure of the performance of a product system at a specific time. Such LCA measures are as vital to environmental management as managerial accounting tools are to business management.

In contrast to the attributional approach, which focuses on the direct impact of the product life cycle activities, one may be interested in the broader impacts of a product system that occur through interactions with economic markets. This sort of analysis is known as a *consequential* LCA. The consequential method recognizes that industrial systems are part of larger economic systems which respond to changes in demand or supply. Economic markets respond with substitution between capital and labor, or products and services, in ways that may be quite unexpected and which have environmental and resource implications. The consequential LCA modeling approach seeks then to describe the consequences of a production decision. The relevant inventory data are marginal and the product system includes many processes that have no direct physical relationship to the product system under study. An example would be that increases in biofuel and biorenewable chemical production could drive up the price of sugar, which would lead some farmers to bypass traditional food and feed markets in order to produce sugar, and as a result farmers on the other side of the planet might then plow up grasslands or cut down forests to plant crops to fill the gap. The desire to capture such “indirect,” market-driven environmental impacts creates a need to incorporate in the analysis economic models such as partial equilibrium or computable general equilibrium models.

Theoretical dimensions of performing consequential LCA have been partially addressed [46, 47], but many practical issues and concerns about the complexity of such analyses remain. Consequential LCA is most applicable to the same sorts of problems that require economic analysis. Many policy questions require an understanding of marginal impacts and impacts mediated by market forces. However, the sorts of models required are not yet fully developed. Most economic models were designed for specific purposes and they will be difficult to adapt to consequential LCA. These models are often complicated as well, and their complexity creates opportunities for non-experts to misuse them.

Both attributional and consequential LCA can be useful in evaluating biorenewable chemical production systems. If one is interested in assessing the direct impacts of a biorenewable chemical, that is, to measure its “environmental footprint” in order to compare it with alternatives, an attributional LCA is appropriate—if production volumes are not expected to be large enough to significantly shift current markets for inputs or products. If instead, one is also interested in the indirect impact of biorenewable products, and production volumes are large enough to shift the markets involved, a consequential analysis is appropriate. It is important that LCA analysts and the consumers of LCA results recognize when each type of LCA is appropriate, and when interpreting results, to draw conclusions that stay within the constraints of the methodology employed. Just as erroneous conclusions are drawn by managers that mistake accounting data for economic data, LCA results are often misinterpreted by decision-makers who are unaware of the underlying assumptions of the different types of LCA.

3.7 Resource Constraints on Biorenewable Chemical Production

One of the consequences of increased production of biorenewable fuels and chemicals that is of keen interest to firms developing new biorenewable processes is how the future availability and cost of resources, particularly feedstock, will be affected by future demand. The feedstocks of most current and proposed biorenewable chemical processes are polysaccharides or sugars. World sugar prices soared to a 29-year high of nearly 30 cents a pound in early 2010 and then fell to around half that level by early summer [48]. The causes of this increase were several: production disruptions due to weather, policy changes, as well as increased sugar consumption which were aggravated by increased industrial sugar use for biorenewable fuels and chemicals. The result has been both price increases—average raw sugar price in 2009 was almost double the long-term average of 11 cents per pound—and price volatility.

The technological uncertainty associated with candidate biorenewable chemical production processes is naturally high due to the difficulty of predicting fac-

tors such as yields and separation costs. This technological uncertainty translates into one source of financial uncertainty. Another important source of financial uncertainty is that introduced by the volatility of sugar or other feedstock costs. This uncertainty is particularly significant because raw material cost is typically of the order of 75% of product value of commodities [49]. The challenge for firms considering commercializing a new biorenewable product then, is to anticipate how much input prices may change due to increasing demand and resource limitations. In this regard sugar may be considered *The New Oil* but oil is actually less subject to production disruptions because it needs only to be extracted, not grown in a field that can be ravaged by pests, disease, or weather.

In addition to being vulnerable to weather and the like, the production of biomass feedstock is dependent on fertilizers, such as nitrogen, phosphorous and potassium, in order to maintain or increase crop yields. Increasingly, the fertilizers that agriculture depends upon are imported. In 2009, the United States imported more than 55% of nitrogen and 81% of potash (i.e., potassium) fertilizer used [50]. Fertilizers are derived from nonrenewable resources which is why in the long-term their prices will likely increase as supplies of nonrenewable inputs dwindle.

For example, modern agriculture is dependent on synthetic nitrogen fertilizer that is produced primarily from natural gas. Phosphorous fertilizer is derived from phosphate rock and current global reserves may be depleted in as little as 50–100 years [51]. The quality of remaining phosphate rock reserves is decreasing and production costs are increasing. As we seek to scale-up biorenewable fuel and chemical production to several times current levels as targeted by the U.S. Renewable Fuels Standard (RFS) and suggested by the U.S. National Research Council [52], very large increases in crop production will be required to provide the necessary feedstock while maintaining food and feed production. Yield increases can come through increasing crop acreage, but the magnitude of this option is limited by a dwindling amount of uncropped fertile land; or by increasing the intensity of production, including irrigation and fertilization. Increased fertilizer use will hasten the depletion of these finite resources, and also aggravate the considerable environmental impacts of fertilizer use.

The use of fertilizers in large quantities across the globe has already significantly perturbed the biogeochemical cycles of the Earth. Rockström et al. [53] have identified thresholds in nine Earth-system processes that if crossed can generate unacceptable environmental change. Two of these processes are the nitrogen and phosphorous cycles, and the nitrogen cycle boundary is one of three boundaries judged to already have been exceeded, as represented graphically in Figure 3.4. Rockström et al. [53] have suggested that a sustainable rate of human fixation of nitrogen would be 25% of the current value.

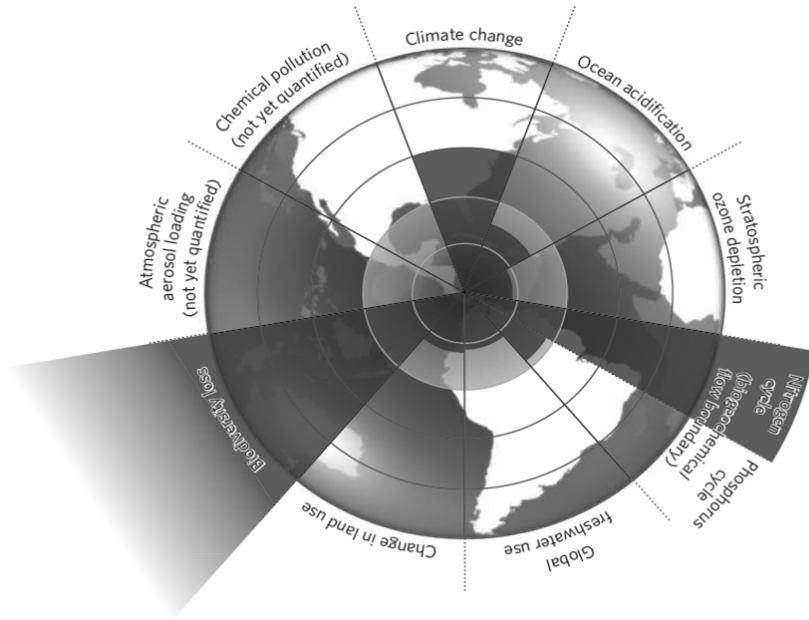


Figure 3.4: The circular boundaries identified for nine planetary systems. The inner circular shading represents the proposed safe operating space and the wedges represent an estimate of the current position for each variable. The boundaries on the level of human interference with the nitrogen cycle, as well as the rate of biodiversity loss and climate change, are deemed to have already been violated.

Through human processes nitrogen is fixed from the atmosphere into reactive forms at a rate of around 120 million metric tons per year of N_2 . This large flow of reactive nitrogen fertilizes crops and then continues through other ecosystems, altering species diversity, accumulating in soils, and forming atmospheric gases that lead to pollution and climate change. Nitrogen impacts are particularly difficult to assess because nitrogen moves through the compartments of environmental systems causing a cascade of impacts [54]. Because in many ecosystem compartments nitrogen is naturally in short supply, it can accumulate there for extended periods of time before being transported to new compartments and causing additional impacts. In this fashion, certain consequences of nitrogen released into the environment can happen many years after the initial release and after the

nitrogen has already produced a long chain of other negative environmental impacts.

Phosphorous is a mineral that is mined from locations where it has accumulated naturally through geological processes. The mined phosphate rock is used for a variety of purposes but around 90% is used as fertilizer [51]. Around 20 million metric tons of phosphorous are produced each year and this is estimated to be approximately eight times the natural background flux rate [53]. The impacts of this are large zones of hypoxia in the world's oceans in the regions where agricultural systems drain.

Although the environmental consequences of fertilizer use are already serious and growing more so, there are a variety of ways to reduce the use of fertilizers in agriculture as well as technologies for recycling nutrients that are removed from agricultural fields. Fertilizer use can be made more efficient through precision application that puts the fertilizer on the field at specific times and locations to improve utilization by plants, thus requiring lower application rates per crop yield [55]. There are also opportunities to recover nutrients from human urine, waste treatment, and emerging biorenewable conversion processes [51, 56].

In addition to fertilizers, other limited resources may be impacted by large increases in demand for crop production to provide industrial feedstock. Many of the less productive lands that have been targeted for biomass feedstock production are marginal lands due to limited soil depth, soil quality, and rainfall. Increased biomass production will require more water for the increased crop growth because plant transpiration is directly related to carbon fixation [57]. Many parts of the world are already experiencing severe water stress. Around 1.2 billion people, or almost one-fifth of the world's population, live in areas of physical water scarcity and another 1.6 billion live where infrastructure and economic systems are unable to deliver sufficient water [58].

Worldwide, agriculture is responsible for around 70% of annual freshwater withdrawals for human use. Agriculture is responsible for generating water scarcity and also for degrading high quality surface and groundwater for marginal output [59]. Impacts of increased water extraction for agriculture include groundwater depletion, reduced river flow, worsening water pollution, reduced habitat, and imperiled human health. It will be increasingly difficult to satisfy the demands for food, feed, and water of a growing global population and protect natural aquatic ecosystems while at the same time meeting large new demands for industrial biomass production.

Resource use is closely coupled to environmental health and the impacts of resource use become more pronounced as resources become scarcer. Natural systems become less resilient and able to absorb disturbances as resource constraints bind more tightly. It is important to consider how increased use of biorenewable

products will impact the supplies of resources that are critical for meeting fundamental human needs. LCA doesn't handle resource limits explicitly as it is commonly practiced because it reports resource use on a specific (i.e., per functional unit) basis, and does not account for the size, location, or nature of resource reserves.

3.8 Conclusion

LCA was developed as a tool to provide information on the full life cycle impact of our consumption choices. To accomplish this at reasonable cost, LCA takes a snap-shot of the product system at a specific time and combines a wide range of impacts into a few measures, often aggregated over time and space. LCA is not intended to be a perfect analysis that reflects the minute details of environmental processes, but rather to introduce environmental considerations in decision-making processes where they are often missing.

As we seek to address ever more complicated environmental questions, we ask more of LCA. We have extended LCA techniques and created specialized LCA tools to meet particular needs. Evaluating candidate biorenewable chemical pathways, such as is required to choose between alternative conversion processes, requires new LCA methods that can provide meaningful results despite highly uncertain process, inventory, and impact data.

LCA is a powerful tool that can inform many important decisions faced by society today. However, as we extend and diversify LCA techniques, we must also train practitioners to understand which tools are appropriate for which questions. Along with our LCA results we must also carefully communicate their limitations and proper use in order to enable society to make better choices and move toward a more sustainable future.

Acknowledgments

This material is based upon work supported, in part, by the National Science Foundation under Award No. EEC-0813570. Any opinions, findings, and conclusions or recommendations expressed in this material are those of the author and do not necessarily reflect the views of the National Science Foundation.

Bibliography

- [1] C.H. Christensen, J. Rass-Hansen, C.C. Marsden, E. Taarning, and K. Egeblad. The Renewable Chemicals Industry. *ChemSusChem* 1 (2008): 283–289.
- [2] B.G. Hermann, K. Blok, and M.K. Patel. Producing Bio-Based Bulk Chemicals Using Industrial Biotechnology Saves Energy and Combats Climate Change. *Environmental Science and Technology* 41 (2007a):7915–7921.
- [3] J. van Haveren, E. Scott, and J. Sanders. Bulk Chemicals from Biomass. *Biofuels, Bioproducts & Biorefining* 2 (2008):41–57.
- [4] A.J. Ragauskas, C.K. Williams, B.H. Davison, G. Britovsek, J. Cairney, C.A. Eckert, W.J. Frederick, J.P. Hallett, D.J. Leak, C.L. Liotta, J.R. Mielenz, R. Murphy, R. Templer, and T. Tschaplinski. The Path Forward for Biofuels and Biomaterials. *Science* 311 (2006):484–489.
- [5] J.J. Bozell and G.R. Peterson. *Green Chemistry* 12 (2010):539–554.
- [6] G. Centi, P. Lanzafame, and S. Perathoner. Analysis of the Alternative Routes in the Catalytic Transformation of Lignocellulosic Materials. *Catalysis Today* 167 (2010):14–30.
- [7] D.R. Dodds and R.A. Gross. Chemicals from Biomass. *Science* 318 (2007): 1250–1251.
- [8] M. Wellisch, G. Jungmeier, A. Karbowski, M.K. Patel, and M. Rogulska. *Biofuels, Bioproducts and Biorefining* 4 (2010):275–286.
- [9] B.J. Nikolau, M.A. Perera, L. Brachova, and B. Shanks. Platform Biochemicals for a Biorenewable Chemical Industry. *The Plant Journal* 54 (2008):536–545.
- [10] Y.-C. Lin and G.W. Huber. The Critical Role of Heterogeneous Catalysis in Lignocellulosic Biomass Conversion. *Energy and Environmental Science* 2 (2009):68–80.
- [11] B.G. Hermann and M.K. Patel. *Applied Biochemistry and Biotechnology* 136 (2007b):361–388.
- [12] C.L. Henn and J.A. Fava. Life Cycle Analysis and Resource Management. In: *Environmental Strategies Handbook*. Ed. by R.V. Kolluru. New York NY: McGraw-Hill, Inc, 1994.

- [13] R.G. Hunt and W.E. Franklin. LCA—How we came about. *International Journal of Life Cycle Assessment* 1 (1996):4–7.
- [14] *Environmental Management. Life Cycle Assessment. Principles and Framework*. 14040. Geneva, 2006.
- [15] *Environmental Management. Life Cycle Assessment. Requirements and Guidelines*. 14044. Geneva, 2006.
- [16] J.A. Fava, R.F. Weston, F. Consoli, R. Denison, K. Dickson, T. Mohin, and B. Vignon. *A Conceptual Framework for Life-Cycle Impact Assessment*. Pensacola, FL: Society of Environmental Toxicology and Chemistry, 1992.
- [17] G.A. Keoleian and D. Menery. *Life Cycle Design Guidance Manual: Environmental Requirements and the Product System, Risk Reduction Engineering Laboratory*. Cincinnati OH: U.S. Environmental Protection Agency, 1993.
- [18] B.W. Vignon, D.A. Tolle, B.W. Cornaby, H.C. Latham, C.L. Harrison, T.L. Boguski, R.G. Hunt, and J.D. Sellers. *Life-Cycle Assessment: Inventory Guidelines and Principles (EPA/600/R-92/245)*. Cincinnati OH: Risk Reduction Engineering Laboratory: U.S. Environmental Protection Agency, 1993.
- [19] M. Akiyama, T. Tsuge, and Y. Doi. Environmental Life Cycle Comparison of Polyhydroxyalkanoates Produced from Renewable Carbon Resources by Bacterial Fermentation. *Polymer Degradation and Stability* 80 (2003):183–194.
- [20] R.P. Anex and A.L. Ogletree. Life-Cycle Assessment of Energy-Based Impacts of a Biobased Process for Producing 1,3-Propanediol. In: *Feedstocks for the Future: Renewables for the Production of Chemicals and Materials*. Ed. by J. Bozell and M. Patel. 921. ACS Symposium. Washington D.C.: American Chemical Society, 2006. 222–238.
- [21] C. Liptow and A.-M. Tillman. *Comparative Life Cycle Assessment of Poly-ethylene Based Sugar Cane and Crude Oil*. PhD thesis. 2009.
- [22] E.T.H. Vink, K.R. Rabago, D.A. Glassner, and P.R. Gruber. Applications of Life Cycle Assessment to Natureworks™ Poly-Lactide (PLA) Production. *Polymer Degradation and Stability* 80 (2003):403–419.
- [23] F. Cherubini and G. Jungmeier. LCA of a Biorefinery Concept Producing Bioethanol, Bioenergy, and Chemicals from Switchgrass. *International Journal of Life Cycle Assessment* 15 (2010):53–66.

- [24] Franklin Associates Ltd. *Resource and Environmental Profile Analysis of Polyethylene and Unbleached Paper Grocery Sacks*. Report prepared for the Council for Solid Waste Solutions. Prairie Village, Kansas, USA, June 1990.
- [25] J.S. Cooper. Specifying Functional Units and Reference Flows for Comparable Alternatives. *International Journal of Life Cycle Assessment* 8 (2003):337–349.
- [26] B.P. Weidema. Multi-User Test of the Data Quality Matrix for Product Life Cycle Inventory Data. *International Journal of Life Cycle Assessment* 3 (1998):259–265.
- [27] R. Frischknecht, N. Jungbluth, H.J. Althaus, G. Doka, R. Dones, R. Hischier, S. Hellweg, T. Nemecek, G. Rebitzer, and M. Spielmann. *Overview and Methodology*. Duebendorf, Switzerland: Swiss Centre for Life Cycle Inventories, 2007.
- [28] Ethanol Can Contribute to Energy and Environmental Goals. *Science* 311 (2006):506–508.
- [29] K. Kodera. *Analysis of Allocation Methods of Bioethanol LCA*. Tech. rep. CML, Leiden University, 2007.
- [30] J.C. Bare, P. Hofstetter, D.W. Pennington, and H.A. Udo de Haes. Midpoint Versus Endpoints: The Sacrifices and Benefits. *International Journal of Life Cycle Assessment* 5 (2000):319–326.
- [31] O. Jolliet, M. Margni, R. Charles, S. Humbert, J. Payet, G. Rebitzer, and R. Rosenbaum. IMPACT 2002+: A New Life Cycle Impact Assessment Methodology. *International Journal of Life Cycle Assessment* 8 (2003): 324–330.
- [32] M. Goedkoop, R. Heijungs, A. Huijbregts, A. De Schryver, J. Struijs, and R. van Zelm. *A Life Cycle Impact Assessment Method which Comprises Harmonized Category Indicators at the Midpoint and the Endpoint Level. Report 1: Characterization*. Tech. rep. ReCiPe 2008. Ruimte en Milieu, Ministeries van Volkshuisvesting, Ruimtelijke Ordening en Milieubeheer, 2009.
- [33] V. Dornburg, I. Lewandowski, and M. Patel. Comparing Land Requirements, Energy Savings, and Greenhouse Gas Emissions Reduction of Bio-based Polymers and Bioenergy. *Journal of Industrial Ecology* 7 (2003): 93–116.

- [34] A. Gehin, P. Zwolinski, and D. Brissaud. *Towards the Use of LCA During the Early Design Phase to Define EOL Scenarios. Advances in Life Cycle Engineering for Sustainable Manufacturing Businesses. Part 2, A1*: 23–28. Springer, 2007.
- [35] D. Millet, L. Bistagnino, C. Lanzavecchia, R. Camous, and T. Poldma. Does the Potential of the Use of LCA Match the Design Team Needs? *Journal of Cleaner Production* 15 (2007):335–346.
- [36] R. Hatti-Kaul, U. Toernvall, L. Gustafsson, and P. Boerjesson. *Trends in Biotechnology* 25 (2007):119–124.
- [37] R. Bretz and P. Rankhauser. Screening LCA for Large Numbers of Products: Estimation Tools to Fill Data Gaps. *International Journal of Life Cycle Assessment* 1 (1996):139–146.
- [38] A.D. Curzons, C. Jimenez-Gonzalez, A.L. Duncan, D.J.C. Constable, and V.L. Cunningham. Fast Life Cycle Assessment of Synthetic Chemistry (FLASC) Tool. *International Journal of Life Cycle Assessment* 12 (2007): 272–280.
- [39] Molecular-Structure-Based Models of Chemical Inventories Using Neural Networks. *Environmental Science and Technology* 42 (2008):6717–6722.
- [40] G. Wernet, S. Papadokonstantakis, S. Hellweg, and K. Hungerbuehler. Bridging Data Gaps in Environmental Assessments: Modeling Impacts of Fine and Basic Chemical Production. *Green Chemistry* 11 (2009):1826–1831.
- [41] M. Pavan and A.P. Worth. Review of Estimation Models for Biodegradation. *QSAR & Combinatorial Science* 27 (2007):32–40.
- [42] J.W. Raymond, T.N. Rogers, D.R. Shonnard, and A.A. Kline. A Review of Structure-Based Biodegradation Estimation Methods. *Journal of Hazardous Materials* B84 (2001):189–215.
- [43] A.C. White, R.A. Mueller, R.H. Gallavan, S. Aaron, and A.G.E. Wilson. A Multiple in Silico Program Approach for the Prediction of Mutagenicity from Chemical Structure. *Mutation Research* 539 (2003):77–89.
- [44] J. Gao, L.B. Ellis, and L.P. Wackett. The University of Minnesota Pathway Prediction System: Multi-Level Prediction and Visualization. *Nucleic Acids Research* 39 (2011):W406–411.

- [45] H. Sugiyama, U. Fischer, K. Hungerbühler, and M. Hirao. Decision Framework for Chemical Process Design Including Different Stages of Environmental, Health, and Safety Assessment. *American Institute of Chemical Engineers* 54 (2008):1037–1053.
- [46] T. Ekvall and B.P. Weidema. System Boundaries and Input Data in Consequential Life Cycle Inventory Analysis. *International Journal of Life Cycle Assessment* 9 (2004).
- [47] B.A. Sanden and M. Karlstom. Positive and Negative Feedback in Consequential Life-Cycle Assessment. *Journal of Cleaner Production* 15 (2007): 1469–1481.
- [48] M. McConnell, E. Dohلمان, and S. Haley. World Sugar Price Volatility Intensified by Market and Policy Factors. *Amber Waves* 8 (2010):28–35. URL: www.ers.usda.gov/amberwaves.
- [49] L.R. Lynd, C.E. Wyman, and T.U. Gerngross. Biocommodity Engineering. *Biotechnology Progress* 15 (1999):777–793.
- [50] USDA. *U.S. Fertilizer Import/Export: Summary of the Data Findings*. Tech. rep. Washington, DC: US Department of Agriculture, Economic Research Service, 2010. URL: <http://www.ers.usda.gov/Data/FertilizerTrade/Summary.htm>.
- [51] D. Cordell, J.-O. Drangert, and S. White. The Story of Phosphorus: Global Food Security and Food for Thought. *Global Environmental Change* 19 (2009).
- [52] NRC. *Biobased Industrial Products: Research and Commercialization Priorities*. ISBN-10: 0-309-05392-7. Washington DC: National Academies Press, 2000.
- [53] J. Rockström, W. Steffen, K. Noone, A. Persson, III F.S. Chapin, E.F. Lambin, T.M. Lenton, M. Scheffer, C. Folke, H.J. Schellnhuber, B. Nykvist, C.A. de Wit, T. Hughes, S. van der Leeuw, H. Rodhe, S. Soerlin, P.K. Snyder, R. Costanza, U. Svedin, M. Falkenmark, L. Karlberg, R.W. Corell, V.J. Fabry, J. Hansen, B. Walker, D. Liverman, K. Richardson, P. Crutzen, and J.A. Foley. A Safe Operating Space for Humanity. *Nature* 461 (2009): 472–475.
- [54] J.N. Galloway, J.D. Aber, J.W. Erisman, S.P. Seitzinger, R.W. Howarth, E.B. Cowling, and B.J. Cosby. The Nitrogen Cascade. *BioScience* 54 (2003):341–356.
- [55] K.G. Cassman. Ecological Intensification of Cereal Production Systems: Yield Potential, Soil Quality, and Precision Agriculture. *Proceedings of the National Academy of Sciences* 96 (1999):5952–5959.

- [56] R.P. Anex, L.R. Lynd, M.S. Laser, A.H. Heggenstaller, and M. Liebman. Potential for Enhanced Nutrient Cycling Through Coupling of Agricultural and Bioenergy Systems. *Crop Science* 47 (2007):1327–1335.
- [57] T.R. Sinclair. Taking Measure of Biofuel Limits. *American Scientist* 97 (2009):400–407.
- [58] United Nations. *Water Scarcity*. Tech. rep. United Nations, 2011. URL: <http://www.un.org/waterforlifedecade/scarcity.html>.
- [59] FAO. *Coping with Water Scarcity*. Tech. rep. Food and Agriculture Organization of the United Nations, 2007. URL: <http://www.fao.org/ag/magazine/0704sp4.htm>.

Chapter 4

Plant Growth: Basic Principles and Issues Relating to the Optimization of Biomass Production and Composition as a Feedstock for Energy

Mark Stitt

4.1 Introduction: The Contribution of Plants to the Global Carbon Cycle

Plants, together with algae and photosynthetic bacteria, are the only living organisms that can use sunlight as an energy source to drive chemical reactions in a process called photosynthesis. They are the basis of all life on earth and play a central role in the global carbon and energy cycles. This chapter provides an overview of the processes involved in photosynthesis and plant growth, analyzes the efficiency of energy conversion in plants, and discusses the consequences for the use of plant biomass as a source of bioenergy.

Biological life depends on the synthesis of myriads of molecules and macromolecules, their organization on many spatial levels to form molecular machines, cells, organs and organisms, the maintenance thereof in the face of a changing environment, and their reproduction. However, human beings and all other animals and most microbes cheat. We gain precursor molecules like sugars, lipids and amino acids by eating other organisms, and we obtain the energy necessary to drive these interconversions by degrading these compounds. Reducing groups that are extracted during their degradation through a series of coupled redox reactions, with oxygen acting as the final acceptor (Figure 4.1A). This process is called respiration. These redox reactions occur in a membrane and release energy that is captured as an electrical gradient across the membrane. This gradient then drives the synthesis of adenosine triphosphate (ATP) from adenosine diphosphate (ADP) and phosphate. ATP is a universal energy carrier that is used to drive a huge variety of biochemical reactions. But where do all the complex molecules in the organisms we eat come from? What energy input drives the biological world?

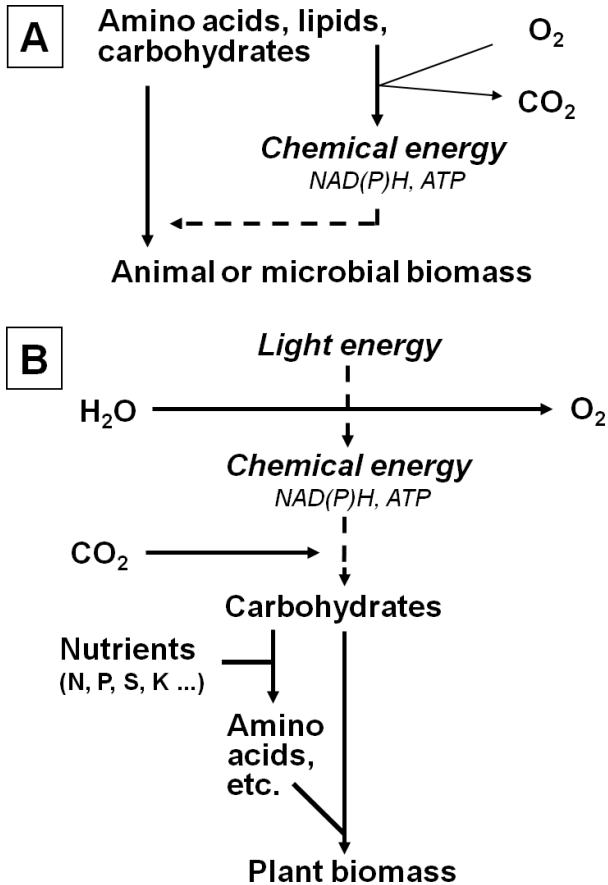


Figure 4.1: A schematic representation of metabolism in non-photosynthetic and photosynthetic organisms. (A) Non-photosynthetic organisms—a microbe or an animal. (B) A photosynthetic organism—an algae or a plant. The flow of energy is indicated as dotted lines. For redox equivalents, this can occur via NADH (especially for use in respiration to produce ATP) or NADPH (especially to provide redox groups for biosynthesis, and in photosynthesis). For simplification, uptake of water (up to 70% of the fresh weight for microbes and animals, and 90% for plants) is omitted.

Many early forms of life used reduced inorganic compounds as a source of energy. Other organisms developed ways to use light energy to oxidize reduced inorganic compounds, thereby generating reducing groups and energy. This is still done today by many bacteria. The decisive step leading to the world as we know it today, however, was the development of what is termed *oxygenic* photosynthesis. In this process, light energy is used to oxidize water to oxygen and hydrogen (Figure 4.1B). This releases very electronegative reducing groups, which pass down a series of redox reactions, releasing energy that is used to make ATP. The reducing groups are ultimately used to generate a molecule called NADPH. The ATP and NADPH are used to drive a plethora of other reactions. The most important reaction is the conversion of CO_2 into carbohydrates. Other reactions include the conversion of nitrate into ammonium, or sulphate into reduced sulphur-containing molecules. The ammonium and reduced sulphur compounds are combined with molecules derived from carbohydrates to generate a multitude of N- and S-containing molecules like amino acids and nucleic acids.

Plants can be viewed as solar-powered chemical factories, which take a range of inorganic compounds (carbon dioxide, nitrate, sulphate, phosphate, iron and many other metals) and use them to produce an enormous range of exquisite organic molecules and macromolecules. Their range and precision far exceed that of chemical factories constructed by men. They do this with a minimum of environmental side effects. Not only the synthesis but also the transport of these chemicals is driven by solar power. For example, nutrients are transported from the soil to the leaves of the plants, up to a hundred meters high in the largest trees, in a flow of water (technically termed the transpiration stream) that is driven by the evaporation of water in the leaves and drawn up as a column of water through fine vessels (technically called the xylem) in the stems.

Oxygenic photosynthesis is the direct or indirect source of almost all life on earth as we see it today. It is the direct source of energy and biological molecules for the growth of plants. It is the indirect source of energy and biological molecules for most bacteria and all fungi and animals. These either feed on plants, or live by degrading dead plant matter, or by eating animals that themselves live off plants.

Oxygenic photosynthesis is also a dominating factor in the global carbon and oxygen cycles that determine the composition of the atmosphere. Briefly, plants use light energy from the atmosphere to assimilate carbon dioxide into reduced organic molecules, thereby releasing oxygen. The plants are themselves eaten by animals, leading to an uptake of oxygen and a release of carbon dioxide. Alternatively, when plants die they decay due to the activity of bacteria, fungi or animals, again leading to an uptake of oxygen and a release of carbon dioxide. Some of the carbon in plants is sequestered in the soil, either because the plant

matter is not degraded, or because it accumulates in residues from the organisms that eat plants or degraded dead plant matter. In the short term, this is an important interim pool of carbon whose disturbance can lead to a sudden release of carbon dioxide into the atmosphere. For example, this occurs when a forest is cleared. In the most extreme case, when plant matter is not degraded, large amounts of organic carbon can accumulate and, over millions of years, be converted into highly reduced forms like coal, oil or gas.

For thousands of years, mankind obtained most of its energy from living or newly dead plant material by burning wood, or by eating plants or animals to provide energy to fuel the muscular system. For some specific tasks, also water (e.g., water wheel driven corn mills) or wind (sailing ships, wind mills) were used. It might be noted that by the 18th century, there was a large-scale use of wood for charcoal production. There were also perceived worries about the lack of wood for other uses such as the building of ships (Dudley Pope, “Life in Nelson’s Navy”¹). This serves as a good example for the potential conflict between the use of plant biomass as a source of material versus its use as a source of energy, which will be discussed later in this chapter and also in other chapters of this book. Starting with the industrial revolution in England in the 18th century, and then accelerating with time and spreading over the entire globe, coal, and later oil and gas, were used as energy sources with a still increasing use. They are often termed *fossil fuels* because they are derived from long-dead plant matter.

By the 1970s there were worries that the finite resources of fossil fuels would become exhausted (see “The Club of Rome”). These worries probably underestimated the amount of undiscovered fossil fuels and the extent to which improved technology and increasing prices for these fuels would allow known but previously inaccessible sources to be used. Research in the last decades, which has led to an increased understanding of the global carbon cycle and the role of carbon dioxide as a greenhouse gas, has led to even more pressing reasons to decrease the use of fossil fuels. Coal, petrol and oil have been accumulating on earth for the last 350 million years. This process is now being reversed at an incredible speed. The amount of carbon dioxide that is currently being released into the atmosphere in a decade is equivalent to the amount of carbon that was sequestered underground over many millions of years. This release is one of the drivers of the present increase in global temperature. It is predicted that if the release of carbon dioxide from fossil fuels continues to increase, there will be a major global change of climate in the coming century. There is an urgent need to radically increase the use of alternative energy sources like wind power, solar power and water power.

¹http://en.wikipedia.org/wiki/Cuthbert_Collingwood,_1st_Baron_Collingwood

Looked at from the point of view of the plant sciences, two questions are pinpointed: First, can bioenergy make a significant contribution to energy production? We might note that this not only requires that living biomass is converted into compounds that can be conveniently used as a source of energy, but also that this is done at a rate that is an order of a million-fold higher than occurred by geological processes in the last 350 million years. Second, can plants be used to reverse or ameliorate the increase in atmospheric CO₂?

4.2 Is the Glass Half Full or Half Empty?

Let us start off by being optimistic. More solar energy reaches the earth's surface every hour (4.3×10^{12} J) than is consumed by humans in a year (4.1×10^{12} J) (Basic Research Needs for Solar Energy Utilization, U.S. Department of Energy Solar Energy Workshop Report²). Plants have been performing photosynthesis for hundreds of millions of years. We might therefore expect them to have become highly optimized for conversion of this solar energy into biomass, which can then be used to generate energy. Further, the CO₂ concentration found in the atmosphere actually limits photosynthesis in most plants. This simple fact can be demonstrated by monitoring the rate of photosynthesis and suddenly increasing the carbon dioxide concentration. It is exploited in the commercial greenhouse industry, which often uses elevated carbon dioxide concentrations to speed up plant growth. Thus, the current increase in atmospheric carbon dioxide concentrations would be expected to allow more photosynthesis globally, and result in an increase in biomass formation and crop yield on agriculturally-used land. Will there be a large enough surplus to provide feedstocks for the large-scale production of bioenergy?

To assess this hope, let us look at the current situation with respect to food production. If there is a large amount of "low hanging fruit" to be used for bioenergy production, we would surely expect there to be a large surplus in food production. This is patently not the case. The following assessment is based on a global perspective and does not address local cases where there is a local surplus, or at least a perceived surplus, as a result of very favorable local terrain and climatic conditions, large financial subsidies, having the wealth to import food, or other economic or political factors. First, despite large increases in crop yield in the last half century as a result of the green revolution, the current global agricultural production is scarcely able to keep pace with the growing demand for food as the world population grows and the standards of living in many parts of the world slowly improve [1]. Second, it is unlikely that more land can be used for agricultural production, neither for food nor for energy purposes [2]. Much

²http://gcep.stanford.edu/pdfs/CTISZRP4nww_77Shjd-A2g/NateLewis_Symposium2009.pdf

of the land that is not currently used has unsuitable terrain or climatic conditions. Other large areas that are not used for agriculture support large scale ecosystems that themselves play a key role in the global carbon and water cycles, such as the tropical rainforests, whose deforestation would lead to the release of so much sequestered carbon that its effect could not be counterbalanced in decades. Third, there are signs that the yield gain is levelling off [3–7].

In the future it will be necessary to find new ways to increase crop yields just to keep pace with the growing global demand for food. The yield increases of the green revolution were achieved by advances in plant breeding and the increased use of water, fertilizers and pesticides. It is thought that these contributed approximately equally to the yield gain, although the contribution may have varied depending on the type of crop and geographical region [3, 6, 8]. In the future, it will be desirable to decrease the use of fertilizers, water and pesticides. Widespread use of fertilizers and pesticides has a significant negative impact on the environment [9, 10]. There are finite reserves of some fertilizers (e.g., phosphates), and the production of others (especially nitrogen fertilizers via the Haber-Bosch process) consumes large amounts of energy. In the context of using bioenergy to decrease the use of fossil fuels and CO₂ release to the atmosphere, this is a serious drawback! Irrigation can lead to a gradual loss of soil quality due to salinisation and contamination with other chemicals. Besides, in areas where irrigation is necessary and widespread, water is often a rare resource and tends to become even more scarce. Agriculture accounts for over 70% of the total water use in most developed countries (World Agriculture: Towards 2015/2030, FAO, 2002³).

This rather disturbing analysis leads to several conclusions with respect to any use of plants as a large-scale source of bioenergy, or as a quantitatively important feedstock for the chemical industry. First, it will be essential that production of bioenergy does not compete with food production. Second, it will be essential to maintain and even increase the yield per unit area of agricultural land, irrespective of whether the plants are going to be used for food only, or for energy and chemical feedstocks as well. Third, this will probably have to be done while decreasing the use of water, fertilizers and pesticides.

Further large advances in either agronomic practice and/or in plant breeding will be required to allow yields to be maintained at current or even higher levels, while decreasing the use of water, fertilizers and pesticides. Although agronomic practice and plant breeding are sometimes seen as alternative routes, it is most likely that it will be the successful fusion of both that will allow further increases in yield [1]. Plant breeders select and optimize crops for their performance in a given cultivation regime. A change in the cultivation regime is likely to create a

³<http://www.fao.org/docrep/005/y4252e/y4252e00.htm>

situation that is not fully exploited by current cultivars, opening a new window of opportunity for plant breeding. Conversely, an advance in breeding or the production of a plant with a major improvement in an existing trait or even a new trait can open up new strategies in agronomic practice.

This interplay between breeding and agronomic practice can be illustrated by two examples from maize breeding. First, the increase in yield per hectare in the last decades has been largely achieved by breeding maize so that it can be packed more densely on the field—i.e., by a very close interaction between breeding and a simple change in agronomic practice [6]. The second example is Roundup Ready maize, a genetically modified organism. This GMO was developed to aid weed control and carries a transgene that confers tolerance to the herbicide glyphosate. However, one of the main advantages of Roundup Ready maize is that it can be sown by drill boring, rather than by ploughing. Previously, maize was sown after ploughing and treatment of the soil with herbicide to remove competing weeds before planting the maize seeds, with the concomitant use of energy for the machines and loss of soil by blow-off. Roundup Ready maize can be drill-sown in small holes bored into unploughed land, and the competing weeds are killed later by the application of glyphosate. Irrespective of the political discussion over the use of GMO crops, this example illustrates how a new trait in the crop can facilitate a change in agricultural practice.

The next sections of this chapter will outline some basic principles underlying the process of photosynthesis and plant growth, which are central to plant yield. At the start of this section, three rather optimistic statements were made:

1. Natural selection over hundreds of millions of years should have optimized the energy conversion and growth rates in plants.
2. The amount of energy needed from plants is minuscule in comparison with the total irradiation intercepted by the earth.
3. Rising atmospheric CO₂ should lead to an increase in photosynthesis and, by implication, to plant growth.

The fact that hardly enough food can be produced for mankind arouses the suspicion that there is a fly in the ointment. In fact, there are several. First, energy conversion in plants is actually inherently inefficient. Second, momentary increases in the rate of photosynthesis often fail to translate into a sustained increase in growth and biomass formation. Third, much of the plant biomass that is produced, even on agricultural fields and even less so in semi-natural or natural ecosystems, cannot be used as food—at least for human consumption—and is also not usable for bioenergy, at least with current technologies. To understand why this is so, we need to look more closely at the processes involved in photo-

synthesis and plant growth and at the function and composition of different parts of the plant.

4.3 Low Energy Conversion Efficiency in Photosynthesis

The energy conversion efficiency of photosynthesis has been the subject of two recent meta-analyses [11, 12], which are summarized in the following section. Although the earth intercepts massive amounts of solar irradiation (120,000 TW per year), several factors mean that only a minute fraction of this energy is actually converted into plant biomass. Before explaining how and why the light energy is used so wastefully, I will first briefly introduce the pathway of photosynthesis.

4.3.1 Photosynthesis

Figure 4.2 provides a schematic overview of the energy and carbon flow during photosynthesis. This is often divided into *light reactions* and *dark reactions* (for a simple introduction, see also Michel [13]).

The first step in the *light reactions* is the absorption of light by chlorophyll. This leads to the excitation of an electron, which moves into a higher orbital. The energy is transferred across an array of chlorophyll molecules to the so-called reaction center. In the reaction center the energized electron drives a redox reaction. There are actually two reaction centers, arranged in series, in oxygenic photosynthesis. Starting with water, the first photochemical reaction (confusingly termed Photosystem II), splits water to release oxygen and hydrogen. The reducing groups of the hydrogen then pass through a series of redox reactions and are ultimately used to reduce NADP^+ to NADPH. At one step during this process, the reducing groups are transferred up to a more electronegative acceptor, using energy from the second light-driven reaction (termed Photosystem I). Energy that is released during this chain of reactions is stored as an electrical or pH gradient across a membrane in which the *light reactions* occur. The electrical or pH gradient is used to convert ADP and orthophosphate into ATP. Two light-driven reactions in series are needed to provide the energy to drive movement of a reducing equivalent from water to NADPH and at the same time to generate ATP.

NADPH and ATP are used in the *dark reactions* to drive the conversion of CO_2 into carbohydrates. The first step in the *dark reactions* is a unique reaction found only in photosynthetic organisms, in which a 5-carbon high-energy acceptor molecule (ribulose-1,5-bisphosphate) reacts with carbon dioxide to form two molecules of glycerate-3-phosphate. This reaction is catalyzed by an enzyme called ribulose-1,5-bisphosphate carboxylase/oxygenase (abbreviated Ru-

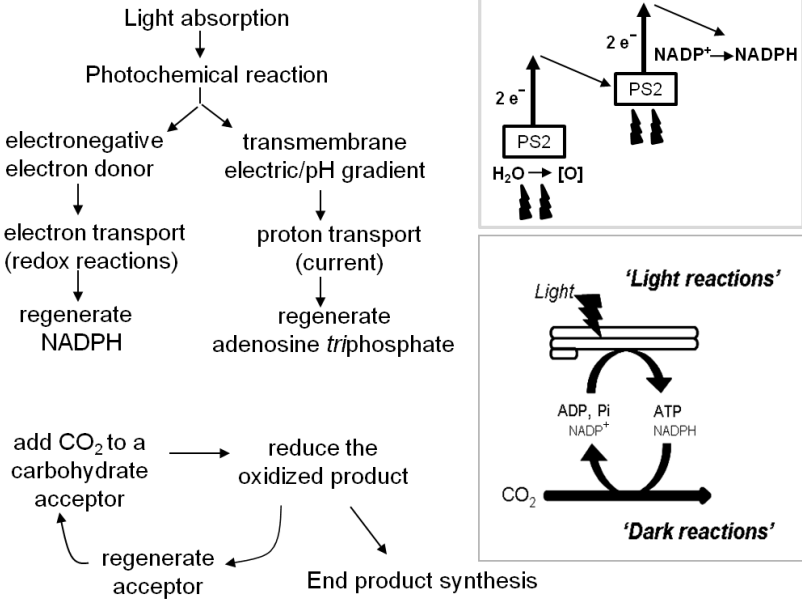


Figure 4.2: A schematic representation of photosynthesis. The lower insert shows the conceptual separation of the *light reactions* in the chloroplast thylakoid membranes and the *dark reactions* in the soluble phase of the chloroplast. The main panel summarizes the main sub-processes in the *light reactions* and in the *dark reactions*. The upper level insert indicates the two sites (photochemical reactions) at which light energy is used to drive the *light reactions*.

bisCO; see later for why it has the additional *oxygenase* in its name). Glycerate-3-phosphate is then reduced to triose-phosphate (triose denotes a carbohydrate with 3-carbons). The reduction of glycerate-3-phosphate to triose phosphate uses almost all the NADPH and most of the ATP that is generated in the *light reactions*. Most of the triose phosphate is used to regenerate the high energy carbon acceptor in a complex multistep pathway that requires ATP. This entire process is called the Calvin-Benson cycle, after the scientists who discovered it (see [14, 15] for historical reviews). The net gain in carbon can be converted to end products like sucrose and starch. Sucrose is exported to the rest of the plant to support

metabolism and growth, while starch is stored during the day and later remobilized at night to support metabolism and growth at night [16].

So where is energy wasted in this process? The rate of plant growth can be modelled as the amount of irradiation intercepted multiplied by the efficiency with which energy in the irradiation is converted into plant matter. The very low global efficiency in the use of solar energy has two reasons; only a small part of the sunlight is actually intercepted by plants or other photosynthetic organisms, and the energy in the intercepted light is not efficiently used to drive carbon dioxide assimilation or (see later sections) plant growth.

4.3.2 Much of the Solar Irradiation is Not Intercepted by Plants

Over half of the total amount of sunlight falls on the oceanic regions of the earth. Although high rates of algal growth are possible in localized areas, much of the ocean is very nutrient-deficient. Nevertheless, it is estimated that about half of the primary photosynthetic biomass production is produced in the oceans [17]. The problem with the use of marine biomass for food and bioenergy is that it is difficult harvesting because almost all of the photosynthetic organisms are unicellular algae. Of course, marine animals grazing on the algae, or on each other, have provided an important source of food and (e.g., whale blubber) energy for millennia. However, this vital energy conversion chain is threatened due to overfishing.

Turning to the solar irradiation that falls on terra firma, a large proportion hits regions without vegetation. This includes areas that are so cold or dry or mountainous or where the soil is so nutrient-poor that plant growth is impossible or very slow at best. Even on land areas that are suitable for plant growth, some of the irradiation arrives during the period of the year that is unsuitable for rapid plant growth. This would include winter in higher latitudes and mountains, and the dry season in Mediterranean-type climate zones and in areas of the subtropics and tropics that experience wet and dry seasons.

Even when climatic and edaphic (soil) conditions are favorable for plant growth, much of the sunlight may not be intercepted by plants because they have not yet developed enough leaves to fully cover the ground area (termed “closing the canopy”). This is especially striking with many crop plants in temperate zones, which are sown early in the year but take almost until mid-summer to grow enough to allow for canopy closure. As a result, the breeding of crops that can be planted early in the year or that can grow under more marginal conditions is one of the most important goals in the breeding of food crops. Developing energy crops that maximize light interception throughout the year or which can be grown in regions with only marginal conditions for the growth of food crops will also

be a vital issue if bioenergy is to make a larger contribution to the global energy mix.

As vegetation becomes increasingly dense, it will start to shade itself with the result that an increasing proportion of biomass is respiring rather than photosynthesizing. This will decrease biomass gain and crop yield. In most natural vegetation systems, some large or tall species take—at least visually—a dominating role and absorb the bulk of the incident radiation, but many others have evolved to occupy niches. Some species have adapted to growing in low light. Others grow early in the year (often from underground bulbs or rhizomes) and flower and complete their life cycle before they become shadowed by the emerging leaves of the trees. In a cereal or maize field, plants start to shade themselves once canopy closure has occurred. Morphological features affecting leaf shape and angle allowing better light penetration into the canopy and decreasing or delaying self-shading in a closely packed stand of plants [18] belong among the most important traits selected by plant breeders in the last century.

4.3.3 Much of the Intercepted Irradiation Cannot be Used to Drive Photosynthesis

Solar irradiation is emitted across a wide wavelength range from under 300 nm (UV) through *visible light* (390–750 nm) to infrared irradiation (up to about 2500 nm). The absorption spectrum of chlorophyll lies between about 360 and 700 nm (there are small variations, depending on the precise structure of the chlorophyll). Irradiance outside this range is not used for photosynthesis, equivalent to a “wastage” of up to half of the incident light energy [11, 13]. Plants have ancillary pigments that can absorb light and transfer its energy to chlorophyll. Some plants and algae that live in water, which preferentially absorbs shorter wavelength irradiation, have modified chlorophyll molecules that slightly extend the absorption spectrum into the infrared region—this can be seen, for example, in the red algae that live near or below the low tide mark. However, there is a limit to which the absorption spectrum of the light absorption pigments can be extended into the infrared. As the light wavelength increases, the energy per photon decreases. At wavelengths above about 700 nm, light (or more precisely, light quanta) does not contain enough energy to drive photosynthetic reactions (see below for more discussion).

Another major inefficiency in energy conversion is the fact that all of the absorbed photons are used to drive the same reaction, irrespective of their wavelength [11, 13]. Blue light at 380 nm contains almost twice as much energy per photon as red light at 700 nm (3.09 and 1.76 eV mol⁻¹, respectively). Absorption of a photon at 380 nm leads to the electron being transferred to a higher orbital but

it falls back immediately to the orbital that would be occupied by an electron after absorption of a photon at 700 nm of red light. In contrast, photovoltaic devices have absorption spectra that closely match incident solar radiation, allowing them to use not only visible but also infrared radiation (see [11]).

Why have living organisms not evolved to use the entire spectrum of solar radiation more efficiently? One reason is probably that photosynthesis evolved relatively late in the history of life, at a time when the basic biochemical machinery for energy conversion had already been established. By that time, universal energy carriers like ATP and NADPH were “established.” A plethora of proteins had already evolved that catalyze reactions in which ATP and NADPH act as energy and redox donors. There had already been a “selection” of reactions whose thermodynamic properties allowed them to be driven by these molecules along with protein structures that were compatible with such reactions. Like societies, the history of biological systems places a constraint on their further development. Photosynthesis evolved via the use and modification of existing proteins and energy carriers, rather than by the *de novo design* of the entire process. Irradiation with a wavelength larger than 700 nm does not have the energy to drive the oxidation of water and the other redox reactions in photosynthetic electron transport. There is interest in the possibility that the long-wavelength irradiation might be used to drive other energetically less expensive processes, for example the synthesis of extra ATP. However, this is an ambitious project, which will require extensive research and further developments in synthetic biology.

4.3.4 Photosynthesis Involves many Sequential Reactions, some Involving Small and others Large Decreases in Free Energy

Energy and metabolic interconversions in biological systems typically occur as a sequence of reactions, each introducing a small change in the molecule. This results in an inherent loss of energy. For example, based on the energy in a photon at 700 nm, the stoichiometry of the *light reactions* and the free energy in ATP and NADPH, it can be calculated that only 37% of the energy in red (700 nm) light is captured as ATP and NADPH [11, 13]. The value falls to 21% for blue light at 380 nm. The *dark reactions* lead to a similar loss of energy, with only about a third of the energy from the ATP and NADPH being captured in the final carbohydrate products of photosynthesis [12].

4.3.5 In Bright Sunlight, Much of the Energy is Dissipated as Heat

The above calculations were made for photosynthesis occurring in low light. Under these conditions, every absorbed photon leads to a reducing equivalent moving through the electron transport chain. Speaking in technical terms, the

“quantum efficiency” is perfect. One oxygen is evolved and one carbon dioxide molecule is fixed for every 8–9 photons absorbed, which reflects the stoichiometry of the pathways.

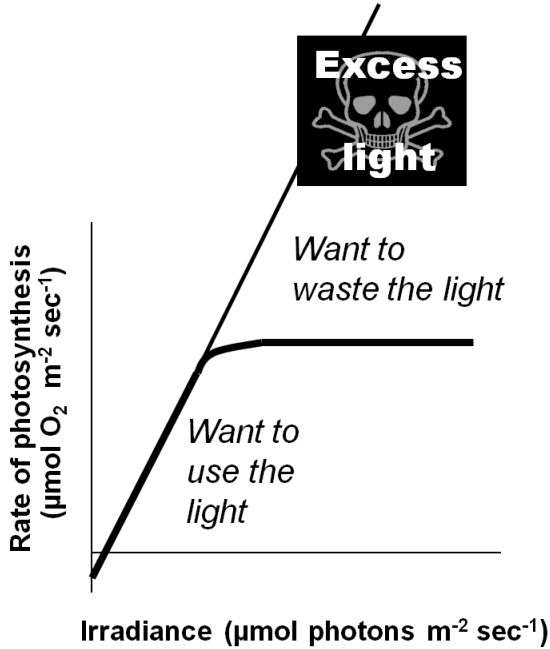


Figure 4.3: The light saturation curve of photosynthesis. The thick line shows schematically the relation between light intensity and the rate of photosynthesis. In darkness, there is net oxygen uptake (respiration). As the light intensity increases, there is initially a strictly proportional increase in the rate of photosynthesis. This reflects the fact that the “quantum yield” is almost perfect, i.e., every photon absorbed is used to drive a photochemical reaction. The slope of this initial line reflects the stoichiometry of the photosynthetic pathways, with 8–9 photons being required to evolve one O_2 (or fix one CO_2). As the light intensity rises further, a region is reached where the rate of photosynthesis reaches a maximum level (i.e., photosynthesis is *light-saturated*). All incident photons above this level are absorbed but the energy is dissipated as heat rather than being used to drive a photochemical reactions.

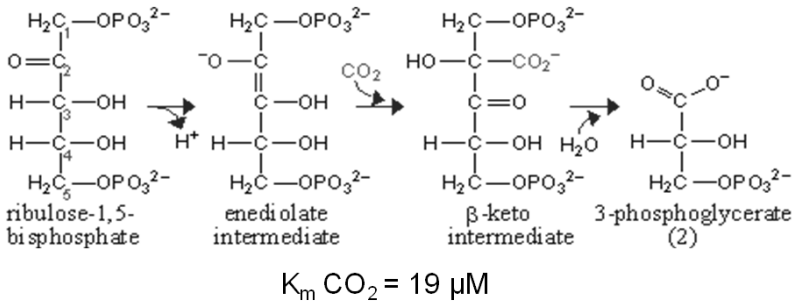
However, as the irradiance intensity is increased, a point is reached where the rate of photosynthesis stops to increase and levels off instead (Figure 4.3). Photosynthesis is then *light-saturated*. The light intensity at which photosynthesis becomes *light-saturated* depends on the temperature, the carbon dioxide concentration, the prehistory of the leaf and the species. In the majority of plants, it is reached well below the light intensities that are experienced on sunny summer days. This means that part of the light energy is not used. It is still absorbed by chlorophyll but, instead of being used to drive photosynthesis, it is dissipated as heat [12].

Energy dissipation occurs via a regulated mechanism, which is turned off at low light intensities and is activated when photosynthesis becomes light saturated. As discussed by Zhu et al. [12], it is important that energy dissipation is switched on and off at the correct light intensities for a given leaf and condition. If energy dissipation is turned on at light intensities that are not yet saturating, the ongoing rate of photosynthesis will be decreased. If it is switched on too late, the un-dissipated light energy results in damage to the photosynthetic apparatus, which will also lead to an inhibition of photosynthesis and requires repair of the apparatus, which is itself an energy-consuming process. This raises the questions if this and other regulatory processes are optimally regulated, if it is possible for a plant to do this across a wide range of different environmental conditions, and if this is a possible target for plant breeding.

4.3.6 An Unspecific Side Reaction of the Key Enzyme RubisCO Leads to a Large Wastage of Energy, Nitrogen and Water

One of the largest sources of inefficiency in photosynthesis revolves around the enzyme RubisCO (Figure 4.4). As already mentioned, RubisCO catalyzes the key reaction in the Calvin-Benson cycle in which the acceptor ribulose-1,5-bisphosphate reacts with carbon dioxide to form two molecules of glycerate-3-phosphate. However, RubisCO has several side reactions, including one in which ribulose-1,5-bisphosphate reacts with oxygen instead of carbon dioxide, resulting in the formation of one molecule of glycerate-3-phosphate and one molecule of 2-phosphoglycolate [19, 20]. Oxygen is a competing substrate to carbon dioxide; as the oxygen concentration increases, the rate of the reaction with oxygen will rise and the rate of the reaction with carbon dioxide will fall. Under current atmospheric conditions (21% oxygen, 78 % nitrogen, 0.038% carbon dioxide), every third reaction uses oxygen instead of carbon dioxide, resulting in the rapid formation of 2-phosphoglycolate. 2-Phosphoglycolate is recycled by a complex metabolic pathway, termed photorespiration, which leads to the release of carbon dioxide and further energy consumption [16, 20, 21]. The oxygenase reaction of RubisCO

and the salvaging of 2-phosphoglycolate lead to a decrease in the rate of photosynthesis of approximately 20–40% and to a 40–50% decrease in the efficiency of energy conversion [12]. This can be seen in a simple experiment, in which the side reaction is suppressed by decreasing the oxygen concentration from 21 to 2%. This leads to an immediate increase in the rate of photosynthesis. The energy loss due to photorespiration increases as the temperature rises [22] because high temperatures favor the reaction of RubisCO with oxygen as compared to carbon dioxide.



Side reaction – oxygenation

O_2 (like CO_2) also reacts with the enediolate intermediate;

$K_m \text{O}_2 = 400,000 \mu\text{M}$.

Products: One molecule of phospho-3-glycerate and one molecule of 2-phosphoglycolate.

The rate of oxygenation rises relative to carboxylation as the O_2 concentration increases or the CO_2 concentration decreases. In current atmospheric conditions the side reaction with O_2 occurs every third to fourth catalytic cycle. The rate of oxygenation also rises relative to the rate of carboxylation as the temperature increases.

Slow catalysis

$K_{\text{cat}} \sim 0.3$ (3 cycles/sec)

30-40% of all the protein in a leaf is RubisCO.

Figure 4.4: Summary of the main features of the reactions catalyzed by ribulose-1, 5-bisphosphate carboxylase/ oxygenase (RubisCO). The scheme shows the reaction sequence with carbon dioxide.

Why does this crucial enzyme perform such a wasteful side reaction, and why have hundreds of millions of years of evolution not solved this “problem”? There are probably two reasons:

One relates to the catalytic mechanism of RubisCO. RubisCO is a very slow catalyst with rates of about three reactions catalyzed per second per catalytic site, compared to typical rates of 10,000 to 100,000 per second that are found for most other enzymes. There is a trade-off between the rate of catalysis and the specificity factor—the specificity for carbon dioxide relative to oxygen, such that an increased specificity for carbon dioxide results in an even lower rate of catalysis [23]. Due to its exceptionally low rate of catalysis, RubisCO already accounts for an incredible 30–40% of all proteins in a leaf. Therefore, there are strong constraints on increasing specificity at the expense of the catalytic rate.

The other reason deals with the way biological systems evolve. Oxygenic photosynthesis evolved in an atmosphere that contained high carbon dioxide and very little oxygen, under which conditions the side reaction of RubisCO with oxygen was quantitatively negligible [22]. This “construction mistake” was not revealed until the gradually falling carbon dioxide and rising oxygen concentrations in the atmosphere led to the side reaction with oxygen becoming quantitatively important. This probably did not occur until the last 400 million years. It is thought that atmospheric conditions will only have favored significant levels of photorespiration during the Carboniferous period (280–340 million years ago) and in the past 35 million years. However, by that time it was too late to change the complex *dark reactions* that had evolved around RubisCO and to develop an oxygen-insensitive pathway for carbon dioxide fixation instead. Citing Sage [22]:

By the Carboniferous, all plants used RubisCO for the net carboxylation step of photosynthesis, and RubisCO was well integrated into the primary metabolism of the plant. Because of this integration, the likelihood of evolutionarily solving the photorespiratory problem within the context of C3 photosynthesis [photosynthesis using the Calvin-Benson cycle] was probably nil. Even if a novel carboxylase could be produced, it would probably be useless because the plant would lack the metabolic pathways to regenerate acceptor molecules and process the carboxylation products.

The costs of this side reaction are not limited to a lower rate of photosynthesis. As mentioned in the last paragraph, RubisCO accounts for 30–40% of total leaf protein. This has a large impact on the so-called *nitrogen use efficiency* of a plant—the amount of nitrogen needed to generate a given amount of biomass. This in practical terms means that crops require more nitrogen fertilizer.

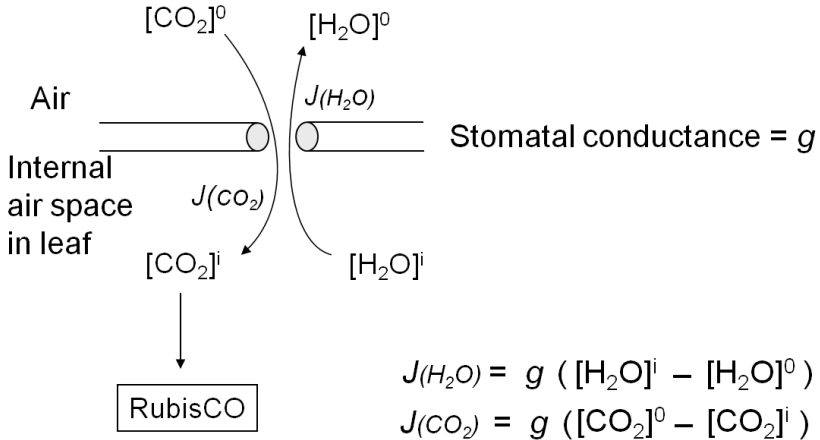


Figure 4.5: Entry of CO_2 into and loss of water from the leaf. The leaf surface is covered with a wax layer and highly impermeable to CO_2 and water vapor. However, it contains many small apertures, called stomata, whose diameter and hence conductance, g , can be changed. The fluxes of CO_2 and water vapor (H_2O) are schematically depicted through a single stomata on the leaf epidermis. For both gases, the flux, J , depends on the concentration gradient and the stomatal conductance, g . The poor affinity of RubisCO for CO_2 and the competitive reaction with O_2 means that $[CO_2]^i$ (the CO_2 concentration in the airspaces inside the leaf) must be maintained at relatively high levels. As $[CO_2]^0$ (the atmospheric concentration of CO_2), is fixed, increased rates of photosynthesis and CO_2 entry can only be achieved by an increase in stomatal aperture, which increases g (stomatal conductance). This is unavoidably accompanied by an increase in the loss of water from the leaf to the atmosphere.

There is an even more important consequence with respect to water use (Figure 4.5). The leaf surface is covered by waxes, making it rather impermeable to gases and water. However, photosynthesis obviously requires entry of carbon dioxide into the plant. This occurs via small regulated apertures on the leaf surface called stomata. Stomata typically open in the light and close in the dark, when no photosynthesis occurs [12]. Carbon dioxide enters by diffusion through the stomata. The rate of entry therefore depends on the concentration gradient between the external atmosphere and the air spaces in the leaf (ΔC) and the con-

ductance (g) of the stomata. Stomatal conductance increases when stomata open. However, other gases and water vapour will also move through the small hole that is conveniently provided by the stomata. Water moves out of the leaf, where the air spaces contain water-saturated air, into the atmosphere. Returning to RubisCO, one of the consequences of the competing side-reaction with oxygen is that a higher carbon dioxide concentration is required inside the leaf to support a given rate of photosynthesis. A higher internal carbon dioxide concentration can only be achieved by increasing g , i.e., opening the stomata further. The option to increase the external carbon dioxide is not available unless the plants are fortunate enough to be growing in a greenhouse with a supply of additional carbon dioxide! Increased opening of the stomata will, in turn, lead to an increased loss of water. In technical terms, the *water use efficiency* of photosynthesis is decreased, i.e., more molecules of water are evaporated per molecule of carbon dioxide fixed.

As can be imagined, there has been enormous evolutionary pressure to ameliorate or get around the self-imposed bottleneck at RubisCO. To date, no plant or any other living organism has managed to evolve a truly alternative way to carry out photosynthetic carbon dioxide fixation. However, there have been small but important gains in the specificity factor when RubisCO is compared in the evolutionarily most primitive organisms (photosynthetic bacteria) and higher plants. Equally important, various strategies have been evolved to “turn back history” and generate a high carbon dioxide concentration around RubisCO. These strategies are collectively termed *carbon dioxide concentration mechanisms* as illustrated in Figure 4.6. These are, in effect, “clamped on” in front of the Calvin-Benson cycle. Plants that operate the Calvin-Benson cycle without a carbon dioxide concentration mechanism are often termed “C3” plants (because the first product of carbon assimilation is the C3 compound glycerate-3-phosphate).

The carbon dioxide concentration mechanism in algae involves active transport of bicarbonate across the cell membrane. In water, carbon dioxide equilibrates with bicarbonate. Algae possess transport proteins that catalyze an energized uptake of bicarbonate from the surrounding medium into the cell. Bicarbonate then equilibrates back to carbon dioxide in the immediate spatial vicinity of RubisCO, which is localized in highly specialized structures (termed carboxysomes in photosynthetic bacteria, and pyrenoids in algae). These subcellular structures may facilitate the concentration of carbon dioxide by decreasing its back diffusion. Their molecular components and organization is still poorly understood. Carbon dioxide accumulation mechanisms are essential for algae, due to the low solubility of carbon dioxide in water.

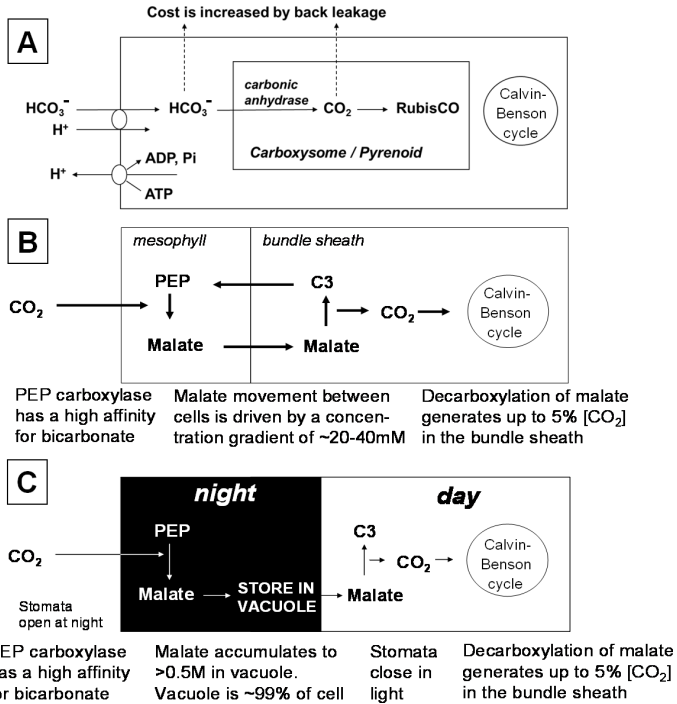


Figure 4.6: *Carbon dioxide concentration mechanisms*. Algae and plants have evolved different mechanisms to concentrate CO_2 in the vicinity of RubisCO, and hence depress the side reaction of RubisCO with oxygen and allow higher rates of photosynthesis at a given external CO_2 concentration. (A) Pumping of bicarbonate and release of CO_2 via a carbonic anhydrase reaction located in the immediate vicinity of RubisCO in subcellular structures (carboxysomes in prokaryotic cyanobacteria, or pyrenoids in eukaryotic algae). (B) C4 Photosynthesis. CO_2 is pumped via a cycle involving the synthesis of 4-carbon acids like malate in external (mesophyll) cells in the leaf and their movement to internal cells (bundle sheath) where they are decarboxylated and the CO_2 is fixed via the Calvin-Benson cycle. (C) CAM Photosynthesis. In the dark, stomata are opened and CO_2 is used for the synthesis of 4-carbon acids like malate which are accumulated in the vacuole. In the light, stomata are closed and malate is decarboxylated to release CO_2 that is fixed via the Calvin-Benson cycle.

Higher plants use a different strategy to concentrate carbon dioxide. So-called C4 plants [24, 25] initially incorporate carbon dioxide (actually bicarbonate) into 4-carbon organic acids like malate via a reaction that is catalyzed by phosphoenolpyruvate carboxylase. This reaction occurs in cells in the outer part of the leaf. The malate diffuses into specially thickened cells in the middle of the leaf, where it is decarboxylated to release carbon dioxide, which is assimilated via RubisCO and the Calvin-Benson cycle. Because phosphoenolpyruvate carboxylase has a very high affinity for bicarbonate and no side reaction with oxygen, photosynthesis can operate with much lower carbon dioxide concentrations in the internal air spaces in the leaf that are in direct contact with the stomata. This means that the stomata do not need to open so wide and that water loss is decreased. In Crassulacean Acid Metabolism (CAM) plants, phosphoenolpyruvate carboxylase incorporates carbon dioxide into malate in the dark. Their cells have an extremely large central water-filled vacuole and can store concentrations of up to 1 molar malate. In the light, the malate is decarboxylated to release carbon dioxide, which is assimilated via RubisCO and the Calvin-Benson cycle. CAM allows water loss to be decreased because the stomata remain closed in the daytime and instead open at night when lower temperatures decrease evaporative water loss.

C4 and CAM plants have evolved multiple times in different taxa and families [22, 25]. This probably occurred in response to intensive selective pressure during periods in the last 20 million years, when the atmospheric carbon dioxide concentration was often lower than today, sometimes falling to below 200 ppm [22]. The most recent “low carbon dioxide periods” were as recent as 10–12,000 years ago. These low carbon dioxide levels would have strongly restricted photosynthesis by C3 plants and provided strong selective pressure for plants with C4 or CAM photosynthesis.

So why do not all plants use one or the other of these mechanisms for carbon dioxide concentration? The answer is that carbon dioxide concentration mechanisms require energy. Under current atmospheric conditions C4 plants and CAM plants actually require more energy than C3 plants except at high temperatures, when the rate of photorespiration rises relative to the rate of photosynthesis [22]. At the present geological time, C3 plants can compete with C4 plants except under hot or dry conditions [12]. Most C4 plants are tropical and subtropical grasses that grow in seasonally dry zones, while most CAM plants are cacti that grow in semi-arid zones.

There is obviously intense interest in decreasing photorespiration because this could lead to an increase in photosynthesis and crop yield and also to a decrease in water use. For the past 30 years, the catalytic mechanism and structure of RubisCO have been studied with the hope of engineering a form with a higher

specificity factor for carbon dioxide [26]. There has also been a longstanding interest in engineering C4 photosynthesis into conventional crops (most major crops are C3 plants, with the exception of maize, sugar cane and sorghum). This is a challenging task because it requires a fundamental change in leaf anatomy and the introduction of many different enzymes and transport proteins into specific cell types. However, the finding that individual components of the C4 pathway exist in C3 plants and the fact that C4 photosynthesis has evolved many times indicates that some basic genetic “switches” exist that underlie these complex morphological and biochemical changes. If the underlying “master genes” can be discovered, it may be possible to use them to engineer the multiple and complex changes that are needed to convert a C3 plant into a C4 plant [24]. Other approaches investigate if a more fundamental reengineering of metabolic pathways could lead to an increase in the efficiency of photosynthesis. Several projects are searching for a more efficient way to salvage 2-phosphoglycolate than the complex pathway that naturally evolved, probably in a piecemeal way as slowly changing atmospheric conditions led to its becoming an increasingly crucial issue for survival [21]. An even more radical approach is to use large scale pathway reconstruction and synthetic biology to try to create a completely novel carbon dioxide fixation pathway that does not require RubisCO [27].

4.4 The Use of Photosynthesis to Drive Plant Growth

Light energy-driven processes lead to the formation of sugars, amino acids, nucleotides, lipids and many other small metabolites. These resources serve to synthesize the macromolecules that build a cell—proteins, lipids and complex polysaccharides. Without going into detail, this involves thousands of biochemical reactions and transport steps, many of which lead to a loss of energy. Further, each reaction and transport step is catalyzed by a specific protein, which has to be synthesized, which again costs energy. For example, proteins are synthesized by molecular machines called ribosomes. In a rapidly growing microbial or plant cell, it is estimated that over half the cell’s resources are actually invested in ribosomes [28]. Cellular growth is a very capital-intensive process. Large scale investment of carbon, nitrogen, phosphate and energy is required to produce the machinery that itself is needed to convert the raw products (the immediate products of photosynthesis and the assimilation of mineral nutrients) into cellular structures. As a result, 30–60% of the assimilated carbon is respired to carbon dioxide in the remainder of the plant to provide energy for growth and for the maintenance of the cellular structures that are needed for growth processes [12].

4.4.1 Vegetative and Reproductive Growth: (Bio)Mass Production versus Quality Products

So far, the biochemical reactions converting the products of photosynthesis into the building procedure of a cell (proteins, lipids and complex polysaccharides) have been considered. However, this only captures one aspect of plant growth. A plant consists of many cells organized in different organs with different functions. This multi-functionality is important for the growth and survival of plants. However, it incurs further costs when plants are considered solely from the perspective of energy conversion. It also has important implications for what kinds of plants can be sensibly used as energy crops and how we must proceed to minimize competition between the production of bioenergy and food.

Figure 4.7 provides a simplified overview of the growth of a young plant. In mature leaves, light and CO_2 are absorbed and converted into carbohydrates like sucrose and starch. The roots absorb nutrients and water from the soil. These are moved in the transpiration stream (as discussed above) to the leaves and used, in combination with the products of photosynthesis, to make amino acids, nucleotides and many other small molecules. Sucrose, amino acids and nucleotides are then exported and used to support the growth of young leaves and roots. As a result, the plant acquires more leaves and a larger root system, which allows the plant to absorb even more light and CO_2 , and access more water and nutrients. This in turn will allow more photosynthesis at the level of the whole plant and even faster growth. This is basically like a bank account that pays compound interest. In contrast to most bank accounts, the interest rate is very high. A young plant under optimal conditions will often increase its weight by 20–30% per day. Thus, young plants typically show an exponential increase in their biomass, which doubles every 4–6 days (see, e.g., [29]).

As the plant becomes larger, this process may slow down because, for example, some of the leaves start to shade each other, or the roots start to exhaust the water or mineral nutrients in the soil, or an increasing proportion of the new growth has to be invested in structures that do not directly allow resource gain (e.g., thicker stems to prevent the plant from falling over). Nevertheless, plants continue to gain weight at rates that would thrill most dealers on Wall Street, if their stocks were to increase in value at a comparable rate.

Later, plants start to produce reproductive organs (Figure 4.7). This can involve the formation of flowers that, after fertilization, develop into seeds, berries or fruits. Some plants produce asexual reproductive organs like potato tubers, thickened storage roots like carrots or sugar beet, or rhizomes (e.g., many grasses).

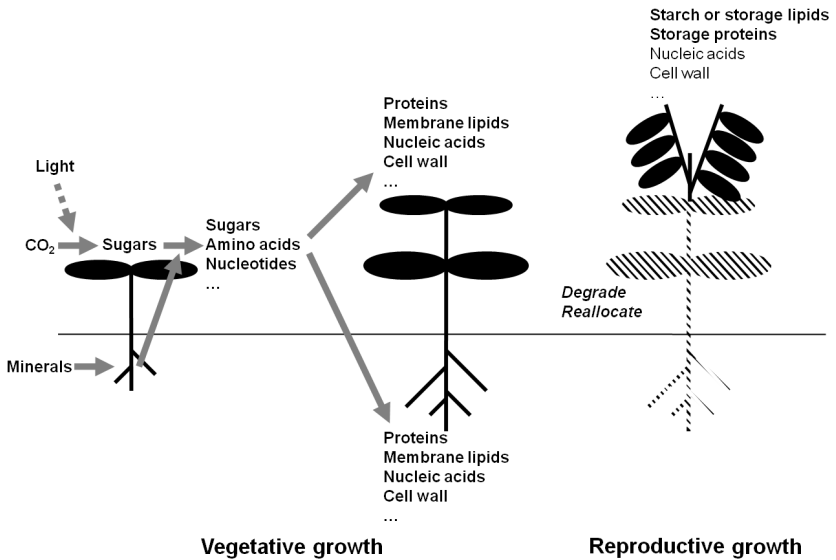


Figure 4.7: Schematic presentation of plant growth. In young plants, light energy drives the assimilation of CO₂ in leaves and the uptake and assimilation of inorganic nutrients by the roots, generating sugars, amino acids and other metabolites that are used to synthesize more leaves and roots. They, in turn, allow the acquisition of even more CO₂, light, minerals and water, which in turn supports even more growth. In a young plant, growth is typically exponential in time, with an increase in biomass of 20% or more per day. Later in the life cycle, growth slows down or stops as resources are used to generate storage and reproductive structures. Investment in the formation of new leaves and roots is curtailed or stopped. This schematic representation reflects the life cycle of determinate annuals (plants that grow, flower and die within one year, i.e., most crop plants). Plants that grow for two or more years have more complex and flexible life cycles.

Reproductive organs are important for at least three reasons. First, they are vital for survival. Seeds and tubers allow annual species (i.e., plants that only live for one year) to survive seasonal periods of weather that would kill the mature plant, like the winter in northern or southern latitudes, or the dry season in climate zones with a hot dry summer. Second, seeds allow distribution of the species. This is important for plants as, unlike animals, they cannot crawl away or walk

about. Seeds can be distributed by the wind (e.g., many grass seeds, dandelions, sycamore seeds), by water (e.g., coconuts) or by animals eating and excreting them. In the last case, the seed is usually surrounded by some attractive food for the animal such as berries and fruits while the seed coat is resistant to the animal's digestive enzymes. The seed is then deposited at some site that the animal has wandered off to, together with a convenient dose of organic fertilizer. Third, sexual reproduction allows the mixing and recombination of chromosomes and thus reshuffles the genetic material and by doing so maintains its diversity.

Seeds contain large amounts of energy-rich storage compounds like starch, lipids and proteins. These nutritive and energy-rich resources are needed to support germination and the growth of the seedling. Starch is a polymer made from glucose and consists of a mix of linear $\alpha(1-4)$ and branched $\alpha(1-4)(1-6)$ glucan chains. It differs from glycogen, which is an important storage carbohydrate in many animals, and in humans as well, because it forms a crystalline structure which is insoluble and more resistant to microbial attacks than free sugar molecules.

Further resources are used to produce surrounding structures like the tough seed coat. In the special case of fruits and berries, resources are also used to make the surrounding nutritional sacrifice that tempts animals to swallow the seed.

An unavoidable result of flowering and seed formation is that plant growth—seen as an increase in weight—slows down or even stops. Indeed, biomass may even decrease. Existing leaves and stems may even enter a process called senescence, in which their protein, lipids and other components are degraded and exported to the growing seeds. Incoming light energy is no longer used to produce more leaves and roots. Instead, existing biomass is used to make high-quality, high-energy long term stores at a specific number of spatially defined sites. These stores are needed to support germination and the growth of the seedling in the following generation. An analogous process occurs during tuber formation.

In effect, instead of continuing to reinvest gains in a high-interest account, funds are cashed in and moved to the vault, incurring large bank charges [30]. The advantage of the plant's strategy to stop growth and allocate resources to seed formation is clear: it is investing in the next generation. The large amounts of protein and energy-intensive storage compounds like starch and lipids will support the growth of the next generation long enough for the seedling to produce the necessary leaves and roots to fend for itself.

The cessation of growth during the formation of seeds and tubers is especially large in many crop plants. Our crop plants are typically annuals in which the vegetative organs die back as the seeds are being filled. They have been selected and bred over thousands of years to maximize the yield of seeds or tubers. One of the major ways in which this has been achieved was the increase of the so-called

harvest index (the proportion of the biomass that is found in the part of the plant that is harvested to be used as food, i.e., the seeds or tubers). They have also often been bred to obtain synchronous flowering and seed growth because this makes it much easier to harvest fields with thousands of plants.

Mankind's major staple foods are seeds from the Gramineae—cereals like wheat, barley and rye—and from related plants like maize, rice and sorghum. Other important staple foods come from the protein-rich seeds of the Leguminosae, like soybean, many different bean cultivars, peas and chick peas. Other important staple foodstuffs are based on starch-containing tubers like potato and cassava. Occasionally, fruits form an important staple, for example starch-rich bananas or plantains in some parts of sub-Saharan Africa. Oils also represent an important and energy-rich component in many diets. These are also largely obtained from seeds (e.g., rape seed oil, sun flower oil) or fruits (e.g., olive oil, palm oil). But why do we rely so much on seeds for food? The answer is three-fold.

First, seeds can be stored. They have evolved to survive not just one winter or dry season, but for many years. This is achieved due to the physical structure of their seed coat, but also to the fact that they are almost completely dried out. This will restrict growth of bacteria and fungi. In addition, many seeds actually contain defence compounds to ward off the unwanted attention of microbes and animals. Examples include derivatives of cyanide in cassava (also called manioc, a starch-rich root that is a major staple crop in sub-Saharan Africa) or strongly allergenic lectins in many legume seeds (beans, peas, etc.). Storability of the staple foodstuff was essential when mankind moved from being a hunter and gatherer to producing food from crops because growth of the latter depended on the season. One interesting cultural side-effect is the immense creativity that has gone into turning an object that is physically inedible (like a wheat grain) into something that is not only edible, but often delicious, and the cultural and culinary diversity that this has engendered.

Second, seeds and, to a lesser extent, tubers and some fruits, especially fruits from the tropics, provide a concentrated source of proteins, carbohydrates and/or lipids. In contrast, the remainder of the plant is mostly inedible. It may provide us with nice flavors, vitamins and roughage, but has very little nutritive or energetic value. This is partly due to another fundamental difference between the growth of plants and animals. Whereas animal cells are full of proteins or lipids, plant cells are like a large balloon: mature plant cells have a large central water-filled vacuole that typically occupies 90% of the cell, with a thin layer of protein around it where metabolism occurs (Figure 4.8).

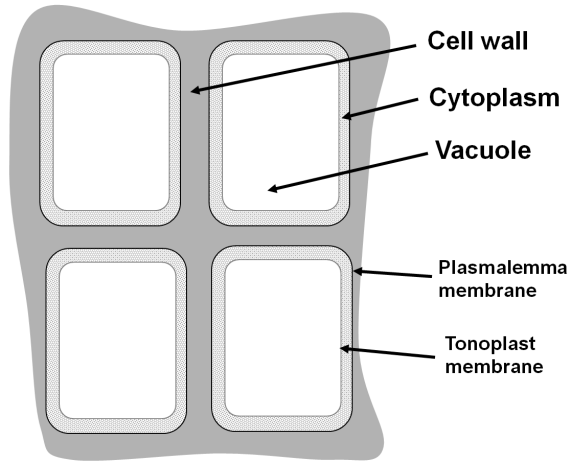


Figure 4.8: A schematic representation of a typical plant cell. The plant cell is surrounded by a thick cell wall that is shared with the neighboring cells. The cell wall consists mainly of cellulose and cell wall matrix components and provides rigidity and physical stability to the cell. The cell itself consists of a layer of cytoplasm and a large central vacuole. The cytoplasm consists mainly of proteins and nucleic acids. It is the site of most metabolic activity but occupies only about 10% of the cell volume. The cytoplasm includes smaller substructures like chloroplasts, mitochondria and the nucleus (not shown). The vacuole consists mainly of water, with dissolved ions and a few metabolites, and occupies about 90% of the cell volume. The cytoplasm is bounded by the plasmalemma, and the cytoplasm and the vacuole are separated by the tonoplast; both are thin membranes that are composed mainly of a phospholipid bilayer with embedded water-insoluble proteins, and provide a semipermeable layer between the cytoplasm and the external surroundings/cell wall, and the cytoplasm and the vacuole, respectively.

This means that, for a given amount of protein, a plant cell occupies a much larger volume and/or can generate a much larger area than an animal cell. This is obviously very useful for a sessile organism that cannot walk about but wants to maximize light and carbon dioxide absorption by generating a large leaf area. Similarly, the plant can generate a physically larger root system underground to access minerals and water in a large soil volume. Third, the bulk of a plant can-

not be degraded by the human intestinal system. Plant cells are surrounded by the so-called plant cell wall (see Figure 4.8), which is indigestible to humans but nevertheless plays an important role by providing roughage to aid digestion. The plant cell wall has many functions in plants, including structural support and defence, which will be described in more detail in the next section.

Many current methods for generating bioenergy also use seeds or tubers as the feedstock to produce alcohol or biodiesel (see below). They do this for the same reason we use seeds and tubers for food; they are a high-quality and energy-intensive product that can be relatively easily processed and degraded. However, the use of carbohydrates and lipids in seeds and tubers as a starting point for bioenergy enters into direct competition with the production of staple foods for nutrition. It is a very wasteful way to produce energy because the production of seeds and tubers is inherently inefficient and because they only represent a small proportion of the total biomass of the plant.

4.5 Vegetative Biomass: What to Do with the Cell Walls?

Why is the rest of the plant not used for bioenergy production? As already mentioned, a typical mature plant cell contains a lot of water and a relatively small amount of proteins, lipids or carbohydrates. The vast bulk of dry vegetative plant biomass derives from the cell walls that surround the cells and are much more difficult to degrade than carbohydrates or lipids. The cell wall provides structure to the plant cell, which otherwise would be a jelly-like bag of water. It also provides structure at the level of the organ and the whole plant. Plants do not have bones, instead, their physical stability results from the walls of all of their individual cells. In small plants, each cell is firm because the ions and small metabolites within the cell act via osmosis to draw water into the cell. This generates a pressure (called turgor) that is exerted against the cell wall. If the cell wall is experimentally removed, the cell will actually explode, unless it is surrounded by a 4–500 mmolar solute. The firmness of a salad leaf is due to all of the cells pushing against their cell walls, and the cell walls of each cell pushing against the cell walls of its neighbors. Plants also possess specialized cells that make especially thick cell walls and provide physical support, which is independent of the interplay with water. These cells play a role in allowing the plant to move water from the roots up into the leaves in a transpiration stream. This is done via a long file of dead cells called xylem vessels, whose thick walls prevent them from collapsing inward as water is sucked up from the roots. In larger plants, these cells become far more numerous and provide large supportive tissues. This is seen most dramatically as wood in the stems of trees.

The plant cell wall is a complex macromolecular structure. As might be expected from its role in providing rigidity and defence, it is extremely difficult to degrade [31–34]. The main component of the cell wall in non-woody plants is cellulose, which is estimated to represent about 30% of the dry weight of a plant. Cellulose, like glycogen or starch (the major carbohydrate stores in animals and plants, as mentioned above), is a polymer made of glucose. However, it differs in that the glucose residues are linked via a $\beta(1-4)$ -glycosidic link rather than an $\alpha(1-4)$ -glycosidic link. This apparently small change in the stereoisometry (spatial structure) of the chemical bond that links the adjacent glucose molecules has a major impact on the spatial organization of the polymer. In glycogen and starch the glucose polymers form a loose helix. In cellulose the $\beta(1-4)$ -glycosidic link is reinforced by an H-bond between the OH-group on the C3 atom of one glucose residue and the oxygen of the O-glycosidic bond. This prevents rotation around the O-glycosidic bond. As a result, the lowest energy conformation for the polymer is that of a linear ribbon-like structure. These can then stack on top of each other, with H-bonds between the adjacent chains leading to the formation of a microfibril. A microfibril is estimated to contain about 36 individual macromolecules, each 500–1400 glucose residues long. These long and inelastic microfibrils wrap around cells in spatially oriented and overlapping layers. They are able to withstand pressures of the same order as those in a car tire [33]. The cellulose microfibrils are held together by several other classes of macromolecules, including hemicelluloses, pectins and glycoproteins. These macromolecules are more flexible, with segments that loop between the cellulose microfibrils, and others that bind onto sites along the cellulose microfibrils [33, 35, 36]. A loose analogy would be to imagine the cell wall as reinforced concrete, with the cellulose being the steel rods and the hemicelluloses, pectins and glycoproteins the concrete that holds them in place.

In wood, the cell wall is further strengthened by the deposition of lignin. Lignin is a highly complex macromolecule formed from various types of aromatic phenylpropanoid molecules. The variety of subunits and the fact that they do not necessarily polymerize in a fixed order makes lignin rather unusual due to its heterogeneity and lack of a defined primary structure. It is even more difficult to degrade than cellulose. Lignin is one of the most abundant organic polymers on earth, exceeded only by cellulose, employing 30% of non-fossil organic carbon and constituting approximately a quarter to a third of the dry mass of wood [37]. Together, lignin and cellulose make up well over half of the plant matter on earth. Jointly, they are often termed *lignocellulose*.

As already mentioned, the digestive tract of humans is not able to degrade cellulose. Vegetables like lettuce and cabbage and fruits like apples and oranges are important sources of vitamins, minerals and roughage, but contain negligible

amounts of energy. However, there are obviously herbivores—animals that eat only plants. Many of these mainly feed on leaves (in particular grass) and are able to digest cellulose. Examples are ruminants like cows, sheep, deer, camels and antelopes whose digestion of cellulose in their rumen depends on a dense population of bacteria, protozoa, and fungi. These produce an enzyme called cellulase that is able to degrade cellulose, and a further cocktail of enzymes that converts cellulose into the disaccharide cellobiose. The latter is fermented in the largely anaerobic rumen to acetate, lactate, propionate, butyrate, carbon dioxide and methane. Other examples of herbivores are the so-called end-gut fermenters like rabbits and horses. They ferment cellulose in an extended large intestine (caecum) and if necessary re-ingest soft pellets (caecal) that contain well fermented microbial products. The relation between such herbivores and their microbial gut inhabitants is a good example of a symbiosis where organisms gain a mutual benefit from a partnership. There is an analogous symbiosis with other microbes in insects that are able to digest the cellulose and lignin in wood; with termites as a well-known example.

This raises the question whether these specialized microbes can be used to convert plant cell wall material and wood into products, which can then be fermented by yeasts to alcohol or other products that can be used as energy. Such processing could, in principle, allow a complete or near-complete conversion of vegetative plant biomass into usable compounds. There is intensive research worldwide into such processes, as described in other chapters of this book. In parallel with research in white biotechnology and chemical engineering, there is also increasing research into the functional properties of the plant cell wall to identify features which might be changed in order to render it less intractable to chemical and enzymatic digestion [32, 38].

There is also interest in developing other ways to use lignocellulose, as an alternative to its conversion to alcohol or other burnable liquid fuels. At this time, biogasification is the most energy efficient way to convert plant biomass into burnable compounds. Biogasification also depends on specialized bacteria and results especially in the formation of methane. Methane is, however, itself a very effective greenhouse gas. This means that widespread use of this technology will depend on engineering and processing methods that near-to-completely prevent its release into the environment. Another approach, which is feasible with dry plant matter, is to burn it. A further interesting process is hydrothermal carbonization to process wet biomass [39]. Low value biomass like garden waste and leaves, crop residue, liquid manure, horse droppings and residues from many industrial food production processes can be converted into products like peat or coal within a few hours. Because the process is exothermic (i.e., producing rather than consuming heat) it requires only a small initial energy input, after which it

produces usable heat. As will emerge later in this chapter, we will probably need to use a wide range of different crops as feedstocks for bioenergy. This will place a premium on having a range of methods to process the plant material, or methods that are robust to changes in the composition of the plant matter.

4.6 Response of Photosynthesis and Plant Growth to Rising Atmospheric Carbon Dioxide

One of the drivers of climate changes is the rising atmospheric carbon dioxide concentration. As already mentioned, the rate of photosynthesis is increased by rising atmospheric carbon dioxide, especially in C3 plants. This opens the hope that in the future, crop yield will increase as a (beneficial) consequence of rising atmospheric carbon dioxide concentrations. Further, we might hope that rising rates of photosynthesis in natural ecosystems could lead to faster growth and sequestration of more carbon in standing plant matter or as dead plant matter in the soil. These hopes were supported by early studies under artificial laboratory or greenhouse conditions, which on average indicated a potential yield gain of over 30% as the atmospheric CO₂ concentration is increased from present-day levels up to 550 ppm CO₂, which is the projected level in 2050. To put this into perspective, projections of the increase in crop yield that will be needed to match the increasing demand for food lie between 40–80%. Does this mean that the increasing carbon dioxide concentration will automatically solve many problems?

In the last 15 years, this possibility has been analyzed more rigorously in a large number of large scale Free Air Carbon dioxide Enhancement (FACE) studies with many crops, including tree plantations, at different locations around the world. These studies have confirmed that there is a stimulation of photosynthesis of ca. 30%, which is in line with predictions made from photosynthesis models. As plant growth is quasi-exponential, this stimulation of photosynthesis should translate into an even larger increase in yield. However, the average yield gain shown in FACE experiments was about 14% [40–42]. Further, in a small number of studies in which elevated carbon dioxide was combined with other predicted changes due to climate change (e.g., increased temperature) or anthropogenic activity (e.g., ozone), the increase in yield was abolished.

The rather small response of yield to elevated carbon dioxide implies that there are major restrictions on growth downstream of photosynthesis. These will include constraints by external factors, like nutrient availability or water, which will become exhausted more rapidly if a plant grows more rapidly. However, there are probably also internal developmental or genetic constraints on the extent to which the growth of a given plant can be increased.

Up to now FACE studies have been performed with one or a very small number of cultivars. It is therefore unclear if the small yield is always due to a weak growth response to carbon dioxide, or also to the specific lines that were used while other lines might respond more. In particular, it is unclear if there is any genetic variation in the breeding populations which would allow the gain in photosynthesis to be transformed into a gain in yield. This raises a dilemma. For many traits, it is possible to carry out breeding trials in different locations to look for lines that will perform better in a given condition. For example, large populations of plants can be screened to identify lines that perform well at low temperatures or with less water by having a set of field sites that differ in temperature or rainfall. At present, there are no FACE sites large enough to perform this kind of large scale screening of our breeding resources for responses to future carbon dioxide levels. Planning and developing such sites is an important challenge for the future [40–42].

4.7 Integrated Model of Energy Use Efficiency during Photosynthesis and Growth

The preceding sections discussed the processes of photosynthesis and growth, and highlighted that the energy conversion efficiency is low, partly due to the inherent need for a loss of energy in any process and partly because of a series of design features which lead to an additional loss—or wastage—of energy. Quantitative analyses by Zhu et al [12] and Blankenship et al. [11] predict that the maximum efficiency of photosynthesis (conversion of energy in the incident light into carbohydrates as the products of photosynthesis) under current atmospheric conditions is of the order of 5 and 8% for C3 and C4 plants, respectively. The predicted maximum efficiency for the conversion of incident light energy into vegetative biomass is below 2 and 2.5% for C3 and C4 plants, respectively. The actual efficiency will be much lower, because the light is sometimes saturating, temperatures may not be optimal for growth and growth may be limited by the availability of nutrients or water. It will become even lower when plants enter the phase of reproductive growth.

Figure 4.9 recapitulates and simplifies the calculations of Zhu et al. [12] and Blankenship et al. [11]. This simplified calculation starts with the value of 120,000 TW of energy, which is the total annual solar energy that is intercepted by the earth. It first considers how much of this irradiation is intercepted by plants and then uses the information about the energy conversion efficiency of photosynthesis and growth to estimate how much of this energy is conserved in plant biomass. Complex and partly unresolved questions about the precise parameterization of the individual process, especially energy conversion in the *dark reac-*

tions and in plant growth, are simplified for the purpose of illustration by setting the energy loss at most of the steps at 50%. They will anyway vary from plant to plant, region to region and day to day. The efficiency cannot be more than two times higher than 0.5, and is also probably not more than two times below it. More precise values are retained for the energy conversion efficiency of light absorption and the light reactions because these processes can be more precisely parameterized with experimental or theoretical values (see [11, 12]).

Process and conversion efficiency		Solar energy intercepted per annum by the earth ~ 120,000 TW
		↓
% going to land with chlorophyll	× 0.2	24000 TW
Seasonality of plant growth	× 0.5	12000 TW
Maximum efficiency of light absorption and the <i>light reactions</i>	× 0.13	1560 TW
Loss due to light saturation	× 0.5	780 TW
Efficiency of the <i>dark reactions</i>	× 0.5	390 TW
Photorespiration	× 0.5	195 TW
Conversion of fixed C to biomass	× 0.5	
		= 98 TW

Figure 4.9: Schematic representation of the conversion of solar energy by the biosphere. This scheme recapitulates and simplifies the calculations of Zhu et al. [12] and Blankenship et al. [11]. Complex, and in part unresolved, questions about the precise parameterization of the individual process like the energy conversion efficiency of the dark reactions and of plant growth are simplified for the purpose of illustration by setting the energy loss as 50%.

This simple exercise predicts that primary biomass production per year will have an energy content of the order of 100 TW. This is only 0.08% of the energy

in the total incoming radiation that arrives at the surface of the earth. The energy content of the resulting biomass is about 0.8% of the energy in the sunlight that is intercepted by plants. This value is about two-fold lower than the maximum values estimated by Zhu et al. [12] because my schematic model already assumes that light is sometimes saturating for photosynthesis.

The calculation in Figure 4.9 puts my earlier optimistic comments about the global availability of solar energy into a stark perspective. Comparison of the estimated primary biomass production (~100 TW p.a.) with the total current (15 TW p.a.) and projected (30 TW p.a.) global energy needs of mankind shows that there are limits to how much of the total energy requirement can be met by bioenergy.

As pointed out by Blankenship et al. [11], the energy conversion efficiency of photosynthesis and plant growth is much lower than the energy conversion efficiency of photovoltaics (in good cases larger than 20%). It is instructive to ask why plants are apparently so inefficient. One reason has already been mentioned, both in the context of the light reactions and of RubisCO. Photosynthesis was not primarily designed to maximize energy conversion efficiency. It was developed in the context of, and had to be compatible with, a pre-existing network of reactions and proteins. Although selection can lead to the evolution of increasing effective living systems, it cannot start again from scratch. However, there are also other and deeper reasons why plants cannot be as efficient in energy conversion per se as a man-made device. Man-made devices are assembled by men (or by machines made by men). The materials needed to construct them are collected and pre-processed by men. The devices are repaired by men (or machines made by men). If the devices are damaged by external events or break down due to wear and tear they are repaired by men. If they break down irretrievably they can be replaced by new machines, which are made by men. Further, machines do not have to improve themselves. This is done by men, who plan and produce the next model, or a new sort of machine that does things in a better way. In contrast, living organisms have to be self-assembling and self-repairing. They have to reproduce themselves and, over time, must evolve to meet the challenges posed by changes in their biological, chemical and physical surroundings. These self-sustaining activities come with an energy cost and place constraints on the design of living organisms.

4.8 What is Needed for Efficient Energy Crops?

The preceding sections lead to the following requirements for an efficient energy crop:

1. It should not compete with food crops.
2. As far as possible the entire biomass of the plant should be used as a feedstock for bioenergy, which will require the development of methods to efficiently utilize lignocellulose.
3. It should be grown using methods that minimize energy-intensive chemical inputs.
4. It should as far as possible be grown on land that is marginal for food crops and/or the feedstocks for energy production should be derived from parts of the plant that are not eaten.

4.9 Current Energy Crops and Their Shortcomings

Most current methods for generating bioenergy use seeds or tubers as feedstock. These are often referred to as “first generation” energy crops. Starch or oil-rich seeds and tubers are used as the feedstock (starting point) for bioenergy production because they provide a concentrated source of high-energy precursors that can be converted to fuel by a combination of physical, chemical and microbial (fermentation) approaches. One major source of biofuels is the use of maize, cereal seeds and sugar beet roots to produce bioethanol. The most widely used procedure to convert sugar- and starch-rich plant matter into ethanol takes advantage of the fact that many yeasts ferment carbohydrates to alcohol. Fermentation is a strategy to cope with anaerobic conditions and allows yeast to convert a small part of the energy in carbohydrates into ATP while producing alcohol as a waste product. Another major source of biofuels is to use oil-rich seeds or fruits like rapeseeds and palm oil to produce biodiesel. Biodiesel is typically made by chemically reacting lipids, for example vegetable oil and animal fat (tallow), with alcohol to generate long-chain alkyl (methyl, propyl or ethyl) esters.

The methods used to produce the majority of these so-called “first generation” biofuels have several major drawbacks. First, the use of seeds and tubers involves direct competition with staple food production. Second, the methods used to produce the feedstock are inherently inefficient. The starting point is a high-quality product whose formation is inherently inefficient because the plant decreases or even stops growth during the formation of seeds and tubers. Further, growth of the crops often occurs in an intensive manner, requiring the use of large amounts of fertilizer. Depending on the crop, the geographical location and

the inputs and outputs used in the analysis, the energy balance can be positive or negative [43].

The most successful current source of bioenergy is sugar cane. The 26 billion liters of ethanol produced in Brazil in 2010 represent about 30% of the total ethanol used as fuel in the world at present [44]. Sugar cane is a successful energy crop for several reasons. First, it is a C4 plant, with inherently high rates of photosynthesis (see above). Second, it is a tropical and subtropical crop that can be grown all year round, maximizing absorption of incident light. Third, sugar cane is unusual in that it stores large amounts of sugars in its stem during vegetative growth. While originally selected and used to produce sugar as a foodstuff, sugar cane also provides an excellent feedstock for the production of ethanol.

However, a large part of sugar cane biomass is not fermented but remains behind as a waste product (bagasse) which consists to about 50% of cellulose, 20% of lignin and the rest mainly made up of other cell wall components. Bagasse is also a waste product of sugar fermentation; for each 10 tons of sugar cane crushed, a sugar factory produces nearly 3 tons of wet bagasse. It often accumulates in large mounds near the sugar mill. There have been large efforts to use bagasse as a starting point for making other products or energy, and these illustrate some general issues in the use of vegetative plant biomass as a feedstock for energy production. First, its composition can be highly variable. Second, its high moisture content (40 to 50%) makes it costly to move and difficult to use as a fuel. Clearly, solving these problems would further improve the energy, economic and ecological balance of sugar cane as a bioenergy crop.

In 2009, the 4.6 Mha of land cultivated for sugar cane in Brazil allowed the production of about 27 giga-liters of alcohol, plus about another 2 gigawatts of electricity via the combustion of bagasse [45]. This is already equivalent to about 40% of the petrol used in Brazil. It is planned to expand sugar cane cultivation to a maximum of 63.5 Mha, mainly by increasing cattle stocking density on a much larger area of about 237 Mha that has already been cleared and is currently being used for cattle ranching (Decree No 6.961, September 17, 2009, Diário Oficial União de 18.9.10, Brazil). This would allow expansion of the area used for this bioenergy crop without further clearing of natural ecosystems. Assuming that advances in the processing of plant biomass also allow the full use of bagasse to produce a liquid fuel, Somerville et al. [38] estimated that Brazil could produce up to approximately 800 giga-liters of ethanol per year, equivalent to approximately 14% of the current world transportation fuel demand (4900 giga-liters) in 2006.

4.9.1 Perspectives for Improving Current Crops to Optimize Bioenergy Production

Two complementary routes are available to improve energy crops. One is to use changes in plant breeding and agronomic practice to improve the energy and ecological balance of existing crops. Another is to develop new dedicated energy crops (see next section).

I will discuss maize as an example of how an existing crop might be made more efficient for energy production. Maize has the advantage that it is already a high-yielding crop which produces a large standing biomass per unit area. In addition, it is one of the crop plants that lends itself relatively easily to crop breeding because it contains a large amount of genetic diversity in its breeding material. In terms of global grain or seed production, maize is the largest crop, producing about 820 million metric tons of grain for food and animal feed purposes. Maize seeds contain a high starch and (in the case of sweet corn) sugar content. There is also a similar amount of stems and stripped cobs (stover) potentially available for fuel production.

One option to increase biomass would be to delay or suppress flowering in order to maximize the duration of vegetative growth and biomass formation. Flowering is a crucial transition in the life of a plant. The timing of flowering is regulated by many inputs including the day length (as an indicator of the time of year), temperature, nutrient status and endogenous signals related to the age of the plant. Maize flowers when the length of day decreases below a critical threshold. This can be seen as a strategy to initiate flowering as autumn approaches. Day length is a more accurate predictor of the time of year than temperature, which fluctuates from day to day and year to year. Within a species, there can be a large genetic diversity in the response of flowering to the length of day. This allows adaptation to the location where the plants are growing. On a given day of the year, the day length depends on the latitude; for example, in the summer months, plants growing at latitudes further away from the equator will experience longer days than plants that grow closer to the equator. Plants at high latitudes are, however, also likely to be subjected to an earlier autumn and winter. They therefore need to flower earlier even though they are experiencing longer days. The wild progenitors of maize grew at different latitudes and altitudes, and different progenitors carried different genes and alleles (variants of genes) that are adapted to these different locations. Enough of this genetic diversity was retained during the domestication of maize to allow the selection of cultivars that are adapted to different latitudes. When plant breeders develop maize cultivars for a particular geographical location, they use this genetic diversity to select an appropriate breeding response to maximize vegetative growth but also ensure that cob maturation is completed before temperatures fall in the autumn. This requires cultivars

that are bred for higher latitudes to flower at longer day lengths than cultivars that are grown nearer the equator. To breed “energy maize” designed for temperate regions like Northern Europe, the selection criteria can be changed and plants selected that do not flower until the day length is much shorter. These plants will not develop cobs because they do not flower until early autumn. This can be achieved by either crossing cultivars adapted to Northern Europe with cultivars selected for lower latitudes (e.g., Italy) or by crossing the Northern European cultivars back into “land” races or wild progenitors from the highlands of Middle America or the equatorial Andes.

A complication is that it is seldom possible to breed for just one trait. At best, other important traits have to be maintained and often several traits need to be improved simultaneously. The growth of maize in higher latitudes is restricted by temperature, especially the low temperatures in late spring which can slow down and even seriously damage young maize seedlings. This is the main reason why maize is not sown until that time. As a consequence, it does not form a closed canopy and absorb all the incident sunlight until early summer—much later compared to cereals like wheat and barley. Over the last decades, considerable progress has been made to improve this low tolerance. Such traits must obviously be retained through the crosses with maize cultivars for the use in warmer climate zones and further improved if possible.

Notwithstanding the possibilities of obtaining energy more effectively from the existing crop plants, the basic problem remains that these will continue to compete for land with food crops. As pointed out by Somerville et al. [38], even the extension of strategies for the use of crop plants like maize to include the harvesting and use of waste products like corn stover (stem and leaf material) may not have a major impact on energy efficiency. This is partly due to the additional financial costs incurred by harvesting and transporting the stover. In addition, the removal of stover may increase soil erosion and decrease the recycling of carbon and nutrients to the soil. For this reason, there is a need for a further and even more radical approach to develop a series of new crops that are specifically designed for the production of energy and chosen for their abilities to grow on land unsuited for food production and to thrive under agronomic methods that minimize energy inputs and negative environmental impact.

4.9.2 Novel Dedicated Energy Crops

Of the over 4000 plant species that humans have used in the past millennia as food, feed or source of other products, almost all were abandoned [46]. Current arable agriculture is based on a small number of species only. The diversification

of the species used for crops is a major future challenge for modern plant science, not only with energy crops but also more widely [47].

The domestication of cereals was the central achievement of the Neolithic revolution 12,000 years ago in southeast Turkey [48]. This and the parallel domestication of maize and members of the Solanaceae (nightshade family) in pre-Columbian America, and rice and soybean in East Asia, shaped the food production on the planet [49]. Recent research has shown that domestication included the choice of alleles of specific genes that support an appropriate timing of seed germination, reduce the influence of the length of day on the timing of fruit ripening, improve seed size, keep the seeds in the ears and aid hand threshing of the ears [50]. Many of these traits are irrelevant, or even counterproductive, for energy crops. It will be an exciting challenge to see whether an increased understanding of plant function and genetics will allow new energy crops to be developed in the next decades, emulating advances that have required thousands of years for today's crop plants.

Perennial grasses, in particular C4 grasses such as sugar cane, energy cane, elephant grass, switchgrass, and *Miscanthus*, are one likely source of future energy plants [38]. Three features of these grasses make them attractive candidates for energy crops. First, they have intrinsically higher light, water, and nitrogen use efficiency than C3 species [51]. Indeed, the highest annual dry-matter production reported for any vegetation to date is for such C4 grasses, including 88 MT/ha per year (MT = metric tons of dry weight) for Napier grass (*Pennisetum purpureum*) in El Salvador and 100 MT/ha per year for natural stands of *Echinochloa polystachya* on the Amazon floodplain [52]. These are rates of biomass production reaching the maximum possible rate of growth, based on incident sunlight and models for energy conversion efficiency developed by Zhu et al. [12]. Second, these plants grow in the warm and/or wet part of the year and develop a large standing above-ground biomass, which then senesces. The majority of the minerals move back from the shoot into storage roots. The above ground biomass can be harvested each year in the dry season or winter for conversion to bioenergy. The following year, shoots re-grow from the roots, using nutrients that are recycled from the previous year. This decreases the need for fertilization and, because ploughing is not necessary, decreases soil erosion. Further, the roots may add carbon to the soil. Third, these types of plants grow in many different types of ecosystems, from river swamps to semi-arid prairies and steppes. This is important, because it may make it possible to develop different crops for different marginal land that is unsuited for the use of food production.

For temperate zones, there is much interest in the perennial C4 grass *Miscanthus x giganteus*. In trials in England, this C4 grass generated a peak biomass of 30 MT/ha per year and a harvestable annual biomass of 20 MT/ha, the high-

est results recorded for a cool temperate climate. In side-by-side trials in central Illinois, unfertilized *Miscanthus x giganteus* produced 60% more biomass than a well-fertilized highly productive maize crop, and across the state, winter-harvestable yields averaged 30 MT/ha per year ([53, 54], see also <http://www.biofuelstp.eu/crops.html>). For warm dry zones, switch grass from the North American prairies is attracting considerable attention. *Arundo donax* (giant reedgrass or Spanish cane) is considered a promising species for biomass production in Europe.

More than 600 Mha of land worldwide has fallen out of agricultural production, mostly in the last 100 years [38]. Some of this area appears suitable for the production of such perennial grasses or other types of energy crops. However, more research is necessary to categorize this abandoned land with respect to its potential for the various types of energy crops. Ironically, in some cases their use may be limited by poor infrastructure for transport of the feedstock or the fuel.

Trees provide a complementary source of biofuel feedstock. The potential of wood is illustrated by the fact that the wood biomass harvested each year in the Northern Hemisphere has an energy content that is equivalent to the annual liquid fuel consumption in the United States [55]. Of course, large natural forest and jungle areas should not be cleared because they form vital ecological habitats, are important for the climate and represent important stores of sequestered carbon (see above). However, there are strategies for sustainable felling of extended forest areas for lumber and paper production, which could be extended to providing feedstock for the production of energy. A major problem may be the lack of transportation and infrastructure in remote forested areas.

There are also considerable land areas that were deforested in the past and used for agriculture but were later abandoned and are now returning to their former forest state. Field and his co-workers estimate that, globally, 89 to 107 Mha of land that were once agriculturally used are now either forests or urban areas [56]. Of these, large tracts of forest land are now mature ecosystems. These are of high intrinsic value for their biological diversity for recreation and also because they are already sequestering carbon. However, more recently abandoned lands have lower ecosystem service values and could be used for the plantation of biomass crops [38].

The best practice to maximize woody biomass production per hectare appears to be coppice harvesting. This practice goes back to ancient times. It involves cutting fast-growing tree species like willow or poplar at near ground level after the end of the growing season every three to five years, depending on the species and the growing conditions. The plants rapidly regenerate shoots from the rootstock without any intervention. This approach minimizes losses of mineral nutrients, soil erosion, and organic carbon emissions. There are many similari-

ties between this approach and the use of perennial grasses (see above). Typically, coppiced woodland is harvested in sections on a rotation with the result that a crop is available each year somewhere in the woodland. When managed this way, coppicing has the added advantage that it generates a variety of habitats, as the woodland always has a range of different-aged coppice growing in it, which is beneficial for biodiversity.

Almost 20% of the global terrestrial surface is classified as semi-arid with 200 to 800 mm of rainfall per year and an average growing season temperature larger than 21°C [43]. This land is little-used for food production, except when artificial irrigation is available. Indeed, much of the land that has fallen out of agricultural production worldwide is semi-arid [56]. There is interest in finding species that could grow under such conditions, even if their growth is relatively slow [38]. One example is the various *Agave* species, which grow well under semi-arid conditions. Like many other plants that are adapted to such conditions, they use CAM photosynthesis (see above). Textbook knowledge states that CAM plants grow slowly. However, some *Agave* species have been reported to exhibit surprisingly high harvested biomass yields of 7–10 MT/ha per year on semi-arid land when harvested at 5 to 6-year cycles [57, 58].

All of the above scenarios are based on the use of plant cell walls as an energy source. These are basically complex carbohydrates and lignin. On a weight basis, however, lipids provide almost double the energy that is provided by carbohydrates. Whereas vegetative plant matter sometimes accumulates large amounts of carbohydrates (e.g., sugar cane, see above) and mutants accumulating large amounts of starch can easily be obtained [16], plants do not accumulate lipids in their vegetative tissues. Lipids are normally stored in seeds. There is considerable interest in understanding why lipids are accumulated only in this manner and also in using this knowledge to develop plants that store large amounts of lipids in mature vegetative tissues (e.g., see <http://www.bch.msu.edu/faculty/benning/fulltextBenning.html>). Another alternative is to identify plants that accumulate large amounts of lipid in their seeds or fruits, but grow on marginal land, like *Camelina sativa*, a plant that is cold-tolerant and has an oil yield of 35–38%, or *Jatropha curcas*, which is a tropical plant with a high drought tolerance and seeds with high oil content (approximately 40%).

There is also large interest in the potential of algae as a bioenergy feedstock. Provided they receive enough sunlight and minerals, algae can have much faster growth rates than terrestrial crops, and some species of algae can even produce up to 60% of their dry weight in the form of oil. Many of the challenges in the use of algae lie in the design and operation of efficient fermenter systems. A key advance would be to breed or engineer algae that secrete oil into the surrounding

medium because this would make it less cost- and energy-intensive to harvest the oil.

Given that it will be an imperative to grow energy crops on marginal land with minimal input, the choice of energy crops will need to be oriented toward the climatic and edaphic conditions in each region. As pointed out by Somerville et al. [38], in many cases water availability may be a key factor, with the less water efficient C3 species like poplar and willow being grown in areas with sufficient rainfall, more water-efficient crops like sugar cane, switch grass and *Miscanthus* being grown where rainfall is not in excess, and specialized plants like *Agave* being grown in more arid regions. Likewise, in higher latitudes, temperature tolerance will be an important determinant.

Quoting Somerville et al. [38]:

Importantly, by focusing on the use of dedicated energy crops—rather than on repurposing food and feed crops—it should be possible to overcome many of the problematic constraints associated with our narrow dependence on a relatively small number of food crops and to develop agroecosystems for fuel production that are compatible with contemporary environmental goals.

This scenario points to the need for a diverse portfolio of species and varieties of these species. It also entails that there will be a wide range of plant feedstocks. Variation in the feedstocks from field-grown plants is probably also unavoidable due to year-to-year changes in the weather and change that may occur during storage for different durations. This, of course, will pose a challenge to the processes further downstream that are required to use these feedstocks.

Acknowledgments

I am grateful to the Max Planck Society for supporting my research, to the members of my research group past and present and to many colleagues with whom I have interchanged ideas about photosynthesis and plant productivity in the last years, especially Julian Hibberd, Steven Long, Thomas Sharkey and Andreas Weber.

Bibliography

- [1] N.E. Borlaug. How to Feed the 21st Century? The Answer is Science and Technology. In: *Genetics and Exploration of Heterosis in Crops*. Ed. by G.J. Coors and S. Pandey. Madison, WI: ASA, CSSA, SSSA, 1999.
- [2] B. Halweil. Farmland Quality Deteriorating. In: *Vital Signs: The Trends that are Shaping our Future*. The Worldwatch Institute in Cooperation with the United Nations Environment Programme. New York: W. W. Norton and Company, 2002. 102–103.
- [3] D.F. Calderini and G.A. Slafer. Changes in Yield and Yield Stability in Wheat During the 20th Century. *Field Crops Research* 57 (1998).
- [4] K.G. Cassman, A. Dobermann, D.T. Walters, and Y. Yang. Meeting Cereals Demand While Protecting Natural Resources and Improving Environmental Quality. *Annual Review of Environment and Resources* 28 (2003): 15–58.
- [5] A.J. Cavalieri and O.S. Smith. Grain Filling and Field Drying of a Set of Maize Hybrids Released from 1930 to 1982. *Crop Science* 25 (1985): 856–860.
- [6] D.B. Egli. Comparison of Corn and Soybean Yields in the United States: Historical Trends and Future Prospects. *Agronomy Journal* 100 (2008): 79–88.
- [7] P.L. Pingali, M. Hossain, and R.V. Gerpacio. *Asian Rice Bowls: The Returning Crisis*. Wallingford, UK: CAB International, 1997.
- [8] D.N. Duvick and K.G. Cassman. Post-Green Revolution Trends in Yield Potential of Temperate Maize in the North-Central United States. *Crop Science* 37 (1999).
- [9] J.M. Beman, K.R. Arrigo, and P.A. Matson. Agricultural Runoff Fuels Large Phytoplankton Blooms in Vulnerable Areas of the Ocean. *Nature* 434 (2005):211–214.
- [10] J. Giles. Nitrogen Study Fertilizes Fears of Pollution. *Nature* 433 (2005): 791.

- [11] R.E. Blankenship, M. David, D.M. Tiede, J. James Barber, G.W. Brudvig, G. Fleming, M. Ghirardi, M.R. Gunner, W. Junge, D.M. Kramer, A. Melis, T.A. Moore, C.C. Moser, D.G. Nocera, A.J. Nozik, D.R. Ort, W.W. Parson, R.C. Prince, and R.T. Sayre. Comparing Photosynthetic and Photovoltaic Efficiencies and Recognizing the Potential for Improvement. *Science* 332 (2011):805–809.
- [12] X.-G. Zhu, S.P. Long, and D.R. Ort. What is the maximum efficiency with which photosynthesis can convert solar energy into Biomass? *Current Opinion in Biotechnology* 19 (2008):153–159.
- [13] H. Michel. Die natürliche Photosynthese: Ihre Effizienz und die Konsequenzen. In: *Die Zukunft der Energie: Die Antwort der Wissenschaft*. Ed. by P. Gruss and F. Schüth. C.H. Beck, 2008.
- [14] J.A. Bassham. Mapping the Carbon Reduction Cycle: A Personal Retrospective. *Photosynthesis Research* 76 (2003):37–52.
- [15] A.A. Benson. Following the Path of Carbon in Photosynthesis: A Personal Story. *Photosynthesis Research* 73 (2002):31–49.
- [16] M. Stitt, B. Usadel, and J. Lunn. Primary Photosynthetic Metabolism – More than the Icing on the Cake. *Plant Journal* 61 (2010):1067–1091.
- [17] C.B. Field, M.J. Behrenfeld, J.T. Randerson, and P. Falkowski. Primary Production of the Biosphere: Integrating Terrestrial and Oceanic Components. *Science* 281 (1998):237–240.
- [18] E.H. Murchie, M. Pinto, and P. Horton. Agriculture and the New Challenges for Photosynthesis Research. *New Phytologist* 181 (2008).
- [19] G.H. Lorimer and T.J. Andrews. Plant Photorespiration – Inevitable Consequence of Existence of Atmospheric Oxygen. *Nature* 243 (1973):359–360.
- [20] C.R. Somerville. An Early Arabidopsis Demonstration. Resolving a Few Issues Concerning Photorespiration. *Plant Physiology* 125 (2001):20–24.
- [21] C. Peterhansel, I. Horst, M. Niessen, C. Blume, R. Kebeish, S. Kuerkcueoglu, and F. Kreuzaler. *Photorespiration. The Arabidopsis Book*. American Society of Plant Biologists, 2010.
- [22] R. Sage. The Evolution of C4 Photosynthesis. *New Phytology* 161 (2004): 341–370.

- [23] G.G. Tcherkez, G.D. Farquhar, and T.J. Andrews. Despite Slow Catalysis and Confused Substrate Specificity, all Ribulose Bisphosphate Carboxylases may be Nearly Perfectly Optimized. *Proceedings of the National Academy of Sciences of the United States of America* 103 (2006):7246–7251.
- [24] N.J. Brown, C.A. Newell, S. Stanley, J.E. Chen, A.J. Perrin, K. Kajal, and J.M. Hibberd. Independent and Parallel Recruitment of Pre-Existing Mechanisms Underlying C4 Photosynthesis. *Science* 331 (2011):1436–1439.
- [25] J.M. Hibberd, E.E. Sheehy, and J.A. Langdale. Using C4 Photosynthesis to Increase the Yield of Rice – Rationale and Feasibility. *Current Opinion in Plant Biology* 11 (2008).
- [26] S.M. Whitney, R.L. Houtz, and H. Alonso. Advancing our Understanding and Capacity to Engineer Nature’s CO₂-Sequestering Enzyme, RubisCO. *Plant Physiology* 155 (2011):27–35.
- [27] A. Bar-Even, E. Noor, N. Lewis, and R. Milo. Design and Analysis of Synthetic Carbon Fixation Pathways. *Proceedings of the National Academy of Sciences of the United States of America* 107 (2010).
- [28] J.R. Warner. The Economics of Ribosome Biosynthesis in Yeast. *Trends in Biochemical Sciences* 24 (1999):437–440.
- [29] Y. Gibon, E.-T. Pyl, R. Sulpice, J. Lunn, M. Hohne, M. Gunther, and M. Stitt. Adjustment of Growth, Starch Turnover, Protein Content and Central Metabolism to a Decrease of the Carbon Supply when Arabidopsis is Grown in Very Short Photoperiods. *Plant Cell & Environment* 32 (2009).
- [30] M. Stitt. Kontrolle des Pflanzenwachstums. In: *Die Zukunft der Energie: Die Antwort der Wissenschaft*. Ed. by P. Gruss and F. Schüth. ISBN: 978-3-406-57639-3. C.H. Beck, 2008.
- [31] B.B. Buchanan, W. Gruissem, and R.L. Jones. *Biochemistry & Molecular Biology of Plants*. 1st ed. Rockville: American Society of Plant Physiology, 2000.
- [32] K. Keegstra. Plant Cell Walls. *Plant Physiology* 154 (2010):483–486.
- [33] C. Somerville. Cellulose Synthesis in Higher Plants. *Annual Review of Cell and Developmental Biology* 22 (2006):53–78.
- [34] C. Somerville, S. Bauer, G. Brininstool, M. Facette, T. Hamann, J. Milne, E. Osborne, A. Paredez, S. Persson, and T. Raab. Toward a Systems Approach to Understanding Plant Cell Walls. *Science* 306 (2004):2206–2211.

- [35] J. Harholt, A. Suttangkakul, and H.V. Scheller. Biosynthesis of Pectins. *Plant Physiology* 153 (2010).
- [36] H.V. Scheller and P. Ulvskov. Hemicelluloses. *Annual Review of Plant Biology* 61 (2010):263–289.
- [37] W. Boerjan, J. Ralph, and M. Baucher. Lignin biosynthesis. *Annual Review of Plant Biology* 54 (2003).
- [38] C. Somerville, H. Youngs, C. Taylor, S.C. Davis, and S.P. Long. Feedstocks for Lignocellulosic Biofuels. *Science* 329 (2010):790–792.
- [39] M.-M. Titirici, A. Thoma, and M. Antonietti. Back in the Black: Hydrothermal Carbonization of Plant Material as an Efficient Chemical Process to Treat the CO₂ Problem? *New Journal of Chemistry* 31 (2007):787–789.
- [40] E.A. Ainsworth, C. Beier, C. Calfapietra, R. Ceulemans, M. Durand-Tardif, D.L. Godbold, G.R. Hendrey, T. Hickler, J. Kaduk, D.F. Karnosky, B.A. Kimball, C. Koerner, M. Koornneef, T. Lafarge, A. D. B. Leakey, K. F. Lewin, S. P. Long, R. Manderscheid, D.L. McNeil, T.A. Mies, F. Miglietta, J.A. Morgan, J. Nagy, R.J. Norby, R.M. Norton, K.E. Percy, A. Rogers, J.F. Soussana, M. Stitt, H.-J. Weigel, and J.W. White. Next Generation of Elevated [CO₂] Experiments with Crops: A Critical Investment for Feeding the Future World. *Plant Cell and Environment* 31 (2008):1317–1324.
- [41] C. Calfapietra et al. “New Challenges and Priorities in the Next Generation of Elevated CO₂ Experiments on Forest Ecosystems and Plantations”. In *Trends in Plant Science*; in press.
- [42] European Science Foundation (ESF). *FACEing the Future: Planning the Next Generation of Elevated CO₂ Experiments on Crops and Ecosystems*. Ed. by R. Ceulemans and M. Stitt. Strasbourg: IREG, 2009.
- [43] United Nations Environment Programme (UNEP). *Towards Sustainable Production and Use of Resources: Assessing Biofuels*. Tech. rep. International Resource Panel, United Nations Environment Programme, 2009.
- [44] URL: <http://www.ethanolrfa.org/pages/statistics#E>.
- [45] URL: <http://faostat.fao.org>.
- [46] E. Sanchez-Monge. *Taxonomia de las Magnoliofitas (Angiospermas) de Interés Agrícola, con Excepción de las Aprovechamientos Exclusivamente Ornamental o Forestal*. Tech. rep. Madrid: Ministerio de Agricultura, Pesca y Alimentación, 1991.

- [47] European Plant Science Organization (EPSO). European Plant Science: A Field of Opportunities. *Journal of Experimental Botany* 56 (2005):1699–1709.
- [48] F. Salamini. Hormones and the Green Revolution. *Science* 302 (2003): 71–72.
- [49] J. Diamond. *Guns, Germs and Steel. The Fates of Human Societies*. London: Random House, 1997.
- [50] C. Pozzi, L. Rossini, A. Vecchiotti, and F. Salamini. Gene and Genome Changes During Domestication of Cereals. In: *Cereal Genomics*. Dordrecht, The Netherlands: Kluwer Academic Publishers, 2004.
- [51] S.P. Long, E.A. Ainsworth, A.D.B. Leakey, J. Nosberger, and D.R. Ort. Food for Thought: Lower-Than-Expected Crop Yield Stimulations with Rising CO₂ Concentrations. *Science* 312 (2006):1918–1921.
- [52] S.P. Long, M.B. Jones, and M.J. Roberts. *Primary Productivity of Grass Ecosystems of the Tropics and Sub-Tropics*. London: UNEP/Chapman & Hall, 1992.
- [53] C.V. Beale and S.P. Long. Can Perennial C4 Grasses Attain High Efficiencies of Radiant Energy Conversion in Cool Climates? *Plant Cell & Environment* 18 (1995):641–650.
- [54] E.A. Heaton, F.G. Dohleman, and S.P. Long. Meeting U.S. Biofuel Goals with Less Land: The Potential of Miscanthus. *Global Change Biology* 14 (2008):2000–2014.
- [55] C.L. Goodale, M.J. Apps, R.A. Birdsey, C.B. Field, L.S. Heath, R.A. Houghton, J.C. Jenkins, G.H. Kohlmaier, W. Kurz, S. Liu, G.-J. Nabuurs, S. Nilsson, and A.Z. Shvidenko. Forest Carbon Sinks in the Northern Hemisphere. *Ecological Application* 12 (2002).
- [56] J.E. Campbell, D.B. Lobell, R.C. Genova, and C.B. Field. The Global Potential of Bioenergy on Abandoned Agriculture Lands. *Environmental Science & Technology* 42 (2008):5791–5794.
- [57] P. Nobel. *Environmental Biology of Agaves and Cacti*. Cambridge: Cambridge University Press, 1988.
- [58] J.W. Purseglove. *Tropical Crops—Monocotyledons*. London, UK: Longman Ltd., 1972.

Chapter 5

Biomass Chemistry

Michael Ladisch, Eduardo Ximenes, Youngmi Kim,

Nathan S. Mosier

5.1 Introduction

The pretreatment of biomass materials for subsequent biological processing requires an understanding of the chemistry of biomass which makes up the feedstock for such processes. The combination of pretreatment and enzyme hydrolysis is a key step in deriving fermentable sugars for the subsequent transformation to ethanol or other fermentation products by either yeast or bacteria. Pretreatment can also impact the chemical processing of biomass materials to synthesis gas containing CO, methane, and other organic molecules. The chemical structure of biomass (lignocellulosic) materials determines the most appropriate combinations of pretreatment and hydrolysis. The types and sources of biomass, their structure and the overall impact of chemistry on pretreatment approaches are presented in this chapter. Recent developments in pretreatment, using water only approaches, as well as the effects of inhibitors on cellulases are also discussed.

5.2 Feedstock Availability

A recent report by the National Academies Committee on America's Energy Future [1] addresses various topics related to sustainable energy supplies in the U.S. This study engaged a broad range of sponsors including the U.S. Department of Energy, Kavli Keck Foundations, Dow Chemical, General Electric, Intel, General Motors, and BP, as well as the National Academies. The overall conclusion of this report was that the only way to meet the concerns of a sustainable fuel supply, environmental consequences, energy security, and economic competitiveness, for the U.S. would be to embark on a sustained effort to transform the manner in which energy is produced and consumed including the conversion of lignocellulosics to fuel ethanol.

Petroleum will continue to be an indispensable transportation fuel. Transportation fuel consumption in terms of gasoline equivalents per day is expected

to rise from about 2.1 billion liters (13 million barrels) in 2009 to 2.4 billion liters (15 million barrels) in 2030 [1]. Cellulosic ethanol is projected to displace about 79 million liters (0.5 million barrels) of gasoline per day by the year 2020 and 270 million liters (1.7 million barrels) per day by 2035. Some of the cellulosic ethanol benefits are that the production of a corn-based ethanol already provides some infrastructure for its distribution, and a life cycle analysis in which CO₂ emissions are one fifth to two fifths that of gasoline. The combination of converting coal and biomass to liquid fuels has even a larger potential to displace gasoline due to the preponderance and availability of coal in the U.S., particularly if CO₂ emissions can be limited by carbon sequestration. With carbon sequestration the amount of CO₂ admitted would be low. The development of coal utilization with carbon sequestration technology is projected to require until 2035 in order to reach the goal of 4 billion liters (2.5 million barrels) of gasoline equivalent per day.

Renewable resources provide the benefit of a low carbon footprint and are available at a number of different sites in a sustainable manner. Conversion efficiency and the amount of biomass, which will be required on a sustainable basis, will be important factors in determining costs. Increased efficiency decreases both costs and the amount of feedstock. The types and sources of biomass include agricultural residues, wood, and purposely grown energy crops of sugarcane, energy cane, switchgrass and poplar. Up to a billion tons per year are generated and are potentially available for biofuels production. The areas of highest growth of biomass and biomass availability are in the Midwest and along the coasts as shown in Figure 5.1. Subsequent to this report, other studies estimated that the amount of the biomass available is about 400 million dried tons (Figure 5.1, American Energy Future Panel Report).

This particular estimate gives current and future (2020) quantities that may be available but does not include woody residues that might be used for the generation of electricity. The majority of the increase in the availability of lignocellulosic feedstocks is assumed to occur from dedicated fuel crops (such as switchgrass or energy cane). Reference to Figure 5.1 also shows that there is significant municipal solid waste (100 million tons per year) but here it is not considered a feedstock for biological conversion of lignocellulosic material to ethanol since a different type of processing technology would be needed. Consequently the total amount of biomass available would be about 448 million dry tons per year in 2020 (Figure 5.1, American Energy Future Panel Report). The report itself estimates that between 400 and 500 million tons of biomass can be sustainably produced in the U.S. without incurring significant direct or indirect greenhouse gas emissions. At the same time, even though the feedstock would be available, timely commercial deployment may depend on adoption of fuel mandates as well as an

accelerated federal investment in essential technologies according to this report [1].

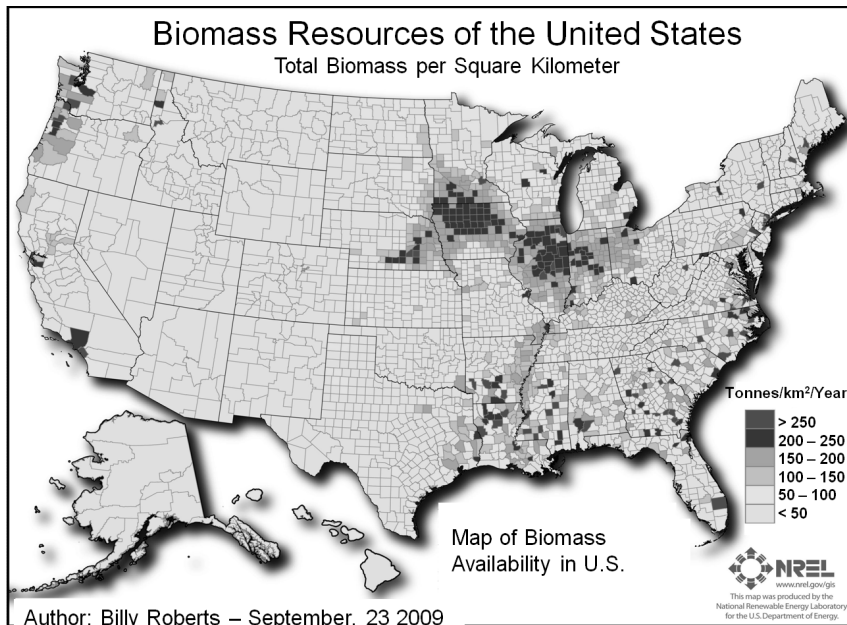


Figure 5.1: Map of biomass availability in the U.S. This study estimates the biomass resources currently available in the United States by county. It includes the following feedstock categories: crop residues (5 year average: 2003–2007), forest and primary mill residues (2007), secondary mill and urban wood waste (2002), methane emissions from landfills (2008), domestic waste water treatment (2007), and animal manure (2002) (<http://www.nrel.gov/gis/biomass.html>).

5.3 The Role of Petroleum

Petroleum will continue to be an indispensable transportation fuel through at least 2035. Transportation fuel consumption in terms of gasoline equivalents per day is expected to rise from about 2.1 billion liters (13 million barrels) in 2009 to 2.4 billion liters (15 million barrels) in 2030. Cellulosic ethanol is expected to displace about 79 million liters (0.5 million barrels) of gasoline per day by the year 2020 and 270 million liters (1.7 million barrels) per day by 2035. These esti-

mates, which are not additives, show that any of these alternative energy sources would provide small but significant additions to the total amount of liquid fuel consumed in the U.S. Some of the benefits of ethanol as a biofuel (presumed here to be cellulosic ethanol) are the production of a liquid fuel that already has infrastructure and a life cycle analysis in which CO₂ emissions are one fifth to two fifths that of gasoline.

Feedstock Type	2008	2020
	Millions of dry tons	Millions of dry tons
Corn stover	76	112
Wheat and grass straw	15	18
Hay	15	18
Dedicated fuel crops	104	164
Woody residues*	110	124
Animal manure	6	12
Municipal solid waste	90	100
TOTAL	416	548

Table 5.1: Estimated U.S. Lignocellulosic Feedstock that could potentially be produced for fuel (*Wood residues currently used for electricity generation are not included in this estimate.)

Renewable resources will provide the benefit of a low carbon footprint, and being available at a number of different sites in a sustainable manner. Conversion efficiency will be important in determining costs.

5.4 The Cost of Biomass Feedstocks

Wood

Wood is a major potential biomass feedstock, with a cost of approximately \$33.00 per green ton (or about \$66.00 per dried ton). Since biomass is local, availability and price will be determined locally as well. Composition of the biomass and the fraction which may be fermented (carbohydrates) varies by biomass. Consequently, the maximum possible ethanol yield itself is a function of composition, and therefore, the yield itself will be locally determined [2–4]. A range of hard wood costs by location is given in Table 5.2 and shows that they range from \$33.00 to \$51.50 per green ton, or approximately double this cost if calculated on a dry ton basis (assuming 50% moisture content).

Region	Hardwood Pulpwood \$/Green Ton
Brazil	40.00
Finland	51.50
Michigan	33.00
Ontario, Canada	38.00
Russia	37.50
Sweden	50.50
U.S. Northeast	36.00

Table 5.2: Cost of Wood (from [5])

A major source of ethanol is the Brazilian sugarcane industry where the sugarcane production is concentrated in the southern part of Brazil and along the coast. Sugarcane ethanol, produced from the sugar itself, accounts for approximately 26 billion liters (7 billion gallons) of fuel ethanol produced annually [6, 7].

The byproduct, sugarcane bagasse, consists of the crushed stalks and cellulosic materials left over after the sugar itself has been extracted from the sugarcane. Bagasse has a composition of 24.4% hemicellulose, 39% cellulose, and 24.8% lignin. The stalks provide energy if burned in a power plant and could also yield significant ethanol with the appropriate pretreatment and conversion technology in place. The maximum ethanol yield for bagasse is approximately 456 L/ton (120 gal/ton).

Agricultural residues

Agricultural residues are globally available in the various agricultural regions of the world, including the U.S. Midwest. Hard wood is available in the upper Midwest in the U.S., as well as in Canada and Europe. Soft woods predominate in the Southeast U.S., and require different types of processing than hard woods if the goal is the fermentation of these woods into ethanol. Purposely grown energy crops may someday be generated in both the U.S. and Brazil, and possibly even in Africa. These could increase the availability of feedstock for biotransformation to fuels and chemicals.

2008/2009		
Planted area	7.8	million ha
Sugarcane	622	million tons
Sugar	31.6	million tons
Ethanol	26.7	billion liters
“Sugarcane brandy”	1.5	billion liters
Employees – direct	1.0	million
Employees – indirect	2.6	million
Future (2012)		
Planted area	> 10	million ha
Sugarcane	1	billion tons
Ethanol	48	billion liters

Table 5.3: Sugarcane ethanol in Brazil (from [8]). Bagasse: 39% Cellulose, 24.4% Hemicellulose and 24.8% lignin. Maximum ethanol yield from sugar: 460 L/ton (121 gal/ton)

The price and availability of these feedstocks are sufficient to support an emerging and sustainable renewable biofuels industry. However, significant development of the infrastructure for both feedstock collection and delivery, as well as distribution of the product will be required. The conversion of the cellulosic materials to fermentable sugars depends on the chemistry and the conditions used to unlock the potential of this chemistry for the production of biofuels through bioprocessing.

5.5 Maximum Yield as a Function of Biomass Composition

A variety of biomass feedstocks is available for conversion of cellulose to ethanol (Figure 5.2). Feedstocks which have been considered and studied include hard woods (poplar and red maple), agricultural residues including corn stover and wheat straw, as well as purposely grown crops such as switchgrass. In addition, there is sugarcane bagasse available in the southern U.S. and also in sugarcane mills that already produce ethanol in Brazil. Based on the assumption that all of the structural carbohydrates that are potentially fermentable to ethanol are hydrolyzed in a 100% efficiency, and fermentation of the formed monosaccharides is 100% efficient, maximal yields would be on the order of 405 liters per ton of

dry biomass (107 gal/dry ton of biomass). However, in the fermentation step a metabolic yield of 90 to 95% should be used as the maximal number, since a small fraction of the sugar is used for growing cell biomass, maintaining cellular metabolism, and providing the energy for other housekeeping functions in the cell. In addition, it is unlikely that a 100% yield would be obtained from hydrolysis, hence a yield of 95% is assumed. As a consequence, the overall maximum practical yield is likely 90% of the total, or corresponding to 364.5 L/ton 96.3 gal/ton.

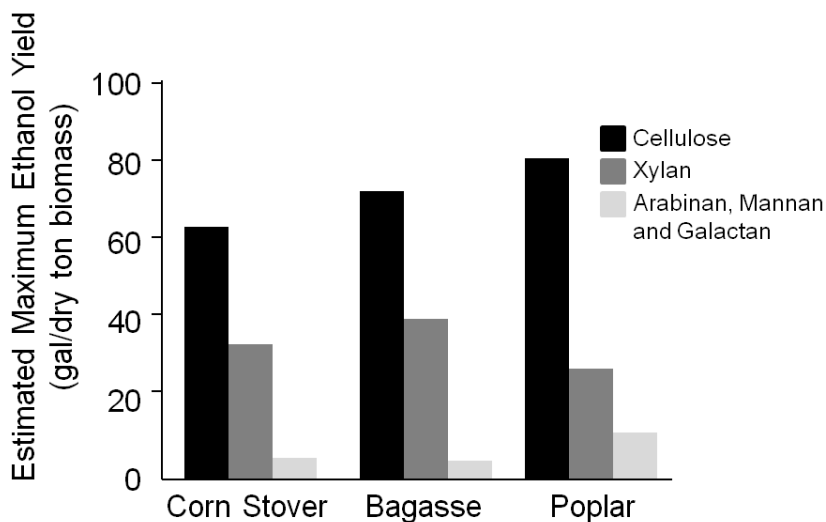


Figure 5.2: Estimated maximum ethanol yield (gal/dry ton biomass) for individual monosaccharides present in corn stover (estimated total maximum ethanol yield of 107 gal/dry ton biomass), bagasse (estimated total maximum ethanol yield of 122 gal/dry ton biomass) and poplar (estimated total maximum ethanol yield of 124 gal/dry ton biomass), (based on information provided in Table 5.4).

Factors which could impact these yields include the efficiency with which arabinose is fermented to ethanol (a newly developed technology for yeast fermentations), as well as the conversion of xylose to ethanol [9–14]. Acetic acid, which is released from many types of lignocellulosic biomass during pretreatment and hydrolysis, may also affect yield due to its inhibitory effects [15].

Feedstock Compositions	Poplar	Red Maple	Corn Stover	Switch grass	Bagasse ***	Pine Wood ****
Cellulose	43.8	41.0	34.6	33.2	39	40
Xylan	14.9	15.0	18.3	21.0	21.8	8.9
Arabinan, Mannan, Galactan	5.6	0.0	2.5	3.2	2.6	19.6
Acetyl	3.6	4.7	3.5	2.5	3.3	N/A
Extractives	3.6	3.0	10.8	10.2	5.7	3.5
Protein	N/A	N/A	N/A	5.7	0.5	N/A
Lignin	29.1	29.1	17.7	17.9	24.8	27.7
Ash	1.1	1.0	10.2	3.7	3.9	N/A
Total	101.7	93.8	97.6	97.4	101.6	99.7
Estimated Maximum Ethanol Yield*, gal/dry ton biomass	124	108	107	111	122	132
Estimated Practical Maximum Ethanol Yield**, gal/dry ton biomass	118	103	102	105	116	125

Table 5.4: Compositions of different types of cellulosic biomass and the maximum ethanol yields possible for each of the compositions. These biomass materials (wood, corn stover (stalks), and switchgrass) are representative of available feedstocks for a cellulosic biorefinery. (* Theoretical maximum yields assuming 100% hydrolysis and 100% fermentation. Data from Laboratory of Renewable Resources Engineering, Purdue University. ** 95% hydrolysis/95% fermentation. *** [16, 17]. **** [18].)

The lignin content of hard wood, poplar, and red maple is greater than that of corn stover, switchgrass, and sugarcane bagasse. This lignin has an energetic value of approximately 21,190 kJ/kg (9111 Btu/lb) [19], and could provide a significant fraction of the power required to run the ethanol plant in addition to providing electricity. Close to theoretical conversion is achievable for all of these feedstocks if enough cellulase enzymes are used with the appropriate pretreatment. However, the challenge is to carry out a pretreatment with minimal addition of chemicals, because chemicals add costs to the production of ethanol. The pretreatment must also minimize the amount of enzymes required in the hydrolysis step. Enzymes are a major cost in the production of ethanol from cel-

lulosic materials. The fermentative microorganisms (whether yeast or bacteria) must be capable of fermenting xylose and arabinose as well as the glucose from cellulose in order to achieve maximal yields. A comparison of ethanol yields from three different feedstocks is shown in Figure 5.2 and illustrates the importance of achieving conversion of cellulose, xylan, and arabinan to ethanol.

5.6 Location

The number of sites that have the potential to supply daily amounts of biomass on a sustainable basis will be a function of the throughput, i.e., the production level of a cellulosic ethanol facility. This is also the case for facilities that would process woody biomass through thermal means to either pyrolysis oil or synthesis gas followed by Fischer Tropsch synthesis [20].

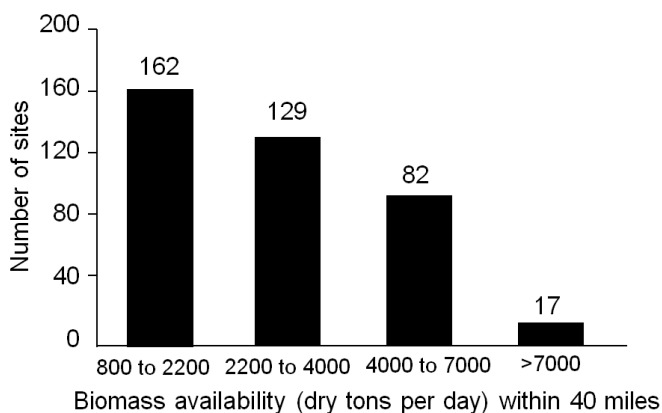


Figure 5.3: Number of sites in the United States with potential to supply indicated daily amounts of biomass within a 40-mile radius (reprinted with permission, National Academies Report, 2009)

Biomass availability in the U.S. based on a combination of wood, agricultural residues and purposely grown energy crops could support approximately 162 processing facilities with throughputs ranging between 820 to 2200 tons per day (approximately 25 to 75 million gal/year production). In addition, there are about 17 sites where facilities are capable of processing more than 7,000 dry tons per day according to the National Academies study on America's Energy Future (Figure 5.3). While these numbers may seem large, the reader should recognize that

large pulp mills in Northern Michigan of the U.S. and in Southern Canada, have ranged in size from 3,000 to 7,000 dry tons per day. In the late nineteenth century through the end of the twentieth century, large wood pulp mills were operated in the hardwood forests of the U.S., namely in New York, Massachusetts, Ohio, and Wisconsin.¹ In Brazil, pulping plants use between 7,000 and 8,000 dry tons/day of eucalyptus for paper making processes. Due to reemergence of large pulping capabilities in developing nations, the pulpwood industry is in decline in the U.S. This provides an opportunity for the production of cellulosic ethanol and biofuels from hard wood feedstocks.

5.7 Metrics for Biochemical vs. Thermochemical Conversion

The productive capacity for generating feedstocks in the U.S. ranges from 2.5–5 tons/hectare/year (1–2 dry tons/acre/year) for corn stover. Purposely grown and fertilized switchgrass could yield 12–17 tons/hectare/year (5–7 dry tons/acre/year) while poplar grown for energy purposes would have a yield of 12–25 tons/hectare/year (5–10 dry tons/acre/year) for poplar grown for energy purposes. The production of fuels may occur from either biochemical or chemical conversion (Figure 5.4), using different types of primary catalysis. Both involve pretreatment and preparation of the biomass material for subsequent conversion steps.

In the biochemical conversion process, the carbohydrates in the feedstock are hydrolyzed into constituent monosaccharides which are converted to ethanol or other valuable chemicals by microorganisms. In the case of thermo-chemical conversion, the feedstock is destroyed or broken down into small building blocks, i.e., CO and hydrogen, are reconstituted or reformed into higher molecular weight hydrocarbons and alcohols, i.e., biofuels. In the thermo-conversion process the lignin is converted into synthesis gas (syngas) along with cellulose and hemicelluloses biomass components. In spite of these differences, both processes (thermo- and biochemical conversion) will potentially convert 1 dry ton of biomass (~20 GJ/ton) to around 6.5 GJ/ton of energy in the form of biofuels, thereby giving an overall biomass to biofuel conversion efficiency of 35% [2] through thermo-chemical volumetric. Thermo-chemical conversion captures approximately 35% of the carbon in the final biofuel molecule, while the remaining carbon is used to provide energy for carrying out the conversion step [4]. Bioprocessing captures 50% of the carbon in the biofuel, although the fuel itself has a lower volumetric energy value (GJ/unit volume) than a hydrocarbon that might be derived from thermo-chemical processing. With either process, pretreatment of the biomass feedstock is required. The difference lies in the type of catalysis which is used to convert the pretreated biomass material into the final fuel products. In either case,

¹<http://business.highbeam.com/industry-reports/wood/pulp-mills>.

understanding the chemistry of biomass and the manner in which the biomass may be deconstructed will help to inform selection of conditions and processing technologies for transforming lignocellulosic materials into renewable fuels.

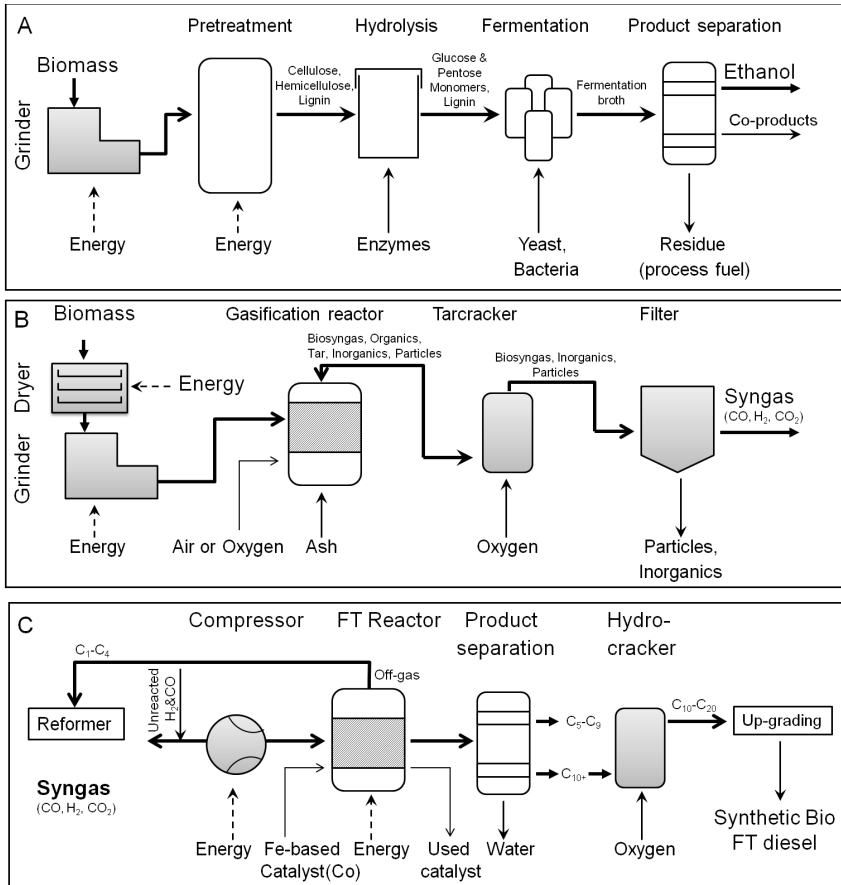


Figure 5.4: Production of fuels can occur from either biochemical or chemical conversion. (A) Process flow diagram for ethanol production from lignocelluloses; (B) Process flow diagram for syngas production and (C) Process flow diagram for synthetic bio FT diesel production using syngas as a feedstock (Figures from [20])

5.8 Biomass Chemistry

5.8.1 Composition

The major constituents of a plant cell wall are cellulose, hemicellulose, and lignin.² The structural carbohydrates, consisting mainly of cellulose and hemicellulose, are organized into the cell wall structure with lignin serving as a binding constituent, improving structural integrity, and protecting the plant against plant pathogens and insects. Composition of the plant biomass will vary between one species and another with ratios of hemicellulose (xylan) to cellulose decreasing as the biomass source moves from agricultural residues and grasses to hardwood to softwood.

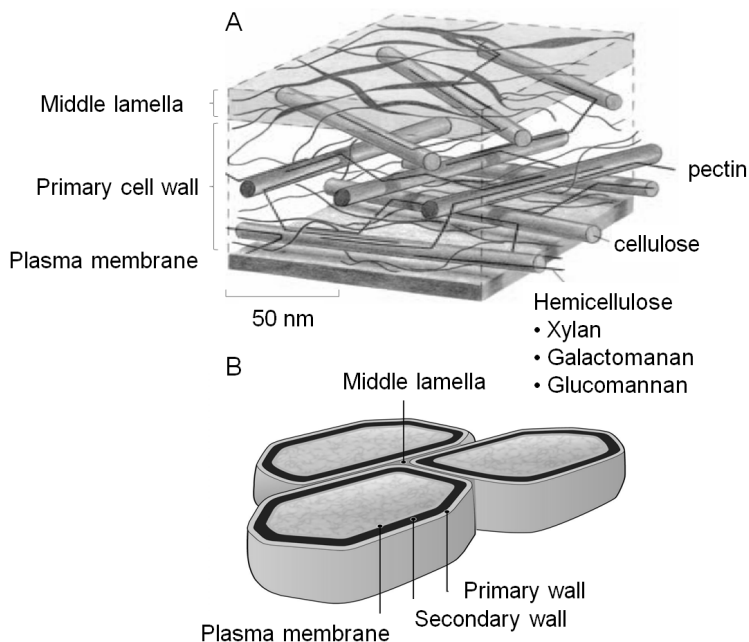


Figure 5.5: Simplified model of the primary cell wall (A) based on McCann and Roberts (1991), and (B) from ORNL (<http://public.ornl.gov/hgmis/gallery/default.cfm?restsection>)

²[21]; see also Figure 5.5A.

Lignin has a polyaromatic structure and makes up 18 to 29% of the lignocellulosic biomass. This component has high energy content due to its relatively low oxygen content compared to carbohydrates and is highly resistant to biochemical conversion. The second major component is hemicellulose which makes up 23 to 32% of lignocellulosic biomass (Figure 5.5A). Hemicellulose is a heterogeneous polymer that is primarily composed of 5-carbon sugars, with xylose being predominant. Previously xylose has been considered a marginal biochemical feedstock because of the prior difficulty of fermenting xylose to ethanol. However since about the year 2000, pentose-fermenting yeasts have been developed and are quite effective in converting the monosaccharides derived from this polymer into ethanol have been developed [10–14]. The third major component in lignocellulosic biomass is cellulose itself, comprising 38 to 50% of the biomass. It is a linear polymer of glucose and is the most abundant form of carbon in the biosphere.

5.8.2 Organization of the Plant Cell Wall

The plant cell wall consists of the primary and secondary wall, in which the cellulose is associated with hemicellulose (Figure 5.5B). The primary wall is separated from the secondary wall by a thin plasma membrane. The cell walls are interspersed with lignin, which is more prevalent in the cell walls of tissues that transport nutrients and water and provide structural integrity to the plant. Lignin helps the plant to resist attack by naturally occurring pathogens by inhibiting hydrolytic action of degradative enzymes. The primary wall is separated from the secondary wall by a thin plasma membrane. The cells themselves are surrounded by the middle lamella, in which the pectin-rich intercellular material cements together the primary walls of adjacent plant cells. Cellulose is protected from degradation by the combination of its crystalline structure, cross-linking by hemicelluloses (xylan), and the lignin that surrounds its multi-polymer structures (i.e., microfibrils, Figure 5.6). The deposition of polysaccharides in a plant illustrated in Figure 5.6 shows how a network of fibers is laid down giving the cell wall a self-assembled complex structure of a multi-layer polymeric network.

One of the objectives of cellulose pretreatment is to expose the cellulosic fraction of the cell wall while removing the hemicellulose fraction in order to substantially improve the accessibility of the cellulose for carrying out enzymatic hydrolysis. In addition, it is known that xylo-oligosaccharides as well as phenolics released by the lignin during pretreatment, cause severe inhibition and deactivation of cellulase enzymes that depolymerize cellulose to glucose [22–26]. The crystalline structure of cellulose (Figure 5.6) further impedes the hydrolytic action of cellulases.

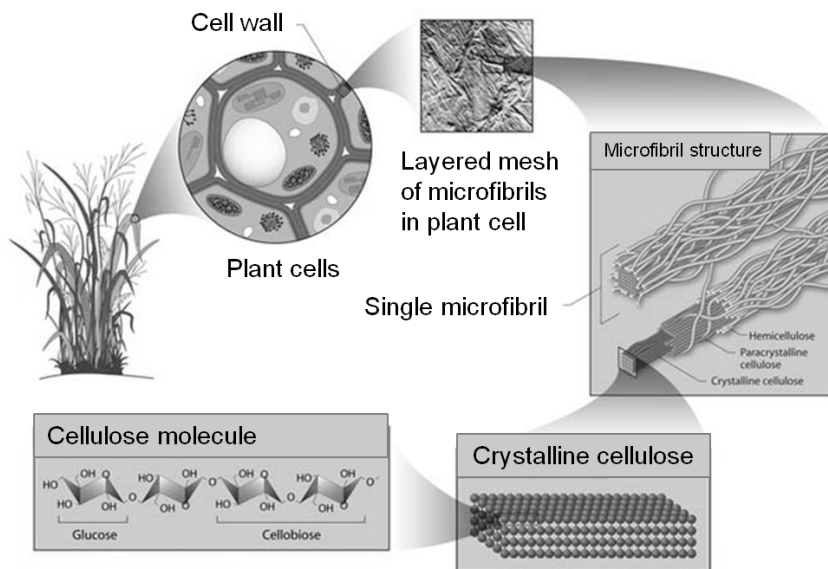


Figure 5.6: Plant Cell Wall Structure ([http:// public.ornl.gov/ hgmis/ gallery/ default.cfm?restsection=](http://public.ornl.gov/hgmis/gallery/default.cfm?restsection=))

5.8.3 Chemical Structures of Hemicellulose, Cellulose, and Lignin

Hemicellulose has a branched chain structure and is chemically heterogeneous while cellulose has a linear structure and is chemically homogeneous. The sources of recalcitrance in the biomass cell structure, and therefore the biomass feedstock itself, are due to the organization of cell wall structure. The role of lignin within the cell wall (as described above), and cellulose crystallinity in which linear chains of cellulose form crystalline regions that protect against hydrolysis. Hemicellulose itself is intercalated between the cellulose structures, and therefore its removal through dissolution or hydrolysis opens up pores to allow more cellulose to become accessible to hydrolytic enzymes or other hydrolytic catalytic agents.

The basic structure of most hemicellulose in biomass materials consists of linked D-xylosyl residues β -1-4 to which various other constituents are attached as short side chains. These include α -4-0-methylglucuronic acid, acetyl, alpha-arabinofuranose, and possibly several other types of uronic acid groups. A schematic representation of the structure, as well as the enzymes that hydrolyze these various structures is given in Figure 5.7.

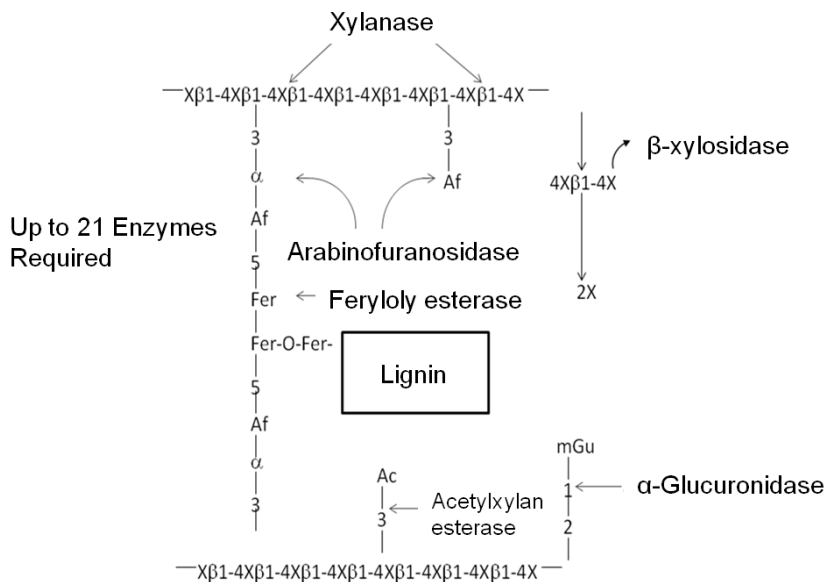


Figure 5.7: Schematic representation of a typical hemicellulose structure and the enzymes that hydrolyze the various bonds (Adapted from [27]). X = xylose, Af = alpha-arabinofuranose, mGu = methylglucuronic acid, Ac = acetyl and Fer = ferulic acid

In most grasses, ferulic acid is known to crosslink plant cell wall polysaccharides to each other and to lignin, limiting the hydrolysis of these substrates by polysaccharide hydrolases (Figure 5.7). Feruloyl esterases (EC 3.1.1.73), also known as ferulic acid esterases, cinnamic acid esterases, or cinnamoyl esterases, are a class of enzymes that are involved in the liberation of ferulic acid and other cinnamic acids from plant cell wall polysaccharides. These enzymes have potential for industrial applications in bioethanol production, and the food, the health, the pulp, and the paper industries [28].

Unlike hemicelluloses, cellulose is a chemical homogeneous polymer consisting of glucose molecules linked through β -1-4 glycosidic bonds (Figure 5.8A). It resists chemical and biological hydrolysis because of its structure. Cellulose in plant cell walls is synthesized as microfibrils with a highly crystalline core [29].

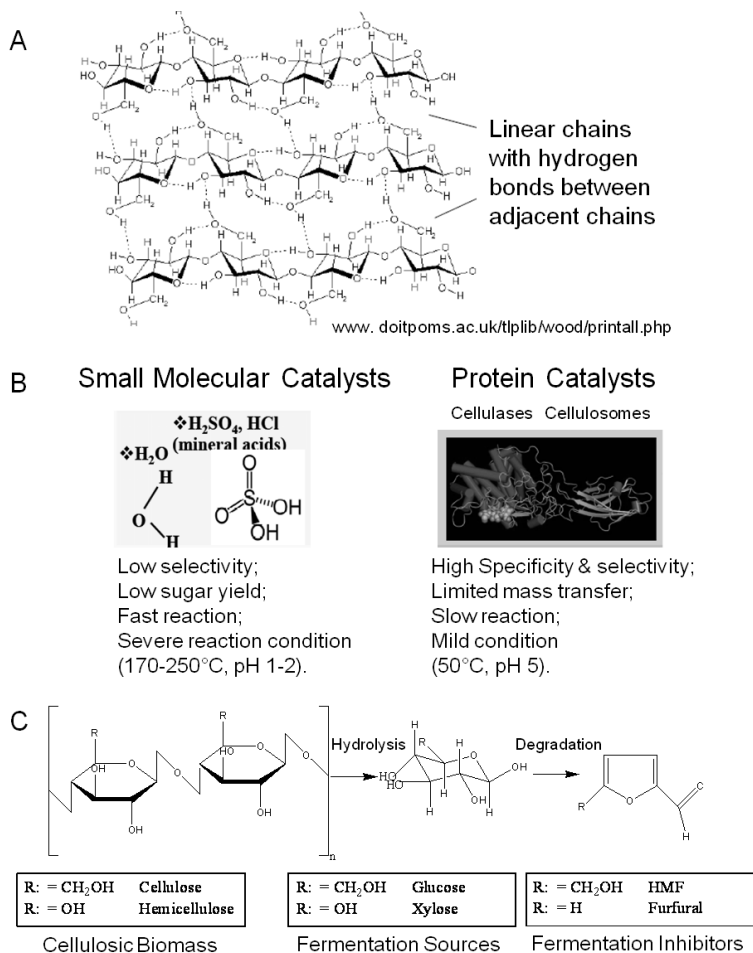


Figure 5.8: A) Representation of the crystalline structure of cellulose and the formation of intra- and inter-chain hydrogen bonds (www.doitpoms.ac.uk/tlplib/wood/printall.php); (B) Representation of catalysts capable of hydrolyzing cellulose into its monomeric units [30]; (C) Hydrolysis by acid results in degradation products. In the case of hemicellulose the sugars formed will again degrade into aldehydes, in this case, furfural inside of hydroxymethyl furfural as would be derived from glucose [30].

The chair conformation of the glucose residues in cellulose forces the hydroxyl groups into radial (equatorial) orientation and the aliphatic hydrogen atoms into axial positions. As a result, there is strong interchain hydrogen bonding between adjacent cellulose chains which form hydrogen-bonded ribbons. Weaker, but significant, hydrophobic interactions between cellulose ribbons result in the crystal structure that resembles a stack of sticky ribbons. The combination of strong interchain hydrogen bonds and hydrophobic stacking effectively excludes water from the structure, thus making crystalline cellulose resistant to acid-catalyzed hydrolysis [31]. The strong interchain hydrogen-bonding network also makes crystalline cellulose resistant to enzymatic hydrolysis [29], unless this structure is disrupted. Hemicelluloses and amorphous cellulose are readily digestible [32].

Lignin is a phenolic polymer composed of three major types of building blocks: p-hydroxyphenyl (H), guaiacyl (G) and syringyl (S) units. Lignin is a major contributor to the recalcitrance of biomass and has been a target for feedstock improvement through genetic engineering. It has been demonstrated in several plant species that a reduction in lignin content using transgenic approaches enhances cell-wall degradability. Plants are amenable to wide ranges in lignin composition changes, including variation in the content of conventional monomers and the incorporation of atypical precursors [33–35]. However, significant improvement in conversion efficiency has often been accompanied by abnormal plant growth and development [36, 37].

5.9 Hydrolysis of Polysaccharides in Cellulosic Biomass

Cellulose hydrolysis may be carried out by small molecule catalysts such as H_2SO_4 and HCl. These particular acids will act at temperatures between 170 and 250 °C and a pH of 1–2. Advantages are fast reaction; disadvantages include low potential sugar yields and low selectivity. In the case of strong acids, protons completely dissociate from the acid catalyst itself in a mechanism known as specific acid catalysts (Figure 5.8B). In this case catalytic efficiency depends only on pH, i.e., proton concentration. The formation of glucose or other monomers occurs rapidly, with the degradation of these monomers by chemical dehydration to form aldehydes and acids also occurring almost as rapidly (Figure 5.8C). These principles apply to cellulose as well as hemicellulose. Consequently, the yields from the acid hydrolysis rarely exceed 60% since a major fraction of the sugars that are formed will degrade. Molecules formed through sugar degradation inhibit fermentations and must be removed or somehow remediated so that the remaining sugars can be efficiently fermented into ethanol using microbial biocatalysts such as yeast.

In comparison, cellulases form a complex mixture in order to hydrolyze cellulose. These particular protein catalysts have the disadvantage of a slow reaction and limited mass transfer. Advantages are hydrolysis at mild conditions with high specificity and selectivity and yield (represented in Figure 5.8B). Cellulases act on carbohydrates through a general acid catalysis mechanism. Both protons and the undissociated forms of the acid catalysts at the active site of the enzyme contribute to the overall catalytic efficiency. Unlike inorganic acids, however, this reaction proceeds at much lower temperatures, with 30 to 50 °C being typical, Figure 5.9 [38].

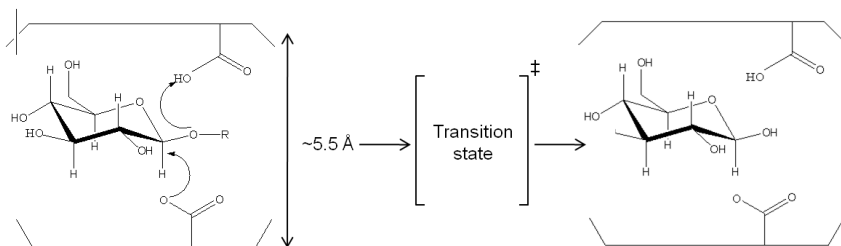


Figure 5.9: Di-acid mechanism of enzymatic hydrolysis of polysaccharides [38]

5.10 Chemistry of Pretreatment

Because of these factors it is important to pretreat cellulose so that it becomes accessible to the catalysts (either acid or enzymes) so that the reaction may occur more rapidly. The schematic representation of pretreatment in Figure 5.10 [30] gives an illustration of how the lignin seal surrounding the cellulose microfibril (heavy black lines) prevents contact of the catalysts with the crystalline structure of the cellulose (straight black lines) within which hemicellulose is intercalated or trapped within these structures (irregularly drawn line). Upon pretreatment, the lignin seal is broken (requires pretreatment to be carried out above the melting temperature of lignin), the xylooligosaccharides are dissolved or removed, and the cellulose itself is partially disrupted.

A preferred method of pretreatment is to cook the cellulose in liquid hot water at high temperatures and pressures. After an exposure of 10–20 minutes at temperatures above 195 °C, the cell wall structure will be disrupted at a submicron scale as in Figure 5.10. For this pretreatment approach, the objective is to maintain the pH between 4 and 7, and to use a temperature between 160 to 210 °C while maintaining the water in liquid state under pressure to minimize degrada-

tion reactions [39–44]; [45] summarized by [46]. This particular approach differs from the hydrothermal pretreatment which has the goal of hydrolysis of the hemicellulose in order to fractionate the biomass into dissolved 5-carbon and insoluble 6-carbon sugar streams [47].

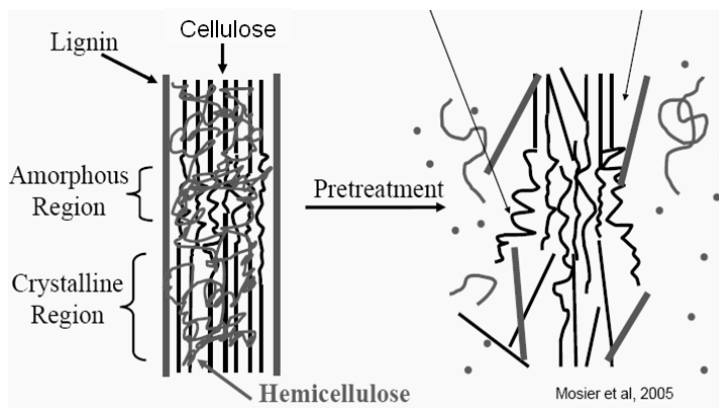


Figure 5.10: Schematic representation of the effect of pretreatment on cellulose structure [30]

Water itself acts as the catalyst with the self-dissociation equilibrium constant (K_w) equal to 0.01×10^{-12} at 25°C and 6×10^{-12} at 230°C . These values represent the dissociation of water into H^+ and OH^- , with higher temperatures resulting in more dissociation and thus higher concentration of catalytic protons. Hence, at temperatures above about 230°C , or at long cooking times (measured in terms of an hour or more), the catalytic action of water will result in acid hydrolysis of cellulose to monosaccharides, and degradation of the formed monosaccharides to organic acids, aldehydes, and humic substances.

5.11 Chemical Degradation and Inhibitor Formation During Pretreatment

Pretreatment carried out in liquid hot water, sulfuric acid, SO_2 or other acids will rapidly degrade any monosaccharides that might be formed, particularly pentoses (5-carbon sugars). Pentoses have a lower energy of activation for the reaction of degradation than glucose (Figure 5.11, [48]). As the hemicellulose is hydrolyzed, xylose will form and then rapidly be degraded to furfural (as shown in the equation in Figure 5.12).

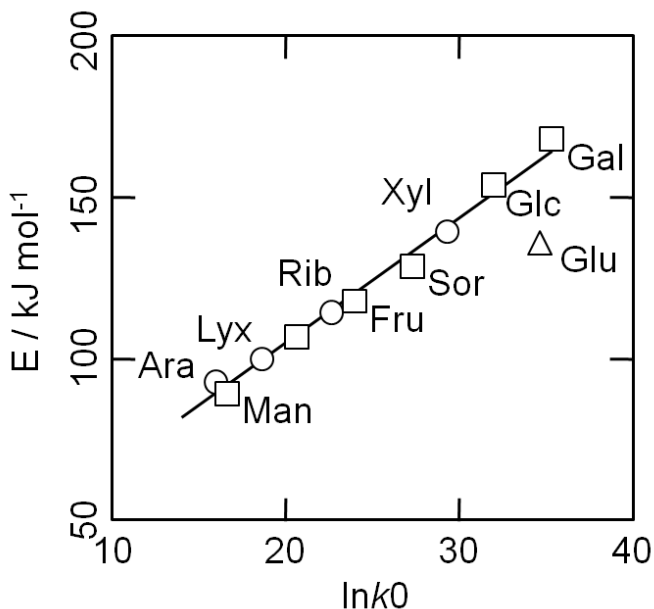


Figure 5.11: Relationships between the activation energy, E , and the natural logarithm of the frequency factor, k_0 , for the degradation of (○) pentoses, (△) hexouronic acids and (□) hexoses in subcritical water [48]. The E and k_0 values were cited from a previous study [49]. The pentoses, hexouronic acids and hexoses are represented by the first three letters of their names, except for glucose – Ara: arabinose, Lyx: lyxose; Rib: ribose, Xyl: xylose; Glu: glucuronic acid; Fru: fructose; Gal: galactose; Glc: glucose and Man: mannose. The plot for the galacturonic acid was beyond the values shown in the figure.

Furfural and acetic acid are significant inhibitors of yeast that ferment these sugars to ethanol [15, 50]. Acetic acid released during hydrolysis of hemicelluloses is also inhibitory.

Liquid hot water pretreatment, when carried out in a media in which the pH is maintained between pH 4 and pH 7 minimizes the formation of xylose, glucose and other monosaccharides, which are a necessary intermediate for the formation of furfural and other sugar degradation products. Consequently, the objective of pretreatment at these conditions is to control severity and pH in order to minimize

formation of monosaccharides, leaving oligosaccharides in liquid solution to be processed separately and selectively to monosaccharides without degradation.

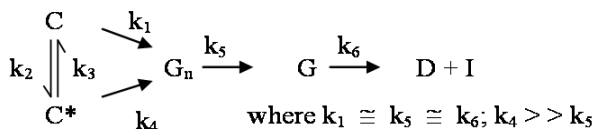


Figure 5.12: Equation 1

Whether the hemicellulose is partially or completely hydrolyzed, pretreatment removes hemicellulose from the lignocellulose structure. Once pretreated, the cellulose is more accessible to cellulases. The benefits of using liquid hot water, other than avoiding the added cost of additional chemicals, is the ability to control and minimize formation of undesirable degradation products through control of time and temperature. The pretreatment process consists of slurring the biomass material with water, pressure cooking it at temperatures between 160 and 220 °C [39–44]; [45] summarized by [46], cooling the material, then recovering and washing it. The washed substrate is then exposed to enzymes or fermentative microorganisms that generate their own enzymes in order to hydrolyze cellulose to glucose and ferment to ethanol. The liquid wash water contains oligosaccharides, which are also fermentable to ethanol upon hydrolysis to their constituent monosaccharides.

The pathway by which degradation products might be formed from the cellulose itself, is illustrated in equations 2 through 6. Native cellulose which is in a crystalline form and exhibits recalcitrance with respect to enzyme hydrolysis is converted to a more reactive form (represented by C* in the equation in Figure 5.13), with both forms being hydrolyzed through the action of water during pretreatment. Both forms of cellulose give oligosaccharides which in turn may be hydrolyzed to glucose. In the absence of degradation, the major product that would accumulate is glucose as illustrated in the equation in Figure 5.13, where degradation products are indicated to be a very small fraction of the overall final solutes in the pretreatment liquid as indicated by the light color. Since hydrolysis during pretreatment is a form of acid catalysis, it would be expected that most of the soluble products derived from the pretreatment would be obtained through the reaction of activated cellulose (C*) which forms oligosaccharides and then glucose (equation in Figure 5.14). However, due to the rapid reactions at high temperatures most oligosaccharides will form a mixture of glucose and degradation products if the hold time at temperature is too long (equation in Figure

5.15). An appropriate pretreatment condition will utilize conditions that separate the two sets of reactions so that the predominant change that occurs during pretreatment is the physical conversion to the reactive form (C to C^*) (equation in Figure 5.16). Once the pretreatment is completed, the material is cooled to room temperature. The reactive cellulosic material is then hydrolyzed to oligosaccharides and glucose by enzymes using the mechanism illustrated in the equation in Figure 5.17. In this manner, the formation of the degradation products that are inhibitory to either enzymes or fermentative microorganisms may be minimized. Any other products that might be formed could also be removed by washing the solid material after cooling and before enzymatic hydrolysis for processing in a separate hydrolysis.

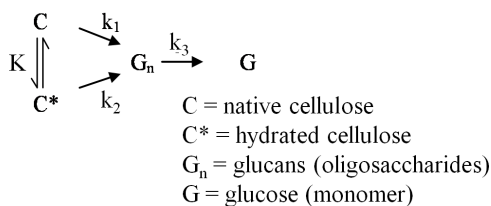


Figure 5.13: Equation 2

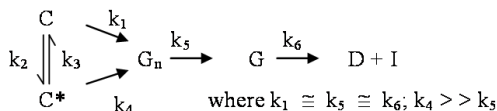


Figure 5.14: Equation 3

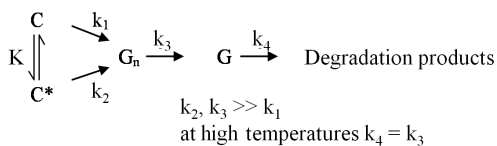


Figure 5.15: Equation 4

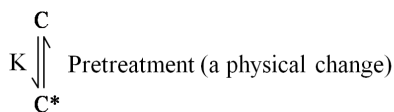


Figure 5.16: Equation 5

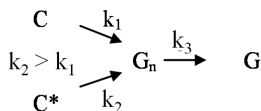


Figure 5.17: Equation 6

5.12 Impact of Formed Inhibitors

The design of effective pretreatment approaches, particularly in the context of bioprocessing, must consider the formation of inhibitors as well as their effects, so that effective hydrolysis of the cellulosic material may be achieved. The enzyme inhibitors may be hydrolysis products such as glucose or cellobiose (from cellulose), phenols (from lignin), and xylose or xylooligosaccharides (from hemicellulose) [22–26].

Figure 5.18 gives the schematic representation of the inhibition of cellulases. The processing of biomass materials also releases acetic acid from the biomass which is a significant inhibitor of ethanol fermentation. Since acetyl groups are associated with hemicellulose, the processing of the hemicellulose and its removal by pretreatment also releases acetic acid through hydrolysis. Consequently, the acetic acid must either be removed, or microorganisms adapted to its presence so that efficient fermentation may occur. Similarly, the mitigation of furfural and 5-hydroxymethyl furfural formed during pretreatment must also be addressed.³

Hydrolysis of lignin and other phenolic compounds during pretreatment of biomass may form inhibitors that may deactivate cellulase enzymes as described by Ximenes (2010, 2011) [23, 25], Kim (2011) [26], and to a greater extent, β -glucosidases (Figures 5.20 and 5.21). The polymeric phenol tannic acid was a

³[30, 50, 51]; see also Figure 5.19.

major inhibitor and deactivator for all of the enzyme activities tested in our studies (filter paper, endoglucanase and β -glucosidase assays), with monomeric phenolic compounds having a less pronounced effect at phenolic : protein ratios of 0.3 and 1.5 mg/mg (equivalent to 0.5-0.7 mg of phenol/units). Our results showed that tannic, ferulic and p -coumaric acids inactivated β -glucosidases from two different microorganisms (*Trichoderma reesei reesei* and *Aspergillus niger*) that are commonly used to produce commercial cellulases.

Hence, the identification and development of β -glucosidases that resist inhibition from both sugars and phenols will enhance cellulose hydrolysis. Alternative strategies include carrying out enzyme hydrolysis over shorter periods of time to decrease time-dependent deactivation, removing phenolics prior to enzyme hydrolysis by separation methods (including washing of the pretreated biomass), or using microbial, enzymatic, or chemical methods of converting the phenolics to an inactive form.

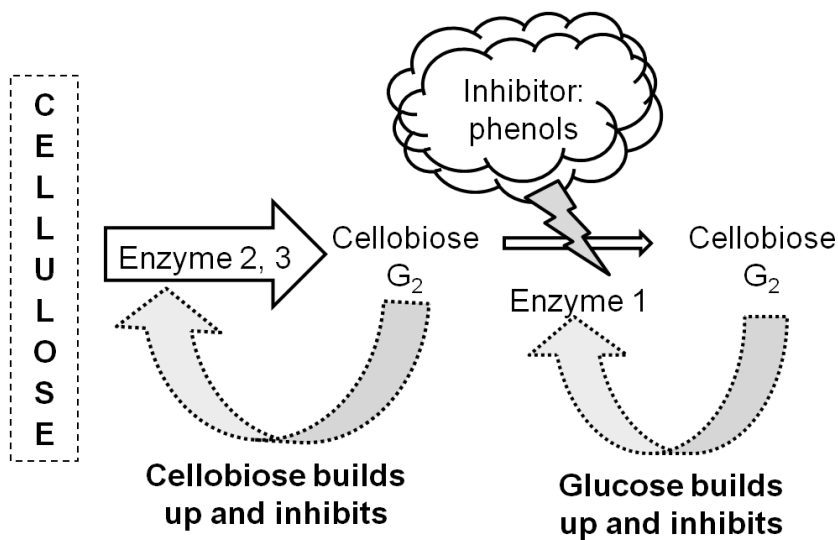


Figure 5.18: Schematic representation of inhibition of cellulase enzymes

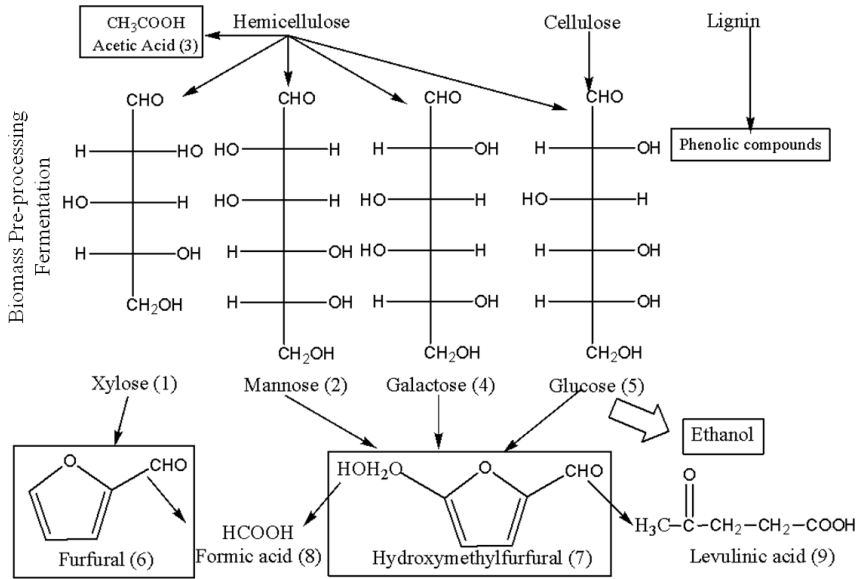
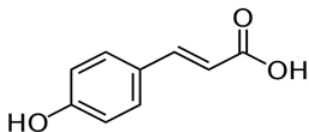
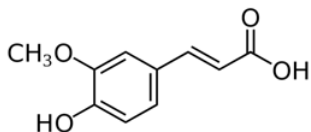


Figure 5.19: Sources of enzyme and fermentation inhibitors in the pretreatment of lignocellulosic materials (adapted from [51]). Inhibitors are derived from phenolics released from lignin, sugar degradation products, and products of hydrolysis (cellobiose and glucose) and fermentation (ethanol).

Monomeric phenol compounds

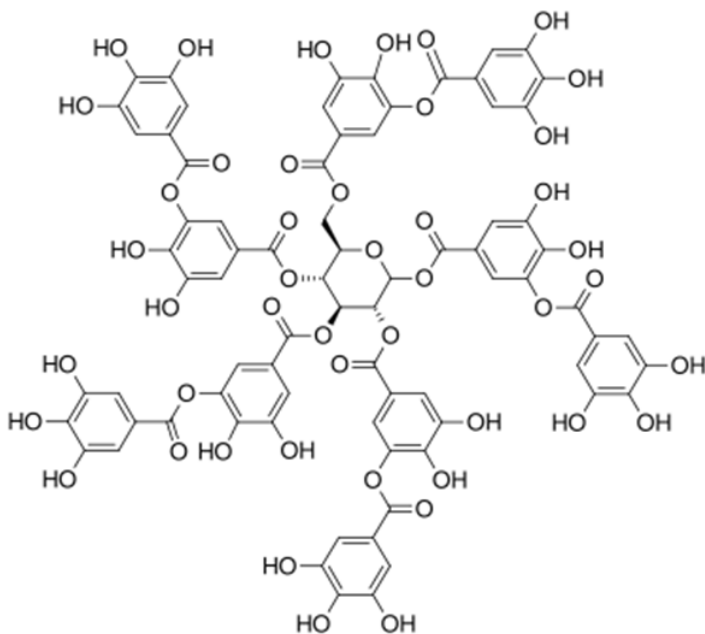


p-coumaric acid



Ferulic acid

Polymeric phenol compound



Tannic acid

Figure 5.20: Structures of phenolic inhibitors [23, 25]

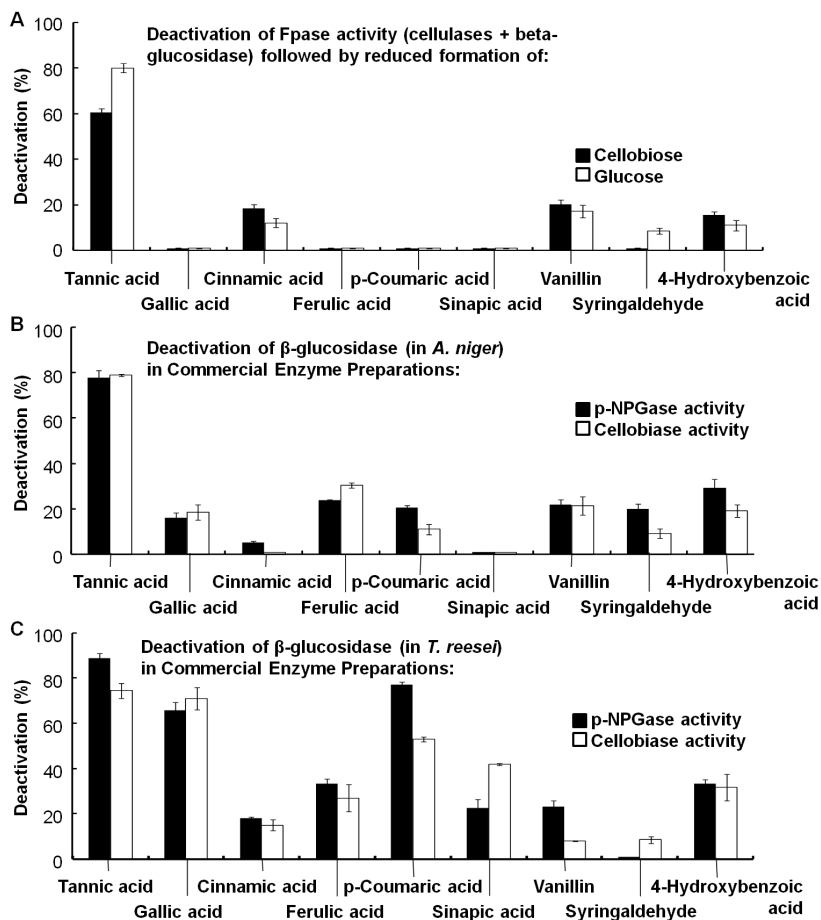


Figure 5.21: Deactivation of cellulase enzymes by phenolic compounds (from [25]). Baseline activities: (A) 100% FPase in Spezyme, (B) and (C) 100% para-NPGase and 100% cellobiase in Novozyme 188 and Spezyme CP, respectively, against which losses in enzyme activity, due to phenolic compounds, are measured.

5.13 Conclusions

The composition of lignocellulosic biomass materials will vary across species, and materials will depend on both species and harvesting methods. Softwoods and hardwoods will be supplied in the form of chips with characteristic dimensions measured in centimeters, while corn stover (ground stalks and leaves) and switchgrass have dimension in the range of millimeters. Sugarcane bagasse is somewhere in between. This chapter, while ignoring the effect of particle sizes of different materials entering the pretreatment process, discussed the chemistry of biomass and how it relates to potential yields of ethanol. Common denominators of recalcitrance found across all species may be addressed by pretreatment. Cooking biomass in water increases accessibility and susceptibility for cellulases that depolymerize, e.g., monosaccharides. An optimal range of temperature and pressure must be identified to enhance reactivity of lignocellulosic materials, while avoiding underived modification into species that are not fermentable.

Acknowledgments

The authors thank Dr. Miroslav Sedlak and Mr Isaac Emery of Purdue University for their internal review of this manuscript. The material in this work was supported by Mascoma Corporation Sponsored Research Grant, Department of Energy Grants GO18103, GO17059-16649, 0012846, DE-SC0000997, and the symposium sponsored by NSF-PIRE (OISE07302270). This work includes information from the National Academies Report on the American Energy Future and the website of Oak Ridge National Laboratory.

Bibliography

- [1] America's Energy Future Panel. *Liquid Transportation Fuels from Coal and Biomass: Technological Status, Costs, and Environmental Impacts*. Washington, DC: The National Academies Press, 2009. 1–370.
- [2] W.E. Mabee, D.J. Greg, C. Arato, A. Berlin, R. Bura, N. Gilkes, O. Mirochnik, X. Pan, E.K. Pye, and J. Saddler. Update on Softwood to Ethanol Process Development. *Applied Biochemistry and Biotechnology* 29 (2006): 55–70.
- [3] ORNL. *Bioenergy conversion factors Oak Ridge National Laboratory, Oak Ridge, Tennessee, USA*, <http://www.ornl.gov/>.
- [4] R.E.H. Sims, W. Mabee, J.N. Saddler, and M. Taylor. An Overview of Second Generation Biofuel Technologies. *Bioresource Technology* 101 (2010):1570–1580.
- [5] Prentiss & Carlisle. *Michigan Timber Market Analysis for the Michigan Department of Natural Resources*. Tech. rep. Michigan Department of Natural Resources, Mar. 2008.
- [6] F.O. Lichts. *Industry Statistics: 2010 World Fuel Ethanol Production*. Renewable Fuels Association, 2010. URL: <http://www.ethanolrfa.org/pages/statistics>.
- [7] A. Eisentraut. *Sustainable Production of Second-Generation Biofuels. Potential and Perspectives in Major Economies and Developing Countries*. Paris: International Energy Agency IEA/OCD, 2010. URL: <http://www.iea.org>.
- [8] E. Sundfeld. *Bionergy Technology Development in Brazil*. <http://www.embrapa.br/english/embrapa>. 2009.
- [9] A.K. Bera, M. Sedlak, A. Khan, and N.W.Y. Ho. Establishment of L-Arabinose Fermentation in Glucose/Xylose Co-Fermenting Recombinant *Saccharomyces Cerevisiae* 424A (LNH-ST) by Genetic Engineering. *Applied Microbiology and Biotechnology* 87 (2010):1803–1811.

- [10] N.W.Y. Ho, Z. Chen, A.P. Brainard, and M. Sedlak. Successful Design and Development of Genetically Engineered *Saccharomyces* Yeasts for Effective Co-Fermentation of Glucose and Xylose from Cellulosic Biomass to Fuel Ethanol. *Advances in Biochemical Engineering/Biotechnology* 65 (1999):163–192.
- [11] N.W.Y. Ho, Z. Chen, A.P. Brainard, and M. Sedlak. Genetically Engineered *Saccharomyces* Yeasts for Conversion of Cellulosic Biomass to Environmentally Friendly Transportation Fuel Ethanol. In: *ACS Symposium series No. 767. Green Chemical Syntheses and Processes*. Ed. by Anastas P.T., Heine L.G., and Williamson T.C. 767. American Chemical Society, 2000. Chap. Washington, DC. 143–159.
- [12] M. Kuyper, H.R. Harhangi, A.K. Stave, A.A. Winkler, M.S. Jetten, W.T. de Laat, J.J. den Ridder, H.J. Op den Camp, J.P. van Dijken, and J.T. Pronk. High-Level Functional Expression of a Fungal Xylose Isomerase: The Key to Efficient Ethanolic Fermentation of Xylose by *Saccharomyces Cerevisiae*. *FEMS Yeast Research* 4 (2003):69–78. URL: <http://www.ncbi.nlm.nih.gov/pubmed?term=%22Kuyper%20M%22%5BAuthor%5D>.
- [13] M. Sedlak and N.W.Y. Ho. Production of Ethanol from Cellulosic Biomass Hydrolysates Using Genetically Engineered *Saccharomyces* Yeast Capable of Co-Fermenting Glucose and Xylose. *Applied Biochemistry and Biotechnology* 113–116 (2004):403–405.
- [14] K. Karhumaa. Investigation of Limiting Metabolic Steps in the Utilization of Xylose by Recombinant *Saccharomyces Cerevisiae* Using Metabolic Engineering. *Yeast* 22 (2005):359–368. URL: <http://www.ncbi.nlm.nih.gov/pubmed?term=%22Karhumaa%20K%22%5BAuthor%5D>.
- [15] E. Casey, M. Sedlak, N.W.Y. Ho, and N.S. Mosier. Effect of Acetic Acid and pH on the Cofermentation of Glucose and Xylose to Ethanol by a Genetically Engineered Strain of *Saccharomyces Cerevisiae*. *FEMS Yeast Research* 10 (2010):385–393.
- [16] D.W. Templeton, C.J. Scarlata, J.B. Sluiter, and E.J. Wolfrum. Compositional Analysis of Lignocellulosic Feedstocks. 2: Method Uncertainties. *Journal of Agricultural and Food Chemistry* 58 (2010):9054–9062.
- [17] M. Kim and D.F. Day. Composition of Sugar Cane, Energy Cane, and Sweet Sorghum Suitable for Ethanol Production at Louisiana Sugar Mills. *Journal of Industrial Microbiology and Biotechnology* (2010). DOI: 10.1007/s10295-010-0812-8.

- [18] B. Du, L.N. Sharma, C. Becker, S.-F. Chen, R.A. Mowery, G.P. van Wal-sun, and C.K. Chambliss. Effect of Varying Feedstock-Pretreatment Chem-istry Combinations on the Formation and Accumulation of Potentially In-hibitory Degradation Products in Biomass Hydrolysates. *Biotechnology and Bioengineering* 107 (2010):430–440.
- [19] E.S. Domalski and T.A. Milne. *Thermodynamic Data for Biomass Ma-terials and Waste Components. The ASME Research Committee on In-dustrial and Municipal Wastes*. New York: The American Society of Me-chanical Engineers, 1987.
- [20] S. Schwietzke, M. Ladisch, L. Russo, K. Kwant, T. Mäkinen, B. Kavalov, K. Maniatis, R. Zwart, G. Shahanan, K. Sipila, P. Grabowski, B. Telenius, M. White, and A. Brown. *Analysis and Identification of Gaps in Research for the Production of Second Generation Liquid Transportation Biofuels*. Paris: International Energy Agency IEA/OCD, www.iea.org, 2008.
- [21] W. Vermerris. Composition and Biosynthesis of Lignocellulosic Biomass. In: *Genetic Improvement of Bioenergy Crops*. New York: Springer, 2008. 89–142.
- [22] R. Kumar and C.E. Wyman. Effect of Supplementation at Moderate Cel-lulase Loadings on Initial Glucose and Xylose Release from Corn Stover Solids Pretreated by Leading Technologies. *Biotechnology and Bioengi-neering* 102 (2009):45–67.
- [23] E. Ximenes, Y. Kim, N. Mosier, B. Dien, and M. Ladisch. Inhibitors of Cellulose Hydrolysis in Wet Cake. *Enzyme and Microbial Technology* 46 (2010):170–176.
- [24] Q. Qing, B. Yang, and C.E. Wyman. Xylooligomers are Strong Inhibitors of Cellulose Hydrolysis by Enzymes. *Bioresource Technology* 101 (2010): 9624–9630.
- [25] E. Ximenes, Y. Kim, N. Mosier, B. Dien, and M. Ladisch. Deactivation of Cellulases by Phenols. *Enzyme and Microbial Technology* 48 (2011): 54–60.
- [26] Y. Kim, E. Ximenes, N.S. Mosier, and M.R. Ladisch. Soluble Inhibitors/ Deactivators of Cellulase Enzymes from Lignocellulosic Biomass. *En-zyme and Microbial Technology* 48 (2011):408–415.
- [27] L.B. Selinger, C.W. Forsberg, and K.-J. Cheng. The Rumen: A Unique Source of Enzymes for Enhancing Livestock Production. *Anaerobe* 2 (1996):263–284.

- [28] I. Benoit, E.G.J. Danchin, R.-J. Bleichrodt, and R.P. de Vries. Biotechnological Applications and Potential of Fungal Feruloyl Esterases Based on Prevalence, Classification and Biochemical Diversity. *Biotechnological Letters* 30 (2008):387–396.
- [29] Y. Nishiyama, P. Langan, and H. Chanzy. Crystal Structure and Hydrogen-Bonding System in Cellulose Ibeta from Synchrotron X-Ray and Neutron Fiber Diffraction. *Journal of the American Chemical Society* 124 (2002): 9074–9082.
- [30] N.S. Mosier, C.E. Wyman, B.E. Dale, R. Elander, M. Holtzapple, and M.R. Ladisch. Features of Promising Technologies for Pretreatment of Lignocellulosic Biomass. *Bioresource Technology* 96 (2005):673–686.
- [31] J.F. Matthews, C.E. Skopec, P.E. Mason, P. Zuccato, R.W. Torget, J. Sugiyama, M.E. Himmel, and J.W. Brady. Computer Simulation Studies of Microcrystalline Cellulose Ibeta. *Carbohydrate Research* 341 (2006): 138–152.
- [32] M.E. Himmel, S.Y. Ding, D.K. Johnson, W.S. Adney, M.R. Nimlos, J.W. Brady, and T.D. Foust. Biomass Recalcitrance: Engineering Plants and Enzymes for Biofuels Production. *Science* 315 (2007):804–807.
- [33] K. Meyer, A.M. Shirley, J.C. Cusumano, D.A. Bell-Lelong, and C. Chapple. Lignin Monomer Composition is Determined by the Expression of a Cytochrome P450-Dependent Monooxygenase in Arabidopsis. *Proceedings of the National Academy of Science USA* 95 (1998):619–6623.
- [34] J. Ralph, C. Lapierre, J.M. Marita, H. Kim, F. Lu, R.D. Hatfield, S. Ralph, C. Chapple, R. Franke, and M.R. Hemm. Elucidation of New Structures in Lignins of CAD- and COMT-Deficient Plants by NMR. *Phytochemistry* 57 (2001):993–1003.
- [35] X. Li, E.A. Ximenes, Y. Kim, M. Slininger, R. Meilan, M. Ladisch, and C. Chapple. Lignin Monomer Composition Impacts Arabidopsis Cell Wall Degradability Following Liquid Hot-Water Pretreatment. *Biotechnology for Biofuels* 3 (2010):1–7.
- [36] X. Li, J.K. Weng, and C. Chapple. Improvement of Biomass Through Lignin Modification. *The Plant Journal* 54 (2008):569–581.
- [37] F. Chen and R.A. Dixon. Lignin Modification Improves Fermentable Sugar Yields for Biofuel Production. *Nature Biotechnology* 25 (2007):759–761.
- [38] A. White and D.R. Rose. Mechanism of Catalysis by Retaining Beta-Glyco- syl Hydrolases. *Current Opinion in Structural Biology* 7 (1997): 645–651.

- [39] K.L. Kohlmann, A. Sarikaya, P.J. Westgate, J. Weil, A. Velayudhan, R. Hendrickson, and M.R. Ladisch. Enhanced Enzyme Activities on Hydrated Lignocellulosic Substrates. In: *207th American Chemical Society National Meeting, ACS Symposium series No. 618. Enzymatic Degradation of Insoluble Carbohydrates*. Ed. by Penner M. and Saddler J. 618. Washington DC: American Chemical Society, 1995. 237–255.
- [40] M.R. Ladisch, K. Kohlmann, P. Westgate, J. Weil, and Y. Yang. “Processes for Treating Cellulosic Material”. 5,846,787. 1998.
- [41] N.S. Mosier, P. Hall, C.M. Ladisch, and M.R. Ladisch. Reaction Kinetics Molecular Action and Mechanisms of Cellulolytic Proteins. *Advances in Biochemical Engineering* 65 (1999):24–40.
- [42] J. Weil, P.J. Westgate, K.L. Kohlmann, and M.R. Ladisch. Cellulose Pretreatments of Lignocellulosic Substrates. *Enzyme and Microbial Technology* 16 (1994):1002–1004.
- [43] J.R. Weil, M. Brewer, R. Hendrickson, A. Sarikaya, and M.R. Ladisch. Continuous pH Monitoring during Pretreatment of Yellow Poplar Wood Sawdust by Pressure Cooking in Water. *Applied Biochemistry and Biotechnology* 68 (1997):21–40.
- [44] J. Weil, A. Sarikaya, S.-L. Rau, J. Goetz, C.M. Ladisch, M. Brewer, R. Hendrickson, and M.R. Ladisch. Pretreatment of Yellow Poplar Sawdust by Pressure Cooking in Water. *Applied Biochemistry and Biotechnology* 68 (1997):21–40.
- [45] J.R. Weil, A. Sarikaya, S.-L. Rau, J. Goetz, C.M. Ladisch, M. Brewer, R. Hendrickson, and M.R. Ladisch. Pretreatment of Corn Fiber by Pressure Cooking in Water. *Applied Biochemistry and Biotechnology* 73 (1998): 1–17.
- [46] Y. Kim, R. Hendrickson, N.S. Mosier, and M.R. Ladisch. Liquid Hot Pretreatment of Cellulosic Biomass. *Methods in Molecular Biology* 581 (2009):93–102.
- [47] W.S.L. Mok and M.J. Antal. Uncatalyzed Solvolysis of Whole Biomass Hemicellulose by Hot Compressed Liquid Water. *Industrial & Engineering Chemistry Research* 31 (1992):1157–1161.
- [48] C. Ususki, Y. Kimura, and S. Adachi. Degradation of Pentoses and Hexouronic Acids in Subcritical Water. *Chemical Engineering & Technology* 31 (2008):133–137.
- [49] S.H. Khajavi, Y. Kimura, R. Oomori, R. Matsuno, and S. Adachi. Degradation Kinetics of Monosaccharides in Subcritical Water. *Journal of Food Engineering* 68 (2005):309–313.

- [50] J.R.M. Almeida, T. Modig, A. Petersson, B.H. Hahn-Haegerdal, G. Liden, and M.F. Gorwa-Grauslund. Increased Tolerance and Conversion of Inhibitors in Lignocellulosic Hydrolysates by *Saccharomyces Cerevisiae*. *Journal of Chemical Technology and Biotechnology* 82 (2007):340–349.
- [51] E. Palmqvist and B. Hahn-Haegerdal. Fermentation of Lignocellulosic Hydrolysates. II: Inhibitors and Mechanisms of Inhibition. *Bioresource Technology* 74 (2000):25–33.

Chapter 6

Chemical and Biological Deconstruction of Aqueous Phase Processing

Charles E. Wyman, Carol J. Wyman

6.1 Introduction

Petroleum is the largest source of energy for the world, supplying about 1/3 of total world energy, and about 2/3 of world petroleum reserves are in the Mideast. Furthermore, about 2/3 of petroleum goes to transportation which in turn relies on petroleum to provide about 97% of its energy. In addition, the transportation sector is a major source of greenhouse gases, contributing more than any other end user in the U.S. [1]. Thus, we need to find sustainable alternatives to petroleum for transportation to avoid future transitions and reduce greenhouse gas emissions.

Over the decades, there has been recurrent talk of reducing our dependence on petroleum. This plea started when the U.S. oil production peaked in 1970 at 9.6 million barrels per day, followed by the *OPEC* oil embargo of 1973 that created economic chaos. Not long after that, on April 18, 1977, President Carter declared the “*moral equivalent of war*” in developing new energy sources with the warning that “*it will get worse every day until we act.*” Virtually every president of the U.S. since that time has committed to reducing petroleum use. However, the real result is anything but convincing. For example, since 1973, the world consumed about 900 billion barrels of oil of the more than 1.1 trillion barrels used to date. In addition, world oil consumption has increased from 56.7 million barrels per day in 1974 to 84.6 million in 2006. For the U.S., consumption has risen to 5.1 million barrels per day. World petroleum reserves now stand at about 1.1 to 1.3 trillion barrels of oil including oil sands in Canada, a total that would last only about 40 years at current world consumption rates. Perhaps even more frightening, atmospheric carbon dioxide levels measured at Mauna Loa rose from about 330 ppm in 1974 to about 380 ppm in 2008, a 17% increase. Few measures have been taken to replace oil other than cane sugar ethanol in Brazil and the now much maligned corn ethanol industry in the U.S., even though they are effective in reducing the use of oil at least somewhat [1].

Faced with this gloomy forecast, what should we do? Some advocate “*Drill baby, drill*” as the answer, but in fact, U.S. energy reserves would only last a few years if we were to rely on them as our only resource. Although new oil is continually discovered, the rate of discovery is lower than the rate of consumption, making this a path of limited opportunity. Against that, we have three options. First, we could change the source of fuels to options such as coal. However, it is vital that the new resource be sustainable such as biomass to avoid GHG emissions and also avoid future transitions. The second option is to use more public transportation and drive less miles. This is an important opportunity but counters historic trends. Finally, we could drive more efficient vehicles, an option that is generally very feasible and synergistic to introducing new fuels that are not likely to be as cheap or as abundant as petroleum.

6.2 Why Cellulosic Biomass?

Petroleum is favored because it is a liquid with high energy density that can be rapidly replenished in vehicles. However, no other abundant resources are high energy content liquids that can be employed in this service. Abundant fossil options include natural gas and coal, but neither is as easily used as petroleum. Oil sands and shale are abundant fossil resources, with the former being now converted into liquid fuels in Canada. However, both have large environmental footprints in access and conversion. Furthermore, none of these fossil alternatives are sustainable and all will contribute greenhouse gas emissions that cause global climate change.

If we turn to sustainable resources, as we must sooner or later, we only have the choices of using the sun, wind, ocean waves, ocean temperature gradients, hydropower, geothermal energy, or nuclear power [2]. However, none of these options are liquids or for that matter lend themselves to mobile applications. Rather we must first capture each as stored energy. For example, all of these resources can be converted into electricity, but we must then store the electrical energy for transportation either by hydrolyzing water into hydrogen or charging batteries or other storage devices. Alternatively, plants can capture the sun’s energy directly by combining water and carbon dioxide through photosynthetic reactions to form biomass. Although biomass itself is a solid that would not lend itself to powering transportation, it can be converted into liquid fuels that are more than capable of powering all classes of vehicles with minimal changes in infrastructure, particularly compared to the major changes needed to accommodate a shift to batteries or hydrogen power. In fact, biomass is the only route to sustainable production of liquid transportation fuels [2]. Thus, while light duty cars and trucks may be able to use hydrogen or batteries if the required infrastructure changes can be made

and consumers are willing to sacrifice the convenience of liquid fuels, heavy duty vehicles and aircraft will be forced to use biofuels to meet their needs sustainably.

Plants come in many shapes and sizes to meet many purposes. Some such as sugar cane and sugar beets are grown to take advantage of their production of sugars that are easily extracted for food uses. Others such as corn capture sugars in long chains as starch and can be used directly as animal feed or human food or readily broken down to their component sugars for use in soft drinks and many other foods. Plants also produce oils in their seeds that can be extracted for food or industrial uses. All three of these forms of solar energy storage in plants, that is, sugar, starch, and oils, can be readily used to produce transportation fuels, but none of them are available in anywhere near enough quantity to impact the vast transportation fuel market in a substantial way. Furthermore, because of their value as food, conversion to transportation fuels sparks controversies about direct and indirect competition with food production, limiting their long term prospects.

Plants also capture the sun's energy in structural carbohydrates known as cellulose and hemicellulose that support plants. Cellulose is a long, linear chain of glucose sugar molecules that form tight hydrogen bonds with neighboring chains to form extensive crystalline regions that become the fibers in plants. Hemicellulose is also a sugar polymer but made up of up to the five sugars arabinose, galactose, glucose, mannose, and xylose as well as other molecules. These chains are branched and not crystalline but serve to glue cellulose chains together. A phenyl propene polymer known as lignin works with hemicellulose in this role, but lignin is not made of sugars. Rather, it resembles coal more closely than sugars. About 40 to 50% of typical plants such as wood, grasses, and agricultural residues is cellulose, another 20 to 30% is hemicellulose, and about 15 to 25% is lignin. Other components including free sugars, minerals, and oils make up the remaining portion, with the amounts depending on such factors as the plant type, harvest season, location, storage conditions, and climate.

Cellulosic biomass is attractive for making fuels because it is more abundant than other biomass types. For example, a recent USDA/DOE sponsored study predicted that well over 1 billion dry tons of biomass could be sustainably available in the long term for making fuels in the United States [3]. This quantity would be sufficient to possibly make enough fuel to displace about 80 billion gallons of gasoline compared to the current U.S. gasoline consumption of 140 billion gallons. Some profess to worry about the density of biomass and the resulting impact on transportation to central processing facilities. Yet, it is easy to show that if cellulosic biomass could be grown at a productivity of 10 dry tons/acre/year and we could realize yields of about 70 gallons of gasoline equivalent per dry ton, approximately 3.5 billion gallons of gasoline could be displaced in a 50 mile radius, which is a distance typically considered acceptable for moving corn or

wood to existing central processing facilities for making corn ethanol and paper products, respectively. Even assuming that some of the land may not be available for growing energy crops or that yields may be lower, it is quite feasible to realize well over a billion gallons of gasoline equivalent within the 50 mile radius. Furthermore, cellulosic biomass is low in cost, with biomass costing \$60 per dry ton equivalent to petroleum at \$20 per barrel on an equal energy content basis [4]. Thus, the challenge is to convert this abundant, low cost resource into liquid transportation fuels at low costs.

6.3 Conversion Options for Aqueous Phase Processing

Although cellulosic biomass is a unique resource for large scale capture and storage of solar energy, it stores energy in a solid while we prefer the convenience of liquid and gaseous fuels, since they are much better suited to transportation applications that now consume much of the petroleum used. Furthermore, liquid fuels from biomass are the only known option for sustainable production of jet and diesel fuels and are virtually certain to have a vital role as we transition to sustainable energy sources. Thus, we must develop low cost processes to convert solid biomass into liquid fuels for transportation.

In simple terms, the composition of cellulosic biomass can be viewed as consisting of fixed carbon, volatile matter, ash, and moisture via what is often called proximate analysis. For example, switchgrass may have typical values of 17.1, 58.4, 4.6, and 20.0 wt%, respectively, and a lower heating value (LHV) of 13.6 MJ/kg and a higher heating value (HHV) of 15.0 MJ/kg. Such information may be sufficient if the intent is simply to burn the material. However, we can also obtain elemental compositions in what is typically designated as ultimate analysis of carbon, hydrogen, oxygen, nitrogen, sulfur, and ash contents, with possible values for switchgrass being 47.0, 5.3, 41.4, 0.5, 0.1, and 5.7 wt%, respectively, on a dry biomass basis. In this case, the LHV and HHV will be greater due to the lack of moisture, with values of 17.0 MJ/kg and 18.7 MJ/kg being representative. This information may be sufficient for thermal conversion approaches that focus on capture of the key elements as fuels. However, cellulosic biomass is made up of a complex network of long cellulose chains that are held together by hemicellulose, lignin and various other components to provide support and promote growth of plants. Cellulose is made up of long chains of covalently bound glucose sugars that are linked to adjacent cellulose chains by hydrogen bonding to form cellulose fibrils, with a large portion being crystalline. Hemicellulose is typically comprised of arabinose, galactose, glucose, mannose, and xylose sugars that are also bound to each other and smaller amounts of other compounds covalently. These compounds can be released from biomass by addition of one molecule

of water to one molecule of the anhydrous sugars known as arabinan, galactan, glucan, mannan, and xylan to form the corresponding sugars in solution through a hydrolysis reaction. Lignin, on the other hand, is not a carbohydrate but is made up of phenyl-propene units. Lignin and hemicellulose work to hold the cellulose structure together in a strong composite material. As one example, switchgrass may contain about 35% glucan, most of it being in cellulose, about 21.8% xylan, 3.5% arabinan, 21.4% lignin, 3.3% ash, and 13.8% other compounds such as free sugars, protein, oils, and starch.

Huber et al. outlined in some detail the variety of routes by which cellulosic biomass can be converted into liquid fuels [5]. These can be divided into thermal routes and aqueous processing approaches. In simple terms, thermal routes involve breakdown of biomass at high temperatures into simple components that can then be recombined to form more complex fuel molecules or directed toward just hydrogen. One set of such thermal routes gasifies biomass to a mixture of carbon monoxide and hydrogen (syngas) that can be converted into diesel fuel via Fischer-Tropsch catalysis or other products including methanol and hydrogen. Other thermal routes employ liquefaction or pyrolysis to form bio-oils that can be upgraded to aromatics and other hydrocarbons by hydrodeoxygenation, zeolite catalysis, and other approaches.

Another set of options is built around aqueous phase processing of cellulosic biomass to release sugars or their dehydration products for subsequent biological or catalytic conversion to fuels. The intent of aqueous processing is to depolymerize biomass into its monomer units, thereby preserving much of the complex structure from which to build fuels. Thus, lower temperatures in the range of 140 to 220 °C are typically applied to avoid loss of these compounds during processing. The sugars that make up hemicellulose can be recovered with good yields of 85% and more by applying dilute sulfuric or other acids at 140 to 170 °C or higher. However, the crystalline structure of cellulose makes it challenging to recover glucose with yields over 60% via thermal routes, and cellulase enzymes are favored to catalyze breakdown of cellulose to glucose with high yields. Unfortunately, high enzyme costs stand in the way of low cost glucose from cellulosic biomass. Alternatively, arabinose and xylose in hemicellulose can be dehydrated to furfural by holding these sugars for longer times at high temperatures, although steps will be needed to achieve higher furfural yields than realized in commercial systems now. Holding reactions for longer times will dehydrate glucose to hydroxymethyl furfural (HMF) that in turn will break down to form levulinic and formic acids in equal molar quantities. It is difficult to capture HMF with high yields, but good yields of levulinic and formic acids can be achieved.

Enzymes are very selective catalysts for the breakdown of cellulosic biomass to form sugars. For example, in the case of cellulase enzymes which attack cel-

lulose to release glucose sugar, these enzymes function as three primary components [6]. The first is called endoglucanase and attacks cellulose chains along their length to form ends to which a second component called exoglucanase can then attach to release sugars from that chain. In fact, it releases mostly combinations of two sugar units called cellobiose into solution as the enzyme progresses along that chain. Cellobiose in turn is broken down by another enzyme component called beta-glucosidase to release single glucose molecules.

Biological routes have a number of potential advantages for the breakdown of biomass to support the production of fuels. First of all, they are highly selective, meaning that they form very few—if any—products other than those intended. In addition, they offer high yields that are critical to economic success for commodity products. There are also opportunities for entirely new organisms and enzymes through the ever evolving techniques of modern biotechnology. There is also substantial experience with the application of biological processing to conversion of starch and sugar into ethanol. In addition, the low temperatures and pressures required make containment relatively inexpensive, and they produce ethanol and other fuels that can replace gasoline. One disadvantage of biological processes is that they are very specific about the substrates they will attack, resulting in some materials being very difficult for them to breakdown. Also cellulosic biomass conversion is not yet commercial, and a lot of work has to be done to prove and apply the technology. In addition, the reactions are very slow. Thermochemical approaches, on the other hand, have a number of advantages including that they can handle a broad range of substrates and that the processes are very robust. There is also substantial commercial experience with thermochemical processes, for example, the Sasol process in South Africa that has been operating for decades converting coal to syngas for the production of diesel fuel substitutes. The reactions are fast and can produce products that can replace conventional fuels. Some of the major challenges facing thermochemical routes, however, include the requirement for very large operations to achieve economies of scale and to be economic, which requires extremely high capital investments. There is also less control of by-product formation from thermochemical processes, so there could be considerable challenges in dealing with some of the streams and waste products. Finally, pressures and temperatures tend to be high, presenting containment challenges.

A major need for producing commodity products is to achieve high yields. For example, for biomass costing \$65 per ton, achieving a yield equivalent to 100 gallons of gasoline per ton would result in a feedstock cost of only 65 cents per gallon of gasoline equivalent. On the other hand, for half that yield, the cost of the feedstock per gallon would double in this particular case to \$1.30 per gallon. Thus, the message here is that high yields are critical to economic success.

6.4 Laboratory Methods to Make Reactive Intermediates

A critical aspect to designing laboratory experiments is to decide what you are looking for in the particular experiments to be conducted. For example, it is often desirable to start by understanding reaction kinetics because the results tell you the potential to make the desired products. On the other hand, we also have to be concerned with effects of heat, mass, and momentum transfer on process scale-up as they can constrain achieving the desired products and yields. Generally, it is preferable to first establish reaction kinetics to determine the potential products that can be made and the maximum yields that are possible. Such kinetic experiments can be successfully carried out on a very small scale. On the other hand, consideration of transport impacts should be done in the context of a commercial design as we are trying to figure out what kind of effects would occur in real commercial equipment. Both present challenges due to the heterogeneity of biomass and the fact that we are dealing with multi-phase systems.

Another challenge to keep in mind is that the biofuels processes we are going to build are very, very large. For example, we can be processing of the order of 2,000 dry tons per day or more of biomass, and process units, therefore, can be quite large. Reactors for the pretreatment of biological cellulose prior to conversion can be of the order of six feet in diameter and over 40 feet long, and there may be several banks of such reactors. Commercial fermentors can be of the order of 500,000 to a million gallons each or so, while our experiments are run at the bench scale or, at best, in a pilot plant. Therefore, typically we are talking about scaling up from experience gained at perhaps a pilot plant with about one ton of biomass to between 1,000 and 2,000 or more tons per day, i.e., three orders of magnitude. The challenge of such a large scale up factor can make investors very nervous as they are concerned about extrapolating data over three orders of magnitude to arrive at a commercial design coupled with investments of the order of \$300 million.

Against this background, the mission of the University of California at Riverside aqueous biomass processing research is first of all to improve the understanding of biomass fractionation, pretreatment, and cellulose hydrolysis to support applications and advances in biomass conversion technologies for the production of low cost commodity products. In addition, we seek to develop advanced technologies that would dramatically reduce the cost of production. To do this, graduate students, post-doctoral candidates, and research engineers on our team conduct such research. We also have developed extensive capabilities for biomass conversion, with particular focus on pretreatment of cellulosic biomass to open up its structure and release sugars followed by application of thermochemical or enzymatic processes to release sugars from the remaining solids for conversion to

ethanol. We have developed equipment for conversion of biomass into furfural, levulinic acid, and formic acid, as reactive intermediates for catalytic processing to drop in fuels. Our equipment ranges in size from what we call a high throughput pretreatment and hydrolysis system, which can process of the order of 3 or 4 milligrams of biomass, up to our steam gun reactor that can process about a pound of biomass at a time. In addition to pretreatment capabilities, we have fermentors that allow us to ferment the sugars we release during pretreatment and hydrolysis to ethanol or other products including continuous trains of reactors.

6.5 Pretreatments and Biological Production of Sugars as Reactive Intermediates Through the Consortium for Applied Fundamentals and Innovation (CAFI)

A number of years ago, a team of researchers who had worked in biomass conversion for some time formed what we called the Biomass Refining Consortium for Applied Fundamentals and Innovation (CAFI) with the goal of better understanding different options for the pretreatment of biomass, followed by the production of sugars by enzymatic processing. This team focused on pretreatment to reduce the natural resistance of biomass to breakdown to sugars followed by a series of biological steps to make enzymes and then break down the polymers in biomass to form sugars. That was followed by fermentation to ethanol or other products with the residue that was left behind, primarily lignin, assumed to be burned to generate heat and power to run the process with excess power left for export. Techno-economic evaluations of this type of process have shown that the most expensive single component in the overall cost of the process is feedstock at about 1/3 of the total cost. However, that is quite low when we keep in mind that feedstocks for commodity products should typically represent of the order of 75 to perhaps 90% of the final product cost. The next biggest process cost was attributed to pretreatment at about 18% of the total. Therefore, working on improvements in pretreatment is critical to coming up with low cost biological processing. Other major costs were the biological conversion steps of making enzymes and using those enzymes for conversion of pretreated material to products, with those two together representing 21% of the total cost. Lesser costs were associated with such steps as distillation and solids recovery at about 10% of the total, waste water treatment at about 4%, and boiler turbo-generator at a net of about 4%; utilities and product storage were also relatively small cost contributors [7].

Pretreatment is critical in this entire operation with its role being to disrupt the orderly structure of biomass to open it up for access to enzymes that can in turn break down cellulose to release glucose sugar. Generally, pretreatment is done by the application of heat and potentially by the addition of chemicals. For

example, pretreatment can be applied to break down hemicellulose to form sugars and disrupt lignin, and the result is cellulose that becomes exposed for enzyme action. When we look at the overall placement of pretreatment, it is pretty much in the center of the entire process and, therefore, has impacts on all surrounding operations. For example, the choice of pretreatment can affect the choice of feedstock and vice versa since not all pretreatments are capable of processing all feedstocks. In addition, pretreatment has an effect on the size reduction requirements as well as potentially on such aspects as harvesting and storage. Enzyme production is influenced by the choice of pretreatment as it determines solid characteristics that the enzymes must attack, and, therefore, the type of activities that are required from these enzymes. Another step impacted by pretreatment is downstream fermentations. For example, we must condition the liquid from pretreatment to make it less inhibitory to fermentation, and the choice of pretreatment has a major impact on the types of inhibitors and removal strategies employed. Similarly, we can show that pretreatment affects product recovery by determining the concentration of the final product and therefore recovery costs and the suitability of the final residues for biological waste treatment or other steps to utilize or dispose of those materials.

When we look at factors affecting enzymatic digestion of cellulose due to pretreatment, there are a number of substrate-related and enzyme-related factors to consider. Substrate-related factors include accessible surface area of the cellulose to enzymes, cellulose crystallinity, lignin and hemicellulose content and modification, the degree of polymerization of cellulose, particle size of the substrate, accessible bonds for breakdown, and deacetylation of biomass. Pretreatment impacts each of these factors. On the other hand, enzyme-related factors are such things as non-specific binding, end product inhibition, thermal inactivation, activity balance for synergism, specific activity, deactivation time, and enzyme immobility.

Numerous pretreatments have been studied to improve enzymatic digestion. These can be characterized in a number of ways. First of all, we can look at the type of additive; for example, none, acid, base, solvent, or enzymes. Also, we can look at the type of system: physical, chemical, thermal, or biological. Another consideration is whether pretreatment is operated in a batch, continuous, flow-through, or counter-current mode. Solids concentration is another important consideration in pretreatment design as is heat-up method and heat-up time. Cool-down method and time must also be considered. Overall, numerous combinations of pretreatment devices have been trialed. In general, such approaches have been long on invention but short on developing fundamental knowledge of such pretreatment systems.

As mentioned, pretreatments can be classified into three major classes. Physical pretreatments are those that require only physical action such as size reduction to prepare material for biological conversion. In general such approaches tend to be very energy-intensive and do not achieve the high yields necessary. A second option is a biological approach which seeks to use enzymes to open up the structure of biomass to prepare it for subsequent downstream operations. However, such biological systems have been difficult to control and be effective. Finally, the third option is what we can call a thermochemical route in which the addition of chemicals is combined with heat to break down biomass and open up its structure. Most successful methods have fallen into the last category.

Pretreatment is faced with a number of important constraints on cost that must be taken into consideration during the development of such technologies. First of all, high yields are critical to distribute operating and capital costs over as much product as possible, and therefore minimize the unit costs for each. Low operating costs are essential to provide a margin for return on capital. This translates into low use of chemicals, energy, and labor. In addition, operating costs must be lower for the overall process than for competing technologies that generally have all their capital already paid for. Finally, low capital costs are essential to minimize exposure. For example, low cost containment meaning small vessel size, low pressures, and low temperatures are very desirable to keep capital costs low. Also, we want to have as few steps as possible to minimize capital costs.

Against this background, the Biomass Refining Consortium for Applied Fundamentals and Innovation (CAFI) was organized in late 1999 and early 2000 to better understand and develop pretreatment technology. The approach of the CAFI team was to employ common feedstocks, shared enzymes, identical analytical methods, same material and energy balance methods, and the same costing methods on leading pretreatment options to provide data that others can use to identify which technologies are best suited to their needs. The CAFI team also wanted to seek to understand mechanisms that influence performance and differentiate pretreatments. This would provide a technology base to facilitate commercial use. It would also facilitate identification of promising paths to advance pretreatment technologies.

Over the years, three different projects were funded for the CAFI team. The first focused on corn stover pretreatment by different methods. The second CAFI project focused on utilization of poplar wood and its conversion to sugars and the fermentation of sugars to ethanol. And the third CAFI project looked at the interaction of all the different steps surrounding pretreatment for application to switchgrass.

Over a period of ten years, the CAFI projects were guided by an Agricultural and Industrial Advisory Board consisting of representatives from about 26

different organizations. This Board met with the CAFI team twice a year to review the CAFI team's progress and offer suggestions for improvements and new approaches. The CAFI technologies studies included ammonia recycle percolation and soaking aqueous ammonia by Y.Y. Lee at Auburn University, dilute active pretreatment by Charles Wyman at the University of California at Riverside, SO₂ pretreatment by Jack Saddler at the University of British Columbia and Charles Wyman at the University of California at Riverside, ammonia fiber expansion (AFEX) by Bruce Dale at Michigan State University, controlled pH pretreatment by Michael Ladisch at Purdue University, and lime pretreatment by Mark Holtzapple at Texas A&M University. In addition, The National Renewable Energy Laboratory through Rick Elander provided logistical support and economic analysis for the CAFI team. Additionally, enzymes were provided by Genencor through Ryan Warner and feedstock by Ceres Corporation through Bonnie Hames and Steve Thomas.

A key aspect of the CAFI project was the development of complete material balances for each pretreatment step. This involved tracking all the major components of biomass, primarily glucose, xylose, and lignin as the material went from size reduction to pretreatment to downstream conditioning and hydrolysis. A unique way to look at yields in the case of the CAFI project was to consider yields on the basis of total glucose plus xylose present in each feedstock and to determine what fraction of the total of those two sugars was released. This approach reflected the fact that most feedstocks are richer in glucose than xylose and to count them equally would not recognize the difference in economic impact.

The first CAFI project focused on corn stover, as mentioned earlier. This project was funded by the U.S. Department of Agriculture Initiative for Future Agriculture and Food Systems (IFAFS) Program through a competitive solicitation with the participation by the National Renewable Energy Laboratory (NREL) supported by additional funds from the DOE Office of the Biomass Program. This project began in September of 2000 and was completed in September of 2004 and found that all the different pretreatments had similar performance and costs. It is particularly noteworthy that when we compare the different pretreatments for corn stover, they all release similar amounts of glucose and xylose, and the major difference was just when such materials were released. For example, dilute acid pretreatment released most of the xylose during the pretreatment step and most of the glucose in the downstream enzymatic hydrolysis step. On the other hand, higher pH pretreatments such as lime would release a fair amount of the lignin as well as some xylose during pretreatment, and the bulk of the glucose during enzymatic hydrolysis. AFEX was unique among the different pretreatments in that it released virtually nothing during pretreatment but made the biomass very accessible to enzymes for a high yield production of sugars downstream.

The second CAFI project started in April of 2004 through funds from the Department of Energy Office of Biomass Program through a competitive solicitation. In this particular project the CAFI team determined more in-depth information on enzymatic hydrolysis of hemicellulose and cellulose in the solid following pretreatment, and also conditioning and fermentation of the hydrolysis liquids. In addition, the University of British Columbia was added to the team to work on sulfur dioxide pretreatment through support of Natural Resources Canada. Again, Genencor supplied commercial and advanced enzymes for the project. Greater differences were found among the different pretreatment technologies for poplar with the highest yields from sulfur dioxide and lime approaches.

The third CAFI project focused on switchgrass as a feedstock. Again, switchgrass was pretreated by all the leading technologies, and material balances were closed by common methods for each pretreatment. Sugar yields were determined versus cellulase enzyme loadings, and the benefits of adding different enzyme activities such as beta-glucosidase and xylanase were evaluated. The CAFI was also able to characterize the effects of key enzyme features and surface characteristics on performance. Furthermore, the effect of switchgrass age, harvest time, and location was explored for the different pretreatments coupled with enzymatic hydrolysis. Three different types of switchgrass were used: one called Alamo, another called Shawnee, and a third known as Dacotah. They were quite similar in many respects, although the Dacotah switchgrass had a higher lignin content and lower free sugars than the other two, primarily due to the Dacotah switchgrass being harvested in the late winter/early spring while the other two were harvested in the fall. In this case, performance was intermediate between that for corn stover and poplar with lime and sulfur dioxide pretreatments achieving the best yields. However, all did reasonably well with switchgrass. In these studies, a wide range of conditions were applied for different pretreatments.

Overall, the different pretreatments have different effects on the substrate. The lowest pH pretreatments with dilute acid or SO_2 remove most of the hemicellulose as monomers and remove low amounts of lignin. At near neutral pH by controlled pH pretreatments with hot water, hemicellulose was hydrolyzed to mostly oligomers in solution, and a limited amount of lignin was removed. Further up the pH scale, ammonia fiber expansion removed almost nothing as noted earlier but opened up the structure for high yield release of sugars by enzymes. Finally lime or soaking with aqueous ammonia pretreatments removed more lignin than hemicellulose and left much of the carbohydrates in the solids.

Key messages from the CAFI project were that first of all it is very important to have transparent material balances to facilitate comparison among different technologies. Also it is clear that pretreatment is still required to achieve high yields from all three substrates; corn stover, poplar and switchgrass. The choice

of pretreatment will also depend on interactions with the rest of the process, such as the type of enzymes used and their activities. CAFI also found that not all pretreatments were equally effective for all feedstocks, and some feedstocks favored certain pretreatments over others. Also, the choice of enzyme formulation and pretreatment technology are linked, and the type of activities needed for enzymes depends upon the characteristics of the solids from pretreatment. In addition, feedstock variability can have a large impact on performance, but the cause and effect between pretreatment alteration of feedstock and enzymatic digestion is not entirely clear. Enzyme loadings are still higher than desired for economic reasons for all the pretreatments, so continued work is needed on pretreatment to find approaches that can reduce enzyme requirements. Hopefully, these results will help others select pretreatment, feedstock, and enzyme combinations that are effective for commercial use.

It is important to note that the results of the CAFI team have been published widely in various journals, with one dedicated volume of *Bioresource Technology* devoted to reporting the CAFI results for corn stover in 2005 [8]. Another special volume in *Biotechnology Progress* reported the CAFI results with poplar in 2009 [9]. Finally, the CAFI team published papers for a targeted volume in *Bioresource Technology* where application of all these different pretreatments to switchgrass was presented in a single volume. At this point, the CAFI project has concluded, and there are no plans to continue [10].

6.6 Thermochemical Processing to Sugars and Other Reactive Intermediates

Key objectives for biomass pretreatment are to capture a large fraction of fermentable hemicellulose sugars to realize high ethanol yields and to minimize formation of degradation products, to minimize inhibition and detoxification needs. It is also critical to realize high yields of glucose from cellulose in pretreatment and enzymatic hydrolysis. In general, dilute acid catalyzes breakdown of hemicellulose to form oligomers which in turn form sugar monomers by that acid as well. However, continued holding of xylose in the presence of dilute acid at high temperatures forms furfural and degradation products. Thus, this sequence represents a classical series reaction, with xylose being the intermediate product between the breakdown of biomass to form oligomers and their breakdown to xylose followed by the breakdown of xylose to furfural and on to degradation products. As a result, sugar generation must be balanced against sugar degradation to maximize yields. Fortunately, in the presence of dilute sulfuric acid at temperatures on the order of 160 to 170 °C or so, we can achieve xylose yields of about 90% before degradation becomes a problem.

In a similar way, cellulose hydrolysis is also catalyzed by dilute acid to form primarily glucose which in turn will breakdown through dehydration to form HMF followed by further dehydration to levulinic acid followed by degradation products. In this case, however, it is much more challenging to obtain high yields that we see for hemicellulose hydrolysis due to the crystalline structure and other aspects of cellulose composition. For example, typically we see glucose yields of the order of 50%, and residence times are only for a few seconds at very high temperatures of the order of 240 °C in the presence of around 1% sulfuric acid to achieve such yields. Unfortunately, it is very difficult to control conditions so precisely in commercial scale equipment to obtain that performance.

However, further consideration of these reactions shows that products formed by breakdown or dehydration of xylose and glucose can be useful for catalytic conversion to other products. For example in the case of xylose, dehydration of xylose in the presence of dilute acid at moderate temperatures of around 160 °C forms furfural, and furfural can be catalytically reacted to form hydrocarbon products. Similarly, holding glucose at high temperatures in the presence of dilute acid forms HMF, which in turn breaks down to levulinic and formic acids which can in turn be converted into hydrocarbon fuels [10].

6.7 Conclusions

Biomass is a unique resource for sustainable production of liquid fuels that we particularly favor to power transportation. Cellulosic biomass offers the low costs and abundance essential to make a meaningful impact on fuel use. A variety of thermal and biological processes can be applied to convert biomass into fuels. However, the natural resistance of cellulosic biomass to breakdown to reactive compounds must be overcome to achieve low costs. Aqueous processing of cellulosic biomass can produce sugars that can be biologically fermented into fuels such as ethanol as well as various other products. In this case, the power of modern biotechnology offers the potential for very low costs. However, aqueous processing can also produce sugar dehydration products such as furfural, HMF, and levulinic acid that can be catalytically reacted to hydrocarbon fuels that are compatible with our existing infrastructure. Thus, aqueous processing of cellulosic biomass offers a versatile route to support low cost production of liquid fuels for transportation and other applications.

Acknowledgments

Support of the Ford Motor Company for the Chair in Environmental Engineering at the Center for Environmental Research and Technology of the Bourns Col-

lege of Engineering at the University of California, Riverside is gratefully acknowledged for making research such as described possible. We also thank the BioEnergy Science Center (BESC), a U.S. Department of Energy Bioenergy Research Center supported by the Biological and Environmental Research Office in the DOE Office of Science, for supporting our research. Other agencies that have made our research possible include the Defense Advanced Research Projects Agency (DARPA) through subcontracts by Logos Technologies and the University of Massachusetts, Amherst; the USDA National Research Initiative Competitive Grants Program, contract 2008-35504-04596; the US Department of Energy Office of the Biomass Program, contract DE-FG36-07GO17102. Finally, it is important to recognize the numerous past and present students, coworkers, and partners who make our research possible.

Bibliography

- [1] U.S. Department of Energy. *Annual Energy Review 2009*. Tech. rep. DOE/EIA-0384(2009). Washington, DC: Energy Information Administration, Aug. 2010.
- [2] L.R. Lynd. Overview and Evaluation of Fuel Ethanol from Cellulosic Biomass: Technology, Economics, the Environment, and Policy. *Annual Reviews of Energy and Environment* 21 (1996):403–465.
- [3] R. Perlack, L. Wright, A. Turhollow, R. Graham, B. Stokes, and D. Erbach. *Biomass as Feedstock for a Bioenergy and Bioproducts Industry: The Technical Feasibility of a Billion-Ton Annual Supply*. Oak Ridge National Laboratory, Oak Ridge, TN. Republished: U.S. Department of Energy, 2010. Annual Energy Review 2009. Report DOE/EIA-0384(2009) August. Washington, DC: Energy Information Administration, 2005.
- [4] L.R. Lynd, C.E. Wyman, and T.U. Gerngross. Biocommodity Engineering. *Biotechnology Progress* 15 (1999):777–793.
- [5] G.W. Huber, S. Iborra, and A. Corma. Synthesis of Transportation Fuels from Biomass: Chemistry, Catalysts, and Engineering. *Chemical Reviews* 106 (2006):4044–4098.
- [6] C.E. Wyman, S.R. Decker, M.E. Himmel, J.W. Brady, C.E. Skopec, and L. Viikari. Hydrolysis of Cellulose and Hemicellulose. In: *Polysaccharides: Structural Diversity and Functional Versatility*. Ed. by S. Dumitriu. 2nd ed. New York: Marcel Dekker, Inc., 2004. 995–1033.
- [7] A. Aden, M. Ruth, and K. Ibsen. *Lignocellulosic Biomass to Ethanol Process Design and Economics Utilizing co-current Dilute Acid Prehydrolysis and Enzymatic Hydrolysis for Corn Stover: National Renewable Energy Laboratory*. NREL/TP-510-32438. Golden, CO: National Renewable Energy Laboratory, 2002.
- [8] C.E. Wyman, B.E. Dale, R.T. Elander, M. Holtzapple, M.R. Ladisch, and Y.Y. Lee. Comparative Sugar Recovery Data from Laboratory Scale Application of Leading Pretreatment Technologies to Corn Stover. *Biore-source Technology* 96 (2005):2026–2032.

- [9] C. Wyman, B. Dale, R. Elander, M. Holtzapple, M. Ladisch, Y. Lee, C. Mitchinson, and J. Saddler. Comparative Sugar Recovery and Fermentation Data Following Pretreatment of Poplar Wood by Leading Technologies. *Biotechnology Progress* 25 (2008):333–339.
- [10] C.E. Wyman, V. Balan, B.E. Dale, R.T. Elander, M. Falls, B. Hames, M.T. Holtzapple, M.R. Ladisch, Y.Y. Lee, N. Mosier, V.R. Pallapolu, J. Shi, and R.E. Warner. Comparative Data on Effects of Leading Pretreatments and Enzyme Loadings and Formulations on Sugar Yields from Different Switchgrass Sources. *Bioresource Technology* 102(24) (2011):11052–11062.

Chapter 7

Analytical Approaches in the Catalytic Transformation of Biomass: What Needs to be Analyzed and Why?

Dmitry Murzin, Bjarne Holmbom

7.1 Introduction

Today, the use of biomass is considered a promising way to diminish negative environmental impact. Moreover, in some future scenarios, renewable raw materials are thought to be able to replace finite mineral-oil-based raw materials before 2050 [1]. This means that new synthetic routes, which should desirably adhere to the principles of green chemistry [2], need to be developed for the production of chemicals.

Lignocellulosic biomass, as a renewable source of energy and chemicals, has attracted a lot of attention recently [3–10]. Wood biomass consists of cellulose (40–50%), lignin (3–10%), hemicelluloses (15–30%) and a variety of extractives (1–10%). Cellulose is a linear polymer of D-glucopyranose and can contain up to 10,000 units ($C_6H_{10}O_5$), connected by glycosidic ether bonds, while the molecular mass for hemicelluloses is lower. Hemicelluloses have a more heterogeneous structure than cellulose, consisting mainly of five-carbon (xylose, arabinose) and six-carbon sugars (galactose, glucose and mannose). Contrary to cellulose lignin is a coniferyl alcohol polymer with coumaryl, coniferyl and sinapyl alcohols as monomers, which are heavily cross-linked, leading to complex structures of large lignin molecules [11].

Chemical treatment of lignocellulosic biomass in general, and wood in particular, can have several targets. One of the options is delignification of the biomass leading to cellulose and some residual hemicelluloses, which are further applied in the production of paper or board, or derivatives of cellulose. Thermal (or catalytic) treatment of biomass, e.g., thermal or catalytic pyrolysis, is a route to bio-based synthesis gas and biofuels [12]. Depolymerization results in the formation of low-molecular-mass components (sugars, phenols, furfural, various aromatic and aliphatic hydrocarbons, etc.), e.g., unique building blocks for further chemical synthesis.

Wood biomass contains many valuable raw materials for producing fine and specialty chemicals (Figure 7.1). These raw materials are carbohydrates, fatty acids, terpenoids and polyphenols, such as stilbenes, lignans, flavonoids and tannins. Some of them can be exuded directly from living trees, while others are extracted and purified via chemical methods.

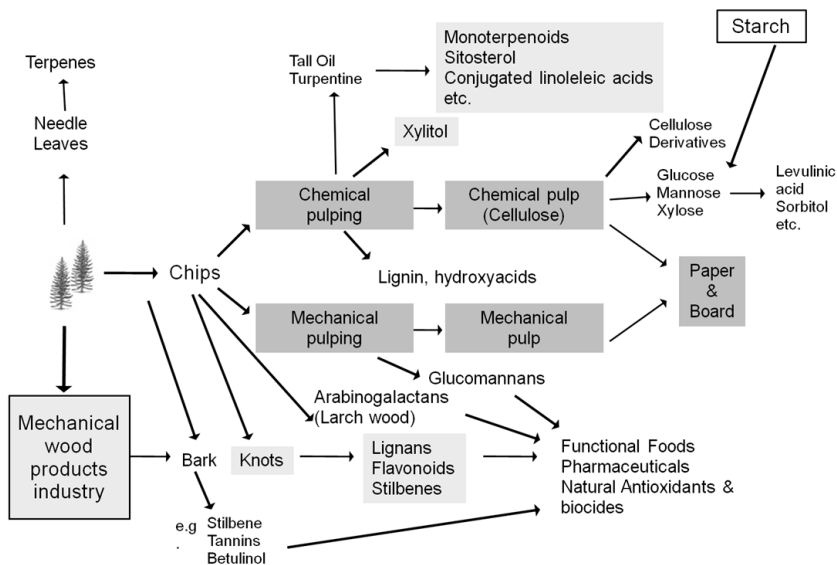


Figure 7.1: Chemical by-products from the forest industry

In this context, applications of catalytic reagents, which are superior to stoichiometric reagents producing stoichiometric amounts of wastes, are worth mentioning. Well-known benefits in using heterogeneous catalysts are associated with easy catalyst separation, regeneration and reuse, as well as relatively low prices compared to homogeneous catalysts. The research regarding catalytic transformations of different wood-derived compounds is currently very active [13].

Because of the complexity associated with the processing of biomass per se or the transformation of biomass-derived chemicals, in-depth chemical analysis of all components and their reactions is difficult to perform. Therefore, most analytical methods will be a result of a compromise between information depth and available resources. It is also obvious that in industrial processes only a limited number of rather fast analytical methods could be utilized since a large number of samples should be processed.

To have in-depth and molecular-level understanding of the chemical reactions occurring during the transformation of biomass not only advanced analytical methods are required, but additionally, a broad spectrum of these methods needs to be applied. Let us consider, for example, the catalytic conversion of cellulose [14–17] in the presence of hydrogen leading to sugar alcohols. During such a depolymerization reaction not only the concentration of carbohydrates and other products in the liquid phase should be measured, but also the crystallinity of cellulose, its morphology, molecular mass distribution and presence of sugar oligomers. The analysis is even more complicated if in this reaction wood is used directly instead of cellulose.

Analytical techniques have made a tremendous progress in recent years giving a possibility to utilize a wide range of modern instrumental methods, including advanced chromatography, microscopy and spectroscopy. It is apparently clear that all the methods currently available cannot be treated in this review, thus a rational selection of them was done by the authors based on their experience, with an understanding that it might not cover all the analytical methods presently utilized in catalytic transformations of biomass-derived chemicals, but focuses mostly on chromatography.

7.2 Analytical Objectives

Any planning of analytical procedures should be based on the goals and scope of the study. The following critical steps in an analytical process can be listed: problem definition and formulation of analytical objectives; set-up of an analytical plan; sampling; sample transport and storage; sample pretreatment; analytical determination; data calculation; evaluation of results to see if the objectives are achieved.

It is apparently clear from this list that the actual analytical determination is just one step among the others and sometimes could not even be the crucial one. Moreover, preparation of the samples, pretreatment and evaluation of data could be more demanding or at least time-consuming. Since in catalytic transformation of lignocellulosic biomass often wood or various streams from pulping are used as raw materials, a special attention should be devoted to sampling. Inappropriate sampling could undermine the value of the whole study, therefore it should be carefully planned. Sampling and sample storage is important since samples may be altered or destroyed due to temperature, light, presence of oxygen, humidity, enzymes or microbes (bacteria, fungi, etc.). For instance, enzymatic and microbiological attack can happen for samples of fresh wood, wet pulp and paper, sludge, process waters and effluents, while polyunsaturated extractives like abietic acid could be subjected to oxidation. Storage in a frozen state ($< -20\text{ }^{\circ}\text{C}$)

gives structural changes in wet, solid materials and physicochemical changes in process waters. Biocides could be added to preserve moist samples. The drying of samples could bring a risk of oxidation, therefore freeze-drying is usually recommended. The latter works by freezing the material and then reducing the surrounding pressure to allow the frozen water in the material to sublime directly from the solid phase to the gas phase.

7.3 Basic Analytical Methods

7.3.1 Chromatography

Chromatographic and spectroscopic methods are widely used today for analytical purposes. Chromatographic techniques are applied not only for off-line analysis, but also for the on-line determination of minute amounts, as well as large-scale preparative separations. In fact, not only monomers, but also polymers and oligomers can be separated by chromatography, although in the former case it is essentially a group separation. There are several forms of chromatography using different mobile and stationary phases, with the two main forms of instrumental chromatography being liquid (LC) and gas chromatography (GC). According to IUPAC definition, chromatography is a physical method of separation in which the components to be separated are distributed between two phases, one of which is stationary, while the other (mobile) moves in a definite direction.

7.3.2 Gas Chromatography

When relating gas chromatography to catalytic transformations of biomass, it can be stated that GC (Figure 7.2) provides qualitative and quantitative determination of organic components such as extractives, hemicellulose building blocks, organic acids, etc. The derivatized and vaporized products are introduced to the column for separation and identified in a detector, whose response is recorded as a chromatogram. Capillary columns made of fused silica with a stationary phase as a thin film of liquid or gum polymer on the inside of the tube are mainly used. The most commonly utilized stationary phases are siloxane polymer gums with different substituents providing different polarity. The polymers are usually cross-linked in the column by photolytic or free-radical reactions, bringing strength to the polymer films. Wall-coated open-tubular columns with a liquid phase coated directly on the inner walls, as well as support-coated open-tubular columns are applied. In the latter case a stationary phase is coated on fine particles deposited on the inner walls. Among non-polar columns, HP-1, DB-1, etc., based on dimethyl, polysiloxane could be mentioned. HP-5 with 95% dimethyl polysilox-

ane and 5% phenyl groups is slightly more polar. Still more polar columns employ polyoxyethylene or polyester liquid phases.

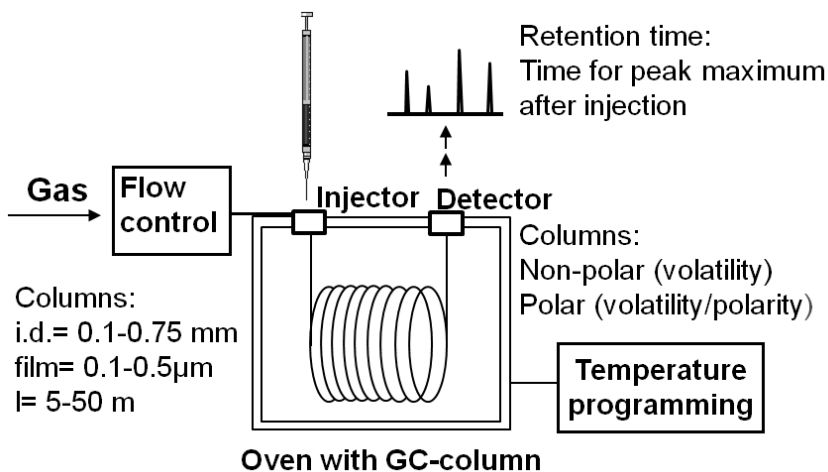


Figure 7.2: The schematic of gas chromatography

Capillary columns are available in a wide range of internal diameters, lengths and liquid film thicknesses (Figure 7.2). Although longer columns provide better separation, they have an increased analysis time which is usually undesired. In addition, longer columns lead to higher pressure and thus to problems with the injection. Columns with thicker films have higher capacity, but usually require higher temperature, while thin-film columns are suited for large molecules with low volatility. In principle, analysis of components with up to 60 carbon atoms is possible.

Different types of injection systems are used in GC. Split mode, where the injected material after evaporation is split between the column and an outlet, affords rapid volatilization and homogeneous mixing with the carrier gas. Most of the sample will pass out through the split vent and only a small proportion will flow into the column. Splitless systems provide a more reliable quantification allowing analysis of even such high-molecular mass compounds as triglycerides and steryl esters. Flame ionization detectors, which are of destructive nature, have high sensitivity to hydrocarbons, but are not able to detect water. On-line coupling of capillary columns with mass spectrometers is routine nowadays and enables convenient structure identification.

An important but sometimes forgotten issue is the fact that the sensitivity for different compounds is varying for a detector; thus, different peak areas are in proportion to the weight concentration. Knowledge of response factors is therefore necessary and calibration for components especially with various functional groups should be properly done. Commonly, internal standard compounds are applied, e.g., compounds which are not present in the sample itself are purposely added. Chemically they should be similar to the sample compounds with close retention time, however, with no peak overlapping (Figure 7.3).

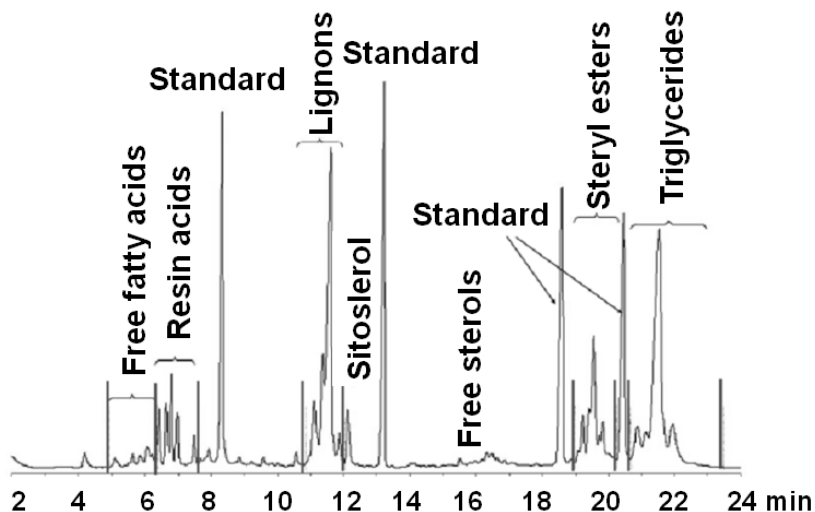


Figure 7.3: Example of a gas chromatogram on a short column with four standards added to a sample (spruce wood extract) [18]

In addition to such advantages of GC as accurate quantification based on internal standards, a possibility to be combined with a mass spectrometer and complete automation regarding injection and analytical runs, the very high resolution should also be mentioned. On the other hand only molecules up to about 1000 mass units can be analyzed, as they should be stable at high temperatures. Therefore, sometimes samples should be processed before the analysis. The last point is important for polar compounds, like for example acids, which should be derivatized. GC and GC-MS analysis in the vapour phase require volatile derivatives that do not adsorb onto the column wall. Different derivatizations

for different substances are recommended, e.g., silylation or methylation for extractives, methanolysis and silylation for carbohydrates. Silyl derivatives of R-O-Si(CH₃)₃ type containing a trimethylsilyl group (TMS) are formed by the displacement of the active proton in -OH, -NH and -SH groups. Thus, protic sites are blocked, which decreases dipole-dipole interactions and increases volatility. Common silylation reagents are listed in Figure 7.4.

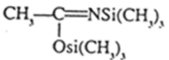
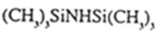
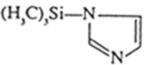
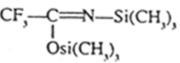
Reagent	Abbreviation	
N, O-Bis-(trimethylsilyl)-acetamide	BSA	
Hexamethyldisilazane	HMDS	
Trimethylchlorosilane	TMCS	
Trimethylsilylimidazole	TMSI	
N,O-Bis-(trimethylsilyl)-trifluoroacetamide	BSTFA	

Figure 7.4: Silylation agents

Methylation relies on the following reactions: utilization of diazometane (CH₂N₂): R-COOH + CH₂N₂ = RCOOMe + N₂; acid-catalyzed esterification: R-COOH + R'OH => RCOOR', as well as *on-column* esterification using tetramethyl ammonium salts R-COOH + N⁺Me₄OH⁻ => RCOOMe.

One of the variants of GC is associated with coupling pyrolysis to it (Figure 7.5). In this arrangement the sample is thermally degraded in an inert atmosphere. The degradation products are introduced to GC or GC-MS for separation and identification allowing qualitative and quantitative determination of semi-volatile and non-volatile components, such as extractives, polymers, paper chemicals, and lignin, etc.

7.3.3 Liquid Chromatography

These chromatographic methods use liquids such as water or organic solvents as the mobile phase. Silica or organic polymers as well as anion-exchange resins are used as stationary phase. Separation is performed either at atmospheric pressure or at high pressure generated by pumps. The last version is often called high-

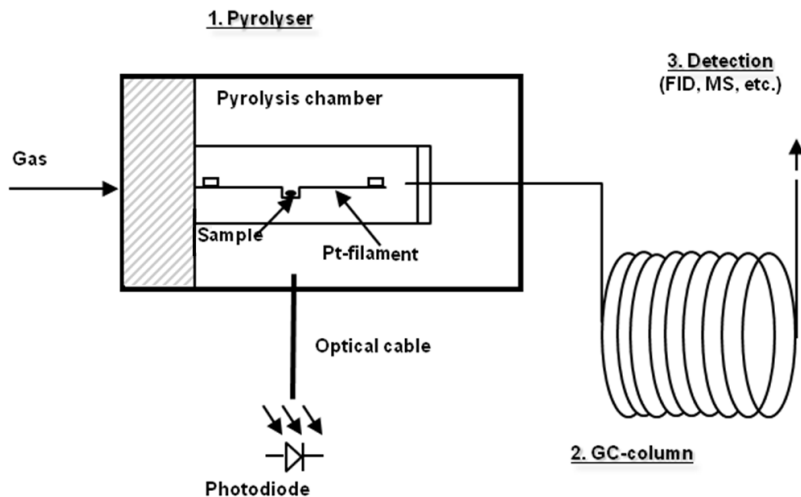


Figure 7.5: Pyrolysis GC

performance liquid chromatography (HPLC) with solvent velocity controlled by high-pressure pumps, giving a constant flow rate of the solvents. Solvents are used not only as single solvents but they can also be mixed in programmed proportions. In fact, even gradient elution could be applied with increasing amounts of one solvent added to another, creating a continuous gradient and allowing a sufficiently rapid elution of all components.

The most commonly used columns contain small silica particles (3–10 μm) coated with a nonpolar monomolecular layer.

For lipophilic (low-polar) compounds the mobile phase is an organic solvent, while reversed phase HPLC employs mixtures of water and acetonitrile or water and methanol as eluents and is applied for non-ionized compounds soluble in polar solvents. As examples, such columns (Figure 7.6) could be mentioned as Agilent Zorbax SB-Aq (4.6 \times 250 mm, 5 μm) allowing the use of highly aqueous mobile phases working in a pH range from 1 to 8 and affording reproducible retention and resolution for polar compounds. Another example is HypercarbTM

(4.6×100 mm, 5 μm) with 100% porous graphitic carbon as a stationary phase, which operates in the pH range 0–14 and can resolve highly polar compounds with closely related structures (e.g., geometric isomers, diastereomers, oligosaccharides). CarboPac PA1 (polymer based) column can be used in mono-, oligo- and polysaccharide analysis by high-performance anion-exchange chromatography combined at high pH with pulsed amperometric detection.

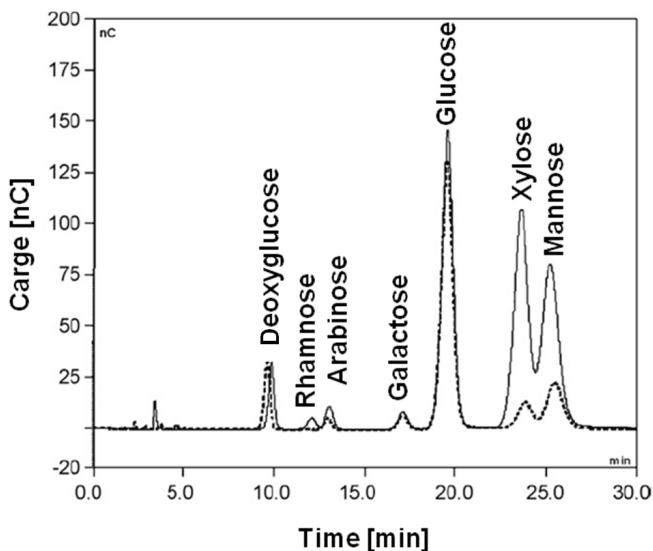


Figure 7.6: Separation of acids and sugars by HPLC using CarboPac PA1 [19]

UV-Vis (Figure 7.7) and diode-array detectors enabling recording of UV-Vis spectra, for example every second, are common nowadays. They can be used for the analysis of conjugated and aromatic compounds, such as phenols. Another popular detector is based on refractive index (RI) monitoring and is well suited, for example, for carbohydrates. High-performance anion-exchange chromatography with pulsed amperometric detection is a common technique for analyzing sugars in wood and pulp hydrolysates.

Another important form of HPLC is size-exclusion chromatography (Figure 7.8), which is widely applied for the determination of molecular-mass distributions of dissolved lignin and hemicelluloses, and even for cellulose dissolved in ionic liquids. The same method can be used for the analysis of extractives and their derivatives, for instance dimers and trimers of fatty acids [20]. In SEC,

solutes in the mobile phase (for example THF) are separated according to their molecular size. Smaller molecules penetrate far into the porous column packing material and thus elute later than larger ones.

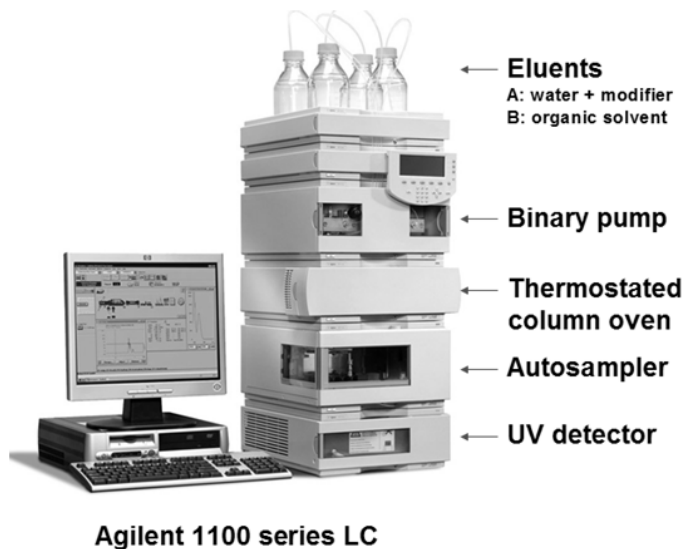


Figure 7.7: A view of LC-UV

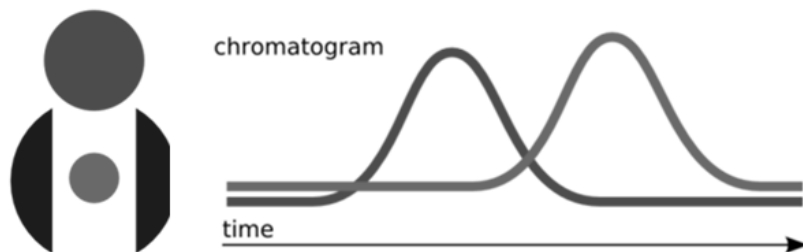


Figure 7.8: Size-exclusion chromatography

The non-destructive character as well as the absence of derivatization could be mentioned among the advantages of LC. This technique can handle both small

and large amounts and it can be used also for preparative isolation of compounds from mixtures. Contrary to GC there are almost no, or at least much fewer, limitations in terms of the molecular size. In addition, LC can be combined with mass spectrometry, once again without derivatization. Thermally unstable and polar compounds can thus be analyzed as such, and the molecular mass in triple quadrupole or ion-trap LC-MS can be up to m/z 3000, while time-of-flight versions allow even up to 16,000.

LC-MS provides better sensitivity and selectivity than GC-MS and is excellent for the quantification of selected substances in complex mixtures. On the other hand, this technique is not very suitable for rapid and reliable identification of unknown compounds mainly because fragmentation is sparse as the conditions of ionization are mild. Furthermore, spectra libraries enabling identification are not available. Other shortcomings of LC-MS are the rather low sensitivity of the detectors for certain compounds. Moreover, it may be difficult to obtain constant pressure, which in turn influences retention; clean, degassed solvents are needed and, finally, it might be challenging to find the optimum solvent mixture.

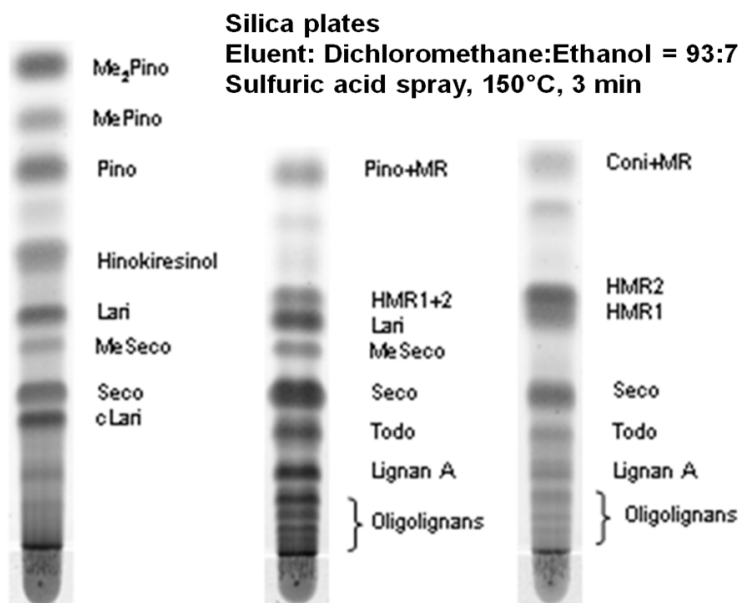


Figure 7.9: TLC of ethanol extracts of knots from: *Araucaria angustifolia* (left), *Abies alba* (center), *Picea abies* trees (right) [21]

Nevertheless, there is a large potential in the application of LC-MS toward analysis of oligosaccharides, lignans and oligolignans, flavonoids, stilbenes and tannins, and even fragments of lignin [21].

One form of LC, which is still used in organic synthesis and was popular until the 1960s in the analysis of monosaccharides obtained by hydrolysis of wood, is the so-called planar chromatography or thin-layer chromatography (TLC), where the separation is done in paper sheets or on particle layers deposited on glass, plastic or aluminium plates. Although these times of analysis of carbohydrates are long gone, TLC is an excellent technique for small scale preparative separation of fractions to be further analyzed by GC or LC. During analysis an eluent and the analytes rise in the stationary phase due to capillary forces. The analytes are separated according to their affinity to the stationary phase, which is most commonly silica (Figure 7.9).

7.3.4 Spectrometric Methods

Besides chromatography a wide variety of other techniques are available, such as capillary electrophoresis (CE), Infra Red spectrometry (IR), Nuclear Magnetic Resonance (NMR), Raman, Near Infra Red Spectrometry (NIR) and Ultra Violet-Visual Light Spectrometry (UV-Vis). Electrophoresis is a separation technique based on the differential transportation of charged species in an electric field through a conductive medium. Capillary electrophoresis (CE) was designed to separate species depending on their size to charge ratio in the interior of a small capillary filled with an electrolyte and can be used for analyzing oligosaccharide and monosaccharide reaction products. In the current review we focus mainly on chromatographic methods although the spectrometric methods listed above are certainly of great importance. For instance, UV spectrometry can be used for the determination of lignins in solutions. Colorimetric methods based on selective complexation with special reagents, which can be determined by spectrometric measurements in the UV-Vis range, are applied for the determination of metal ions, hemicelluloses and pectins. IR is a possibility to identify such functional groups as hydroxyls, carbonyls, carboxyls and amines.

For example, the analysis of products in rapeseed oil hydrogenation was conducted by IR [22]. However, IR spectra of large biomolecules are complex, moreover spectra of component mixtures could be difficult to interpret. An advantage of Raman spectroscopy for the transformation of biomass occurring often in water solutions is the easy detection of double and triple carbon-carbon bonds while the adsorption of water is weak. Thus, in contrast to FTIR, wet pulp and wood samples can be analyzed with signals related to extractives, lignin and carbon hydrogen bonds of the polysaccharides, while in FTIR signals of the hy-

droxyl groups of wood polysaccharides are dominating. NMR is an important method as it provides structural information about complex molecules, therefore it is frequently used for structural analysis of lignins and even hemicelluloses. Crystalline cellulose requires the application of solid-state NMR, as utilized for instance recently in the hydrolytic hydrogenation of cellulose [17].

7.3.5 Selection of Analytical Methods

Summarizing shortly the methods described above, it can be stated that the choice of analytical methods in general depends on sample characteristics, matrix complexity, the aim of the analysis, accessible equipment and the amount of resources available.

For instance in order to be analyzed by GC, compounds in the samples must be able to get volatilized and additionally possess thermostability. In case of LC, solubility in the mobile phase is important as well as size, structure and hydrophobicity, presence of functional groups, etc.

Regarding matrix complexity it could be also mentioned that chromatography can be used both for the separation of a compound from the matrix and for quantification and identification. It is important but rarely considered that no residual matter should remain in the samples; especially heavy compounds, which are difficult to evaporate in the GC columns, could significantly influence subsequent analyses. Thus, regular control of retention times and response factors, as well as column cleaning or replacement in due time should not be overlooked. For some samples related to the analysis of biomass even prefractionation could be necessary.

7.4 Analytical Examples

7.4.1 Analysis of Carbohydrates and their Transformation Products

Let us consider first the analysis of a sample of hemicelluloses dissolved in water. The general analytical strategy is given in Figure 7.10. An analytical procedure using GC based on acid methanolysis consists of the following steps [23]. Freeze drying of a 2 mL solution of hemicellulose in water with the subsequent addition of 2 M HCl in water-free methanol, is followed by keeping the sample at 100 °C for three hours of neutralization with pyridine, addition of internal standard (sorbitol), evaporation, silylation (hexamethyldisilazane and trimethylchlorosilane), and finally GC analysis. The latter could use, for instance, a split injector (260 °C, split ratio 1:15) with a 30 m/0.32 mm i.d. column coated with dimethyl polysiloxane (DB-1, HP-1), hydrogen or helium as a carrier gas and FID with a following temperature programme: 100–280 °C and ramping 4 °C/min.

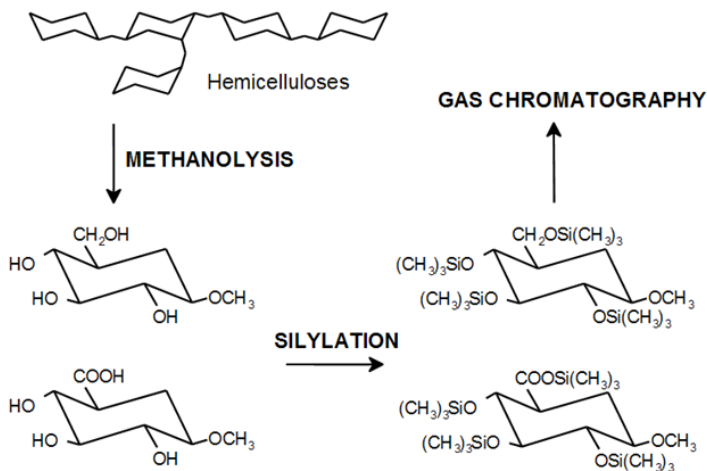


Figure 7.10: Analysis of sugar units in hemicellulose

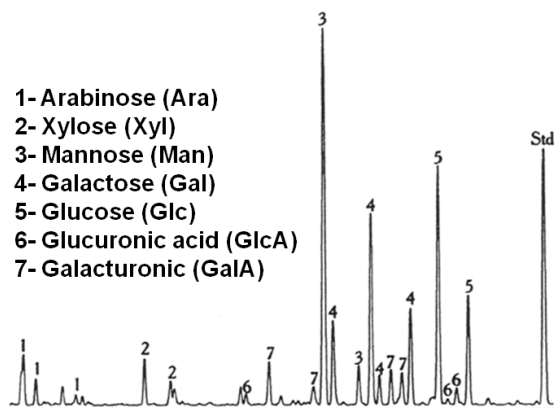


Figure 7.11: Typical gas chromatogram showing the major sugar units released upon methanolysis of a sample (spruce wood) containing hemicelluloses (Std = internal standard, sorbitol)

An advantage of direct methanolysis of wood samples is that essentially only hemicelluloses are cleaved and very little cellulose. Moreover, contrary to hydrolysis, it allows less degradation of released monosaccharides. Methanolysis can be used also for direct analysis of solid wood and fiber samples. A typical chromatogram is presented in Figure 7.11, showing several peaks for a particular sugar due to the presence of α & β anomers of pyranoses & furanoses (Figure 7.12).

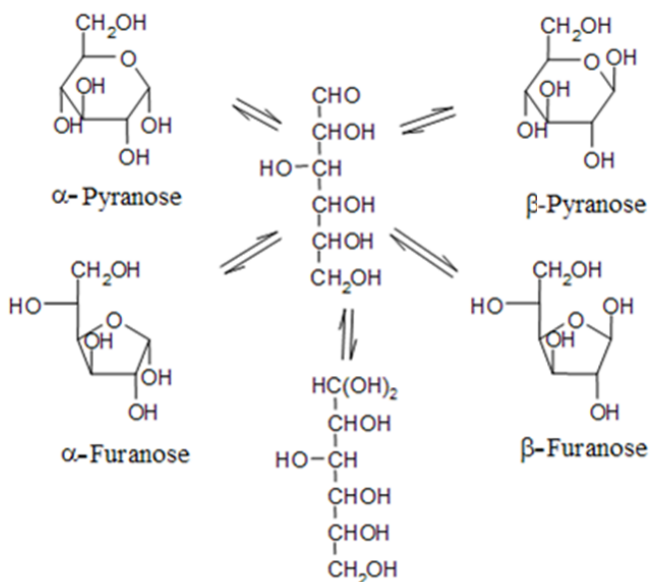


Figure 7.12: Equilibrium of different forms of sugars

Due to the complexity of the product mixture and the analytical procedure correction factors are needed. For instance, cleavage (the methanolysis) could be incomplete for certain glycosidic bonds, such as the Xyl-MeGlcA bond. Some degradation of formed sugars, especially uronic acids may happen and the products can have different detector responses. In order to determine correction factors it is recommended to perform methanolysis, silylation and GC analysis on a sample containing equal amounts of Ara, Xyl, Man, Glc, Gal, GlcA, GalA, etc., and pure hemicelluloses and pectins (if present) and to compare peak areas with the area of the internal standard.

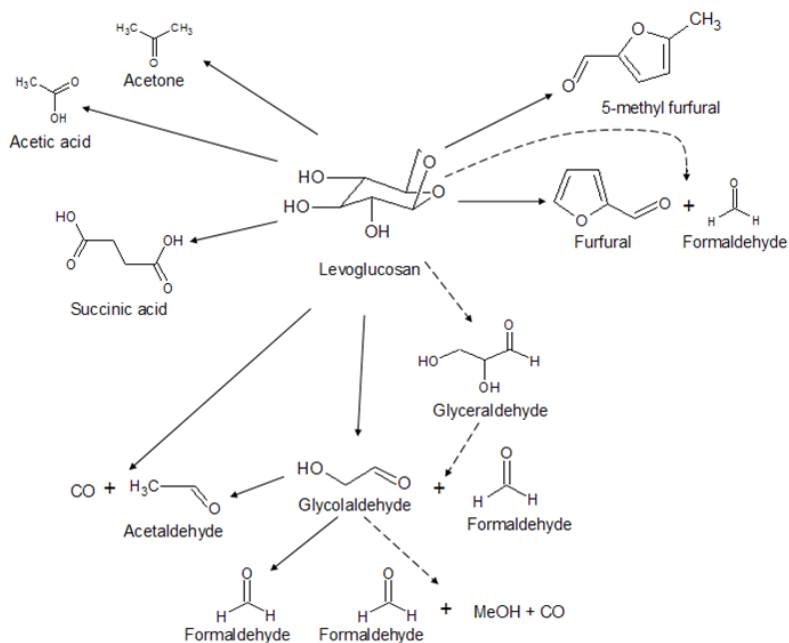


Figure 7.13: Transformations of levoglucosan [24]

Another example worth considering is the gas-phase catalytic transformation of levoglucosan over zeolites [24, 25]. The reaction scheme is given in Figure 7.13. In [24, 25] for HPLC analysis an acid Aminex cation H^+ column with sulfuric acid (0.005 M) as a mobile phase with a flow of 0.5 ml/min at 338 K was used, along with an Aminex HPX-87C column and mobile phase-calcium sulfate (1.2 mM) with a flow rate of 0.4 ml/min at 353 K. A refractive index detector was applied. Figure 7.14 illustrates that the separation is very much dependent on the analytical conditions.

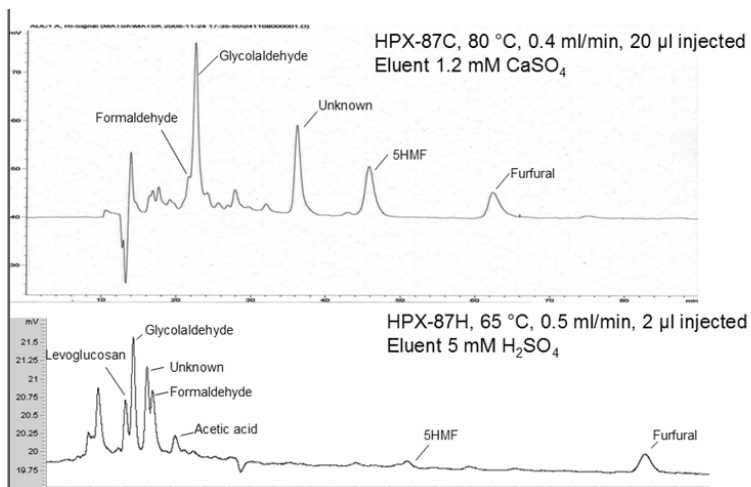


Figure 7.14: Analysis of a levoglucosan transformation mixture by HPLC with two different columns [26]

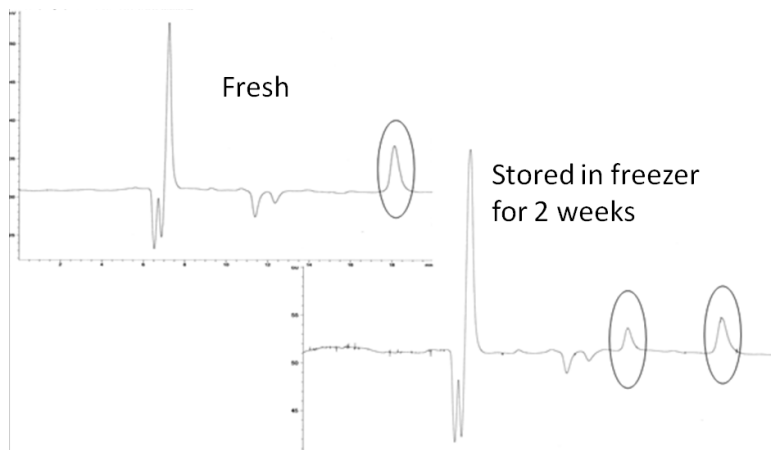


Figure 7.15: HPLC data showing instability of reaction products in levoglucosan transformations [26]

Stability of the samples is another important issue, which should also be carefully considered, as illustrated in Figure 7.15. Samples stored in a freezer exhibited another peak, which is certainly a result of transformations happening during storage.

An even more prominent difference in analysis was noticed in the aqueous reforming of sorbitol [27–29]. Comparison of the analysis for different columns is given in Figure 7.16 demonstrating that for the identification of reaction products tedious and time-consuming analytical work is required.

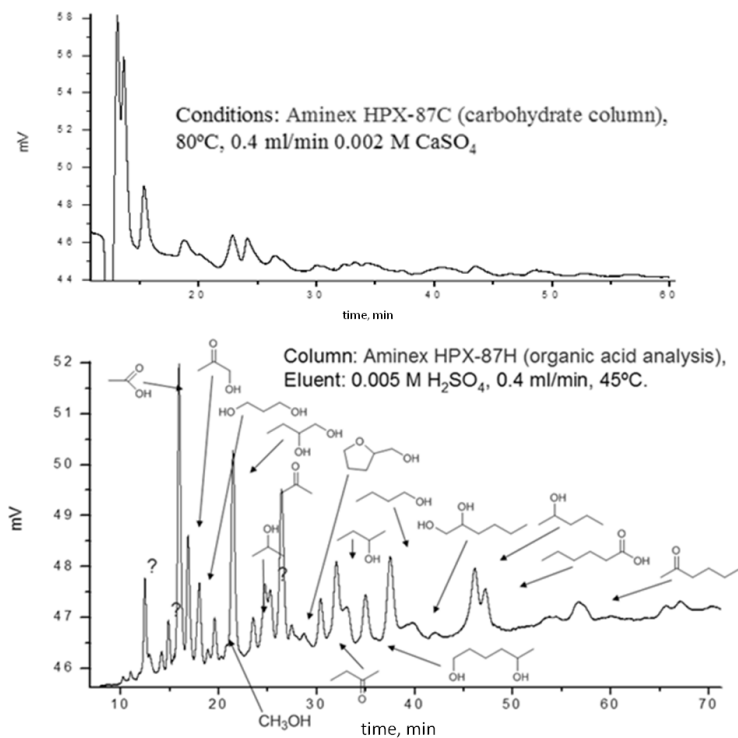


Figure 7.16: HPLC analysis of aqueous phase reforming products [29]

7.4.2 Analysis of Lignin

Structural information on lignins could be obtained by wet-chemical and spectroscopic methods using the approach for analysis of wood given in Figure 7.17.

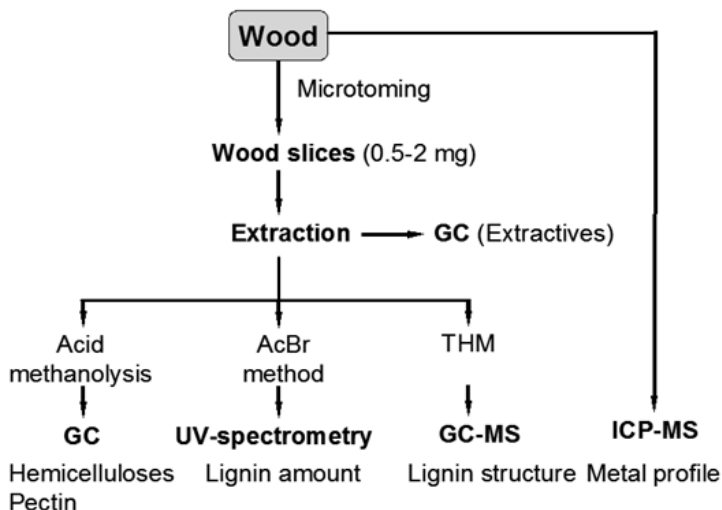


Figure 7.17: A scheme for the microanalysis of wood [30]

Here, 5 mL 20% AcBr in pure acetic acid is added to ca. 1–10 mg of wood followed by the addition of 0.1 mL perchloric acid (70%) and keeping the mixture for 3 hours at 50 °C, with subsequent neutralization with NaOH, dilution and UV-Vis analysis at 280 nm.

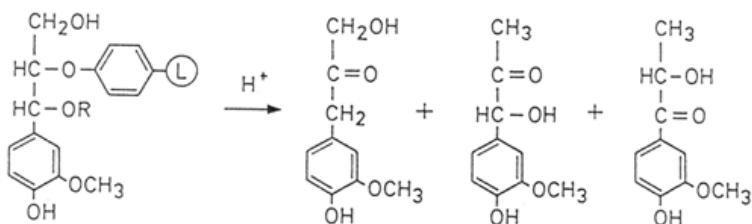


Figure 7.18: Acidolysis of lignin

Direct analysis of lignin in wood can be performed by selective / specific degradation followed by GC analysis. Among degradation methods acidolysis,

thioacidolysis, permanganate oxidation and pyrolysis can be mentioned. Acidolysis (Figure 7.18) cleaves predominantly β -O-4-ether bonds by acid hydrolysis and gives many degradation products with a rather low yield of ca. 60%.

Thioacidolysis (Figure 7.19) gives selective cleavage of β -O-4-ether bonds and results in less complex mixtures than acidolysis and also gives higher yields (> 80%) being able to quantify units with β -O-4-ether bonds and a free hydroxyl. This reaction is performed in dioxane-ethanethiol with boron trifluoride etherate. The degradation products are silylated prior to analysis by GC.

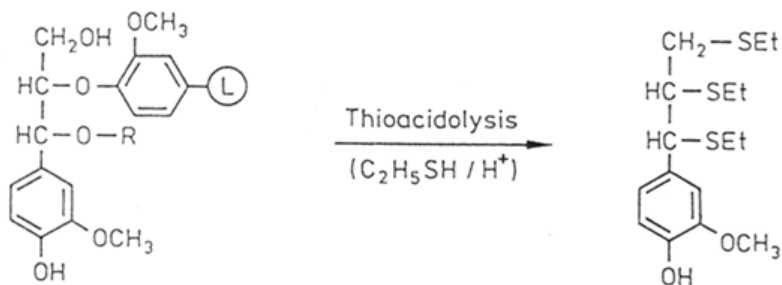


Figure 7.19: Thioacidolysis of lignin

Oxidation by permanganate ($\text{KMnO}_4 - \text{NaIO}_4$ at 82°C for 6 hours) in acidic solution of ethylated (at $\text{pH} = 11$ and 25°C with diazoethane for 25 hours) samples with further oxidation by alkaline peroxide for 10 min at 50°C and final methylation results in samples which can be analyzed by GC (Figure 7.20). This method gives information only on aromatic units with a free hydroxyl, comprising about 10% of lignin in wood and ca. 70% of lignin after kraft cooking.

Another method for the analysis of lignin is pyrolysis combined with GC-MS (Py GC-MS) allowing even a simultaneous determination of lignin and carbohydrates. Py GC-MS can be combined with advanced chemometric methods such as principal component analysis to enable a more complete identification of various lignin fragments. In summary, it can be stated that because of the heterogeneity of lignin there is no universal degradation method giving all desired information on the lignin structure, however, by combination of several methods the structure of lignin can be described fairly well.

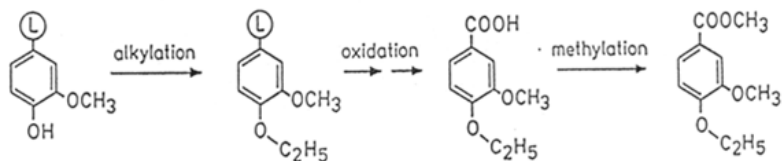


Figure 7.20: Oxidation method for the analysis of terminal units (free phenolic groups) in lignin

7.4.3 Wood Extractives

Wood contains a wide variety of components that are extractable with various organic solvents or water. Non-polar and semi-polar solvents (hexane, dichloromethane, diethyl ether, MTBE etc.) extract lipophilic oleoresin and fat components, while polar solvents (acetone, ethanol, water, etc.) extract hydrophilic phenolics, sugars, starch and inorganic salts. Acetone and ethanol extract also lipophilic extractives.

Location in the wood	Resin canals (Oleoresin)	Parenchyma cells	Heartwood	Cambium and growth zone	Ascending water Sap
Major compound classes	Resin acids Monoterpenoids Other terpenoids	Fats, fatty acids Steryl esters Sterols	Phenolic substances	Glycosides Sugars, starch proteins	Inorganics
Main function in the tree	Protection	Physiological food reserve, cell membrane comp.	Protection	Biosynthesis Food reserve	Photosynthesis Biosynthesis
Solubility					
Alkanes	+++	+++	0	0	0
DCM	+++	+++	++	0	0
Acetone	+++	+++	+++	++	+
Water	0	0	0	+++	++

Figure 7.21: Classification of wood extractives [31]

A classification of wood extractives is given in Figure 7.21, while the analytical procedure for extractives is outlined in Figure 7.22. Group analysis of fatty acids, resin acids, triglycerides, lignans and sterols can be done using a short column GC (5–7 m/0.53 mm capillary column with 0.15 μm film thickness), or by HP-SEC (Figure 7.23) as well as thin layer chromatography.

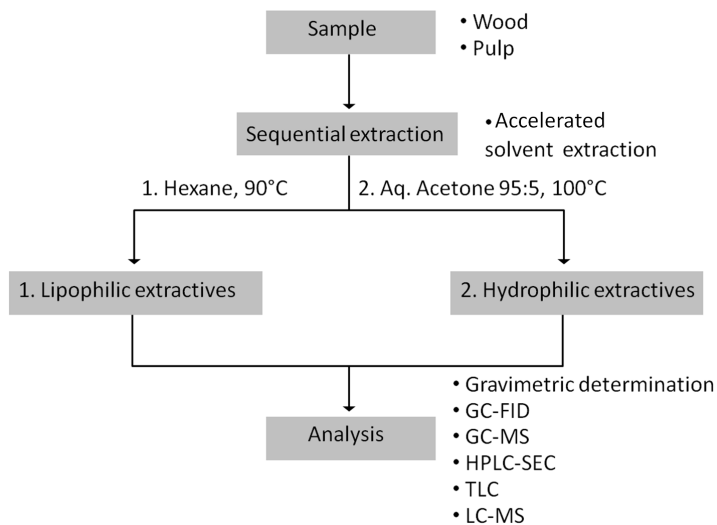


Figure 7.22: Analytical procedures for wood extractives

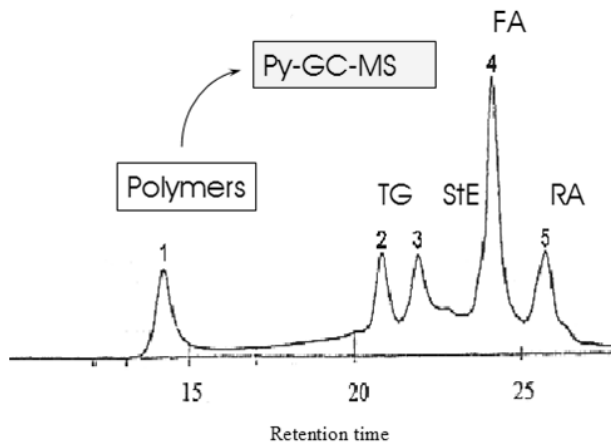


Figure 7.23: Separation of wood extractives with SEC. TG, StE, FA and RA stand for triglycerides, sterols, fatty acids and resin acids respectively [32].

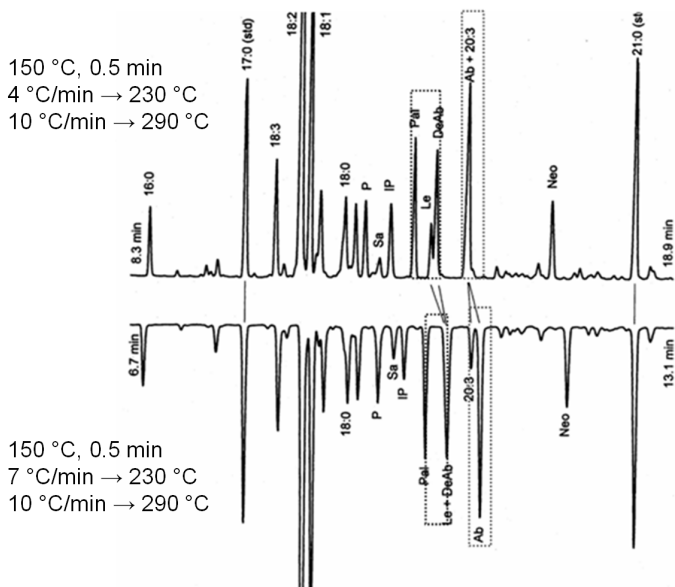


Figure 7.24: GC of fatty acids and resin acids with HP-1, 30 m, 0.32 mm i.d. column with different temperature gradients [31]

The analysis of individual compounds can be done by GC on a longer column (20–30 m/0.20–0.32 mm capillary columns) and reverse phase HPLC, while the identification of compounds can be performed by GC-MS, LC-MS, and NMR of isolated substrates. In case of a poor separation between compounds, the following parameters could be modified: temperature gradient, column polarity, type of derivative used in derivatization. As seen in Figure 7.24 a better separation, for example, between abietic acid and tri-unsaturated C20 fatty acid, is achieved with somewhat higher ramping. The HP-1 column usually follows a boiling point order, however, columns with different polarity could also be used (Figure 7.25) to allow better separation.

As previously mentioned, derivatization of fatty and resin acids is needed for accurate quantitative analysis. Although methylation is a commonly used method, silylation can sometimes afford better separation (Figure 7.26). In addition, for some GC columns peak-tailing is more severe for methyl esters than for silyl esters.

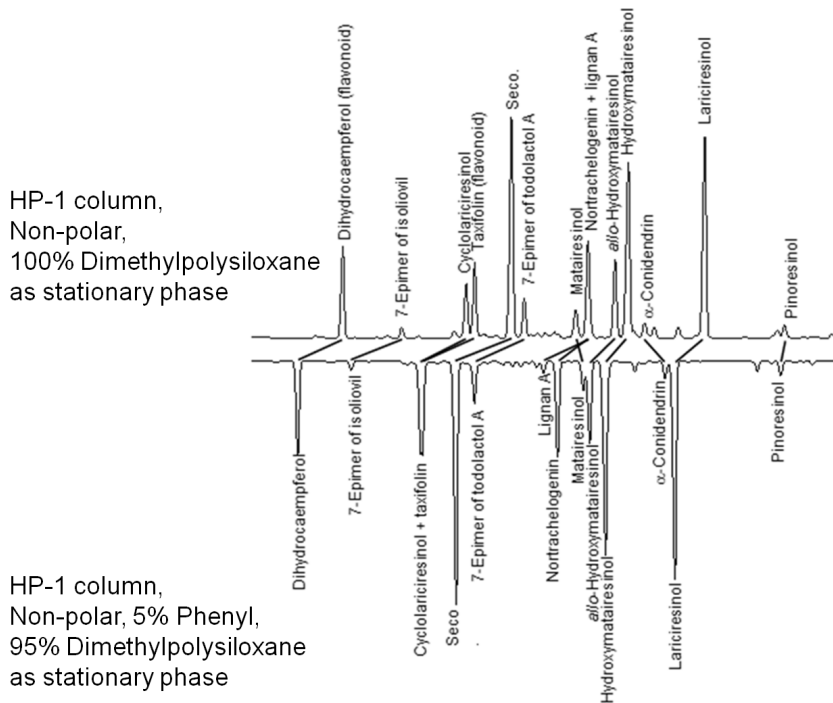


Figure 7.25: GC separation of phenolic extractives (flavonoids and lignans) using columns of different polarity [21]

7.5 Final Words

This chapter describes some of the contemporary methods for the chemical analysis of biomass-derived chemicals. All available methods could not have been treated in this review, therefore the focus was mainly on chromatographic methods. A more comprehensive overview of analytical methods was published several years ago by one of the authors [31, 33]. In the current work, detailed procedures were discussed for only a few cases as the emphasis was laid more on general approaches.

The analytical procedure depends very much on the objective of a particular study as well as the available resources in terms of instruments, time, costs and human skills.

The main hurdles on the way toward the development of a reliable analytical method for a particular application are associated with a lack of time to check methods described in literature, a certain trust in already published procedures, even if they are far from being perfect, as well as a pressure from granting agencies/sponsors to get “real” catalytic results rather than means to develop or check analytical methods. In the latter case there is certainly more glory in developing new methods compared to just checking the old ones.

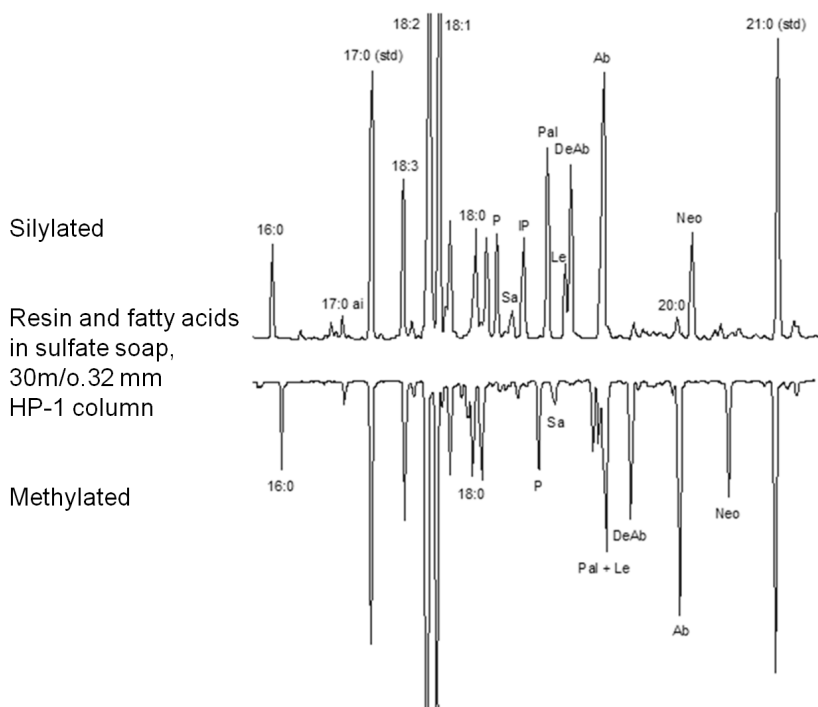


Figure 7.26: Comparison between GC analysis of methylated and silylated fatty and resin acids [31]

Finally, we should stress that no single method works perfectly for all kinds of samples. Moreover, dubious methods are sometimes presented in literature, which means that the results are not reliable. It can thus be emphasized once more that improving analytical methods, not only in the particular case of the catalytic transformation of biomass, but in general improves the quality of science.

Bibliography

- [1] C. Okkerse and H. van Bekkum. From Fossil to Green. *Green Chemistry* 4 (1999):107–114.
- [2] P.T. Anastas and J.C. Wagner. *Green Chemistry Theory and Practice*. New York: Oxford University Press, 1998.
- [3] T. Werpy and G. Petersen. *Top Value Added Chemicals from Biomass, Vol 1: Results of Screening for Potential Candidates from Sugars and Synthesis Gas*. Battelle: US Department of Energy, Energy Efficiency and Renewable Energy, 2004. URL: <http://www1.eere.energy.gov/biomass/pdfs/35523.pdf>.
- [4] G.W. Huber, S. Iborra, and A. Corma. Synthesis of Transportation Fuels from Biomass: Chemistry, Catalysts, and Engineering. *Chemical Reviews* 106 (2006):4044–4098.
- [5] L. Petrus and M.A. Noordermeer. Biomass to Biofuels, a Chemical Perspective. *Green Chemistry* 8 (2006):861–867.
- [6] G.W. Huber and A. Corma. Synergies between Bio- and Oil Refineries for the Production of Fuels from Biomass. *Angewandte Chemie International Edition* 46 (2007).
- [7] S. Lestari, P. Mäki-Arvela, J. Beltramini, G.Q. Max Lu, and D.Yu. Murzin. Transforming Triglycerides and Fatty Acids to Biofuels. *ChemSusChem* 2 (2009):1109–1119.
- [8] R. Rinaldi and F. Schüth. Design of Solid Catalysts for the Conversion of Biomass. *Energy & Environmental Science* 2 (2009):610–626.
- [9] D.M. Alonso, J.Q. Bond, J.C. Serrano-Ruiz, and J.A. Dumesic. Catalytic Conversion of Biomass to Biofuels. *Green Chemistry* 12 (2010):1493.
- [10] J. Zakzeski, P.C.A. Bruijninx, A.L. Jongerius, and B.M. Weckhuysen. The Catalytic Valorization of Lignin for the Production of Renewable Chemicals. *Chemical Reviews* 110 (2010):3552–3599.
- [11] E. Adler. Lignin Chemistry - Past, Present and Future. *Wood Science and Technology* 11 (1977):169–218.

- [12] A. Atutxa, R. Aguado, A.G. Gayubo, M. Olazar, and J. Bilbao. Kinetic Description of the Catalytic Pyrolysis of Biomass in a Conical Spouted Bed Reactor. *Energy Fuels* 19 (2005):765–774.
- [13] P. Mäki-Arvela, B. Holmbom, T. Salmi, and D.Y. Murzin. Recent Progress in Synthesis of Fine and Specialty Chemicals from Wood and Other Biomass by Heterogeneous Catalytic Processes. *Catalysis Reviews, Science and Engineering* 49 (2007):197.
- [14] A. Fukuoka and P.L. Dhepe. Catalytic Conversion of Cellulose into Sugar Alcohols. *Angewandte Chemie International Edition* 45 (2006):5161–5163.
- [15] P.L. Dhepe and A. Fukuoka. Cellulose Conversion under Heterogeneous Catalysis. *ChemSusChem* 1 (2008):969–975.
- [16] A. Fukuoka and P.L. Dhepe. Sustainable Green Catalysis by Supported Metal Nanoparticles. *The Chemical Record* 9 (2009):224–235.
- [17] V. Jolle, F. Chambon, F. Rataboul, A. Cabiac, C. Pinel, E. Guillon, and N. Essayem. Non-Catalyzed and Pt/Gamma- Al_2O_3 -Catalyzed Hydrothermal Cellulose Dissolution–Conversion: Influence of the Reaction Parameters and Analysis of the Unreacted Cellulose. *Green Chemistry* 11 (2009):2052–2060.
- [18] F. Oersa and B. Holmbom. A Convenient Method for the Determination of Wood Extractives in Papermaking Process Waters and Effluents. *Journal of Pulp and Paper Science* 20 (1994):J361–J365.
- [19] S. Willför, A. Pranovich, T. Tamminen, J. Puls, C. Laine, A. Suurnaekki, B. Saake, K. Uotila, H. Simolin, J. Hemming, and B. Holmbom. Carbohydrate Analysis of Plant Materials with Uronic Acid-Containing Polysaccharides - A Comparison between Different Hydrolysis and Subsequent Chromatographic Analytical Techniques. *Industrial Crops and Products* 29 (2009):571–580.
- [20] P. Tolvanen, P. Mäki-Arvela, N. Kumar, K. Eraenen, R. Sjoeholm, J. Hemming, B. Holmbom, T. Salmi, and D.Yu. Murzin. Thermal and Catalytic Oligomerisation of Fatty Acids. *Applied Catalysis A: General* 330 (2007):1–11.
- [21] S.M. Willför, A.I. Smeds, and B.R. Holmbom. Chromatographic Analysis of Lignans. *Journal of Chromatography A* 1122 (2006):64–77.

- [22] I.V. Deliy, N.V. Maksimchuk, R. Psaro, N. Ravasio, V. Dal Santo, S. Racchia, E.A. Paukshtis, A.V. Golovin, and V.A. Semikolenov. Kinetic Peculiarities of cis/trans Methyl Oleate Formation during Hydrogenation of Methyl Linoleate over Pd/MgO. *Applied Catalysis A: General* 279 (2005):99–107.
- [23] A. Sundberg, K. Sundberg, C. Lillandt, and B. Holmbom. Determination of Hemicelluloses and Pectin in Wood and Pulp Fibres by Acid Methanolysis and Gas Chromatography. *Nordic Pulp & Paper Research Journal* 226 (1996):216–219.
- [24] M. Käldestrom, N. Kumar, T. Heikkilä, M. Tiitta, T. Salmi, and D.Yu. Murzin. Formation of Furfural in Catalytic Transformation of Levoglucosan over Mesoporous Materials. *ChemCatChem* 2 (2010):539–546.
- [25] M. Käldestrom, N. Kumar, T. Salmi, and D.Yu. Murzin. Levoglucosan Transformation over Aluminosilicates. *Cellulose Chemistry and Technology* 44 (2010):203–209.
- [26] M. Käldestrom and D.Yu. Murzin. *unpublished data*.
- [27] A.V. Kirilin, A.V. Tokarev, E.V. Murzina, L.M. Kustov, J.-P. Mikkola, and D.Yu. Murzin. Reaction Products and Intermediates and their Transformation in the Aqueous Phase Reforming of Sorbitol. *ChemSusChem* 3 (2010):708–718.
- [28] A.V. Tokarev, A.V. Kirilin, and D.Yu. Murzin. *unpublished data*.
- [29] A.V. Tokarev, A.V. Kirilin, E.V. Murzina, K. Eraenen, L.M. Kustov, D.Yu. Murzin, and J.-P. Mikkola. The Role of Bioethanol in Aqueous Phase Reforming to Sustainable Hydrogen. *International Journal of Hydrogen Energy* 35 (2010):12642–12649.
- [30] A. Pranovich, J. Konn, and B. Holmbom. Methodology for Chemical Microanalysis of Wood. In: *Proceedings 9th European Workshop on Lignocellulosics and Pulp*. Vienna: BOKU, 2006. 436–439.
- [31] B. Holmbom. Extractives. In: *Analytical Methods on Wood Chemistry, Pulping and Papermaking*. Berlin: Springer Verlag, 1998. 125–148.
- [32] B. Holmbom. *unpublished data*.
- [33] B. Holmbom and P. Stenius. Papermaking Science and Technology. In: *Forest Products Chemistry*. 3. ISBN 952-5216-03-9. Fapet Oy, 2000. 105–169.

Chapter 8

Methods for Biomass Compositional Analysis

Amie Sluiter, Justin Sluiter, Edward J. Wolfrum

8.1 Introduction

Biomass, or plant derived material, is of interest as a fuel source for several reasons. Foremost, when managed wisely, it has the potential to become a sustainable source of hydrocarbon fuels. It is a leading near-term solution to fill the gap between growing global energy demand and dwindling petroleum availability. The conversion of biomass to renewable fuels has the potential to be carbon neutral, where carbon dioxide produced during fuel production and consumption is utilized by the next generation of plants during growth cycles [1]. Finally, many geographic areas contain some type of plant material that can be utilized as a fuel source, eliminating the need for long-distance fuel transport.

Many types of biomass are inherently heterogeneous, especially lignocellulosic biomass, or non-edible plant material. Biomass derives from living, growing plants that change during their life cycle. Since plants are a living organism, the polymer matrix of the material is very complex and difficult, or impossible to control [2]. Figure 8.1 demonstrates the variety of constituents within the anatomical fractions of a single plant. The variable nature of biomass feedstocks represent a risk in processing environments, as processes can be difficult to optimize without steady state input.

Cellulosic biomass feedstocks can be processed in several ways to make fuels. In the biochemical conversion process, the cellulosic biomass is converted to monomeric carbohydrates, which are then fermented to ethanol, butanol, or other liquid fuels. Alternative conversion techniques include thermochemical conversion to either pyrolysis oil or synthesis gas, or catalytic conversion of the monomeric carbohydrates in aqueous solution. The techniques for biomass feedstock compositional analysis are largely independent of the conversion process, although the analyses of process intermediates are obviously dependent on the conversion process. We are writing this work from the perspective of our experience in biochemical conversion research.

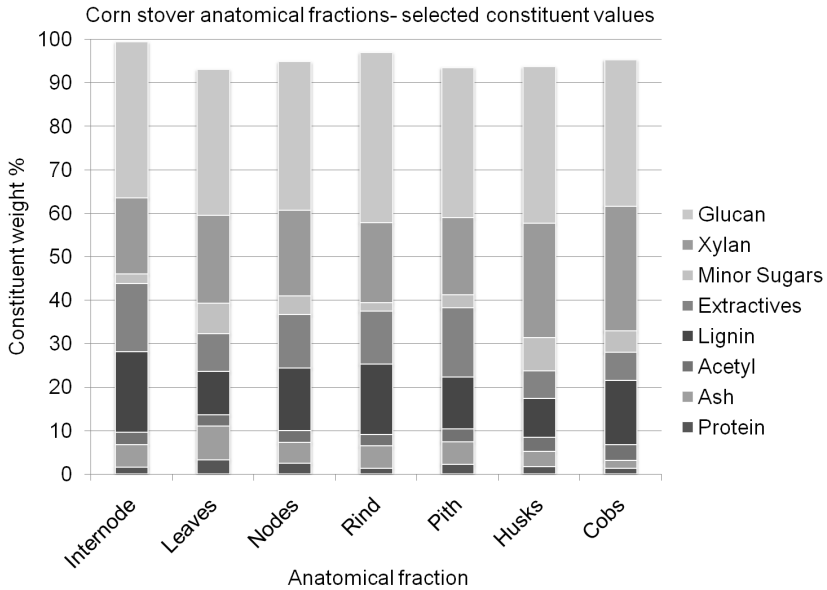


Figure 8.1: This figure demonstrates the variety of constituents within a single type of biomass separated into individual fractions. This sample of corn stover was separated by hand into anatomical fractions, and each fraction was individually analyzed. For visual simplicity, some constituents have been grouped, such as extractives and minor sugars.

In this chapter, we first review the constituents of biomass, and then discuss methods used to measure both feedstocks and biochemical conversion process intermediates, concentrating primarily on the so-called *fiber analysis methods* used in our laboratories. We discuss the uncertainties associated with these methods, and the influence of these uncertainties on derived values from experiments. Finally, we briefly discuss new developments in the rapid analysis of biomass using spectroscopic methods.

8.2 Biomass Composition

Plant derived biomass consists of many different constituents. A detailed description of biomass composition can be found at <http://www1.eere.energy.gov/>

biomass/feedstock_glossary.html, but the principal constituents are structural carbohydrates, lignin, protein, ash, and non-structural materials.

The structural carbohydrates are typically divided into two groups, cellulose and hemicellulose. Cellulose is a polymer with a rigid structure of repeating glucose units, and is highly stable and resistant to chemical attack. It has a high degree of hydrogen bonding, which contributes to the rigidity of the structure [3]. Hemicellulose is a polymer consisting of shorter, highly branched chains of sugars. Hemicellulose can contain five-carbon sugars, such as xylose and arabinose, as well as six-carbon sugars, such as glucose, galactose, and mannose. The backbone may be mannose or xylose, with a variety of side chain sugars [4]. The branched character of hemicellulose causes it to be more amorphous and easier to break down compared to cellulose.

Aside from carbohydrates, the major structural materials present in lignocellulosic biomass include lignin, ash, and protein. Lignin is a polymeric structure that is highly aromatic and branched. It has a high molecular weight and a complex structure. Lignin assists in holding the cells together, provides the plant with rigidity, and gives it some resistance to insect and biological degradation. Ash is any inorganic matter, typically silica. Protein is a compact structure made up of chains of amino acids.

Materials that are not a part of the cellular structure and can be removed with solvents are termed extractives for the purpose of biomass compositional analysis. This is an inexact definition; extractives can include waxes, saps, and fats. Different solvents remove different portions of the soluble material. For example, a water extraction can remove surface material such as soil and fertilizers and can also remove non-structural, low molecular weight carbohydrates, like sucrose, that were present in the plant when it was harvested. Extractions with ethanol, toluene, or other organic solvents can isolate waxes, fats, and resins.

8.3 Measuring Biomass Composition: Forage and Fiber Analysis

Determining the composition of biomass is a detailed and complex undertaking when all of the constituents are individually measured. The goal of most biomass analysis for fuels is summative mass closure, where all of the constituents are accounted for and 100% of the weight of the material is classified. Quantifying all of the constituents is vital to calculate fuel conversion yields and mass balance [5]. Though a single constituent may make up a very small portion of the biomass, when dealing with tens or hundreds of tons of material in a processing environment, even one or two weight percent of the material can comprise a significant amount of material. Without analysis, the planning for disposal or potential use of every fraction becomes impossible.

8.3.1 Forage Analysis Methods

Forage analysis methods are widely used in agriculture to assess the quality of feedstocks for animal nutrition. The two most widely used forage analysis methods are neutral detergent fiber (NDF) and acid detergent fiber (ADF). A complete discussion of all forage analysis methods can be found at the National Forage Testing Association [6].

The NDF and ADF analysis methods are essentially extraction techniques; the reported value is the mass fraction remaining after contacting the biomass samples with an acidic or neutral surfactant solution, rinsing, and drying. Acid detergent lignin (ADL) is a classical Klason lignin analysis performed on the ADF residue. These methods are sometimes combined to provide estimates of hemicellulose (NDF-ADF) and cellulose (ADF-ADL). The assumption behind the hemicellulose calculation is that NDF removes all non-structural material while ADF removes non-structural material and hemicellulose, so the difference between these results is hemicellulose. The cellulose calculation assumes that ADF leaves behind only cellulose and lignin, which is subsequently removed by ADL.

Because they are extractive techniques, NDF and ADF methods do not provide information about the structural carbohydrates in the same manner as the fiber analysis methods discussed below. We recently attempted to correlate forage and fiber analysis measurements and found that the highest correlations between NDF and/or ADF was with the extractives measurement performed as part of the fiber analysis method [7]. We found little correlation between the forage analysis results and the fiber analysis results when the latter were calculated on an extractives-free basis. Thus, we found the forage analysis methods relatively uninformative for the purposes of structural carbohydrate analysis.

8.3.2 Fiber Analysis Methods

Fiber analysis methods for biomass have a long history, dating back more than 100 years. The methods we use are built on the knowledge gleaned from decades of biomass analysis research [4, 8]. Essentially, all fiber analysis methods begin with an extraction step to remove the non-structural material from the biomass sample. The extracted material then undergoes acid hydrolysis (typically a concentrated acid hydrolysis step performed at room temperature followed by a dilute acid hydrolysis step at elevated temperature) to break down the structural carbohydrates to their monomeric forms, which can then be measured chromatographically. Lignin is typically measured gravimetrically as the acid-insoluble residue.

Many different laboratories use fiber analysis methods. Recently, ten different laboratories participated in a round-robin analysis [9] of the four biomass reference materials available from the National Institute of Standards and Technology (sugarcane bagasse, poplar, pine, and wheat straw) [10]. Not surprisingly, different laboratories got different results during the analysis.

Fiber analysis methods are empirical in nature; if they are executed with care they will provide repeatable results over time. However, our experience is that small deviations in a standard method can have large impacts on the measured constituent values. For example, we have found that inadequate mixing of the hydrolysate during the dilution from the very viscous first stage hydrolysis to the less viscous and more dilute second stage acid hydrolysis will lead to irreproducible results due to uneven hydrolysis, and failure to adequately mill pretreated solids results in skewed lignin and carbohydrate values due to incomplete hydrolysis.

In the following sections, we discuss the fiber analysis methods in use at the National Renewable Energy Laboratory for biomass compositional analysis. Again, other laboratories have developed fiber analysis methods that can also provide robust, reproducible results. Our goal in this work is to describe in detail the methods we use to give the reader an in-depth understanding of the details of these methods and to help researchers using these methods to improve their techniques by learning about the issues we have faced using these methods.

8.4 Summative Compositional Analysis of Biomass Feedstocks

Researchers at the National Renewable Energy Laboratory (NREL) have developed a system of individual published methods for the summative mass closure analysis of biomass based on classical fiber analysis methods. Figure 8.2 demonstrates the high level of interest in these procedures. A detailed lineage of these methods can be found in a recent publication [11]. We refer to these incremental methods as Laboratory Analytical Procedures (LAPs). The LAPs are publicly available at http://www.nrel.gov/biomass/analytical_procedures.html, and updates are posted as they are available. A number of these procedures have been adopted as ASTM standards as well.

By combining the appropriate LAPs, the goal is to break the biomass sample down into constituents that sum up to 100% by weight. Some of these constituents are individual components, such as individual carbohydrates, and some are groups of compounds, such as extractable material. However, the goal of these analyses is to characterize all of the material in the sample. If the constituents do not sum up to 100%, the analysis should be revisited to determine missing or incorrectly quantified components. There are several points within the compositional

analysis where decisions must be made to optimize the analysis. Some of these decisions are based on the type of biomass present, and some decisions must be made to accurately measure all components that are present. We provide a discussion to aid these decisions below. The Summative Mass Closure LAPs provide an overview of the individual LAPs, detail how the individual LAPs integrate, and highlight many of the pitfalls that can cause an analysis to fail [12, 13].

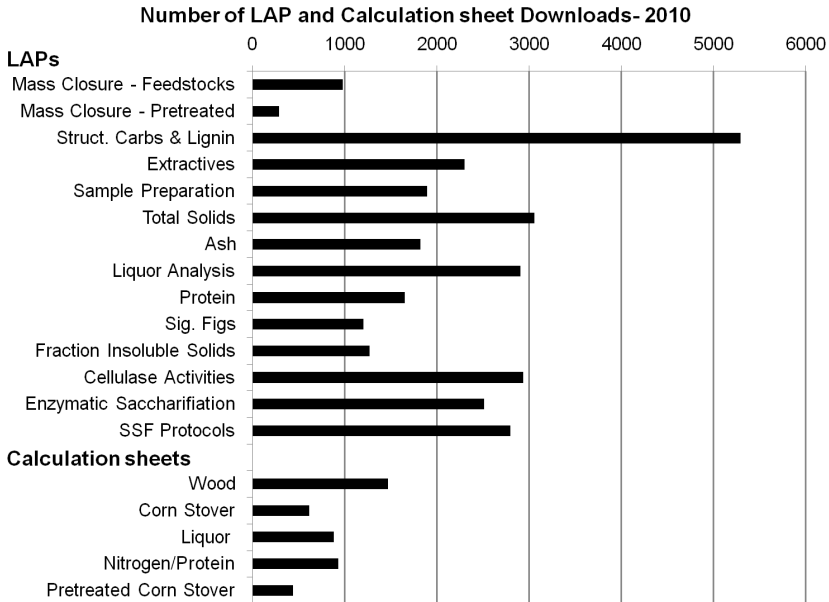


Figure 8.2: The high level of interest in NREL's Laboratory Analytical Procedures is captured by the number of downloads of the LAPs in 2010. The core hydrolysis procedure is contained in the Structural Carbohydrates and Lignin LAP, which alone was downloaded over 5000 times. The calculation *sheets* designed to accompany the LAPs were downloaded a combined 4000 times. Interestingly, the majority of downloads were for woody feedstocks.

In the following sections we summarize the process we use to perform biomass compositional analysis. Reading these sections carefully and completely is NOT a substitute for reading and understanding the complete procedures. The LAPs have been optimized for corn stover and generally work well on woody

feedstocks and herbaceous materials such as switchgrass, sorghum, and miscanthus, although minor adjustments may be necessary. Some LAPs are not appropriate for chemically or thermally altered material. Unusual feedstocks will typically require some method development to capture constituents not included in the LAP suite.

8.4.1 Sample Preparation

The details of sample preparation are found in the NREL LAP *Preparation of Samples for Compositional Analysis* [14]. The first step in biomass analysis is preparing the sample for analysis. Biomass samples typically arrive from the field in an intact or semi-intact state that includes soil or other debris and a significant moisture content. Proper sample preparation will minimize interferences in subsequent compositional analyses. Sample drying, particle size reduction, and potential sieving are discussed in this LAP.

To be accurately analyzed, the sample must be less than 10% moisture by weight and be milled to a certain particle size. This LAP covers several methods for drying the sample. Air-drying, the simplest option, can be used when ambient humidity and temperature allow the sample to dry to specified conditions without degrading. When ambient humidity is too high to permit this technique, samples must be monitored for degradation and microbial growth until the moisture content is less than 10% by weight. Samples can also be dried at 45 °C in a convection oven. This method should be used with care, as temperatures exceeding 45 °C can cause thermal degradation. Lyophilization, or freeze-drying, is also covered. This method can be used for samples that need to be dried under mild conditions or are very wet. Lyophilization is an unsuitable technique for large or bulk samples and those with large pieces of biomass.

After drying, the sample needs to be reduced to a uniform specific particle size. Since the subsequent methods are optimized for a -20/+80 mesh particle size, milling the sample will likely be necessary [15, 16]. Knife milling is the preferred method, as screens can ensure consistent particle size. Prior to milling, the sample must meet moisture requirements discussed above. Milling wet samples can result in the degradation of the sample during milling. The mill must be monitored to ensure that it is operating at optimal temperature. An overheated mill can cause extractable material to separate from the biomass and deposit on the heated metal portions of the mill or may partially degrade the biomass. Milling with dry ice is not recommended, as contaminants potentially present in dry ice leave a residue on the biomass. Care should also be taken to ensure that the biomass fed into the mill has been reduced to an appropriate size, and that the mill does not bind or overheat.

Sieving a sample is occasionally necessary, but the composition of the biomass may change with sieving. Specifically, the fraction of the biomass removed during sieving may be higher in ash content than the bulk sample. Sieving should only be used when necessary, such as with samples containing an ash content high enough to interfere with later analyses. Sieving of biomass prior to acid hydrolysis was introduced to prevent excessive degradation of small particles during analysis. The acid hydrolysis steps were optimized for a -20/+80 mesh particle size, and deviation to a larger particle size distribution can cause structural carbohydrates to be incompletely dissolved into solution. Such deviation will result in higher acid insoluble lignin values and lower overall structural carbohydrates, especially cellulose. Deviation from the recommended particle size to a smaller particle size may result in degradation of the structural carbohydrates, contributing to an overproduction of sugar degradation products, which can complicate the acid soluble lignin measurement.

Sieving was originally developed for the analysis of very homogeneous materials, such as wood samples. However, when herbaceous feedstocks were first analyzed it became apparent that the heterogeneity of the feedstock caused partitioning of components during sieving. Therefore, for feedstocks with a high degree of heterogeneity, such as herbaceous materials, sieving is not recommended. Also, reactor processes usually require whole sample composition, and mathematically adding the measured composition of a sieved fraction back into the bulk sample can be complicated.

Sieving can be performed to purposefully remove a portion of the higher ash content fraction. This should only occur when the ash content of the extracted biomass is high enough to interfere with hydrolysis. Further discussion of ash interference is included with the hydrolysis discussions.

Once prepared, the biomass should be carefully stored. Airtight storage containers will prevent unwanted moisture changes. However, biomass can settle and separate into fractions while stored, even for a short while. When sampling a stored sample, homogenize the sample well prior to removing an aliquot, to ensure a representative sample. Large samples may need specific homogenization procedures, such as riffle splitting or the *cone and quartering* technique, prior to removing a subsample.

8.4.2 Measuring Total Solids

The details of determining moisture content, or total solids content, are found in LAP *Determination of Total Solids in Biomass and Total Dissolved Solids in Liquid Process Samples* [17]. Since all measured constituents are reported on a dry weight basis, the moisture content of the sample must be measured several

times throughout the analysis. Reporting values on a dry weight basis means that the water weight of the sample has been mathematically removed from the constituent value. That is, the ash content of a biomass sample that contains 50% moisture and 10% ash is 20% on a dry-weight basis. We believe that this is the best way to compare samples on a consistent basis. As this measurement is used to correct all other measurement during the analysis, it is one of the most critical measurements. Any errors made during measurement of moisture will propagate through the remaining values and lead to increased uncertainties.

The moisture content of biomass can change very quickly (sometimes within minutes), depending on how the sample is stored as well as ambient conditions in the laboratory. Therefore, every time a sample is weighed for an analysis, a concurrent moisture determination must be performed. The LAP describes two methods of moisture determination, one using a 105 °C convection oven and one using an automatic infrared moisture analyzer. This LAP should not be used for samples that may chemically change when heated, such as for pretreated biomass samples that contain residual acid or base.

This LAP also discusses the measurement of the total solid material in pretreated slurries. That portion of the method is discussed in the slurry analysis section. The sample aliquot used for %*Total Solids* analysis has been exposed to elevated temperatures and thermal degradation, and should not be used in further analyses, with the exception of determining ash content.

8.4.3 Measuring Ash

Inorganic materials are present in both whole and structural, or extracted, biomass samples. They are the result of inorganic matter bound into the plant structure or external additions such as surface fertilizer. In addition to contributing significantly to total mass closure, inorganic material may interfere with acid hydrolysis. LAP *Determination of Ash in Biomass* describes two methods for the determination of %*Ash* in biomass [18]. The LAP provides instructions for ash determination in a muffle furnace set to 575 °C with prior preignition, and describes the use of a ramping muffle furnace with no preignition. Our experience has shown that, when executed correctly, the two methods provide equivalent results.

8.4.4 Measuring Protein

Herbaceous feedstocks can contain a significant amount of protein in the stalks and leaves. Measurement of protein in biomass is performed indirectly by measurement of nitrogen content and the use of a nitrogen-to-protein conversion multiplier. The typically used nitrogen-to-protein conversion value of 6.25 is not accurate for biomass proteins [19–21]. Instead, an appropriate conversion factor is

determined by measuring the individual amino acids in the feedstock of interest. Because a portion of the protein is often removed during the extraction process, protein analysis is performed on both whole and extractives-free materials. Details of this procedure can be found in LAP *Determination of Protein Content in Biomass* [19].

Protein can potentially interfere with lignin measurements in subsequent analyses, since lignin is determined gravimetrically as the acid insoluble residue after analytical hydrolysis, and not all protein in the sample is still soluble after hydrolysis. By measuring the protein prior to hydrolysis, we can correct for this interference. Determining the amount of protein condensed with the acid insoluble residue is difficult, as the protein will have been altered during condensation. The nitrogen content of the acid insoluble residue and the hydrolysate can be determined and the amount of protein in the acid insoluble residue estimated from these values. Alternately, all of the protein can be assumed to be in the acid insoluble fraction or the hydrolysate fraction, and all analyses can be compared on a consistent, if not accurate, basis.

8.4.5 Measuring Extractives

The details of extracting biomass samples are found in NREL LAP *Determination of Extractives in Biomass* [21]. Extractives are the non-structural portion of biomass, those constituents that are not chemically bound to the structure of the material. Some biomass types can contain over thirty percent by weight extractable material. Since some extractives are destroyed in subsequent analyses, and some interfere with downstream procedures, the extractable material must be removed and quantified prior to further analyses. Different solvents remove different types of non-structural material [20, 22]. We typically use sequential water and ethanol extractions, although a single step ethanol extraction is sometimes adequate. Extraction with ethanol is required for all biomass types to ensure the removal of waxy materials that co-precipitate during filtration of the acid hydrolysate. When analyzing woody feedstocks, ethanol extraction alone is generally sufficient to remove interfering extractable material, including sap and resins. Herbaceous feedstocks require water extraction prior to the ethanol extraction. We use two different types of extraction apparatus: the traditional Soxhlet technique and automated Accelerated Solvent Extractor (Dionex ASE). The automated unit provides higher sample throughput than the Soxhlet method.

Nonstructural water soluble components commonly removed include inorganic material in the form of soil or fertilizers, proteins that are easily washed from the biomass, and a diverse array of carbohydrates, especially sucrose. Sucrose, a dimer of glucose and fructose, is of particular interest to fermentation and

can be abundant in herbaceous plants, but it is easily degraded during acid hydrolysis. Measurement of the water-soluble sucrose from biomass allows for better quantification of the structural glucose present in a feedstock as well; during acid hydrolysis sucrose will break down to fructose and glucose. The LAP describes the sampling of the water extractable material to determine sucrose concentration. While the remaining array of small quantity analytes can be individually determined [23], the process is generally too expensive and time consuming for a standard analysis, so they are grouped into a single category.

Although extraction is the first major step in the analysis process, compositional data are typically reported on a “whole biomass” basis. Since extraction values, like the moisture determinations discussed above, are used to correct subsequent measurements, the extractives content is a critical measurement. Any errors made in the determination of the extractives content will propagate through all structural material and increase the uncertainties of those components.

Note that herbaceous feedstocks are typically higher in inorganic materials (commonly soil or fertilizer) and protein than woody feedstocks. The water extraction process will remove some of these materials; therefore ash and protein measurements are recommended both before and after extraction.

8.4.6 Measuring Structural Carbohydrates and Lignin

Structural carbohydrates and lignin make up the bulk of most feedstocks and often represent the most interesting portions. *LAP Determination of Structural Carbohydrates and Lignin in Biomass* describes the acid hydrolysis and subsequent analyses of acid soluble and acid insoluble portions [24]. It describes the preparation and two-stage sulfuric acid hydrolysis of the sample. After hydrolysis the solids are separated from the liquid and the fractions are analyzed separately. Acid soluble lignin and acid insoluble lignin are combined to calculate total lignin content. This LAP also describes carbohydrate analysis of the liquid fraction via high pressure liquid chromatography (HPLC), including preparation of standards, hydrolysate neutralization, HPLC method setup, and acetyl analysis. The LAP includes the use of sugar recovery standards, which are used to correct for loss of carbohydrates during hydrolysis.

The determination of carbohydrates using this method requires that all carbohydrates be in monomeric form. The presence of carbohydrate oligomers indicates incomplete hydrolysis, and those carbohydrates will not be measured. During hydrolysis, the conversion of polymers to monomers in the carbohydrates results in the addition of a hydrogen and a hydroxyl group to each monomer. An anhydro correction is used to mathematically convert the monomeric values back to a structural polymeric value.

Sugar recovery standards (SRSs) are used to account for sample sugar degradation during the dilute sulfuric acid step. SRSs are used to mimic the behavior and degradation of sample monomers. Since these values can fluctuate depending on a variety of factors, SRSs are included with every sample analysis. They are independent from the sample but are run in parallel. Because carbohydrate concentration will affect degradation levels, it is imperative to mimic the sample carbohydrate concentrations as closely as possible in the SRSs. Since this correction is critical to all measured sugar concentrations, duplicate or triplicate SRSs are recommended. It is understood that monomeric sugars behave differently during hydrolysis than polymeric sugars. Due to the difficulty of obtaining pure polymeric sugars, monomeric versions are used for the SRS determination.

LAP Determination of Structural Carbohydrates and Lignin in Biomass also details the steps necessary to determine acid insoluble residue, including filtration of the hydrolysate and determination of the ash content of the residue. Acid insoluble residue, frequently referred to as Klason lignin, is considered high molecular weight lignin which is a behavior-based definition. A more detailed structural analysis would require further characterization of the material. Acid insoluble residue must be corrected for ash, as a significant portion of the ash in the whole biomass is acid insoluble. Some herbaceous feedstocks may need to have the acid insoluble residue corrected for protein as well, as a significant portion of the protein from the feedstock can condense into that fraction. The specific amount of protein that will co-condense can vary between feedstocks. Individual feedstocks need to be evaluated for protein condensation into the acid insoluble residue. This evaluation is not included in the method.

Acid soluble lignin is low molecular weight lignin that is solubilized in the acidic hydrolysis solution. Inclusion of acid soluble lignin in the total lignin value is necessary, as acid soluble lignin can represent a significant portion of the lignin. The LAP describes the measurement of acid soluble lignin by UV-Visible spectroscopy, but does not detail the determination of the proper extinction coefficient for feedstocks. A short list of common extinction coefficients is included in the LAP.

This LAP discusses several notable interferences, such as high moisture or ash content in the sample. High moisture content, above 10% by weight, can dilute the acid concentration beyond the tolerances of the LAP, possibly resulting in incomplete hydrolysis. Similarly, ash content above 10% by weight may buffer the acid, causing an effective reduction in acid concentration. However, not all inorganic material in biomass has this buffering effect, so the buffering effect of excessive inorganic material should be determined prior to analysis if this problem is suspected.

Analytical hydrolysis of unextracted biomass feedstock is *not* recommended. Extractives can deposit on the filter during separation of the acid soluble and acid insoluble fractions, resulting in excessive filtration time. In addition, our experience has clearly shown that the extractives partition irreproducibly between the acid soluble and acid insoluble fractions, compromising the measured lignin values.

8.4.7 Measuring Starch

Starch, a glucose polymer, is often found in biomass feedstocks that contain grain, or in young plants. NREL recommends use of an adapted version of the Megazyme Total Starch Assay (amylglucosidase/ α -amylase method) [25]. The major difference in the NREL adaptation is the use of HPLC detection for quantification of glucose after enzymatic hydrolysis as opposed to color assay. The quantification of glucose is not specific to starch, therefore extraction of the biomass is recommended prior to the starch assay to remove any nonstructural free glucose or sucrose. Failure to remove free glucose and sucrose will artificially elevate the apparent starch content of the biomass sample. If this procedure is performed in conjunction with carbohydrate (cellulose and hemicellulose) determination, the contribution of glucose from starch can be used to correct the structural glucan value.

8.4.8 A Typical Analysis

The flow chart of biomass compositional analysis, Figure 8.3, provides an example of a complete biomass feedstock analysis. In this section we step through an analysis of a whole feedstock sample and discuss the typical decisions an analyst will face at each step, using a hypothetical herbaceous feedstock as an example. This hypothetical feedstock is a potential dedicated bioenergy crop that is harvested off of the ground. The plant is known to produce grain late in life, but we were told by the researchers who did the harvesting that this particular sample should not contain grain. Before being shipped to us for analysis the sample was dried and milled through a 2-mm screen and sealed in a plastic bag.

As this sample has already been milled to an appropriate particle size, the first decision to be considered for this sample is whether sieving is necessary. Initial ash measurements indicate an ash content of 12%, which is greater than the recommended 10%, and may interfere with the acid hydrolysis steps.

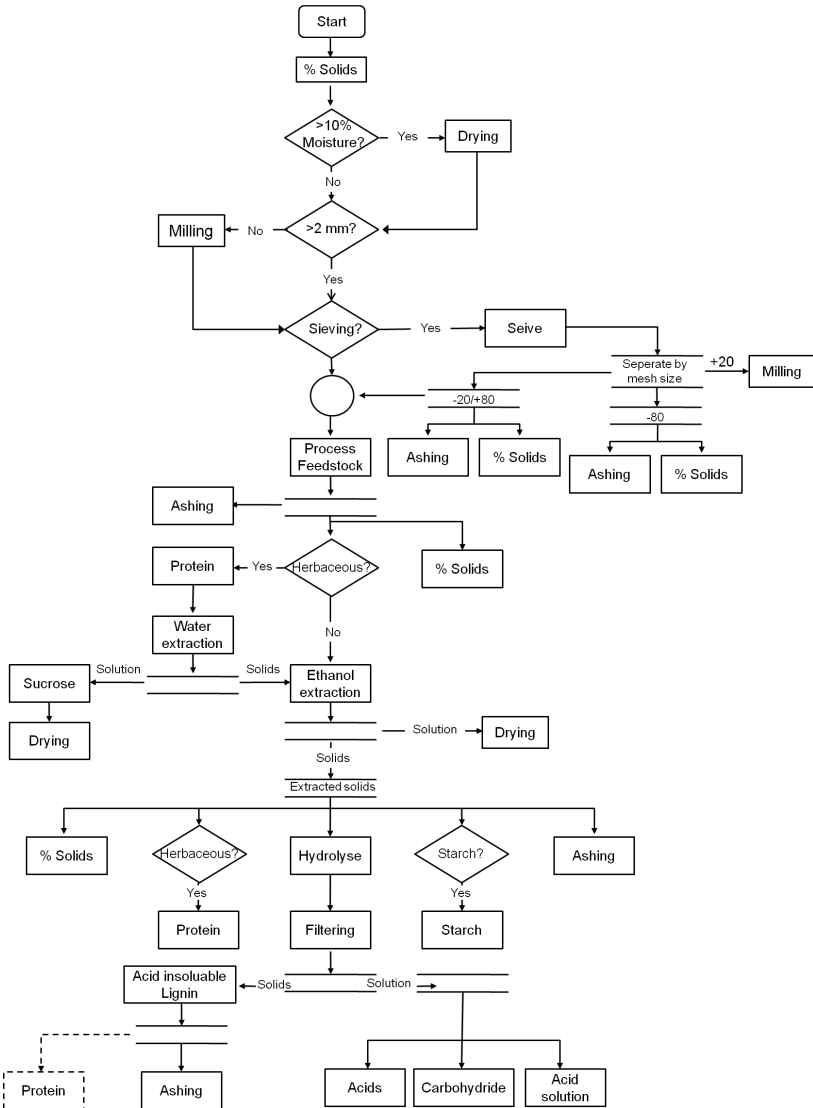


Figure 8.3: This figure is a flow chart for the analysis of feedstocks using NREL LAPs. The decision making process is outlined to assist the analyst in putting together the individual LAPs in the correct order and achieving summative mass closure.

Sieving could be tested to determine if some of the ash could be partitioned into the fines (-80 mesh), but as the plant was harvested off of the ground, the high ash content is likely soil and can be reduced by water extraction. Since the sample is herbaceous, water extraction is already part of the analysis suite.

Extraction is the next major consideration for the sample. As discussed above, we extract all herbaceous materials with water and ethanol. Prior to extraction with water, samples must have protein and total solids measurements performed, in addition to the ash measurement, which has already been done. Water extraction is required to quantify sucrose levels for herbaceous materials, but it also proves to be efficient at reducing the ash content to 5%. If it had not, sieving would need to be reconsidered to reduce the ash content to less than 10% before hydrolysis. Ethanol extraction follows the water extraction to ensure no complications regarding acid insoluble lignin measurements. The sample is now extractives-free and ready for hydrolysis.

Prior to hydrolysis the sample must again have total solids, protein, and ash measurements performed. Total solids will be used to convert values to a dry weight basis. Protein and ash measurements are used to determine the amount of these constituents removed during the extraction process.

Two-stage acid hydrolysis is performed, but the sample seems to have difficulty filtering while removing the acid insoluble residue. Carbohydrate analysis, acetyl analysis, and acid soluble lignin measurement of the hydrolysate are performed.

Once the data are compiled, the glucan measurement seems unusually high and the mass closure is significantly below 100%. Other constituent values seem to be typical of similar herbaceous feedstocks. Additionally, the acid soluble lignin results seem to have higher than expected variability between replicate analyses. These problems may stem from one issue or a combination of problems. Two potential areas of interference will be examined.

If the plant did contain grain that was not detected in the field, the sample may contain starch that was not accounted for. Since starch present during analytical hydrolysis is measured as glucan in the analysis, the starch content would explain the high glucan values, but not the low mass closure.

The unusually slow filtration of the acid insoluble lignin and the high acid insoluble residue variability are often related. In this case, further solvent extractions would be a good consideration to remove additional fractions of extractable material.

8.5 Summative Compositional Analysis of Pretreated Biomass Slurries and Liquors

Most lignocellulosic feedstocks cannot be directly fermented from a whole feedstock state. Some chemical or physical decomposition of the constituents is necessary to liberate carbohydrates from the plant structure. One common approach is pretreatment. The chemical pretreatment of biomass, followed by saccharification, is a common process in the bioethanol industry [26]. A wide array of pretreatment conditions allows the tuning of components released from the biomass [27]. LAPs developed at NREL have been optimized to provide compositional analysis for biomass feedstocks as well as intermediary products of dilute acid pretreatment.

The LAPs are optimized for woody or herbaceous species that have been pretreated with dilute acid at elevated temperatures. These LAPs have been successfully applied to biomass pretreated with steam or hot water at neutral pH. Biomass pretreated under alkaline conditions may require substantial method adjustment before compositional analysis may be performed. Biomass that has been mildly treated or degraded (i.e., during ensiling) is not suitable for this type of analysis and may be better considered a feedstock for analysis purposes.

Dilute acid pretreatment yields what is termed *slurry*. Slurry is composed of undigested biomass solids and an aqueous phase. The aqueous phase, or *liquor*, typically will contain large portions of the xylans, some of the lignin, and any degradation products from the acid pretreatment. The cellulose typically remains in the solid fraction of the slurry along with whatever lignin did not dissolve during pretreatment. Minor constituents, such as ash and protein, are usually split between the two phases.

Discussions of the LAPs necessary to obtain complete compositional analysis of a pretreated biomass slurry sample are included below. Slurries are generally separated into two fractions for analysis. The first is a filtered liquor sample. The second is the solids fraction of the slurry that has been washed to remove any liquor traces and then dried. There are many subtleties in the analytical suite of LAPs, and this summary is not meant to replace a careful reading of the relevant LAPs in any way.

8.5.1 Sample Preparation

One of the only considerations for preparing a pretreated biomass slurry for analysis is representative sampling. Slurries can range in consistency from a thick paste to a highly liquid sample, and may contain chunks of partially digested biomass or condensation products. Pretreated slurries are usually very heterogeneous and sampling can be a major hindrance to analysis. We recommend that the slurry be

thoroughly mixed immediately before sampling. Failure to immediately sample after mixing will not change the composition of the washed solids or the liquors, but can significantly bias any attempts to determine fraction allocations, as solid/liquid separation begins immediately. Figure 8.4 demonstrates the separation of liquor and solid in several slurry samples.

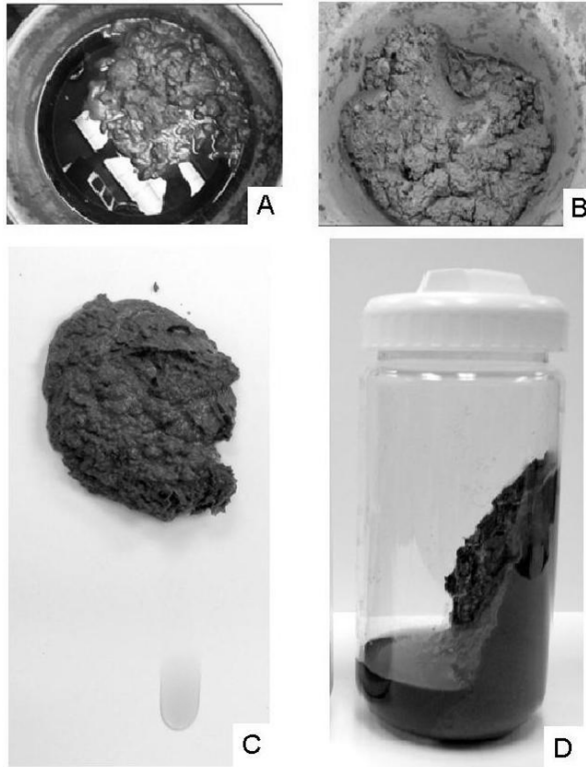


Figure 8.4: (A) A dilute acid pretreated corn stover slurry in a 55 gallon drum that has been left to settle for several months. A clear separation of the solid and liquid phases is evident. (B) The slurry from photo A, homogenized by mixing. (C) A well-mixed pretreated corn stover slurry left on the benchtop for 30 minutes has already begun to separate. (D) A pretreated corn stover slurry after centrifugation, separating the solid and liquid phases for further analysis.

8.5.2 Measuring Insoluble Solids

Due to the varied components present in the slurry, the solid and liquid phases are separated for parallel analyses. *LAP Determination of Insoluble Solids in Pretreated Biomass Material* is used to separate these fractions as well as determine the fraction of insoluble solids (f_{IS}) that is present in the pretreated slurry [28]. It describes the detailed measurement of solids and liquids that is necessary to relate measured component concentrations back to the slurry as a whole. The wash water from the rinsing process must be kept if f_{IS} is to be determined. This process may also be used to simply isolate liquor or washed solids samples. In this case, many of the measurements and calculations can be eliminated.

Two methods are detailed for the separation of the liquid and solid fractions, centrifugation and filtration. Both methods separate a sample of liquor from the slurry for analysis, prior to washing of the solids. Both methods detail steps for washing the solids free of soluble materials by repeated rinsing with water. An alternative for the isolation of the liquor from the slurry is pressing with a pneumatic or hydraulic press.

Centrifugation is our recommended method for most biomass samples. A large capacity centrifuge is required to process enough pretreated biomass for subsequent compositional analysis or further experiments (e.g., saccharification and fermentation of the solid material). Care should be taken to retain as much of the fine solids during the washing procedures as is practical, as these materials may have a significantly different chemical makeup.

Filtration can be faster than centrifugation for samples that are lightly pretreated, or samples with an undigested consistency. Care should be taken when using the filtration method to prevent exposure of the liquors to excessive vacuum, as evaporation of the water will cause concentration of the solubilized components in the filtrate. Samples that are more easily washed by filtration often require pneumatic or hydraulic pressing to remove the liquor fraction in a separate step.

Washing of the solids is critical, as the residual liquor present in the solids contains acid that will concentrate as the solids dry, causing chemical degradation of the solids. Additionally, the sugars dissolved in the liquor can significantly bias the measured sugars in the solids. To ensure complete removal of soluble sugars, the concentration of sugars is monitored in the rinses. Xylose liberated from the hemicellulose is the most concentrated sugar in the liquor, but if glucose is easier to monitor it may be substituted, as it is present in the liquor as well.

The procedure detailed above is specifically designed for the isolation of materials for compositional analysis. If samples are to be isolated for saccharification or fermentation, there are additional considerations. Washed pretreated solids should not be dried before saccharification or fermentation, as this can

cause cell wall collapse. Cell wall collapse limits the availability of the surfaces to enzyme and fermentation agents.

Unwashed pretreated solids should not be pressed at excessive pressures as this may also lead to cell wall collapse. We have performed tests up to ~600 psig of direct pressure that show no detrimental effect on enzymatic hydrolysis. We recommend further testing be done before exceeding this pressure.

8.5.3 Measuring Liquors

The procedures for detailed analysis of liquor samples can be found in LAP *Determination of Sugars, Byproducts, and Degradation Products in Liquid Fraction Process Samples* [29]. This LAP covers the analysis of monomeric carbohydrates and carbohydrate degradation products by HPLC, and acid soluble lignin via UV-Vis spectroscopy. It also covers the determination of oligomeric carbohydrates in solution through a single stage acid hydrolysis and subsequent HPLC analysis. It describes the preparation of HPLC standards, HPLC method setup, and the use of sugar recovery standards, which are used to correct for loss of carbohydrates during hydrolysis.

8.5.4 Measuring Washed Solids

The procedure for chemical compositional analysis of washed and dried pretreated solids is very similar to that of an extracted feedstock sample, detailed earlier, in Section 8.4. However, washed pretreated solids do not require extraction, as the extractable material is considered to be removed by the pretreatment and the washing of the slurry. Additionally, chemical changes in the biomass will result in most extraction methods removing more material than anticipated, some of which cannot be characterized. However, the analytical methodology is substantially similar. The differences between the procedures for compositional analysis of extracted feedstock and washed pretreated solids are discussed here. A flow chart of analysis (Figure 8.5) provides an example of a complete slurry analysis. Included are steps for solid/liquid separation and analyses of the fractions.

Milling of *feedstock* samples is carefully controlled to avoid degradation of small particles during hydrolysis. Washed pretreated solids are much harder to mill to a specific particle size because there is usually significant degradation of the structure of the biomass. It is still necessary to mill the solids, but fines are never removed by sieving. Generally, a smaller particle size is accepted for pretreated material.

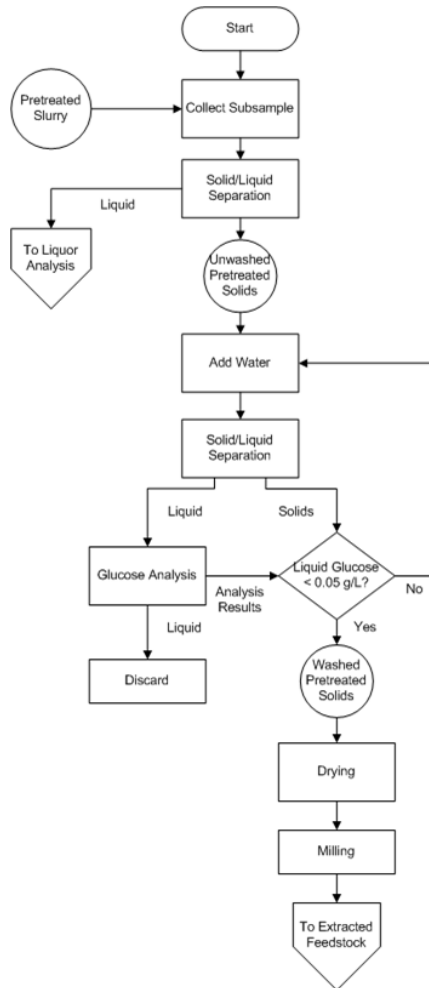


Figure 8.5: This figure is a flow chart for the analysis of acid pretreated slurries using NREL LAPs. The decision making process is outlined to assist the analyst in putting together the individual LAPs in the correct order and achieving summative mass closure. It includes the separation of the solid and liquid fractions of slurries. The analysis of washed dried solids references the analyst to the extracted feedstock flow chart, as the analyses are identical after that point.

Protein analysis is performed on the washed pretreated solids, but it is difficult to determine a conversion factor for nitrogen to protein due to the degradation of the proteins during acid pretreatment. The protein content is still reported, but it is important to realize that this is best viewed as an estimate.

Extractives remaining in very mildly pretreated feedstocks will interfere with LAP *Determination of Structural Carbohydrates and Lignin in Biomass* [24]. As with the analysis of feedstocks, extractives can deposit on the filter during separation of the acid soluble and acid insoluble fractions, resulting in excessive filtration time and potential concentration of the liquid fraction. Extractives can also partition irreproducibly between the acid soluble and acid insoluble fractions, compromising the lignin values. We recommend that the extinction coefficient used for the originating feedstock also be used for the pretreated materials when determining the acid soluble lignin content.

8.6 Summative Mass Closure-Calculations, Troubleshooting, and Errors

Performing a comprehensive mass balance across a process, including determining the composition of feedstocks, intermediate materials, and end products, can require dozens of individual measurements and hundreds of calculations. All of the calculations are listed in the appropriate LAP. To minimize the risk of one calculation error spoiling a set of analyses, NREL has developed Excel spreadsheets that automatically calculate all necessary equations on measured data. These spreadsheets are available for download [30]. These sheets also flag samples that do not replicate analyses within specified error tolerances. While these sheets are an invaluable tool for an analyst, it is important to understand the mathematics behind the calculations to better identify analytical problems.

After the data have been compiled, the analyst should closely examine them for problems. While the aim of summative mass closure is to characterize 100% of the constituents, inherent error in measurements usually provides a range of 97–103% mass characterization. Summative values outside of that range require examination. Further, the analyst should always review values to ensure that they are reasonable. Some analytical issues can cause analyte values to shift inversely, making the individual values wrong, but the mass closure appropriate. For example, incomplete hydrolysis can cause carbohydrate values to be low, and the lignin value to be high.

A variety of problems can be identified through data examination. Some problems, such as entering measured values incorrectly, can be quickly spotted and rectified. In the feedstock analysis section above, an example problem including low mass closure, disproportionately high glucan values, acid soluble

lignin values with high errors, and unusually slow filtration is presented. This is an excellent example of multiple issues compounding problems.

Other issues that may arise when examining data are: errors in duplicate values, mass closure values out of range, and the presence of oligomers in the carbohydrates. Areas to investigate for each of these problems are presented. The first step in data review should be a careful review of the standards run during the analyses. Generally, a well-characterized material of similar matrix is run concurrently with the samples. This can be an in-house sample, or one purchased externally, for example the biomass reference standards from NIST [10]. An analysis may only be deemed successful if the standard's values are within acceptable tolerances, as determined by historical values. If these values are outside of acceptable tolerances, the entire run must be examined.

Errors in duplicate values can be due to basic data entry errors or instrument malfunctions. They may also be due to heterogeneous sampling. This is a particular issue with biomass, as sample settling can occur rapidly. If the cause cannot be pinpointed, we recommend that duplicate analyses are performed again.

Mass closure issues, when the mass closure is under 97% or over 103%, can be the result of single or multiple constituents. A high mass closure indicates that one or more constituents have been counted twice during analyses. For example, if the protein value of a feedstock is measured, but condensed protein is not removed from the lignin value, the protein will be counted twice. A low mass closure indicates that constituents have been missed. This is a particular problem with extractives, such as sucrose, which will degrade beyond measurability if not captured at the start of the process.

Problems that may be noticeable during analysis are slow filtration after hydrolysis and the presence of oligomers in the carbohydrate solutions after hydrolysis. Slow filtration is generally caused by the presence of extractives. If one or more groups of extractives (e.g., waxes or fats) are not removed prior to hydrolysis, they can clog the filter and impede filtration. Remaining extractives will frequently manifest as artificially high lignin values.

If oligomers are noted in post hydrolysis carbohydrate chromatograms, incomplete hydrolysis has occurred. Incomplete hydrolysis may be the result of poor technique, autoclave malfunction, or low acid concentration. Many of the noted interferences can result in incomplete hydrolysis, and a careful examination of these interferences should be undertaken with the specific sample matrix in mind.

8.7 Uncertainty in the Primary Measurements

Uncertainty is inherent in every measurement, and it is important to understand sources of uncertainty and quantify them if possible. This is especially true with fiber analysis methods for biomass compositional analysis as they are empirical methods. The final results from compositional analysis are very dependent on how the methods were performed; minor variations in methods can cause significant changes to the results.

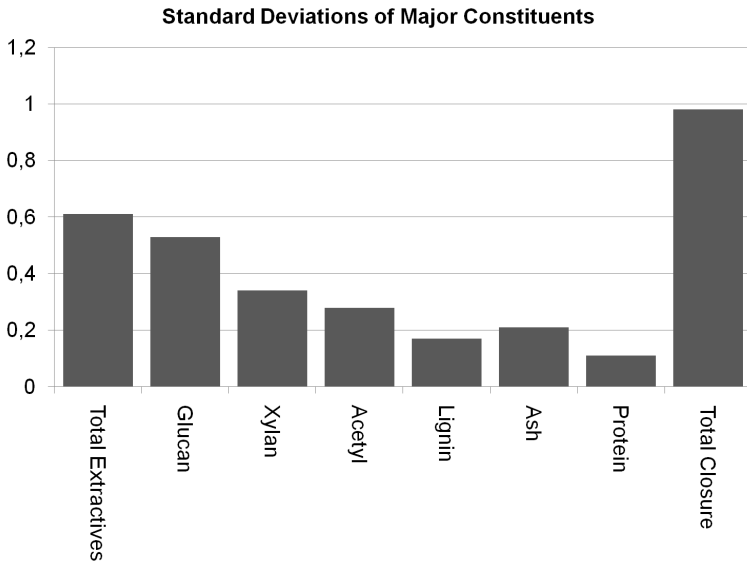


Figure 8.6: The uncertainties for each constituent measured during the NREL round robin of corn stover indicate that extractives contribute significantly to the uncertainty of the mass closure.

NREL recently published the results of an internal round-robin style determination of the uncertainties associated with the measurement described in the LAPs [31]. Seven different analysts operating in two different laboratories performed a total of 156 replicate analyses on a common corn stover sample. The results of that study are discussed below. It should be noted that the errors discussed here are uncertainty, which is the result of random error inherent in measurements. This is different from a bias, which is the result of a systematic error that causes results to be constantly high or low.

The primary contributor to the uncertainties for total mass closure was extraction, as seen in Figure 8.6. As described in the text above, a large number of the measurements are performed on an extractives-free sample and the con-

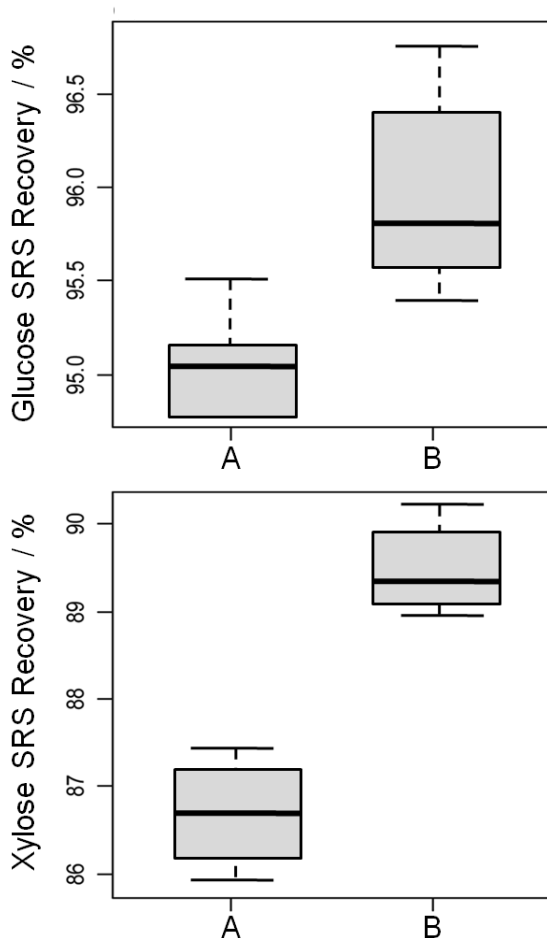


Figure 8.7: Recoveries of glucose and xylose from SRSs. A and B represent two different autoclaves. Not only can the difference in recovery per autoclave be noted, but the differences in standard deviation demonstrate the disparity in autoclave performance.

stituents are mathematically corrected back to a whole biomass basis. Since that correction is based on the extraction and moisture measurements, extraction has high leverage on a large number of constituents.

Another major contributor to uncertainty was the variability inherent between batches of analyses. Each analyst in the study performed batches that contained 12 corn stover samples and one method control. The variability within each batch was found to be much smaller than the variability between batches. This indicates that the specific conditions during a single analysis cause small but measurable variations in the results of the compositional analysis.

One uncontrollable source of method variation is the heating and cooling profile of the autoclave during the second stage of acid hydrolysis. From one autoclave to another this heating profile is likely to be different. Figure 8.7 shows the compiled variability for two autoclaves used during the round robin. The two autoclaves do not exhibit the same sugar degradation factors. While it is common to use a “historical” factor for sugar degradation, these data clearly indicate that there is a bias between autoclaves and that each autoclave should be evaluated independently. In addition to the bias, each autoclave has a range over which the loss factor varies. This range is likely related to a number of aspects, including autoclave function on a specific day, promptness of the analyst at removing the samples from the autoclave following hydrolysis, and cooling rate of the vessels once removed. These considerations also make it difficult to argue for the use of a “historical” factor. The sugar recovery standards attempt to control for autoclave variability, but in doing so become very high leverage measurements. We recommend that triplicate SRSs be run to mitigate some of the uncertainty in this measurement.

8.8 Propagation of Uncertainty in Primary Measurements

All primary analytical measurements have some amount of uncertainty associated with them, and measurements associated with biomass analysis are no exception. For example, five repeated measurements of the concentration of glucose and xylose in a single pretreated liquor sample using HPLC will not produce exactly the same value. The same is true for any repeated empirical measurement. When multiple primary analytical measurements are combined in a calculation, the individual uncertainties in the primary measurements are propagated in the calculation. We have discussed the uncertainties associated with the biomass compositional analysis methods used at NREL, and now we consider the effect of these uncertainties on calculated values. This is important because the purpose of making primary analytical measurements is almost always to use them in subsequent calculations, and it is important to understand the precision with which

we can make claims about these calculated values. Of particular interest is the calculation of component yields from specific unit operations, such as the yield of glucose from saccharification, the yield of ethanol from fermentation, or the yield of xylose from pretreatment.

As a specific example of interest to biomass researchers, consider a batch pretreatment reaction where a biomass feedstock is treated with dilute acid to break down the hemicellulose into soluble xylose. It is common to calculate the yield of xylose from this chemical reaction; what fraction of the xylan originally in the biomass feedstock was hydrolyzed to monomeric xylose? The yield of xylose from a batch pretreatment can be written as:

$$Y_x = \frac{m_s(1-f_{IS})}{m_F} \frac{c_X}{x_X} \frac{1}{\rho_L} \frac{MW_{xylan}}{MW_{xylose}} \frac{1}{10^3} \quad (8.1)$$

where m_S is the mass of the pretreated slurry produced in the experiment, m_F is the mass of feedstock used, f_{IS} is the fraction insoluble solids in the pretreated slurry, ρ_L is the liquor density (g/mL), c_X is the concentration of xylose (monomeric or total) in the liquor (g/L), x_X is the mass fraction of xylan in the feedstock, MW_{xylan} is the molecular weight of xylan, MW_{xylose} is the molecular weight of

Parameter	Value	Units	SD	RSD (%)
Fraction insoluble solids f_{IS}	0.25	Mass fraction	0.01	4
Liquor xylose concentration c_X	60	g/l	1	2.5
Feedstock xylan content	0.20	Mass fraction	0.005	2.5
Liquor density	1.11	g/mL	NA	NA
Xylose yield (analytic)			0.0235	3.29
Xylose yield (MC, 10000 iterations)	0.713	NA	0.0235	3.29

Table 8.1: Uncertainty propagation in the yield of xylose from biomass feedstock during pretreatment. The analytic and Monte Carlo (MC) approaches to calculating the uncertainty in xylose yield during pretreatment produce essentially identical results. SD = Standard deviation; RSD = Relative standard deviation (SD/Value).

xylose, and the term 103 is simply for unit conversion (mL to L). For typical values of these parameters (shown in Table 8.1) the yield of xylose is 71.3%; almost three quarters of the xylan originally present in the feedstock is released as xylose in the pretreated liquor.

How can we calculate the uncertainty in the xylose yield from the uncertainty in the primary analytical measurements? There are two general approaches to the propagation of uncertainty. First is a classical approach that uses differential calculus, and second is a Monte Carlo approach that uses uncertainty distributions of the primary measurements to calculate the uncertainty distribution of the calculated value.

Typically, the standard deviation of repeated measurements collected over time is used as a measure of uncertainty. If we can assume that the measurement errors that contribute to the uncertainty are normally distributed, then by using the standard deviation as our measure of uncertainty, we can safely assume that a single measurement will be within 1 standard deviation of the “true” value 69% of the time, and within 1.96 standard deviations 95% of the time.

As an aside, another option for expressing uncertainty is to use a confidence interval. If the standard deviation of n repeated measurements from a given experiment is known (s_n), then the confidence interval can be expressed as

$$t_n \frac{s_n}{\sqrt{n-1}} \quad (8.2)$$

where t_n is the value of Student’s t-distribution for n measurements. This formulation is useful because repeated independent measurements decrease the value of the confidence interval. However, the measurements must be truly independent and must include all the steps required to make the measurement: sample collection, sample manipulation, and finally measurement. For example, replicate HPLC injections of a corn stover analytical hydrolysate to measure structural carbohydrates would not count as independent measurements of carbohydrate content because all of the steps required to make this measurement were not performed independently (e.g., the extraction of the feedstock, the two-stage analytical hydrolysis, and the filtration prior to HPLC analysis). All steps used to generate and measure the sample must be independently replicated.

The classical uncertainty propagation differential equation can be written as:

$$U_F(x_1, x_2, \dots, x_N) = \sqrt{\sum_{i=1}^n \left(\frac{\partial F}{\partial x_i} \right)^2 U_{x_i}^2} \quad (8.3)$$

where U_F is the uncertainty in the value of the value F which is calculated analytically from the primary measurements x_1 through x_N . The uncertainty of the calculated value depends on the influence each primary measurement has on the calculated quantity (the $\partial F/\partial x$ terms) and the uncertainty of the primary measurement itself (the U_x terms). Thus, the uncertainty in a primary measurement can have a large influence on the uncertainty of a calculated value if a small change in the primary measurement causes a large change in the calculated value (e.g., $F = x^2$, $F = \exp(x)$) or if there is a large uncertainty in the primary measurement itself.

To simplify this example problem, we will assume that the liquor density and the feedstock and slurry mass measurements have negligible uncertainty compared to the other terms, since these quantities (m_S, m_F, ρ_L) are typically measured to 3 or 4 significant figures. With this assumption, the uncertainty in the calculated xylose yield depends only on the uncertainty in three primary measurements: the fraction insoluble solids (f_{IS}) of the pretreated biomass slurry, the xylose concentration of the pretreated liquor (c_X), and the xylan content in the solid (x_X). We can rewrite the xylose yield equation as:

$$Y_x = A(1 - f_{IS}) \frac{c_X}{x_X} \quad (8.4)$$

where the parameter A now groups all the terms not directly associated with the uncertainty. If we apply the uncertainty partial differential equation to the xylose yield equation using the standard deviation s as the measure of uncertainty, this works out to be:

$$s_{Y_x} = \sqrt{\left(\frac{\partial Y_x}{\partial f_{IS}} s_{f_{IS}}\right)^2 + \left(\frac{\partial Y_x}{\partial c_X} s_{c_X}\right)^2 + \left(\frac{\partial Y_x}{\partial x_X} s_{x_X}\right)^2} \quad (8.5)$$

Calculating the partial derivatives and doing some simple algebra gives us:

$$s_{Y_x} = \sqrt{\left(-A \frac{c_X}{x_X} s_{f_{IS}}\right)^2 + \left(A(1 - f_{IS}) \frac{1}{x_X} s_{c_X}\right)^2 + \left(-A(1 - f_{IS}) \frac{c_X}{x_X^2} s_{x_X}\right)^2} \quad (8.6)$$

Thus, the expected standard deviation of xylose yield calculation can be expressed as the combination of the uncertainties of the primary measurements. For any given set of primary measurements (c_X, x_X, f_{IS}) with associated uncertainties ($s_{c_X}, s_{c_X}, s_{f_{IS}}$), we can calculate not only the value of the xylose yield standard deviation of Y_x but also the uncertainty of this calculation s_{Y_x} . Note that applying

the uncertainty partial differential equation to the simple summation $a = b + c$ yields the expression

$$s_c = \sqrt{s_a^2 + s_b^2} \quad (8.7)$$

which is the familiar *sum of squares rule* for adding standard deviations.

While these results show that we can calculate a closed-form algebraic approach to calculating uncertainty, for very complex formulas this is not always possible. Monte Carlo techniques provide distributions of expected values of a calculated value based on distributions of expected values of the primary measurement variables. These techniques are most useful for calculating the uncertainty of very complex formulas where the calculation of partial derivatives would be unwieldy, such as techno-economic (TE) or life cycle assessment (LCA) models. Nonetheless, it is a useful technique and we will demonstrate it using the same xylose yield equation.

To perform a Monte Carlo uncertainty calculation, we need to assume some type of distribution of expected values for all primary measurements. In this example, we used normal distributions using the same standard deviation values for each of the three primary measurements. We used the open source programming language R¹ to do these calculations. We used 10,000 iterations which were calculated in approximately 1 second on a standard desktop computer, but simulations with 100–10,000,000 iterations provided similar results.

Part one of Section 8.11 shows the R-code used to generate both the algebraic and Monte Carlo estimates of uncertainty, and part two of Section 8.11 shows the R-code used to generate the plot shown in Figure 8.8, which shows the calculated distributions of the uncertainties of the three primary measurements (c_X , x_X , f_{IS}) and the distribution of calculated xylose yield values Y_X . The bars represent histograms of the results of the Monte Carlo calculations with 10,000 iterations, while the smooth curves are normal distributions fitted to the mean and standard deviations of the Monte Carlo calculation results. Table 8.1 shows the parameters used and the calculated parameters.

¹www.r-project.org

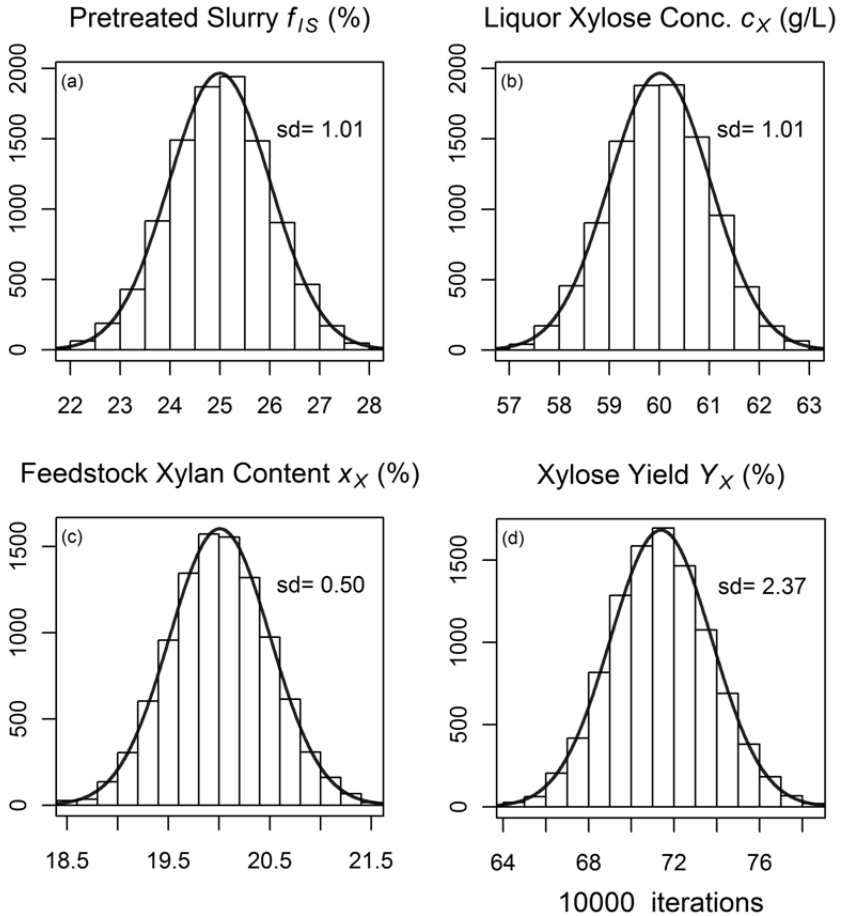


Figure 8.8: Histograms from Monte Carlo uncertainty calculations. (a) to (c) are primary measurement uncertainties of fraction insoluble solids, xylose liquor concentration, and feedstock xylan content (f_{IS} ; c_X ; x_X), and (d) is the uncertainty histogram of the calculated xylose yield (Y_X): Bars represent histograms of the results of the Monte Carlo calculations, while curves are normal distributions fitted to the mean and standard deviations of the Monte Carlo calculation results.

Both the algebraic and the Monte Carlo methods provide essentially equivalent estimates of uncertainties; about 2.35% of the calculated yield of xylose from xylan, or 3.3% relative standard deviation (RSD). So how can we interpret these results? We can conclude that replicate experiments will provide calculated xylose yield results within $\pm 1.96 \times 2.35\%$ or 4.6% about 95% of the time. Put another way, two experiments with calculated yield values that differ by less than about 4.6% are not statistically significantly different. Thus, before performing a long series of pretreatment experiments, we can estimate the smallest experimentally-determined yield difference that is statistically significant.

It is interesting that the RSD of the final yield calculation is smaller than the largest relative uncertainty of the primary variables, in this case f_{IS} which has an RSD value of 4%. How can this be? It turns out that the yield calculation actually uses the mass fraction of the liquor and soluble solids ($1-f_{IS}$) and not f_{IS} . This is an important distinction, because the relative uncertainty in the term $1-f_{IS}$ is 1.3% ($0.01/0.75$) not 4.0% ($0.01/0.25$). As the value of f_{IS} increases, the relative uncertainty in the term $1-f_{IS}$ increases; at a (nonsensical) value of 0.90 the relative uncertainty is 10%; at 0.95 it is 20%. Again, this surprising result is independent of the technique used to calculate the uncertainty in the xylose yield; both the algebraic and Monte Carlo approaches provide the same results.

The algebraic approach has one advantage over the Monte Carlo approach in that we can use the intermediate calculation results to identify primary measurement variables responsible for the majority of the uncertainty. In the case of our calculation, the liquor xylose concentration uncertainty is responsible for ~60% of the total uncertainty, the xylan feedstock content measurement uncertainty is responsible for ~25%, and the f_{IS} uncertainty for about 15%. Thus, if we wish to decrease the uncertainty associated with the xylose yield calculation, we should begin with decreasing the uncertainty in the liquor xylose concentration measurement.

A rigorous calculation of uncertainty for calculated values is relatively easy to perform using either the partial derivative approach or the Monte Carlo approach; all that is needed is a good understanding of the uncertainties in the primary variables. Such calculations provide a solid understanding of the accuracy of the calculated values, which is important when one is making claims regarding these calculated values.

8.9 Room for Improvement in Biomass Compositional Analysis

While the analysis of biomass is not a new science, it still has many areas that offer opportunity for improvement. Some improvements are in the form of faster

analysis time and higher throughput. Others include more accurate characterization of components that are already measured.

Increased throughput, a certain improvement, could be achieved by shortening necessary instrumentation or analyst time. Instrumentation improvements can come in the form of better HPLC column resolution, shorter run times, and increased accuracy. When minutes are shaved off of each instrumentation characterization, time savings can quickly add up. It also may be possible to optimize current methods by altering lengthy hydrolysis steps, concentrating acid, or changing other parameters. Other time consuming steps, like the separation of a slurry into liquor and washed dried solids, would benefit from time reducing steps [32]. Some research has been done in these areas, but new methods must be exhaustively compared to current methods. There is a wealth of historical data generated by current procedures, and it is imperative that the results from new optimized methods be comparable to historical data.

Discovering fast and simple ways to further characterize the components in extractives, especially water extractives, could again offer the added benefit of upgraded co-products. Currently, the detailed examination of the water extractives fraction of biomass is lengthy [23], and not conducive to adoption into a traditional biomass analysis.

More accurately characterizing certain constituents offers a large area for improvement. For example, the lignin content of a feedstock may be used as a fuel source via combustion, or may be upgraded to valuable co-products. More accurate analysis of the lignin content would allow for better decisions on the fate of lignin. Since lignin is a complex structure, and unique to each biomass type, specific characterization of the lignin can be difficult.

The SRSs introduce a high leverage measurement, meaning that this measurement affects all of the carbohydrate measurements, and this measurement has been subjected to recent reexamination. It is necessary to include SRSs with each sample set to correct for sugars lost during the hydrolysis of oligomeric sugars to monomeric sugars. Due to the difficulty of obtaining representative oligomeric sugars to use as SRS standards, monomeric sugars are used. However, monomeric sugars are not a truly representative standard. If high purity representative oligomeric sugars were readily available, this measurement could be improved and lead to greater certainty of sugar concentrations. Figure 8.9 clearly demonstrates the differences between true liquor samples and synthetic liquors, which is as close as we can get with readily available commercial compounds.

Alternatively, the sugar loss could be measured by direct measurement of the degradation products of all sugars in the sample solution. This technique would account for any matrix effects and oligomer behavior. For this to become a reality, a reliable method for measurement of all degradation products would need to be

developed. Current methods are limited by an inability to differentiate beyond products derived from C5 sugars or C6 sugars. In biomass types with multiple sugars of the same carbon length, this can lead to overcorrection of one sugar and undercorrection of others.

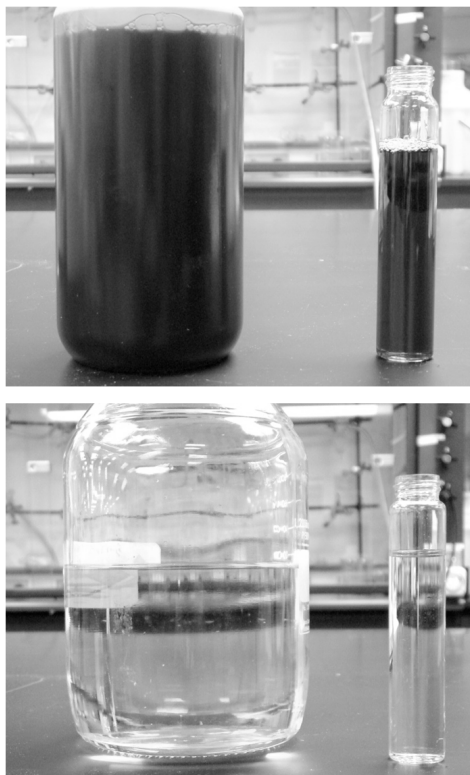


Figure 8.9: A hydrolysate liquor sample isolated from a pretreated corn stover slurry, top photo, has a dark brown color and is opaque. By comparison, a synthetic hydrolysate prepared to similar concentrations, lower photo, has a much lighter and less opaque appearance. The darker color in a real hydrolysate liquor sample is due to constituents not included in the synthetic, as well as matrix effects that are impossible to account for.

8.10 Rapid Biomass Analysis via NIR

Full chemical characterization of a biomass sample can take weeks, which is both cost- and time-prohibitive in industrial processes. Using near infrared (NIR) spectroscopy coupled with chemometric modeling software can make composition analysis faster and non-destructive. NIR can be applied to solids, liquids, and slurries. It can also be adapted to bulk samples in an on-line environment. Rapid biomass characterization can be utilized in the field to manage crop conditions, at the destination to determine a purchase price based on constituent value and blend feedstocks, and during conversion processes to monitor intermediates and end products. NIR calibration methods are widely used to characterize food, animal feed, and an assortment of agricultural products [33].

In order to develop a working NIR predictive model, much work must be done to characterize an appropriate calibration set. An ideal calibration set should contain samples with constituent values that are evenly distributed across the range of expectation for each constituent. That is, the calibration set should span constituent values expected for future samples. Some minor constituents may not contain enough variability to produce robust models. The uncertainties associated with the wet chemical methods used will translate directly to the NIR predictive method, so care should be taken to minimize chemical analysis uncertainties.

When building a predictive model, mathematically altering the data, also called pretreating or preprocessing, prior to modeling can minimize certain problems. Pretreating can remove much of the spectroscopic noise due to particle size differences and scatter, as well as highlight important peaks and information. A variety of pretreatment techniques is available that correct different spectroscopic issues [34].

Once data are sufficiently pretreated, Partial Least Square (PLS) models can be created to regress the spectroscopic data against the wet chemical information. PLS-1 or PLS-2 models can be used, depending on the data set and desired end models. The PLS-1 algorithm regresses the spectral data against the constituent data one constituent at a time, while the PLS-2 algorithm regresses all constituents simultaneously [35].

All predictive models must be validated. Several statistical validations are used to determine model performance. The root mean square error of prediction (RMSEP), root mean square error of calibration (RMSEC), and correlation coefficient (R^2), provide a good estimator of future model performance. Cross validation is a commonly used method for validation. It is the process of removing a single sample or a group of samples from the calibration set and recreating the model to predict the removed samples. It is a conservative estimator of final model performance. Cross validation provides RMSEP. Predicting the calibration set

on the final model provides RMSEC and R^2 . Deviations from the perfect target line should approximate wet chemical uncertainties. Independent blind validation samples are the best gauge of model accuracy, and should be used as a final check. Models should also be periodically validated with independent samples to ensure continuing accuracy and performance.

Once NIR predictive models have been built and validated, they can be used to predict new samples. Models can only be used to predict samples of a similar matrix and are therefore usually specific to a feedstock or pretreated biomass intermediate type. Models, being mathematical equations, will predict any data input. It is up to the operator to determine the appropriateness of the model, and to monitor the model uncertainties. Samples that do not belong to the calibration population (e.g., different species or samples with constituent values outside of the population range) should not be predicted. This represents the difference between interpolation and extrapolation. As the models are multi-dimensional, linearity is not ensured beyond the calibration range. It is imperative to remember that the user is responsible for assessing the uncertainties associated with the predictions and determining if the sample is a good fit in the calibration population. We also cannot stress enough that the predictions will only be as good as the original data used to create the calibration set. Secondary methods are only as good as the primary methods used to create them.

8.11 Conclusions

The accurate determination of the composition of lignocellulosic feedstocks and process intermediates is an often understated challenge. The individual operations in the methods, such as filtration and weighing, are not difficult to perform. The understanding of the intricacies of the methods and the proper sequencing of the different methods are where the challenge lies. Here we have tried to relate some of the experiences that we have had with a variety of feedstock and pretreatment types.

We have also tried to stress the empirical nature of the methods. What may seem to be a minor change to a procedure can lead to a bias between data sets. If a direct comparison of data is necessary, undetected biases could lead to misinterpretation of results. Our colleagues in the field have published alternate methods that have both advantages and disadvantages as compared to the methods we present here. Those methods are also highly empirical. Therefore, it is important to know and understand the methods used to generate any data and the characteristics of the data they produce. Again, an undetected bias could make a true comparison impossible.

Finally, we recognize that there is room to improve the techniques for determining the composition of biomass. It is our hope that the reader will be inspired to contribute to the development of these future methods. Improvements of methods for the chemical characterization and rapid analysis of feedstock and process intermediates will play important roles in the biorefineries of tomorrow. As one esteemed colleague once said: “You cannot control what you cannot measure.”

Acknowledgments

Sections 4–6 are based on two recent NREL technical publications: the Summative Mass Closure LAPs [12, 13] provide an overview of the individual LAPs, detail how the individual LAPs integrate, as well as highlight many of the pitfalls that can cause an analysis to fail. Summative Mass Closure LAPs are available for the analysis of lignocellulosic feedstocks and acid pretreated intermediates for fuel production.

Figure 8.4: photos A and B taken by students from the David Koch School of Chemical Engineering Practice at MIT, C and D taken by Justin Sluiter and Courtney Payne, NREL. Figure 8.9: photos taken by Justin Sluiter, NREL.

We acknowledge students from the David Koch School of Chemical Engineering Practice at MIT for their work investigating the effect of uncertainty in primary measurements on yield calculations. This work will be published in the near future.

We appreciate the review of this chapter by Ms. Courtney Payne, Mr. Chris Scarlata, and Dr. Angela Ziebell.

Bibliography

- [1] E.D. Larson. A review of life-cycle analysis studies on liquid biofuel systems for the transport sector. *Energy for Sustainable Development* 10(2) (2006):109–126.
- [2] C. Somerville, S. Bauer, G. Brininstool, M. Facette, T. Hamann, J. Milne, E. Osborne, A. Paredes, S. Persson, and T. Raab. Toward a Systems Approach to Understanding Plant Cell Walls. *Science* 306 (2004):2206–2211.
- [3] EERE. *Feedstock Composition Glossary*. 2011.
- [4] B.R. Hames. Biomass Compositional Analysis for Energy Applications. In: *Biofuels*. Ed. by Jonathan R. Mielenz. 581. Humana Press, 2009.
- [5] EERE. *Theoretical Ethanol Yield Calculator*. 2011.
- [6] N.F.T. Association. URL: <http://www.foragetesting.org>.
- [7] E. Wolfrum, A. Lorenz, and N. deLeon. Correlating detergent fiber analysis and dietary fiber analysis data for corn stover collected by NIRS. *Cellulose* 16(4) (2009):577–585.
- [8] T.A. Milne, H.L. Chum, F. Agblevor, and D.K. Johnson. Standardized analytical methods. *Biomass and Bioenergy* 2(1-6) (1992):341–366.
- [9] D.W. Templeton, J.H. Yen, and K.E. Sharpless. *Compositional Analysis of Biomass Reference Materials: Results from an Interlaboratory Study*. 2011.
- [10] NIST. *NIST Standard Reference Materials*. 2011.
- [11] J.B. Sluiter, R.O. Ruiz, C.J. Scarlata, A.D. Sluiter, and D.W. Templeton. Compositional Analysis of Lignocellulosic Feedstocks. 1. Review and Description of Methods. *Journal of Agricultural and Food Chemistry* 58(16) (2010):9043–9053.
- [12] J. Sluiter and A. Sluiter. *Summative Mass Closure, Laboratory Analytical Procedure (LAP) Review and Integration: Feedstocks*. 2010.
- [13] J. Sluiter and A. Sluiter. *Summative Mass Closure, Laboratory Analytical Procedure (LAP) Review and Integration: Pretreated Slurries*. 2010.

- [14] B. Hames, R. Ruiz, C. Scarlata, A. Sluiter, J. Sluiter, and D. Templeton. *Preparation of Samples for Compositional Analysis Laboratory Analytical Procedure (LAP)*. 2008.
- [15] H. L. Chum, D.K. Johnson, F.A. Agblevor, R.J. Evans, B.R. Hames, T.A. Milne, and R.P. Overend. *Status of the IEA Voluntary Standards Activity - Round Robins on Whole Wood and Lignins*. Nov. 1994.
- [16] F. Agblevor, H.L. Chum, and D.K. Johnson. Compositional Analysis of NIST Biomass Standards from the IEA Feedstock Round Robins. In: *Energy from Biomass and Wastes XVI*. Ed. by D.L. Klass. Orlando, FL: Institute of Gas Technology, 1992. 395–421.
- [17] A. Sluiter, B. Hames, D. Hyman, C. Payne, R. Ruiz, C. Scarlata, J. Sluiter, D. Templeton, and J. Wolfe. *Determination of Total Solids in Biomass and Total Dissolved Solids in Liquid Process Samples Laboratory Analytical Procedure (LAP)*. 2008.
- [18] A. Sluiter, B. Hames, R. Ruiz, C. Scarlata, J. Sluiter, and D. Templeton. *Determination of Ash in Biomass Laboratory Analytical Procedure (LAP)*. 2008.
- [19] B. Hames, C. Scarlata, and A. Sluiter. *Determination of Protein Content in Biomass Laboratory Analytical Procedure (LAP)*. 2008.
- [20] G. Lindstedt. Constituents of Pine Heartwood. *Acta Chemica Scandinavica* 3 (1949):1375–1380.
- [21] A. Sluiter, R. Ruiz, C. Scarlata, J. Sluiter, and D. Templeton. *Determination of Extractives in Biomass Laboratory Analytical Procedure (LAP)*. 2008.
- [22] TAPPI. *TAPPI 264 cm-07 Preparation of Wood for Chemical Analysis*. 2007.
- [23] S.-F. Chen, R.A. Mowery, C.J. Scarlata, and C.K. Chambliss. Compositional Analysis of Water-Soluble Materials in Corn Stover. *Journal of Agricultural and Food Chemistry* 55(15) (2007):5912–5918.
- [24] A. Sluiter, B. Hames, R. Ruiz, C. Scarlata, J. Sluiter, D. Templeton, and D. Crocker. *Determination of Structural Carbohydrates and Lignin in Biomass Laboratory Analytical Procedure (LAP)*. 2010.
- [25] Megazyme. *Total Starch Assay Procedure (Amyloglucosidase/ α -Amylase Method)*. 2009.

- [26] A. Aden, M. Ruth, and K. Ibsen. *Lignocellulosic Biomass to Ethanol Process Design and Economics Utilizing co-current Dilute Acid Prehydrolysis and Enzymatic Hydrolysis for Corn Stover: National Renewable Energy Laboratory*. NREL/TP-510-32438. Golden, CO: National Renewable Energy Laboratory, 2002.
- [27] C.E. McMillan. *Processes for Pretreating Lignocellulosic Biomass: A Review*. Tech. rep. National Renewable Energy Laboratory, 1992.
- [28] A. Sluiter, D. Hyman, C. Payne, and J. Wolfe. *Determination of Insoluble Solids in Pretreated Biomass Material Laboratory Analytical Procedure (LAP)*. 2008.
- [29] A. Sluiter, B. Hames, R. Ruiz, C. Scarlata, J. Sluiter, and D. Templeton. *Determination of Sugars, Byproducts, and Degradation Products in Liquid Fraction Process Samples Laboratory Analytical Procedure (LAP)*. 2008.
- [30] NREL. *Standard Biomass Analytical Procedures*. 2011. URL: http://www.nrel.gov/biomass/analytical_procedures.html.
- [31] D.W. Templeton, C.J. Scarlata, J.B. Sluiter, and E.J. Wolfrum. Compositional Analysis of Lignocellulosic Feedstocks. 2: Method Uncertainties. *Journal of Agricultural and Food Chemistry* 58 (2010):9054–9062.
- [32] N. Weiss, J. Stickel, J. Wolfe, and Q. Nguyen. A Simplified Method for the Measurement of Insoluble Solids in Pretreated Biomass Slurries. *Applied Biochemistry and Biotechnology* 162(4) (2010):975–987.
- [33] B. Hames, S. Thomas, A. Sluiter, C. Roth, and D. Templeton. Rapid biomass analysis. *Applied Biochemistry and Biotechnology* 105(1) (2003): 5–16.
- [34] C.A. Roberts, J. Workman Jr., and J.B. Reeves III. *Near-Infrared Spectroscopy in Agriculture*. Agronomy. Madison, WI: American Society of Agronomy, Inc., Crop Science Society of America, Inc., Soil Science Society of America, Inc., 2004.
- [35] E. Wolfrum and A. Sluiter. Improved multivariate calibration models for corn stover feedstock and dilute-acid pretreated corn stover. *Cellulose* 16(4) (2009):567–576.

Appendix

R-code used to calculate the uncertainties in xylose yield calculations using both the analytic and Monte Carlo methods:

The yield of xylose from pretreatment is defined as follows

FIS = fraction insoluble solids

c = xylose concentration in liquor

x = xylan fraction in solid

```
y<-function(FIS,c,x,A)A*(1-FIS)*c/x/1000
```

number of iterations for monte-carlo simulation

vary this parameter to see effect on symmetry of distribution

```
num <-10000
```

set the mean and SD for FIS, c, and x

FIS mean value & standard deviation

```
FIS_mean <-0.25 no units
```

```
FIS_sd <-0.01
```

xylose liquor concentration mean value & standard deviation

```
c_mean <-60 g/L
```

```
c_sd <-01
```

xylan feedstock mass fraction mean value & standard deviation

```
x_mean <-0.200 no units
```

```
x_sd <-0.005
```

typical liquor density & xylan/xylose MWs

```
A <-1/1.11 * 132/150 units of g/mL
```

typical slurries are about 25% solids, so 500 g of feedstock yields 2000 g of slurry

```
A <- A * 2000/500
```

create arrays of normally-distributed random variables

```
FIS <-rnorm(num,FIS_mean,FIS_sd)
```

```
c <-rnorm(num,c_mean,c_sd)
```

```
x <-rnorm(num,x_mean,x_sd)

create an array of xylose yield values
yy <-y(FIS,c,x,A)
sd_yy <-sd(yy)

asdf <-y(FIS_mean,c_mean,x_mean,A)

use the PDE for uncertainty to calculate sdYY
compare sdYY to sd(yy) above

a1<- -A/1000*c_mean/x_mean*FIS_sd
a2<- A/1000*(1-FIS_mean)/x_mean*c_sd
a3<- -A/1000*(1-FIS_mean)*c_mean/x_mean2*x_sd
sdYY<- sqrt(a12+a22+a32)
```

R-code used to produce the plots in Figure 8.8:

```
layout(matrix(c(1,2,3,4), 2, 2, byrow = TRUE))
par(mar=c(4,4,3,2)+.1)
FIS<-100*FIS convert to percent
h1<-hist(FIS,plot=FALSE)
xfit<-seq(min(FIS),max(FIS),length=400)
yfit<-dnorm(xfit,mean=mean(FIS),sd=sd(FIS))
yfit <- yfit*diff(h1$mids[1:2])*length(FIS)
plot(xfit, yfit, col="blue", lwd=2,type="l",main=expression(paste("Pretreated
  Slurry ",italic(f[IS])," (%))),xlim=c(mean(FIS)-
  3*sd(FIS),mean(FIS)+3*sd(FIS)),xlab="",ylab="")
text(mean(FIS)+2*sd(FIS),max(yfit)*.8,paste("sd=",format(sd(FIS),digits=2,
  nsmall=2)))
mtext(" (a)",3,cex=0.66,adj=0,line=-1)
lines(h1)

h2<-hist(c,plot=FALSE)
xfit<-seq(min(c),max(c),length=400)
yfit<-dnorm(xfit,mean=mean(c),sd=sd(c))
yfit <- yfit*diff(h2$mids[1:2])*length(c)
plot(xfit, yfit, col="blue", lwd=2,type="l",main=expression(paste("Liquor
  Xylose Conc. ",italic(c[X])," (g/L))),xlim=c(mean(c)-
```

```

3*sd(c),mean(c)+3*sd(c)), xlab="", ylab="")
text(mean(c)+2*sd(c),max(yfit)*.8,paste("sd=",format(sd(c),digits=2,nsml=2)))
mtext(" (b)",3,cex=0.66,adj=0,line=-1)
lines(h2)

```

```

x<-100*x convert to percent
h3<-hist(x,plot=FALSE)
xfit<-seq(min(x),max(x),length=400)
yfit<-dnorm(xfit,mean=mean(x),sd=sd(x))
yfit <- yfit*diff(h3$mids[1:2])*length(x)
xfit<-xfit
plot(xfit, yfit, col="blue", lwd=2,type="l",main=expression(paste("Feedstock
  Xylan Content ",italic(x[X])," (%))),xlim=c(mean(x)-
3*sd(x),mean(x)+3*sd(x)),xlab="", ylab="")
text(mean(x)+2*sd(x),max(yfit)*.8,paste("sd=",format(sd(x),digits=2,nsml=2)))
mtext(" (c)",3,cex=0.66,adj=0,line=-1)
lines(h3)

```

```

yy<-100*yy convert to percent
h4<-hist(yy,plot=FALSE)
xfit<-seq(min(yy),max(yy),length=400)
yfit<-dnorm(xfit,mean=mean(yy),sd=sd(yy))
yfit <- yfit*diff(h4$mids[1:2])*length(yy)
plot(xfit, yfit, col="blue", lwd=2,type="l", main=expression(paste("Xylose
  Yield ", italic(Y[X])," (%))),xlim=c(mean(yy)-
3*sd(yy),mean(yy)+3*sd(yy)),xlab="", ylab="")
text(mean(yy)+2*sd(yy),max(yfit)*.8,paste("sd=",format(sd(yy),digits=2,
  nsml=2)))
mtext(" (d)",3,cex=0.66,adj=0,line=-1)
lines(h4)

```

```

mtext(paste(format(num,scientific=FALSE)," iterations"),side=1,outer=F,
  line=2.5)

```

```

if(to.print) dev.off()

```

Chapter 9

Reaction Engineering Concepts for the Catalytic Conversion of Biorenewable Molecules

Robert J. Davis

9.1 Introduction

Proper design of a catalytic process for the conversion of any chemical species, including biorenewable molecules, requires accurate knowledge of the rate of the reaction, stability of the catalyst, the influence of reactor configuration, and the potential role of transport phenomena. Each of these reaction engineering concepts will be addressed briefly in this chapter, with each concept illustrated with examples involving biorenewable molecules. The goal of this chapter is to help new researchers to the field avoid common pitfalls in the study of reactions catalyzed by solid materials.

Reaction engineering is a broad field with many excellent textbooks dedicated to both undergraduate and graduate courses in the area. Commonly used textbooks include *Elements of Chemical Reaction Engineering* by H.S. Fogler [1], *Chemical Reaction Engineering* by O. Levenspiel [2], *Introduction to Chemical Reaction Engineering and Kinetics* by R.W. Missen et al. [3], *Chemical Reactions and Chemical Reactors* by G. Roberts [4], *The Engineering of Chemical Reactions* by L.D. Schmidt [5], and *Chemical Reactor Analysis and Design* by G.F. Froment et al. [6]. Many of the concepts in this chapter can be found in the recent book *Fundamentals of Chemical Reaction Engineering* by Davis and Davis [7], which is currently available as a PDF file free of charge at <http://caltechbook.library.caltech.edu/274/>.

This chapter is divided into two broad themes, the proper evaluation of the kinetics of catalytic reactions involving biorenewable molecules followed by a discussion of reactor types and transport phenomena that can influence observed reaction kinetics.

9.2 Measurement of Reaction Rates

The reaction rate, r , is defined simply as the time derivative of the extent of reaction:

$$\frac{d\xi}{dt} = r, \quad (9.1)$$

where the extent of reaction ξ is unique to each reaction, i.e., it does not depend on which species in the reaction you follow:

$$\xi(t) = \frac{[n_i(t) - n_i^0]}{\theta_i} \quad (9.2)$$

In the expression above, n_i is the number of moles and θ_i is the stoichiometric coefficient of species i in the reaction. The superscript 0 refers to the initial amount in the reactor. For example, in the reaction of A and B to form product C according to the following equation:



the extent of reaction is calculated by:

$$\xi(t) = \frac{[n_A(t) - n_A^0]}{(-1)} = \frac{[n_B(t) - n_B^0]}{(-2)} = \frac{[n_C(t) - n_C^0]}{(+3)}, \quad (9.4)$$

and the rate is determined by the time derivative of ξ . A very common way to evaluate the rate of a reaction is to load the reactants into a batch reactor together with the catalyst and then measure the loss of reactants or the formation of products over time. A hypothetical plot of the amount of C produced with time after charging 1 mole of A and 2 moles of B to a batch reactor can be found in Figure 9.1. The rate is calculated from the initial slope of the curve divided by the stoichiometric coefficient of the product, which in this case is +3. The rate determined from the slope of a reaction profile at an early time is called an “initial” rate because it will generally decrease as reactants are consumed. Therefore, a rate is specific to a particular set of reaction conditions (concentrations, partial pressures, and temperature) at which it is evaluated. Many researchers unfortunately report product yields instead of rates or reaction profiles. For example, some papers would describe the yield of product C in Figure 9.1 as approximate-

ly 99% after 2 hours, which does nothing to help quantify the rate since the yield after 1 hour is nearly the same.

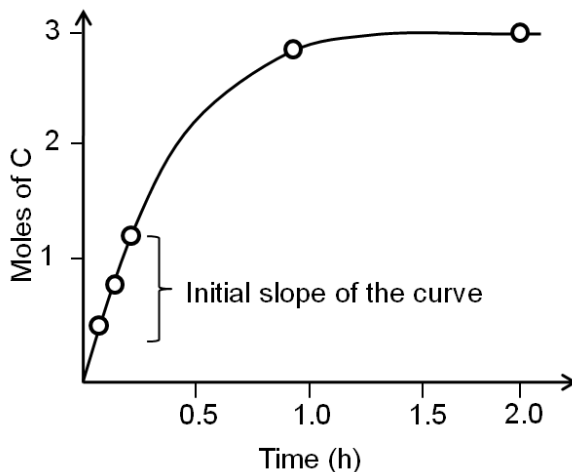


Figure 9.1: Evolution of product with time in a batch reactor for the reaction of $A + 2B \rightarrow 3C$

Since catalysis is a kinetic phenomenon, it is proper to report a rate instead of a yield, preferably normalized by some property of the catalyst relevant to the reaction. If possible, a rate should be reported as a turnover frequency, or TOF, which requires some measure of the active sites on the catalyst. The catalytic conversion of biorenewable molecules generally involves metal catalysts for reactions such as hydrogenation, dehydrogenation, oxidation, decarboxylation, decarbonylation and reforming as well as acid/base catalysts for dehydration, (trans)esterification, hydrolysis and condensation reactions. Thus, characterization of the catalysts used in the conversion of biorenewable molecules should include a measure of the metal dispersion determined either by chemisorption of probe molecules such as CO or H₂, or by direct imaging of the particles by electron microscopy. For counting the number of acid and base sites on catalysts, standard probes such as ammonia and carbon dioxide, respectively, are often used. Some catalysts cannot be appropriately pretreated for gas adsorption studies, so adsorption of species from solution can be performed instead. For example, a recent study by Xi and Davis on the transesterification of tributyrin with methanol over basic hydrotalcite catalysts utilized the adsorption of phenol onto

the hydrotalcites in cyclohexane solvent to count the number of base sites on the catalysts [8]. A turnover rate for transesterification was based on the active site density evaluated by the amount of phenol adsorbed on the samples. Expressing reaction rates as turnover frequencies enables a straightforward comparison of catalyst activity among different samples and different laboratories.

9.3 Kinetics of Chemical Reactions

The rate of reaction is often a strong function of reactant concentrations and, although the order of reaction with respect to various reagents is often positive, it can also be negative because of strong adsorption on the catalyst surface. This can be easily understood from the basic Langmuir-Hinshelwood expression for the rate of reaction of A and B to irreversibly form products in the presence of a solid catalyst. The rate can be written as:

$$r = k[*]_0\theta_A\theta_B, \quad (9.5)$$

where θ_A and θ_B represent the coverage of species A and species B on the catalyst surface, k is the surface reaction rate constant, and $[*]_0$ is the density of active sites on the surface. If the reactants A and B are equilibrated with the surface according to the adsorption equilibrium constants K_{adsA} and K_{adsB} , and the surface reaction is one way, or irreversible, then the above rate expression can be expressed as:

$$r = \frac{kK_{adsA}K_{adsB}[*]_0[A][B]}{(1 + K_{adsA}[A] + K_{adsB}[B])^2} \quad (9.6)$$

Depending on the magnitude of the equilibrium constants, the order of reaction in either A or B can vary between +1 and -1. For the specific case of $K_{adsB}[B] \gg K_{adsA}$ and $K_{adsB} \gg 1$, the rate reduces to:

$$r = \frac{kK_{adsA}[*]_0[A]}{K_{adsB}[B]}, \quad (9.7)$$

which illustrates how the reaction orders in A and in B can be +1 and -1, respectively. The rate should be expressed as a turnover frequency if possible; so if $[*]_0$ can be measured from chemisorption, then the TOF can be calculated:

$$TOF = \frac{r}{[*]_0} = \frac{kK_{adsA}[A]}{K_{adsB}[B]} \quad (9.8)$$

The rates of some catalytic reactions can also be inhibited by the products; for example, the rate of alcohol oxidation is sometimes claimed to be inhibited by adsorption of the acid products on the catalyst. This phenomenon complicates the measurement of initial rates since the product concentration changes significantly at the beginning of a reaction. For the reaction profile in Figure 9.1, which describes the evolution of product C from the reaction of A and B, product inhibition would complicate the calculation of the rate from the initial slope of the reaction profile. In cases involving product inhibition, initial rates should be evaluated with various levels of C in the reactor to quantify the influence of the product on the conversion process.

When more than one reaction occurs, the selectivity of the desired chemical transformation should be reported together with the rate. The *overall selectivity* of a reaction sequence is often defined as the ratio of the total amount of desired species formed to the total amount of all products formed. However, the amount of product can be based on a variety of factors, such as the number of moles of the products, the number of moles of carbon in the products, the mass of the products, etc. Therefore, it is imperative for researchers to report the exact definition of selectivity used in their work. A term that is sometimes referred to as the *instantaneous selectivity* is defined as the ratio of the rate of desired product formation over the sum of the rates of formation of all of the products. The difference between the overall selectivity and instantaneous selectivity is illustrated by a simple example involving parallel and sequential reactions. The reaction of A to form either desired product B or undesired product C via two parallel, irreversible first order reactions ($A \rightarrow B$ and $A \rightarrow C$) with rate constants k_1 and k_2 , respectively, has an overall selectivity to product B that is identical to the instantaneous selectivity:

$$\text{selectivity of } B = \frac{k_1}{k_1 + k_2}, \quad (9.9)$$

because the selectivity in this case does not depend on conversion. A very different result is found when reactions are sequential. Consider the irreversible first order reaction of A to form B which subsequently reacts to form C ($A \rightarrow B \rightarrow C$). At a very early time in the reaction (or low conversion of A), the rate of formation of B is far greater than the rate of formation of C so both the overall selectivity to B and the instantaneous selectivity to B are very high. However, at a late stage of the reaction (high conversion A), B is actually being consumed (negative rate of formation) and there is little B left in the reactor compared to C. Clearly, the selectivity to B and C, regardless of the definition of selectivity, changes throughout the progress of the reaction. This example illustrates the importance of reporting

product selectivities at identical levels of conversion when trying to compare the effectiveness of particular catalysts or operating conditions.

The conversion of biorenewable molecules usually involves more than one reaction, so selectivity needs to be appropriately reported in all published papers. A convenient feature of complex reaction networks is that they consist of assemblies of either parallel or series reactions. Consider, for example, the oxidation of the sugar-derived 5-hydroxymethylfurfural (HMF) to 2,5-furandicarboxylic acid (FDCA) according to the network in Figure 9.2.

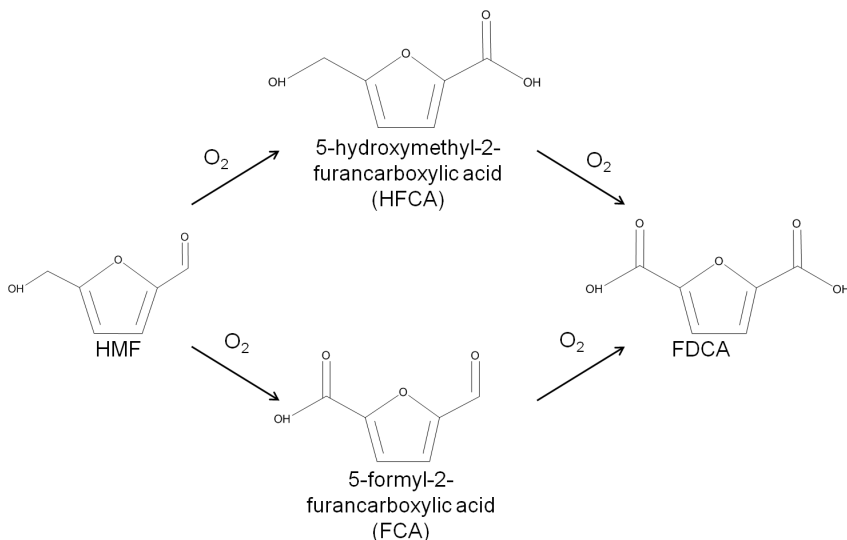


Figure 9.2: Schematic of the reaction network for the catalytic oxidation of 5-hydroxymethylfurfural (HMF) to 2,5-furandicarboxylic acid (FDCA) in aqueous solution

The reactant HMF has two side chains where oxidation can take place. The initial conversion of HMF occurs in the two parallel reactions that oxidize either the aldehyde side chain to form 5-hydroxymethyl-2-furancarboxylic acid (HFCA) or the alcohol side chain to form 5-formyl-2-furancarboxylic acid (FCA). The sequential oxidation of both HFCA and FCA produces the final product FDCA. Figure 9.3 illustrates the reaction profile of HMF oxidation with O_2 in basic aqueous solution over a carbon-supported Pt catalyst. The parallel and sequential nature of the network is illustrated by the early formation of HFCA and FCA followed by their conversion to the final product FDCA. Over Au catalysts, the

initial reaction of HMF to HFCA was found to be very rapid, whereas the subsequent conversion of HFCA to FDCA was quite slow [9]. This reaction network shows the critical importance of comparing selectivity at identical levels of conversion. If it all possible, reporting the entire reaction profile is preferable.

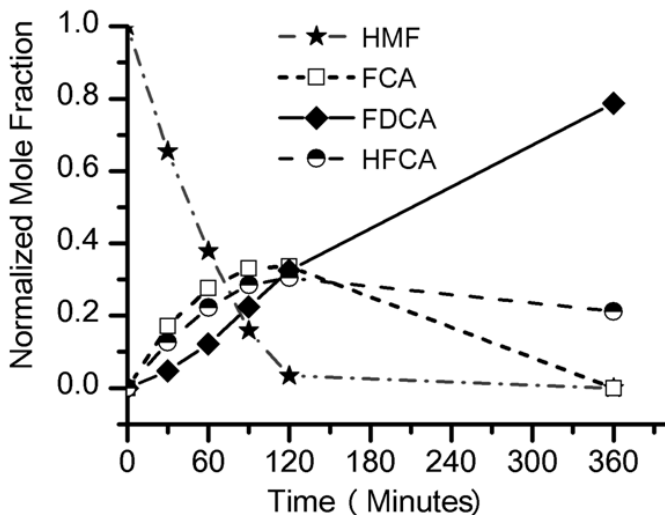


Figure 9.3: Reaction profile of HMF oxidation in 0.15 M HMF, 0.3 M NaOH aqueous solution over a supported Pt catalyst at 295 K and 690 kPa O_2 , adapted from Davis [9]

When reporting reaction rates and selectivities, it is very useful to also report the overall carbon balance in the system. Many of the reactions of interest in the conversion of biomass create tars or light gases that are difficult to quantify. Therefore, the overall carbon balance of the system provides some indication of how important unreported side reactions are in the system. Researchers in this field do not expect the balance to close to 100% because of the difficulty of identifying unknown compounds derived from complex biomass feeds and the formation of carbonaceous residues. Thus, attempts to quantify and report the carbon balance should be made so that others can better understand the overall catalytic process being investigated.

9.4 Deactivation of Catalysts

In a perfect world, catalysts would function forever and never need to be replaced. In reality, however, catalysts lose their activity and/or selectivity over time and eventually become ineffective. Thus, it is just as important to evaluate the stability of catalysts as it is to evaluate their activity and selectivity. The definition of stability depends on one's perspective. Industrial researchers often explore the stability of catalysts over the time frame of months, whereas academic researchers shorten that period to hours or perhaps days.

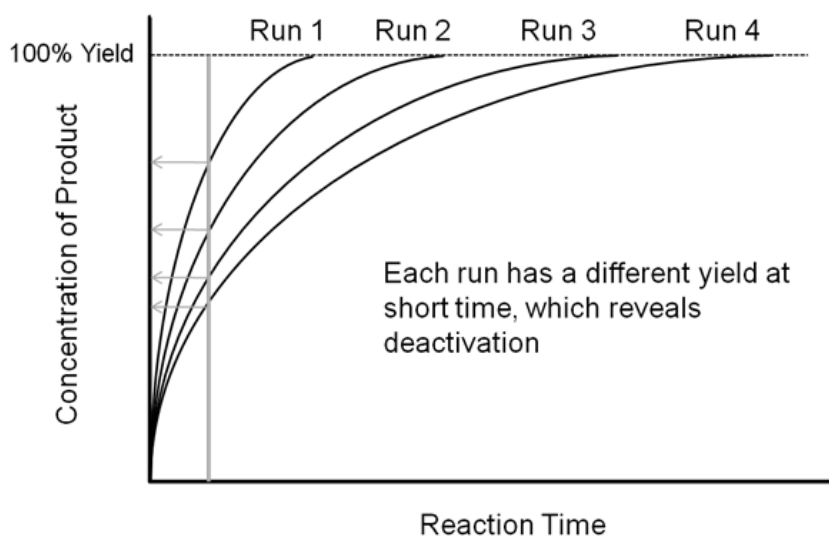


Figure 9.4: Schematic of the reaction profiles associated with the classic recycle test. After each run, the catalyst is recovered and reused in the subsequent run.

Since many studies with biomass-relevant feeds are performed with batch reactors, a common stability probe is known as the recycle test in which catalyst performance is examined after repeated recovery and reuse cycles. Figure 9.4 shows four reaction profiles corresponding to four reaction runs that involve recovery and reuse of the exact same catalyst in each subsequent run. The product is formed in very high yield in all four runs. Thus, if the products are only sampled after long reaction times, very high yield will be reported after each run and

the incorrect conclusion that the catalyst is stable will be presented. However, if the reaction products are sampled at a shorter time (as shown in Figure 9.4) then each run will have less product formed than the previous run, demonstrating the deactivation of the catalyst. This example illustrates the importance of reporting reaction rates during the recycle test instead of simply reporting product yields.

Deactivation is caused by a variety of phenomena, including migration of metal atoms during reaction, adsorption of poisons onto the active sites, and leaching of active species into the reaction medium. Although nanometer-size metal particles are often used as catalysts, they can agglomerate or sinter on the support during reactions at elevated temperature or when the support is transformed in the reaction medium. Moreover, the surface composition of bimetallic nanoparticles can be influenced by the nature of the reaction medium, which can result in a severe restructuring of a bimetallic catalyst in the reactor compared to its structure immediately after preparation. Adsorption of poisons onto a catalyst is particularly problematic when processing impure feed streams such as those derived from raw biomass. For example, trace organic acids can poison catalytic base sites, which is a special concern in the base-catalyzed transesterification of triglycerides with a short chain alcohol to produce biodiesel. The free fatty acid content of biodiesel feedstocks needs to be very low to prevent neutralization of the base catalyst. Since carbon dioxide is also a poison for many solid base catalysts, air-free handling of solid-base catalyzed reactions is required. The influences of base impurities on the performance of acid catalysts are analogous to those mentioned for acid impurities on base catalysts. Some components of biomass contain sulfur, which can severely poison transition metal catalysts when it is present in a reduced form. Although the acid, base, and inorganic components of biomass are potential causes of catalyst deactivation, the carbon backbone of the biomass itself can also be converted into strongly adsorbed carbonaceous deposits that can block active sites on the catalyst.

Ketchie et al. explored the stability of ruthenium metal particles on various supports in liquid water at 473 K at high pH [10]. In that study, ruthenium was supported on γ -alumina, carbon, titania, and silica and reduced in gaseous H_2 at 473 K to generate highly-dispersed supported Ru particles of 1 to 2 nm in average diameter as determined by X-ray absorption spectroscopy and chemisorption of hydrogen. For the particles supported on γ -alumina and silica, the Ru particle size increased substantially after subsequent reduction by H_2 in liquid water at 473 K, indicating a critical role of water on the restructuring of the catalyst. The silica catalyst actually dissolved in 0.4 M NaOH solution at 473 K and the Ru particle size on alumina continued to grow in the basic solution. The X-ray diffraction patterns of the alumina-supported catalyst after the various aqueous treatments revealed a transformation of the support into lower surface area, crys-

talline, bohemite. Interestingly, the Ru particles on carbon and titania were little affected by the aqueous treatments at 473 K, which suggests that these supports are good candidates for further study in the conversion of biomass feeds under aqueous conditions. Clearly, the use of silica and transitional alumina supports should be avoided if at all possible in studies involving liquid water at elevated temperature since the poor stability of these supports can allow the metal particle size to increase.

Maris et al. examined the influence of reaction conditions on the structure of bimetallic Pt-Ru and Au-Ru catalysts used for the hydrogenolysis of glycerol to ethylene glycol, propylene glycol, and (sometimes) lactic acid [11]. The bimetallic catalysts were prepared by selective reduction of HAuCl_4 and H_2PtCl_6 onto a monometallic carbon-supported Ru catalyst. Catalysts were analyzed by electron microscopy, chemisorption of hydrogen, and X-ray absorption spectroscopy to evaluate particle size and distribution of the metals. Single particle elemental analysis in the electron microscope confirmed the selective reduction of Pt by Ru since both elements were present in individual metal particles. However, single particle analysis revealed the presence of monometallic Au and Ru particles as well as bimetallic Au-Ru particles after the attempted reduction of Au selectively onto Ru. Evidently, the synthesis of Pt-Ru generated a more uniformly bimetallic sample than the synthesis of Au-Ru. To confirm the presence of Au on the Ru, ethane hydrogenolysis at 473 K was performed over the parent Ru/C and the bimetallic Au-Ru/C sample. The presence of Au suppressed the turnover frequency on Ru by a factor of 4–5. Interestingly, the turnover frequency on the Pt-Ru sample was similar to that on Ru, even though a monometallic Pt/C catalyst was inactive under identical conditions. Analysis of the X-ray spectra associated with the Pt, Au and Ru components of the catalysts after reduction of the catalysts by gaseous H_2 at 473 K confirmed that first-shell Pt-Ru and Au-Ru interactions were present in the fresh materials, as expected. These catalysts were then used for glycerol hydrogenolysis with 40 bar H_2 in liquid water at 473 K at neutral and high pH. Both of the bimetallic samples catalyzed the glycerol hydrogenolysis reaction with an activity and selectivity similar to that of the monometallic Ru catalyst. A post-mortem analysis of the Au-Ru sample by electron microscopy and X-ray absorption spectroscopy revealed a severe restructuring of the catalyst after the harsh conditions of the glycerol hydrogenolysis reaction. The Au-Ru interaction, which was observed in the X-ray analysis of the fresh catalyst, was completely absent in the used catalyst, and electron microscopy revealed new large gold particles on the support after the reaction. Since X-ray absorption spectroscopy of the Pt-Ru catalyst was nearly identical to the fresh catalyst, the bimetallic Pt-Ru particles were claimed to be much more stable to the aqueous phase reaction conditions than the Au-Ru particles.

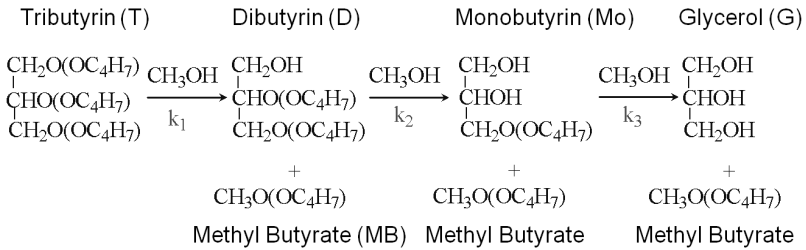


Figure 9.5: Sequential transesterification reactions during the conversion of tributyrin to methyl butyrate and glycerol over solid base catalysts [8, 12]

The transesterification of triglycerides with methanol provides an excellent example to illustrate the poisoning influence of acids on base catalysts. Xi and Davis studied the transesterification of a model triglyceride known as tributyrin with methanol over a hydrotalcite base catalyst to produce methyl butyrate (a short chain biodiesel analogue) in the sequential reaction depicted in Figure 9.5 [8, 12]. Hydrotalcite is a magnesium-aluminum hydroxycarbonate with brucite-type layers of magnesium hydroxide that have some of the magnesium cations replaced with aluminum cations, thus generating a positive charge on the layers. Interlayer anions such as carbonates are therefore needed to maintain electroneutrality of the sample. The upper left portion of Figure 9.6 represents the layered structure typical of hydrotalcite together with carbonate anions and water molecules in the interlayer region. The carbonate form of hydrotalcite, however, is a very weak base and is therefore not effective in catalysis. Conversion of the charge-balancing carbonate anions to hydroxide anions creates a powerful solid Brønsted base that can be utilized in catalytic reactions. Simple ion-exchange of hydroxide for carbonate does not occur because of the high affinity of hydrotalcite for carbonate anions. Therefore, hydrotalcite was decomposed to a mixed oxide of magnesia and alumina followed by rehydration with CO_2 -free water to regenerate the hydrotalcite with hydroxide as the charge balancing anion instead of carbonate, as depicted in Figure 9.6.

This procedure was used to generate a variety of hydrotalcite base catalysts in the work of Xi and Davis [8, 12]. After ensuring that CO_2 -free handling procedures were sufficient, they observed that the water content of the newly-prepared hydrotalcite in the OH^- form was a critical parameter that influenced the transesterification activity of the catalyst. As the OH^- form of hydrotalcite was progres-

sively dried under increasingly rigorous conditions while maintaining the layered structure, the activity of the catalyst was found to decline.

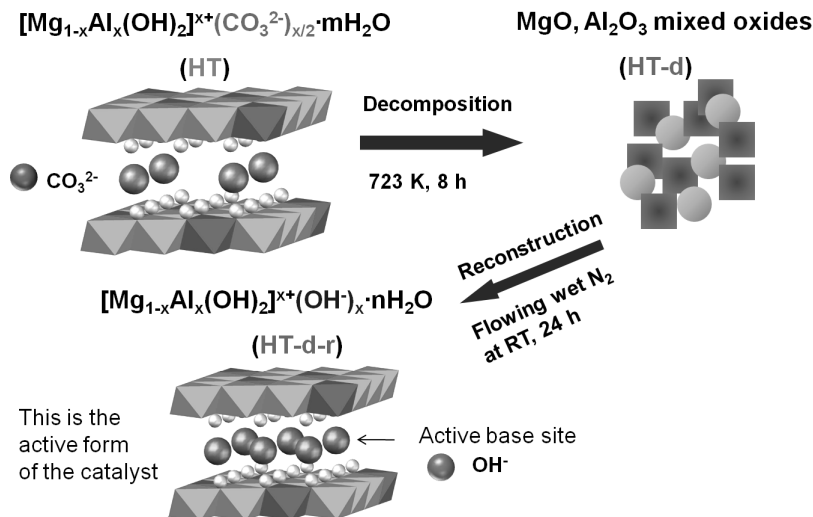


Figure 9.6: Synthesis of hydrotalcite base catalyst by sequential decomposition and rehydration to the OH^- form [courtesy of Y. Xi]

Thus, catalysts that contained the highest loadings of water were the most active. Unfortunately, these active catalysts also deactivated very quickly. Characterization of the used catalysts by X-ray diffraction and FT-IR spectroscopy revealed a significant expansion of the interlayer spacing of the used material compared to a fresh catalyst and the presence of carboxylate species on the used catalyst. Those results pointed to the idea that water or hydroxide facilitated the hydrolysis of tributyrin (or its reaction products) to butyric acid, which would subsequently neutralize the base sites of the hydrotalcite and deactivate the catalyst. Control experiments with butyric acid were consistent with the characterization results. In this case, water accelerated both the desirable transesterification of tributyrin with methanol as well as the undesirable side reaction of hydrolysis to carboxylic acid. The intercalation of butyric acid into the hydrotalcite layers and reaction with the base sites, as depicted in Figure 9.7, is consistent with the observed deactivation of the catalyst and the characterization results by diffraction and spectroscopy. In this particular example, the deactivating species was generated by a side reaction with the active phase of the catalyst.

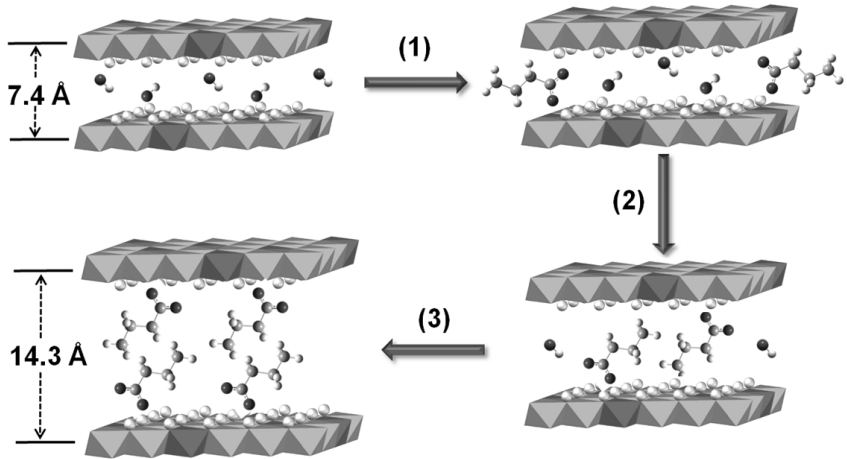


Figure 9.7: Expansion of hydrotalcite layers during catalyst deactivation by reaction with butyric acid [courtesy of Y. Xi]

Leaching of the active phase from a solid catalyst will impact its long term viability as well as the purity of the product stream. Therefore, some evaluation of catalyst leaching should be performed when solid catalysts are utilized in liquid reaction media. For example, the hydrotalcite catalyst described previously was removed by filtering the hot solution after about 60% conversion of the tributyrin was accomplished [12]. The partially reacted mixture was then returned to the reactor to see if further conversion of tributyrin was accomplished. Since the reaction was completely halted after removal of the catalyst, Xi and Davis concluded that the reaction was catalyzed by the hydrotalcite and not any trace components that might have leached from the solid into solution [12]. The opposite conclusion was reported in a paper by those authors for the same reaction catalyzed by layered yttrium hydroxide containing intercalated ethylene glycol [13]. In that study, the catalyst was removed from the reactor after about 40% conversion of tributyrin, but the reaction mixture continued to react in the absence of any catalyst. Evidently, a significant fraction, if not all, of the observed activity resulted from components that leached from the solid into the reactant mixture.

The hot filtration test described above is only one test often used by researchers to explore catalyst leaching. Many researchers also submit both the catalyst and reaction medium to analysis for various elements responsible for the active phase. When supported metal catalysts are used, analysis of the trace metal

content in solution as well as the metal loading on the catalyst before and after reaction can be used to evaluate movement of active metal from the solid to the solution. Another test for leaching involves recovery and reuse of the catalyst in subsequent runs. Although deactivation of the catalyst may or may not be caused by leaching, a constant activity with multiple uses is often claimed to be good evidence that the solid catalyst is effective for reaction and that leaching is not important.

Phan et al. recently published a comprehensive review of Pd-catalyzed Mizoroki-Heck and Suzuki-Miyaura coupling reactions with a critical assessment of whether or not leached Pd species in solution are the active sites [14]. A complication with these coupling reactions is that very low levels of Pd can facilitate the transformations, so a major issue in the field involves the idea that solid-supported metal particles or metal complexes can serve as reservoirs that may release molecular Pd species into solution as the active species. Elemental analyses of the reactant mixtures are generally inconclusive since extremely low levels of Pd, perhaps as low as parts per billion, can be active for the reaction. Extensive research has confirmed that Pd metal does indeed leach into solution during the reactions but then re-deposits back onto the supports upon completion. This phenomenon of leaching and re-deposition during the course of a reaction is precisely why the hot filtration test is best performed in the middle of the reaction when all of the reagents and products are still present in the medium. For the case of the Pd-catalyzed coupling reactions, the rapid deposition of molecular Pd species onto the support during the filtration process could also provide misleading results. Nevertheless, correlation of the coupling rate with the amount of soluble Pd suggests that molecular Pd species are important in the reaction. For cases such as this one in which there are indications that soluble species are critical for reactivity, additional tests need to be performed. Phan et al. describe a poisoning test and a three-phase test to probe the activity of soluble species [14]. In the poisoning test, a solid material that binds the active species in solution is added to the reaction medium—if the reaction is halted by the presence of the solid poison, then the reaction is probably catalyzed exclusively by species in the liquid phase. The three-phase test is a great one for a reaction that involves two reagents and a catalyst. It involves the anchoring of one of the reagents to a solid support and running the reaction with a solid catalyst in the presence of the second liquid phase reagent. Analysis of the supported reagent is used to verify if any reaction occurred in the presence of the catalyst. If there is any conversion of the supported reagent, then the solution phase must have been involved in the catalytic transformation since solid-solid interactions are not favored. A negative test is inconclusive, however, if the anchored reagent is the one that causes leaching of the active phase.

The catalytic transformations of biomass are often performed in the presence of a liquid phase, so evaluation of the solution phase activity should always be performed. Even if the catalyst under investigation does not leach into solution, an understanding of its deactivation profile is important to the field. Although characterization of catalysts under working conditions is best, post-mortem characterization studies can still yield useful insights into the potential causes of catalyst deactivation.

9.5 Reactors Used to Evaluate Catalysts

A common reactor used to study catalytic reactions in a solvent is a stirred vessel or a stirred autoclave reactor. Autoclave reactors for research purposes can be readily purchased at a very modest cost. This type of reactor is termed a batch or semibatch reactor, depending on whether or not reagents are continually added or removed. For example, hydrogenation of a biorenewable molecule that takes place in an autoclave that has been pressurized, and then sealed, is said to occur in a batch mode. However, if the autoclave is connected to a continuous source of hydrogen to maintain a constant pressure in the reactor, then the reactor is operated in a semi-batch mode. In either case, the biorenewable substrate is consumed in the reactor and the reaction rate is evaluated by monitoring the concentrations of the reactants and products with time in the reactor. Batch or semibatch reactors are simple to operate and the solid catalyst can be recovered by simple filtration. Batch reactors are used commercially to produce small-volume, high-value chemicals where the economics of a massive scale are not needed to ensure profitability. Moreover, monitoring of batch processes for quality assurance is straightforward since products are produced in well-separated lots that can be individually-analyzed and tracked. Thus, batch processes are very common in the production of specialty chemicals and pharmaceuticals.

In contrast to batch reactors, flow reactors offer the opportunity to convert reagents in a continuous manner, thus allowing the reacting system to theoretically achieve a stationary state, or steady state, operating condition in which reactants are continually fed to the reactor and products are continually removed. In its simplest form, a catalytic flow reactor consists of a tube packed with catalyst pellets. This configuration, termed a packed bed or fixed bed reactor, requires the catalyst pellets to be immobilized in the tube by mesh screens, glass beads, or some other sort of mechanical device. Catalyst particles can also be fixed to the walls of a reactor. Flow reactors can process very large volumes of material in an efficient manner, which is appropriate for the production of commodity chemicals and the refining of fuels. Moreover, since flow reactors can reach a steady state, kinetic studies that involve changing parameters such as reactant concen-

tration and reaction temperature can be easily performed without having to reload the reactor and restart the reaction. Deactivation in a flow reactor is evaluated by simply monitoring the decline in product concentration exiting the reactor with time, while keeping all other process variables constant. The mathematical treatment of chemical transformations in flow reactors is beyond the scope of this chapter, so the reader is referred to the many textbooks on reaction engineering that were cited in the Introduction for additional information.

In the conversion of biorenewable molecules, the reacting system will often include three phases: a solid catalyst, reagents dissolved in a liquid medium, and a mixture of products in the liquid phase as well as the gas phase. The proper operation and analysis of three-phase systems is quite complex and researchers should strive to simplify their particular configuration if at all possible. One simple example of the possible complexity of three-phase operations involves the choice of whether to flow the liquid reagents in a downflow mode or an upflow mode. Although this looks like a trivial choice at first glance, the realization that gaseous products could be generated as the liquid flows over the catalyst particles in the reactor complicates the flow pattern. In the downflow configuration, gas bubbles that form in the reactor could possibly travel upward, countercurrent to the fluid, because of their buoyancy. Thus, the size of the gas bubbles formed and the velocity of the fluid flowing down through the reactor will determine how the gas exits the reactor. In the upflow configuration, the fluid velocity is in the same direction as the buoyant forces on the gas bubbles, so that both the liquid and the gas will exit the top of the column. Although there is no “correct” way to operate, researchers need to realize that simple physical phenomena can affect the observed behavior in a reactor.

9.6 Mass and Heat Transfer Artifacts

Since multiple phases of matter can exist in a catalytic reactor, the transport of reagents and products between those phases can limit the rate of chemical reaction of those species. Likewise, the rate of transport of heat to a catalyst (for an endothermic reaction) or away from a catalyst (for an exothermic reaction) can affect the observed rate of a reaction. To properly evaluate the intrinsic reaction rate of a chemical reaction occurring in the presence of a solid catalyst, which is certainly the desired goal when comparing a set of catalysts or designing a new process, some estimation of the mass and heat transfer artifacts in the observed rate should be performed. If the rate of mass (or heat) transfer through the reactor limits the observed rate, then the experimental parameters must be adjusted to either lower the reaction rate (i.e., lower reaction temperature, different reactant concentrations) and/or increase the rate of mass (or heat) transfer (i.e., increase

agitation rate, increase flow rate, decrease catalyst particle size). The following sections describe how mass or heat transfer limitations can affect observed reaction rates.

9.6.1 Gas-Liquid Transport

For reactions in which a gaseous reagent is consumed in a liquid solvent in the presence of a solid catalyst, there are several regions in which mass transfer can affect the rate of conversion: the dissolution of gas into the liquid, the transport of dissolved gas through the stagnant boundary layer surrounding a catalyst particle, and the diffusion of dissolved gas through the pores of a catalyst particle. The importance of gas-liquid mass transfer will be discussed first.

Supported gold particles are extremely active catalysts for the oxidation of substrates such as glycerol and hydroxymethylfurfural (HMF) in liquid water at high pH [9, 15]. Very high observed turnover frequencies that exceed 1 s^{-1} for the oxidation reaction on supported Au suggest that the transport of O_2 could limit the reaction rate. Therefore, a check on the mass transfer characteristics within the reactor is warranted.

The oxidation of glycerol and HMF over supported gold catalysts was accomplished in a semi-batch reactor in which a slurry of gold catalyst and reactant in aqueous solution at high pH were stirred under a constant pressure of O_2 [9, 16]. Transport of oxygen across the small interface between the headspace in the reactor and the agitated solvent could possibly limit the observed reaction rate. Therefore, a recommended practice is to evaluate the maximum rate of oxygen transfer under exactly the same conditions of liquid volume, gas pressure and agitation in the system by performing a separate reaction in which oxygen transfer is known to be rate-limiting. A comparison of the maximum flux of oxygen to that observed under catalytic conditions will demonstrate whether or not mass transfer from the gas to the liquid is limiting the observed rate. An effective way to determine the flux of oxygen in a chemical reactor is to utilize a reaction known to biochemical engineers for the evaluation of the volumetric mass transfer coefficient during aerobic fermentation [15]. Specifically, the oxidation of sulfite anions to sulfate anions by O_2 can be used to measure the maximum flux of oxygen into the liquid phase. The sodium sulfite oxidation experiments confirmed that indeed the transfer rate of oxygen could sometimes limit the oxidation rate over Au catalysts, so the amount of Au in the reactor was decreased to appropriate levels prior to reporting rates.

9.6.2 Gas-Solid and Liquid-Solid Transport

For reactions catalyzed by solid particles, transport of reagents through the stagnant boundary layer surrounding the particles (Region 1 in Figure 9.8) and transport within the pore network (Region 2 in Figure 9.8) can potentially limit the observed reaction rate. Thus, researchers need to ensure that artifacts in kinetic studies resulting from transport limitations involving the catalyst particles are minimized.

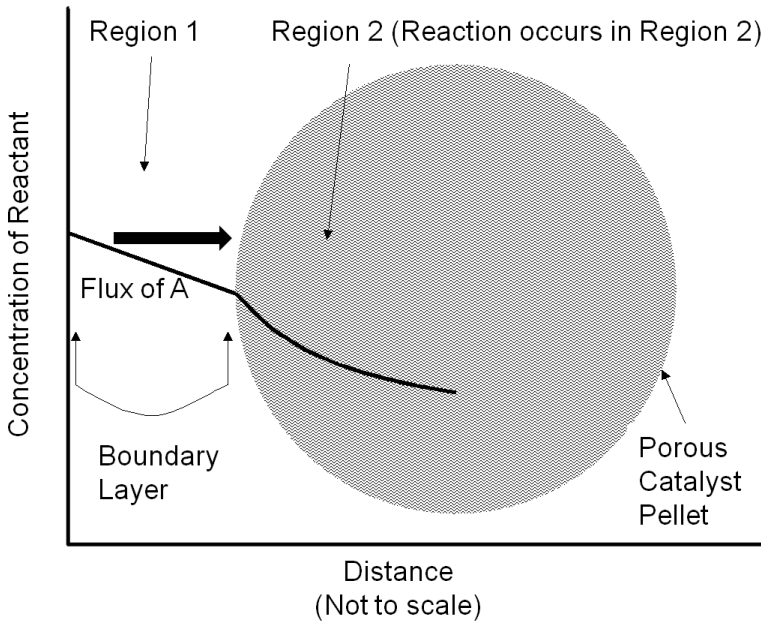


Figure 9.8: Concentration profile of a reactant A in the vicinity of a porous solid catalyst particle. Region 1 depicts the stagnant boundary layer surrounding the particle and Region 2 depicts the porous interior of a catalyst particle where active sites are located. Adapted from Davis [7]

A simple mathematical analysis (not presented here) illustrates that the flux of a reactant to a catalyst particle is directly proportional to the concentration difference between the bulk fluid phase surrounding a particle and the external surface of the catalyst, as represented in Region 1 of Figure 9.8, with a propor-

tionality constant assigned as the mass transfer coefficient k_c . The linearity of the concentration profile in this region results from the assumption that no chemical reactions occur in the boundary layer. According to this analysis, mass transfer characteristics of the system can be improved by simply adjusting system variables that increase the mass transfer coefficient. The following relationship between the mass transfer coefficient associated with flow around spherical particles and a variety of process variables can be derived from engineering correlations:

$$k_c \propto \frac{D_{AB}^{\frac{2}{3}} u^{\frac{1}{2}} \rho^{\frac{1}{6}}}{R_p^{\frac{1}{2}} \mu^{\frac{1}{6}}}, \quad (9.10)$$

where D_{AB} , u , ρ , R_p and μ represent the diffusivity of A in medium B, the linear fluid velocity, the fluid density, the radius of the catalyst particle, and the viscosity of the fluid, respectively. Properties such as diffusivity, fluid density, and fluid viscosity are very difficult to change in a reacting system and are not usually considered as adjustable process variables. In contrast, increasing the linear fluid velocity (by stirring faster or flowing faster) and decreasing catalyst particle size are often used to increase the mass transfer coefficient of a catalytic system. It should be emphasized that pressure drop through a packed bed of particles is often the limiting process variable since utilizing smaller catalyst particles and increasing the flow of reagents can potentially cause an unacceptably high pressure drop in a flow reactor.

Assuming the mass transfer characteristics surrounding a catalyst particle are acceptable, reagents and products still need to navigate the internal pore network of the catalyst as depicted in Region 2 of Figure 9.8. The concentration profile within the particle is non-linear because the reagent is consumed as it proceeds into the catalyst interior. The analysis of mass transfer characteristics in porous catalysts is complicated by the fact that both reaction and diffusion occur simultaneously.

Figure 9.9 summarizes how the diffusivity of gaseous molecules is affected by the pore size of a catalyst particle. Most importantly, diffusion in very large pores is controlled by molecule–molecule collisions and is termed molecular diffusion in Figure 9.9. However, as the pore size decreases to the same size as the mean free path of the gaseous molecules, collisions between the gas and the pore walls become increasingly important. This type of diffusion, known as Knudsen diffusion, is obviously a strong function of the size of the pore, as illustrated in Figure 9.9. Single file diffusion involves pores that are too narrow to allow molecules to pass each other, which can be important in biomass-related systems involving very large molecules. It should be noted that Figure 9.9 summarizes the diffusivity of gaseous molecules in porous systems. The molecular diffusivity of

most compounds in the liquid phase is often in the range of $10^{-5} \text{ cm}^2 \text{ s}^{-1}$, which is significantly less than the molecular diffusivity and the Knudsen diffusivity for gas-solid systems as represented in Figure 9.9. The lower diffusivity of molecules in a liquid medium results from the frequent collisions with solvent molecules in a condensed phase. For liquids, molecule-fluid collisions always dominate over molecule-pore collisions until pores become so small that only single file diffusion can occur.

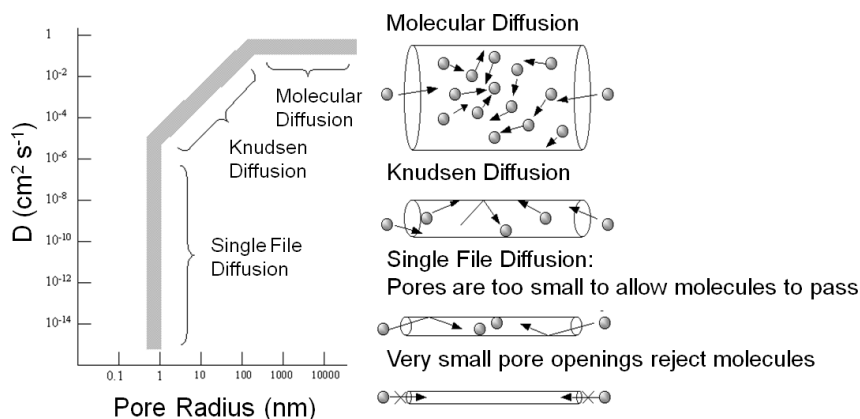


Figure 9.9: Influence of pore size on the diffusivity (D) of gaseous molecules in porous materials. From Davis [7]

If both the reaction rate constant and the diffusivity of a reacting species are known or can be estimated, the concentration of that species undergoing reaction in a catalyst pellet can be calculated by the simultaneous solution of the differential equations that describe the reaction (mole balance in the pore) and diffusion (Fick's Law) in the pore. This well-known system of equations in reaction engineering reveals a non-dimensional quantity that relates the characteristic rate of reaction to the characteristic rate of diffusion in the pore. For a first order reaction in a cylindrical catalyst pore, this quantity ϕ (also known as the Thiele modulus) is simply:

$$\phi = L \sqrt{\frac{k}{D}}, \quad (9.11)$$

where L is the length of the catalyst pore, k is the first order rate constant and D is the diffusivity of the reacting species in the medium. The Thiele modulus for

reactions other than first order can also be derived, but are not presented here for the sake of brevity. The concentration profile for a species A undergoing a first order reaction in a catalyst pore is presented in Figure 9.10 for different values of the Thiele modulus. The concentration of A in the pore (C_A) is normalized by the concentration at the pore mouth, which is at the external surface of the catalyst (C_{AS}). The profiles in Figure 9.10 show that, for high values of the Thiele modulus, the reactant A is consumed rapidly in the pore and that diffusion of A into the pore is not fast enough to replace the A that is converted. Thus, for a value of $\phi=10$ in Figure 9.10, the reactant A converts completely in the first half of the pore.

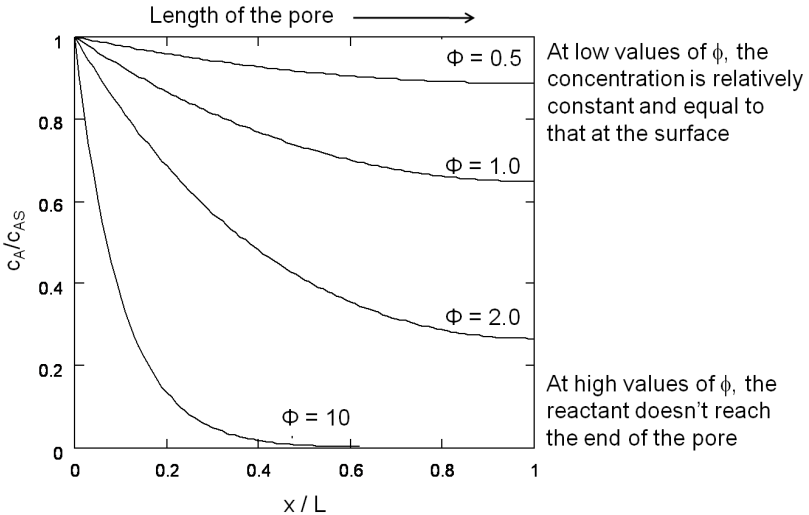


Figure 9.10: Concentration profiles of reactant A converting in a first order reaction along the pore of a catalyst pellet, for various values of the Thiele modulus. Adapted from Davis [7]

This example illustrates the importance of properly balancing the rate of reaction to the rate of diffusion in a solid catalyst. If nanoparticles of an expensive catalytic metal, such as Pt, were deposited along the length of the pore to catalyze a desired reaction, half of the Pt would not even be involved in the reaction for the case in Figure 9.10 when $\phi=10$, which is a very inefficient use of such a precious resource. Moreover, the observed rate of reaction is convoluted with the rate of diffusion when the concentration profile varies greatly down the length of a pore

because the rate is a function of the reactant concentration. To measure the intrinsic rate of a catalytic reaction, one needs to ensure that all of the active sites in the catalyst pore are accessed and that there is a negligible concentration gradient of the reactants (and products, if there is product inhibition) along the length of the pore. The profile in Figure 9.10 for $\phi=0.5$ shows that the concentration of reactant A is nearly constant along the length of the pore, which is the preferred circumstance for measuring the intrinsic reaction rate on a catalyst.

The Thiele modulus for any shape of catalyst pellet, ϕ_0 , is defined by

$$\phi_0 = L_p \sqrt{\frac{k}{D}}, \quad (9.12)$$

where L_p is the characteristic length associated with the catalyst particle shape determined by the ratio of the volume of the particle to its external surface area. The Thiele modulus is used to estimate how effectively a catalyst is being used in a reaction by calculating a term known as the effectiveness factor, η , which is defined as the observed reaction rate in a catalyst particle divided by the rate if it were not influenced by diffusion of the reactants. Figure 9.11 illustrates the relationship between the effectiveness factor and the Thiele modulus for a first order reaction in a porous catalyst of any geometry. The effectiveness factor approaches unity at low values of the Thiele modulus ($\phi_0 \ll 1$), indicating that the rate is unaffected by diffusional limitations under these conditions. However, at high values of the Thiele modulus ($\phi_0 \gg 1$), the effectiveness factor becomes much less than one and approaches the relationship defined by $\eta=1/\phi_0$, as depicted in Figure 9.11. Thus, to operate in a condition that is not influenced by the effects of mass transfer along the pore length, parameters such as catalyst particle size (which determines L) and reaction temperature (which affects k) need to be selected so that the Thiele modulus is much less than unity.

If the intrinsic reaction rate constant is unknown, then estimation of the Thiele modulus is quite difficult. Fortunately, Weisz and Prater developed a dimensionless parameter Φ based on observable quantities to ascertain whether or not diffusional artifacts are influencing the observed rate [17]. If the so-called Weisz-Prater criterion shown below is satisfied, then there are no significant diffusional limitations in the system:

$$\Phi = \frac{r_{obs} R_p^2}{D^e C_{AS}} < 1, \quad (9.13)$$

where r_{obs} is the observed reaction rate for an irreversible first order reaction, R_p is the radius of a spherical catalyst pellet, D^e is the effective diffusivity (the

diffusivity multiplied by the porosity of the catalyst, typically 0.5, divided by its tortuosity, typically 3–4; see any text on reaction engineering for additional details) and C_{AS} is the concentration of A at the external surface of the catalyst pellet.

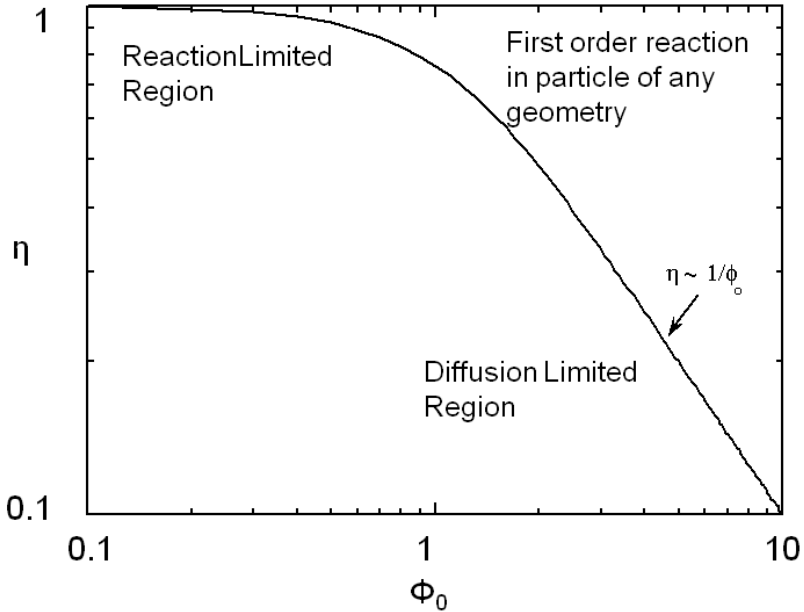


Figure 9.11: Plot showing how the effectiveness factor η is influenced by the Thiele modulus ϕ_0 . From Davis [7]

As an example, Xi and Davis used the Weisz-Prater criterion to evaluate the potential for diffusional limitations in their study of the transesterification of tributyrin with methanol to produce methylbutyrate, which was introduced earlier [12]. The reaction was run in a great excess of methanol so that the reaction profiles of tributyrin conversion to dibutyryn, monobutyryn, and eventually glycerol, as illustrated in Figure 9.5, could be easily modeled as pseudo-first order consecutive reactions. The initial reaction rate for the conversion of tributyrin in the first step was observed to be $8.0 \times 10^{-5} \text{ mol s}^{-1} \text{ g}^{-1}$ at 333 K over a hydrotalcite catalyst. An estimate of the catalyst particle size derived from sieve trays was 0.038 mm and the initial tributyrin concentration was 0.7 mol L^{-1} . The catalyst density and effective diffusivity of tributyrin in methanol were estimated to be

2 g cm^{-3} and $10^{-5} \text{ cm}^2 \text{ s}^{-1}$. Substituting the appropriate values into the Weisz-Prater criterion resulted in a value of $\Phi=0.3$, which is less than unity and thus satisfies the criterion. A value of $\Phi=0.3$ corresponds to an effectiveness factor greater than 0.95, which indicates that effects of mass transfer limitations on the observed rate were negligible.

Temperature gradients in reactors and catalyst particles can also affect the observed reaction rate. Since the rate of most reactions increases exponentially with absolute temperature, a small gradient in temperature can impact the observed reaction rate in a major way. An interesting illustration of this phenomenon can be found in the work of Kehoe and Butt [18]. The temperature profile across the external film surrounding a catalyst pellet, as well as within the pellet itself, was monitored during the exothermic hydrogenation of benzene over a kieselguhr-supported Ni catalyst.

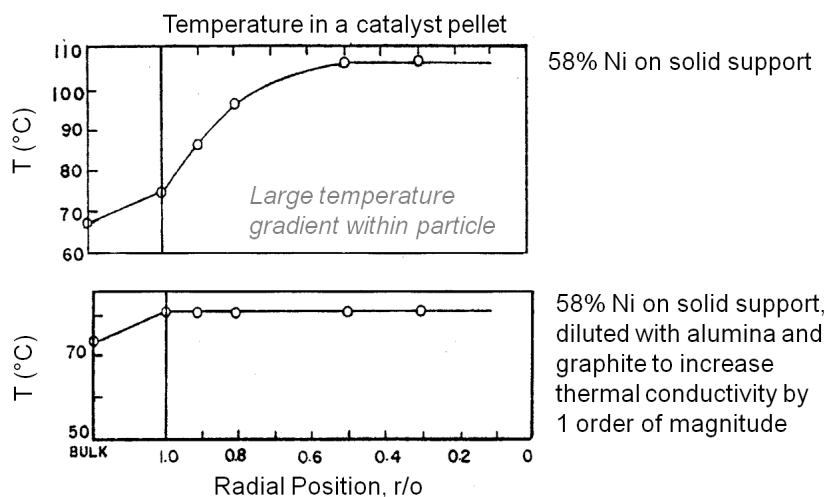


Figure 9.12: Measured external and internal temperature profiles during benzene hydrogenation over Ni catalysts. Feed conditions: 14% C_6H_6 , 86% H_2 , $T_{\text{feed}}=338\text{--}340 \text{ K}$, $P=1 \text{ atm}$, H_2 flow $9.0(\pm 1.2) \times 10^{-3} \text{ mol s}^{-1}$. Measured rate: $2.44 \pm 0.08 \times 10^{-6} \text{ mol s}^{-1} \text{ g}^{-1}$. Adapted from Kehoe [18]

The upper portion of Figure 9.12 illustrates a 10 K temperature gradient across the external film, where the catalyst surface is hotter than the surround-

ing bulk fluid. However, the temperature increase within the catalyst particle itself was about 30 K because the heat generated inside the pellet, where most of the active Ni catalyst was located, could not be removed fast enough. The lower portion of Figure 9.12 illustrates how increasing the thermal conductivity of the catalyst pellet by adding alumina and graphite eliminated the temperature gradient in the pellet. However, the gradient across the external film still remained. The thermal gradients sometimes present during exothermal catalytic reactions raise the temperature of the catalyst pellet above that of the surrounding fluid. Therefore, the catalyst might be operating at an internal temperature that is much hotter than is realized or monitored, and the observed rate can be much higher than one would expect for a reaction taking place at the bulk fluid conditions. Indeed, the effectiveness factor of a pellet accomplishing an exothermic reaction can exceed unity because of this phenomenon.

$$\frac{r_{\text{obs}} R_p^2}{D^e C_{AS}} < \frac{1}{n}$$

Weisz-Prater criterion used to confirm a lack of significant mass transfer limitations inside spherical catalyst particles (r_{obs} is the observed rate of an irreversible reaction, R_p is the radius of the catalyst particle, D^e is the effective diffusivity, C_{AS} is the concentration at the particle surface, and n is the reaction order).

$$\frac{r_{\text{obs}} R_p}{k_c C_{AB}} < \frac{0.15}{n}$$

Criterion used to confirm that mass transfer from the surrounding fluid to the particle surface does not affect the observed rate (C_{AB} is the concentration in the bulk fluid and k_c is the mass transfer coefficient).

$$\frac{|\Delta H_r| r_{\text{obs}} R_p^2}{\lambda^e T_s} < 0.75 \frac{R_g T_s}{E}$$

Anderson criterion used to confirm a minimal intraparticle temperature gradient (ΔH_r is heat of reaction, λ^e is the effective thermal conductivity of the particle, T_s is the surface temperature, R_g is the gas constant, and E is the true activation energy)

$$\frac{|\Delta H_r| r_{\text{obs}} R_p}{h_t T_B} < 0.15 \frac{R_g T_B}{E}$$

Mears criterion used to confirm a minimal temperature gradient between the fluid phase and the particle (h_t is the heat transfer coefficient and T_B is the bulk fluid temperature)

Figure 9.13: Commonly-used criteria to check for the influences of mass and heat transfer artifacts in measured catalytic reaction rates. See Davis [7]

As discussed above, the Weisz-Prater criterion was developed to ascertain the importance of an intrapellet concentration gradient on the observed rate of a catalytic reaction. Likewise, criteria have been developed to elucidate the role of a concentration gradient through the external film surrounding a catalyst particle. Moreover, additional criteria analogous to those used for exploring mass transfer effects have been proposed to determine the importance of heat transfer effects in catalytic systems. A summary of commonly-used mass and heat transfer criteria is provided in Figure 9.13.

All of the criteria discussed previously were derived for rather specific conditions and require the knowledge of various system properties such as diffusivity, mass transfer coefficient, thermal conductivity, and heat transfer coefficient. Perhaps the best experimental verification for the lack of mass and heat transfer effects in kinetic data associated with solid catalyst particles is known as the Koros-Nowak criterion, which is sometimes referred to as the Madon-Boudart criterion. In this criterion, the turnover frequency of a reaction is measured on catalysts with at least two different loadings of active sites. If the turnover frequency is invariant with active site density and the same comparison is repeated at another temperature, then the measured rates are guaranteed to be free of artifacts from mass and heat transfer limitations.

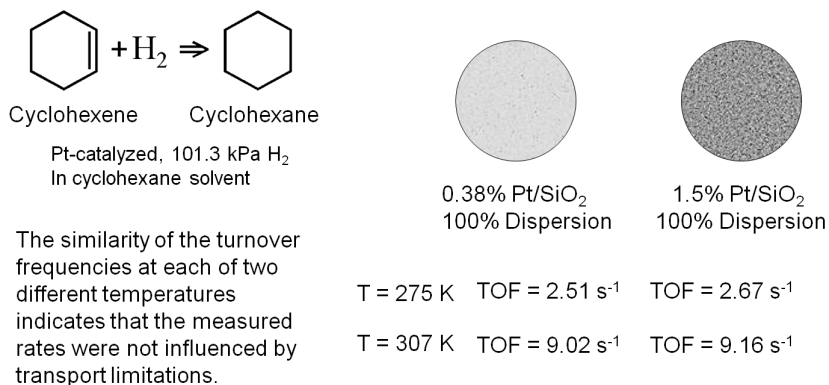


Figure 9.14: Example of the Koros-Nowak criterion or the Madon-Boudart criterion for cyclohexene hydrogenation, based on data in [18]

Figure 9.14 illustrates the implementation of this criterion by Madon and Boudart, who studied cyclohexene hydrogenation over two different supported Pt catalysts, with a factor of 4 difference in Pt loading while maintaining a high

dispersion [19]. As revealed in Figure 9.14, the turnover frequency on both catalysts was the same ($\sim 9.1 \text{ s}^{-1}$) at 307 K, within experimental error. There is a minor complication that occurs with exothermic reactions since heat transfer limitations can sometimes compensate for mass transfer limitations and give an overall effectiveness factor of one. Therefore, if the TOF is the same for the two catalysts at another temperature, then the system is surely free of transport artifacts. Indeed, Figure 9.14 shows that the two Pt catalysts have a TOF of $\sim 2.6 \text{ s}^{-1}$ for cyclohexene hydrogenation at 275 K, confirming that kinetic results at 307 K and 275 K were not influenced by transport limitations.

Maris et al. used a form of the Koros-Nowak or Madon Boudart criterion to evaluate the kinetics of glucose hydrogenation to sorbitol over Ru nanoparticles supported silica and carbon [20]. In that study, a 50 wt% aqueous solution of glucose was hydrogenated with 80 bar H_2 at 373 K in a batch autoclave reactor containing the supported Ru catalyst. The rate was calculated from the initial slope of the sorbitol profile. Three different synthetic Ru/ SiO_2 catalysts with Ru loadings ranging from 0.56 wt% to 4.47 wt% were tested, as well as a commercial sample of 5 wt% Ru/carbon. The particles of Ru on all of the silica-supported samples ranged from 1 to 2 nm as determined by H_2 chemisorption, whereas the Ru/carbon sample had slightly larger particles. The TOF of the reaction over all four samples was reported to be $\sim 0.25 \text{ s}^{-1}$, which is consistent with the idea that the kinetics are free from transport artifacts. It would have been preferable to have the same experiment reported at a different temperature. However, it is very unlikely that the compensation of heat and mass transfer would have occurred in exactly the same fashion over all four catalysts with two different supports. It should be noted that ideally the Koros-Nowak or Madon-Boudart criterion should be performed with identical metal particle sizes. This requirement originates from the fact that some reactions are structure sensitive, i.e., their TOF varies significantly as the metal particle size varies between 1 and 10 nm. Since hydrogenation reactions on transition metals are generally considered to be structure insensitive, small variations in metal particle size, such as the Ru catalysts in the previously discussed example, should not appreciably affect the observed TOF.

An excellent example of how transport criteria can be used to evaluate the kinetic data for a biomass-related chemical conversion can be found in the recent work of the Dumesic lab. Shabaker et al. studied the aqueous phase reforming of methanol and ethylene glycol at 483–493 K to produce hydrogen and carbon dioxide over alumina-supported Pt catalysts in an upflow, fixed-bed reactor attached to a gas-liquid separator at the reactor outlet [21]. The overall reaction network is quite complicated since side reactions such as the water gas shift reaction and hydrocarbon formation reactions can be observed. The Pt/alumina catalysts were prepared by incipient wetness impregnation followed by calcination and sieving

to an appropriate pellet size. In this manner, the Pt loading within the powders could be controlled and the overall size of the supported catalyst pellets could be selected from a judicious choice of sieve trays. Chemisorption of CO was used to evaluate the dispersion of Pt on the alumina support as well as the Pt particle size. Conversions of 10 wt% solutions of methanol or ethylene glycol were kept below 3% to ensure that the concentration profile of reactants throughout the bed was fairly constant. Shabaker et al. explored the transport characteristics of the system under the most severe conditions of high temperature and high catalyst tortuosity. For the highest Pt-loaded catalyst with the largest pellet size, the Weisz-Prater parameter was calculated to be 6.7 and the internal effectiveness factor was reported to be 0.78, confirming that mass transfer within the Pt/alumina pellets limited the rate. However, pellets with much smaller size and Pt loading were not limited at all by transport artifacts. The authors concluded from their analysis that mass transfer limited the kinetics before heat transfer, and that the transport limitations through the external film surrounding the pellets is important only after resistance to mass transfer in the pores of the catalyst became significant. It should be noted that heat transfer limitations did not come into play in this particular system since the reaction medium was a liquid, which has a much higher thermal conductivity than a gas. Since the smaller pellet sizes appeared to be free of transport limitations, Shabaker et al. performed a Koros-Nowak or Madon-Boudart test on two small pellet Pt catalysts with Pt loadings of 0.16 wt % and 0.59 wt%. The TOF to produce H₂ at 483 K was similar at 4.3 and 4.2 min⁻¹, respectively, which also suggests that the results are free of transport limitations. The TOF at 498 K was again similar at 9.4 and 9.0 min⁻¹, which strictly satisfies the Madon-Boudart criterion for the invariance of TOF at two different temperatures.

9.7 Influence of Reactor Configuration

Private discussions among researchers reveal that sometimes different reactivity results are observed for biomass-related conversions in flow reactors compared to batch reactors. In principle, however, there should be little or no difference as long as the details of mixing and transport artifacts are correctly accounted for. In this section, a couple of recent examples will be discussed to highlight the major areas of concern when performing reactions in various reactor configurations.

Zhang et al. reported a detailed Langmuir-Hinshelwood kinetic expression for lactic acid (LA) hydrogenation/hydrogenolysis to propylene glycol in aqueous solvent over a supported Ru catalyst [22]:

$$r_{LA} = \frac{kC_{LA}P_{H_2}}{(1 + K_{H_2}P_{H_2} + K_{LA}C_{LA})^2}, \quad (9.14)$$

where the K values represent fitted adsorption constants and k is an overall rate constant. The authors performed an extensive analysis of the transport characteristics of their system and confirmed that their kinetic data were not significantly influenced by mass transfer artifacts. Therefore, the constants in their expression could be derived from reaction profiles in the batch reactor. Moreover, reasonable values of the heats of adsorption of LA and H_2 that were determined from the temperature dependence of the adsorption constants illustrated the thermodynamic consistency of the kinetic model. In follow-up work, Xi and Miller directly compared the conversion of lactic acid to propylene glycol over supported Ru in a multi-well batch system to that in a downflow trickle bed reactor in which gas and liquid are co-fed to a tube packed with the same catalyst [23]. The temperature was lowered to the point at which the researchers were satisfied that mass transfer limitations within the catalyst particles were not limiting the rates. Although the behavior of the batch reactor agreed very well with earlier work from the lab [22], the results from the trickle bed system deviated from the expected performance. The observed reactivity in a trickle bed reactor needs to account for the fact that some parts of the solid catalyst particles can be totally wetted by the liquid medium whereas other parts of the catalyst particles can be dry [24]. In the case of hydrogenation reactions, diffusion of hydrogen through the liquid film will be important in the wetted sections only. Thus, Xi and Miller explored by numerical methods four different models of the trickle bed reactor:

1. A partially wetted catalyst in which one rate is used for the wetted fraction and another rate is used in the non-wetted fraction;
2. a fully wetted catalyst;
3. a partially wetted catalyst in which reaction only occurs in the wetted fraction;
4. a fully wetted catalyst in which there are no gas-liquid or liquid-solid mass transfer resistances that affect the rate (the standard plug flow model).

The rigorous, partially wetted catalyst model agreed well with the experimental observations in the trickle bed reactor since the other models either underpredicted or overpredicted conversion of lactic acid. In summary, conditions of high liquid flow and low temperature (i.e., low rate and low conversion), allow results in the trickle bed reactor to approach those of fully wetted behavior so that the kinetics are similar to those in a batch reactor. However, under high conversion conditions, partial wetting of the catalyst and limitations from mass transfer can disguise the reaction kinetics. Additional analysis of trickle bed behavior accom-

plishing the conversion of a biorenewable molecule can be found in the recent published work of Xi et al., which involves the hydrogenolysis of glycerol to propylene glycol in alkaline aqueous solution over a Co/Pd/Re catalyst [25].

A particularly intriguing case of influencing reactivity by altering the reactor configuration is the oxidation of glycerol over supported Au catalysts. Gold is an excellent catalyst for the oxidation of glycerol in aqueous solution at mild conditions, but the reaction requires the presence of added base [26]. The reaction is generally believed to occur by formation of a glyceraldehyde intermediate that rapidly interconverts to dihydroxyacetone in basic solution. These reactive intermediates are then oxidized primarily to glyceric acid, with some researchers also reporting the presence of the product glycolic acid formed by C–C bond cleavage. Interestingly, very little of the diacids (tartronic and oxalic) are observed, even at high conversions of glycerol. A simplified schematic diagram of this sequence is presented in Figure 9.15.

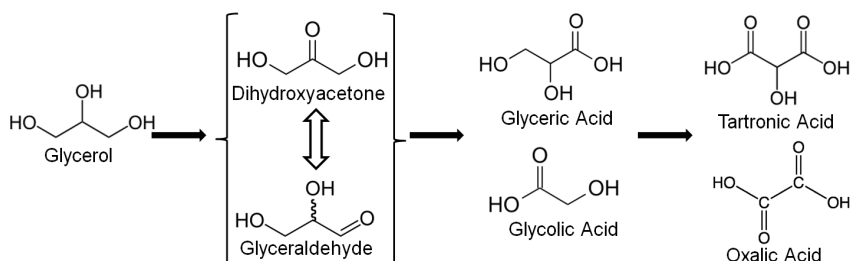


Figure 9.15: Simplified schematic representation of the reaction network for glycerol oxidation in alkaline water solution on Au catalysts

Pollington et al. performed glycerol oxidation utilizing a Au catalyst in a meso-scale structured downflow slurry bubble column reactor and compared the results to those obtained in a standard batch autoclave reactor [27]. The researchers were interested in exploring how the hydrodynamics of a three-phase system in which the Au catalyst was present in a moving slurry would affect activity and selectivity of the oxidation reaction. Their closed-loop recirculating flow reactor system involved passing the reactant liquid through the reactor after which the product stream was collected in a receiver vessel and then pumped back to the reactor. The oxygen was introduced at the top of the reactor where it was mixed with the liquid spray before entering the reaction zone. It should be noted that the receiver vessel was depressurized so that high pressure gas was only present in the reaction zone. The powder catalyst, 1 wt% Au on carbon,

was evaluated for glycerol oxidation in a standard batch reactor at 333 K with a 0.6 mol L^{-1} aqueous solution of glycerol containing NaOH at the same concentration [28]. Under their particular conditions, glyceric acid was produced with nearly 100% selectivity at 30% conversion of glycerol. When the same catalyst powder was placed in the receiver vessel of the closed loop recirculating reactor, the measured activity and selectivity were substantially altered. In this reactor configuration, the Au/carbon powder catalyst was transported with the liquid to the reaction zone in which high pressure gas was added. The specific rate in the flow reactor was higher by several orders of magnitude compared to that observed in a batch autoclave at the same temperature and reactant concentration. Moreover, the selectivity of the reaction at 30% conversion of glycerol was about 50% glyceric acid with the remaining 50% being mostly dihydroxyacetone. The report claims that higher oxygen availability through improved oxygen transport in the three-phase recirculating loop reactor is responsible for the large difference in observed activity and selectivity compared to a standard batch autoclave reactor [27]. It should be noted, however, that a recent report by Zope et al. indicates the role of oxygen during glycerol oxidation is mainly that of an electron scavenger for the Au, whereas the hydroxyl species present in the alkaline solution is critical for the oxidation reaction [26]. Therefore, a complex interplay of oxygen, hydroxyl, gold, and glycerol is involved in structured reactors.

At about the same time as the work by Pollington et al. was published, Zope and Davis reported a comparison of glycerol oxidation in a batch reactor and in a fixed bed flow reactor, both containing Au nanoparticles supported on titania [29]. The flow reactor in this particular case was operated in a single pass, up-flow mode in which high pressure oxygen was added to a pressured liquid stream that was fed to the fixed bed of Au/TiO₂ catalyst pellets. The optimum pellet diameter of 180 μm was used to provide the lowest resistance to mass transfer without causing an unacceptable pressure drop in the reactor. Optimal liquid and gas flow rates were also determined to minimize impacts of transport limitations while limiting the conversion through the reactor. Despite the best attempts to facilitate mass transfer in the system, the rate of oxidation on supported Au was too high to guarantee all kinetic results were free of transport limitations. Nevertheless, important differences in glycerol reactivity between the flow reactor and the batch reactor were observed. In the autoclave reactor, the primary product was glyceric acid over Au/titania as expected, but substantial amounts of glycolic acid and trace amounts of diacids were also observed. The selectivity to diacid products (tartronic and glycolic) increased substantially in the fixed bed reactor compared to the very low values in the autoclave reactor. More specifically, diacid selectivity in a batch reactor was always less than 10% of the product mixture (and sometimes less than 5%) for various concentrations of NaOH and

conversion levels of glycerol up to 83%. However, diacids were found in the effluent from the flow reactor at levels greater than 30% for even low levels of glycerol conversion and otherwise identical conditions. The turnover frequency in the flow reactor was about a factor of three lower than that in the batch system, which was likely the result of differences in the mass transfer characteristics of the two systems.

In summary, the results presented in Ref. 29 show how moving a Au catalyst from a batch system to a flow system can enhance diacid formation (the end of the reaction network in Figure 9.15) whereas the results in Ref. 27 illustrated how moving a Au catalyst from a batch system to a recirculating slurry reactor can shift the product distribution back to dihydroxyacetone (the beginning of the reaction network in Figure 9.15). In principle, the reaction should be entirely predictable from one reactor configuration to another as long as the details of the mechanism of the complex reaction network are known. In the case of Au-catalyzed oxidation of glycerol, important roles of solution phase reactions, alkalinity, oxygen transfer, and the Au catalyst in the reaction network prevent the use of simplistic reactor engineering models of performance.

9.8 Conclusions

The goal of this chapter is to emphasize important reaction engineering principles that need to be followed in the growing field of catalytic conversion of biorenewable molecules. The following list summarizes the key points regarding evaluation of catalytic reaction rates for chemical transformations in a variety of chemical reactors.

1. Always report reaction rates instead of overall product yields or conversions. If possible, normalize the rate to the number of active sites in the reactor, thus producing a turnover frequency for the reaction.
2. Always report the selectivity of a reaction together with the level of conversion. When comparing catalysts or reactors, be sure to compare selectivities of different systems at identical levels of conversion.
3. Always evaluate the overall material balance in the system. This is especially important in the conversion of complex biorenewable molecules that can form a broad spectrum of products such as light gases, polar oxygenates, hydrocarbons, and tars.
4. In addition to measuring the activity and selectivity of a particular catalyst, the stability should also be evaluated. Characterizing the catalyst during or after the reaction provides important clues to the modes of deactivation.

5. For solid catalysts functioning in a liquid reaction medium, the reactivity of the solution needs to be evaluated as well as the amount of material leached from the solid.
6. The reactor used to evaluate a particular chemical transformation should be selected based on the desired measurement. Reactors used for evaluating fundamental reaction kinetics, maximizing product yields, and performing pilot-plant scale tests are not necessarily the same.
7. To evaluate intrinsic kinetics of a catalytic reaction, serious efforts to minimize or eliminate transport artifacts are needed, such as using a small catalyst pellet size, a high flow rate or high agitation rate, and a set of reaction conditions that ensures that the rate is not too high.
8. In kinetic studies, an experimental check of the reaction rate by the Koros-Nowak or Madon-Boudart criterion should be performed to ensure the observed rates are not convoluted with transport phenomena.
9. If the Koros-Nowak or Madon-Boudart criterion cannot be performed, empirical criteria should be used to estimate the importance of transport artifacts in the catalytic system.
10. Transport phenomena in a catalytic system can cause unanticipated changes in activity and selectivity of a catalyst because of the complexity of the reaction mechanism. Since the observed behavior of a catalyst in one type of reactor may not translate to another type of reactor, a complete description of the reactor configuration needs to be provided.

Acknowledgments

The author acknowledges support for this work by grants from the U.S. National Science Foundation (CTS-0624608, OISE 0730277 and EEC-0813570).

Bibliography

- [1] H.S. Fogler. *Elements of Chemical Reaction Engineering*. 4th ed. Part of the Prentice Hall Professional Technical Reference Series. Upper Saddle River, NJ: Prentice Hall, 2006.
- [2] O. Levenspiel. *Chemical Reaction Engineering*. 3rd ed. New York: Wiley, 1999.
- [3] R.W. Missen, C.A. Mims, and B.A. Saville. *Introduction to Chemical Reaction Engineering and Kinetics*. New York: Wiley, 1999.
- [4] G.W. Roberts. *Chemical Reactions and Chemical Reactors*. New York: Wiley, 2009.
- [5] L.D. Schmidt. *The Engineering of Chemical Reactions*. New York: Oxford, 1998.
- [6] G.F. Froment, K.B. Bischoff, and J. De Wilde. *Chemical Reactor Analysis and Design*. 3rd ed. New York: Wiley, 2011.
- [7] M.E. Davis and R.J. Davis. *Fundamentals of Chemical Reaction Engineering*. New York: McGraw-Hill, 2003.
- [8] Y. Xi and R.J. Davis. Influence of Textural Properties and Trace Water on the Reactivity and Deactivation of Reconstructed Layered Hydroxide Catalysts for Transesterification of Tributyrin with Methanol. *J. Catal.* 268 (2009):307–317.
- [9] S.E. Davis, L.R. Houk, E.C. Tamargo, A.K. Datye, and R.J. Davis. Oxidation of 5-hydroxymethylfurfural over supported Pt, Pd and Au Catalysts. *Catalysis Today* 160 (2011):55–60.
- [10] W.C. Ketchie, E.P. Maris, and R.J. Davis. In-situ X-ray Absorption Spectroscopy of Supported Ru Catalysts in the Aqueous Phase. *Chemistry of Materials* 19 (2007):3406–3411.
- [11] E.P. Maris, W.C. Ketchie, M. Murayama, and R.J. Davis. Glycerol Hydrogenolysis on Carbon-Supported PtRu and AuRu Bimetallic Catalysts. *Journal of Catalysis* 251 (2007):281–294.
- [12] Y. Xi and R.J. Davis. Influence of Water on the Activity and Stability of Activated Mg-Al Hydrotalcites for the Transesterification of Tributyrin with Methanol. *J. Catal.* 254 (2008):190–197.

- [13] Y. Xi and R.J. Davis. Intercalation of Ethylene Glycol into Yttrium Hydroxide Layered Materials. *Inorganic Chemistry* 49 (2010):3888–3895.
- [14] N.T.S. Phan, M. Van Der Sluys, and C.W. Jones. On the Nature of the Catalytic Species in Palladium Catalyzed Heck and Suzuki Couplings—Homogeneous or Heterogeneous Catalysis, a Critical Review. *Advanced Synthesis & Catalysis* 348 (2006):609–679.
- [15] B. Maier, C. Dietrich, and J. Buchs. Correct Application of the Sulphite Oxidation Methodology of Measuring the Volumetric Mass Transfer Coefficient $k_L a$ under Non-Pressurized and Pressurized Conditions. *Trans. IChemE* 79 (2001):107–113.
- [16] W.C. Ketchie, M. Murayama, and R.J. Davis. Promotional effect of hydroxyl on the aqueous phase oxidation of carbon monoxide and glycerol over supported Au catalysts. *Topics in Catalysis* 44 (2007):307–317.
- [17] P.B. Weisz and C.D. Prater. Interpretation of Measurements in Experimental Catalysis. *Advances in Catalysis* 6 (1954):143–196.
- [18] J.P.G. Kehoe and J.B. Butt. Interactions of Inter- and Intrapphase Gradients in a Diffusion Limited Catalytic Reaction. *AIChE J (American Institute of Chemical Engineers Journal)* 18 (1972):347–355.
- [19] R.J. Madon and M. Boudart. Experimental Criterion for the Absence of Artifacts in the Measurement of Rates of Heterogeneous Catalytic Reactions. *Industrial & Engineering Chemistry Fundamentals* 21 (1982):438–447.
- [20] E.P. Maris, W.C. Ketchie, V. Oleshko, and R.J. Davis. Metal Particle Growth During Glucose Hydrogenation over Ru/SiO₂ Evaluated by X-ray Absorption Spectroscopy and Electron Microscopy. *Journal of Physical Chemistry B* 110 (2006):7869–7876.
- [21] J.W. Shabaker, R.R. Davda, G.W. Huber, R.D. Cortright, and J.A. Dumesic. Kinetics of Aqueous-Phase Hydrogenation of Lactic Acid to Propylene Glycol. *Journal of Catalysis* 215 (2003):344.
- [22] Z. Zhang, J.E. Jackson, and D.J. Miller. *Industrial & Engineering Chemistry Research* 41 (2002):691.
- [23] Y. Xi and D.J. Miller. Correlation of Reaction Rates for Lactic Acid Hydrogenation in Batch and Trickle Bed Reactors. In: *Proc. 2009 Annual Meeting of the American Institute of Chemical Engineers*. Nashville, Tennessee, November 9–13, 2009.

- [24] A. Dietz, A.M. Julcour, A.M. Wilhelm, and H. Delmas. Selective Hydrogenation in Trickle-Bed Reactor: Experimental and Modelling including Partial Wetting. *Catalysis Today* 79-80 (2003):293.
- [25] Y. Xi, J.E. Holladay, J.G. Frye, A.A. Oberg, J.E. Jackson, and D.J. Miller. A Kinetic and Mass Transfer Model for Glycerol Hydrogenolysis in a Trickle-Bed Reactor. *Organic Process Research & Development* 14 (2010): 1304–1312.
- [26] B.N. Zope, D.D. Hibbitts, M. Neurock, and R.J. Davis. Reactivity of the Gold/Water Interface During Selective Oxidation Catalysis. *Science* 330 (2010):74–78.
- [27] S.D. Pollington, D.I. Enache, P. Landon, S. Meenakshisundaram, N. Dimitratos, A. Wagland, G.J. Hutchings, and E.H. Stitt. Enhanced Selective Glycerol Oxidation in Multiphase Structured Reactors. *Catalysis Today* 145 (2009):169–175.
- [28] S. Carrettin, P. McMorn, P. Johnston, K. Griffin, C.J. Kiely, and G.J. Hutchings. Oxidation of Glycerol using supported Pt, Pd and Au Catalysts. *Physical Chemistry Chemical Physics* 5 (2003):1329–1336.
- [29] B.N. Zope and R.J. Davis. Influence of Reactor Configuration on the Selective Oxidation of Glycerol over Au/TiO₂. *Topics in Catalysis* 52 (2009):269–277.

Chapter 10

Catalytic Strategies and Chemistries Involved in the Conversion of Sugars to Liquid Transportation Fuels

Elif I. Gürbüz, James A. Dumesic

10.1 Introduction

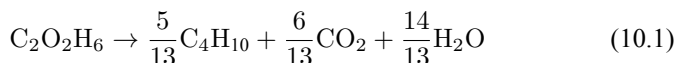
Biomass is an attractive renewable resource as an alternative to diminishing fossil fuels for the production of hydrogen and liquid transportation fuels. In this chapter, we outline recent processes for the production of hydrogen and fuels from biomass-derived platform molecules, such as sugars, sugar alcohols and derivatives. We start by discussing thermodynamic issues for converting oxygenated hydrocarbons to alkane species. This analysis helps us formulate strategies for the conversion of sugars to alkane fuels. We show that the main strategy to be followed is the deconstruction of lignocellulose through controlled deoxygenation reactions to obtain platform molecules and monofunctional species that retain functionalities for further upgrading reactions, such that molecules with carbon chains longer than the platform molecules (5–6 carbons) can be obtained. These upgrading reactions generally require C–C coupling reactions through reactive functional groups, such as C=C, C=O, and acid groups. We also introduce the concept of catalytic coupling at multiple length scales, to aid in the design of catalysts and/or catalytic systems to achieve cost-competitive biorefining strategies, in which the number of processing steps for reactions and separations is minimized.

10.2 Thermodynamic Considerations

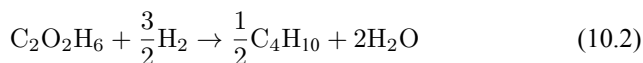
We start this section by discussing some of the thermodynamic issues involved in the conversion of oxygenated hydrocarbons, such as sugars and sugar alcohols derived from biomass to alkane species as presented by Simonetti [1]. Even though hydrogenation of these oxygenated species is very favorable thermodynamically, it is important to remember that the maximum carbon chain length of the alkane product species is limited to the carbon number of the sugar or polyol feed, such as glucose (6 carbon sugar), xylose (5 carbon sugar), sorbitol (6 carbon

sugar alcohol) and xylitol (5 carbon sugar alcohol). Therefore, we will address issues involved in the production of alkanes with longer carbon chain lengths than present in the carbohydrate reactant. To illustrate the concepts, we use ethylene glycol as a model reactant, because this molecule is the smallest molecule containing a C–C bond and having a C:O stoichiometry equal to 1:1, representing a sugar alcohol. To study the C–C bond formation step, we investigate the production of butane from ethylene glycol. This thermodynamic analysis is also applicable to the larger C5 and C6 sugars and sugar alcohols derived from lignocellulose to be used as feedstocks for the production of fuels.

The conversion of ethylene glycol to butane can be represented by the following stoichiometric equation:



This conversion can be described as a combination of two reactions



where the H_2 required for the reduction of ethylene glycol (Equation 10.2) is supplied by the reforming of ethylene glycol with water to form H_2 and CO_2 (Equation 10.3). The enthalpy change (at 500 K) for the reduction of ethylene glycol in Equation 10.2 is equal to $-37 \text{ kcal mol}^{-1}$, while the enthalpy change for ethylene glycol reforming in Equation 10.3 is equal to 6 kcal mol^{-1} , such that the conversion of ethylene glycol to butane in Equation 10.1 is exothermic by 24 kcal mol^{-1} . Due to the exothermic nature of this reaction, the energy contained in the butane product obtained from 1 mol of ethylene glycol is lower than that of ethylene glycol. The energy content of a compound is expressed by the heat of combustion to form water vapor and CO_2 . Figure 10.1 shows the enthalpy changes for the combustion of various compounds that can be derived from ethylene glycol to form water vapor and CO_2 (at a typical reaction temperature of 500 K). The decrease in enthalpy for the conversion of ethylene glycol to butane is sufficiently small that 91% of the energy content of the ethylene glycol reactant is preserved in the alkane product. On the other hand, the mass of butane is approximately 36% of the mass of ethylene glycol, which leads to an increase in energy

density. Furthermore, the alkane product is more volatile and less hydrophilic than the oxygenated reactant, which changes the combustion characteristics.

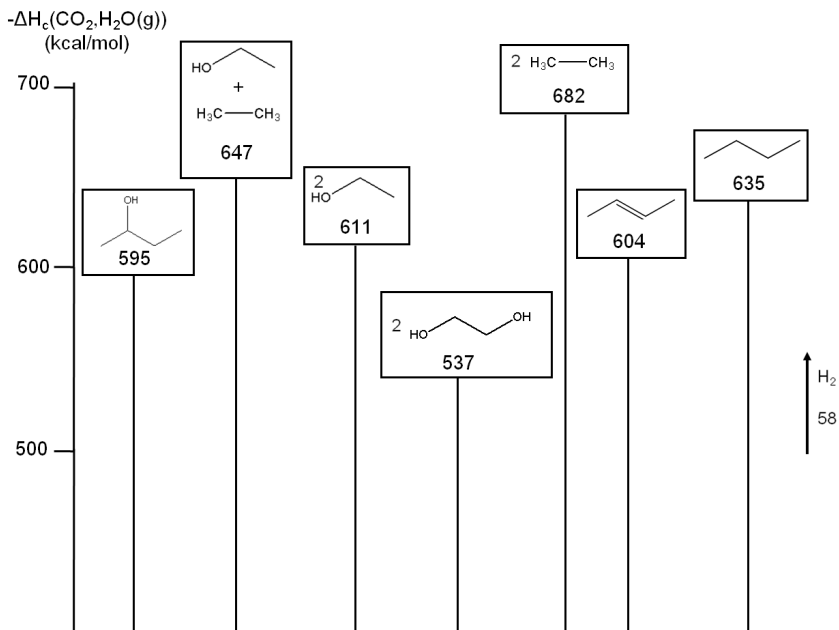
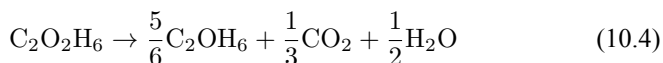
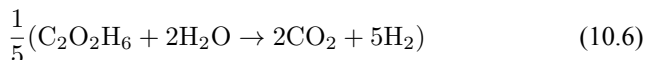
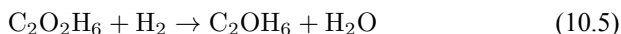


Figure 10.1: Energy content (negative value of enthalpy of combustion at 500 K, kcal mol⁻¹) for various compounds derived from ethylene glycol. The co-products of the combustion, CO₂ and water vapor have zero energy content. Adapted from [1]

The conversion of two ethylene glycol molecules to ethanol molecules results in an increase in the energy content of the molecules, from 537 kcal mol⁻¹ to 611 kcal mol⁻¹. This conversion also requires the use of H₂ (which has an energy content of 58 kcal mol⁻¹), which must be provided by reforming of ethylene glycol to produce H₂ and CO₂ according to Equation 10.6. The stoichiometric equation for the conversion of ethylene glycol to ethanol is given by



which is a combination of the following two reactions:



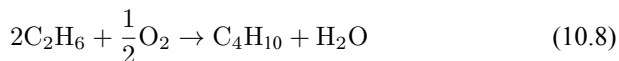
Equation 10.5 is exothermic by 21 kcal mol⁻¹ and Equation 10.6 is endothermic by 4 kcal mol⁻¹. As a result, the conversion of ethylene glycol to ethanol according to Equation 10.4 has an enthalpy change of -14 kcal mol⁻¹. With a high equilibrium constant due to the exothermic nature of the reaction, high conversions are achievable. The conversion of ethylene glycol to ethanol demonstrates that the more reduced product has a higher energy content per mol compared to the reactant. Moreover, heat integration can be achieved in a single catalytic reactor by the coupling of the endothermic heat for the reforming reaction to produce H₂ with the exothermic heat of the reduction step. The conversion of ethanol to ethane, similar to the ethylene glycol conversion to ethanol, is a combination of reduction and reforming reactions and results in an increased energy content of ethane compared to ethanol, as can be seen in Figure 10.1.

As mentioned earlier with respect to the reduction reactions discussed above, the carbon chain length of the alkane product will be the same as that of the reactant. For instance, starting with glucose, the longest carbon chain alkane that can be obtained is hexane. Similar to the case for ethylene glycol conversion, the reduction of glucose to hexane is exothermic, and the reforming of glucose with water to form the required H₂ for the reduction reaction is endothermic, such that the overall conversion of glucose to hexane, CO₂ and H₂O is exothermic (-45 kcal per mole of glucose). If the endothermic energy for the reforming reaction is provided by the exothermic reduction reaction, then the liquid hexane product retains 93% of the energy content of the glucose reactant and only 30% of the original mass of glucose. Even though this conversion to hexane represents a significant increase in the energy density, larger alkanes are required for gasoline, jet, and diesel fuel applications. Therefore, it is now important to focus on reactions employed to increase the length of the alkane chain. At first, we look at the conversion of ethane to butane by the following reaction:



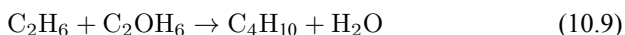
As can be seen from Figure 10.1, the conversion of ethane to butane is an endothermic reaction (10 kcal mol⁻¹). Due to the endothermic nature of this reac-

tion, the equilibrium constant would be low, such that high conversions would not be achievable in a single-pass reactor. Another possibility to obtain butane from ethane is oxidative coupling by producing water as a by-product, as demonstrated below:

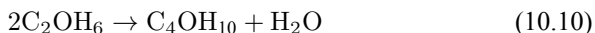


This reaction is exothermic with an enthalpy change of $-47 \text{ kcal mol}^{-1}$, resulting in a favorable equilibrium constant. However, in practice, it is difficult to achieve high yields of butane because of the high reactivities of alkanes to undergo combustion reactions in the presence of O_2 . As demonstrated, the production of longer chain alkane molecules by coupling of light alkane molecules remains a challenge in the field of heterogeneous catalysis.

By studying Figure 10.1, it can be seen that various coupling reactions involving partially oxygenated reactants are exothermic in nature. Such reactions have favorable equilibrium constants, while not requiring the use of O_2 as an oxidizing agent. One example is the coupling between ethane and ethanol to form butane and water ($-12 \text{ kcal mol}^{-1}$):



The coupling between two ethanol molecules leads to butanol and water in another exothermic reaction ($-16 \text{ kcal mol}^{-1}$):



This butanol product can then undergo dehydration to butene, followed by hydrogenation to butane, which in the end will lead to an increase in the energy content (from $595 \text{ kcal mol}^{-1}$ to $635 \text{ kcal mol}^{-1}$). The dehydration can be accomplished with high conversion due to the positive entropy change. The conversion of butene to butane then requires the addition of H_2 , and in an ideal case, the endothermic production of the required H_2 by reforming (accompanied by the production of CO_2) would be coupled with the exothermic heat of the olefin hydrogenation step.

In addition to the coupling of an ethanol molecule with itself or an ethane molecule, other catalytic scenarios can be imagined to achieve C–C coupling to obtain longer carbon chain alkanes. For instance, two molecules of ethanol can undergo dehydrogenation to form acetaldehyde molecules, which can be coupled

by aldol condensation. The aldol product can then be dehydrated and hydrogenated to form the alkane product [2]. It is also possible to dehydrate ethanol to obtain ethylene, coupled with ethylene dimerization followed by hydride transfer with ethane over acid catalysts [3].

Comparing the C–C coupling reactions of light alkanes to those of partially oxygenated compounds, we can conclude that partially oxygenated compounds offer new routes for C–C coupling that are unavailable for C–C coupling reactions between alkanes. Thus, the strategy that should be followed to produce alkanes with longer carbon chains than the biomass derived carbohydrate feeds is to utilize the oxygen-containing moieties in the functional reaction intermediates to form C–C bonds, prior to formation of the final alkane product.

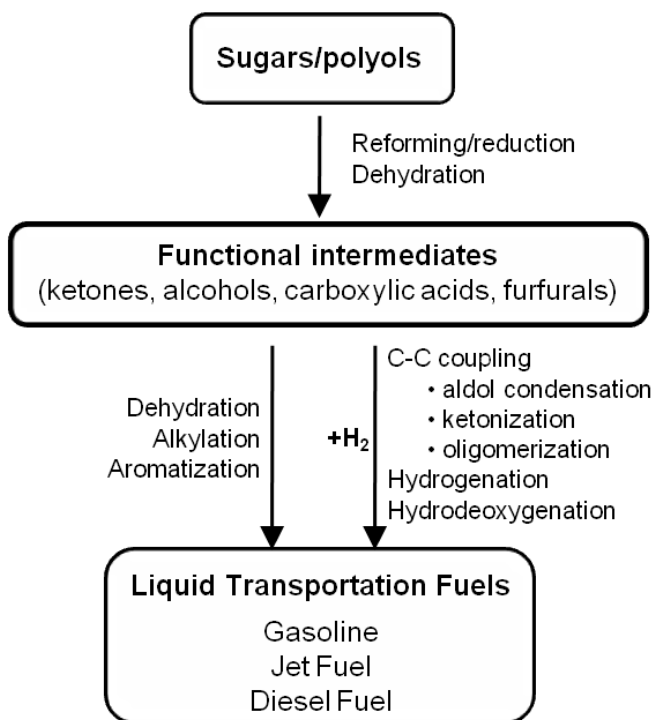


Figure 10.2: The overall strategy for the production of liquid fuels from sugars and sugar alcohols. Adapted from [1]

These functional intermediates can be obtained from carbohydrates by the combination of reforming and reduction reactions, and/ or by selective dehydration processes. These intermediates can then be converted directly to liquid transportation fuels through processes that do not require the addition of hydrogen, such as dehydration, alkylation and aromatization reactions to produce alkanes, olefins, and aromatic compounds. Alternatively, some intermediates might have desired functionalities to undergo C–C coupling reactions, such as aldol-condensation and ketonization processes, followed by hydrogenation and hydrodeoxygenation reactions to produce higher molecular weight alkanes. The H_2 required for these hydrogenation and hydrodeoxygenation steps could be generated by the reforming of the carbohydrate feed. This overall strategy for the production of liquid fuels from carbohydrates is demonstrated in Figure 10.2.

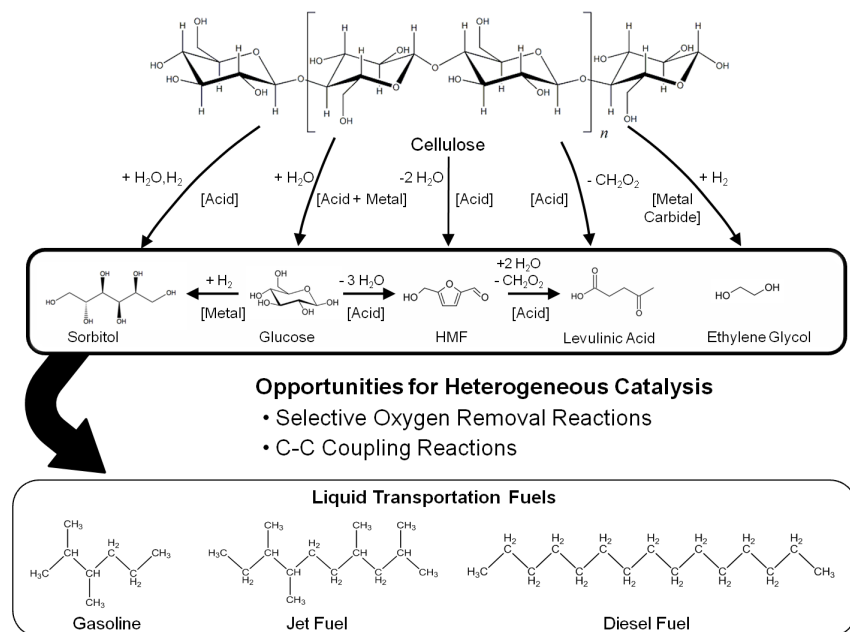


Figure 10.3: Examples of platform molecules that can be obtained from cellulose and the overall strategy for the production of liquid fuels from biomass through the formation of platform molecules. HMF-5-Hydroxymethylfurfural

10.3 Formulating Strategies for the Conversion of Sugars to Alkane Fuels: Platform Molecules

As discussed in the previous section, a useful strategy for the production of liquid fuels from biomass is to start with controlled oxygen removal reactions to produce functional intermediates, which have sufficient functional moieties to carry out C–C bond forming reactions to obtain long carbon chain alkanes.

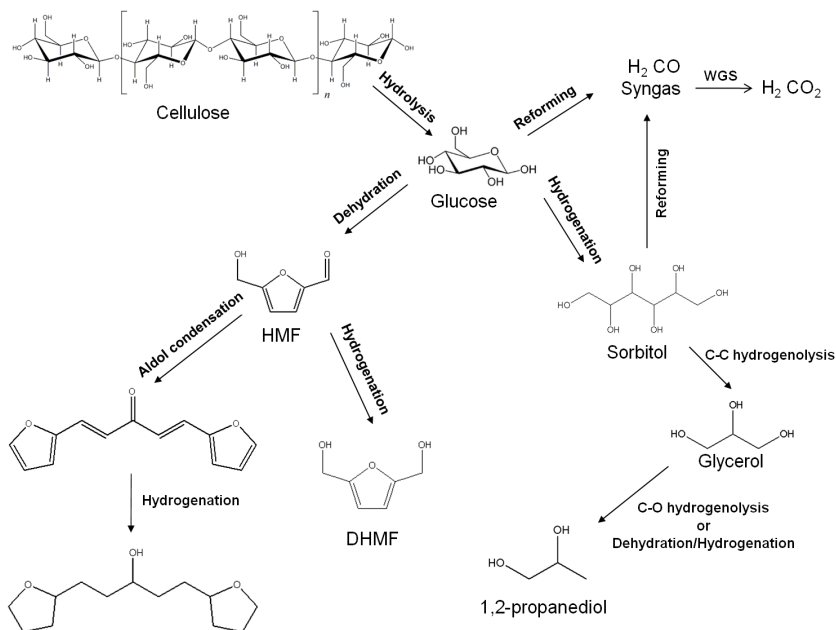


Figure 10.4: Examples of main chemical reaction classes involved in the production of transportation fuels and chemicals from carbohydrate based feedstocks in a bio-refinery. HMF-5-Hydroxymethylfurfural; DHMF-Di(hydroxymethyl)furan. Adapted from [4]

Prior to obtaining these less-reactive intermediates that can be subsequently upgraded to the desired products, biomass (cellulose, hemicellulose and lignin) needs to be converted to molecules that are easier to process but at the same time have sufficient functionalities to allow the production of a wide range of simpler molecules. These functional intermediates can also be referred to as platform molecules, some examples of which include glucose, sorbitol, 5-hydroxymethyl-

furfural and levulinic acid. Figure 10.3 demonstrates some platform molecules that can be obtained from cellulose and summarizes the strategy for producing liquid fuels from biomass through the formation of platform molecules. Several reactions can be carried out to obtain these platform molecules and convert them into liquid fuels. In this section, we will outline the main reactions that would be required in biorefining strategies. Figure 10.4 shows some examples of these reactions.

10.3.1 Reaction Classes

1. **Hydrolysis:** Hydrolysis is a major reaction adopted in many biorefining strategies starting from lignocellulosic biomass. It is generally carried out in upstream processing to cleave the glycosidic bonds between the sugar units in cellulose and hemicellulose to obtain simple sugar molecules. Hydrolysis reactions can be carried out using acid or base catalysts at temperatures ranging from 370–570 K, depending on the structure and nature of the polysaccharides. Hydrolysis of cellulose, the most abundant polysaccharide and the major component of lignocellulose, is carried out mostly by using enzymes or dilute mineral acids. High yields of glucose (>90% of theoretical maximum) can be achieved by enzymatic hydrolysis of cellulose after biomass pretreatment [5, 6]. Harsher conditions using solutions of mineral acids (H_2SO_4) at elevated temperatures can be applied to hydrolyze cellulose to obtain lignocellulose degradation products such as 5-hydroxymethylfurfural (HMF) and levulinic acid, which are also platform molecules [7, 8]. Hemicellulose can be hydrolyzed at more modest temperatures and dilute acid concentrations, thereby minimizing degradation of the simple sugars obtained, consisting mainly of xylose [8].
2. **Dehydration:** Dehydration reactions take place in the presence of acid catalysts and result in the formation of C=C bonds following the loss of a water molecule. For instance, sugar molecules can be dehydrated to generate furan compounds such as furfural and HMF, which have functional groups suitable for further upgrading reactions to obtain liquid fuel additives [9]. Another example is the dehydration of alcohols to obtain alkene molecules that can be converted to liquid fuels through oligomerization reactions [10, 11].
3. **Hydrogenation:** Hydrogenation reactions are used to saturate C=C and C=O bonds in molecules over metal catalysts, such as Pd, Pt, Ni, or Ru. Some examples in biorefining strategies include hydrogenation of sugars to sugar alcohols and ketones and aldehydes to secondary and primary alcohols, respectively. When hydrogenation is coupled with dehydration over a

bifunctional acid/metal catalyst, high molecular weight ketones, aldehydes and alcohols can be converted to alkanes suitable for fuel applications [4, 12].

4. Hydrogenolysis: Cleavage of C–C and C–O bonds by hydrogen is referred to as hydrogenolysis. This reaction requires the presence of a metal catalyst, such as Pd, Pt, Ni, Ru or Cu and can be carried out under basic conditions [13]. Selective C–O bond cleavage can be used for controlled oxygen removal from highly oxygenated species to obtain monofunctional species such as carboxylic acids and alcohols [14].
5. Reforming: Reforming reactions involve the production of CO and hydrogen from carbohydrates by the cleavage of C–C bonds of the carbohydrate backbone. The mixture of CO and H₂ is referred to as synthesis gas and can be used for methanol synthesis as well as for the production of liquid fuels via Fischer-Tropsch synthesis. In the presence of water, water-gas shift reaction can take place to convert CO to CO₂ while generating additional H₂. Steam reforming is utilized to generate hydrogen from alkanes (especially methane) and carbohydrates, whereas aqueous-phase reforming is favorable for hydrogen production starting from aqueous solutions of sugars and sugar alcohols [15]. The thermodynamic and kinetic considerations for hydrogen production by aqueous-phase reforming are discussed in the following sections.
6. C–C coupling: As presented earlier, C–C bond formation reactions are crucial for the production of liquid fuels with appropriate molecular weights for gasoline, diesel fuel and jet fuel applications, starting with biomass-derived feedstocks. The most common C–C coupling reactions to be used in a biorefinery are Fischer-Tropsch synthesis, aldol condensation, ketonization and oligomerization. These reactions are shown with representative species in Figure 10.5.

In Fischer-Tropsch synthesis, CO is catalytically hydrogenated to produce mainly alkanes and alkenes. The mixture of CO and H₂ is referred to as synthesis gas and can be produced from reforming reactions. Fischer-Tropsch synthesis is a polymerization reaction; thus, the product stream consists of compounds with a wide molecular weight distribution. This distribution among the product species depends on feed gas composition, pressure, temperature, catalyst and promoters [16, 17]. A detailed example will be provided in the following sections for the Fischer-Tropsch synthesis using the synthesis gas generated from the reforming of glycerol.

Aldol condensation is used to couple two ketone/aldehyde molecules to form a higher molecular weight homologue [18]. This reaction can take place in the presence of either acid or base catalysts and can be used for fine chemical syn-

thesis as well as for the production of fuels. In terms of fuel production, prior to the aldol condensation step, ketones and aldehydes (such as 2-hexanone, acetone, furfural, and HMF) need to be obtained as functional molecules from biomass-derived carbohydrates using controlled C–C and C–O cleavage or dehydration [14, 19]. A detailed example will be discussed in the following sections for the conversion of sugars and polyols to monofunctional species such as ketones, alcohols and carboxylic acids over a bimetallic PtRe/C catalyst [14]. The aldol condensation step should be followed by oxygen removal steps to obtain branched or linear, long carbon chain alkanes suitable for gasoline, diesel and jet fuel.

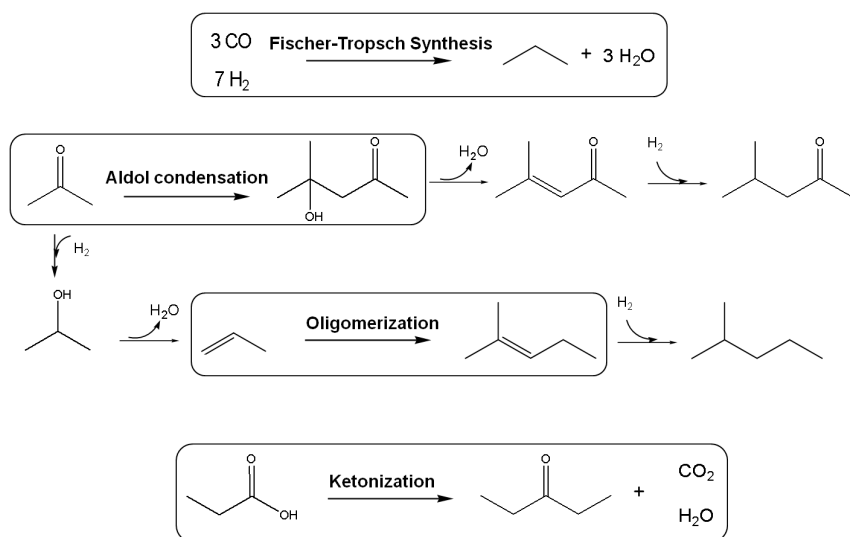


Figure 10.5: Examples of most common C–C coupling reactions to be used in the production of transportation fuels from carbohydrate based feedstocks in a bio-refinery

In ketonization reactions, two carboxylic acid molecules are combined to form a higher molecular weight ketone molecule, yielding CO_2 and water molecules as the co-products. The product ketone molecules can be converted to alkanes by oxygen removal steps, such as dehydration coupled with hydrogenation. Various studies on the ketonization of carboxylic acids have been presented using several oxides as catalysts such as Cr_2O_3 , Al_2O_3 , PbO_2 , TiO_2 , ZrO_2 , CeO_2 , iron oxide, and manganese oxide, as well as Mg/Al hydrotalcites [20].

The oligomerization of light alkenes to produce petrochemicals and fuels is commonly practiced in petroleum-based refineries with high conversion at moderate temperatures (e.g., 470 K). Because it is a well studied and understood reaction, oligomerization is a favorable C–C coupling reaction in biomass processing, making alkenes desirable reaction intermediates [21].

As an example, alkenes can be obtained by dehydration of alcohols in the presence of acid catalysts.

10.3.2 Catalytic Coupling at Multiple Length Scales

The establishment of a biorefinery for the production of fuels and chemicals that is cost competitive with the current petroleum-based refineries requires the development of strategies with a reduced number of processing and separation steps and increased activity and selectivity toward the target products [22]. In order to accomplish these objectives, we consider the possibilities of couplings between catalytic processes at various length scales. Different types of catalytic couplings that will be discussed in further detail are:

1. Functional coupling at the active site level,
2. active site coupling between different active sites in the same reactor,
3. chemical reaction coupling between surface reactions and homogeneous reactions for liquid-phase processes, and
4. phase coupling between multiple phases (e.g., aqueous and organic liquids) in liquid-phase processes.

1. Functional Coupling

Functional coupling takes place at the level of the active site and is achieved by chemical bonding interactions that lower the energy of the transition state relative to the reactants and/or products [23]. This lowering in energy, in turn, increases the rate of the overall reaction and the selectivity toward the desired product. Catalytic sites can be created at the subnanometer scale with controlled properties [24]. For instance, active sites can be coupled at the molecular level leading to organic-inorganic hybrid materials (e.g., silica materials functionalized with organic acid and/or base groups) to replace homogeneous acids and bases [24–42]. In these hybrid catalysts two active groups (e.g., an acid and a base) can work cooperatively [34, 37–39, 43], or a controlled environment around the active center (e.g., changing the steric or electronic environment by incorporating non-polar/polar surface moieties or modifying pore size) can be created [44–52].

One example involves the esterification of fatty acids with alcohols and polyols to form fatty acid esters. The esterification reaction is important for the pro-

duction of fatty acid esters (which have multiple applications in the food and drug industry), the conversion of vegetable oils and animal fats into biodiesel, and the selective removal of free fatty acids from triglyceride feedstocks [53]. It has recently been demonstrated that the surface hydrophobicity and steric surroundings of the catalytic sites can be tuned to synthesize multifunctional mesoporous silica catalysts for these esterification reactions [50]. For example with glycerol, it is desired to selectively produce monoesters instead of diesters and triesters. Even though conventional homogeneous catalysts, such as *p*-toluenesulfonic acid, result in high activity, the mono-esters cannot be produced with desired selectivity [50]. On the other hand, high activities coupled with increased selectivity to monoesters can be achieved by using mesoporous silica functionalized with organic sulfonic acid groups. Sulfonic acid groups provide the sufficient acid strength for high rates, while the pore size of the mesoporous silica can be tuned to prevent the formation of bulky diesters and triesters [47–49].

2. Active Site Coupling

Active site coupling can be described by the incorporation of two different types of catalytic sites in the same reactor. This type of catalytic coupling can improve the overall process in different ways. For instance, a rate-controlling reaction step that leads to a reactive intermediate can be coupled with a thermodynamically favorable reaction that converts the reactive intermediate to the final product with increased yield. In such a case, the active sites are generally coupled in a bi- or multifunctional catalyst. One example for this case is the coupling of aldol condensation with hydrogenation using a bifunctional catalyst consisting of base (metal oxide) and metal sites [9, 54–57].

This type of approach has been used for the production of methyl isobutyl ketone (MIBK) from acetone. Acetone can undergo aldol condensation over basic catalysts, such as $Mg_xAl_yO_z$ to form diacetone alcohol (DAA) or mesityl oxide (MO) through a consecutive dehydration. MO can later be hydrogenated over a metal catalyst to generate MIBK. However, the production of DAA or MO from acetone is equilibrium limited; and thus, high yields of MIBK cannot be achieved if the hydrogenation takes place in a separate reactor. On the other hand, over a bifunctional catalyst that has both metal and base sites, such as Cu or Pd supported over $Mg_xAl_yO_z$, MO can be hydrogenated to MIBK in the same reactor [55, 57]. The conversion of acetone to MIBK is thermodynamically more favorable, and as a result, high yields of MIBK can be obtained in a single stage. The conversion of acetone to MIBK through DAA and MO is shown in Figure 10.6 with corresponding thermodynamic information. Using a bifunctional catalyst not only improves the overall yield of the desired product, but also decreases

the number of reaction steps, which in turn decreases the capital and operating costs [9, 54, 55, 57].

Another approach for active site coupling is the coupling of two or more reactions in a single reactor, even though individual reactions can be carried out with high yields in separate reactors. Coupling these reactions in a dual-bed or mixed bed system decreases the number of processing steps together with capital and operating costs. The catalytic conversion of glycerol to H_2/CO combined with Fischer-Tropsch synthesis for the production of liquid fuels from biomass-derived feedstocks is an example of such a catalytic coupling approach. Because the production of synthesis gas from aqueous glycerol solutions can be accomplished in the same temperature range as Fischer-Tropsch synthesis, the endothermic production of synthesis gas can be coupled with exothermic Fischer-Tropsch synthesis, leading to an energy-integrated process [58, 59]. This coupling is described in further detail in the following sections.

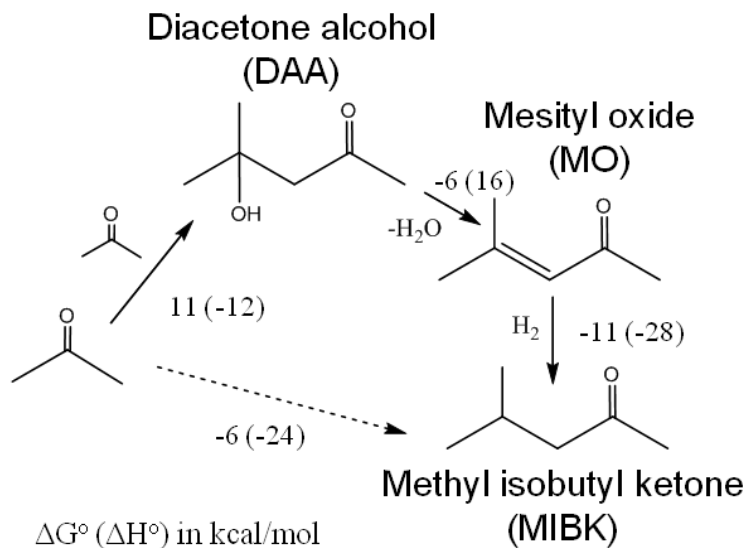


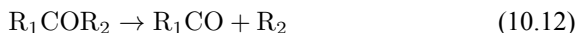
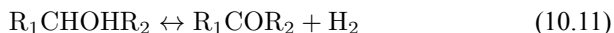
Figure 10.6: The conversion of acetone to methyl isobutyl ketone (MIBK) through diacetone alcohol (DAA) and mesityl oxide (MO) with corresponding values for ΔG° and ΔH° of reaction (kcal mol^{-1}) of individual steps

3. Chemical Reaction Coupling

As stated earlier, sugar alcohols or polyols, such as glycerol and sorbitol, are common platform molecules, from which fuels and chemicals can be produced. Unlike the production of fuels, the production of fine chemicals requires selective reaction pathways, which can be difficult to achieve due to the high degree of functionality in polyol molecules [60, 61]. One example is the hydrogenolysis of glycerol or sorbitol to produce a mixture of glycols and alcohols [60, 62–70]. Hydrogenolysis involves multiple reaction steps, such as H-abstraction, C–C bond cleavage and hydrogenation. In addition, the polyol molecules have low volatilities which make them easier to process in the liquid phase than in the gas phase. The presence of these two features opens up the possibility that the conversion of the biomass derived polyols may proceed as a combination of surface reactions as well as homogeneously catalyzed liquid-phase reactions, thereby improving the economics of the process [71–74].

Coupling of surface reactions with homogeneous reactions in the liquid phase is referred to as chemical reaction coupling. In such a case, the reaction in the liquid phase can increase the overall rate of a reaction by lowering the energy barrier for the formation of a key reaction intermediate.

As stated earlier, the aqueous phase hydrogenolysis of polyols leads to a mixture of products resulting from the cleavage of C–O versus C–C bonds [60, 64, 65]. For instance, the cleavage of C–O bonds in glycerol leads to propanediols, while C–C cleavage generates ethylene glycol and methanol [64, 65]. C–O bond cleavages followed by C–C bond breaking can produce mono-alcohols and alkanes [64, 65]. According to literature, hydrogenolysis of polyols can go through the following pathways (R_1 and R_2 represent alkyl groups, hydroxyl groups, alkyl-hydroxyl groups, or H) [75]:



Step 1 (Equation 10.11) represents the dehydrogenation of a hydroxyl group to an aldehyde or a ketone, which takes place over metal sites. Step 2 (Equation 10.12) shows the C–C cleavage by retro-aldol reaction, whereas step 3 (Equation 10.13) shows the C–O cleavage by dehydration. Both of these steps are catalyzed by base in the liquid solution. Finally, step 4 (Equation 10.14) represents the hydrogenation of C=O and C=C bonds over a metal catalyst [64, 65, 68, 75]. It is important to note that C–C and C–O bond breaking steps (Equations 10.12 and 10.13) can also be catalyzed by metal sites [64, 65].

Recent work from Davis and co-workers on hydrogenolysis of glycerol over both Pt and Ru has provided insight into the roles of surface metal sites and base catalysis in solution [64, 65, 76]. Even though it is believed that C–C and C–O bond cleavages proceed via base catalyzed retro-aldol reaction and dehydration respectively [75], Davis and coworkers showed that a metal must be present for hydrogenolysis to take place [65]. In these studies, Ru showed a higher overall activity compared to Pt for all conditions tested [65].

The authors also showed that the addition of a base, NaOH in this case, leads to an order of magnitude increase in Ru activity and a 50-fold increase in Pt activity. The authors also reported that the rate of ethylene glycol formation was increased over Pt but stayed unchanged over Ru [65]. In addition, the propylene glycol production rate was increased by an order of magnitude over Ru and by a factor of 50 over Pt [65].

These results demonstrate that C–C bond breaking is metal-catalyzed over Ru and base-catalyzed over Pt, while C–O bond breaking is catalyzed by the base over both metals [65]. Finally, the authors propose that initial dehydrogenation of hydroxyl groups in glycerol is metal-catalyzed and results in the formation of glyceraldehydes. However, the H-abstraction step in dehydrogenation is catalyzed by the base, which in turn enhances the dehydrogenation step [65]. As a result, the mechanism for the hydrogenolysis of glycerol contains chemically coupled steps in which the homogeneous reaction enhances the overall rate in various ways. First of all, the presence of the homogenous catalyst lowers the energy barrier between reactants and transition states by the abstraction of H in the dehydrogenation step. Furthermore, the base-catalyzed retro-aldolization and dehydration reactions generate intermediates for a thermodynamically favorable step (hydrogenation over metal sites).

4. Phase Coupling

In phase coupling, a reaction in one phase generates an intermediate for the reaction in a different phase. Phase coupling can also occur when the reactants and the

catalyst exist in different phases. Finally, it is also possible that the second phase is used as an extracting solvent to improve the overall thermodynamics and/or prevent further reaction of the intermediate obtained in the first phase. An example for this approach is the dehydration of sugars to furanic compounds in a biphasic system. High yields can be achieved when monosaccharides, such as glucose, fructose and xylose or polysaccharides, such as sucrose, cellobiose and xylan are dehydrated in the presence of acid catalysts to generate furanic compounds like 5-hydroxymethylfurfural (HMF) and furfural. The dehydration takes place with an acid catalyst, such as HCl or H₂SO₄ in the aqueous phase, whereas the second phase, a partially miscible organic solvent like butanol, methyl-isobutyl ketone, or dichloromethane, continuously extracts the furanic product to prevent further degradation [2, 4, 77–79]. It is desirable to utilize low boiling point solvents to eliminate the need of energy intensive separation steps.

Detailed studies have been presented in literature for fructose dehydration to generate HMF. The capacity of extracting HMF by the organic phase from the aqueous phase is measured by the ratio of the HMF concentration in the organic phase to that in the aqueous phase after the reaction is completed, and is denoted by R . Experimental results suggests a direct relation of HMF selectivity with the value of R [77, 78]. Even though the value of R can be increased by using a combination of different organic solvents, it has also been shown that the addition of salt to the aqueous phase can increase R due to the salting-out effect. With the addition of the salt, electrolytes change the intermolecular bonding interactions between liquid components, thereby decreasing the solubility of the two phases in each other. Compared to experiments without salt, a 30 wt% fructose solution saturated with NaCl and 2-butanol as the extracting solvent (with initial ratio of organic and aqueous phase volumes $V_{org}/V_{aq} = 1.6$) results in an increase in R from 1.6 to 3.3, resulting in an increase in HMF selectivity from 66% to 79% [78]. It is important to note that other than altering the solvent properties, the salt remains inert for the chemical reaction.

10.4 The Conversion of Sugars and Polyols to H₂ and Alkanes

In this section, we present a strategy for the production of H₂ and alkanes from sugar feedstocks. We first look at the thermodynamics of the production of H₂ from sugars and polyols in the gas phase as well as in the aqueous phase as demonstrated by Davda et al. [80] previously. Following that, we present kinetic considerations with some examples and discuss how the selectivity toward H₂ can be shifted toward making alkanes.

10.4.1 Thermodynamic Considerations for H₂ Formation

The steam reforming reaction of alkanes to generate CO and H₂ is described in Equation 10.15.

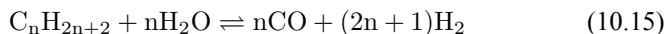
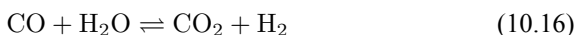
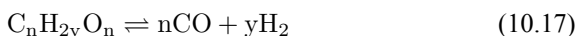


Figure 10.7 shows changes in the standard Gibbs free energy ($\Delta G^\circ/RT$) for the steam reforming reaction of different alkanes (methane, ethane, propane and hexane), from which it can be seen that the reaction becomes thermodynamically favorable at temperatures higher than 700 K. This temperature is as high as 900 K for the steam reforming of methane. The production of H₂ can be increased by the water-gas shift (WGS) reaction, which is shown in Equation 10.16.



The reforming of carbohydrates (C:O ratio being 1:1), such as methanol, ethylene glycol, glycerol and sorbitol, is represented by the equation below (Equation 10.17):



The value of $\Delta G^\circ/RT$ with changing temperature is plotted as well for various carbohydrates in Figure 10.7. Comparison with the values for alkanes shows that the steam reforming of carbohydrates starts to become thermodynamically favorable at considerably lower temperatures. Furthermore, the water-gas shift reaction is also thermodynamically favorable at these lower temperatures. This behavior opens the possibility that hydrogen can be obtained from steam reforming of oxygenated hydrocarbons with a low-temperature route in a single reactor, in which the WGS reaction can also take place. Even though the steam reforming of alkanes generally takes place in the vapor phase, at low temperatures, when WGS is thermodynamically favorable, carbohydrate feeds might have low volatility, which limits the reaction in the vapor phase in return. The vapor phase steam reforming can be carried out for methanol, ethylene glycol and glycerol at temperatures around 500 K. On the other hand, the reforming of heavier carbohydrates such as glucose and sorbitol should be carried out in the liquid phase in order to be coupled with WGS reaction in the same reactor.

Hydrogen production from carbohydrates in the liquid phase is referred to as aqueous phase reforming (APR) and has several advantages over steam reform-

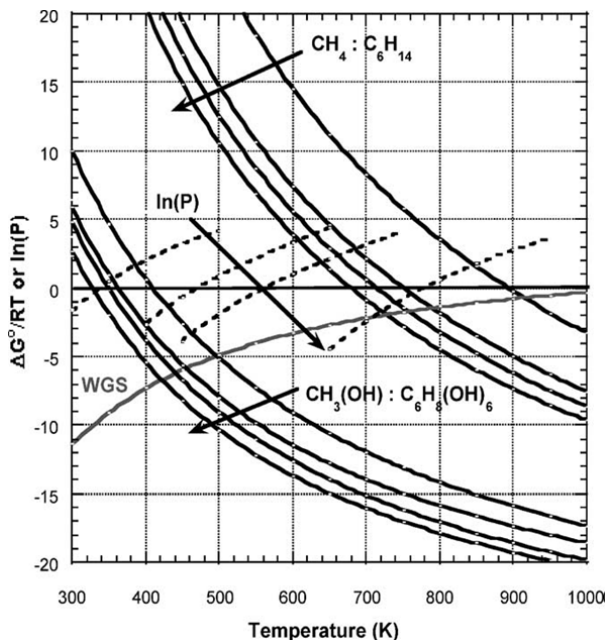


Figure 10.7: $\Delta G^\circ/RT$ values with changing temperature for water-gas shift reaction and production of CO and H_2 through vapor phase reforming of methane, ethane, propane, hexane, methanol, ethylene glycol, glycerol and sorbitol. Adapted from [80]

ing. Firstly, the energy requirement is minimized, since neither water nor the carbohydrate feed needs to be vaporized. In addition, as mentioned earlier, the water-gas shift reaction can take place in the same reactor as aqueous reforming and makes it possible to obtain high hydrogen yields with minimal CO levels. Finally, APR takes place at pressures around 15–50 bar where hydrogen purification strategies such as pressure-swing adsorption are effective.

10.4.2 Kinetic Considerations

Even though the thermodynamics of APR reactions seem to be favorable, it is also important to discuss kinetic considerations, such as selectivity issues for this reaction. Firstly, it is known in literature that at low temperatures the formation of alkanes is favorable from H_2 , CO and CO_2 mixtures through methanation and

Fischer-Tropsch synthesis reactions [81]. In addition, C–O bond breaking, which leads to alkanes by consecutive hydrogenation reactions, is a competitive pathway to the desired C–C bond cleavage reactions. In short, in order to reach high yields toward H_2 , an efficient catalyst is required that promotes reforming reactions (C–C scission followed by water-gas shift) and inhibits alkane-formation reactions (C–O scission followed by hydrogenation) as well as methanation and Fischer-Tropsch synthesis reactions. A high activity for the water-gas shift reaction is also important in terms of removing CO from the metal surface at low reforming temperatures. Parallel and series reaction pathways that affect the selectivity toward the production of H_2 from oxygenated carbohydrate feeds are shown in Figure 10.8.

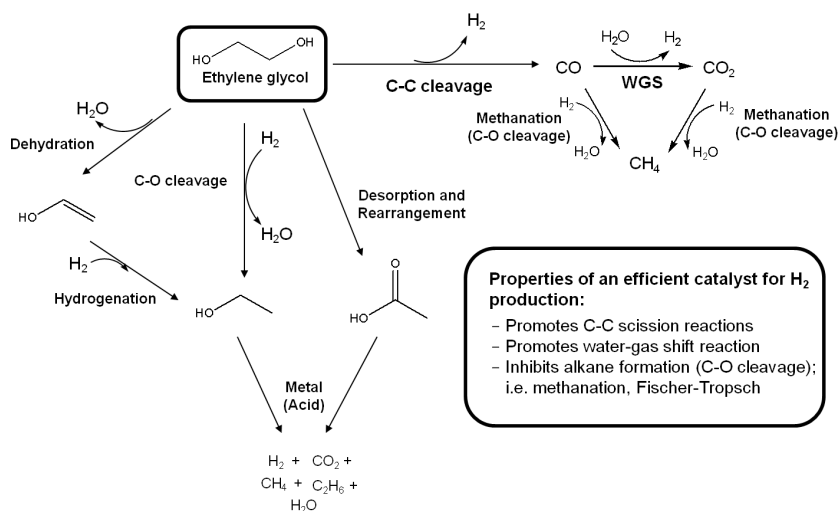


Figure 10.8: Parallel and series reaction pathways involved in the catalytic conversion of biomass-derived oxygenated compounds to H_2 and alkanes over supported metal catalysts. Adapted from [15]

Previous studies on the C–C bond cleavage activity over different metals show that Ru, Ni, Ir and Rh demonstrate high activity followed by Pt [82]. In terms of water-gas shift activity, over an alumina support, Cu exhibits the highest activity followed by Pt, Ru and Ni [83]. Finally, in terms of methanation activity, it has been reported in literature that Ru, Ni and Rh exhibit the highest rates of methanation, whereas Pt, Ir and Pd show lower catalytic activities. When all this kinetic information is combined, it can be concluded that by being active for C–

C bond cleavage and water-gas shift reaction as opposed to methanation (C–O cleavage), Pt and Pd should be suitable for the selective production of H₂ by aqueous-phase reforming of oxygenated carbohydrates [84].

As predicted above, Pt-black and Pt supported on various supports like Al₂O₃, TiO₂, and ZrO₂ showed high activity and selectivity toward H₂ for the APR reaction of methanol and ethylene glycol [80]. Pd supported catalysts have shown similar selectivity, although with a lower activity compared to Pt-based materials. It has also been reported that Rh, Ru, and Ni favor the production of alkanes from polyols over hydrogen [81], because C–O bond cleavage is favored over the C–C bond cleavage over these metals. Experimental results for the APR of glucose, sorbitol, glycerol, ethylene glycol, and methanol over a Pt/Al₂O₃ catalyst at 498 and 538 K show that the selectivity for H₂ production improves in the order glucose < sorbitol < glycerol < ethylene glycol < methanol.

Acidity, introduced by the use of solid acid supports (i.e., SiO₂/Al₂O₃), increases dehydration rates, which in turn increases the selectivity toward alkanes at the expense of hydrogen [15].

In order to describe the kinetics of the reforming of oxygenates in terms of competitive C–C and C–O bond breaking pathways, we provide two example studies (i.e., ethanol and ethylene glycol reforming), in which density functional theory (DFT) calculations have been used together with experimental data.

Example: The Reforming of Ethanol

Ethanol has been chosen for study because it is the simplest oxygenated hydrocarbon, possessing both C–C and C–O bonds. Alcalá et al. [85] carried out DFT calculations to investigate the nature of the surface intermediates and transition states formed from ethanol reforming as a result of C–C and/or C–O bond cleavage pathways over Pt(111) surfaces. The main aim of this investigation was to understand which pathways were most favorable for the reforming of oxygenated hydrocarbons over Pt surfaces.

The DFT studies were initiated by determining the most stable surface intermediates that can be formed from ethanol by removal of hydrogen atoms (no breaking of C–C or C–O bonds) as a first step. Out of many possible species with stoichiometry of C₂H_xO, the most stable species were determined as ethanol, 1-hydroxyethyl (CH₃CHOH), 1-hydroxyethylidene (CH₃COH), acetyl (CH₃CO), ketene (CH₂CO), ketyl (CHCO), and CCO species. Following this analysis, surface energies of all the possible products of C–C and C–O bond cleavages (i.e., stabilities of adsorbed O, OH, C₂H_x, and CH_xO species) were determined. Finally, with the results from DFT calculations and through Brønsted-Evans-Polanyi correlations, the energies of the transition states for C–C and C–O cleavage reac-

tions were determined [85, 86]. These correlations relate the energy of the transition state to the energy of the products (final state) with each surface reaction being defined in the exothermic direction. The energies of the transition states (TS) and final states (FS) are relative to the energy of the corresponding initial state in the gas phase. It was determined that among the dehydrogenation products of ethanol on the surface, 1-hydroxyethylidene (CH_3COH) species had the lowest energy transition state for C–O bond cleavage, and the ketenyl (CHCO) species had the lowest-energy transition state for C–C bond cleavage.

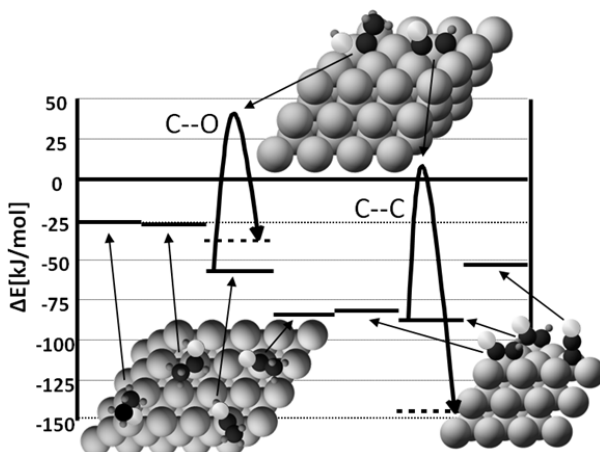


Figure 10.9: Simplified potential energy diagram of the stabilities and reactivities of dehydrogenated species derived from ethanol on Pt(111). The reference state is gas-phase ethanol and clean slab. Only the most stable species and transition states for C–O and C–C bond cleavage are shown. The black, orange (or light gray) and small blue (or dark grey) balls represent carbon, oxygen and hydrogen atoms, respectively. Adapted from [85]

Figure 10.9 presents a simplified potential energy diagram of the stabilities and reactivities of dehydrogenated species derived from ethanol on Pt(111). Only the most stable species and transition states for C–O and C–C bond cleavage are shown in this schematic potential energy diagram. It can be seen in this figure that C–O bond cleavage occurs on more highly hydrogenated species compared to C–C bond cleavage. In addition, it is shown that the energy of the lowest transition state of C–C bond breaking with respect to ethanol is 4 kJ/mol, whereas it is 42 kJ/

mol for C–O bond cleavage. This difference indicates that C–C cleavage should occur at a faster rate compared to C–O cleavage for species derived from ethanol.

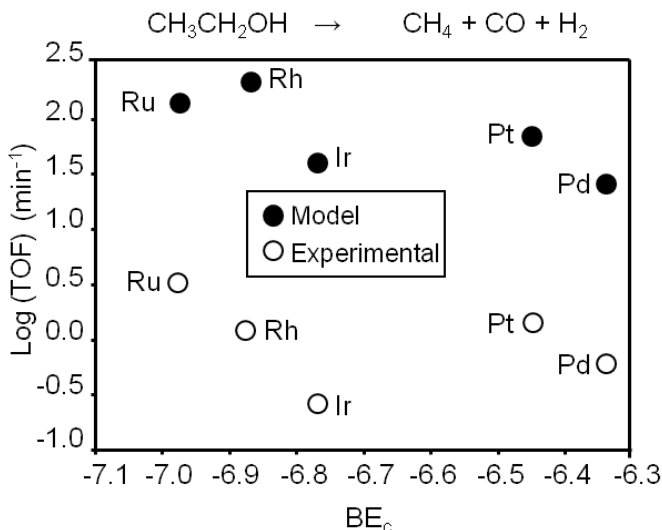


Figure 10.10: Experimental rates in terms of turnover frequency (TOF) in comparison with the predictions from DFT calculations for C–C bond cleavage of ethanol over Pt, Pd, Ir, Rh and Ru. Open and solid circles show the experimental data and model calculations, respectively. Adapted from [86]

Ferrin et al. [85, 86] studied the decomposition of ethanol over various supported metal catalysts, such as Cu, Pt, Pd, Ir, Rh and Ru. The experimental results show that for all the metals except for Cu, the rate of methane and CO formation is 1 to 2 orders of magnitude higher than the rate of the formation of ethane. This behavior indicates that the rate of C–C bond cleavage is considerably higher than that of C–O cleavage, which supports the conclusions reached from DFT studies presented above. Cu does not show activity of C–C or C–O bond cleavage due to low stability of surface intermediates and transition states on the Cu surface. Figure 10.10 presents the experimental rates in terms of turnover frequency (TOF) in comparison with the predictions from DFT calculations for C–C bond cleavage over Pt, Pd, Ir, Rh and Ru. It can be seen from Figure 10.10 that for each metal, the value of the TOF predicted by the model is consistently higher than the value measured experimentally. This difference is acceptable, given the uncertainty in

DFT and the correlations used. However, it is evident that the model captures the trends observed in different metals experimentally. It is stated by the authors that the selectivity toward C–C cleavage is due to the weaker bonding of O compared to C on these metal surfaces. With any C–O cleavage step, one of the resulting species will be bound to the surface through the oxygen atom. If binding of this species to the surface is weak, then the final state of C–O cleavage step will be less stable compared to that of C–C cleavage step. This conclusion suggests that in order to be able to cleave the C–O bond selectively, a metal catalyst with stronger binding of O is required.

Example: The Reforming of Ethylene Glycol

Next we look at the kinetics of the reforming of ethylene glycol. Ethylene glycol (EG) is an important model compound to study, because with a C–C bond and having a C:O stoichiometry equal to 1:1, it represents a sugar alcohol. We focus on work carried out by Kandoi et al. [87], in which experimental data (Pt supported on alumina) as well as results of DFT calculations (Pt(111)) are reported for the reforming of EG in vapor as well as in the aqueous phase. Using the experimental and DFT results, microkinetic models were developed for the reaction in both phases, providing insight into the similarities and differences in the reforming chemistries taking place in both phases.

Similar to the analysis of ethanol reforming, DFT calculations were carried out to find the surface energies of all intermediates that can be derived from the dehydrogenation of EG on Pt(111). The most stable $C_2H_xO_2$ (x being from 0 to 6) species derived from the subsequent dehydrogenation of EG (with respect to EG in the gas phase and clean slab) are $HOCH_2CH_2OH$, $HOCH_2CHOH$, $HOCH_2COH$ or $HOCHCHOH$, $HOCHCOH$, $HOCCOH$, $HOCCO$, and $OCCO$. With the use of Brønsted-Evans-Polanyi type correlations developed for C–H/O–H and C–C bond scissions in other oxygenated compounds on Pt(111) together with DFT calculations, activation barriers for C–C and C–O bond cleavage reactions were calculated over Pt(111). Figure 10.11 shows the Gibbs free energy changes (at 483 K) for these reaction steps (relative to EG in the gas phase and the clean slab). The most stable species resulting from dehydrogenation of EG and the most stable transition states for C–H/O–H and C–C bond scission are included in this figure. The DFT calculations show that at an intermediate value of x (around $C_2H_3O_2$), the activation energy barriers to break the C–C bond become similar to those for C–H/O–H cleavage. This comparison suggests that after this point, C–C cleavage becomes a kinetically competitive pathway.

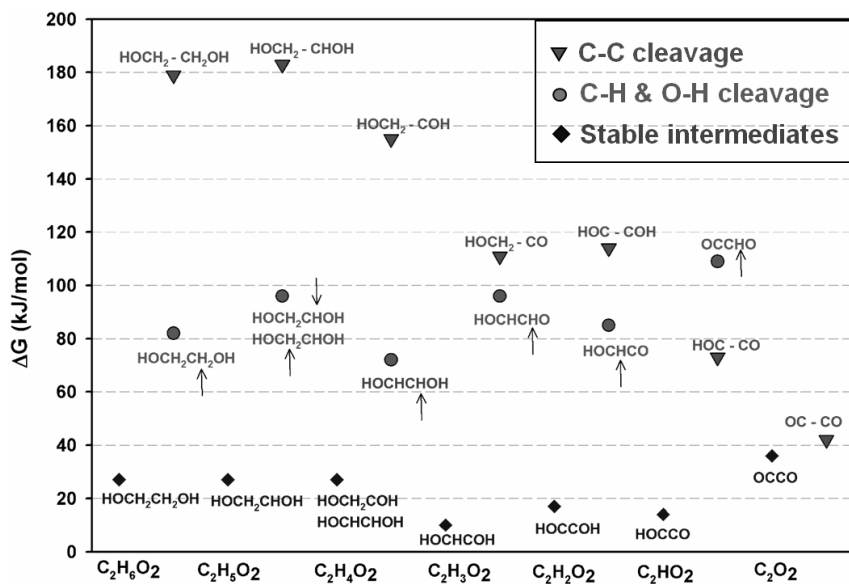
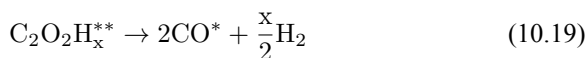
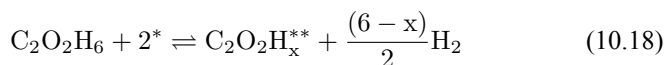
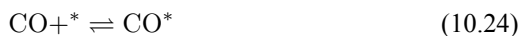
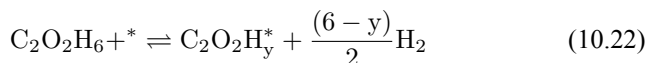
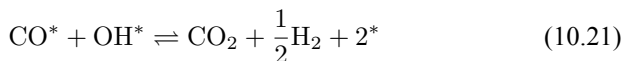
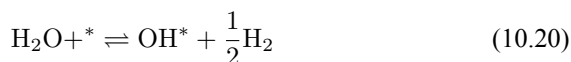


Figure 10.11: The Gibbs free energy changes (at 483 K) for C–H/O–H and C–C bond scission steps (relative to ethylene glycol in the gas phase and the clean slab) starting from ethylene glycol. The most stable species resulting from dehydrogenation of ethylene glycol (diamonds) and the most stable transition states for C–H/O–H (circles) and C–C bond (inverted triangles) scission are included. The location of C–H cleavage is shown by a small arrow above or below the corresponding hydrogen atom. Adapted from [87]

A microkinetic model, based on the results from the DFT calculations, was developed to understand the vapor and aqueous phase reforming kinetics of EG on Pt. The model was simplified by combining various elementary steps, which resulted in a 7-step reaction mechanism. The simplified mechanism is shown below (Equations 10.18–10.24). Note that, A^* and B^{**} denote monodentate and bidentate adsorbed species, respectively.





Step 1 (Equation 10.18) is the dehydrogenation of EG to generate a surface intermediate $\text{C}_2\text{H}_x\text{O}_2^{**}$. This surface species then decomposes into CO and H_2 in Step 2 (Equation 10.19). Steps 3 and 4 (Equations 10.20 and 10.21) represent the WGS reaction steps, where CO reacts with H_2O (dissociatively adsorbed) to generate CO_2 and H_2 . EG forms a spectator species ($\text{C}_2\text{H}_y\text{O}_2^*$) in step 5 (Equation 10.22). Finally, Steps 6 and 7 (Equations 10.23 and 10.24) are the adsorption-desorption of H_2 and CO, respectively. The same reaction mechanism was used to build the two models in both phases. Two additional equations were added to develop the aqueous phase model to account for the formation of gas bubbles during aqueous-phase reforming. It is reported that these models describe the experimental kinetic data reasonably well using similar values of the kinetic parameters, suggesting that the vapor phase and aqueous phase reforming chemistry is similar on platinum. The microkinetic model also suggests that the C–C bond in EG is broken on platinum at an intermediate value of x in $\text{C}_2\text{H}_x\text{O}_2$, thus supporting results from DFT calculations.

10.4.3 Changing Selectivity toward Alkanes

Until now, we have discussed the selective production of hydrogen by aqueous phase reforming of oxygenated hydrocarbons. However, it is possible to tailor aqueous phase reforming of highly oxygenated hydrocarbons, such as sorbitol,

to produce a clean stream of heavier alkanes consisting of butane, pentane and hexane. This conversion requires the formation of hydrogen and CO_2 through reforming over a metal catalyst, such as Pt, as well as dehydration over a solid acid catalyst (such as silica-alumina) or with a mineral acid. Following that, the generated hydrogen is used to hydrogenate the dehydrated intermediates over the metal sites. Alkanes are produced through consecutive cycles of dehydration/hydrogenation. When the reforming, dehydration and hydrogenation steps are balanced properly, the hydrogen generated through reforming can be completely consumed for the hydrogenation of dehydrated intermediates. The alkanes formed are straight-chain compounds with only minor amounts of branched isomers (less than 5%). The selectivity toward alkanes can be modified by changing the catalyst composition, pH of the feed (when mineral acids are present), and the reaction conditions [56].

It has been reported by Huber et al. [56] that for an aqueous sorbitol feed, the H_2 selectivity decreases from 43 to 11% for a $\text{Pt}/\text{Al}_2\text{O}_3$ catalyst when a solid acid catalyst ($\text{SiO}_2\text{-Al}_2\text{O}_3$) is added, and also decreases from 43 to 6% upon the addition of a mineral acid (HCl) to the feed to change the pH from 7 to 2. These results demonstrate that with the presence of an acid catalyst, the hydrogen generated by the reforming reaction is consumed for the production of alkanes. When 4 wt% $\text{Pt}/\text{SiO}_2\text{-Al}_2\text{O}_3$ was used for the conversion of the aqueous 5 wt% sorbitol feed, the H_2 selectivity was less than 5%, indicating that most of the H_2 generated was consumed in the production of the alkanes. It was observed that decreasing the reaction temperature from 538 to 498 K did not have a significant effect on product selectivity. On the other hand, at 498 K, when the system pressure was increased to about 40 bar from 26 bar, the hexane selectivity was increased to 40 from 21%. The authors reported that co-feeding of H_2 could improve the alkane production further. At 498 K and 35 bar, co-feeding of H_2 resulted in an increase in hexane selectivity to 78 from 55%. At these conditions, it was calculated that 90% of the effluent gas-phase carbon was present as alkanes. Based on these results, it can be concluded that increasing the hydrogen partial pressure in the reactor increases the rate of hydrogenation as opposed to C–C bond cleavage over metal sites. Finally, it is noteworthy that co-feeding of H_2 with the aqueous feed opens the possibility of using bifunctional catalysts (metal/acid) with metals (such as Pd) that by themselves show low activities for hydrogen production by APR reactions.

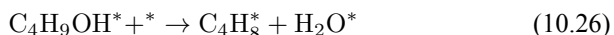
As can be seen in this section, dehydration followed by hydrogenation is a significant reaction sequence for aqueous-phase reforming to form alkanes from oxygenated hydrocarbons. For this reason, we look into the kinetics of dehydration reactions in further detail with the example of dehydration/hydrogenation of 2-butanol in aqueous environment.

Example: Dehydration/Hydrogenation of Butanol

As mentioned above, successive dehydration/hydrogenation in the aqueous phase leads to the production of straight chain alkanes such as butane, pentane and hexane from oxygenated hydrocarbons [56]. When metal catalysts such as Pt supported on acidic supports (silica-alumina or niobium phosphate) are used under conditions, such as 520 K and 50 bar, olefinic species are not observed in the outlet stream [56]. These results suggest that hydrogenation is fast and the rate limiting step is dehydration. West et al. [88] studied the kinetics of dehydration of 2-butanol in the presence of water (liquid as well as vapor) over different acid catalysts and developed a kinetic model to understand the pathways of dehydration in both phases. 2-butanol was chosen as a model compound. The authors first confirmed that dehydration was the rate limiting step by reacting 2-butanol over Pt/SiO₂-Al₂O₃ as well as the support only (SiO₂-Al₂O₃) to convert to butane and butenes, respectively. The rates of production of butane and butenes were the same on these two catalysts, indicating that dehydration was the rate limiting step.

The vapor pressures of water and 2-butanol at 513 K are 33 and 30 bar, respectively. With a total system pressure of 53 bar, in a closed system, water should remain as a liquid. However, when there is a gas flowing through the water, the gas bubbles carry water vapor to the outlet stream of the reactor. In addition, the butene produced by the dehydration reaction is present only in the gas phase. Therefore, the rate of butene production will also affect the extent of the sparging of liquid water. When there is no butene formation, all of the 2-butanol and water can be sparged into the gas phase at a gas flow (He) inlet to the reactor of 74 cm³(STP)/min. The extents of vaporization of water and 2-butanol were quantified by using vapor-liquid equilibrium expressions and the Antoine equation.

Two adsorption models were used for kinetic modeling to explain the reaction kinetics data for the effect of the flow rate of inert gas on the rates of dehydration over SiO₂-Al₂O₃ and NbOPO₄. The first mechanism investigated is a Langmuir-Hinshelwood (L-H) mechanism, which consists of the surface reaction of adsorbed butanol with a vacant site to form adsorbed butene and water. This mechanism is shown below:





Steps 1, 3, and 4 (Equations 10.25, 10.27 and 10.28) are the adsorption-desorption steps of butanol, butene, and water, respectively, and thus are assumed to be quasi-equilibrated steps. Step 2 (Equation 10.26) is the surface reaction for the production of butene and water on the surface from adsorbed 2-butanol.

The second pathway is based on the BET adsorption isotherm, in which the possibility of multilayer water adsorption is also included. Equation 10.29 shows the fractional coverage for the first adsorbed water molecule on the surface, whereas equations 10.30 and 10.31 show the fractional coverage of two-stack and n-layer stack of water molecules, respectively. $K_{\text{H}_2\text{O}}$ is the equilibrium constant for the adsorption of water and $K_{\text{W}1}$ is the equilibrium constant for the adsorption of water on an already adsorbed water molecule. The $K_{\text{W}1}$ constant is actually the equilibrium constant for liquefaction of water (inverse of the saturation pressure of water at the reaction temperature).

$$\theta_{\text{H}_2\text{O}} = K_{\text{H}_2\text{O}} P_{\text{H}_2\text{O}} \theta_v \quad (10.29)$$

$$\theta_{(\text{H}_2\text{O})_2} = K_{\text{H}_2\text{O}} P_{\text{H}_2\text{O}} K_{\text{W}1} P_{\text{H}_2\text{O}} \theta_v \quad (10.30)$$

$$\theta_{(\text{H}_2\text{O})_n} = K_{\text{H}_2\text{O}} P_{\text{H}_2\text{O}} (K_{\text{W}1} P_{\text{H}_2\text{O}})^{n-1} \theta_v \quad (10.31)$$

It is also possible to derive expressions for the hydration of butanol adsorbed on the surface. In such a case, the adsorption of butanol on a dry site and adsorption of water onto an adsorbed butanol molecule is added with corresponding equilibrium constants.

Figure 10.12 shows the change in butanol dehydration reaction rates in terms of TOF (1/s) with changing flow rates of the inert gas. For both solid acid catalysts (only the data for NbOPO_4 are shown in the figure), the general trend observed is an increase of the reaction rate at inert gas flow rates below and above $70 \text{ cm}^3(\text{STP})/\text{min}$ approximately. Higher flow rates of inert gas increase the reaction rate by decreasing the partial pressure of water. On the other hand, with flow rates

lower than $70 \text{ cm}^3(\text{STP})/\text{min}$, liquid water is present in the reactor and, increasing the inert gas flow rates, results in preferential vaporization of 2-butanol due to the non-ideality of the butanol-water system and high value of the butanol activity coefficient.

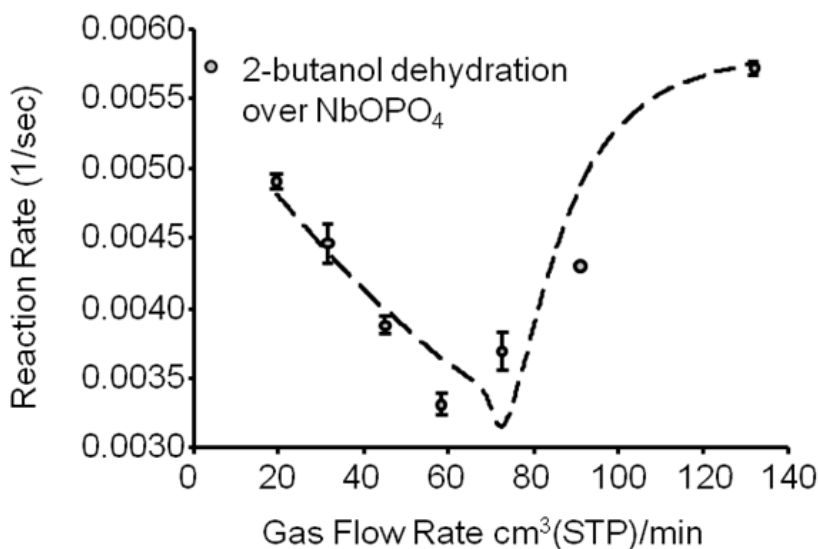


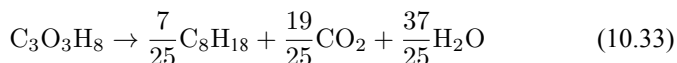
Figure 10.12: The change in 2-butanol dehydration reaction rates in terms of TOF ($1/\text{s}$) with changing flow rate of the inert gas over NbOPO_4 at 513 K and 52 atm total system pressure. BET multilayer adsorption mechanism with two surface reactions (adsorbed butanol with a vacant site, and adsorbed-hydrated butanol with a hydrated site) is used for the model (shown with the dashed line). Adapted from [88]

The simplest description of the surface reaction chemistry is the L-H mechanism in which adsorbed butanol reacts with a vacant site to produce adsorbed butene and water. However, this mechanism fails to predict accurately the behavior of the liquid/water system, because it does not include the formation of liquid water on the surface. On the other hand, for the model including the BET adsorption isotherms, a second surface reaction step can be included in which a hydrated site can also react with adsorbed-hydrated butanol to form butene and water. It can be seen in Figure 10.12, that the BET multilayer adsorption mechanism with

two surface reactions (adsorbed butanol with a vacant site, and adsorbed-hydrated butanol with a hydrated site) correctly predicts the trends seen in experiments.

10.4.4 Glycerol Reforming and Fischer-Tropsch Synthesis

This section will conclude our introduction to the reforming of biomass derived oxygenated hydrocarbons. We present a process for the conversion of aqueous glycerol feeds over platinum-based catalysts to produce synthesis gas (mixture of H_2 and CO) through reforming at low temperatures (498–620 K). The generated synthesis gas can subsequently be used for the production of liquid hydrocarbon fuels and/or chemicals by means of Fischer-Tropsch and methanol syntheses, respectively. This integrated process is a good example of active site coupling. The decomposition of glycerol into CO and H_2 is shown by Equation 10.32, and the reforming of glycerol combined with Fischer-Tropsch reaction to form alkanes (octane in this case) is shown in Equation 10.33.



The endothermic enthalpy change of this reaction is 350 kJ mol^{-1} and the heat generated by Fischer-Tropsch conversion of the CO and H_2 to liquid alkanes such as octane is -412 kJ mol^{-1} . When these two reactions are combined, the overall reaction becomes exothermic with an enthalpy change of $(-63 \text{ kJ mol}^{-1})$. This value corresponds to about 4% of the heating value of the glycerol ($-1480 \text{ kJ mol}^{-1}$).

As explained earlier, APR can take place at conditions where the water-gas shift reaction is favored. Water-gas shift is an important step when the aim is to produce high yields of hydrogen in $\text{H}_2:\text{CO}_2$ gas mixtures containing low levels of CO ($\sim 100 \text{ ppm}$). However, when the aim is to generate synthesis gas ($\text{H}_2:\text{CO}$ mixtures), the water-gas shift reaction is an undesirable reaction. Therefore, glycerol reforming is carried out in the vapor phase at higher temperatures, where it is possible to control the extent of the water-gas shift reaction and the $\text{H}_2:\text{CO}$ ratio in the outlet stream. It may also be desirable to use catalysts that do not promote the water-gas shift reaction.

Glycerol is a platform molecule that can be derived from various biomass conversion routes. One source of glycerol is the low value waste stream obtained from the production of biodiesel by transesterification of plant oils [53, 89] and

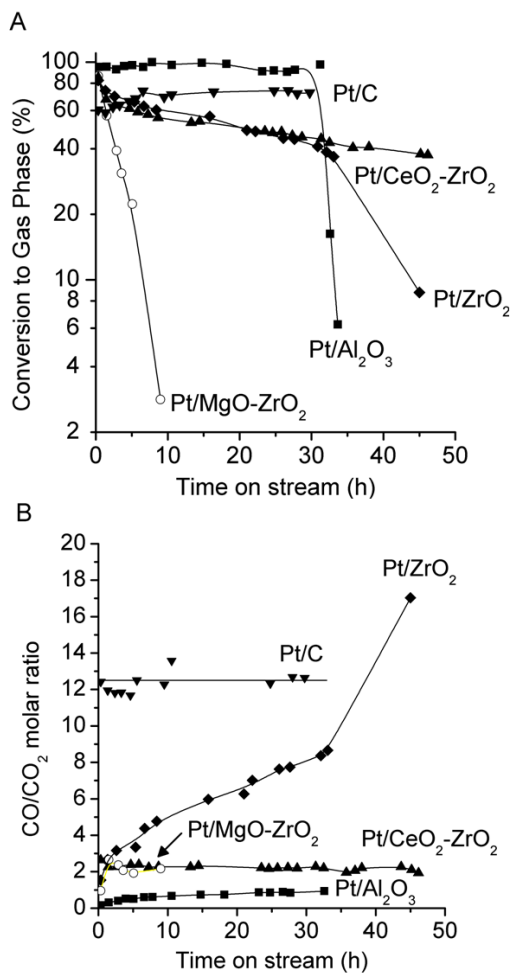


Figure 10.13: A) The conversion of glycerol to gas-phase products and B) the CO/CO₂ molar ratio for catalysts consisting of Pt supported on Al₂O₃ (solid squares), ZrO₂ (solid diamonds), CeO₂/ZrO₂ (solid triangles), MgO/ZrO₂ (open circles) and carbon (solid inverted triangles) with time on stream. Reactions were carried out at 623 K and 1 bar with 30% aqueous glycerol solution. Adapted from [59]

animal fat [53]. We first present studies carried out for the synthesis gas production from glycerol, and then we will discuss the combination of reforming with Fischer-Tropsch synthesis for the production of liquid fuels. Soares et al. [59] studied the gas-phase conversion of glycerol into synthesis gas over supported Pt catalysts using a feed of glycerol: H₂O solution (30 wt% glycerol) at 623 K and atmospheric pressure. Figure 10.13 shows the conversion of glycerol and the CO/CO₂ molar ratio for catalysts consisting of Pt supported on Al₂O₃, ZrO₂, CeO₂/ZrO₂ and MgO/ZrO₂ and carbon with time on stream. As it can be seen from Figure 10.13A all the catalysts except Pt/C showed deactivation with time on stream. Pt/C remained stable for at least 30 hours on stream. The different deactivation profiles suggest that the support has an important effect on the stability of the catalyst. The authors tracked the rate of formation of C₂-hydrocarbons (ethane and ethylene) for the Pt supported catalysts. They recorded measurable amounts of ethane and ethylene over the Pt catalysts with oxide supports, whereas negligible amounts were detected over Pt/C. They also observed that the C₂-TOF/H₂-TOF ratio increased with time on stream for the oxide supported catalysts. These observations suggest that a possible cause of deactivation is the deposition of carbonaceous species caused by unsaturated species formed through dehydration of glycerol or intermediates over oxide supports. It has also been reported that the water-gas shift activity was increased in the presence of oxide supports. As can be seen in Figure 10.13B, the initial CO/CO₂ ratio for Pt/C is 12:1, whereas for the other catalysts it is less than 3:1. When the glycerol conversion is decreased by increasing space velocity or glycerol concentration, the CO/CO₂ ratio is also increased, suggesting that the reforming of glycerol to CO and H₂ is a primary reaction, whereas the water-gas shift reaction is a secondary reaction. As a consequence of this behavior, it becomes possible to adjust the H₂/CO ratio to be suitable for Fischer-Tropsch reaction, while reaching almost complete conversions of glycerol.

To achieve the most efficient combination of glycerol reforming with Fischer-Tropsch synthesis, the glycerol reforming step should take place at a lower temperature, such that heat integration between the endothermic reforming and exothermic Fischer-Tropsch reaction can be realized. Therefore, the glycerol conversion reaction was also studied at 498–573 K. As explained earlier, the conversion of polyols to H₂ and CO requires selective C–C cleavage versus C–O bond breaking [15], and Pt is preferred for its ability to do so. However, at these low temperatures CO desorption may limit the reforming reaction due to high coverages of CO on the surface. This high coverage of CO on the surface may also increase the rate of the water-gas shift reaction, which is not a desirable reaction when the purpose is to generate synthesis gas.

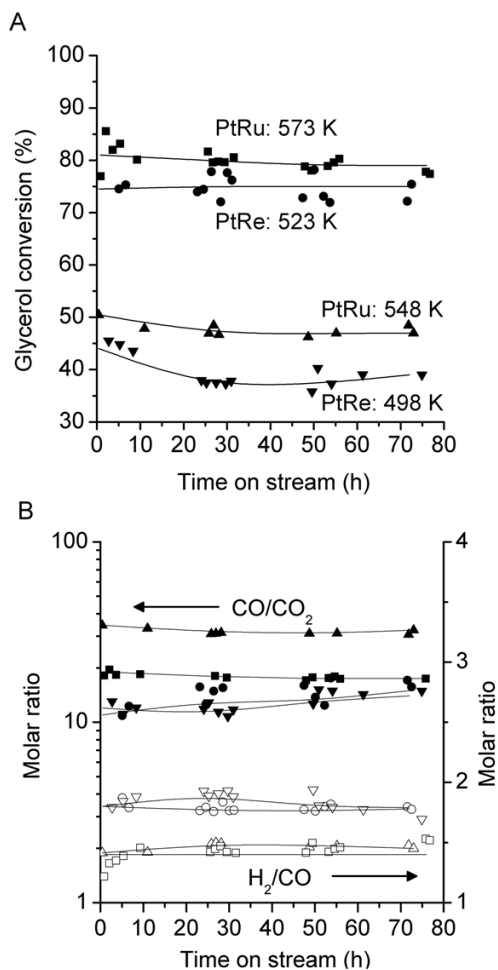


Figure 10.14: A) The glycerol conversion to gas-phase products and B) molar ratios of CO/CO₂ (solid symbols) and H₂/CO (open symbols) with time on stream at low temperatures over PtRu and PtRe (atomic ratio 1:1) bimetallic catalysts. Reactions were carried out at 1 bar with 30% aqueous glycerol solution. Triangles: PtRu/C, 548 K, squares: PtRu/C, 573 K, inverted triangles: PtRe/C, 498 K, and circles: PtRe/C 523 K. Adapted from [59]

Therefore, it is crucial to find a catalyst that is still active and selective for C–C cleavage, and that can weaken the CO bonding to catalyst surface. The binding energy of CO can be reduced by using appropriate metal alloys, such as PtRu and PtRe alloy catalysts [90]. Figure 10.14 shows the glycerol conversion and molar ratios of CO/CO₂ and H₂/CO with time on stream at low temperatures over PtRu and PtRe (atomic ratio 1:1) bimetallic catalysts.

These results demonstrate that the conversion of glycerol to synthesis gas can be accomplished at temperatures within the ranges used for Fischer-Tropsch synthesis [91]. It is important to note that the H₂/CO ratio can be adjusted to be suitable for Fischer-Tropsch synthesis (H₂/CO=2 stoichiometrically) if necessary through a water-gas shift reaction. Over 10 wt% PtRe/C (atomic ratio 1:1), higher pressures and feed concentrations were studied to allow for an efficient combination of two processes. Simonetti et al. [58] investigated the formation of liquid alkanes by the integration of glycerol conversion with Fischer-Tropsch synthesis. These experiments employed a two-bed catalyst system using 1.0 g of 10 wt% PtRe (1:1)/C followed by 1.7 g of 1.0 wt% Ru/TiO₂, with an 80 wt% glycerol feed at 548 K and total pressures between 5 and 17 bar. Figure 10.15 demonstrates the coupling of glycerol reforming and Fischer-Tropsch synthesis to produce liquid fuels, and Figure 10.16 shows the results of the experiments carried out at different pressures. At 5 bar, only 32% of the carbon is converted to alkanes and the primary product is observed to be CO. When pressure is increased to 11 and 17 bar, the carbon distribution is shifted toward C₁–C₅₊ alkanes, such that selectivities of alkanes are 42% and 51% at 11 bar and 17 bar, respectively. In addition to the C₅₊ alkanes, the organic liquid effluent also contains oxygenates, such as acetone, pentanones, hexanones, and heptanones. The amount of carbon in these oxygenates increases by a factor of 5 with increasing pressure. At the highest pressure studied, the amount of CO decreased by more than an order of magnitude and total selectivity to alkanes increased. On the other hand, compared to 11 bar, selectivity toward C₅₊ alkanes is slightly reduced. This change is due to increased water-gas shift activity as well as overall Fischer-Tropsch activity with increased pressure. The percentage of carbon in the organic liquid-phase product was 43% at 17 bar, 35% at 11 bar, and 15% at 5 bar, with the percentage of carbon in gaseous products (CO, CO₂, and C₁–C₉ alkanes) decreasing from 71% at 5 bar to approximately 50% at 11 and 17 bar. At 5 and 11 bar, 14% of the carbon is contained as oxygenated species in the aqueous effluent (acetone, methanol, and ethanol), and at 17 bar, this value decreases to 10%. These aqueous liquid effluents contain between 5 wt% and 15 wt% methanol, ethanol, and acetone. It is noted that these species are at similar concentrations as aqueous ethanol streams produced by fermentation of glucose (e.g., 5 wt%). Therefore, it might be desirable to separate the components by distillation for use in the chemical industry.

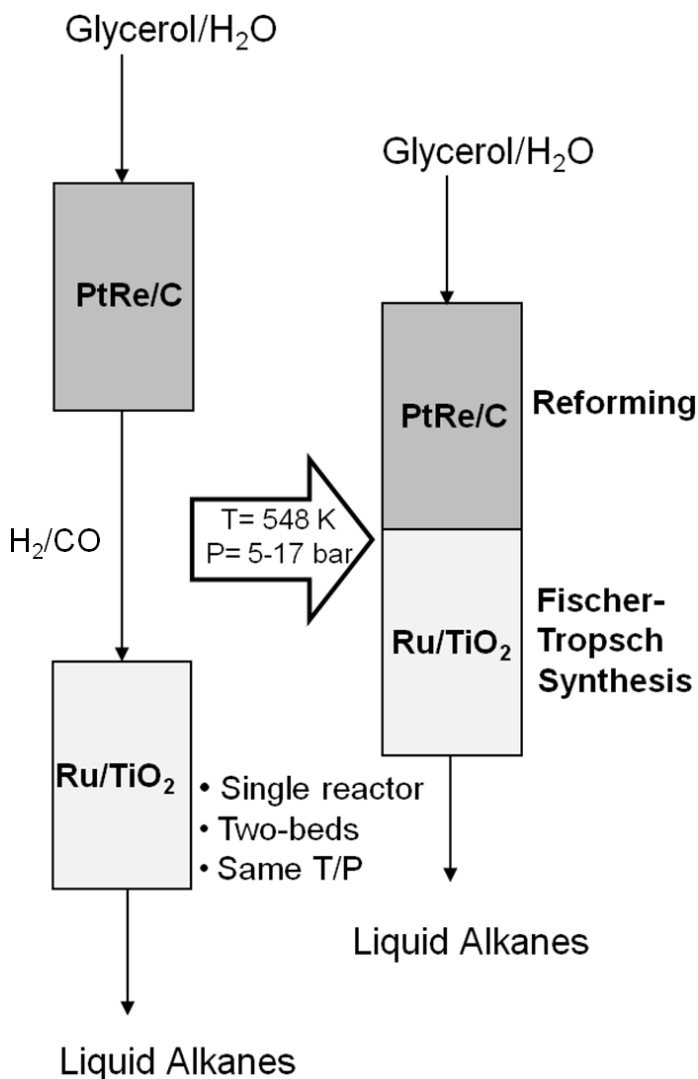


Figure 10.15: Schematic representation of the dual-bed catalytic reactor used for the combined glycerol reforming and Fischer-Tropsch synthesis to produce liquid alkanes

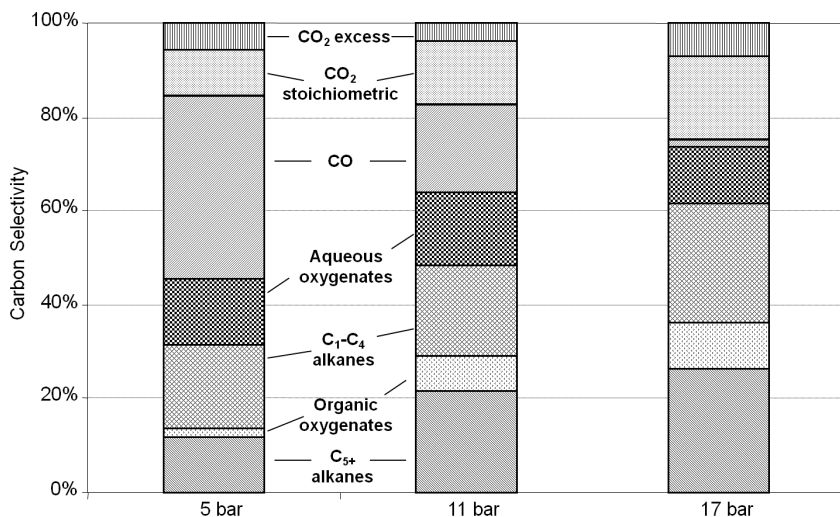


Figure 10.16: Carbon distribution in the effluent from glycerol conversion over a two-bed catalytic reactor containing PtRe/C followed by Ru/TiO₂ at 548 K at pressures of 5, 11 and 17 bar. Adapted from [58]

10.5 Conversion of Sugars/Polyols to Liquid Fuels via the Formation of Monofunctional Intermediates

Until now, we have presented the utilization of aqueous-phase or gas-phase reforming reactions to form H₂, synthesis gas (H₂ and CO) or alkanes (C₄–C₆) through selective C–C or C–O cleavage steps. Even when the alkanes are obtained selectively, the carbon number of the heaviest alkane is limited to the carbon number of the sugar or polyol feed. As we concluded in the previous sections, the production of heavier liquid fuels from sugars and/or polyols can be accomplished by controlled oxygen removal reactions (controlled C–O and C–C cleavage reactions) to obtain functional intermediates that can undergo C–C bond forming reactions. Kunkes et al. [14] recently reported a process in which sugars and polyols are converted to monofunctional intermediates over a carbon-supported PtRe bimetallic catalyst in a single reactor. By operating at moderate temperatures (283–523 K) and pressures (20–30 bar) with concentrated aqueous polyol (60 wt% sorbitol) or sugar (40 wt% glucose) feeds, 80% of the initial oxygen content of the sugars and polyols is removed by controlling C–C cleavage (leading to CO₂ and H₂) and C–O cleavage (leading to alkanes) rates. As a result, an organic

phase is formed that spontaneously separates from water and consists of a mixture of C_4 – C_6 monofunctional species (carboxylic acids, alcohols, ketones and heterocyclic species). Cleavage of C–O bonds takes place through hydrogenolysis, which is promoted by Re [92, 93]. As oxygen is progressively removed from the intermediates, the binding of these intermediates to the catalyst surface becomes weaker, resulting in the production of monofunctional species, such as acids, alcohols, ketones and heterocycles before alkanes are generated. One of the most significant features of this process is that the deoxygenation (C–O bond cleavage) is accomplished by using the hydrogen generated in situ by the endothermic partial reforming of the carbohydrate feed. The exothermic deoxygenation reactions are balanced with endothermic reforming reactions in the same reactor, such that the overall conversion is mildly exothermic and more than 90% of the energy content of the carbohydrate feed is stored in the reaction products. The overall process is illustrated schematically for sorbitol in Figure 10.17.

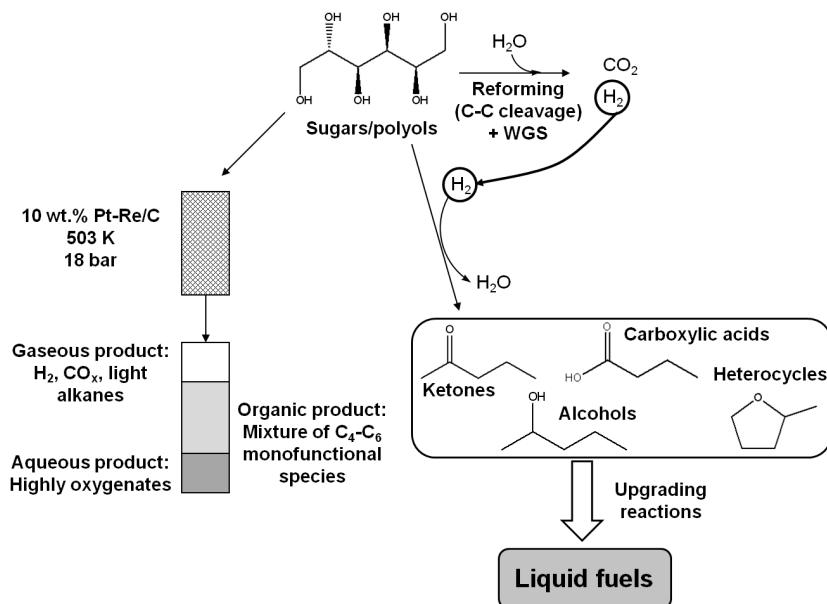


Figure 10.17: Schematic representation of the conversion of sugars and polyols over PtRe/ C to produce an organic liquid consisting of C_4 – C_6 monofunctional species (ketones, alcohols, carboxylic acids and heterocyclic species). Adapted from [14]

The gas-phase effluent consists of CO_x and light alkanes ($\text{C}_1\text{--C}_6$), the aqueous phase consists of higher oxygenates such as isosorbide, and the organic phase effluent consists of the monofunctional species and alkanes ($\text{C}_4\text{--C}_6$). The conversion of a 60 wt% sorbitol solution over a 10 wt% PtRe(1:1) catalyst supported on carbon was studied in a fixed bed flow reactor at pressures of 18–27 bar, temperatures of 483–523 K, and weight hourly space velocities (WHSV) of 0.6 to 2.4 hr^{-1} . The effluent carbon from the aqueous phase species is shifted to organic phase species when pressure is increased from 18 to 27 bar at 483 K. At a higher temperature (503 K), the pressure increase from 18 to 27 bar results in a shift from aqueous phase species to gaseous species, whereas it is observed that pressure has a negligible effect on the carbon distribution, when the temperature is increased further to 523 K. The production of alkanes increases at the expense of oxygenated species as pressure or temperature is increased when the other is kept constant. At constant temperature and pressure, when the space velocity is increased from 0.60 to 1.2 h^{-1} , the production of organic phase species, specifically ketones, alcohols and carboxylic acids, increases at the expense of alkanes in the gaseous phase as well as in the liquid organic phase. However, a further increase of space velocity to 2.4 h^{-1} shifts the carbon distribution toward the aqueous phase oxygenates. At 503 K and 18 bar, with WHSV of 0.6 h^{-1} , PtRe/C showed good stability for longer than one month time on stream. The organic outlet stream at these conditions contains 52% of the carbon found in the 60 wt% sorbitol feed, when the gaseous and aqueous streams contain 36% and 12%, respectively.

Kunkes et al. [14] also showed that glucose can be converted directly to mixtures of monofunctional species without the need for initial formation of sorbitol through a hydrogenation step. An aqueous solution containing 40 wt% glucose was used with slightly different reaction conditions (483 K, 18 bar, and 0.6 hr^{-1} WHSV) to ensure stable catalyst activity. The most significant difference in product distributions compared to sorbitol conversion is the higher selectivity towards carboxylic acids. Carboxylic acids constitute 14% of total carbon, or 35% of organic product from glucose conversion as opposed to 6% of the total carbon, or 13% of the organic product from sorbitol conversion.

10.5.1 Upgrading Strategies for Monofunctional Intermediates to Obtain Liquid Fuels

As stated earlier, the monofunctional species obtained in the organic effluent from the conversion of sugars and polyols over PtRe/C catalyst have sufficient functional moieties to undergo various upgrading reactions to form high-molecular weight compounds suitable for gasoline, diesel and jet-fuel applications. These upgrading strategies are summarized in Figure 10.18. Diesel fuels consist primar-

ily of hydrocarbons with a linear carbon chain and minimal branching to achieve high cetane numbers, whereas gasoline typically contains more highly branched hydrocarbons and aromatic compounds having high octane numbers [94, 95].

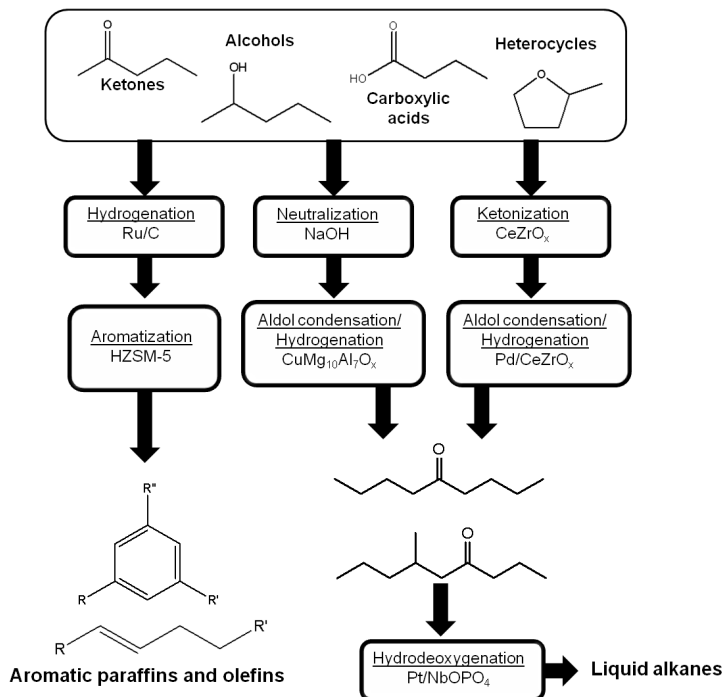


Figure 10.18: Upgrading strategies for the production of liquid fuels starting from monofunctional species obtained from sugars/polyols over PtRe/C. Adapted from [14]

With respect to gasoline components, Kunkes et al. [14] showed that the organic liquid produced from sorbitol can be converted to aromatic compounds or to a distribution of branched olefins centered at C₁₂. The first step for both conversions is the hydrogenation of ketones and carboxylic acids to alcohols. Using a 5 wt% Ru/C catalyst at 433 K, under 55 bar H₂, most of the ketones, carboxylic acids and some of the heterocyclic species in the sorbitol-derived organic liquid can be hydrogenated into corresponding alcohols. It is important to note that the heterocycles present in the organic liquid can be used as high-octane additives in gasoline [94, 96, 97]. In order to obtain aromatic species, the mixture of al-

cohols is reacted over HZSM-5 at 673 K and atmospheric pressure [98]. When hydrogenation is combined with the aromatization step, 25% and 29% of the carbon in the sorbitol-derived organic phase is converted to paraffins and olefins containing 3 and 4 carbon atoms, respectively. Almost 40% of the inlet carbon is converted to aromatic species, consisting of benzene, toluene, C₂-benzene (a benzene with two additional carbon atom substituents such as xylenes or ethyl benzene) and C₃–C₆ substituted benzene. In addition, it is possible to dehydrate secondary alcohols obtained by hydrogenation over an acidic niobia catalyst to form C₄–C₆ branched olefins. These olefins can later undergo an oligomerization reaction combined with cracking reactions over HZSM-5 to produce a distribution of branched olefins centered at C₁₂. Approximately 50% of the carbon present in the secondary alcohols can be converted into fuel-grade compounds overall [14].

To produce C₈–C₁₂ compounds that have minimal branching to be used in diesel fuel applications, C–C coupling by aldol condensation can be applied to the organic effluent obtained from sorbitol solution over PtRe/C. However, when this organic liquid is subjected to aldol condensation/hydrogenation in the presence of H₂ over a bifunctional CuMg₁₀Al₇O_x catalyst (has both base and metal sites), it was observed that the small amounts of carboxylic acids and esters caused deactivation of the basic CuMg₁₀Al₇O_x catalyst [99]. Therefore, the esters were hydrolyzed and the acids were neutralized by refluxing the organic mixture with a 20 wt% NaOH solution at 343 K. Following this step, the aldol condensation/hydrogenation of the C₄–C₆ ketones and secondary alcohols was carried out over CuMg₁₀Al₇O_x at 573 K and 5 bar pressure with H₂ co-feed [55, 57]. 45 % of the inlet carbon was converted to C₈–C₁₂ species containing 1 or no oxygen atoms. The remaining carbon is in the form of light species (C₄–C₆) with 1 or no oxygen atoms. The 3-ketones showed low reactivity for aldol condensation [100], while heterocyclic species were mostly inert. The product stream of the aldol condensation step can be subjected to hydrodeoxygenation over a metal/acid bifunctional catalyst to form an alkane stream [19].

As an alternative to the neutralization/ester hydrolysis step (NaOH refluxing), the carboxylic acid molecules can be upgraded by coupling through ketonization reactions to form higher molecular weight ketones (releasing CO₂ and H₂O), prior to the aldol condensation step. Ketonization reactions are advantageous especially for the organic liquids obtained from glucose, since the carboxylic acid production is significant. Ketonization of the monofunctional mixture obtained from glucose over CeZrO_x achieved greater than 98% conversion of the carboxylic acids in the feed to C₇–C₁₁ ketones. During the ketonization reaction, the remainder of the monofunctional species remains unreacted, and therefore, the product stream of this step can be subjected to further C–C coupling by aldol condensation of ketones and secondary alcohols. Even though the

$\text{CuMg}_{10}\text{Al}_7\text{O}_x$ catalyst still deactivated due to trace amounts of organic acids and esters, a bifunctional catalyst consisting of 0.25 wt% Pd on CeZrO_x was stable at 623 K with time on stream for aldol condensation. The feed used for aldol condensation over the Pd/ CeZrO_x catalyst consisted of 34% C_7 – C_{11} ketones and 66% C_4 – C_6 monofunctionals and alkanes. When the ketonized organic liquid was reacted over Pd/ CeZrO_x at 573 K and 5 bar pressure with H_2 co-feed, 57% of the total carbon in the liquid organic product stream was in the form of C_{7+} ketones, with 34% and 23% generated in ketonization and aldol condensation reactions, respectively. Products with a carbon chain length greater than C_{12} were also observed, due to aldol condensation of C_6 ketones with C_{7+} ketones formed during ketonization [14].

10.5.2 Integration of C–C Coupling Reactions of Monofunctional Intermediates

As mentioned earlier, ketonization is an effective strategy for decreasing the acidity of the aldol condensation/hydrogenation feed, allowing for the integration of the two steps using a basic aldol condensation catalyst. Since the reaction conditions for ketonization and aldol condensation/hydrogenation reactions are similar, it is possible that they could be integrated in a single reactor with a dual-bed system consisting of CeZrO_x to perform ketonization followed by a downstream bed of Pd/ CeZrO_x to perform aldol condensation/hydrogenation. Integrating the aldol condensation and ketonization steps into a single reactor system is an example of active site coupling that would streamline the overall C–C coupling process. To effectively accomplish the integration of ketonization and aldol condensation/hydrogenation in a single reactor, it is necessary to understand the effects of the co-products, i.e., CO_2 and water, produced during the ketonization of carboxylic acids on the downstream aldol condensation/hydrogenation reaction. To study the effect of CO_2 and water on aldol condensation activity, experiments with pure 2-hexanone as the feed were carried out. When 10 mol% CO_2 in H_2 stream was co-fed with 2-hexanone feed over 0.25 wt% Pd/ CeZrO_x , 2-hexanone self-condensation conversion decreased from 60% to 5%. Since the basic sites are poisoned by CO_2 , the reactions that can take place on acid and metal sites become more pronounced, causing higher yields to alkanes through dehydration/hydrogenation and reforming reactions. When water was introduced with a 2-butanone feed (12 wt%), a 40% decrease in self-condensation conversion was recorded [101].

Literature shows that the nature of the interaction of CO_2 with a mixed oxide surface can be altered by changing the composition of mixed oxides [102, 103]. To permit the integration of ketonization and aldol condensation reactions

in a single reactor, $Ce_aZr_bO_x$ mixed oxide catalysts with different compositions were synthesized to find a catalyst, over which inhibition by CO_2 and H_2O was minimal [104]. It was observed that the conversion of 2-hexanone increases with increasing zirconia content in mixed oxide catalysts and pure ZrO_2 displays the highest conversion of 90%. When 10% CO_2 in H_2 co-feed was introduced instead of a pure H_2 stream, all ceria containing catalysts lost significant activity. On the other hand, Pd/ZrO_2 showed significant resistance to inhibition by CO_2 , with only a 20% decrease in condensation activity (corresponding to 72% conversion of 2-hexanone). In addition, when water was introduced in a 2-butanone feed, the catalytic activity decreased by about 10% for the case of Pd/ZrO_2 compared to a 40% decrease for $Pd/CeZrO_x$. Thus, it was concluded that Pd/ZrO_2 was a suitable catalyst for integrating ketonization and aldol condensation/hydrogenation in a single reactor due to the diminished inhibition of aldol condensation activity by water and CO_2 . This conclusion was then tested over a dual-catalyst bed system consisting of $CeZrO_x$ (upstream bed for ketonization) and Pd/ZrO_2 (downstream bed for aldol condensation/hydrogenation) using a feed mixture of 20 mol% butanoic acid in 2-hexanone in comparison to a feed mixture of 20 mol% heptane in 2-hexanone at 623 K and 5 bar with H_2 co-feed. The difference between the aldol condensation activity and selectivity values for the two runs were found to be insignificant, suggesting that Pd/ZrO_2 showed resistance to the CO_2 and water generated in the ketonization step when butanoic acid was present in the feed [104].

Following these results, the dual-catalyst bed system was implemented to process the organic liquid of monofunctionals obtained from a 60 wt% aqueous sorbitol solution over $PtRe/C$. Specifically, the performance of the dual-bed system was compared to that of a cascade system, in which two separate reactors are used for ketonization ($CeZrO_x$) and aldol condensation/hydrogenation (Pd/ZrO_2), with removal of CO_2 and water between the reactors [12]. The reactor set-ups are shown in Figure 10.19. The overall conversion of monofunctional species was approximately 70% for both systems, with a 42% overall yield to C_{7+} products. Accordingly, the selectivity to C_{7+} products was approximately 60%, the remainder of the products being in the form of C_4 – C_6 products. Effluent streams from both set-ups can be subjected to dehydration/hydrogenation reactions over Pt/SiO_2 – Al_2O_3 to obtain alkane streams. It was concluded in this work that the dual-bed, single reactor system is the preferred mode of operation, because the energy consumption as well as the reactor infrastructure associated with cooling and re-heating the products in between two C–C coupling steps can be eliminated, decreasing operating and capital costs [12].

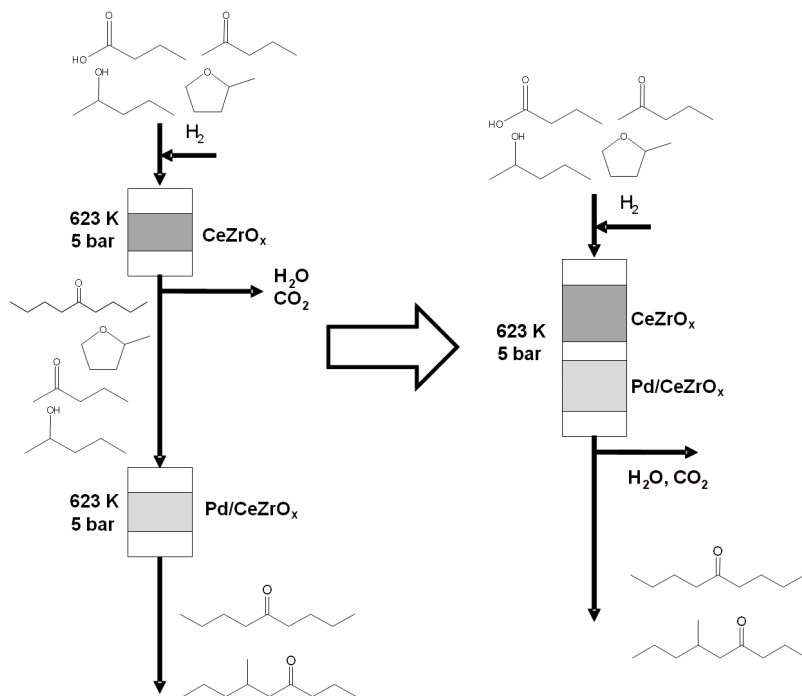


Figure 10.19: Schematic representation of the dual-bed catalytic reactor used for the combined ketonization and aldol condensation to produce liquid alkanes starting from monofunctional species obtained from sugars/polyols over PtRe/C. Adapted from [12]

In the final product stream from both set-ups, the ratio of linear alkanes to branched alkanes was determined to be approximately equal to 1. The majority of the branched ketones have minimal branching, i.e. methyl-branched species, which are formed from the coupling of 2-ketones and/or secondary alcohols. Only small amounts of ethyl-branched alkanes were observed, suggesting that coupling of 2-ketones/alcohols with 3-ketones/alcohols is not as favorable. The linear alkanes are formed by coupling of 2-ketones/alcohols with aldehydes generated from ring-opening of heterocycles over Pd/ZrO_2 . These results show that C–C coupling through ketonization and aldol condensation is desirable for the production of diesel fuel, since the extent of branching in the long carbon chain alkanes is minimal and can be controlled [12].

10.6 Levulinic Acid and γ -Valerolactone Platforms for the Production of Liquid Fuels

Levulinic acid (LA) is an attractive platform molecule from which a range of fine chemicals (δ -aminolevulinic acid, diphenolic acid, etc.) and fuel additives (levulinate esters, methyltetrahydrofuran, etc.) can be produced [105]. Levulinic acid can be obtained from the decomposition of 5-hydroxymethylfurfural (HMF) or direct hydrolysis of lignocellulosic biomass [106, 107] and cellulose [108] through dilute sulfuric acid hydrolysis. In all of these conversions, equimolar amounts of formic acid are generated with levulinic acid. Levulinic acid production by hydrolysis of cellulose can be carried out through different strategies, such as by using dilute sulfuric acid [108], concentrated hydrochloric acid [109], solid acids [110] and ionic liquids [111]. Among these strategies, hydrolysis by dilute sulfuric acid appears to have the optimum balance of cost, yield, and scalability for the preparation of levulinic acid. The Biofine process produces levulinic acid from lignocellulose at a pilot level production via dilute sulfuric acid hydrolysis [106, 107]. Final yields to levulinic acid are around 70–80% of the theoretical maximum, and correspond to 50% of the mass of the C_6 sugars. The remaining mass is collected as formic acid (20%), which is separated from levulinic acid by evaporation, and humins (30%), which are solid polymers produced by degradation reactions of [112].

A specifically valuable derivative of LA is γ -valerolactone (GVL) [112], another platform molecule, from which fine chemicals, fuel additives, and gasoline, jet fuel and diesel fuel components can be produced [10, 108, 113, 114]. LA can be converted to GVL through consecutive dehydration/hydrogenation reactions. If dehydration takes place first, angelica lactone is the intermediate, and if reduction takes place first, 4-hydroxy-pentanoic acid is the intermediate. The conversion of LA to GVL can take place at relatively low temperatures (373–543 K) and high pressures (50–150 bars) with either homogeneous or heterogeneous catalysts [115]. High yields of GVL (97%) can be obtained using a Ru/C catalyst. The reduction of LA to GVL generally takes place in the presence of molecular H_2 ; however, the use of H_2 generated in situ from the decomposition of formic acid is a promising alternative. The use of formic acid as a hydrogen source in aqueous solutions also eliminates the need for purification of LA. When obtained through mineral acid hydrolysis from cellulose, the separation of levulinic acid from the mineral acid becomes energy intensive. A recent strategy for the production of GVL starting from cellulose, starts with the hydrolysis of cellulose with dilute sulfuric acid solution to generate an equimolar mixture of levulinic and formic acids in water. Levulinic acid is then reduced to GVL over a Ru/C catalyst using the H_2 generated in situ by formic acid decomposition. Even

though sulfuric acid inhibits the reduction activity significantly, the Ru/C shows stable activity. The GVL product is more hydrophobic than levulinic acid, and therefore, selective separation of GVL from sulfuric acid becomes possible using a hydrophobic extracting solvent. This way, most of the sulfuric acid can be recycled back to the cellulose deconstruction reactor. For example, using an equal mass of ethyl acetate with aqueous GVL solution, 76% of the GVL can be extracted, while only 3% of the sulfuric acid and 6% of water is transferred into the organic solvent [108].

In terms of chemicals, some compounds that can be produced from GVL are α -methylene- γ -valerolactone [116], caprolactone [117] or adipic acid [117]. In terms of fuel applications, GVL itself can be directly used as a fuel additive (i.e., it has a similar capacity to ethanol [118]) or can be converted to methyltetrahydrofuran. In addition to forming fuel additives, two recent strategies have been reported in which GVL can be converted to liquid fuels in the range of diesel and jet fuel. In the first strategy, GVL is converted over bifunctional metal/acid catalysts (e.g., Pd/Nb₂O₅) to form pentanoic acid, which is used to produce 5-nonanone by ketonization at high yields (92%) [114]. 5-Nonanone can undergo hydrodeoxygenation to nonane for use in diesel fuel blends, or it can be hydrogenated/dehydrated to produce nonene, which can be converted to C18 olefins through oligomerization reactions [114, 119]. In the second strategy, GVL is converted to butene through decarboxylation over an acidic catalyst, such as SiO₂/Al₂O₃. Butene can be oligomerized to obtain jet fuel range olefins [10]. These strategies derived from GVL are summarized in Figure 10.20, which includes the production of GVL from levulinic acid. We now explore these two strategies in further detail.

The production of pentanoic acid from aqueous solutions of GVL (50 wt%) over Pd/Nb₂O₅ takes place at 623 K and under 35 bar with H₂ co-feed and goes through pentenoic acid intermediates obtained by ring-opening of GVL [114]. Pentenoic acids can be hydrogenated to form pentanoic acid over the metal sites (Pd) in the presence of H₂. Due to its low solubility in water, pentanoic acid can be obtained as an organic layer that spontaneously separates from water. The metal loading of the catalyst is crucial to obtain pentanoic acid with high selectivity. When the metal loading is increased, the production of byproducts, such as butane and pentane, is increased. Butane is formed through decarboxylation/decarbonylation of pentanoic acid followed by hydrogenation, and pentane can be obtained by hydrogenation/dehydration/hydrogenation of the pentanoic acid with the use of both acid and metal sites. Increasing hydrogen pressure has the same effect as increasing the metal loading. Approximately 92% yield to pentanoic acid can be achieved when the metal loading is 0.1 wt% and the H₂ partial pressure is 17 bar (35 bar of total pressure) at 598 K. Pentanoic acid is a monofunctional molecule

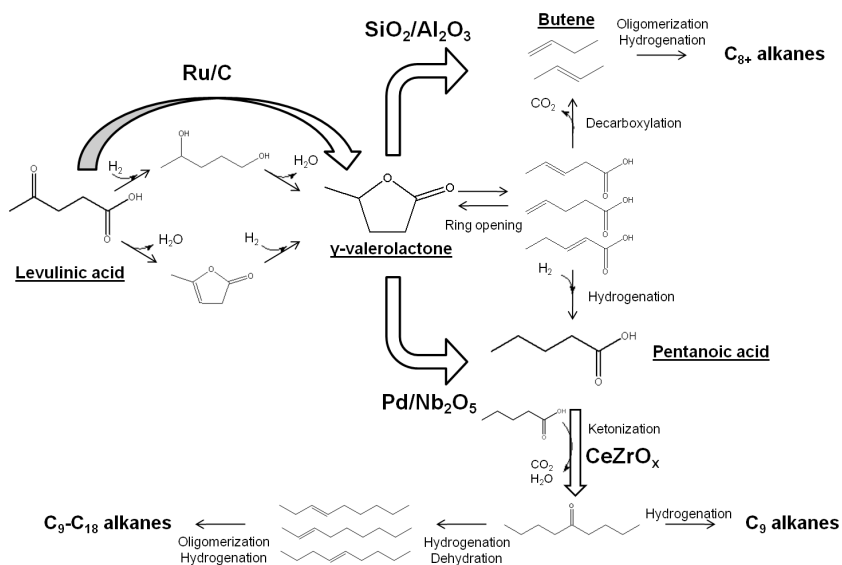


Figure 10.20: Reaction pathways for the production of γ -valerolactone (GVL) derived from levulinic acid and the production of targeted molecular weight alkanes via the catalytic upgrading of GVL through the formation of pentanoic acid and butene isomers. Adapted from [119]

and can further be upgraded selectively through C–C coupling reactions. Similar to the acids obtained from sorbitol/glucose over PtRe/C bimetallic catalyst, pentanoic acid can be ketonized over a CeZrO_x catalyst at 698 K and pressures from 1 to 20 bar to form 5-nonanone, CO_2 and water. When reaction conditions for both steps are optimized for highest yields, 84% overall yield to 5-nonanone can be obtained in a cascade mode, with a 6% yield to lower molecular weight ketones, i.e., 2-hexanone and 3-heptanone [114]. These latter ketones are obtained by α and β scissions of 5-nonanone. As noted above, the 5-nonanone can be a precursor for fuels suitable for gasoline and diesel fuel.

When GVL is reacted over an acid catalyst, like $\text{SiO}_2/\text{Al}_2\text{O}_3$ without the presence of metal sites, decarboxylation of GVL is the most favorable reaction, leading to butene and CO_2 as the main products. High yields of butene can be achieved from aqueous solutions (30–60 wt%) of GVL at 648 K and pressures ranging from 1 to 36 bar [10]. When 80% GVL in water is used as the feed at 648 K and 36 bar, a 99% conversion of GVL and 96% yield of butene can be obtained.

As mentioned earlier, butene can be oligomerized to obtain high molecular weight olefins suitable for jet fuel. However, before going into details of that reaction, we present studies on thermodynamics and kinetics involved in the production of pentenoic acid, butene/ CO_2 , and pentanoic acid from GVL.

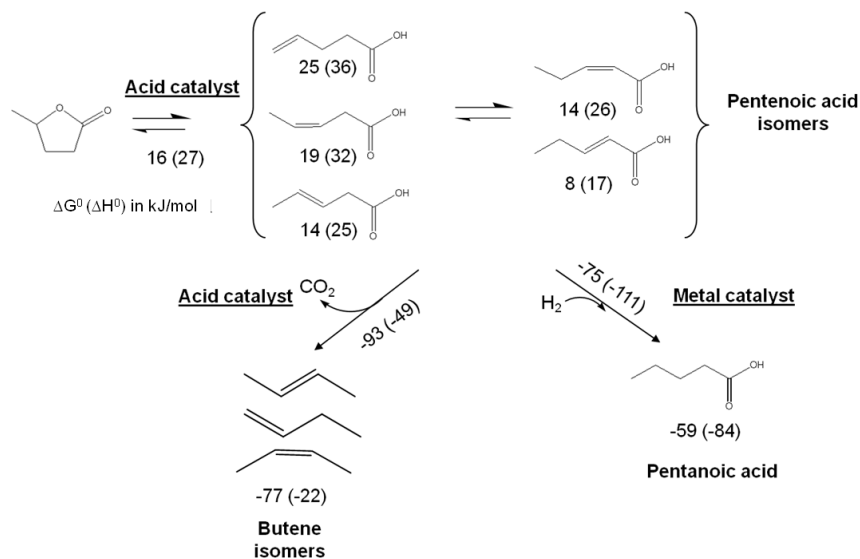


Figure 10.21: Values of ΔG° and ΔH° (kJ mol^{-1}) for γ -valerolactone (GVL) ring-opening reaction to isomers of pentenoic acid, and decarboxylation and hydrogenation of pentenoic acids to butene and pentanoic acid, respectively. Adapted from [120]

GVL conversion is initiated by ring-opening over acid sites to form an isomeric mixture of pentenoic acids. These unsaturated acids can be hydrogenated over metal sites to form pentanoic acid or can be decarboxylated over acid sites to form butene and CO_2 . Bond et al. [120] carried out thermodynamic calculations at standard conditions, and values of ΔG° and ΔH° for GVL ring-opening reactions to various isomers of pentenoic acid, and decarboxylation and hydrogenation of pentenoic acids are shown in Figure 10.21.

Pentenoic acid isomers consist of 4-, 2-trans, 3-trans, 2-cis, and 3-cis pentenoic acids. The enthalpy changes for the production of 4-, 2-trans, 3-trans, 2-cis, and 3-cis pentenoic acids are estimated to be 36, 17, 25, 26, 32 kJ/mol , respectively. Similarly, changes in Gibbs free energy at 298 K are estimated to be 25,

8, 14, 16, and 19 kJ/mol for 4-, 2-trans, 3-trans, 2-cis, and 3-cis pentenoic acids, respectively. These values indicate that formation of GVL is thermodynamically

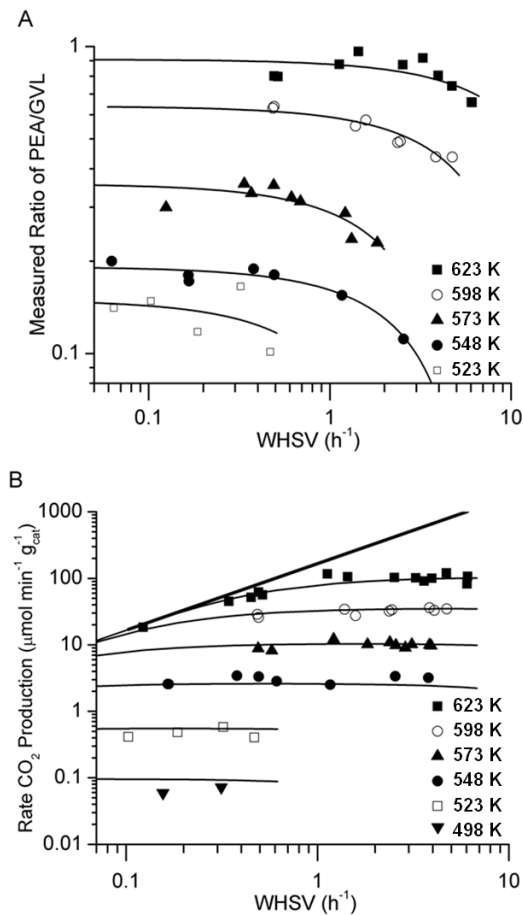


Figure 10.22: A) Measured ratio of pentenoic acids (PEA) to γ -valerolactone (GVL) in the outlet stream and B) the rate of CO₂ production at different weight hourly space velocities (WHSV, h⁻¹) and temperatures (K) for GVL conversion over SiO₂/Al₂O₃. Solid inverted triangles: 498 K, open squares: 523 K, solid circles: 548 K, solid triangles: 573 K, open circles: 598 K, and solid squares: 623 K. Adapted from [120]

avored over pentenoic acid isomers at standard conditions. However, since the ring-opening reaction is endothermic and entropically favored, the ratio of pentenoic acid isomers to GVL is expected to increase with temperature. This behavior is demonstrated in Figure 10.22A. As shown in Figure 10.21, hydrogenation of pentenoic acid (using an average distribution of isomers) to pentanoic acid is thermodynamically favorable with an enthalpy change of -111 kJ/mol and a Gibbs free energy change of -75 kJ/mol. This conversion makes the overall conversion of GVL to pentanoic acid favorable, with values of ΔH° and ΔG° for reaction being -84 and -59 kJ/mol, respectively. Decarboxylation of pentenoic acid to butene is also favorable, with a value of ΔG° being -93 kJ/mol. Starting from GVL, ΔG° is equal to -77 kJ/mol. Thus, the conversions of both GVL and pentenoic to butene and CO_2 are essentially irreversible.

In terms of the kinetics of ring-opening and decarboxylation of GVL, Figure 10.22 shows the values of the ratio of pentenoic acid to GVL, and the CO_2 production rate with changing weight hourly space velocity (WHSV) and temperature [120]. As temperature increases from 523 K to 623 K, the pentenoic acid (PEA)/GVL ratio increases as mentioned earlier. At a constant temperature, the PEA/GVL ratio remains constant for low to moderate space velocities, indicating the presence of an equilibrium controlled reaction. At high space velocities, the ratio begins to decrease, because the rate of ring-opening becomes slower relative to the inlet feed rate. Figure 10.22B shows that the CO_2 production rate is increased as temperature is increased. At a constant temperature, when the space velocity is changed, the CO_2 production rate does not seem to be affected. This behavior results because the conversion of GVL to pentenoic acid isomers is quasi-equilibrated and the partial pressures of GVL and pentenoic acid remain approximately at the same ratio. The decarboxylation step is kinetically controlled; therefore, the production rate of CO_2 remains the same with constant partial pressure of pentenoic acid and GVL [120].

Bond et al. [121] in a different work investigated the significance of the direct pathway of decarboxylation of GVL to form butene, as opposed to the indirect pathway, in which pentenoic acid isomers are generated prior to butene formation. The overall reaction scheme is shown in Figure 10.23. The relative rates of the direct and indirect decarboxylation pathways were studied by measuring the production rate of butene and CO_2 together with the concentration of pentenoic acids with changing weight hourly space velocity. Using a 10 wt% GVL solution in water as the feed, the partial pressure of pentenoic acid continuously decreases with increasing space velocity and extrapolates to zero at infinite WHSV ($1/\text{WHSV}=0$). Similarly, the partial pressure of butene approaches to zero when $1/\text{WHSV}$ approaches to zero, whereas the GVL partial pressure approaches to that of the inlet feed. As the space velocity increases, the rate of

decarboxylation remains constant and starts to decrease at lower space times ($< 0.01h$). This behavior suggests that the ring-opening reaction to pentenoic acids is quasi-equilibrated at relatively low space velocities, and the rate of decarboxylation is controlled by direct and indirect rates of decarboxylation. In the limit of zero space time, when there is no pentenoic acid, the rate of decarboxylation can be extrapolated to a finite number, proving the presence of a direct pathway from GVL. This value of the rate of decarboxylation at the limit of infinite space velocity is equal to the rate of direct decarboxylation of GVL to butene, and at higher space times when the indirect pathway also becomes significant, the direct pathway contributes considerably to the total butene production rate.

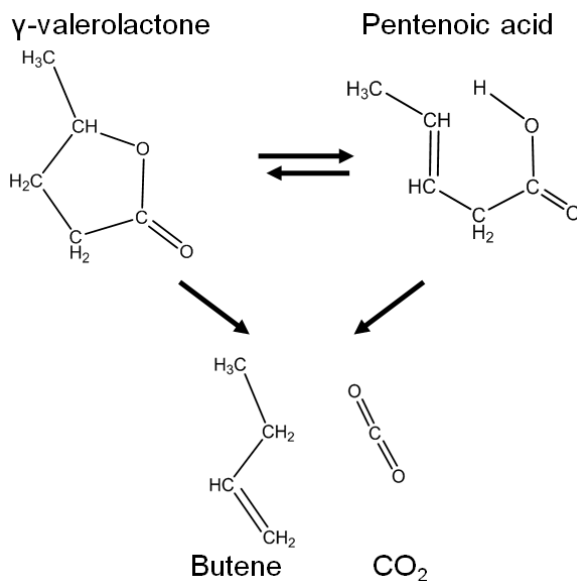


Figure 10.23: The reaction schemes for the indirect and direct pathways for the production of butene/ CO_2 from γ -valerolactone (GVL). Adapted from [121]

Following the formation of butene, in a second reactor connected in series, butene molecules can undergo C–C coupling reactions through oligomerization over an acid catalyst to form C_{8+} alkenes that can be used as jet fuel upon hydrogenation. Good yields were obtained from butene oligomerization at elevated pressures (35 bar) over Amberlyst 70. It was presented by Bond et al. [10] that

the two reactors could operate at the same system pressure and therefore could be integrated in series. In the integrated system, the outlet of the first reactor is used as the feed for the second reactor. Because CO_2 and water are present in the outlet stream with butene from the first reactor, the effects of these species on the oligomerization activity over Amberlyst 70 were investigated.

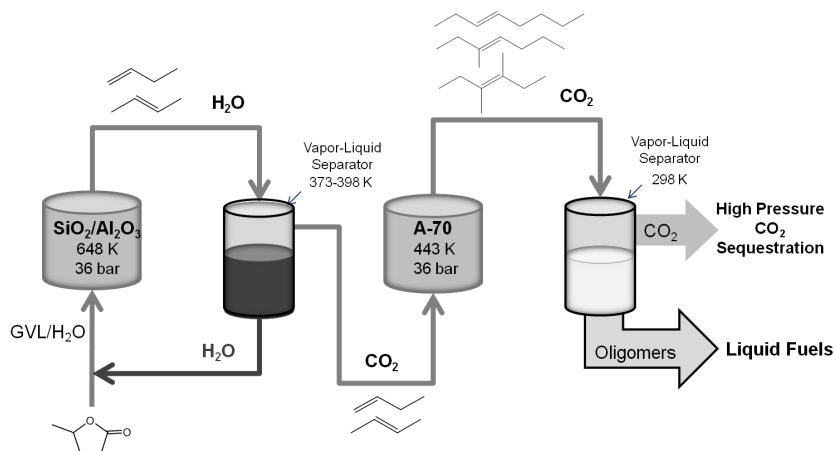


Figure 10.24: The overall process scheme for the production of liquid fuels starting from aqueous solutions of γ -valerolactone (GVL). Adapted from [10]

Experiments showed that the presence of CO_2 in the butene stream only affects the oligomerization reaction due to the dilution of the reactant (butene). On the other hand, when water was introduced to the inlet stream, a significant inhibition of the oligomerization activity was observed. In fact, for an equal molar feed of butene with CO_2 and water, the catalytic activity was completely suppressed. The negative effect of water required that it be removed from the gas stream prior to the oligomerization reaction. This removal was achieved by using a liquid-vapor separator operated at system pressure (36 bar) prior to the oligomerization reactor. The temperature of the separator was adjusted (373–393 K) such that most of the water would be condensed (97%) with all of the butene remaining in the vapor phase. When decarboxylation of GVL and oligomerization of butene take place over $\text{SiO}_2/\text{Al}_2\text{O}_3$ and Amberlyst-70, respectively, with a liquid-vapor separator in between, C_{8+} liquid alkenes can be obtained with 75% overall yield.

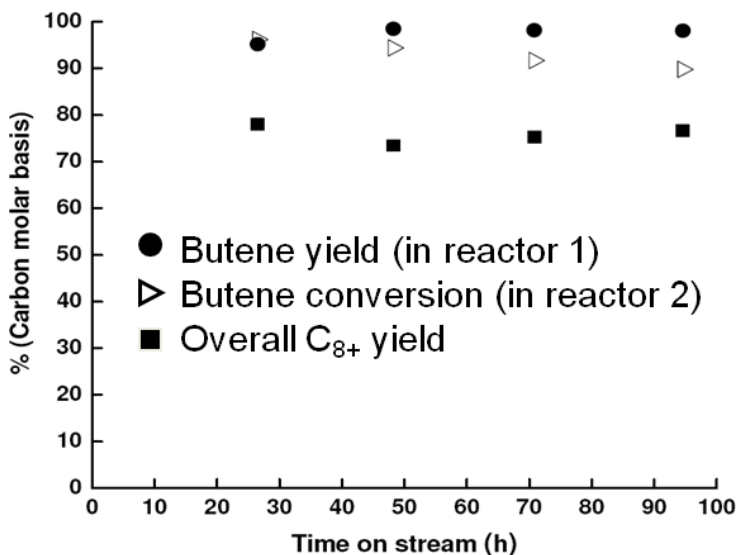


Figure 10.25: The butene yield from reactor 1, butene conversion in reactor 2 and overall C₈₊ yields obtained in the operation of the integrated catalytic system for conversion of γ -valerolactone (GVL) to liquid fuels. First reactor is operated at 36 bar, 648 K with SiO₂/Al₂O₃. First separator is operated at 36 bar and 398 K. Second reactor is at 36 bar, 443 K with Amberlyst-70. Second separator is at 36 bar and 298 K. Adapted from [10]

The effluent of the oligomerization reactor is fed to another vapor-liquid separator in series at system pressure and room temperature to obtain alkene oligomers in the condensed phase and CO₂ in the gas phase [10]. The process scheme is shown in Figure 10.24 and the butene yield, butene conversion and C₈₊ yields from the operation of the integrated catalytic system are shown in Figure 10.25. It is important to note that the conversion of GVL to alkene oligomers does not require an external source of hydrogen. Furthermore, the CO₂ stream obtained is at high pressure suitable for sequestration. The C₈₊ oligomers or the corresponding saturated alkanes are ideal to be used in gasoline and jet-fuel applications, while retaining 95% of the energy content of the glucose molecules that make up cellulose.

10.7 Concluding Remarks

In this chapter, we have outlined strategies for the conversion of carbohydrates to hydrogen or alkane fuels by providing thermodynamics analyses and various examples from recent catalytic processes. First, we indicate how lignocellulosic biomass can be deconstructed to form platform molecules that can be processed further and upgraded to specific fuels and chemicals. Some examples of these platform molecules include glucose, sorbitol and levulinic acid. Even though these species are simpler compared to cellulose, hemicellulose or lignin, they still have sufficient functionality for additional catalytic processing options. These species can be completely deoxygenated to obtain alkanes with 4–6 carbons; however, if alkanes with longer carbon chains than feed molecules are desired, then the deoxygenation reaction should not be carried to completion. Instead, the platform molecules should be processed to produce targeted functional groups (e.g., C=C, C=O, and acid groups), such that these species are easily upgradable through C–C coupling reactions, such as oligomerization, aldol condensation/hydrogenation and ketonization to form higher molecular weight species. We showed with various examples of processes, that this overall strategy can be followed starting with different platform molecules and generating various mono-functional molecules. Therefore, when formulating a new processing strategy, one should decide what useful functional molecules can be obtained, what reactions can be used for controlled removal of oxygen from the platform molecules, and how the C–C coupling between the functional intermediates can be achieved.

Throughout this chapter, we also presented with examples, how the feasibility of a new catalytic process can be explored. As shown for the conversion of carbohydrates to hydrogen, synthesis gas or alkanes, it is important to determine the conditions for which the desired reaction is thermodynamically favorable. In addition, it is required to address the selectivity issues for the desired product by identifying series or parallel competing reactions. Finally, it is necessary to determine overall yields and types of separation steps that would be required.

In order to maximize the yield of the desired products, the factors that control the selectivity should be identified. We demonstrated through examples that selectivity can be altered by changing reaction conditions, the phase of the reaction (liquid- versus gas-phase), types of active sites (metal/acid/base), intrinsic properties of the active sites (e.g., whether C–C or C–O cleavage is favored on a metal), and by using promoters to overcome inhibition and poisoning caused by the reactants, intermediates or products.

We also presented in this chapter the different types of catalytic coupling strategies at different length scales to develop more efficient processing strategies. One easily applicable catalytic coupling strategy is active site coupling that

enables the integration of multiple reactions in a single reactor by the use of multi-functional catalysts in a single catalyst bed, and/or by the use of dual catalyst beds. The examples show that there are several factors to be considered to integrate two reactions in a single reactor. First of all, it should be determined if the reaction conditions would allow such an integration. If the integration is possible, then the selectivity in the first reaction should be controlled to provide a suitable feed for the second reaction. Accordingly, the effects of the by-products or co-products of the first reaction on the activity of the second reaction should be investigated. The integration of reactions in such a manner opens new strategies for the efficient production of hydrogen and fuels from lignocellulosic biomass with fewer reaction and separation steps, thereby leading to more cost-competitive biorefining strategies.

Acknowledgments

The results from the University of Wisconsin reported here were supported in part by the U.S. Department of Energy Office of Basic Energy Sciences, by the National Science Foundation Chemical and Transport Systems Division of the Directorate for Engineering, by the DOE Great Lakes Bioenergy Research Center,¹ and by the Defense Advanced Research Projects Agency (Surf-cat: Catalysts for Production of JP-8 range molecules from Lignocellulosic Biomass). This chapter was written with the support from Partnerships for International Research and Education (PIRE) program funded by National Science Foundation grant OISE-0730277.

¹www.greatlakesbioenergy.org.

Bibliography

- [1] D.A. Simonetti and J.A. Dumesic. Catalytic Strategies for Changing the Energy Content and Achieving C–C Coupling in Biomass-Derived Oxygenated Hydrocarbons. *ChemSusChem* 1 (2008):725–733.
- [2] J.N. Chheda and J.A. Dumesic. An Overview of Dehydration, Aldol-Condensation and Hydrogenation Processes for Production of Liquid Alkanes from Biomass-Derived Carbohydrates. *Catalysis Today* 123 (2007):59–70.
- [3] C.-D. Chang and A.J. Silvestri. The Conversion of Methanol and other O-Compounds to Hydrocarbons over Zeolite Catalysts. *Journal of Catalysis* 47 (1977):249–259.
- [4] J.N. Chheda, G.W. Huber, and J.A. Dumesic. Liquid-Phase Catalytic Processing of Biomass to Fuels and Chemicals. *Angewandte Chemie International Edition* 46 (2007):7164–7183.
- [5] T.A. Lloyd and C.E. Wyman. Total Sugar Yields for Pretreatment by Hemicellulose Hydrolysis Coupled with Enzymatic Hydrolysis of the Remaining Solids. *Bioresource Technology* 96 (2005):1967–1977.
- [6] C.E. Wyman, B.E. Dale, R.T. Elander, M. Holtzapple, M.R. Ladisch, and Y.Y. Lee. Comparative Sugar Recovery Data from Laboratory Scale Application of Leading Pretreatment Technologies to Corn Stover. *Bioresource Technology* 96 (2005):2026–2032.
- [7] R. Rinaldi and F. Schüth. Acid Hydrolysis of Cellulose as the Entry Point into Biorefinery Schemes. *ChemSusChem* 2(12) (2009):1096–1107.
- [8] C.E. Wyman, S.R. Decker, M.E. Himmel, J.W. Brady, C.E. Skopec, and L. Viikari. Hydrolysis of Cellulose and Hemicellulose. In: *Polysaccharides: Structural Diversity and Functional Versatility*. 2nd ed. New York: Marcel Dekker INC, 2005.
- [9] G.W. Huber, J.N. Chheda, C.J. Barrett, and J.A. Dumesic. Production of Liquid Alkanes by Aqueous-Phase Processing of Biomass-Derived Carbohydrates. *Science* 308 (2005):1446–1450.

- [10] J.Q. Bond, D.M. Alonso, D. Wang, R.M. West, and J.A. Dumesic. Integrated Catalytic Conversion of γ -Valerolactone to Liquid Alkenes for Transportation Fuels. *Science* 327 (2010):1110–1114.
- [11] R.M. West, E.L. Kunkes, D.A. Simonetti, and J.A. Dumesic. Catalytic Conversion of Biomass-Derived Carbohydrates to Fuels and Chemicals by Formation and Upgrading of Mono-Functional Hydrocarbon Intermediates. *Catalysis Today* 5 (2008).
- [12] E.I. Gürbüz, E.L. Kunkes, and J.A. Dumesic. Dual-bed Catalyst System for C–C Coupling of Biomass-Derived Oxygenated Hydrocarbons to Fuel-Grade Compounds. *Green Chemistry* 12 (2010):223.
- [13] J. Chaminand, L. Djakovitch, P. Gallezot, P. Marion, C. Pinel, and C. Rosier. Glycerol Hydrogenolysis on Heterogeneous Catalysts. *Green Chemistry* 6 (2004):359–361.
- [14] E.L. Kunkes, D.A. Simonetti, R.M. West, J.C. Serrano-Ruiz, C.A. Gaertner, and J.A. Dumesic. Catalytic Conversion of Biomass to Monofunctional Hydrocarbons and Targeted Liquid-Fuel Classes. *Science* 322 (2008):417–421.
- [15] R.D. Cortright, R.R. Davda, and James A. Dumesic. Hydrogen from Catalytic Reforming of Biomass-Derived Hydrocarbons in Liquid Water. *Nature* 418 (2002):964.
- [16] M.E. Dry. The Fischer-Tropsch Process: 1950–2000. *Catalysis Today* 71 (2002):227.
- [17] L. Caldwell. *Selectivity in Fischer-Tropsch Synthesis: Review and Recommendations for Further Work*. 1980. URL: http://www.fischer-tropsch.org/DOE/DOE_reports/81223596/pb81223596.pdf.
- [18] D. Tichit, D. Lutic, B. Coq, R. Durand, and R. Teissier. The Aldol Condensation of Acetaldehyde and Heptanal on Hydrotalcite-type Catalysts. *Journal of Catalysis* 219 (2003):167–175.
- [19] R.M. West, Z.Y. Liu, M. Peter, and J.A. Dumesic. Liquid Alkanes with Targeted Molecular Weights from Biomass-Derived Carbohydrates. *ChemSusChem* 1 (2008):417–424.
- [20] O. Nagashima, S. Sato, R. Takahashi, and T. Sodesawa. Ketonization of Carboxylic Acids over CO₂-based composite oxides. *Journal of Molecular Catalysis A* 227 (2005):231–239.
- [21] J.F. Knifton, J.R. Sanderson, and P.E. Dai. Olefin Oligomerization via Zeolite Catalysis. *Catalysis Letters* 28 (1994):223–230.

- [22] A.J. Ragauskas, C.K. Williams, B.H. Davison, G. Britovsek, J. Cairney, C.A. Eckert, W.J. Frederick, J.P. Hallett, D.J. Leak, C.L. Liotta, J.R. Mielenz, R. Murphy, R. Templer, and T. Tschaplinski. The Path Forward for Biofuels and Biomaterials. *Science* 311 (2006):484–489.
- [23] P.M. Holmblad, J.H. Larsen, I. Chorkendorff, L.P. Nielsen, F. Besenbacher, I. Stensgaard, E. Laegsgaard, P. Kratzer, B. Hammer, and J.K. Nørskov. Designing Surface Alloys with Specific Active Sites. *Catalysis Letters* 40 (1996):131–135.
- [24] A.P. Wight and M.E. Davis. Design and Preparation of Organic-Inorganic Hybrid Catalysts. *Chemical Reviews* 102 (2002):3589–3614.
- [25] A. Bhaumik and T. Tatsumi. Organically Modified Titanium-Rich Ti-MCM-41, Efficient Catalysts for Epoxidation Reactions. *Journal of Catalysis* 189 (2000):31–39.
- [26] V.L. Budarin, J.H. Clark, J.J.E. Hardy, R. Luque, K. Milkowski, S.J. Tavener, and A.J. Wilson. Starbons: New Starch-Derived Mesoporous Carbonaceous Materials with Tunable Properties. *Angewandte Chemie International Edition* 45 (2006):3782–3786.
- [27] V.L. Budarin, J.H. Clark, R. Luque, D.J. Macquarrie, A. Koutinas, and C. Webb. Tunable Mesoporous Materials Optimised for Aqueous Phase Esterifications. *Green Chemistry* 9 (2007):992–995.
- [28] V.L. Budarin, J.H. Clark, R. Luque, and D.J. Macquarrie. Versatile Mesoporous Carbonaceous Materials for Acid Catalysis. *Chemical Communications* (2007):634–636.
- [29] V.L. Budarin, R. Luque, D.J. Macquarrie, and J.H. Clark. Towards a Bio-Based Industry: Benign Catalytic Esterifications of Succinic Acid in the Presence of Water. *Chemistry - A European Journal* 13 (2007):6914–6919.
- [30] M.E. Davis. Ordered Porous Materials for Emerging Applications. *Nature* 417 (2002):813–821.
- [31] D.J. Macquarrie, D.B. Jackson, J.E.G. Mdoe, and J.H. Clark. Organomodified Hexagonal Mesoporous Silicates. *New Journal of Chemistry* 23 (1999):539–544.
- [32] D.J. Macquarrie. Direct Preparation of Organically Modified MCM-Type Materials. Preparation and Characterisation of Aminopropyl-MCM and 2-cyanoethyl-MCM. *Chemical Communications* (1996):1961–1962.

- [33] D.J. Macquarrie and D.B. Jackson. Aminopropylated MCMs as Base Catalysts: A Comparison with Aminopropylated Silica. *Chemical Communications* (1997):1781–1782.
- [34] E.L. Margelefsky, R.K. Zeidan, V. Dufaud, and M.E. Davis. Organized Surface Functional Groups: Cooperative Catalysis via Thiol/Sulfonic Acid Pairing. *Journal of the American Chemical Society* 129 (2007):13691.
- [35] D. Margolese, J.A. Melero, S.C. Christiansen, B.F. Chmelka, and G.D. Stucky. Direct Syntheses of Ordered SBA-15 Mesoporous Silica Containing Sulfonic Acid Groups. *Chemistry of Materials* 12 (2000):2448–2459.
- [36] M. Toda, A. Takagaki, M. Okamura, J.N. Kondo, S. Hayashi, K. Domen, and M. Hara. Green Chemistry: Biodiesel made with Sugar Catalysts. *Nature* 438 (2005):178.
- [37] R.K. Zeidan, V. Dufaud, and M.E. Davis. Enhanced Cooperative, Catalytic Behavior of Organic Functional Groups by Immobilization. *Journal of Catalysis* 239 (2006):299–306.
- [38] R.K. Zeidan, S.J. Hwang, and M.E. Davis. Multifunctional Heterogeneous Catalysts: SBA-15 Containing Primary Amines and Sulfonic Acids. *Angewandte Chemie International Edition* 45 (2006):6332.
- [39] R.K. Zeidan and M.E. Davis. The Effect of Acid-Base Pairing on Catalysis: An Efficient Acid-Base Functionalized Catalyst for Aldol Condensation. *Journal of Catalysis* 247 (2007):379–382.
- [40] R. Zhang, W. Ding, B. Tu, and D. Zhao. Mesoporous Silica: An Efficient Nanoreactor for Liquid-Liquid Biphasic Reactions. *Chemistry of Materials* 19 (2007):4379–4381.
- [41] D.Y. Zhao, J.L. Feng, Q.S. Huo, N. Melosh, G.H. Fredrickson, B.F. Chmelka, and G.D. Stucky. Triblock Copolymer Syntheses of Mesoporous Silica with Periodic 50 to 300 Angstrom Pores. *Science* 279 (1998):548–552.
- [42] X.S. Zhao and G.Q. Lu. Modification of MCM-41 by Surface Silylation with Trimethylchlorosilane and Adsorption Study. *Journal of Physical Chemistry* 102 (1998):1556–1561.
- [43] V. Dufaud and M.E. Davis. Design of Heterogeneous Catalysts via Multiple Active Site Positioning in Organic-Inorganic Hybrid Materials. *Journal of the American Chemical Society* 125 (2003):9403–9413.

- [44] J.D. Bass, A. Solovyov, A.J. Pascall, and A. Katz. Acid-Base Bifunctional and Dielectric Outer-Sphere Effects in Heterogeneous Catalysis: A Comparative Investigation of Model Primary Amine Catalysts. *Journal of the American Chemical Society* 128 (2006):3737.
- [45] J.D. Bass, S.L. Anderson, and A. Katz. The Effect of Outer-Sphere Acidity on Chemical Reactivity in a Synthetic Heterogeneous Base Catalyst. *Angewandte Chemie International Edition* 42 (2003):5219–5222.
- [46] J.D. Bass and A. Katz. Bifunctional Surface Imprinting of Silica: Thermolytic Synthesis and Characterization of Discrete Thiol-Amine Functional Group Pairs. *Chemistry of Materials* 18 (2006):1611–1620.
- [47] I.K. Mbaraka, K.J. McGuire, and B.H. Shanks. Why are Proteins Charged? Networks of Charge-Charge Interactions in Proteins Measured by Charge Ladders and Capillary Electrophoresis. *Industrial & Engineering Chemistry Research* 45 (2006):3022.
- [48] I.K. Mbaraka, D.R. Radu, V.S.Y. Lin, and B.H. Shanks. Mesoporous Silicas for the Esterification of Fatty Acids. *Journal of Catalysis* 219 (2003): 329–336.
- [49] I.K. Mbaraka and B.H. Shanks. Acid Strength Variation due to Spatial Location of Organosulfonic Acid Groups on Mesoporous Silicas. *Journal of Catalysis* 244 (2006):78–85.
- [50] I.K. Mbaraka and B.H. Shanks. Conversion of Oils and Fats using Advanced Mesoporous Heterogeneous Catalysts. *Journal of the American Oil Chemists' Society* 83 (2006):79.
- [51] I.K. Mbaraka and B.H. Shanks. Design of Multifunctionalized Mesoporous Silicas for Esterification of Fatty Acids. *Journal of Catalysis* 229 (2005):365–373.
- [52] J.M. Notestein and A. Katz. Enhancing Heterogeneous Catalysis through Cooperative Hybrid Organic-Inorganic Interfaces. *Chemistry - A European Journal* 12 (2006):3954–3965.
- [53] D.L. Klass. *Biomass for Renewable Energy, Fuels, and Chemicals*. San Diego, CA: Academic Press, 1998.
- [54] C.J. Barrett, J.N. Chheda, G.W. Huber, and J.A. Dumesic. Single-Reactor Process for Sequential Aldol-Condensation and Hydrogenation of Biomass-Derived Compounds in Water. *Applied Catalysis B: Environmental* 66 (2006):111–118.

- [55] J.I. DiCosimo, G. Torres, and C.R. Apesteguia. One-Step MIBK Synthesis: A New Process from 2-Propanol. *Journal of Catalysis* 208 (2002): 114–123.
- [56] G.W. Huber, R.D. Cortright, and J.A. Dumesic. Renewable Alkanes by Aqueous-Phase Reforming of Biomass-Derived Oxygenates. *Angewandte Chemie International Edition* 43 (2004):1549–1551.
- [57] A.A. Nikolopoulos, B.W.L. Jang, and J.J. Spivey. Acetone Condensation and Selective Hydrogenation to MIBK on Pd and Pt Hydrotalcite-Derived Mg-Al Mixed Oxide Catalysts. *Applied Catalysis A: General* 296 (2005): 128.
- [58] D.A. Simonetti, J. Rass-Hansen, E.L. Kunkes, R.R. Soares, and J.A. Dumesic. Coupling of Glycerol Processing with Fischer-Tropsch Synthesis for Production of Liquid Fuels. *Green Chemistry* 9 (2007):1073–1083.
- [59] R.R. Soares, D.A. Simonetti, and J.A. Dumesic. Glycerol as a Source for Fuels and Chemicals by Low-Temperature Catalytic Processing. *Angewandte Chemie International Edition* 45 (2006):3982.
- [60] T. A. Werpy, J. G. Frye, A. H. Zacher, and D. J. Miller. 6841085 B2. 2005.
- [61] C.H.C. Zhou, J.N. Beltramini, Y.X. Fan, and G.Q.M. Lu. Chemoselective Catalytic Conversion of Glycerol as a Biorenewable Source to Valuable Commodity Chemicals. *Chemical Society Reviews* 37 (2008):527–549.
- [62] D.G. Lahr and B.H. Shanks. Effect of Sulfur and Temperature on Ruthenium-Catalyzed Glycerol Hydrogenolysis to Glycols. *Journal of Catalysis* 232 (2005):386.
- [63] D.G. Lahr and B.H. Shanks. Kinetic Analysis of the Hydrogenolysis of Lower Polyhydric Alcohols: Glycerol to Glycols. *Industrial & Engineering Chemistry Research* 42 (2003):5467.
- [64] E.P. Maris and R.J. Davis. Hydrogenolysis of Glycerol over Carbon-Supported Ru and Pt Catalysts. *Journal of Catalysis* 249 (2007):328–337.
- [65] E.P. Maris, W.C. Ketchie, M. Murayama, and R.J. Davis. Glycerol Hydrogenolysis on Carbon-Supported PtRu and AuRu Bimetallic Catalysts. *Journal of Catalysis* 251 (2007):281–294.
- [66] C. Montassier, J.C. Menezes, L.C. Hoang, C. Renaud, and J. Barbier. Aqueous Polyol Conversions on Ruthenium and on Sulfur-Modified Ruthenium. *Journal of Molecular Catalysis* 70 (1991):99.

- [67] C. Montassier, J.C. Menezo, J. Moukolo, J. Naja, L.C. Hoang, J. Barbier, and J.P. Boitiaux. Polyol Conversions into Furanic Derivatives on Bimetallic Catalysts: Cu-Ru, Cu-Pt and Ru-Cu. *Journal of Molecular Catalysis* 70 (1991):65.
- [68] C. Montassier, J.C. Menezo, J. Naja, P. Granger, J. Barbier, P. Sarrazin, and B. Didillon. Polyol Conversion into Furanic Derivatives on Bimetallic Catalysts; Nature of the Catalytic Sites. *Journal of Molecular Catalysis* 91 (1994):119–128.
- [69] K. Wang, M.C. Hawley, and T.D. Furney. Mechanism Study of Sugar and Sugar Alcohol Hydrogenolysis Using 1,3-Diol Model Compounds. *Industrial & Engineering Chemistry Research* 34 (1995):3766.
- [70] Z. Zhang, Y.-W. Dong, and G.-W. Wang. Efficient and Clean Aldol Condensation Catalyzed by Sodium Carbonate in Water. *Chemistry Letters* 32 (2003):966.
- [71] M. Besson and P. Gallezot. Selective Oxidation of Alcohols and Aldehydes on Metal Catalysts. *Catalysis Today* 57 (2000):127–141.
- [72] P. Gallezot. Selective Oxidation with Air on Metal Catalysts. *Catalysis Today* 37 (1997):405–418.
- [73] J.H.J. Kluytmans, A.P. Markusse, B.F.M. Kuster, G.B. Marin, and J.C. Schouten. Engineering Aspects of the Aqueous Noble Metal Catalysed Alcohol Oxidation. *Catalysis Today* 57 (2000):143–155.
- [74] T. Mallat and A. Baiker. Oxidation of Alcohols with Molecular Oxygen on Platinum Metal Catalysts in Aqueous Solutions. *Catalysis Today* 19 (1994):247–284.
- [75] D.K. Sohounloue, C. Montassier, and J. Barbier. Catalytic Hydrogenolysis of Sorbitol. *Reaction Kinetics and Catalysis Letters* 22 (1983):391–397.
- [76] W.C. Ketchie, M. Murayama, and R.J. Davis. Promotional effect of hydroxyl on the aqueous phase oxidation of carbon monoxide and glycerol over supported Au catalysts. *Topics in Catalysis* 44 (2007):307–317.
- [77] J.N. Chheda, R. Roman-Leshkov, and J.A. Dumesic. Production of 5-Hydroxymethylfurfural and Furfural by Dehydration of Biomass-Derived Mono- and Poly-Saccharides. *Green Chemistry* 9 (2007):342–350.
- [78] Y. Roman-Leshkov, C.J. Barrett, Z.Y. Liu, and J.A. Dumesic. Production of Dimethylfuran for Liquid Fuels from Biomass-Derived Carbohydrates. *Nature* 447 (2007):982–985.

- [79] Y. Roman-Leshkov, J.N. Chheda, and J.A. Dumesic. Phase Modifiers Promote Efficient Production of Hydroxymethylfurfural from Fructose. *Science* 312 (2006):1933–1937.
- [80] R.R. Davda, J.W. Shabaker, G.W. Huber, R.D. Cortright, and James A. Dumesic. A Review of Catalytic Issues and Process Conditions for Renewable Hydrogen and Alkanes by Aqueous-Phase Reforming of Oxygenated Hydrocarbons over Supported Metal Catalysts. *Applied Catalysis B: Environmental* 56 (2005):171–186.
- [81] R.R. Davda, J.W. Shabaker, G.W. Huber, R.D. Cortright, and James A. Dumesic. Aqueous-Phase Reforming of Ethylene Glycol on Silica-Supported Metal Catalysts. *Applied Catalysis B: Environmental* 43 (2003): 13–26.
- [82] J.H. Sinfelt and D.J.C. Yates. Catalytic Hydrogenolysis of Ethane over the Noble Metals of Group VIII. *Journal of Catalysis* 8 (1967):82.
- [83] D.C. Grenoble, M.M. Estadt, and D.F. Ollis. The Chemistry and Catalysis of the Water Gas Shift Reaction. 1. The Kinetics over Supported Metal Catalysts. *Journal of Catalysis* 67 (1981):90–102.
- [84] M.A. Vannice. The Catalytic Synthesis of Hydrocarbons from Hydrogen/Carbon Monoxide Mixtures over the Group VIII Metals V. The Catalytic Behavior of Silica-Supported Metals. *Journal of Catalysis* 50 (1977):228.
- [85] R. Alcalá, M. Mavrikakis, and James A. Dumesic. DFT Studies for Cleavage of C–C and C–O Bonds in Surface Species Derived from Ethanol on Pt(111). *Journal of Catalysis* 218 (2003):178–190.
- [86] P. Ferrin, D. Simonetti, S. Kandoi, E. Kunkes, J.A. Dumesic, J.K. Norskov, and M. Mavrikakis. Modeling Ethanol Decomposition on Transition Metals: A Combined Application of Scaling and Bronsted-Evans-Polanyi Relations. *Journal of the American Chemical Society* 131 (2009):5809.
- [87] S. Kandoi, J. Greeley, D. Simonetti, J. Shabaker, J.A. Dumesic, and M. Mavrikakis. Reaction Kinetics of Ethylene Glycol Reforming over Platinum in the Vapor versus Aqueous Phases. *Journal of Physical Chemistry C* 115 (2011):961.
- [88] R.M. West, D.J. Braden, and J.A. Dumesic. Dehydration of Butanol to Butene over Solid Acid Catalysts in High Water Environments. *Journal of Catalysis* 262 (2009):134–143.
- [89] J.M. Encinar, J.F. Gonzales, and A. Rodriguez-Reinares. Biodiesel from Used Frying Oil. Variables Affecting the Yields and Characteristics of the Biodiesel. *Industrial & Engineering Chemistry Research* 44 (2005): 5491–5499.

- [90] E. Christoffersen, P. Liu, A. Ruban, H.L. Skriver, and J.K. Norskov. Anode Materials for Low Temperature Fuel Cells. *Journal of Catalysis* 199 (2001):123–131.
- [91] E. Iglesia, S.C. Reyes, R.J. Madon, and S.L. Soled. Selectivity Control and Catalyst Design in the Fischer-Tropsch Synthesis: Sites, Pellets and Reactors. *Advances in Catalysis* 39 (1993):221–302.
- [92] E.L. Kunkes, D.A. Simonetti, J.A. Dumesic, W.D. Pyrz, L.E. Murillo, J.G. Chen, and D.J. Buttrey. The Role of Rhenium in the Conversion of Glycerol to Synthesis Gas over Carbon Supported Platinum-Rhenium Catalysts. *Journal of Catalysis* 260 (2008):164–177.
- [93] V. Pallassana and M. Neurock. Reaction Paths in the Hydrogenolysis of Acetic Acid to Ethanol over Pd(111), Re(0001), and PdRe Alloys. *Journal of Catalysis* 209 (2002):289–305.
- [94] M. T. Barlow, D. J. H. Smith, and D. G. Gordon. 82689 A2. 1983.
- [95] C.H. Bartholomew and R.J. Farrauto. *Fundamentals of Industrial Catalytic Processes*. Hoboken, NJ: Wiley, 2006.
- [96] D. J. Barratt and J. Lin. 5,925,152. 1999.
- [97] T. H. Takizawa, S. A. Shimizu, S. S. Yamada, S. H. Ikebe, and S. H. Hara. 5,925,152. 1994.
- [98] A.G. Gayubo, A.T. Aguayo, A. Atutxa, R. Aguado, and J. Bilbao. Transformation of Oxygenate Components of Biomass Pyrolysis Oil on a HZSM-5 Zeolite. I. Alcohols and Phenols. *Industrial & Engineering Chemistry Research* 43 (2004):2610–2618.
- [99] J. Lopez, J. Valente, J.-M. Sanchez, J.M. Clacens, and Francois Figueras. Hydrogen Transfer Reduction of 4-Tert-Butylcyclohexanone on Basic Solids. *Journal of Catalysis* 208 (2002):30–37.
- [100] S.G. Powell and A.T. Nielsen. Condensation of Butanal with 4-Heptanone and 3-Hexanone and Attempted Condensation of 2-Ethyl-2-hexenal with 4-Heptanone. *Journal of the American Chemical Society* 70 (1948):3627.
- [101] E.L. Kunkes, E.I. Gürbüz, and J.A. Dumesic. Vapour-Phase C–C Coupling Reactions of Biomass-Derived Oxygenates over Pd/CeZrOx Catalysts. *Journal of Catalysis* 206 (2009):236–249.
- [102] J.I. DiCosimo, V.K. Diez, M. Xu, E. Iglesia, and C.R. Apesteguia. Structure and Surface and Catalytic Properties of Mg-Al Basic Oxides. *Journal of Catalysis* 178 (1998):499–510.

- [103] V.K. Diez, J.I.D. Cosimo, and C.R. Apesteguia. Study of the Citral/Acetone Reaction on Mg_yAlO_x Oxides: Effect of the Chemical Composition on Catalyst Activity, Selectivity and Stability. *Applied Catalysis A: General* 345 (2008):143–151.
- [104] E.I. Gürbüz, E.L. Kunkes, and J.A. Dumesic. Integration of C–C Coupling Reactions of Biomass-Derived Oxygenates to Fuel-Grade Compounds. *Applied Catalysis B: Environmental* 94 (2010):134–141.
- [105] J.J. Bozell, L. Moens, D.C. Elliott, Y. Wang, G.G. Neuenschwander, S.W. Fitzpatrick, R.J. Bilski, and J.L. Jarnefeld. Production of Levulinic Acid and Use as a Platform Chemical for Derived Products. *Resources, Conservation and Recycling* 28 (2000):227–239.
- [106] S. W. Fitzpatrick. 4897497. 1990.
- [107] S. W. Fitzpatrick. 5608105. 1997.
- [108] J.C. Serrano-Ruiz, D.J. Braden, R.M. West, and J.A. Dumesic. Conversion of Cellulose to Hydrocarbon Fuels by Progressive Removal of Oxygen. *Applied Catalysis B: Environmental* 100 (2010):184–189.
- [109] M. Mascal and E.B. Nikitin. High-Yield Conversion of Plant Biomass into the Key Value-Added Feedstocks 5-(Hydroxymethyl)Furfural, Levulinic Acid, and Levulinic Esters via 5-(Chloromethyl)Furfural. *Green Chemistry* 12 (2010):370–373.
- [110] P. Wang, S. Zhan, and H. Yu. Production of Levulinic Acid from Cellulose Catalyzed by Environmental-Friendly Catalysts. *Advanced Materials Research* 96 (2010):183.
- [111] F. Tao, H. Song, and L. Chou. Catalytic Conversion of Cellulose to Chemicals in Ionic Liquid. *Carbohydrate Research* 346 (2011):58–63.
- [112] J. Horvat, B. Klaić, B. Metelko, and V. Sunjic. Mechanism of Levulinic Acid Formation. *Tetrahedron Letters* 2 (1985):2111–2114.
- [113] J.P. Lange, R. Price, P.M. Ayoub, J. Louis, L. Petrus, L. Clarke, and H. Gosselink. Valeric Biofuels: A Platform of Cellulosic Transportation Fuels. *Angewandte Chemie International Edition* 49 (2010):4479–83.
- [114] J.C. Serrano-Ruiz, D. Wang, and J.A. Dumesic. Catalytic Upgrading of Levulinic Acid to 5-Nonanone. *Green Chemistry* 12 (2010):574–577.
- [115] H. Heeres, R. Handana, D. Chunai, C.B. Rasrendra, B. Girisuta, and H.J. Heeres. Combined Dehydration/(Transfer)-Hydrogenation of C6-Sugars (D-Glucose and D-Fructose) to γ -Valerolactone using Ruthenium Catalysts. *Green Chemistry* 11 (2009):1247–1255.

- [116] L.E. Manzer. Catalytic Synthesis of α -Methylene- γ -Valerolactone: A Biomass-Derived Acrylic Monomer. *Applied Catalysis A: General* 272 (2004): 249–256.
- [117] J.P. Lange, J.Z. Vestering, and R.J. Haan. Towards “Bio-Based” Nylon: Conversion of γ -Valerolactone to Methyl Pentenoate under Catalytic Distillation Conditions. *Chemical Communications* 33 (2007):3488–3490.
- [118] I.T. Horvath, H. Mehdi, V. Fabos, L. Boda, and L.T. Mika. γ -Valerolactone - A Sustainable Liquid for Energy and Carbon-Based Chemicals. *Green Chemistry* 10 (2008):238–242.
- [119] D.M. Alonso, J.Q. Bond, J.C. Serrano-Ruiz, and J.A. Dumesic. Production of Liquid Hydrocarbon Transportation Fuels by Oligomerization of Biomass-Derived C(9) Alkenes. *Green Chemistry* 12 (2010):992–999.
- [120] J.Q. Bond, D.M. Alonso, R.M. West, and J.A. Dumesic. γ -Valerolactone Ring-Opening and Decarboxylation over $\text{SiO}_2/\text{Al}_2\text{O}_3$ in the Presence of Water. *Langmuir* 26 (2010):16291–16298.
- [121] J.Q. Bond, D. Wang, D.M. Alonso, and J.A. Dumesic. Interconversion between γ -Valerolactone and Pentenoic Acid Combined with Decarboxylation to form Butene over Silica/Alumina. *Journal of Catalysis* 281 (2011): 290–299.

Chapter 11

Design of Heterogeneous Catalysts for the Conversion of Biorenewable Feedstocks

Brent H. Shanks

11.1 Introduction

Designing heterogeneous catalysts for the conversion of biorenewable feedstocks, e.g., carbohydrates, lipids, and lignins, creates new challenges and opportunities for catalyst technology. The development of the science and technology of heterogeneous catalysis has been performed largely in concert with the development of the science and technology associated with the production of fuels and petrochemicals from crude oil and natural gas with the one notable exception being the treatment of the gaseous effluent from combustion processes. In general, the crude oil and natural gas-based feedstocks used for fuel and petrochemical production are not particularly reactive, so they typically are “activated.” The most common means of activation is through cracking-type reactions. This cracking is performed at elevated temperatures and leads to shorter chain molecules and compounds that contain a small fraction of unsaturated C–C bonds, which can be exploited for subsequent catalytic transformations. In contrast, biorenewable feedstocks already contain quite a number of functional groups that can be used for chemical transformations, which necessitates a new paradigm of how to design heterogeneous catalysts that can do selective chemistry in the presence of multiple reactive functional groups within a reactant molecule.

The fine and specialty chemical market has been confronted with the challenge of selectively converting substrates containing multiple reactive groups, which has commonly been addressed through the use of homogeneous catalysts or biocatalysts. Given the high value of fine and specialty chemicals, these types of catalyst systems can be economically deployed. However, the cost, temperature limitations, and separation issues that can be created by using homogeneous catalysts and biocatalysts will undoubtedly restrict their use in biorenewable feedstock conversions when the target products are lower-valued products such as fuel and industrial chemicals.

While the reactive moiety generated in cracking hydrocarbons for use in subsequent reactions is an unsaturated C–C bond, the multiple reactive functional groups within biorenewable feedstocks usually involve oxygen. Therefore, chemical transformations of biorenewable feedstocks will need to be performed in the presence of hydroxyl, carbonyl, carboxylic acid, ester, and/or ether groups. One outcome from this difference is that well established heterogeneous catalyst technology developed for hydrocarbon feedstocks, which are efficient for selective hydrogenation, selective oxidation, isomerization, reforming, etc., has not been designed for the dehydration, decarboxylation, decarbonylation, hydrogenolysis, esterification, ketonization, etc., reactions that are needed for converting biorenewable feedstocks to desirable products.

A second challenge introduced due to the presence of multiple functional groups in biomass-derived compounds is the poor volatility of the compounds at relevant reaction temperatures. This property commonly leads to the requirement of condensed phase reaction systems, which is in marked contrast to the primarily gas-phase reaction systems used for hydrocarbon processing. The resulting liquid-solid interfaces place new demands on catalytic materials relative to catalytic properties, catalyst stability and transport properties, which are further exacerbated when the condensed phase solvent is water. Due to their high oxygen content, biorenewable feedstocks are effectively hydrogen deficient relative to hydrocarbons, so three-phase reaction systems consisting of a solid catalyst, liquid solvent/reactant mixture and hydrogen gas will commonly need to be employed to generate products that replace those from hydrocarbons.

As discussed in previous chapters, biorenewable feedstocks can take many different forms, so it is important to define the range of molecules to be discussed in the current chapter. The primary focus of the heterogeneous catalyst design issues to be considered will be carbohydrates and their derivatives as these represent the most significant departure in chemistry from hydrocarbon feedstocks. There will be limited discussion of triglyceride and fatty acid reactions as examples for demonstrating some of the concepts. Increasingly, lignin and its aromatic building blocks are receiving attention, but they will not be discussed explicitly in this chapter.

Carbohydrates exist in nature primarily as polymeric species, so these polymers must be sufficiently deconstructed to create soluble compounds if heterogeneous catalysts are used for further transformations. The deconstruction of carbohydrates can be loosely categorized by the temperature in which it is performed (see Figure 11.1). Under high temperature conditions (~ 800 °C), carbohydrates can be gasified to produce CO and H₂ also known as syngas. The catalytic chemistry associated with converting syngas to fuels and chemicals has received significant attention over quite a number of years. Neglecting tar compounds, trace

contaminants and the CO:H₂ ratio (admittedly, these are important properties that in practice cannot be ignored), syngas is a carbon-based feedstock agnostic, so obtaining it from carbohydrate gasification does not introduce new syngas chemistry. At intermediate temperatures (350–550 °C), solid carbohydrates can be converted to a liquefied form. High-pressure liquefaction can be accomplished at about 350 °C and pyrolysis, either fast thermal or catalytic, typically employs temperatures ranging from 450–550 °C. These intermediate temperature processes when using established technology cause non-selective deconstruction of carbohydrate polymers leading to a liquid product, known as bio-oil, that is composed of numerous oxygenated chemical species. Given the compositional complexity of bio-oil, attention has largely been focused on upgrading it to fuels rather than for converting and purifying it to specific chemical products. Selective deconstruction of carbohydrates can be achieved at 35–170 °C by hydrolyzing the glycosidic bond between glucosyl rings. This approach, which can utilize enzymes, ionic liquids, or acids, results in the liberation of predominantly monomeric carbohydrates if the proper reaction conditions are imposed. The sugars released, glucose, xylose, arabinose, and mannose, can in principle be converted to fuels or chemicals. The primary focus of the discussion in the current chapter will be on the catalyst properties that need to be considered in the conversion of the monomeric sugars from hydrolysis or the oxygenated species in bio-oil into fuels and chemicals.

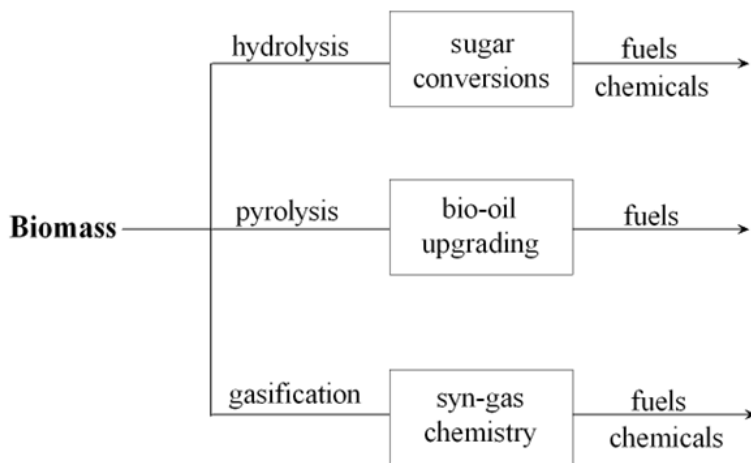


Figure 11.1: Biomass deconstruction and upgrading pathways

The conversion of carbohydrate-derived species in the condensed phase using heterogeneous catalysts introduces a broad array of interesting questions ranging from those concerning fundamental reaction mechanisms to reaction systems. How do molecules with a high level of oxygen functionality adsorb on metal/metal oxide surfaces? Can specific C–C or C–O bonds be targeted for conversion when multiple reactive functional groups are present? How will water play a role in these condensed phase reactions? How should catalytic materials be modified for use in converting carbohydrates and their derivatives? Can solid catalysts be constructed that can withstand hydrothermal conditions? Can heterogeneous catalyst systems be designed to deal with biorenewable feedstocks impurities? Can the catalytic reaction systems be coupled with separations to improve efficiencies? Rather than categorizing by specific reaction classes, this chapter will discuss these questions. Examples of some studies that have begun to examine these questions will be given as illustrations.

11.2 Adsorption of Carbohydrates and Their Derivatives on Solid Surfaces

Through a combination of experimental and theoretical work, the adsorption of hydrocarbons on catalytic surfaces has received sufficiently extensive attention such that the interaction between unsaturated C–C bonds and metal or metal oxide surfaces is reasonably understood. The interaction of other functional groups such as hydroxyls with catalytic surfaces has also been examined. However, carbohydrates and their derivatives contain multiple functional groups and the adsorption behavior of these types of molecules has only received a limited amount of attention. While only considering the adsorption interaction of a single molecule possessing multiple functional groups with a metal or metal oxide surface is challenging to characterize, the added complexity of probing this adsorption behavior under reaction conditions is even more daunting. Excellent *in situ* characterization techniques have been developed that can probe adsorbate-surface interactions under gas-phase conditions, but effective *in situ* characterization approaches for characterizing condensed phase reaction systems are only beginning to be developed.

Rather than attempting an exhaustive treatment of all types of functional groups that can arise in carbohydrates and species derived from carbohydrates, the interaction between hydroxyl groups and surfaces will be discussed for the case when multiple hydroxyl groups are present in the adsorbing molecule. A limiting case of this situation is the adsorption of 1,2-propylene glycol and glycerol. Peereboom *et al.* [1] examined the adsorption of these species on Ru at ambient temperature due to its implication on the hydrogenolysis of glycerol to

produce propylene glycol. Over extended adsorption times, they found that the total amount of glycerol or propylene glycol adsorbed on a clean Ru surface was roughly equivalent. The competitive adsorption of the two species was also evaluated. First, the clean Ru surface was exposed to an aqueous solution of one of the species and then the second was added at a later time point (Figure 11.2). For the data in Figure 11.2A), Ru was exposed to a propylene glycol aqueous solution for about 17 hours and then glycerol of equal concentration was introduced. An uptake of glycerol was immediately observed. In contrast, the initial addition of a glycerol aqueous solution followed by propylene glycol introduction at about 17 hours, as shown in Figure 11.2B), was found to inhibit the adsorption of propylene glycol. This apparent stronger adsorption affinity for glycerol was consistent with previous literature. Based on fitting kinetic parameters to reaction data for glycerol hydrogenolysis using a Ru supported on a carbon catalyst, the glycerol adsorption constant was found to be five times higher than the constant for propylene glycol [2]. While purely speculative, the significant difference in adsorption behavior would seem to be related to either the presence of three hydroxyl groups in glycerol or the alkyl group at the end of propylene glycol.

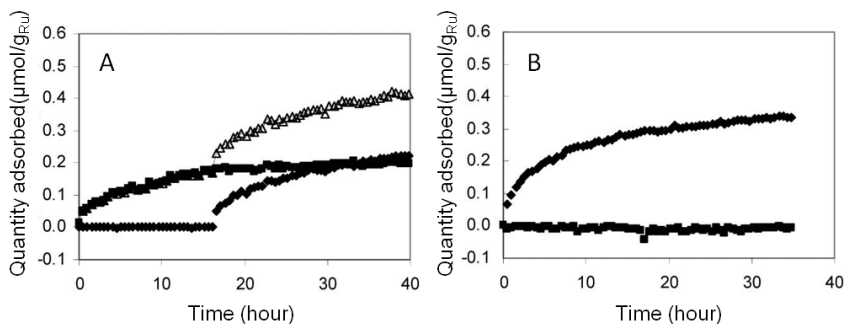


Figure 11.2: Polyol adsorption (propylene glycol - squares; glycerol - diamonds; total moles adsorbed - triangles) on Ru at ambient temperature: (A) initial propylene glycol adsorption followed by glycerol introduction at 15 hours, (B) initial glycerol adsorption followed by propylene glycol introduction at 15 hours [1]

As demonstrated by the above example, the adsorption behavior for relatively simple polyhydroxylated species is not well understood. When considering the adsorption behavior of carbohydrates, additional complexity is introduced by the fact that carbohydrates can exist in different conformations. In the

case of D-glucose, it exists in aqueous solution at ambient temperature almost exclusively in the glucopyranose form in which the five carbons and an oxygen form a six-membered ring with the oxygen linkage between the C1 and C5 carbons. However, when D-glucose is allowed to equilibrate in an aqueous solution, α - and β -glucopyranose isomers exist in the ratio of 36:64, where the isomers correspond to whether the hydroxyl group on the C1 carbon is above or below the plane of the ring. In contrast, fructose in an aqueous solution exists at ambient temperature in four cyclic and one acyclic isomer form, with six-membered ring fructopyranose (70%) and five-membered ring fructofuranose (22%) being the dominant forms. Although it might be expected that the interaction between a specific carbohydrate, such as D-glucose, and a catalytic surface would lead to a single type of adsorbed species, which presumably would be the most favorable energetically, no systematic study has been performed to validate this presumption.

Given the stereogenic centers present in carbohydrates, a family of carbohydrate stereoisomers exist that have the same molecular formula. This family represents molecules with different configurations. Since carbohydrates with different configurations do not spontaneously isomerize to a different configuration, the different stereoisomers can be used to gain some information about how carbohydrates adsorb.

One such example is a study that examined the adsorption behavior of a range of sugars in aqueous solution onto hydrous zirconium oxide and iron oxide at ambient temperature [3]. In an experimental approach that employed Langmuir monolayer adsorption, aldohexoses, aldopentoses, and ketohexoses as well as several of their derivatives were evaluated (shown in Figure 11.3 are the sugars used in the study). The Langmuir equilibrium constant as well as the maximum amount of a sugar required to form a monolayer on the solid surface were found to be strongly dependent on the stereoisomer used. D-ribose had a Langmuir equilibrium constant that was five times that for D-glucose and a maximum amount of molecules in the resulting monolayer that was 50% higher. A general trend was found in which the stereochemistry of the three neighboring hydroxyl groups on either the C2, C3, C4 carbon atoms for aldohexoses or the hydroxyl groups on the C2, C3, C4 carbon atoms in ketohexoses strongly correlated with the resulting adsorption behavior. Interestingly, the differences in adsorption behavior between the sugars examined was significantly more pronounced when the surface was hydrous zirconium oxide rather than hydrous iron oxide. The surface-specific response was speculated to be due to the difference between the ionic radii of the metal ions in the two hydrous metal oxides.

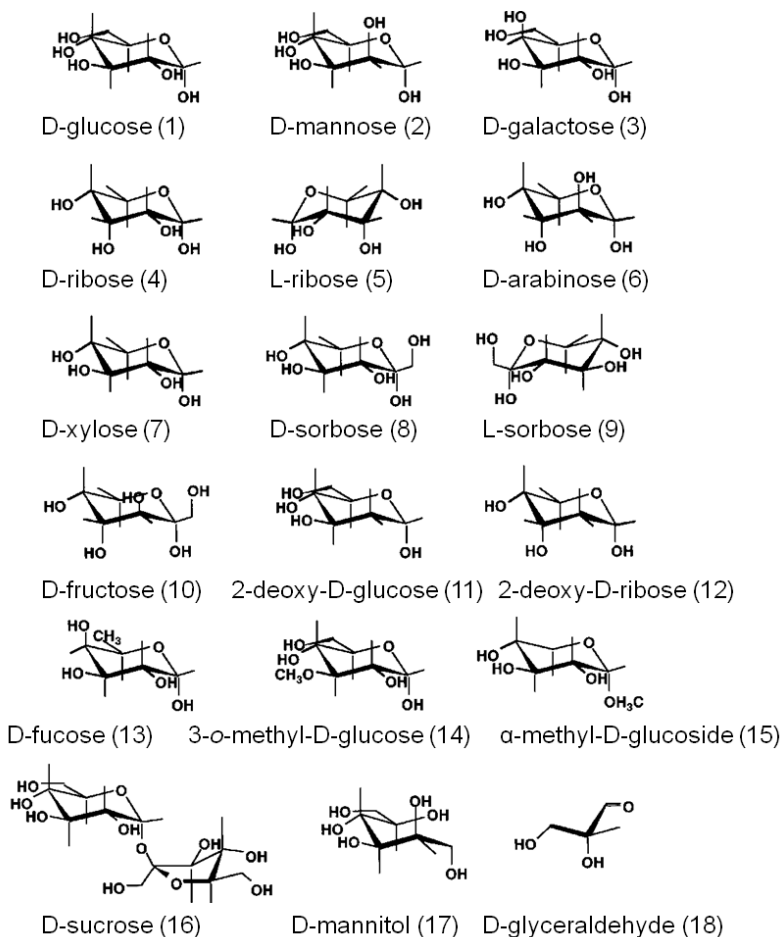


Figure 11.3: Carbohydrate species used in a Langmuir adsorption study over hydrous zirconium oxide and iron oxide [3]

As the preferred conformation of an adsorbed carbohydrate could be a function of temperature, ambient temperature adsorption studies of carbohydrates might not directly correlate with their adsorbed conformation at the elevated temperatures used in reactions. Unfortunately, no reliable methods are currently available to examine carbohydrate adsorption from an aqueous solution at elevated

temperatures. An indirect method to examine adsorption behavior is through reactivity studies.

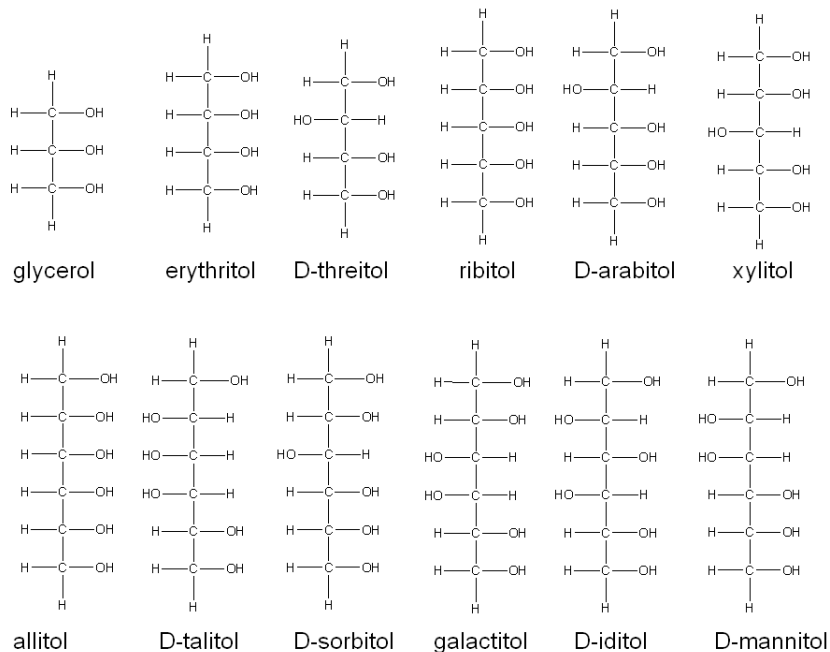


Figure 11.4: Fischer projections of the alditols from C3 to C6

An example of this approach was a study of the initial reactivity of alditol stereoisomers, corresponding to the hydrogenated forms of sugars, under hydrogenolysis conditions [4]. In this study, the relative initial rate of disappearance of alditols in an aqueous system was compared over a Ru on a carbon catalyst. Shown in Figure 11.4 are the Fischer Projections of the C3–C6 alditols. As several of the C6 alditols have limited solubility in water, Table 11.1 gives the initial hydrogenolysis rates for those with sufficient solubility grouped according to their carbon number. As can be seen from this grouping, the initial reaction rates did not correlate with the alditol carbon number as stereoisomers had different reactivities. As demonstrated in the carbohydrate adsorption study discussed above, the stereoisomers for a given carbon number likely have somewhat different ad-

sorption characteristics, which would be expected to be manifest in their resulting reactivity.

Compound	Reaction Rate (205 °C, mmol/min)	Reaction Rate (240 °C, mmol/min)
Glycerol	3.9	10.3
Erythritol	3.4	10.1
Threitol	2.0	5.0
Ribitol	3.3	11.0
Arabitol	3.0	9.5
Xylitol	2.5	6.4
Mannitol	2.8	7.8
Sorbitol	2.5	6.7
Galactitol	N/A	3.5

Table 11.1: Initial reaction rates for alditols over a Ru/C catalyst (0.5 M alditol concentration, 100 bar H₂, and pH adjusted to 11.5 using CaO)

One could ask whether the reactivity data could correlate better to configuration rather than carbon number. Consider the three pentitols stereoisomers as shown again in their Fischer Projections in Figure 11.5.

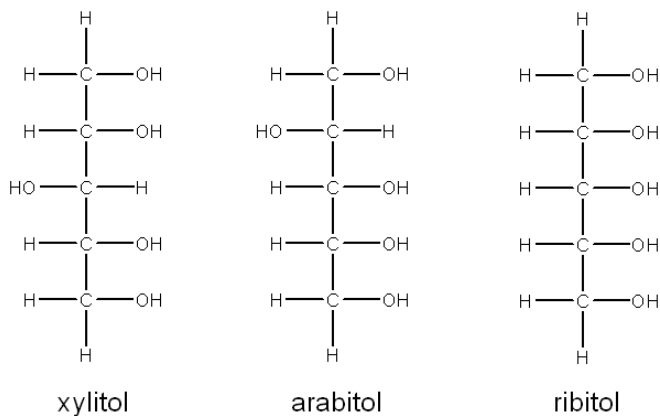


Figure 11.5: Fischer projections of the C₅ alditols, which provide a comparison of their different configurations

These molecules consist of three chiral carbons as the two terminal carbons can freely rotate. A simple classification would be to count the number of hydroxyl group inversions for the chiral carbons, corresponding to C2, C3 and C4. For ribitol, all of the hydroxyl groups reside on the same side, so it can be categorized as having zero inversions. Using the same categorization approach, xylitol possesses two inversions and arabitol has one. Shown in Table 11.2 are the initial reaction rate data now categorized by the number of inversions rather than carbon number (glycerol has no chiral carbon, so it cannot have an inversion). While not perfectly correlated, this categorization does a better job of lumping similar observed reaction rates than does carbon length.

Alditol	Reaction Rate (mmol/min)	Inversion	Alditol Length
Glycerol	10.3	0	3
Erythritol	10.2	0	4
Ribitol	11.0	0	5
Threitol	5.0	1	4
Arabitol	9.5	1	5
Mannitol	7.8	1	6
Xylitol	6.4	2	5
Sorbitol	6.7	2	6
Galactitol	3.5	2	6

Table 11.2: Groupings of initial alditol reaction rates relative to their configurations (Ru/C, 0.5 M polyol concentration, 100 bar H₂, and pH adjusted to 11.5 using CaO)

A second aspect that could play a role in the adsorption and reactivity of the alditols is the conformation of the molecules upon adsorption. C5 and C6 alditols can adopt either zig-zag or sickle conformation in solution. Shown in Figure 11.6 are xylitol and ribitol in these two conformations. As can be seen from the figure, xylitol in the zig-zag conformation has all of the hydroxyl groups on the chiral carbons pointing in the same direction, while in the sickle conformation, at most two hydroxyl groups on the chiral carbons are in the same direction. This situation is exactly reversed for ribitol. Under ambient temperatures and in aqueous solution, NMR analysis has shown that the zig-zag conformation dominates for alditols [5]. When the complexation of xylitol and ribitol with Ca(II) was examined at ambient temperature, xylitol was found to more readily complex than ribitol. This difference might be attributed to the hydroxyl group location for xylitol, which

point in the same direction in the zig-zag conformation leading to more potential interaction points between the molecule and the surface. If it is presumed that the reactivity of xylitol and ribitol is correlated with adsorption, then the higher reactivity of ribitol might suggest that the preferred adsorption conformation at the elevated temperatures used for hydrogenolysis is the sickle form as ribitol has all of the hydroxyls on the chiral carbons pointing in the same direction. Clearly, this postulate is highly speculative, but it points to the lack of understanding that currently exists with regard to the adsorption behavior of carbohydrates and their derivatives on solid surfaces under reaction conditions.

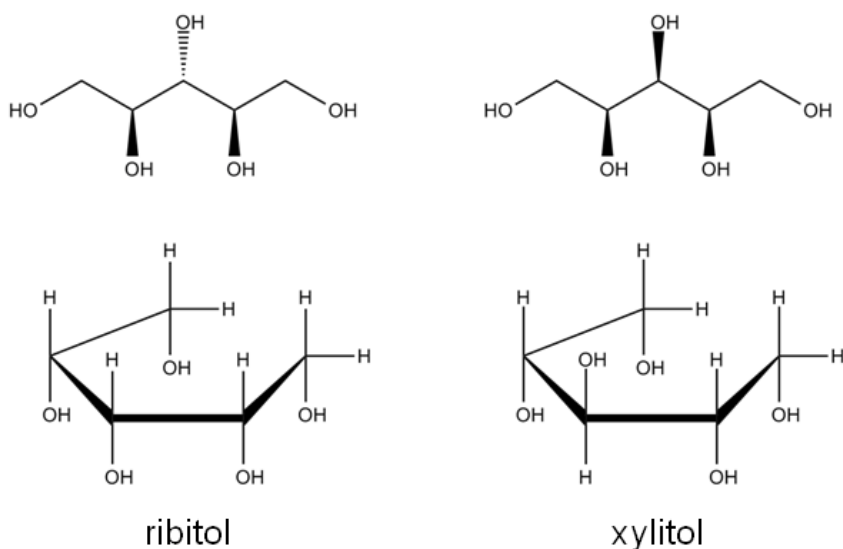


Figure 11.6: Possible conformations for ribitol and xylitol, which are zig-zag (top) and sickle (bottom)

11.3 Selective Bond Cleavage

For most targeted products from biomass, the biorenewable feedstocks will typically contain excess oxygen, so there is a desire to develop catalytic transformations that can selectively remove oxygen. Examples of reaction classes that have been examined for oxygen removal from biorenewable feedstocks are dehydration, decarbonylation/decarboxylation, condensation and ketonization. Not only are these reactions not the typical ones that have been the focus of catalyst

development for hydrocarbon processing, but they have the added complication in biorenewable feedstock conversion of needing to be achieved in the presence of multiple reactive groups.

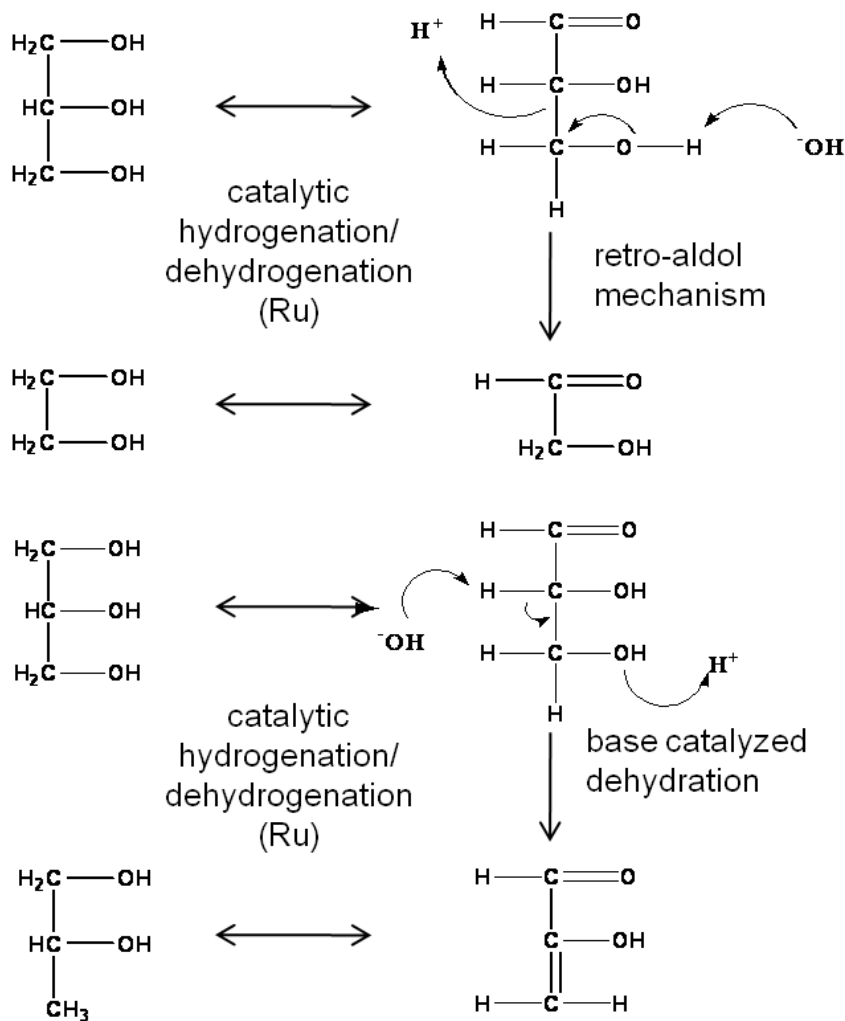


Figure 11.7: Mechanism that has been proposed for the hydrogenolysis of glycerol to ethylene glycol and propylene glycol

For example, when dehydrating a polyhydroxylated compound it could be a goal to not only control C–O bond cleavage without C–C bond cleavage, but to control which C–O bond is cleaved. A reaction demonstrating these challenges is the hydrogenolysis of alditols with sorbitol, xylitol, and glycerol having received particular attention. This reaction is thought to be initiated by dehydrogenation of the sugar alcohol to either an aldehyde or ketone, so a kinetic mechanism for the system must address the relative reactivity of the hydroxyl groups at the different carbon positions in the molecule as well as the adsorption behavior of the reactant. Hydrogenolysis of alditols provides a useful representative reaction system for the range of reaction considerations that can be encountered in the catalytic conversion of many carbohydrate-derived species, so the reaction can be used to examine the potential of using heterogeneous catalysts for the selective cleavage of C–C and C–O bonds at specific locations within a molecule.

The reaction sequence that has been postulated for the hydrogenolysis of alditols is shown in Figure 11.7, with glycerol as the reactant. The sequence is thought to be initiated by the dehydrogenation of a hydroxyl group to form either an aldehyde or ketone depending on the hydroxyl group affected [6–8]. This intermediate species can then undergo a C–O bond cleavage through a dehydration reaction, C–C bond cleavage through a retro-aldol reaction, or re-hydrogenation to the initial alditol. The catalyst system most extensively examined for this reaction is Ru on a carbon support, which is used in a highly basic solution. For the previously proposed reaction sequence, the metal function serves to catalyze the dehydrogenation/hydrogenation reactions and the hydroxyls from the basic solution to catalyze the dehydration/retro-aldol reactions. While this straightforward demarcation of catalytic functions for the reaction system is mechanistically attractive, more recent work on glycerol hydrogenolysis has shown that the metal function also plays a role in the cascade of reactions resulting in glycerol dehydration to propylene glycol [2, 9, 10]. Further complicating the hydrogenolysis reaction, studies with C5 alditols suggest that C–C bond cleavage can potentially occur through decarboxylation as well as through the retro-aldol reaction [4].

While the alditol hydrogenolysis reaction is quite complicated, the fact that the C4 and higher alditols can exist as different stereoisomers (Figure 11.4) can be exploited to gain more insight into the reaction mechanism. For the case of glycerol hydrogenolysis, whether the retro-aldol mechanism (Figure 11.8A) or the decarboxylation mechanism (Figure 11.8B) is the primary path for C–C bond scission cannot be easily resolved as either require formation of glyceraldehyde.

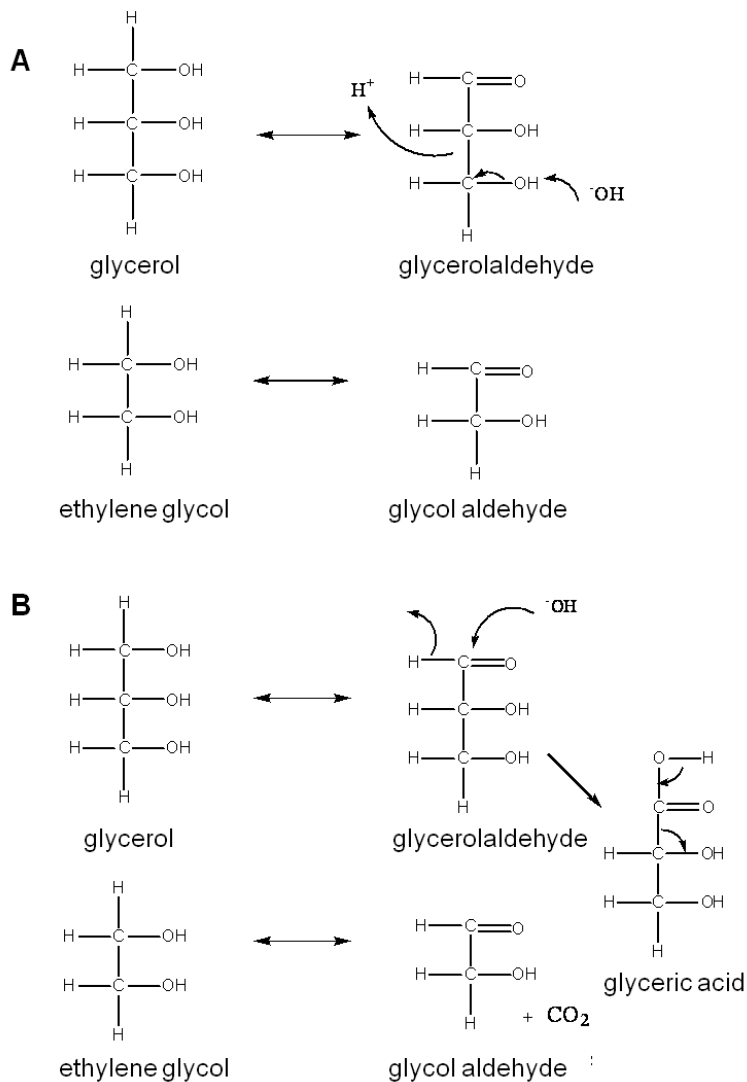


Figure 11.8: Possible C–C bond scission reactions in polyols: A) retro-aldol reaction, B) decarboxylation reaction

However, consider the case of C–C bond cleavage in xylitol hydrogenolysis where C4 alditols are obtained as products. If decarboxylation was the primary mechanism, the initial step would need to be dehydrogenation of a terminal hydroxyl group (C1 or C5) to yield an aldehyde intermediate. As can be seen from the Fisher Projection of xylitol, cleavage of the C–C bond between either the C1–C2 or C4–C5 would lead to only D-threitol as the product.

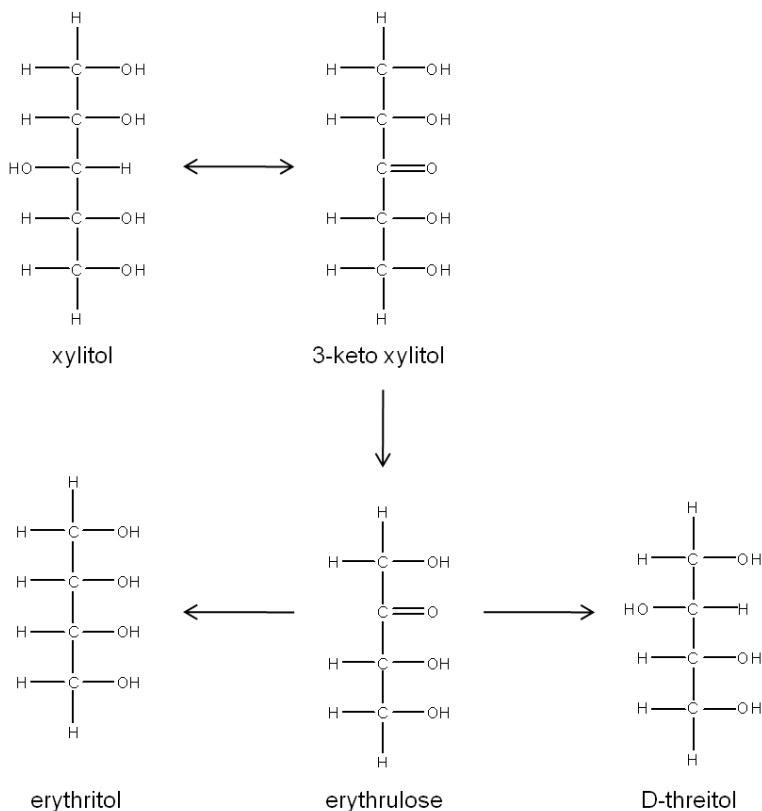


Figure 11.9: Possible C4 alditols that could result from xylitol when the retro-aldol reaction is initiated by dehydrogenation of the interior hydroxyl group

The only way in which a C4 alditol could be obtained from xylitol via the retro-aldol reaction would be if the hydroxyl group on the C3 had been dehydro-

generated, as dehydrogenation of the hydroxyls at the other carbon positions could only lead to the formation of C2 and C3 polyols. Therefore, the only possibility for C4 alditol formation from xylitol via the retro-aldol mechanism can be shown in Figure 11.9. The first step would be dehydrogenation of the hydroxyl on C3 to form 3-keto xylitol followed by C–C cleavage at C1–C2 or C4–C5, either of which would yield erythrulose. Since the subsequent hydrogenation of the keto group could occur with equal probability from above and below the keto plane, both C4 alditols would be equally likely to form. Therefore, C–C bond scission to C4 alditols via decarboxylation or retro-aldol from xylitol would necessarily yield different product distributions.

Extending from the xylitol example, the possible products resulting from C–C bond scission through hydrogenolysis of C4, C5, and C6 alditols can be mapped as a network of possible products if it is assumed that dehydrogenation of a hydroxyl group is the initiating step. This map is shown in Figure 11.10.

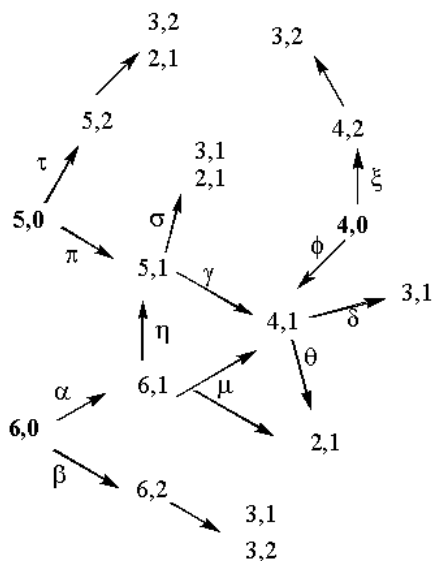


Figure 11.10: Possible reaction pathways occurring during C–C bond scission in the hydrogenolysis of alditols

To simplify the map visualization, only dehydrogenation of the hydroxyl groups located at the terminal carbons or the carbon one position in from the terminal carbons are shown. In the map, the first number represents the number

of carbon atoms in the molecule and the second number the position of the hydroxyl group that is dehydrogenated. For clarification, consider the case of a C5 alditol (5,0). This alditol can dehydrogenate at a terminal carbon to form an aldehyde (5,1), which upon decarboxylation would go to an aldehyde (4,1) or upon retro-aldol reaction to two aldehydes (3,1 and 2,1). Alternatively, the C5 alditol could have dehydrogenation of the hydroxyl group one carbon in from the terminal carbon (5,2), which could only undergo C–C scission via retro-aldol leading to an aldehyde (2,1) and a ketone (3,2). Under the reaction conditions used for hydrogenolysis, the aldehydes and ketones will readily hydrogenate due to the presence of hydrogen and Ru, so only polyhydric alcohols will be observed.

Temp/(S/Ru)	OAL = 6	OAL = 5	OAL = 4
205/0	0.44	0.46	0.52
205/1	0.20	0.15	0.25
240/0	0.44	0.37	0.59
240/1	0.21	0.07	0.32

Table 11.3: Calculated fraction of dehydrogenation taking place on the primary hydroxyl groups based on selectivity mapping of the hydrogenolysis reaction. OAL = Original Alditol Length

Initial conversion studies were performed using most of the C3–C6 alditols [4]. Both their initial rates, as discussed in the previous section, and their reaction products were measured. Importantly, no isomerization was observed from the initial reactant, e.g., when xylitol was used as the reactant no ribitol or arabitol was observed in the product. By combining all of the product distribution data using the mapping approach discussed in conjunction with Figure 11.10, it was possible to calculate whether the hydroxyl group on the terminal carbons were the most readily dehydrogenated under the assumption that only decarboxylation or retro-aldol could give C–C scission. Shown in Table 11.3 are the estimates for the fraction of dehydrogenation occurring at the terminal carbon for two different reaction temperatures (205/0 and 240/0) and three different alditol carbon numbers. As indicated by these results, there is not an equal probability for each of the hydroxyl groups to dehydrogenate as dehydrogenation of the hydroxyl groups on the terminal carbons was somewhat favored.

Several alditol hydrogenolysis studies with Ru on carbon have shown that the addition of sulfur to the reaction system significantly affects the resulting product distribution. For example, sulfur introduction into the glycerol hydrogenolysis reaction system caused the selectivity to propylene glycol to increase relative

to ethylene glycol, and its introduction into the xylitol reaction system suppressed the formation of C4 alditols [4, 6, 9]. To examine this effect, initial conversion studies were performed with the C3-C6 alditols in the presence of sulfur. Shown in Table 11.3 in the 205/1 and 240/1 rows are estimates for the fraction of the dehydrogenation occurring at the terminal carbons when sulfur was added at the level of one mole of sulfur per mole of Ru. These experiments and the analysis mirrored what was discussed in the previous paragraph with the exception of adding sulfur to the reaction system. The addition of sulfur diminished the activity of the catalyst, as reported previously [9], but it also had a large impact on which hydroxyl groups appeared to dehydrogenate most readily. As can be seen by comparison to the 205/0 and 240/0 data, the presence of sulfur appeared to depress dehydrogenation of the hydroxyl groups on the terminal carbons. While the reaction data are phenomenological rather than directly mechanistic, the results clearly demonstrate that the selectivity of bond cleavage can be altered in the hydrogenolysis of alditols with a heterogeneous catalyst.

Several companies have announced the development of commercial processes that are claimed to economically convert either glycerol or sorbitol to propylene glycol. Therefore, the potential exists to cleave selectively C–O and C–C bonds in the presence of multiple hydroxyl groups. However, there is still a need for significantly better understanding of how this cleavage can be achieved selectively and, as such, remains an important research challenge for biorenewable feedstocks.

11.4 Aqueous Phase Considerations

Carbohydrates and their derivatives typically have limited volatility, so their conversion will likely require reactor operation using a condensed phase. As the deconstruction of starch or cellulose to produce monosaccharides is performed in water, subsequent condensed phase processing will likely also involve the aqueous phase. Since heterogeneous catalyst technology has been developed primarily for gas-phase conversions, the determination of how the presence of condensed water at the catalyst/solution interface can influence the kinetics and mechanisms of the resulting reactions has received limited attention. These aqueous phase considerations have implications for both supported metal catalysts as well as solid acid catalysts.

As an example of how the presence of a metal/water interface can influence reaction systems, Neurock and co-workers have used *ab initio* molecular dynamics to examine several aqueous-phase, metal-catalyzed reaction systems including the dissociation of acetic acid over Pd [11], the hydrogenation of formaldehyde over Pd [12], and the oxidation of CO to CO₂ over Pt/Ru [13, 14]. Their simula-

tions considered the metal surface and adsorbates as well as an extended ensemble of water molecules. In these computational studies, the presence of the aqueous phase was found to change the thermodynamics and kinetics for many of the elementary reaction steps including adsorption, diffusion, desorption and surface reactions. Perhaps not surprisingly, the reaction steps that involved charge transfer were most strongly affected. One would expect that water would have a solvation effect thereby affecting the thermodynamics and kinetics of the reaction. However, they also found that the condensed phase could play an important role in the reaction mechanism through direct participation in the catalytic pathways.

One example from their work was the analysis of the possible hydrogenation pathways involved in the Pd-catalyzed hydrogenation of formaldehyde [12], which serves as a potential model for the hydrogenation of the aldehyde groups that could be required in the conversion of carbohydrate-derived species. The presence of the aqueous media was found to reduce the activation barrier for hydrogen addition at either the carbon or oxygen end of the molecule. Perhaps of more interest is that a new energetically favorable pathway enabled by the aqueous phase was found. The new pathway involved a surface hydrogen atom transferring an electron to the surface and then migrating into solution as a proton where the water phase network of local hydrogen bonds facilitated its movement to the active site. The proton then is available to hydrogenate the surface intermediate at the active site. In this new pathway, the metal surface both bonded the adsorbate to the surface and assisted in charge transfer. The charge transfer, which facilitated the electron release from an adsorbed hydrogen creating a proton in solution, was possible because the Pd surface had a work function that was high enough to accept an electron.

The potential for altering a reaction mechanism due to the presence of an aqueous phase was also demonstrated computationally for the dissociation of acetic acid over Pd(111) [11]. When acetic acid was dissociated over Pd in the gas phase, the most energetically favorable pathway was found to be homolytic dissociation with an activation barrier of 468 kJ/mol. Heterolytic dissociation with a computed activation barrier of 1483 kJ/mol did not appear to be possible. When the same reaction system was examined with a condensed aqueous phase the possibility of heterolytic dissociation into an acetate ion and proton was found to be not only energetically attractive with an activation barrier of only 37 kJ/mol, but also favored over homolytic dissociation.

Many reactions of interest in the conversion of biorenewable molecules involve acid catalysis, e.g., hydrolysis, esterification, dehydration, etc., in which a Brønsted acid site is the catalytic moiety. Brønsted acids in aqueous solutions are significantly impacted by solvation through modifying acid strength with the most extreme case being leveling of the acid strength, which occurs when the

Brønsted acid sites are completely deprotonated and the acid moiety in the reaction system becomes H_3O^+ . An additional consideration is that Lewis acid sites when placed in an aqueous medium can be converted to Brønsted acid sites.

An example of the effect of proton solvation on catalyst activity was nicely demonstrated in the case of carboxylic acid esterification with methanol [15]. The esterification reaction converts the carboxylic acid and methanol to a methyl ester and water. The condensed phase reaction system used was a starting solution of the carboxylic acid in excess methanol with a solid Brønsted acid catalyst. Studies were also performed in which the starting solution was doped with different low levels of water. It was found that the addition of even small amounts of water into the reacting solution dramatically decreased catalyst activity. This loss in activity was attributed to a decrease in acid strength due to the acidic protons being solvated by the water molecules.

For many reactions catalyzed with Brønsted acids, the activity of the catalyst will correlate with the strength of the acid site, so it is important to be able to measure reliably the $\text{p}K_{\text{a}}$ values for solid acid catalysts. While reactivity results can be used to indirectly examine acidic site strength, the danger of relying solely on reaction results for characterizing heterogeneous catalysts is that the intrinsic catalytic properties can be obscured due to convolution with mass transfer effects. A number of characterization techniques have been developed to measure independently the strength of acidic sites on solid materials including temperature programmed desorption (TPD), in situ FT-IR and 2-D solid-state NMR, which all primarily make use of adsorbed probe molecules such as carbon monoxide, ammonia, triethylphosphine oxide (TEPO) and pyridine. Unfortunately, these commonly used characterization techniques are based on the interactions of gas-phase probe molecules and cannot account for solvent effects such as proton solvation.

An example of the challenge associated with measuring acid strength for solid acid catalysts to be used in condensed phase reactions is the measurement of the acidic properties of organic acid functionalized materials. A number of studies have examined the acidic properties of propylsulfonic ($-\text{PrSO}_3\text{H}$), ethylphosphonic ($-\text{EtPO}_3\text{H}$), butylcarboxylic ($-\text{BuCOOH}$) and arenesulfonic ($-\text{ArSO}_3\text{H}$) functional groups covalently bonded to silica surfaces [16–20]. In a TPD study using pyridine as the probe molecule, the $-\text{PrSO}_3\text{H}$ and $-\text{ArSO}_3\text{H}$ groups were found to have similar acidic strengths with the $-\text{PrSO}_3\text{H}$ group shown to be a slightly stronger acid [21]. In contrast, a ^{31}P -MAS NMR study with TEPO as the probe molecule indicated that $-\text{ArSO}_3\text{H}$ was the stronger acidic moiety [20]. This discrepancy was also seen in other studies, where the acidic trends among the functional groups were dependent on the method employed and/or the probe molecule used. Additionally, the solvent used in the reaction system can affect the acidic strength of the catalytic sites. A study comparing the acid strength of

sulfonated polystyrene resin and sulfonated mesoporous silica in both aqueous and non-aqueous media [22] found molar enthalpies of neutralization suggesting that the sulfonated polystyrene material was more acidic than the sulfonic-acid functionalized silica material in water, but the result was found to be the opposite in a non-aqueous media.

A computational study was performed to compare how the acidic properties for organic acid functionalized silica were impacted by the presence of a single water molecule versus several water molecules [23]. This comparison began to examine how acidic strength can be influenced by the presence of a single *probe* molecule relative to an ensemble of molecules, which is in the direction of a condensed phase calculation. In this work, the interaction of the $-\text{PrSO}_3\text{H}$, $-\text{EtPO}_3\text{H}$, $-\text{BuCOOH}$, $-\text{ArSO}_3\text{H}$ functional groups with water was examined using the Effective Fragment Potential method with density functional theory (DFT). The simulations were performed for the cases in which the functional groups were bound to a silicon atom that was either capped with hydroxyl groups or linked to an oxygen-silicon structure. The optimized structures for each of the functional groups and silicon (capped using the two different models) and one water molecule is shown in Figure 11.11.

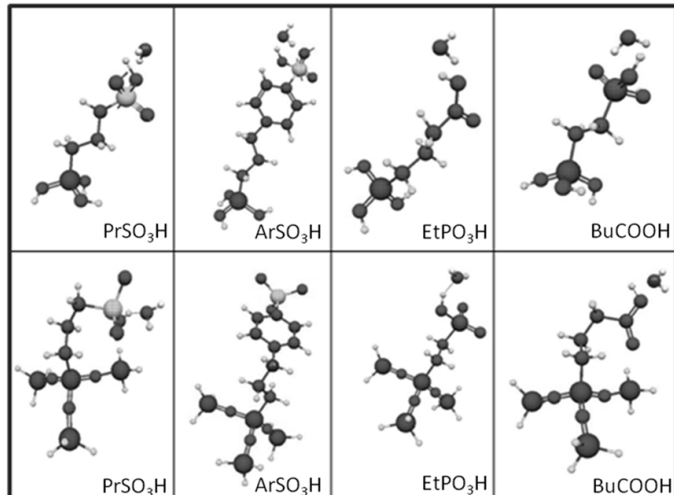


Figure 11.11: DFT optimized acid functional group structures with one water molecule; top row with silanol groups and bottom row without

The elongation of the O-H bond in the acidic moiety has been used in literature to predict pK_a values with greater elongation of this bond correlated with lower pK_a values [24]. Shown in the first row in Table 11.4 is the O-H bond distance for each of the tethered functional groups without water present. The second row gives the elongated bond length after a single water molecule was introduced into the computation. The elongated bond length was calculated in a ratio with the initial bond length to get the percent elongation for the O-H bond due to a single water molecule. As can be seen from the table, the computational results suggested that acidic strength of the functional groups followed the trend of $-\text{PrSO}_3\text{H} > -\text{ArSO}_3\text{H} > -\text{EtPO}_3\text{H} > -\text{BuCOOH}$.

	PrSO ₃ H w/ SiOH	PrSO ₃ H w/o SiOH	PhSO ₃ H w/ SiOH	PhSO ₃ H w/o SiOH
O-H bond distance (Å)	0.9761	0.9706	0.9700	0.9629
elongated O-H distance (Å)	1.0455	1.0384	1.0381	1.0299
elongation %	7.11	6.99	7.02	6.96

	EtPO ₃ H w/ SiOH	EtPO ₃ H w/o SiOH	BuCOOH w/ SiOH	BuCOOH w/o SiOH
O-H bond distance (Å)	0.9689	0.9661	0.9584	0.9570
elongated O-H distance (Å)	1.0204	1.0159	1.0027	1.0002
elongation %	5.32	5.16	4.62	4.51

Table 11.4: Calculated bond distances and O-H bond elongation resulting from the interaction of a single water molecule with the functional group

The trend predicted for the interaction of the different organic acid functional groups did not follow that observed from aqueous phase titration of the acids, which gave an acid strength ordering of $-\text{ArSO}_3\text{H} > -\text{PrSO}_3\text{H} > -\text{EtPO}_3\text{H} > -\text{BuCOOH}$ [25]. Therefore, the computational work was extended by adding water molecules up to a total of four with the optimized structures (minimized energy) shown in Figure 11.12. While four molecules were still considerably short of representing a continuous condensed phase, the O-H bond elongation percent was

calculated. As shown in Table 11.5, the relative ordering of the O-H bond length elongation for these four functional groups now followed the same pK_a trend that was observed from experimental titrations with the $-\text{ArSO}_3\text{H}$ group having the longest O-H bond elongation. These results demonstrate the challenge associated with characterizing Brønsted acid catalysts relative to their use in the aqueous phase, or other solvent phases, as traditional acid site characterization techniques might not adequately represent how the catalytic moiety might be expected to perform under condensed phase conditions.

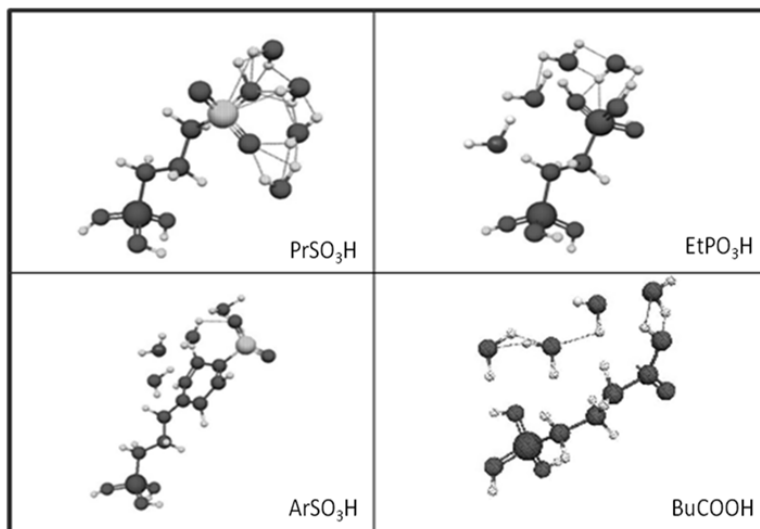


Figure 11.12: DFT optimized acid functional group structures with four water molecules

	PrSO ₃ H	PhSO ₃ H	EtPO ₃ H	BuCOOH
O-H bond distance (Å)	0.9761	0.9700	0.9689	0.9584
elongated O-H distance (Å)	1.0555	1.0553	1.0225	1.0077
elongation %	8.13	8.79	5.53	5.15

Table 11.5: Calculated bond distances and O-H bond elongation resulting from the interaction of four water molecules with the functional group in the presence of silanol groups.

Overall, the presence of an aqueous phase in a catalytic reaction system dictates that catalyst characterization approaches developed for catalysts used in gas-phase reactions need to be carefully considered when applied to catalysts that are to be used in aqueous-phase applications. Additionally, there is a need to develop new methodologies that are appropriate for characterizing how catalysts might be expected to perform in the presence of an aqueous solvent.

11.5 Novel Catalytic Materials for Biomass Conversion

It is reasonable to expect that catalyst materials that were developed for gas-phase applications with hydrocarbons will not likely be the best catalysts for condensed phase applications with biomass-derived molecules. While there is only a limited precedent for translating standard heterogeneous catalysts into their effective use for converting biorenewable feedstocks, there are catalyst systems that have developed to be efficient in this application. Enzymes have evolved to be quite active and selective in the conversion of biorenewable molecules with an important aspect being the creation of a reaction sphere around the active site. These active domains in enzymes consist of amino acid residue groupings in which the amino acid residues surrounding the specific active site amino acid residue can modify the reaction sphere thereby modifying the reactivity and selectivity of the active site.

Shown in Figure 11.13 is a rendering of a cellobiohydrolase enzyme, which is active for hydrolyzing the glycosidic bond in a cellobiose molecule [26]. It is interesting to see how this enzyme has evolved to create an active and selective catalytic domain. First, the enzyme has a folded tunnel that creates a hydrogen bonding gradient, which can effectively “pull” the cellobiose substrate to the active domain within the enzyme. When reaching the active domain, the cellobiose substrate docks into a configuration that places torsional pressure on the glycosidic bond, thereby lowering its activation barrier for the hydrolysis reaction. Within the active domain there are two amino acid residues that act in concert to catalyze the reaction. Figure 11.14 shows the mechanism thought to be occurring in this enzyme for the hydrolysis reaction (known as the inverting mechanism). In the inverting mechanism, a deprotonated amino acid residue activates a water molecule by nucleophilic attack, which activates the water to interact with carbon next to the glycosidic bond. Since the water molecule is donating electron density to this carbon, the glycosidic C–O bond is weakened sufficiently such that a proton from a carboxylic acid group on another amino acid residue can more easily break the bond. The activation barrier for glycosidic bond cleavage with a typical cellobiohydrolase enzyme is about 35 kJ/mol compared to about 120 kJ/mol

with a mineral acid ([27]), which demonstrates how an enzyme can dramatically modify reaction activation barriers by controlling the entire reaction domain.

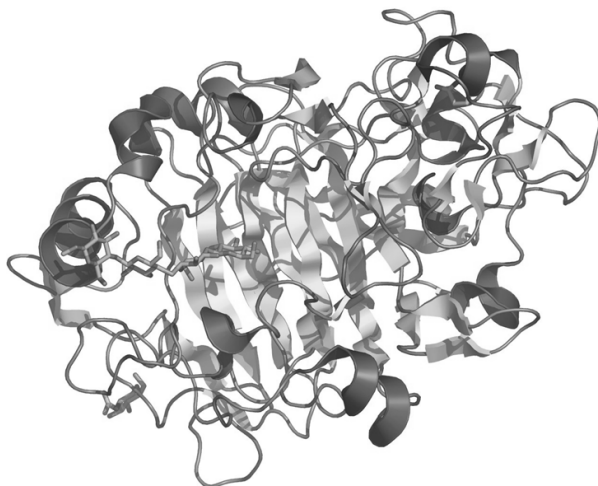


Figure 11.13: Representation of a glycoside hydrolase, family 7 cellobiohydrolase, with the cellobiose substrate entering the reactive domain

Examination of the cellobiohydrolase enzyme shows that the enzyme controls the reaction domain by providing preferential access of the desired substrate to the active site, adsorbing the substrate in a form that activates the compound for the reaction, and providing cooperative action between two catalytic sites for improved activity. Taking this cue from nature, catalytic materials in which both the active site and the broader reaction domain are carefully controlled may prove to be types of materials that are particularly effective for the active and selective conversion of biorenewables. In gas-phase reactions, there is precedent for heterogeneous materials that have some of the same elements of reaction domain control, but the catalytic requirements for these reaction domains when used in converting biorenewable feedstocks in the condensed phase will undoubtedly be different.

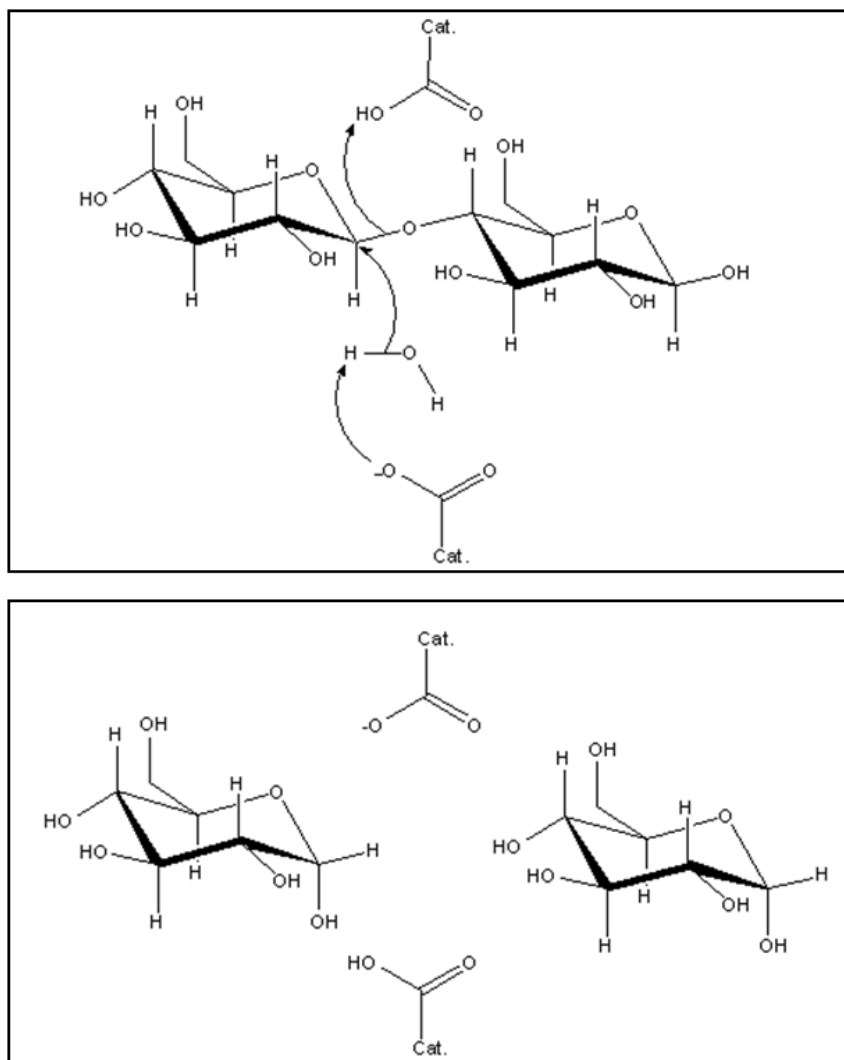


Figure 11.14: Proposed inverting mechanism reaction for the hydrolysis of a β -1,4 glycosidic bond with a hydrolase enzyme

The esterification reaction with biorenewable feedstocks has been the subject of several studies focused on improving catalytic performance by controlling

the reaction environment in solid materials, Diaz et al. [28, 29] examined glycerol esterification with fatty acids using organic acid-functionalized mesoporous silicas. The goal of the reaction was preferentially to produce monoglycerides while minimizing subsequent esterification reactions, which lead to the formation of di- or triglycerides. They used three attributes within the mesoporous materials to control their catalytic performance. First, propylsulfonic acid groups were tethered to the interior of the pores within the mesoporous materials.

Mesoporous silica was used as the support so that only a narrow pore size distribution existed. Additionally, the average pore diameter of these pores was controlled by choice of the surfactant template used in the synthesis of the mesoporous support. By using a strong acid group in conjunction with a tuned pore diameter, a MCM-41-SO₃H catalyst having both high activity and selectivity for glycerol esterification to monoglycerides only was identified. The good catalytic performance of the propylsulfonic acid-functionalized mesoporous silica catalyst was attributed to a combination of strong acidic sites located inside the mesopores and to the narrow pore size distribution, which diminished the formation of secondary di- and triglyceride products. The catalytic activity of the propylsulfonic acid-functionalized mesoporous silica catalyst was compared to that of a homogeneous acid (p-toluenesulfonic acid). The homogeneous acid had high activity but poor selectivity to the desired monosaccharide. A third attribute that was examined was the introduction of a second organic group within the pore through functionalizing MCM-41 materials with alkyl groups as well as propylsulfonic acid groups. It was found that the esterification reaction rate was improved with an increase in alkyl group loading, which was speculated to be due to water being excluded from the reaction environment within the pore. The methylated propylsulfonic acid-functionalized MCM-41 catalyst had a three-fold increase in catalytic activity relative to the non-methylated organosulfonic acid-functionalized mesoporous silica material.

Mesoporous scaffolds, having uniform sized pores, offer the opportunity to control the reaction environment around an active site throughout the catalytic material by controlling the placement of functional groups within the pores and/or on the exterior of the metal oxide particles. Controlled placement of functional groups in and on mesoporous silicas was examined, with the resulting catalysts tested in the esterification of fatty acids with methanol [30–32]. The esterification reaction, which produces an alkyl ester and water as the reaction product, is reversible. While the equilibrium constant at typical esterification reaction temperatures strongly favors the products over the fatty acid and methanol reactants, the constraint imposed by equilibrium becomes important at high conversion levels of the reactants. For organosulfonic acid functionalized mesoporous silicas, the tethered functional groups within the pores are surrounded by silanol groups, so

the pores are hydrophilic. As it is desirable to exclude water from the catalytically active domain, a material having hydrophobic pores would be preferred. A set of catalytic materials were synthesized to control the hydrophilicity/hydrophobicity of the pores in mesoporous particles by introducing tethered alkyl groups.

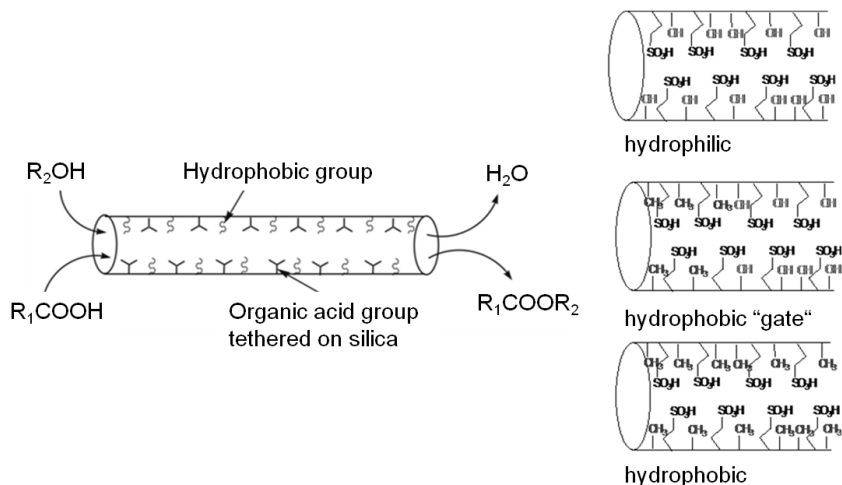


Figure 11.15: Schematics of propylsulfonic acid functionalized mesoporous silicas with different incorporation of alkyl groups either no incorporation (top), post-grafted (middle), and co-condensed (bottom)

Shown in Figure 11.15 are idealized schematics of the materials resulting from three different synthesis approaches [30]. Hydrophilic pores result from co-condensation of organosulfonic acid and silica precursors in the presence of a surfactant template. Studies have shown that the co-condensation synthesis creates materials in which all of the tethered functional groups reside on the interior of the pores. This material would represent the most hydrophilic case. Grafting an alkyl group onto these sulfonic acid functionalized silicas via condensation of an alkyl alkoxy silane precursor with the surface silanols will result in tethering the alkyl group to the external surface of the particles as well as to the pore mouth since the silanol groups at these locations are the most readily accessible. This material will effectively have a hydrophobic “gate” as the external surface of the particle and entrance to the pore will still be hydrophobic, while most of the interior of the pore will still be hydrophilic. Alternatively, the organosulfonic acid, alkyl, and silica precursors can all be co-condensed leading to a material

that has a more hydrophobic pore. The mesoporous silica catalyst that was synthesized by co-condensing all of the precursors, which placed the hydrophobic groups within the pores, gave significantly higher catalytic performance than the catalyst without hydrophobic group incorporation and the grafted catalyst, which would preferentially place the hydrophobic groups on the particle surfaces and near the pore mouths [30].

Another interaction effect exploited by enzymes is the interaction between multiple amino acid residues, which can modify the acid strength of the residue that directly serves as the active site. This cooperativity effect can be seen with heterogeneous catalysts as well as it has been shown that the location of propylsulfonic acid groups within a mesoporous material can alter the acidity of the resulting material. Intentionally forcing sulfonic acid groups to be in close proximity through the use of a disulfide precursor decreased the pK_a value relative to the same number of acidic sites incorporated using a propyl thiol precursor, which would not force two sulfonic acid groups to be in close proximity (see schematic in Figure 11.16) [19, 32].

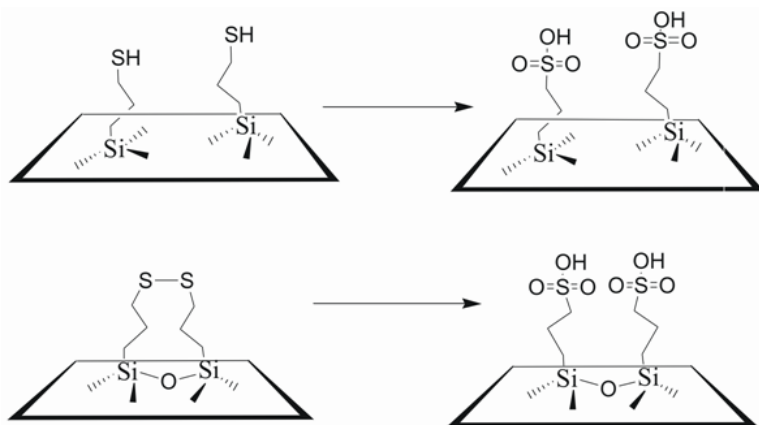


Figure 11.16: Controlled spatial placement of propylsulfonic acid groups through the use of a propyl thiol precursor (top) or a propyl disulfide precursor (bottom)

Enhanced reactivity due to cooperative effects between catalytic moieties can also be seen for cases in which two different catalytic moieties are interacting as shown in a study involving a bifunctional catalyst with both strong acid and metal sites [33]. One method to deconstruct solid biomass into smaller molec-

ular species existing in the condensed phase is the fast pyrolysis process. Fast pyrolysis generates a “bio-oil” that is a mixture of over 200 chemical species resulting from the thermal deconstruction of lignocellulose. While these bio-oils hold potential for upgrading to fuels, they are too acidic and unstable. Aldehydes and organic acids in the bio-oil are important contributors to the instability and acidity, so their removal would be desirable. In principle, the aldehydes and organic acids could be simultaneously removed by hydrogenating the aldehydes to alcohols, which could then be esterified with the organic acids to form esters. Metal catalysis is required for the hydrogenation step and acid catalysis for the esterification reaction. This concept is shown schematically in Figure 11.17.

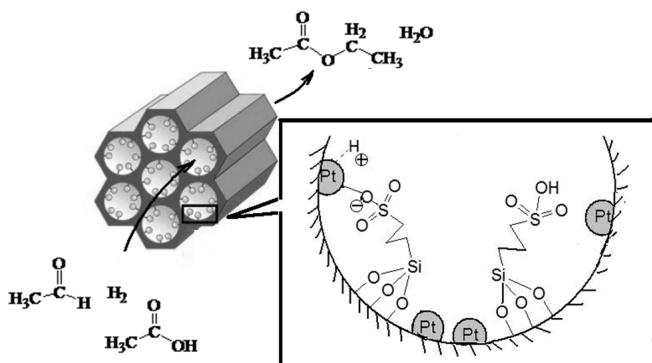


Figure 11.17: Schematic of the bifunctional catalyst used in the simultaneous hydrogenation and esterification of aldehydes and organic acids

To accomplish combined hydrogenation/esterification a mesoporous catalyst was synthesized in which propylsulfonic acid groups were tethered to the interior pores through co-condensation followed by incorporation of Pt through reductive deposition [33]. A TEM image of the resulting bifunctional catalyst is shown in Figure 11.18. Upon titration characterization of the bifunctional catalysts, the presence of Pt was found to lower the pK_a of the acidic groups as shown in Table 11.6, where the pK_a of the propylsulfonic acid functionalized silica was 3.91, which was subsequently lowered to 3.55 and 3.31 when nominal loadings of 1 wt% and 5 wt% Pt were incorporated, respectively. Shown in Table 11.7 are comparative reactivity results for the monofunctional catalyst and the bifunctional catalysts. As can be seen from the first column the hydrogenation activity was only dependent on whether Pt was present on the catalyst as the monofunctional Pt

and bifunctional catalysts had the same activities. However, the bifunctional catalyst had superior esterification activity than the monofunctional propylsulfonic acid catalyst as well as a physical mixture of the monofunctional Pt and propylsulfonic acid catalysts. These results were in complete agreement with the acid strength measurements and confirmed that the Pt and propylsulfonic acid groups had to be in close proximity to achieve the cooperative acid strength effect.

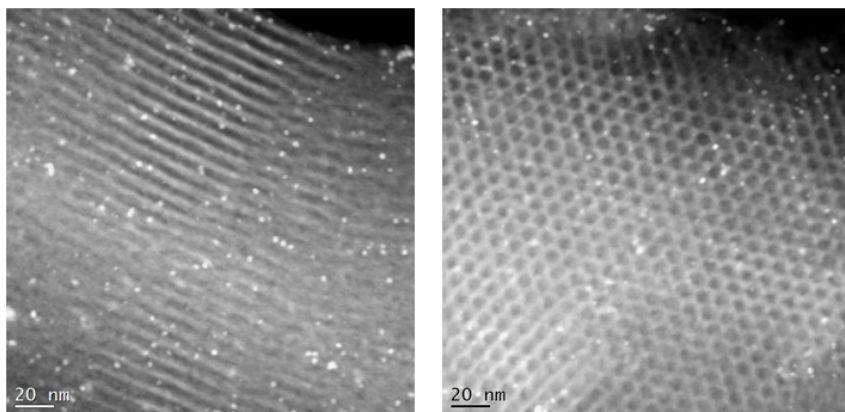


Figure 11.18: TEM images of Pt impregnated on propylsulfonic acid functionalized mesoporous silica

Catalysts	Acid sites mmol/g	pK_a
SBA15-PrSO ₃ H	0.89	3.91
Pt(1)/SBA15-PrSO ₃ H	0.69	3.55
Pt(5)/SBA15-PrSO ₃ H	0.57	3.31

Table 11.6: Number of acid sites and pK_a values for propylsulfonic acid functionalized mesoporous silicas upon incorporation of Pt

Catalyst	Hydrogenation (CH ₃ CHO conv., 24 h)	Esterification (TON of HAc)	Esterification (HAc conv., 24 h)
SBA15-PrSO ₃ H	–	3000	–
Pt/SBA15	8.1%	–	–
PtSBA15- PrSO ₃ H	7.9%	8000	8.4%
Physical mixture: SBA15-PrSO ₃ H +Pt/SBA15	–	–	3.5%

Table 11.7: Activity comparison for a series of mesoporous silica catalysts with various functional groups (150 °C and 15 bar H₂)

11.6 Hydrothermally Stable Catalytic Materials

Reaction systems in the condensed phase create a new challenge involving developing catalysts that possess adequate physical stability. This challenge is magnified when the reaction is being performed in the aqueous phase. Hydrothermal stability of heterogeneous catalysts has received a great deal of attention as it is a longstanding issue for typical metal oxide based catalysts. Even so, much of the work on creating hydrothermally stable solid catalysts has focused on their recalcitrance to water vapor and not condensed water. Aqueous-phase catalytic conversions of biorenewables are demanding as they will necessitate solid catalysts that can maintain their stability to temperatures as high as 230 °C.

An attractive feature of metal oxide supports is that they provide high surface area to disperse catalytic species and can be readily functionalized due to the presence of surface hydroxyls. Unfortunately, both of these characteristics diminish the hydrothermal stability of the metal oxides as high surface area coupled with high surface hydroxyl content makes the metal oxides more easily hydrolyzed. One approach to improving hydrothermal stability is to calcine the metal oxides at elevated temperatures, which will remove surface hydroxyls and decrease surface area. This effect can be seen in Figure 11.19, where mesoporous SBA-15 silicas were tested for hydrothermal stability in liquid water at 145 °C for 2 hours. Shown on the left in the figure is the pore size distribution of the mesoporous silicas, as synthesized and calcined (500 °C for 1 hour), prior to hydrothermal treatment. The overall pore volume diminished slightly upon calcination, but the average pore diameter remained essentially the same. After the hydrothermal treatment, the pore structure of the uncalcined mesoporous silica completely collapsed while

the calcined material maintained its structure. When the hydrothermal treatment was performed at 175 °C in water for 2 hours, even the structure of the calcined mesoporous silica collapsed.

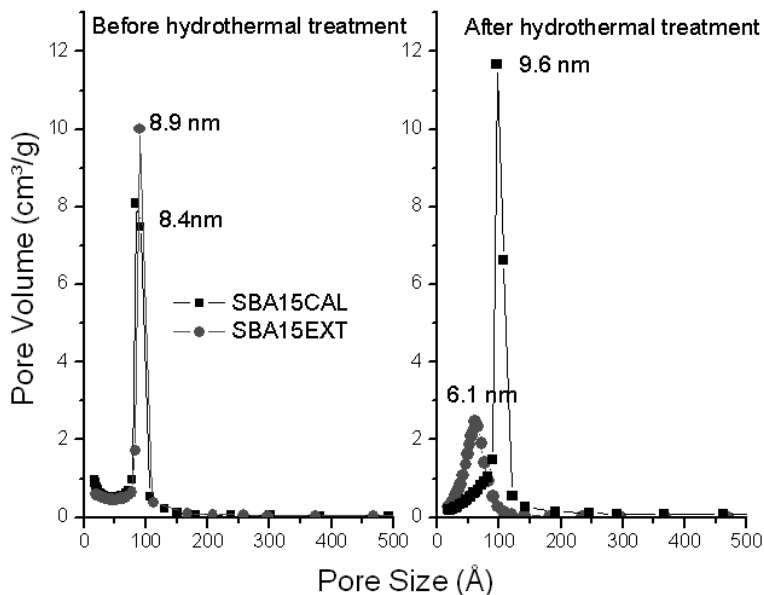


Figure 11.19: Pore size distribution of SBA-15 as synthesized and after calcination with subsequent hydrothermal treatment

As discussed in previous sections, many transformations of carbohydrates and their derivatives will require the use of Brønsted acid catalysts. Unfortunately, acidic aqueous solutions further exacerbate the hydrothermal stability problem as the acidic proton can catalyze the hydrolysis of metal oxides. When a calcined mesoporous silica was subjected to hydrothermal treatment at 145 °C in water for 2 hours with the water at pH4, the pore structure of the silica was found to collapse. Therefore, metal oxides are not promising supports for use in aqueous reactions at elevated temperatures particularly if acid catalysis is desired.

An interesting class of acidic materials that has been examined for use in the conversion of biorenewable molecules is sulfonated carbons. Using glucose or sucrose carbonization followed by sulfonation with concentrated sulfuric acid,

sulfonated carbons were produced [34, 35]. Depending on the carbonization conditions, carbon-based materials with acid content of up to 1.34 mmol/g were reported. It was speculated that the carbonized carbohydrate formed polycyclic aromatic sheets with the sulfonic acid groups bound to the edges of the sheets [34]. The sulfonated carbon materials were found to have good activity for fatty acid esterification with methanol and were stable to repeated batch reaction testing at temperatures of 80–180 °C. However, it should be noted that the water content was fairly low as the only water present was that produced in the esterification reaction.

In a more rigorous test of the stability of sulfonated carbons in aqueous media, the materials were tested using the cellulose hydrolysis reaction at 150 °C [34]. For this study, the sulfonated carbon catalysts were synthesized by sulfonating activated carbon rather than carbonized carbohydrates. While the catalyst was found to maintain its activity through three hydrolysis cycles, an independent measure of the number of sulfonic acid groups remaining at the end of the three cycles was not performed to determine whether sulfur loss had occurred.

While using sulfonated carbonized carbohydrates appeared to yield catalysts with good stability in condensed phase reactions, these materials were not easily amenable for producing materials in which the pore size distribution could be controlled. Therefore, several alternative synthesis approaches were explored for creating mesoporous sulfonated carbons with narrow and tunable pore size distributions. In one approach, sucrose was impregnated onto preformed SBA-15 and then the combined material was carbonized [36]. After carbonization, the original silica framework was removed using HF washing and the resulting mesoporous structured carbon was sulfonated. The carbon-based catalytic material was reported to be stable when used for multiple reaction cycles in the liquid-phase Beckmann rearrangement of cyclohexanone oxime. A similar approach was used to make sulfonated carbon-silica mesoporous composites in which the silica was not removed [37]. The MCM-48-based composite materials were found to maintain their ordered mesoporous structure upon being exposed to boiling water for 48 hours, whereas the MCM-48 mesoporous structure when not coated with carbon collapsed within 3 hours when exposed to boiling water. Additionally, the sulfonated carbon-silica material was found to be an active esterification catalyst.

The studies with the sulfonated carbon materials appear to suggest that these materials have promising hydrothermal stability properties. However, key characterization validating the long-term stability of the materials has still not been reported. While reproducible activity through 3–5 batch reaction cycles is important, the limited number of cycles is inadequate to determine whether the sulfonic acid groups are still slowly being lost. Catalyst activity is an indirect measure of sulfonic acid group content so small losses of active sites can be obscured by

other reaction factors such as reactant and product measurement accuracy, etc. Therefore, it is desirable to have an independent measure of the number of active sites retained. Additionally, acid-catalyzed biorenewable reactions can require that the catalysts be stable in the aqueous phase at temperatures as high as 230 °C, so the sulfonated carbon materials need to be tested at temperatures above boiling water to determine their potential range of application.

Sample	Acidic sites mmol H ⁺ /g	Sample II	Acidic sites mmol H ⁺ /g
SC0	1.21	SC0	1.37
SC1	1.18	SC1	1.28
SC2	1.08	SC2	1.22
SC3	1.07		
SC(175)	1.10		

Table 11.8: Stability of acid sites on sulfonated carbon subjected to hydrothermal treatment in liquid water (145 °C for 2 hours in each treatment)

Shown in Table 11.8 and Figure 11.20 are results for the stability of a sulfonated carbon catalyst, which was made by sulfonation of carbonized sucrose following the method of Toda et al. [35]. The fresh sulfonated carbon sample was found via titration to have an acid site content of 1.37 mmol H⁺/g. The starting material was split into 5 samples, which were subjected to different hydrothermal treatment conditions. Sample SC0 had no hydrothermal treatment, while SC1, SC2, and SC3 were subjected to 1, 2, and 3 hydrothermal treatment cycles, respectively, at 145 °C in water for 2 hours. SC(175) had one hydrothermal treatment at 175 °C in water for 2 hours. Shown in Figure 11.20 is the performance of these sulfonated carbon materials in the acetic acid esterification reaction with methanol. This reaction was used to evaluate the catalysts as it has been found to be quite sensitive to the number of acidic groups and the strength of the acidic groups. Within the experimental error, SC0, SC1, and SC2 all appeared to have comparable activities from the reaction studies, but as can be seen from Table 11.8 there was a slight loss of acidic sites from SC0 to SC1 to SC2. A large decrease in activity was observed for SC3 and SC(175), which was accompanied with a significant decrease in the number of active sites. This example is illustrative of the risk associated with characterizing catalyst stability only according to its performance under reaction conditions as the reaction results would suggest stability for SC0, SC1, and SC2 when more complete characterization demonstrated that the materials were not ultimately stable for extended use.

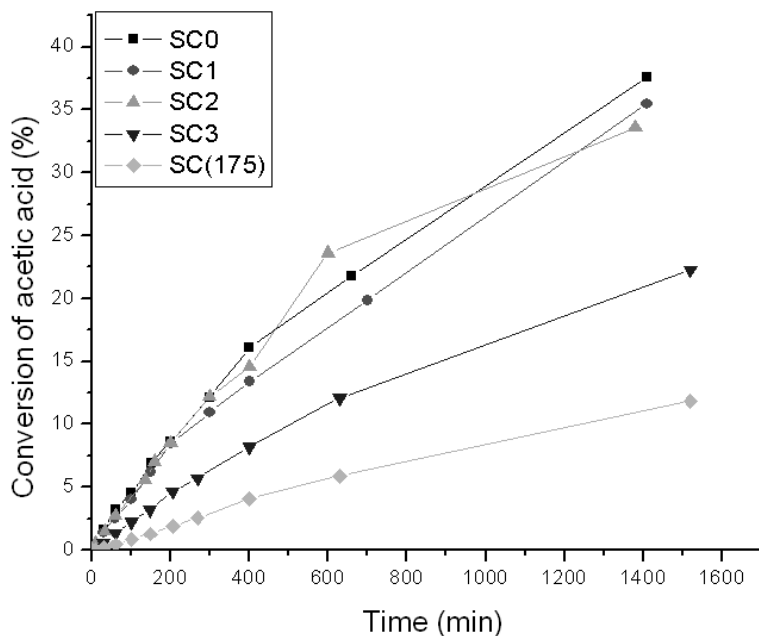


Figure 11.20: Esterification activity of sulfonated carbons after hydrothermal treatment

Finding solid catalysts that are stable under condensed phase hydrothermal conditions remains an important challenge. The challenge is more significant when attempting to synthesize a solid Brønsted acid catalyst, as the acidity has an adverse affect on stability. In exploring hydrothermal stability of solid catalysts it is important to ensure that the characterization techniques being used are truly representative of determining whether the catalytic material is hydrothermally stable for the prolonged use needed in a real catalytic process.

11.7 Impurity Tolerant Catalysts

Frequently, the development of catalysts for converting new feedstocks focuses on how to accomplish the transformation of these new reactants to the desired products. There is no doubt that demonstrating successful transformation chem-

istry is vital when evaluating new types of feedstocks. However, new feedstocks can introduce the additional issue of low-level impurities that are intrinsic to that feedstock. For example, the primary low-level impurities of concern in processing crude oil are sulfur and nitrogen heteroatoms. Biorenewable feedstocks introduce a new array of low-level impurities that can have significant impact on heterogeneous catalyst performance.

Triglyceride transesterification and fatty acid esterification to alkyl esters, which are used as biodiesel, have received a great deal of attention. The primary catalysts used commercially in these conversions, sodium methoxide for transesterification and sulfuric acid for esterification, are homogeneous, which necessitates a downstream catalyst removal step. There has been a large number of papers examining possible heterogeneous catalysts capable of replacing the homogeneous catalysts. While catalyst activity and stability against leaching of the active sites are critical properties for the heterogeneous catalysts, dealing with impurities in the feedstocks will also play a role in developing viable heterogeneous catalyst systems.

An example demonstrating the importance of impurities for alkyl esters production is the esterification of fatty acids in lipid feedstocks containing elevated levels of free fatty acids, i.e., a portion of the triglycerides have been hydrolyzed creating fatty acids that are not bound up as esters. Typically, the first step in processing such a feedstock is to use a homogenous acid, commonly sulfuric acid, to esterify the free fatty acids to alkyl esters, with the remaining triglycerides then transesterified with a strong base catalyst. Using model feedstocks in which 15 wt% of a fatty acid was doped into purified triglycerides, it was shown that an organosulfonic acid functionalized mesoporous silica catalyst was an effective replacement for sulfuric acid in the esterification reaction [38]. However, when the solid catalyst was used for esterifying free fatty acids in a real feedstock, beef tallow with 7 wt% free fatty acid, the catalyst deactivated quite rapidly [31]. In successive batch reactor runs with the same catalyst, the catalyst activity was halved from the first cycle to the second cycle and then halved again in the third cycle (see Figure 11.21A). The most likely source of this deactivation was adsorption of polar compounds, such as phospholipids or proteins, that are known to exist at low levels in unpurified lipid feedstocks. A simple purification of the beef tallow accomplished by passing it over a bed of activated silica, which had a highly hydroxylated surface that would provide for adsorption of polar compounds, dramatically improved the performance of the catalyst, as now the activity of the solid esterification catalyst decreased by only about 15% from the first cycle to the second. Although an improvement, the activity loss was still too high for the catalyst to be of practical relevance. Therefore, a catalytic material was made in which organosulfonic acid and alkyl precursors were co-condensed with the

silica precursor leading to mesoporous silica with tethered organosulfonic acid and alkyl groups (see schematic in Figure 11.21B). The alkyl groups were introduced to make the surface more hydrophobic and thereby less likely to adsorb polar compounds.

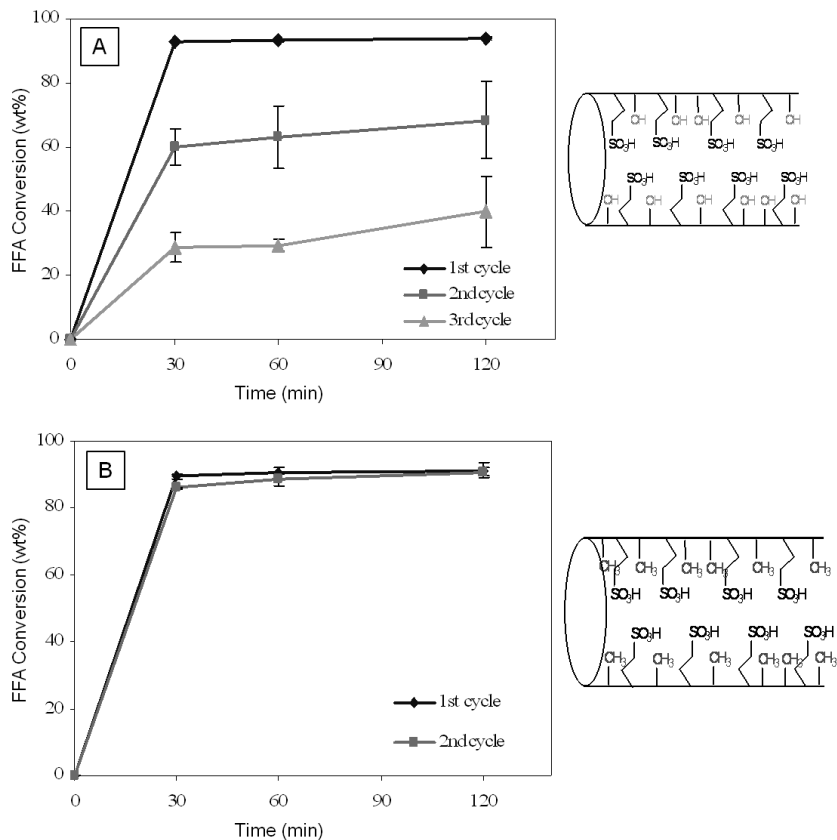


Figure 11.21: Performance of propylsulfonic acid mesoporous silica in the conversion of beef tallow: A) loss of activity when the catalysts is used in multiple cycles, B) activity of resulting when incorporating alkyl groups in the pores and pretreating the feed with activated silica

Shown in Figure 11.21B is the performance of the catalyst system in which the activated silica was used prior to the alkyl-modified organosulfonic acid functionalized mesoporous silica catalyst. As can be seen in the figure, this combination led to a catalyst system in which no loss of activity was observed between the first and second cycles. While two cycles were insufficient to demonstrate long term stability, a clear improvement in performance was realized.

Another type of impurity that is present to varying levels in lignocellulosic feedstocks is metal ions. Shown in Table 11.9 are metal ions commonly present in lignocellulosic biomass. Included in the table are the most common forms in which the metal ions exist, which includes both as salts and as organically associated species [39]. A more quantitative determination of impurity content in a lignocellulosic feedstock is shown in Table 11.10 [40]. For these data, switchgrass was combusted and the resulting ash analyzed for its metal oxide content. Of particular importance for the use of heterogeneous catalysts with biomass is the significant presence of alkalis and alkaline earths, which are known to be poisons for many types of metal catalysts. Therefore, catalysts must be developed that can either tolerate these impurities or a pretreatment system needs to be employed that can remove the impurities prior to exposure to the catalyst. This issue becomes important in processes in which lignocellulosic biomass is thermally deconstructed such as by gasification or pyrolysis with subsequent catalytic upgrading to desired products. In general, pretreatment to remove alkalis and alkaline earths from biomass is quite expensive, so there will be a need to deal with these species downstream from the gasification or pyrolysis step.

Element	Compound	Share of the total element (%)
Ionic form, water soluble		
Na	NaCl, NaNO ₃	> 90
K	KCl, KNO ₃	> 90
Mg	Mg(NO ₃) ₂ , MgCl ₂ , Mg ₃ (PO ₄) ₂	60–90
Ca	Ca(NO ₃) ₂ , CaCl ₂ , Ca ₃ (PO ₄) ₂	20–60
Organically Associated		
Mg	Chlorophyll	8–35
Ca	Ca-oxalate, Ca-pectate	30–85
Mn, Fe	Other macromolecules	> 80

Table 11.9: Typical forms of metal ions in biomass materials

Compound	Content (wt%)
SiO ₂	72.2
Al ₂ O ₃	3.74
Fe ₂ O ₃	1.28
SO ₃	0.39
CaO	6.19
MgO	2.33
Na ₂ O	0.77
K ₂ O	6.17
P ₂ O ₅	2.63
TiO ₂	0.18
SrO	0.02
BaO	0.01

Table 11.10: Composition of the ash resulting from the combustion of switchgrass

11.8 Novel Reaction Systems

As reaction systems for biorenewables will frequently involve a condensed phase, separation processes will also need to be developed that can purify the desired products from the reaction medium. To improve the economic viability of biorenewable conversions, it is useful to design catalysts in concert with reaction systems such that the subsequent separation can be facilitated. While the goal of integrating separation considerations with the reaction system typically involves producing a product that can be more easily removed from the reaction medium, another objective can be to enhance product selectivity. The multifunctional nature of biorenewable-derived molecules makes selective conversion to a desired product more difficult since the product will often have significant reactivity as well. Therefore, removal of the product from the reaction medium can have the advantage of improved selectivity beyond what might be possible just from catalyst modifications.

One example of integrating reaction and separation is work from the Dumesic lab that examined the conversion of aqueous-phase carbohydrates to monofunctional hydrocarbons (alcohols, ketones, heterocyclics, and acids) using a Pt-Re catalyst [41, 42]. In this work, C₄ and higher monofunctional species were produced that were sufficiently hydrophobic such that they formed an organic phase, which was then immiscible from the reactant-containing aqueous phase. Starting with a 60 wt% solution of sorbitol in water, they were able to recover as much as

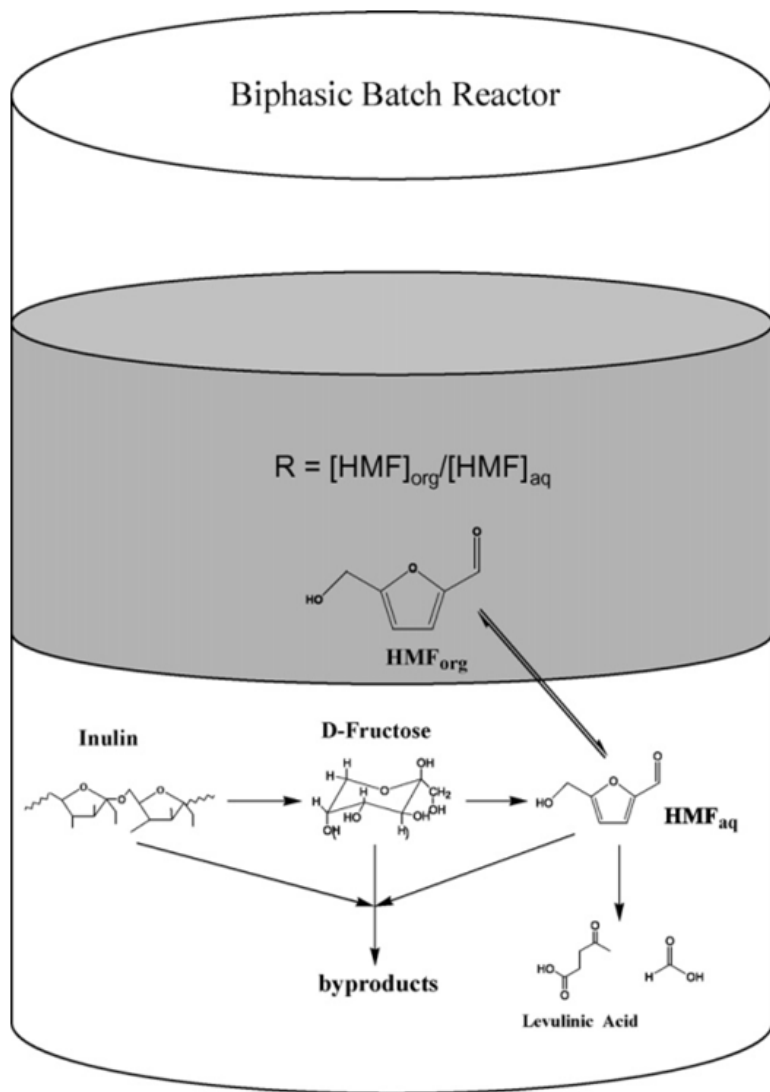


Figure 11.22: Schematic of biphasic reactor system for converting fructose to HMF [43]

60 mol% of the original feedstock carbon within an organic phase using a reaction system that was operating at 230 °C, 27 bar and a space velocity of 1.2 hr⁻¹ [41]. Therefore, a simple separation of the product was achieved by operating the system at conditions leading to the formation of hydrophobic monofunctional hydrocarbons. The monofunctional hydrocarbons could then be directly upgraded to fuels through aldol condensation and ketonization C–C coupling reactions to produce fuels without any further intermediate separation [44–48].

A second example in which separation considerations were effectively incorporated into the design of a biorenewable reaction system was the biphasic production of hydroxymethylfurfural (HMF) from fructose [43, 49, 50]. It is difficult to achieve high selectivity in the dehydration of fructose to HMF, since the acid catalyst needed for dehydration is also quite active for the further reaction of HMF to undesirable products. By using a biphasic reaction system (see schematic in Figure 11.22), the reactive aqueous phase, which contained the fructose feedstock and the acid catalyst, was immiscible with an extracting phase, which contained an organic solvent having high HMF solubility. The extraction of the HMF to the nonreactive organic phase greatly reduced the subsequent conversion of HMF, which both increased the yield to the desired product and increased the fructose conversion. By appropriate selection of the extracting solvent and the addition of a salt or phase modifiers (DMSO and 1-methyl-2-pyrrolidinone) to the aqueous phase to further improve the partitioning of HMF into the extracting phase, high selectivities to the HMF product were achieved. For example, a 30 wt% fructose solution saturated with NaCl using 1-butanol as the extracting solvent gave an HMF selectivity of 82% whereas in a simple single phase reaction the HMF selectivity was only about 28%.

11.9 Summary

Over the past several years there has been a rapid acceleration of studies aimed at understanding how to tailor heterogeneous catalysts and the reaction systems utilizing them for the efficient conversion of biorenewable feedstocks with a number of them given in this chapter. It is clear that the catalytic materials needed to convert successfully biorenewable feedstocks must address reaction characteristics that are distinctly different from those encountered when developing catalytic materials for the refining and petrochemical industry. While catalyst development for biorenewables can build from knowledge for hydrocarbon conversions, there is a need to develop evaluation techniques that can adequately address the new attributes imposed through this alternative feedstock, which have been discussed in the current chapter. The economic hurdle to replace fossil carbon with renewable carbon in chemical and fuel applications is quite demanding, so sig-

nificant improvements in catalyst technology are required. To achieve the necessary heterogeneous catalyst advancements, more advanced fundamental knowledge about how catalysts can be designed specifically for converting biorenewable feedstocks is still needed and, as such, the unique challenges associated with designing catalysts for this application will be a rich source of new research directions for heterogeneous catalysis.

Bibliography

- [1] L. Peereboom, J.E. Jackson, and D.J. Miller. Interaction of Polyols with Ruthenium Metal Surfaces in Aqueous Solution. *Green Chemistry* 11 (2009):1979–1986.
- [2] D.G. Lahr and B.H. Shanks. Kinetic Analysis of the Hydrogenolysis of Lower Polyhydric Alcohols: Glycerol to Glycols. *Industrial & Engineering Chemistry Research* 42 (2003):5467.
- [3] M.K. Koshikawa and T. Hori. Adsorption Selectivity of Sugars toward Hydrous Zirconium(IV) and Hydrous Iron(III) Oxide Surfaces. *Physical Chemistry Chemical Physics* 2 (2000):1497–1502.
- [4] D.G. Lahr and B.H. Shanks. Effect of Sulfur and Temperature on Ruthenium-Catalyzed Glycerol Hydrogenolysis to Glycols. *Journal of Catalysis* 232 (2005):386.
- [5] R.J. Ferrier. Carbohydrate Chemistry. Monosaccharides, Disaccharides, and Specific Oligosaccharides. *Carbohydrate Chemistry* 26 (1994):1.
- [6] C. Montassier, J.C. Menezo, L.C. Hoang, C. Renaud, and J. Barbier. Aqueous Polyol Conversions on Ruthenium and on Sulfur-Modified Ruthenium. *Journal of Molecular Catalysis* 70 (1991):99.
- [7] E. Tronconi, N. Ferlazzo, P. Forzatti, I. Pasquon, B. Casale, and L. Marini. A Mathematical Model for the Hydrogenolysis of Carbohydrates. *Chemical Engineering Science* 47 (1992):2451–2356.
- [8] K. Wang, M.C. Hawley, and T.D. Furney. Mechanism Study of Sugar and Sugar Alcohol Hydrogenolysis Using 1,3-Diol Model Compounds. *Industrial & Engineering Chemistry Research* 34 (1995):3766.
- [9] D.G. Lahr. *Mechanistic Insight into the Production of Ethylene Glycol and Propylene Glycol from Biorenewable Resources*. PhD thesis. Iowa State University, 2005.
- [10] E.P. Maris and R.J. Davis. Hydrogenolysis of Glycerol over Carbon-Supported Ru and Pt Catalysts. *Journal of Catalysis* 249 (2007):328–337.

- [11] S.K. Desai, P. Venkataraman, and M. Neurock. A Periodic Density Functional Theory Analysis of the Effect of Water Molecules on Deprotonation of Acetic Acid over Pd(111). *Journal of Physical Chemistry B* 105 (2001):9171–9182.
- [12] S.K. Desai. *Theoretical Investigations of Solution Effects on Metal Catalyzed Hydrogenation and Oxidation Processes*. PhD thesis. University of Virginia, 2002.
- [13] S.K. Desai and M. Neurock. A first Principles Analysis of CO Oxidation over Pt and Pt66.7 Ru33.3 (111) Surfaces. *Electrochimica Acta* 48 (2003): 3759–3773.
- [14] S.K. Desai and M. Neurock. First-Principles Study of the Role of Solvent in the Dissociation of Water over a Pt-Ru Alloys. *Physical Review B* 68 (2003):075420.
- [15] E. Lotero, Y. Liu, D.E. Lopez, K. Suwannakarn, D.A. Bruce, and J.G. Goodwin. Synthesis of Biodiesel via Acid Catalysis. *Industrial & Engineering Chemistry Research* 44 (2005):5353–5363.
- [16] S. Hamoudi, S. Royer, and S. Kaliaguine. Propyl- and Arene-Sulfonic Acid Functionalized Periodic Mesoporous Organo Silicas. *Microporous and Me-soporous Materials* 71 (2004):17–25.
- [17] V. Herledan-Semmer, S. Dakhlaoui, F. Guenneau, E. Haddad, and A. Gedeon. Spectroscopic Evidence of SBA-15 Mesoporous Solids Functionalization. *Studies in Surface Science and Catalysis* 154 (2004):1519–1524.
- [18] S. Koujout and D.R. Brown. Calorimetric Base Adsorption and Neutralization Studies of Supported Sulfonic Acids. *Thermochimica Acta* 434 (2005):158–164.
- [19] R.K. Zeidan, V. Dufaud, and M.E. Davis. Enhanced Cooperative, Catalytic Behavior of Organic Functional Groups by Immobilization. *Journal of Catalysis* 239 (2006):299–306.
- [20] R. Kanthasamy, I.K. Mbaraka, B.H. Shanks, and S.C. Larsen. Solid-State MAS NMR Studies of Sulfonic Acid-Functionalized SBA-15. *Applied Magnetic Resonance* 32 (2007):513–526.
- [21] S. Hamoudi, D.T. On, and S. Kaliaguine. Mesostructured Solid Acids. *Studies in Surface Science and Catalysis* 14 (2003):15–22.
- [22] S. Koujout, B.M. Kiernan, D.R. Brown, H.G.M. Edwards, J.A. Dale, and S. Plant. The Nature of the Internal Acid Solution in Sulfonated Poly(styrene-co-divinylbenzene) Resins. *Catalysis Letters* 85 (2003):33–40.

- [23] B. Cinlar. *Acid Catalyzed Carbohydrate Degradation and Dehydration*. PhD thesis. Iowa State University, 2010.
- [24] P. Lorente, I.G. Shenderovich, N.S. Golubev, G.S. Denisov, G. Buntkowsky, and H.H. Limbach. $1\text{H}/15\text{N}$ NMR Chemical Shielding, Dipolar 15N , 2H Coupling and Hydrogen Bond Geometry Correlations in a Novel Series of Hydrogen-Bonded Acid-Base Complexes of Collidine with Carboxylic Acids. *Magnetic Resonance in Chemistry* 39 (2001):18–29.
- [25] B. Cinlar and B.H. Shanks. Characterization of the Acidic Sites in Organic Acid Functionalized Mesoporous Silica in the Aqueous Phase. *Applied Catalysis A: General* (in press).
- [26] P. Reilly. *Courtesy of Professor Peter Reilly, Iowa State University*.
- [27] J.A. Bootsma and B.H. Shanks. Cellobiose Hydrolysis Using Organic-Inorganic Hybrid Mesoporous Silica Catalysts. *Applied Catalysis A: General* 327 (2007):44–51.
- [28] J. Perez-Pariente, I. Diaz, F. Mohino, and E. Sastre. Selective Synthesis of Fatty Monoglycerides by Using Functionalized Mesoporous Catalysts. *Applied Catalysis A: General* 254 (2003):173–188.
- [29] I. Diaz, C. Marquez-Alvarez, F. Mohino, J. Perez-Pariente, and E. Sastre. Combined Alkyl and Sulfonic Acid Functionalization of Mcm-41 Type Silica Part 1. Synthesis and Characterization. *Journal of Catalysis* 193 (2000):283–294.
- [30] I.K. Mbaraka and B.H. Shanks. Design of Multifunctionalized Mesoporous Silicas for Esterification of Fatty Acids. *Journal of Catalysis* 229 (2005):365–373.
- [31] I.K. Mbaraka and B.H. Shanks. Conversion of Oils and Fats using Advanced Mesoporous Heterogeneous Catalysts. *Journal of the American Oil Chemists' Society* 83 (2006):79.
- [32] I.K. Mbaraka and B.H. Shanks. Acid Strength Variation due to Spatial Location of Organosulfonic Acid Groups on Mesoporous Silicas. *Journal of Catalysis* 244 (2006):78–85.
- [33] Y. Tang, S. Miao, B.H. Shanks, and X. Zheng. *Applied Catalysis A: General* 375 (2010):310–317.
- [34] M. Okumura, A. Takagaki, M. Toda, J.N. Kondo, K. Domen, T. Tatsumi, M. Hara, and S. Hayashi. Acid-Catalyzed Reactions on Flexible Polycyclic Aromatic Carbon in Amorphous Carbon. *Chemistry of Materials* 18 (2006):3039–3045.

- [35] M. Toda, A. Takagaki, M. Okamura, J.N. Kondo, S. Hayashi, K. Domen, and M. Hara. Green Chemistry: Biodiesel made with Sugar Catalysts. *Nature* 438 (2005):178.
- [36] R. Xing, Y.M. Liu, Y. Wang, L. Chen, W.H. Wu, Y.W. Jiang, M.Y. He, and P. Wu. Active Solid Acid Catalysts Prepared by Sulfonation of Carbonization-Controlled Mesoporous Carbon Materials. *Microporous and Mesoporous Materials* 105 (2009):41–48.
- [37] Y. Liu, J. Chen, J. Yao, Y. Lu, L. Zhang, and X. Liu. Preparation and Properties of Sulfonated Carbon-Silica Composites from Sucrose Dispersed on MCM-48. *Chemical Engineering Science* 148 (2009):201–206.
- [38] I.K. Mbaraka, D.R. Radu, V.S.-Y. Lin, and B.H. Shanks. Organosulfonic Acid Functionalized Mesoporous Silicas for the Esterification of Fatty Acid. *Journal of Catalysis* 219 (2003):329–336.
- [39] W.R. Livingston. *Biomass Ash Characteristics and Behaviour in Combustion, Gasification and Pyrolysis Systems*. Tech. rep. Doosan Babcock Energy Limited, 2007.
- [40] P.R. Patwardhan, J.A. Satrio, R.C. Brown, and B.H. Shanks. Influence of Inorganic Salts and Switchgrass Ash on Primary Pyrolysis Products of Cellulose. *Bioresource Technology* 101 (2010):4646–4655.
- [41] E.L. Kunkes, D.A. Simonetti, R.M. West, J.C. Serrano-Ruiz, C.A. Gaertner, and J.A. Dumesic. Catalytic Conversion of Biomass to Monofunctional Hydrocarbons and Targeted Liquid-Fuel Classes. *Science* 322 (2008):417–421.
- [42] R.M. West, E.L. Kunkes, D.A. Simonetti, and J.A. Dumesic. Catalytic Conversion of Biomass-Derived Carbohydrates to Fuels and Chemicals by Formation and Upgrading of Mono-Functional Hydrocarbon Intermediates. *Catalysis Today* 147 (2009):115–125.
- [43] Y. Roman-Leshkov, J.N. Chheda, and J.A. Dumesic. Phase Modifiers Promote Efficient Production of Hydroxymethylfurfural from Fructose. *Science* 312 (2006):1933–1937.
- [44] J.N. Chheda and J.A. Dumesic. An Overview of Dehydration, Aldol-Condensation and Hydrogenation Processes for Production of Liquid Alkanes from Biomass-Derived Carbohydrates. *Catalysis Today* 123 (2007):59–70.
- [45] J.N. Chheda, G.W. Huber, and J.A. Dumesic. Liquid-Phase Catalytic Processing of Biomass to Fuels and Chemicals. *Angewandte Chemie International Edition* 46 (2007):7164–7183.

- [46] C.A. Gaertner, J.C. Serrano-Ruiz, D.J. Braden, and J.A. Dumesic. Catalytic Coupling of Carboxylic Acids by Ketonization as a Processing Step in Biomass Conversion. *Journal of Catalysis* 266 (2009):71–78.
- [47] D.A. Simonetti and J.A. Dumesic. Catalytic Strategies for Changing the Energy Content and Achieving C–C Coupling in Biomass-Derived Oxygenated Hydrocarbons. *ChemSusChem* 1 (2008):725–733.
- [48] R.M. West, Z.Y. Liu, M. Peter, C.A. Gaertner, and J.A. Dumesic. Carbon-Carbon Bond Formation for Biomass-Derived Furfurals and Ketones by Aldol Condensation in a Biphasic System. *Journal of Molecular Catalysis A: Chemical* 296 (2008):18–27.
- [49] J.N. Chheda, R. Roman-Leshkov, and J.A. Dumesic. Production of 5-Hydroxymethylfurfural and Furfural by Dehydration of Biomass-Derived Mono- and Poly-Saccharides. *Green Chemistry* 9 (2007):342–350.
- [50] R. Roman-Leshkov and J.A. Dumesic. Solvent Effects on Fructose Dehydration to 5-Hydroxymethylfurfural in Biphasic Systems Saturated with Inorganic Salts. *Topics in Catalysis* 52 (2009):297–303.

Chapter 12

Tailor-Made Fuels and Chemicals from Biomass

Thorsten vom Stein, Jürgen Klankermayer, Walter Leitner

12.1 Introduction

Individual mobility together with automotive cargo transportation represents one of the fundamental incentives for economic stability and growth. However, the energy supply within the transport sector is currently facing major changes due to the urgent need to accomplish increasing independence from fossil raw materials and to reduce the associated carbon dioxide emission. Scenarios based on these assumptions predict an increasing technological diversification of the transportation sector including the use of various alternative energy carriers, such as natural gas, ethanol, or hydrogen, and the application of electrically powered automobiles. All possible scenarios have in common that electrically powered vehicles are expected to impact mostly on urban transportation, whereas internal combustion engines will remain the prevailing propulsion systems for long-distance and heavy-duty applications. Due to their superior energy density as well as proven storage and distribution concepts, liquid chemical compounds represent the energy carrier of choice for these applications.

Projections of the International Energy Agency (IEA) predict that the use of fuels from biomass will continuously increase, providing up to 27% of all transportation fuels in 2050, compared to only 3% today. The competition to the food supply chain as well as the critical energy and CO₂-balance have triggered intensive research on sustainable biofuel production beyond the established first generation products based on sugarcane, corn, maize or palm oil. These established processes only use certain parts of the plant material for fuel production. With the exception of specific regional situations such as sugarcane in Brasil, they therefore imply severe limitations on the way to a sustainable long-term solution. Significant progress has been achieved on large-scale implementation of second generation biofuels, which intend to use the non-food relevant part of the plant material. One prominent example is the Biomass-to-Liquid (BtL) approach, where biomass materials are converted to syngas and subsequently transformed to alkane mixtures. In mid-term, second generation biofuels are expected to con-

tribute up to 4% of all utilized fuels in Europe in 2020. However, current efforts are aiming mainly at the substitution of fossil fuels based on hydrocarbon mixtures without capitalizing on the potential of innovative fuel design and improved engine systems. In order to fully exploit the engine potential in terms of emissions and fuel efficiency, the ideal properties of future fuels may differ considerably from those of current conventional fuels, making it attractive to concomitantly tailor the combustion systems to the fuel properties and vice versa.

The Cluster of Excellence *Tailor-Made Fuels from Biomass* at RWTH Aachen University addresses the fundamental scientific and technological challenges associated with this approach toward next generation biofuels.¹ Researchers from RWTH Aachen and the Max-Planck-Institut für Kohlenforschung have formed an interdisciplinary, integrated network comprising scientific expertise in the fields of chemistry, biology, reaction and process engineering, and combustion engineering. Complementary to current state-of-the-art biofuel concepts, the Cluster's research program aims at the selective (bio-)chemical conversion of lignocellulosic biomass into molecularly defined fuel compounds that are not merely viewed as substitutes for existing products, but recognized as an opportunity to improve the performance of internal combustion engines.

12.2 Conceptual Approach to Tailor-Made Fuels via Combined Product and Process Design

The initial step in developing production pathways for the desired new fuel candidates is to define target molecules comprising the envisaged physical properties, which are beneficial for the application in internal combustion engines. Based on these novel fuel molecules, potential production pathways have to be identified. For this task we have proposed to apply a design strategy in analogy to the retrosynthetic approach commonly used in organic chemistry [1]. In such an analysis, the targeted molecules are traced back to the starting materials step by step through building blocks and intermediates that are readily available (Figure 12.1). In organic synthesis based on the current petrochemical supply chain, the retrosynthetic analysis typically reduces the complexity and functionality of the products on the way to the starting materials. Synthetic methods for the formation of carbon-carbon and carbon-heteroatom bonds connect the simpler building blocks with the more complex product structures. In contrast, the target products of the biomass-based supply chain are typically less oxidized and of lower molecular weight than the biopolymer feedstocks. Therefore, new catalytic methods for selective de- and re-functionalization (mainly deoxygenation) in liquid

¹<http://www.fuelcenter.rwth-aachen.de>

phase have to be developed to connect the structures along the possible pathways identified in the retrosynthetic analysis.

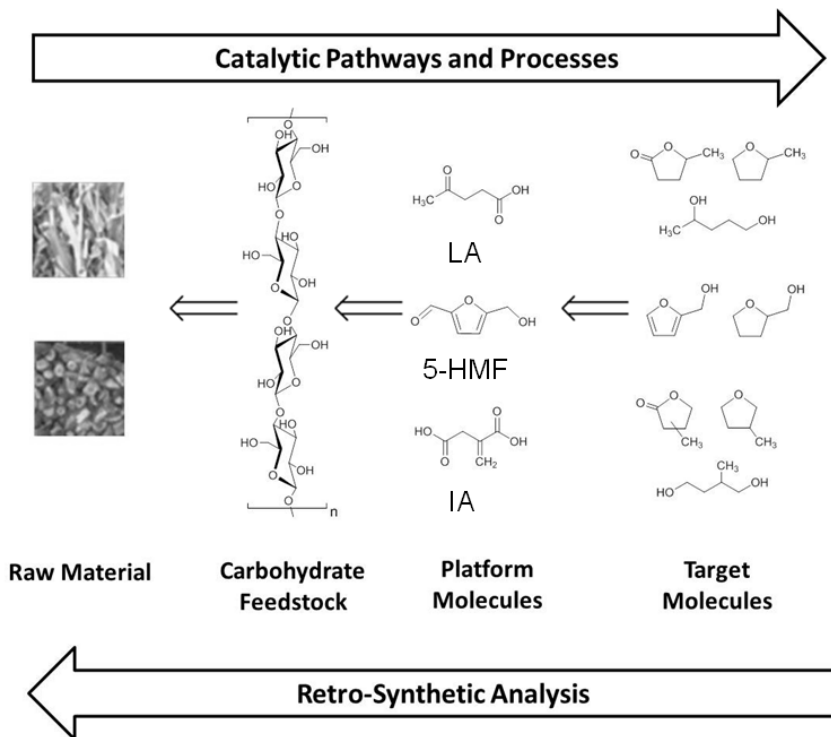


Figure 12.1: Concept for the targeted development of new routes to potential fuel compounds based on lignocellulose as raw material

Figure 12.1 exemplifies this approach for cyclic esters, ethers and furan derivatives as products. Based on the literature background [2], these molecular structures have been identified as promising targets for potential fuel components and continue to be refined further through the interdisciplinary collaboration within the Cluster. The specific structures can be traced back to well-defined intermediates, levulinic acid (LA), itaconic acid (IA) and 5-hydroxymethylfurfural (5-HMF), which have been selected from the range of so-called *platform chemicals* available from the carbohydrate feedstock of biomass. Finally, the required cellulose and hemicellulose fractions can be obtained by the disintegration of the

diverse lignocellulosic raw material coupled with selective separation processes. The following sections will describe some selected recent developments and advances for these steps to highlight the challenges and opportunities for catalysis research resulting from this targeted and rational approach to next generation biofuels and biomass-derived chemicals.

12.3 From Intermediates to Products

12.3.1 Chemicals and Fuels from the Platform Chemicals Levulinic and Itaconic Acid

2-Methyltetrahydrofuran (2-MTHF) and γ -valerolactone (GVL) can be obtained from levulinic acid (LA), whereas the isomeric compounds 3-MTHF and methylbutyrolactone (MBL) are accessible from itaconic acid (IA). Even for these seemingly direct conversions, a large number of pathways are possible. For example, as many as nineteen different connections are conceivable to lead from IA to 3-MTHF. Researchers within the Cluster have developed a mathematical model for the reaction network flux analysis that allows characterization of such competing pathways according to criteria such as yield, mass-, or energy efficiency [3]. Thus, the possible solutions can be ranked accordingly, and the most desirable pathways can be selected a priori as primary goals for the catalysis research.

A prerequisite to enable these sustainable pathways from platform molecules to tailored fuel candidates represents the development of flexible catalytic systems. The envisaged systems for the highly selective defunctionalisation can be based on catalytic dehydration-hydrogenation, decarboxylation, decarbonylation, or dehydroxylation strategies. For example, the defunctionalization pathway of LA to 2-MTHF, that was selected according to the criteria defined above, comprises a series of consecutive hydrogenation and dehydration steps. Therefore, it requires a multifunctional catalytic system, which was not available at the beginning of the study [1]. Thus, the conceptually combined analysis of the energetic balance and the required molecular transformations allows identification of defined challenges for catalyst development.

The sequence of molecular transformations from LA via γ -valerolactone (GVL), to 1,4-pentanediol (1,4-PDO), and finally 2-MTHF is shown in the scheme in Figure 12.2. The stepwise process consists of a consecutive series of hydrogenations (green) and dehydrations (blue) via well-defined, but short-lived intermediates (in brackets). Initially, the keto function of LA is reduced to γ -hydroxy carboxylic acid, and spontaneous intramolecular esterification yields γ -valerolactone (GVL). The reduction of the C=O bond gives a hemiacetal, which is in equilibrium with the open hydroxy aldehyde. A further hydrogenation step then

forms 1,4-pentane-diol (1,4-PDO). Finally, acid catalyzed intramolecular etherification yields 2-MTHF.

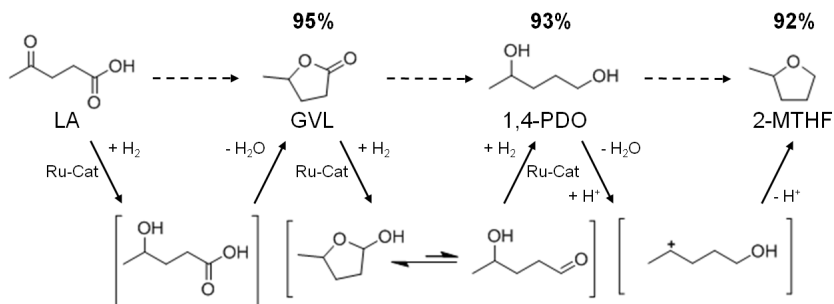


Figure 12.2: Reaction sequence and maximum yields for the selective conversion of levulinic acid (LA) into γ -valerolactone (GVL), 1,4-pentanediol (1,4-PDO), and 2-methyltetrahydrofuran (2-MTHF)

For the initial hydrogenation step of LA to GVL, heterogeneous systems were applied previously with great success and ruthenium catalysts supported on carbon showed favorable selectivity [4]. Recently, the combination of ruthenium on silica and supercritical CO₂ as reaction and extraction media even enabled the continuous production of GVL from LA [5]. Horvath and co-workers were able to apply a homogeneous ruthenium system based on Ru(acac)₃ and a monodentate phosphine ligand for this transformation. This system promoted quantitative conversion of LA to GVL after 8 hours at a moderate reaction temperature of 135 °C [6]. Based on these pioneering studies [6, 7], a multifunctional system based on the ruthenium precursor Ru(acac)₃, a phosphine ligand, and suitable additives were developed. As LA has a melting point of 31–33 °C and a high thermal stability, it provides a suitable reaction medium for the homogeneously catalyzed processes without the need of the addition of any external solvent. The key feature of this new system represents the tuneable product selectivity by control of the hydrogenation activity through the choice of ligand combined with adjustment of the acidity of the reaction medium through the additives (Figure 12.3). With the monodentate ligand trioctylphosphine P(*n*-Oct)₃, GVL is formed in almost quantitative yield in agreement with literature data [6–8]. The use of the tripodal phosphine ligand 1,1,1-tris(diphenylphosphinomethyl)ethane (triphos) leads to a significantly more active hydrogenation catalyst that reduces the cyclic ester further. In absence of additives, 1,4-PDO is formed in 95% yield. The addition of the acidic ionic liquid (4-sulfobutyl)imidazolium-p-toluenesulfonate shifts the

hydrogenation beyond the diol stage giving 2-MTHF in 87% yield. This could be even further improved to 92% yield by using additional stabilization by NH_4PF_6 in catalytic amounts. With this modular catalyst system, three valuable products are accessible in excellent yields from one substrate, emphasizing the potential of the selective defunctionalization approach. The scheme in Figure 12.2 summarizes the optimum yields for the direct conversion of LA and the remarkable control and flexibility offered by the multifunctional molecular catalyst system.

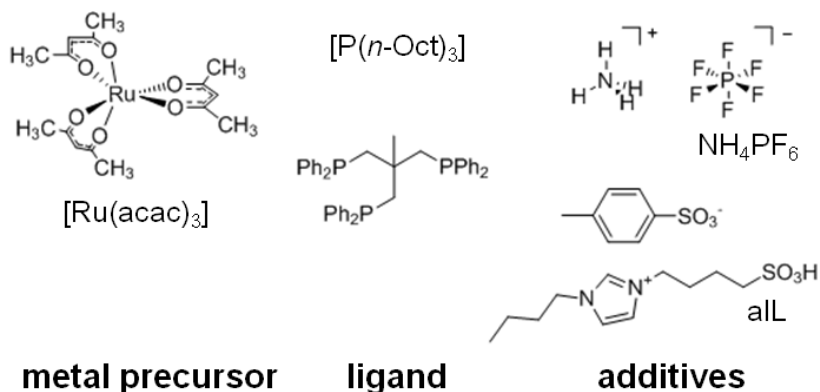


Figure 12.3: Components for the generation of the multifunctional catalyst. aIL: acidic ionic liquid

While 1,4-PDO is primarily interesting for applications in the polymer industry [9], GVL and 2-MTHF are discussed as promising fuel candidates. GVL has been employed as additive in diesel and gasoline fuels with a RON of 96 [7]. 2-MTHF has a lower oxygen content as well as a higher combustion enthalpy and therefore should exhibit beneficial engine properties. In fact, a blend of 70% 2-MTHF and 30% dibutylether showed promising results in diesel engine tests. In comparison to standard EN595 diesel, the oxygenate blend allowed a nearly soot-free combustion even at high engine loads. Furthermore, hazardous NO_x emissions could be significantly reduced due to the low internal combustion temperature [10]. Previously, 2-MTHF has been already approved by the U.S. Department of Energy as an additive in gasoline blends which consist of 35% liquids from natural gas and 45% ethanol. These P Type series fuels exhibit octane numbers ranging from 89 to 93.

The ruthenium/triphos catalyst system, which efficiently promoted the conversion of the C_6 -sugar derived platform molecule LA, could also be readily

adapted to the intermediate itaconic acid (IA), which can be assessed at least in principle by fermentation routes from C₆ or C₅-sugars. This substrate cannot be used for neat reactions, but bio-based MTHF could be used as a reaction solvent. The detailed transformation sequence is shown in Figure 12.4. In analogy to the LA reduction, the transformation of IA to 3-methyltetrahydrofuran (3-MTHF) involves a series of hydrogenation and dehydration steps. The hydrogenation of the C=C bond in IA to form methyl succinic acid (MSA) is straightforward with ruthenium phosphine catalysts, but the reduction of the free carboxylic acid function with molecular hydrogen is very challenging for a homogeneous organometallic catalyst. Reduction of one carboxyl group and subsequent intramolecular esterification yields 2- and 3-Methyl- γ -butyrolactone (3- and 2-MGBL). At 180 °C selective formation of the two isomeric lactones was obtained in a combined yield of about 80% with the Ru/triphos catalyst in the absence of any additives. Once this lactone stage is reached, further conversion into 2-methylbutanediol (2-MBDO) and the tetrahydrofuran derivative 3-MTHF is achieved by increasing the temperature above 195 °C and can be controlled as for LA through the choice of additives. The diol 2-MBDO could be obtained in excellent yield of up to 93% and the combination of p-toluenesulfonic acid (p-TsOH) and NH₄PF₆ as additive afforded 3-MTHF in 95% yield.

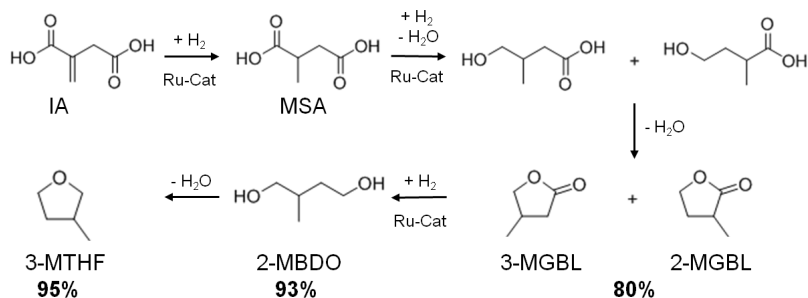


Figure 12.4: Reaction sequence and maximum yields for the selective conversion of itaconic acid (IA) into lactones (MGBL), 2-methylbutanediol (2-MBDO), and 3-methyltetrahydrofuran (3-MTHF)

In order to gain insight into the mechanistic details of the catalytic cycle, a density functional theory (DFT) study was performed and corroborated with experimental data from catalytic processes and NMR investigations. For the cationic fragment [Ru(triphos)H]⁺ as catalytically active unit, a common mechanistic pathway for the reduction of the C=O functionalities in the various substrates

could be identified (Figure 12.5) [11]. The reduction results from hydride transfer on to the carbonyl or carboxyl carbon via transition states typical for migratory insertion. The subsequent hydrogenolysis of the metal-oxide unit involves proton transfer via σ -bond metathesis from a coordinated dihydrogen molecule, regenerating at the same time the catalytically active Ru-H unit. The interplay between the classical and the non-classical metal hydride coordination provides an overall pathway that does not require changes in the formal oxidation state of the ruthenium center. The energetic spans for the reduction of the different functional groups increase in the order aldehyde < ketone < lactone \approx carboxylic acid. Although other mechanistic principles cannot be excluded at this stage, this reactivity pattern as well as the absolute values for the energy barriers are in full agreement with experimentally observed activities and selectivities, forming a rational basis for further catalyst development.

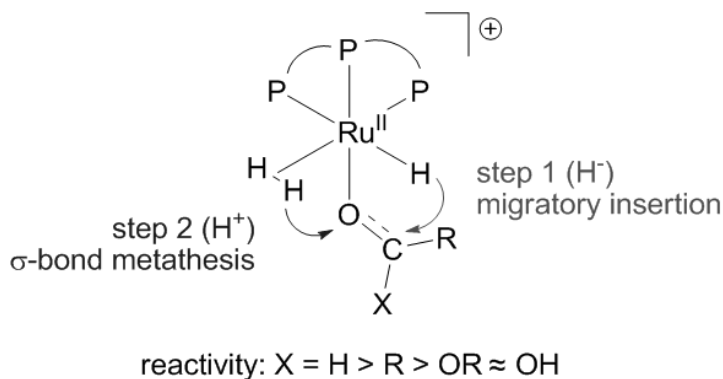


Figure 12.5: Possible common mechanism for the reduction of carbonyl and carboxyl groups using the Ru-triphos catalytic system

Based on the optimized reaction conditions, a flow sheet for a possible continuous production process for 2-MTH from LA was developed with methods of conceptual process design (Figure 12.6, [1]). In the optimum process scenario, hydrogen and levulinic acid are heated and compressed to reaction conditions and fed into a plug flow reactor. The homogeneous catalyst system is introduced with the liquid substrate in the starting phase of the process. The solvent-free conditions greatly facilitate the isolation and downstream processing of the 2-MTHF product. Under continuous conditions the reactor effluent is vaporized and the remaining liquid stream containing the catalyst and additives is recycled into the

reactor. The vapour stream from the flash distillation, which consists of the products 2-MTHF and the water formed from the dehydration steps, is condensed and fed to the decanter of a hetero-azetropic distillation system. The product is recovered in high purity at the bottom of the respective column.

Heat integration between the catalyst recycling and the product recovery can significantly reduce the energy demand of the process, which is in the order of 3% of the energy content of the recovered 2-MTHF. A preliminary economic evaluation revealed that the production costs are dominated mainly by raw materials and catalyst costs. Catalyst productivities corresponding to a turnover number in the order of 10^5 mol product/mol Ru were estimated to be necessary for the process to become feasible. Although a challenging target, this is well in the range of TON values obtained with transition metal phosphine catalysts in industrial applications [12] or with advanced immobilization concepts [13, 14]. It is also important to note that the process does not critically depend on the economy of scale, in contrast to conventional refinery or BTL units. This makes this approach well compatible with the logistics of biomass utilization, which are expected to be more decentralized than current refinery technology due to the large areal distribution of typical lignocellulosic feedstock.

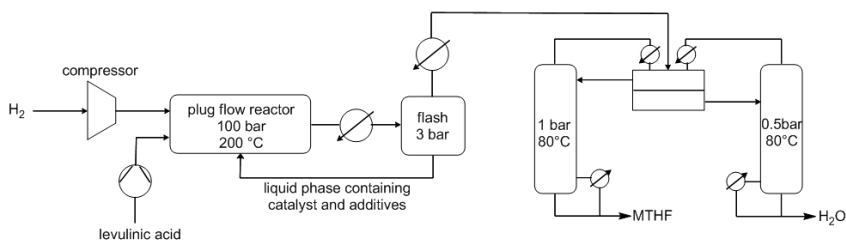


Figure 12.6: Flow sheet for a possible LA to 2-MTHF process

12.3.2 Chemicals and Fuels from the Platform Molecules Furfural and 5-HMF

As can be seen in Figure 12.1, further derivatives from tetrahydrofuran or furan structures can be obtained starting from 5-HMF. Iterative progress in the product design suggests that these compounds provide access to further potential fuels, in particular by variation of the carbon number and potential esterification or etherification of the -OH groups [15]. The currently established production route of tetrahydrofurfuryl alcohol (THFA) is based on the hydrogenation of furfural (FF), which is produced on industrial-scale through dehydration of C₅-sugars. In

light of the larger availability of the C₆-sugars over C₅-sugars in biomass feedstock, it would be attractive to gain access to THFA and its follow-up products from the C₆-sugar platform if fuel applications are envisaged. In this respect the decarbonylation of 5-hydroxymethylfurfural (5-HMF) would represent a viable entry point (Figure 12.7). 5-HMF is accessible from C₆-sugars via dehydration processes, albeit the currently employed starting material to obtain high yields is fructose. Due to the high functionalization of 5-HMF, the compound is very reactive and prone to polymerization yielding tar-like humins at higher temperatures. Additionally, the further transformation to the coupled products levulinic acid and formic acid often leads to complex mixtures and only modest yields.

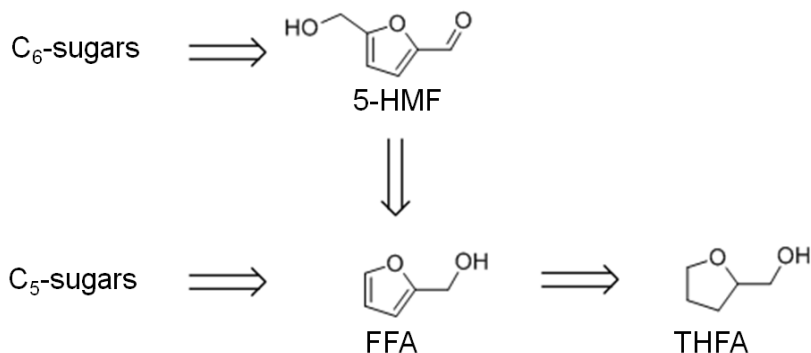


Figure 12.7: Retrosynthetic connection of the C₆ and C₅ sugar process chains for furfuryl alcohol (FFA) and tetrahydrofurfuryl alcohol (THFA)

The combination of an efficient iridium-based catalyst in combination with an optimized reaction medium enabled to overcome these limitations at least partly, opening for the first time access to the cyclic C₅ alcohols from the C₆ feedstock via decarbonylation. The catalyst system was prepared from the iridium precursor [Ir(COD)Cl]₂ and a monodentate phosphine ligand (tricyclohexylphosphine or trioctylphosphine) [16]. In this decarbonylation reaction the addition of 50 bar CO₂ pressure successfully suppressed the undesired polymerization/decomposition processes, most likely by formation of an expanded liquid phase [14]. Thus, full conversion of 5-HMF to FFA could be obtained with 95 % selectivity after 12 hours (Figure 12.8). Beyond the specific target molecule, this result demonstrates that decarbonylation provides a useful route for the reduction of the oxygen content in bio-based supply chains, avoiding the use of high-energy and costly hydrogen equivalents.

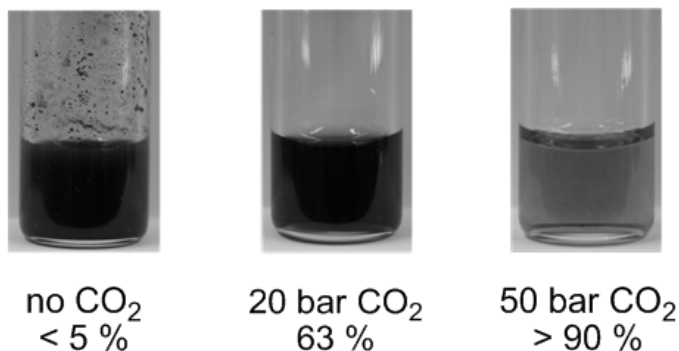


Figure 12.8: Product mixtures and FFA yields of the decarbonylation after reaction under different CO₂ pressures

The resulting furfuryl alcohol (FFA) is readily hydrogenated by ionic liquid stabilized Ru-nanoparticles to obtain tetrahydrofurfuryl alcohol (THFA), yet another target molecule for engine applications. In addition, THFA could also be used as a solvent for the decarbonylation as well as for the hydrogenation reaction, highly facilitating subsequent downstream processing (Figure 12.9). A reasonably high octane number of 83 was reported for both FFA and THFA and detailed properties as fuel additives are consequently under current investigation.

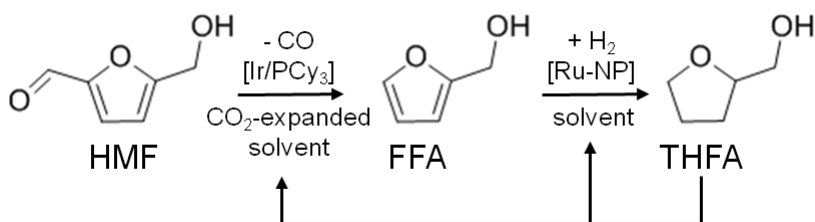


Figure 12.9: The integrated development and optimization of catalysts and reaction media lead to a highly selective decarbonylation of 5-HMF to FFA with an iridium/phosphine-catalyst in the presence of compressed carbon dioxide. Subsequent hydrogenation over ruthenium nanoparticles leads to THFA, a possible solvent for the decarbonylation reaction.

Another furan-derivative based on 5-HMF, which has shown interesting combustion properties is 2,5 Dimethylfuran (2,5-DMF) [17]. Dumesic and co-workers developed an integrated catalytic system, which enabled the direct conversion of fructose to 2,5-DMF [18]. First, fructose is dehydrated to 5-HMF by HCl in aqueous media, while a second organic layer allows in-situ extraction leading to a high selectivity toward 5-HMF. Once HCl and water are removed by evaporation, this extracting phase is fed directly to a hydrogenolysis reactor. Here, a carbon-supported copper-ruthenium catalyst efficiently promotes the deoxygenation of 5-HMF with four equivalents of hydrogen to afford 2,5-DMF. Finally, the product and water contaminants are evaporated from the reaction solution, which can be recycled back to the dehydration reactor. Since 2,5-DMF is not miscible with water, it separates spontaneously and therefore can be easily isolated. In this way the bio-catalytic formation of fructose, followed by homogeneously acid-catalyzed dehydration and heterogeneously catalyzed deoxygenation of 5-HMF are efficiently coupled into an integrated process concept.

In addition, the key intermediates of the C₆ and C₅ carbohydrate platform, 5-hydroxymethylfurfural (5-HMF) and furfural, can also be further modified by the incorporation of additional building blocks, for example through aldol-condensation with acetone, leading to compounds with higher carbon numbers (Figure 12.10). Such compounds are promising targets, in particular for blending, to account for limitations in ignition delays and evaporation properties of the fuel molecules discussed up to now [19].

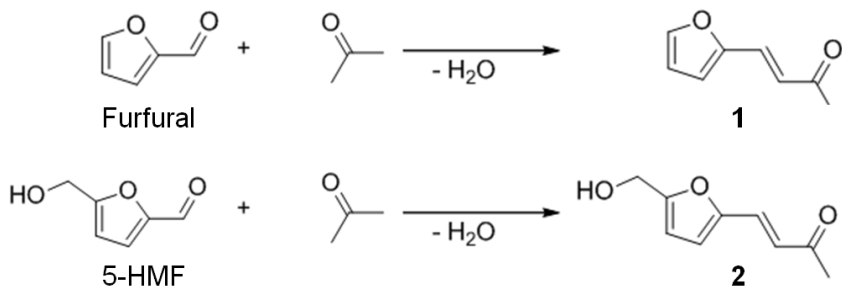


Figure 12.10: Aldol-condensation of biomass-derived furfuryl derivatives with acetone

Selective hydrogenation of the primary products 1 and 2 gives access to a range of increasingly saturated structures. Deep hydrogenation to the corresponding alkanes has been achieved by heterogeneously catalyzed reactions for both

furfuryl derivatives and proposed as a selective route to individual linear alkanes [20]. The intermediate hydrogenation products are also of interest, as they offer various options for further derivatization depending on the remaining functionalities (aromatic, olefinic, C=O, C–OH). Figure 12.11 shows possible hydrogenation products that have not been deoxygenated, highlighting the challenge for the development of selective catalysts and processes to control their formation.

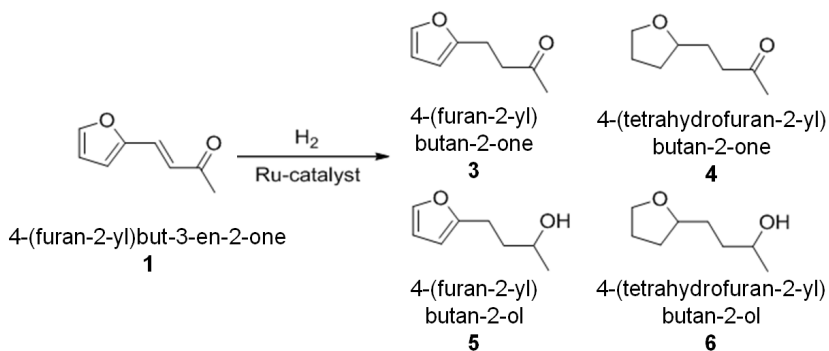


Figure 12.11: Hydrogenated target structures derived from the aldol-condensation product (**1**) of furfural with acetone (4-(2-furyl)-3-butene-2-one)

For the selective hydrogenation of the biomass-derived 4-(furan-2-yl)but-3-en-2-one (**1**) catalysts based Ru-nanoparticles stabilized in ionic liquid matrices (Ru@IL) were investigated [21]. The size of the nanoparticles, as well as their catalytic activity and selectivity can be controlled by variation of the respective IL. The novel catalyst systems were highly active and therefore excellent catalysts for the hydrogenation of C=O and C=C bonds, as well as for the heteroaromatic ring. Moreover, they show interesting selectivities, which differ from classic homogeneous and heterogeneous Ru-catalysts. The catalytic performance of Ru@[C₁₂MIM][BTA] was compared with the catalytic behavior of classic heterogeneous (ruthenium on alumina) and homogeneous ([RuHCl(PPh₃)₃]) catalysts under identical reaction conditions. The Ru@[C₁₂MIM][BTA] catalyst allowed production of either product **4** or **6** with high selectivity, whereas the homogeneous organometallic complex is very selective for the C=C bond hydrogenation to give **3**. At high temperature and hydrogen pressure, the classical heterogeneous catalysts Ru on alumina leads to **6** as the major product. At mild conditions, Ru@[C₁₂MIM][BTA] gave a more selective system that allowed ac-

cess to the individual products in fair to good yields. Monitoring the course of reaction showed that the hydrogenation of **2** with Ru@[C₁₂MIM][BTA] occurred as a consecutive reaction (Figure 12.12). Initially the C=C double bond of the substrate was hydrogenated, followed by the hydrogenation of the heteroaromatic ring and finally the reduction of the carbonyl group.

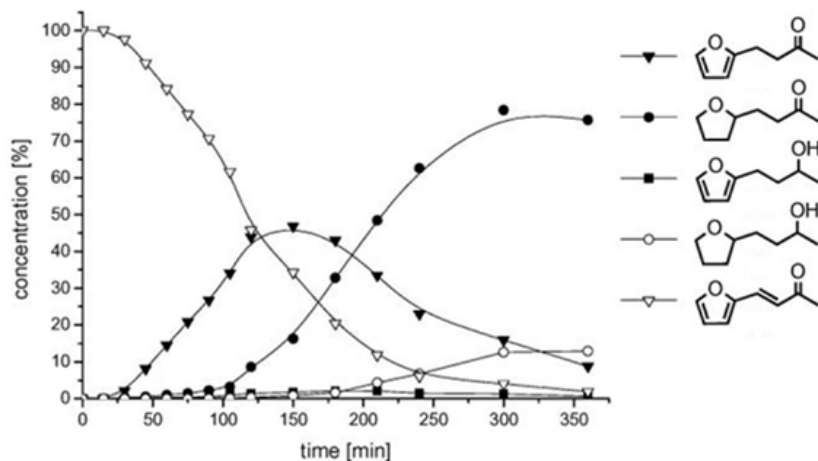


Figure 12.12: Conversion-time profile for the hydrogenation of 4-(2-furyl)-3-buten-2-one **1** using Ru@[C₁₂MIM][BTA] at T = 60 °C and p(H₂) = 60 bar, indicating high selectivity toward product **4**. Compound **6** can be obtained in 90% yield under more forcing conditions (T = 120 °C, p(H₂) = 120 bar)

The IL-stabilized nanoparticles were found to be readily separated from the products, showing excellent stability and recyclability. The products can be efficiently extracted from the ionic liquid phase by supercritical CO₂, opening the possibility for continuous-flow processes [13, 14]. In repetitive batch-mode, the immobilized ruthenium nanoparticles led to full conversion under standard conditions even after several consecutive cycles. This finding was also supported by TEM measurements, which showed no apparent agglomeration of the nanoparticles. Furthermore, inductively-coupled-plasma mass-spectrometry (ICP-MS) analysis of the isolated products showed a ruthenium contamination below 5 ppm in the product samples, indicating efficient prevention of metal leaching.

12.4 From Lignocellulosic Raw Materials to Carbohydrate Feedstock and Platform Molecules

A preliminary economic and ecologic analysis of the pathways shown in Figure 12.1 indicates that they provide viable options for sustainable production routes, provided that the platform chemicals are accessible at economic and energetic costs required for typical bio-refinery concepts. The fractionation of the complex and highly functionalized raw material lignocellulose to generate the three main feedstock streams cellulose, hemicellulose and lignin imposes a crucial challenge in this context [22]. As the initial pre-treatment of the raw material represents the entry point into every production route of renewable chemicals and fuels, it is essential to develop highly efficient and selective fractionation processes [23]. This implies the fractionation and separation of hemicellulose (mostly pentose sugars like xylose), cellulose (purely glucose) and the aromatic polymer lignin for subsequent transformation in the production of biofuels, commodities and other high-added-value products. Due to the recalcitrant nature of lignocellulose, current pre-treatment processes are often performed at harsh reaction conditions, leading to concomitant biomass degradation and waste formation. Thus, in order to enable an efficient and sustainable valorization of biomass, an ideal fractionation process should achieve the disentanglement of lignocellulose in a single step, while employing mild reaction conditions and ideally renewable reactants. In a recent approach toward this goal, the catalytic pretreatment of lignocellulose was performed in a biphasic reaction system comprising an aqueous phase containing oxalic acid as catalyst and 2-MTHF as biogenic organic solvent [24]. The conceptual process scheme, combining the selective hydrolysis of hemicellulose with a biphasic separation of lignin is illustrated in Figure 12.13.

In a typical reaction setup, a slurry of beech wood in a biphasic solvent system comprised of dilute aqueous oxalic acid solution (0.1 M) and 2-methyltetrahydrofuran (2-MTHF) is heated at temperatures ranging from 80–125 °C. Under these conditions the hemicellulose fraction is quantitatively depolymerized to sugar monomers (mainly xylose) via acid catalyzed hydrolysis of the glycosidic bonds. The cellulose fraction is not depolymerized and precipitates as solid residue. Subsequent enzymatic depolymerization of the obtained cellulose pulps with the commercially available enzymatic catalysts, Accellerase-1500 R (Genencor), showed promising activities giving 3.5 g of soluble reducing-end sugars per liter and hour. This indicates that lignin is efficiently removed from the pulp during the process. Indeed, a water insoluble lignin fraction, which is released during the disintegration of the hemicellulose fraction, is extracted into the organic layer and can be isolated by the subsequent removal of the volatile organic 2-MTHF phase.

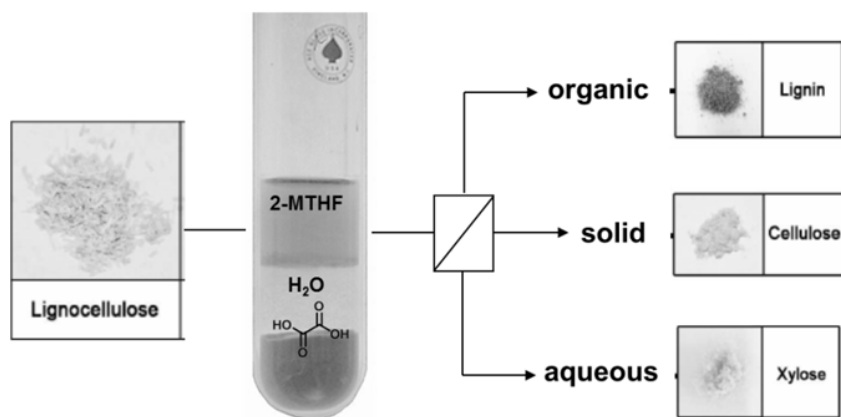


Figure 12.13: Process scheme of one-step lignocellulose fractionation system

The basic principle of this approach is based on the combination of molecular selectivity and selective extraction of the catalytic system: the applied catalyst oxalic acid is able to depolymerize only the amorphous hemicellulose regions under these conditions, whereas the partly crystalline areas of cellulose-pulp are not cleaved at the applied temperatures. At the same time, the second organic phase enables an efficient in-situ extraction of lignin. With this approach, lignocellulose can be disintegrated into its three major constituents in a single step. With respect to sustainability criteria, this concept benefits from the exclusive use of bio-derived solvents and reagents. Furthermore, recrystallization of the oxalic acid from the aqueous effluent enables straightforward catalyst recycling.

Whatever the most efficient process for the disintegration of biomass ultimately will be, the next important step on the pathway from lignocellulosic raw material to the desired platform chemical relates to the conversion of cellulose (the most abundant renewable feedstock) to glucose. In principle, the catalytic cleavage of the glycosidic bonds in cellobiose or cellulose can be achieved with enzymes or Brønsted acids [25]. However, due to its highly crystalline structure, the essential hurdle is the limited accessibility of cellulose, which is responsible for the low reactivity in such systems. Consequently, reagents able to disrupt the crystalline network before catalytic depolymerization are needed. In this respect, the use of ionic liquids (ILs) in biomass pretreatment enabled the facile disruption of the intrinsic hydrogen bonding between cellulose fibres, and promoted the subsequent dissolution [26].

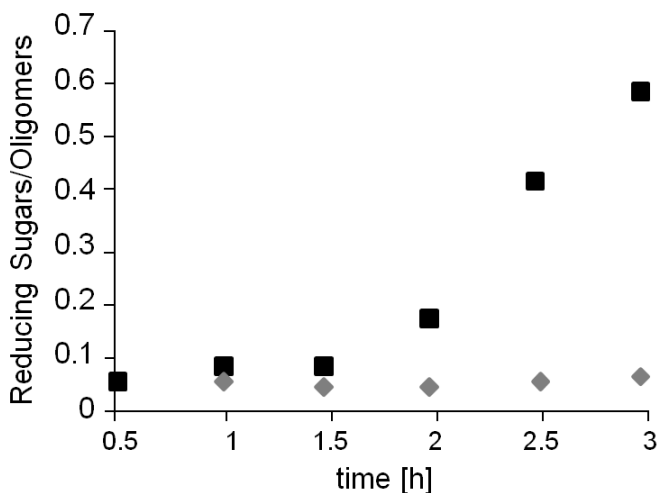


Figure 12.14: Effect of sodium chloride on hydrolysis of crystalline Avicel®. Diamond: Only oxalic acid. Square: Oxalic acid with 30 wt% NaCl. Reaction conditions: 20 mg Avicel®, 1 mL aqueous NaCl solution (30 wt%), 0.1 M oxalic acid, 105 °C.

Ionic liquids are organic salts with melting points below 100 °C, exhibiting interesting physico-chemical properties that can be tuned widely by molecular design of the cations and anions. Especially acetate and chloride based ILs were found to exhibit unique solvent properties for cellulose and even wooden biomass [27]. Accordingly, ionic liquids greatly enhance the activity in cellulose depolymerization. For example, Schüth et al. reported the combination of the solid acid catalyst Amberlyst 15-Dry and ionic liquid 1-butyl-3-methylimidazolium chloride (BMIMCl), promoting an efficient depolymerization of cellulose to water soluble glucose oligomers under mild conditions [28].

Based on the understanding of the interaction of ILs with the hydrogen bonding network of cellulose, other systems have been developed to mimic the solubility properties with cheaper and more readily recycled materials. Thus, the combination of a simple sodium chloride solution with oxalic acid as catalyst enabled the hydrolysis of highly crystalline Avicel® cellulose at mild reaction conditions (see Figure 12.14, [29]). Even concentrated seawater could be used as processing medium in combination with suitable mild acids. In general, the combination of strong electrolytes that disrupt the hydrogen bonding network of cellulose [30]

together with mild acidic media for the selective cleavage of the glycosidic bonds provides an interesting alternative to enzymatic depolymerization processes.

The techniques to produce carbohydrate fractions and feedstocks from lignocellulose are constantly improving and new innovations are emerging, strongly stimulated also by the increasing efforts to implement second generation bioethanol on a commercial scale [31]. In addition to these challenges, de-bottlenecking is also necessary for the production of the intermediate platform chemicals derived thereof. While the fermentative production of itaconic acid from green biomass is currently in a very preliminary stage [32], levulinic acid and 5-HMF are accessible at least in principle via already established processes, albeit economic constraints are still to be overcome.

Especially levulinic acid is of increasing interest as a primary platform chemical due to its relatively simple production from acid treatment of fructose or glucose (Figure 12.15). The required dehydration reaction is promoted by a number of catalysts, and recent developments include examples ranging from simple Brønsted acids and Lewis acids to heterogeneous catalysts (e.g., zeolites) [33]. The major drawback in this transformation is associated with the thermal instability of the intermediately formed 5-HMF, which tends to polymerize at elevated temperatures. Therefore, the catalyst, reaction media and reaction conditions have to be carefully adapted. In addition, while glucose represents the most abundant hexose, its susceptibility for the dehydration reaction is largely inferior to that of fructose and consequently effective isomerization reactions have been developed in recent years. Especially the combination of chromium dichloride (CrCl_2) and the ionic liquid 1-ethyl-3-methylimidazolium chloride (EMIMCl) showed high conversions for the direct transformation of glucose, presumably via in situ isomerization [34].

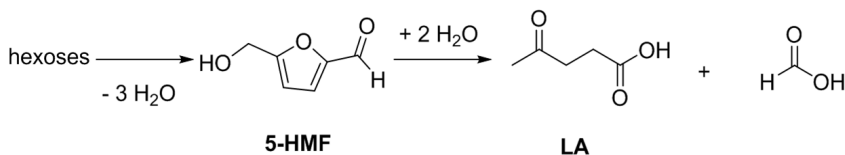


Figure 12.15: Production of 5-HMF and LA from hexoses

12.5 Conclusion and Outlook

The selective conversion of lignocellulosic biomass provides a possible approach to the sustainable production of fuels and chemical products. Studies of the Clus-

ter of Excellence as well as from other groups around the world demonstrate that the synthetic pathways can be competitive in terms of energy and carbon efficiency to the conventional routes of second generation biofuels. Whereas the latter search mainly for substitutes of existing products, the new approaches aim at improved and tailor-made products. This paradigm shift overcomes the purely limitation-driven (resources or economics) approach to biomass research, opening the field for innovative solutions that may go way beyond a mere feedstock alternative. However, long-term fundamental research is clearly required to reach this ambitious, yet highly attractive goal, which may equally apply to fuels and chemical products.

1. Product design: although significant progress has been made in certain areas such as pharmaceuticals, our understanding of the relationship between molecular structures and application properties is still often severely limited for many chemical products. The fuel sector, where properties are largely described via lumped parameters such as octane or cetane numbers, provides a very illustrative example. This becomes even more challenging when several sustainability criteria such as performance, costs, toxicity, and eco-toxicity have to be combined and balanced within a multi-parameter optimization problem.
2. Pathway design: The retrosynthetic approach described herein offers a general guideline for the identification and selection of promising pathways. However, the toolbox of classical organic chemistry is currently not widely applicable in these scenarios, as it aims at functionalization, rather than de- and re-functionalization in most cases. Hence, new catalytic methodologies have to be developed, capitalizing on the huge potential of homogeneous, heterogeneous, and bio-catalytic methods. Along the value chain, it is likely that enzymatic and fermentative processes will have to be combined with chemo-catalytic methods in order to create flexible supply networks. As highlighted in the present chapter, the carbohydrate fraction of lignocellulose shows already some promising possibilities in this respect. Lignin, however, the third major constituent of biomass, is fundamentally different and the very heterogeneous structure of the aromatic biopolymer and its linkages make it difficult to envisage a similar strategy based on platform chemicals [35]. Selective bond cleavage reactions have to be developed if defined molecular structures need to be carved out from the complex lignin structures [36].
3. Process design: Entering a chemical or energetic supply chain with high molecular weight and highly functional starting materials requires process strategies that are fundamentally different from current refinery concepts. Liquid-phase processes will prevail, and hence separation processes have

to be based more on differences in solubility rather than on volatility. Consequently, extraction will gain increasing importance in early stages of the supply chain relative to rectification. The use of advanced fluids such as ionic liquids or supercritical fluids can provide novel approaches for liquid-type processes, albeit the economic constraints are obviously very stringent in this sector. Again, however, several seemingly conflicting aspects have to be balanced, disconnecting for example the classical strategy of economy of scale in refineries from the decentralized logistics of biomass production.

In addition to these specific challenges for the selective conversion approach, the sustainable cultivation and supply with biomass as raw material is a key issue for all scenarios concentrating on renewable resources. Although it is clear that biomass cannot provide enough energy carriers for a full replacement of the entire current fuel consumption, it provides a viable option to address the areas where liquid fuels are inevitable (see Introduction) [37]. Increasing productivity of biomass generation, reducing the land use that might compete with other needs, and any strategy that reduces the consumption of soil and water will all have an enormous impact on the sustainability of a future bioeconomy. Ultimately, however, these necessary improvements can only be exploited if suitable processes are available to convert the raw material into the final products that are required to fulfill the needs of mankind in the energetic and material supply chain.

Acknowledgments

The work from our group described in this conceptual review was funded within the Initiative of Excellence of the German Government as part of the Cluster of Excellence *Tailor-Made Fuels from Biomass (TMFB, EXC 236)*. The fruitful collaboration within the Cluster is gratefully acknowledged, especially with Profs. Wolfgang Marquardt, Stefan Pischinger, Ferdi Schüth, and Regina Palkovits, and Drs. Pablo Dominguez de Maria, Markus Hölscher, Nils Theyssen, Roberto Rinaldi, and Martin Müther.

Bibliography

- [1] F.M.A. Geilen, B. Engendahl, A. Harwardt, W. Marquardt, J. Klankermayer, and W. Leitner. Selective and Flexible Transformation of Biomass-Derived Platform Chemicals by a Multifunctional Catalytic System. *Angewandte Chemie International Edition* 49 (2010):5510–5514.
- [2] G.W. Huber, S. Iborra, and A. Corma. Synthesis of Transportation Fuels from Biomass: Chemistry, Catalysts, and Engineering. *Chemical Reviews* 106 (2006):4044–4098.
- [3] A. Voll and W. Marquardt. Reaction Network Flux Analysis: Optimization-Based Evaluation of Reaction Pathways for Biorenewables Processing. *American Institute of Chemical Engineers Journal* (2011).
- [4] L.E. Manzer. Catalytic Synthesis of α -Methylene- γ -Valerolactone: A Biomass-Derived Acrylic Monomer. *Applied Catalysis A: General* 272 (2004): 249–256.
- [5] R.A. Bourne, J.G. Stevens, J. Ke, and M. Poliakoff. Maximising Opportunities in Supercritical Chemistry: The Continuous Conversion of Levulinic Acid to γ -Valerolactone in CO_2 . *Chemical Communications* 44 (2007):4632–4634.
- [6] H. Mehdi, V. Fabos, R. Tuba, A. Bodor, L. T. Mika, and I. T. Horvath. Integration of Homogeneous and Heterogeneous Catalytic Processes for a Multi-step Conversion of Biomass: From Sucrose to Levulinic Acid, γ -Valerolactone, 1,4-Pentanediol, 2-Methyl-tetrahydrofuran, and Alkanes. *Topics in Catalysis* 48 (2008):49–54.
- [7] I.T. Horvath, H. Mehdi, V. Fabos, L. Boda, and L.T. Mika. γ -Valerolactone - A Sustainable Liquid for Energy and Carbon-Based Chemicals. *Green Chemistry* 10 (2008):238–242.
- [8] L. Deng, J. Li, D.-M. Lai, Y. Fu, and Q.-X. Guo. Catalytic Conversion of Biomass-Derived Carbohydrates into γ -Valerolactone without Using an External H_2 Supply. *Angewandte Chemie International Edition* 121 (2009):6651–6654.
- [9] A. Corma, S. Iborra, and A. Velty. Chemical Routes for the Transformation of Biomass into Chemicals. *Chemical Reviews* 107 (2007):2411–2502.

- [10] A.J. Janssen, F.W. Kremer, J.H. Baron, M. Muether, S. Pischinger, and J. Klankermayer. Tailor-Made Fuels from Biomass for Homogeneous Low-Temperature Diesel Combustion. *Energy Fuels* (2011).
- [11] F.M.A. Geilen, B. Engendahl, M. Hoelscher, J. Klankermayer, and W. Leitner. Selective Homogeneous Hydrogenation of Biogenic Carboxylic Acids with [Ru(TriPhos)H](+): A Mechanistic Study. *Journal of the American Chemical Society* 133 (2011):14349–14358.
- [12] H.-U. Blaser. The Chiral Switch of (S)-Metolachlor: A Personal Account of an Industrial Odyssey in Asymmetric Catalysis. *Advanced Synthesis & Catalysis* 344 (2002):17–31.
- [13] U. Hintermair, T. Hoefener, T. Pullmann, G. Francio, and W. Leitner. Continuous Enantioselective Hydrogenation with a Molecular Catalyst in Supported Ionic Liquid Phase under Supercritical CO₂ Flow. *ChemCatChem* 2 (2010):150–154.
- [14] U. Hintermair, G. Francio, and W. Leitner. Continuous Flow Organometallic Catalysis: New Wind in Old Sails. *Chemical Communications* 47 (2011): 3691–3701.
- [15] M. Hechinger, A. Voll, and W. Marquardt. Towards an Integrated Design of Biofuels and their Production Pathways. *Computers and Chemical Engineering* 34 (2010):1909–1918.
- [16] F.M.A. Geilen, T. vom Stein, B. Engendahl, S. Winterle, M.A. Liauw, J. Klankermayer, and W. Leitner. Highly Selective Decarbonylation of 5-(Hydroxymethyl)furfural in the Presence of Compressed Carbon Dioxide. *Angewandte Chemie* 123 (2011):6963–6966.
- [17] G. Tian, R. Daniel, H. Li, H. Xu, S. Shuai, and P. Richards. Laminar Burning Velocities of 2,5-Dimethylfuran Compared with Ethanol and Gasoline. *Energy Fuels* 24 (2010):3898–3905.
- [18] Y. Roman-Leshkov, C.J. Barrett, Z.Y. Liu, and J.A. Dumesic. Production of Dimethylfuran for Liquid Fuels from Biomass-Derived Carbohydrates. *Nature* 447 (2007):982–985.
- [19] R. Xing, A.V. Subrahmanyam, H. Olcay, W. Qi, G.P. van Walsum, H. Pendse, and G.W. Huber. Production of Jet and Diesel Fuel Range Alkanes from Waste Hemicellulose-Derived Aqueous Solutions. *Green Chemistry* 12 (2010):1933–1946.
- [20] E.L. Kunkes, D.A. Simonetti, R.M. West, J.C. Serrano-Ruiz, C.A. Gaertner, and J.A. Dumesic. Catalytic Conversion of Biomass to Monofunctional Hydrocarbons and Targeted Liquid-Fuel Classes. *Science* 322 (2008):417–421.

- [21] J. Julis, M. Hoelscher, and W. Leitner. Selective Hydrogenation of Biomass Derived Substrates using Ionic Liquid-Stabilized Ruthenium Nanoparticles. *Green Chemistry* 12 (2010):1634–1639.
- [22] B. Kamm, P.R. Gruber, and M. Kamm. *Biorefineries—Industrial Processes and Products. Status Quo and Future Directions*. 1st ed. Weinheim: Wiley-VCH, 2006.
- [23] J.-P. Lange. Lignocellulose Conversion: An Introduction to Chemistry, Process and Economics. *Biofuels, Bioprod. Bioref.* 1 (2007):39–48.
- [24] T. vom Stein, P.M. Grande, H. Kayser, F. Sibilla, W. Leitner, and P. Dominguez de Maria. From Biomass to Feedstock: One-Step Fractionation of Lignocellulose Components by Selective Organic-Acid Catalyzed Depolymerization of Hemicellulose in a Biphasic System. *Green Chemistry* 13 (2011):1772–1777.
- [25] R. Rinaldi and F. Schüth. Acid Hydrolysis of Cellulose as the Entry Point into Biorefinery Schemes. *ChemSusChem* 2(12) (2009):1096–1107.
- [26] D.A. Fort, R.C. Remsing, R.P. Swatloski, P. Moyna, G. Moyna, and R.D. Rogers. Can Ionic Liquids Dissolve Wood? Processing and Analysis of Lignocellulosic Materials with 1-n-Butyl-3-Methylimidazolium Chloride. *Green Chemistry* 9 (2007):63–69.
- [27] C. Sievers, M.B. Valenzuela-Olarte, T. Marzialetti, I. Musin, P.K. Agrawal, and C.W. Jones. Ionic Liquid Phase Hydrolysis of Pine Wood. *Industrial & Engineering Chemistry Research* 48 (2009):1277–1286.
- [28] R. Rinaldi, R. Palkovits, and F. Schüth. Depolymerization of Cellulose by Solid Catalysts in Ionic Liquids. *Angewandte Chemie* 120 (2008):8167–8170.
- [29] T. vom Stein, P. Grande, F. Sibilla, U. Commandeur, R. Fischer, W. Leitner, and P. Dominguez de Maria. Salt-Assisted Organic-Acid-Catalyzed Depolymerization of Cellulose. *Green Chemistry* 12 (2010):1844–1849.
- [30] A. Pinkert, K.N. Marsh, S. Pang, and M.P. Staiger. Ionic Liquids and Their Interaction with Cellulose. *Chemical Reviews* 109 (2009):6712–6728.
- [31] J. Larsen, M. Ostergaard Petersen, L. Thirup, H. Wen Li, and F. Krogh Iversen. The IBUS Process—Lignocellulosic Bioethanol Close to a Commercial Reality. *Chemical Engineering & Technology* 31 (2008):765–772.
- [32] J. J. Bozell. Connecting Biomass and Petroleum Processing with a Chemical Bridge. *Science* 329 (2010):522–523.

- [33] B.F.M. Kuster. 5-Hydroxymethylfurfural (HMF). A Review Focussing on its Manufacture. *Starch/Stärke* 42 (1990):314–321.
- [34] H.B. Zhao, J.E. Holladay, H. Brown, and Z.C. Zhang. Metal Chlorides in Ionic Liquid Solvents Convert Sugars to 5-Hydroxymethylfurfural. *Science* 316 (2007):1597–1600.
- [35] J. Zakzeski, P.C.A. Bruijninx, A.L. Jongerius, and B.M. Weckhuysen. The Catalytic Valorization of Lignin for the Production of Renewable Chemicals. *Chemical Reviews* 110 (2010):3552–3599.
- [36] J.M. Nichols, L.M. Bishop, R.B. Bergman, and J.A. Ellman. Catalytic C–O Bond Cleavage of 2-Aryloxy-1-arylethanol and its Application to the Depolymerization of Lignin Related Polymers. *Journal of the American Chemical Society* 132 (2010):12554–12555.
- [37] C. Somerville, H. Youngs, C. Taylor, S.C. Davis, and S.P. Long. Feedstocks for Lignocellulosic Biofuels. *Science* 329 (2010):790–792.

Chapter 13

Solution-Based Deconstruction of (Ligno)-Cellulose

Roberto Rinaldi, Jennifer Reece

13.1 Introduction

The supramolecular structure of cellulose is perhaps the most difficult hurdle facing processes starting from cellulosic fibers. Nonetheless, the supramolecular structure can be disassembled, for example, by dissolving the biopolymer. As a result, cellulose, a recalcitrant polymer in solid-state, becomes a reactive macromolecule in solution. For instance, the hydrolysis of cellulose can proceed even at room temperature in solution; however, the reaction sounds inapplicable below 180 °C when starting from cellulose slurries in water. Although processing cellulose in solution could well hold the key to its efficient conversion into bio-fuels and bio-based chemical assets, the use of solvents may carry considerable costs. The economics surrounding the use of solvents is beyond the scope of this chapter. Herein, the fundamental challenges facing the hydrolysis of cellulose in solution are discussed. This chapter aims to aid in the chemical understanding of

1. cellulose recalcitrance,
2. cellulose in solution,
3. homogeneous hydrolysis of cellulose, followed by
4. final remarks.

13.2 Understanding Cellulosic Recalcitrance

Cellulose is a special polymer. Although it is made of sugar, it is not soluble in water. Moreover, the biopolymer is much less reactive than glucose, its building unit. *What makes cellulose so unique?* The answer to this question does not lie solely in the structural aspects of a single polymeric chain, but depends also on the supramolecular structure of cellulose, i.e., the chemical system made up of several cellulosic chains commonly called *cellulosic microfibril*.

Cellulose is a linear polymer, which can be defined either as a syndiotactic polymer of β -D-glucose or as an isotactic polymer of cellobiose [1]. However,

defining cellulose as a syndiotactic polymer of β -D-glucose is more common. Thus, the formula of cellulose is $(C_6H_{10}O_5)_n$, where n is the number of repeating units or degree of polymerization (DP). Cellulose can exhibit DP as high as 10,000 anhydroglucose units (AGU) [1]. The AGUs are bonded via 1,4- β -glycosidic linkages. This key feature distinguishes cellulose from amylose, another polymer of glucose linked by 1,4- α -glycosidic bonds. The different stereochemistry of the glycosidic linkages leads to a straight chain structure in cellulose and a helical structure in amylose (Figure 13.1) [2].

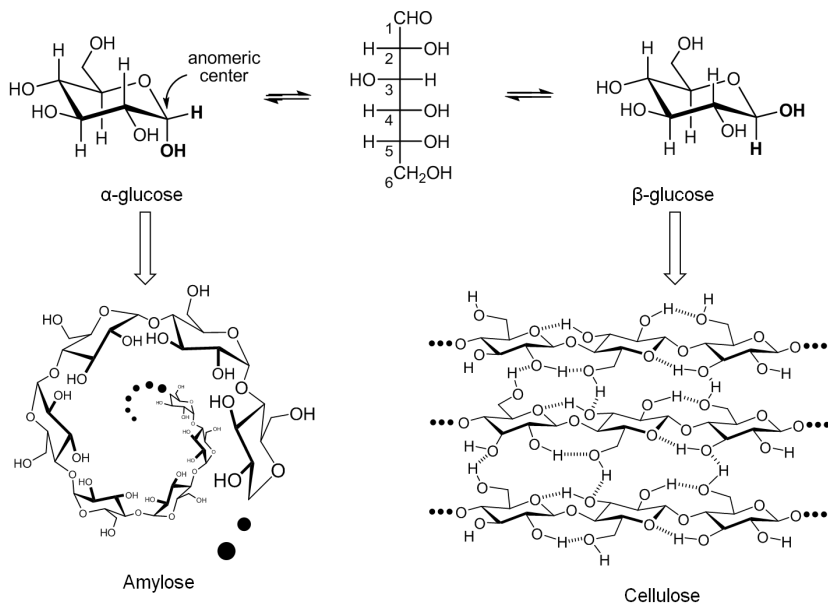


Figure 13.1: Amylose and cellulose, the polymers of glucose [2]

The 1,4- β -glycosidic linkage enables an intense intramolecular H-bonding among the groups around the glycosidic bond (Figure 13.1) [1]. This makes the polymeric chains assume a straight conformation, which allows them to be packed side-by-side through intermolecular H-bonding [1]. As a result, a planar sheet composed of cellulosic chains is formed. In the polymorph of cellulose found in nature, *cellulose I*,¹ these planar sheets are stacked on one another and held to-

¹The term *cellulose I* describes two polymorphs, I_α and I_β . The polymorph I_α is found in the cell wall of some algae and in bacterial cellulose, whereas the polymorph I_β is predominant in cotton, wood,

gether by van der Waals forces [5]. This supramolecular structure forms the crystalline domain of the microfibrils. In this chemical system, only the cellulosic chains exposed on the surface of the microfibril are easily accessible to solvents, reactants and enzymes (Figure 13.2²) [5]. For this reason, the reactivity of cellulose toward hydrolysis is markedly low. Indeed, the half-life of cellulose in water at 25 °C (non-catalyzed hydrolysis) is estimated at 5–8 million years [6].

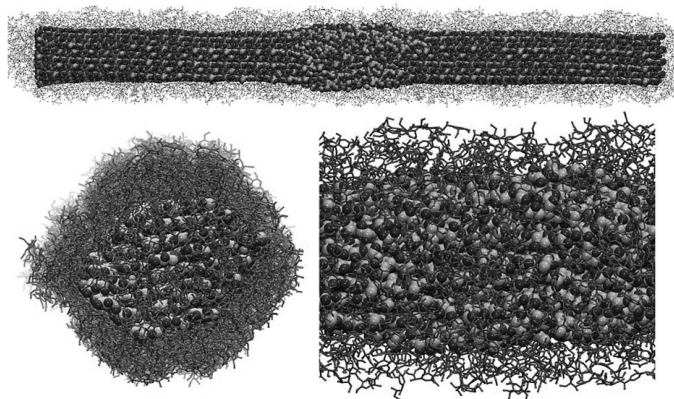


Figure 13.2: A computational model of a cellulose microfibril in aqueous solution. At the top, a complete system showing an amorphous region (in the center of the top image) is presented. At lower left, a cross section of the fibril is shown. At lower right, a close-up of the amorphous region is given. Courtesy of Xiaolin Cheng, Oak Ridge National Laboratory

Along the same microfibril both crystalline and amorphous domains are present [3, 4]. Considering the catalytic hydrolysis, the reaction proceeds with ease in the amorphous domains, where the structural restrictions are to some extent relaxed [7]. This results in a rapid rate of hydrolysis at the beginning of the reaction. Upon hydrolyzing the amorphous domains, however, the reaction rate progressively slows down reaching negligible rates when only the crystalline domains remain in the suspension [5].

and ramie fibers. However, both polymorphs can be found in the same sample and along the same microfibril. This made the first investigations of the crystalline structure of *Cellulose I* cumbersome and controversial [3, 4].

²Source: <http://ascr-discovery.science.doe.gov/kernels/ligno1.shtml>.

To improve the performance of hydrolytic processes, the supramolecular structure of cellulose should be disrupted, i.e., the crystalline domains should be converted into amorphous ones. For this purpose, several pretreatments of ligno-cellulosic materials have been extensively explored (e.g., chemical degradations, mechanical comminution, activation by swelling, ammonia fiber expansion and water-vapor explosion of the wooden fibers) [8, 9]. As will be discussed later on, the dissolution of cellulose offers an alternative to the conventional pretreatments.

13.3 Cellulose in Solution

For nearly a century, processes to dissolve cellulose as well as regenerate the processed polymer from its solutions were developed to reshape the native polymer into fibers and films [10]. Nowadays, most of the manmade cellulose-based fibers are produced by the viscose and Lyocell processes. In the viscose process, cellulose becomes a soluble derivative in 5–8% aqueous NaOH solutions upon treating the fibers with CS₂ and NaOH [10]. In the Lyocell process, *N*-methylmorpholine-*N*-oxide (NMNO) is a non-derivatizing solvent that dissolves cellulose [10]. Despite efficacy, these solvents are expensive and not environmentally friendly. Thus, advances toward improved processes for the dissolution of cellulose are necessary not only for the production of fibers, but also in the biorefining of lignocellulose. In fact, solvents could play an important role in driving down the costs involved in the pretreatment of lignocellulose. Nowadays, the lignocellulose pretreatment (via two stage, dilute sulfuric acid hydrolysis [11]) accounts for about 20% of the direct costs involved in the production of cellulosic ethanol [9]. Considering enzymatic hydrolysis, the pretreatment costs can reach 40–50% of the final price of cellulosic ethanol [9]. In this scenario, improving the knowledge either in the dissolution or in the swelling of lignocellulose could provide the key to alternative, less expensive pretreatment processes. In this section, a discussion on the main aspects of the dissolution of cellulose is given.

13.3.1 Physical Chemical Aspects of the Dissolution Process

The solubility of 1,4- β -glucans is related to their DP [5]. Oligomers composed of 2 to 6 AGUs are quite soluble in water, whereas molecules comprising 7 to 13 AGUs are partially soluble in hot water [5]. As the size of the cellulosic chain grows, packing up the polymeric chains by a dense network of intermolecular H-bonds becomes energetically favorable [12]. In general, microfibrils comprising polymeric chains greater than 30 AGUs are insoluble in most of the typical polar solvents and highly resistant to chemical and biological transformations, displaying the typical properties of cellulose [1, 5].

The dissolution of cellulose begins with the molecules of solvent diffusing through the polymeric matrix. Accordingly, the polymer swells becoming highly solvated, forming a gel. However, the dissolution process is only complete when the structure of the gel is broken, dispersing the macromolecules into the solvent. It is important to keep in mind that a polymeric solution is indeed a colloidal system because of the dimensions of the macromolecule (e.g., a straight chain of cellulose comprising 200 AGUs measures ca. 100 nm in length [5]).

The dissolution of cellulose is a spontaneous process, at a given temperature, only if the free energy of solution, $\Delta G (= \Delta H - T\Delta S)$, is negative. The entropy of solution, ΔS , always assumes a positive value because of the increased conformational mobility of the polymeric chains in solution. Thus, the term “ $-T\Delta S$ ” contributes toward an exergonic process ($\Delta G < 0$). In this manner, the sign of ΔG is determined by the enthalpy of solution, which is approximately equal to the heat of mixing. In turn, the heat of mixing, ΔH_{mix} , is given by Equation 13.1:

$$\Delta H_{mix} = V_{mix}(\delta_1 - \delta_2)\phi_1\phi_2, \quad (13.1)$$

where V_{mix} is the volume of the mixture, ϕ_1 and ϕ_2 are the volume fractions of the two components, and δ is the solubility parameter (or also called Hildebrand parameter).

Analyzing Equation 13.1 shows that the term $(\delta_1 - \delta_2)$ defines the extent to which ΔH_{mix} is a positive value. Hence, to obtain an enthalpy of mixing near to zero, it is required that $\delta_1 \approx \delta_2$. Under this condition, solely entropic effects will govern the dissolution process. As a result, the free energy of solution will invariably assume a negative value, i.e., the dissolution is spontaneous at a given temperature.

The δ parameter is defined by Equation 13.2:

$$\delta = \left(\frac{E}{V}\right)^{1/2} = \left(\frac{\Delta H_{vap} - RT}{V}\right)^{1/2}, \quad (13.2)$$

where ΔE and V stand for the energy of vaporization and the molar volume of the component respectively. Because $E = \Delta H_{vap} - RT$ (where ΔH_{vap} is the latent heat of vaporization, R is the gas constant, and T is the absolute temperature in Kelvin), δ can be directly determined from ΔH_{vap} for volatile solvents.

The term (E/V) is known as *cohesive energy density*. The physical meaning of this term is the energy required to remove a molecule from its nearest neighbor. For compounds having negligible vapor pressure such as cellulose, the cohesive energy density can be determined via direct and indirect methods (e.g., gas-solid

chromatography [13], mechanical measurements [14], from calculations using group molar attraction constants [14] and from known relationships with the free energy of surface [14]).

To date, there has been little agreement on the values of the δ parameter of microcrystalline cellulose. The value determined by a direct method, based on inverse gas chromatography, is $39.9 \text{ MPa}^{1/2}$ (Table 13.1, entry 34) [13]. Questions were raised about the method because the material needs to be preconditioned at $80 \text{ }^\circ\text{C}$ for 48 hours removing water from the surface of the cellulose [14]. An indirect mechanical measurement revealed a much lower value of the δ parameter, $25.7 \text{ MPa}^{1/2}$ (Table 13.1, entry 35) [14]. Furthermore, the calculation of the δ parameter using the group molar attraction constants results in a value of $30.2 \text{ MPa}^{1/2}$ (Table 13.1, entry 36) [14]. In turn, Hansen considered that amorphous cellulose would have a δ parameter close to the value found for Dextran C, $38.6 \text{ MPa}^{1/2}$ (Table 13.1, entry 37) [15]. Finally, the solubility of cellulose in the ionic liquid 1-butyl-3-methylimidazolium chloride, [BMIM]Cl, suggests that the value of δ should be about $35.0 \text{ MPa}^{1/2}$.

Entry	Molecular solvents	δ	δ_p	δ_D	δ_H (MPa) ^{1/2}	R _a (34)	R _a (36)	R _a (37)
1	<i>n</i> Hexane	14.9	14.9	0	0	35	25.8	29.7
2	Diethylether	15.8	14.5	2.9	5.1	29.7	20.2	26.8
3	Ethyl acetate	18.1	15.8	5.3	7.2	26.2	17.7	23.2
4	Toluene	18.2	18.0	1.4	2.0	31.5	23.8	24.1
5	Methyl ethyl ketone	19.0	16.0	9.0	5.1	27.3	19.8	24.4
6	Tetrahydrofuran	19.4	16.8	5.7	8	24.9	17.0	21.1
7	Cyclohexanone	19.6	17.8	6.3	5.1	27.2	20.1	21.8
8	Acetone	20.0	15.5	10.4	7.0	25.6	18.2	23.9
9	1,4-Dioxane	20.5	19.0	1.8	7.4	26.3	19.2	18.5
10	Carbon disulfide	20.5	20.5	0	0.6	33.3	26.8	23.2
11	Acetic acid	21.4	14.5	8.0	13.5	20.9	11.7	22.2
12	Pyridine	21.8	19.0	8.8	5.9	25.7	20.1	19.7
13	<i>N</i> -Methyl-2-pyrrolidone	22.9	18.0	12.3	7.2	24.3	19.0	19.9
14	2-Propanol	23.5	15.8	6.1	16.4	17.8	8.4	18.5
15	DMF	24.8	17.4	13.7	11.3	20.4	15.5	17.9
16	Formic acid	24.9	14.3	11.9	16.6	17.9	10.1	21.6
17	Ethanol	26.5	15.8	8.8	19.4	14.5	5.8	17.8
18	Dimethylsulfoxide	26.7	18.4	16.4	10.2	21.5	18.2	17.1

Entry	Molecular solvents	δ	δ_P	δ_D	δ_H (MPa) ^{1/2}	$R_a(34)$	$R_a(36)$	$R_a(37)$
19	NMNO	26.9	19.0	16.1	10.2	21.4	18.5	16.3
20	Triethyleneglycol	27.5	16.0	12.5	18.6	14.4	8.4	17.5
21	Methanol	29.6	15.1	12.3	22.3	12.5	6.2	19.0
22	Diethyleneglycol	29.9	16.2	14.7	20.5	12.7	9.0	16.7
23	Propyleneglycol	30.2	16.8	9.4	23.3	10.1	3.6	15.3
24	Ethanolamine	31.5	17.2	15.6	21.3	11.3	9.9	14.5
25	Dipropyleneglycol	31.7	16.0	20.3	18.4	16.5	14.9	17.5
26	Ethyleneglycol	32.9	17.0	11.0	26.0	7.4	5.0	15.3
27	Glycerol	36.1	17.4	12.1	29.3	4.6	7.7	15.6
28	Formamide	36.6	17.2	26.2	19.0	18.8	20.4	14.9
29	Water	47.8	15.6	16.0	42.3	13.8	19.8	26.7
Ionic liquids								
30	[BMIM]PF ₆	29.3	21.0	17.2	10.9	21.1	20.2	13.4
31	[OMIM]PF ₆	27.8	20.0	16.5	10.0	21.7	19.6	15.2
32	[BMIM]BF ₄	31.5	23.0	19.0	10.0	23.3	24.0	13.1
33	[BMIM]Cl	35.0	19.1	20.7	20.7	13.3	15.9	10.6
Substrates							R_0	
34	Cellulose	39.3	19.4	12.7	31.3	-		
35	Cellulose	24.7	-	-	-	-		
36	Cellulose	30.2	15.8	6.8	24.8	-		
37	Dextran C	38.6	24.3	19.9	22.5	17.4		

Table 13.1: Solubility parameters of selected solvents and polysaccharides [13–18]

Considering 39.9 MPa^{1/2} as the value of the δ parameter of cellulose, the analysis of Table 13.1 reveals that only the molecular solvent, formamide (Table 13.1, entry 26), and the ionic liquid [BMIM]Cl (Table 13.1, entry 26) would have similar solubility parameters to cellulose. Formamide does not dissolve cellulose, whereas [BMIM]Cl does. Actually, the Hildebrand parameter often fails in the prediction of the solubility of highly H-bonded compounds such as cellulose [17].

The cohesive energy, δ^2 , is indeed the sum of three distinct cohesive energies resulting from (1) nonpolar, atomic (dispersion) interactions, δ_D^2 , (2) permanent dipole-dipole molecular interactions, δ_P^2 , and (3) hydrogen bonding interactions, δ_H^2 , as indicated in Equation 13.3 [17]:

$$\delta^2 = \delta_D^2 + \delta_P^2 + \delta_H^2 \quad (13.3)$$

The solubility parameters δ_D , δ_P and δ_H are known as *Hansen Solubility Parameters* or *HSP*. Analyzing separately the terms that contribute to the overall cohesive energy, δ^2 , helps to understand why solvents having the same value of δ parameter, such as 1,4-dioxane and CS_2 (Table 13.1, entries 9 and 10), sometimes possess totally different properties. In this case, the term δ_H clearly differentiates 1,4-dioxane from CS_2 .

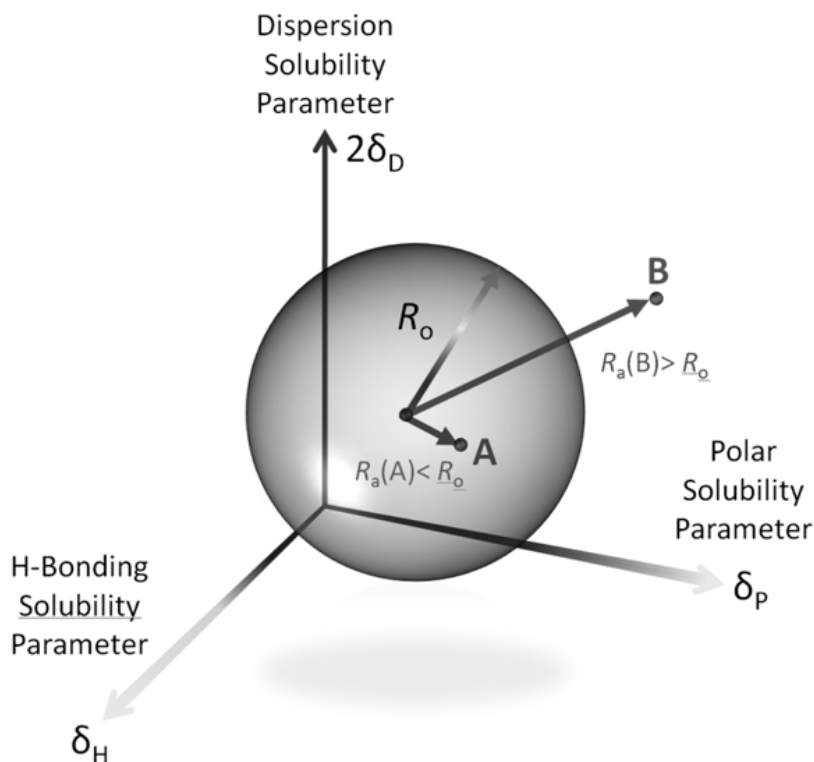


Figure 13.3: Three-dimensional visualization of the Hansen Solubility Parameters (HSP) in the characterization of a good solvent (A) and a poor solvent (B). Adapted from [17]

According to Hansen [17], dissolution or swelling takes place when a solvent has the values of δ_D , δ_P and δ_H close to those of the polymer. Figure 13.3 shows

a three-dimensional representation of the HSP characterization. The HSP of the polymer are at the center of the sphere. The radius of the sphere, R_o , indicates the maximum difference in affinity that is tolerable for a “good” interaction between solvent and solute. This parameter is empirically determined by comparing the solubility of a solute in several solvents [15]. Good solvents are within the sphere, whereas the poor ones are outside. For instance, solvent A is a good solvent for the solute, but solvent B does not have the adequate HSP, as illustrated in Figure 13.3 [15].

The dissolution or the swelling of the polymer is predicted to occur if the condition $R_a < R_o$ is satisfied (Figure 13.3). The interaction distance between the solvent and the center of the sphere, R_a , is calculated as indicated in Equation 13.4 [15, 17]:

$$R_a = [4(\delta_{D,p} - \delta_{D,s})^2 + (\delta_{P,p} - \delta_{P,s})^2 + (\delta_{H,p} - \delta_{H,s})^2]^{1/2}, \quad (13.4)$$

where the letters p and s are the descriptors for the HSP values of the polymer and the solvent, respectively.

Table 13.1 shows the interaction distances R_a (entry 34), R_a (entry 36) and R_a (entry 37) that were calculated considering the HSP values of microcrystalline cellulose (entries 34 and 36) and dextran C (entry 37). It is clear from Table 13.1 that [BMIM]Cl is one of the solvents with a short interaction distance. However, the solvents listed in the entries 21 to 24, 26 and 27 have shorter distance values than the one found for [BMIM]Cl. Although cellulose swells in some of these solvents, they are not capable of dissolving it. Considering that the HSP values of amorphous cellulose are the same as those of dextran C [15], a better differentiation of solvents can be achieved using a value of R_o equal to 17.4. Due to the structural differences between cellulose and dextran C, caution must be applied in this analysis as the HSP values of dextran C might not be transferable to amorphous cellulose. For example, the ionic liquids assume quite similar values of R_a , but only [BMIM]Cl dissolves cellulose.

The HSP is a *thermodynamic approach* to predict solubility. It may happen that the prediction indicates that the material is soluble in a solvent, but in reality the material is only swollen or even insoluble in the solvent. Several reasons may account for the “incorrect” prediction. First, if the solvent molecules are too large to penetrate the pore structure of the polymer, the swelling of the polymer as well as its dissolution will be *extremely* slow. Second, although $\Delta G < 0$ implies that the process is spontaneous, this gives no information about the rate of the process, i.e., a spontaneous process may never happen due to a kinetic barrier between the

initial and the final states. Third, the HSP approach considers a solution as an ideal mixture. Thus, specific interactions between a solvent and a polymer are not considered in the analysis. Finally, the prediction may be false. This may be the case for cellulose because of the supposed inaccuracy of the HSP determined for this polymer.

Class	Type	Examples
Mineral acids	Concentrated mineral acids	H ₂ SO ₄ , HCl, HF, H ₃ PO ₄
Aqueous systems	Transition metal complexes containing NH ₃ and/or amine ligands (excess of NH ₃ or amine is required)	<i>Cadoxen</i> – [Cd(H ₂ N(CH ₂) ₂ NH ₂) ₃](OH) ₂ , <i>Cupren</i> – [Cu(H ₂ N(CH ₂) ₂ NH ₂) ₂](OH) ₂ , <i>Cuam</i> – [Cu(NH ₃) ₄](OH) ₂ , <i>Zincoxen</i> – [Zn(H ₂ N(CH ₂) ₂ NH ₂) ₂](OH) ₂
	Transition metal tartrates	<i>FeTNa</i> – NA ₆ [Fe(C ₄ H ₃ O ₆) ₃]
	Quaternary ammonium hydroxides	<i>Triton B</i> , <i>TEOH</i> , <i>Triton F</i> , <i>Guanidinium hydroxide</i>
	Alkali hydroxides	NaOH, LiOH
Molten salt hydrates	Tertiary amines oxides	<i>N</i> -Methylmorpholine- <i>N</i> -oxide
	Swelling agents	LiCl• <i>x</i> H ₂ O (2 ≤ <i>x</i> ≤ 5), Zn(NO ₃) ₂ •6H ₂ O, NaClO ₄ •H ₂ O, Mg(ClO ₄) ₂ •H ₂ O, LiClO ₄ •3H ₂ O/CaCl ₂ ±6H ₂ O
	Solvent media	ZnCl ₂ •4H ₂ O, LiClO ₄ •3H ₂ O, Zn(NO ₃) ₂ • <i>x</i> H ₂ O (<i>x</i> < 6), FeCl ₃ •6H ₂ O, LiSCN•2H ₂ O, LiI•2H ₂ O, LiClO ₄ •3H ₂ O/MgCl ₂ •6H ₂ O, LiClO ₄ •3H ₂ O/Mg(ClO ₄) ₂ /H ₂ O, LiClO ₄ •3H ₂ O/NaClO ₄ /H ₂ O, LiCl/ZnCl ₂ /H ₂ O, NaSCN/KSCN/LiSCN/H ₂ O
Non-aqueous systems	Alkyl imidazolium ionic liquids	[EMIM]Cl: 1-ethyl-3-methylimidazolium chloride, [BMIM]Cl: 1-butyl-3-methylimidazolium chloride

Class	Type	Examples
Non-aqueous systems	Alkyl imidazolium ionic liquids	[EMIM][AcO]: 1-ethyl-3-methylimidazolium acetate, [EMIM][OP(O)(OMe) ₂]: 1-ethyl-3-methylimidazolium dimethylphosphate
Non-aqueous systems	<i>N</i> Alkylpyridinium salts	<i>N</i> -Ethylpyridinium chloride
	Tertiary amine oxides	<i>N</i> -Methylmorpholine- <i>N</i> -oxide, Triethylamine- <i>N</i> -oxide, <i>N</i> -Methylpiperidine- <i>N</i> -oxide
	DMSO based-solvent media	DMSO/methylamine, DMSO/ KSCN, DMSO/CaCl ₂ , DMSO/ tetrabutylammonium fluoride (TBAF)
	Liquid NH ₃ based-solvent media	NH ₃ /NaI(NH ₄ I), NH ₃ / NaSCN(NH ₄ SCN)
	Dipolar aprotic solvents/ LiCl	<i>N,N</i> -Dimethylacetamide/LiCl, <i>N</i> -Methylpyrrolidone/LiCl
	Tricomponent solvent media	NH ₄ /NaCl/DMSO, Ethylenediamine/ NaI/ <i>N,N</i> -Dimethylformamide, Diethylamine/SO ₂ /DMSO

Table 13.2: Some solvents for cellulose. Adapted from [10, 19–21]

13.3.2 Solvents for Cellulose

There are several solvents or solvent systems that fulfill the thermodynamic and kinetic requirements to dissolve cellulose. A short list of solvent systems for cellulose is given in Table 13.2 [10, 19–21].

In the solvent systems listed in Table 13.2, cellulose plays the following roles in solution [21]:

1. Cellulose acts as a base (when solvents such as H₂SO₄, HCl or H₃PO₄ are employed);
2. Cellulose acts as an acid (when solvents such as urea/NaOH/water or ionic liquids are used);

nocellulose. The use of ionic liquids (ILs) as solvents for cellulose is the most important example in the current RD [18, 22, 23]. ILs are salts that melt below 100 °C [22]. The 1-alkyl-3-methylimidazolium-based ILs comprising good H-bond acceptor anions (e.g., Cl^- , CH_3COO^- and $[\text{CH}_3\text{O}]_2\text{P}[\text{O}]\text{O}^-$ to mention some [24, 25]) can dissolve cellulose [22, 26] and even wood [18, 23]. However, the high cost related to the use of ILs still hinders their applicability in biorefineries. Moreover, the recycling of ILs is a big challenge due to the lack of efficient separation processes to extract highly polar compounds (e.g., sugars or 5-hydroxymethylfurfural) from ILs [18, 23].

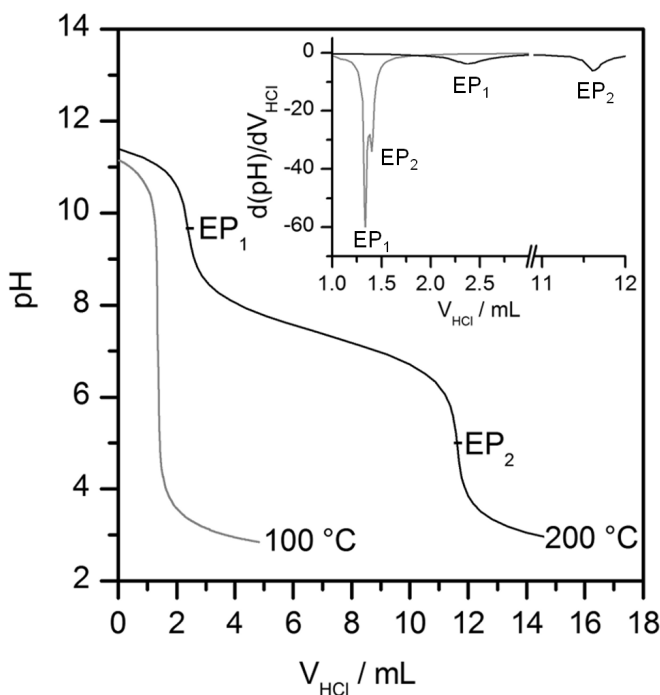


Figure 13.5: Back-titration curves obtained from the samples of [BMIM]Cl heated at 100 and 200 °C for 24 hours [27]

In process development, primary criteria for the selection of ILs are not only price, toxicity and recyclability, but also the degradation temperature of the IL is important in the final decision. The first serious discussions on the thermal stabil-

ity of ILs emerged from investigations using thermogravimetric analysis (TGA) [28]. Although efforts to determine the degradation temperature of several ILs were undertaken, the reported data are rather controversial, and there is no general agreement about the published degradation temperatures for the same ionic liquid [28]. For instance, degradation temperatures between 235 and 450 °C are published for 1-methyl-3-butylimidazolium bis(trifluoromethylsulfonyl)imide [28].

Recently, the potentiometric titration of alkylimidazoles was used to assess the deterioration of the ILs' quality occurring upon thermal aging [27]. Figure 13.5 shows the curves of back-titration obtained from the samples of [BMIM]Cl heated at 100 and 200 °C for 24 hours. The first equivalent point, EP₁, is due to the neutralization of the excess of NaOH solution dosed in the direct titration. The second equivalent point, EP₂, is associated with the amount of free imidazoles in the samples.

The potentiometric titration of the [BMIM]Cl sample treated at 200 °C for 24 hours revealed decomposition of ILs already at much lower temperatures than those inferred from TGA [27]. Table 13.3 lists the imidazole titers found in the untreated samples of some ILs and in those heated at 200 °C for 24 hours [27].

IL	T_{onset} (°C)	Imidazoles ($\mu\text{mol g}^{-1}$) as purchased	Imidazoles ($\mu\text{mol g}^{-1}$) 200 °C
[EMIM]Cl	222	16 ± 1	332 ± 4
[BMIM]Cl	214	7 ± 1	874 ± 10
[BMIM] [CH ₃ SO ₃]	295	14 ± 1	31 ± 1
[BMIM] [Tf ₂ N]	367	5 ± 1	21 ± 2

Table 13.3: Thermal stability of IL samples aged at 200° C for 24 hours [27]. The onset decomposition temperature, T_{onset} , was determined by TGA [27].

The long-term stability of ILs is an important issue for industrial use. Figure 13.6 shows the evolution of the imidazole content in [BMIM]Cl (99.9%) samples heated at 100 or 140 °C for 10 days. Although the [BMIM]Cl samples heated at 100 °C show no degradation over 10 days, the imidazoles content increases from 13 to 62 $\mu\text{mol g}^{-1}$ after heating the samples over 10 days at 140 °C under anhydrous conditions. On the other hand, a titer of 78 $\mu\text{mol g}^{-1}$ was found upon aging a sample containing 2 wt% water at 140 °C for 10 days. This shows that water also affects the ionic liquid thermal stability [27].

The solubility of cellulose in ILs is another important aspect to be considered. Currently, the ILs available in the market cannot dissolve more than 25 wt% of cellulose, which results in very viscous solutions or even “sticky” gels [18, 22, 26]. Furthermore, a typical difficulty experienced while dissolving cellulose in ILs is the agglomeration of the cellulosic fibers. The resulting clumps take very long to dissolve. Slowly pouring the biopolymer into the IL under vigorous mechanical stirring helps to break up the clumps of cellulose to a certain extent, however, this unit operation is rather energy demanding.

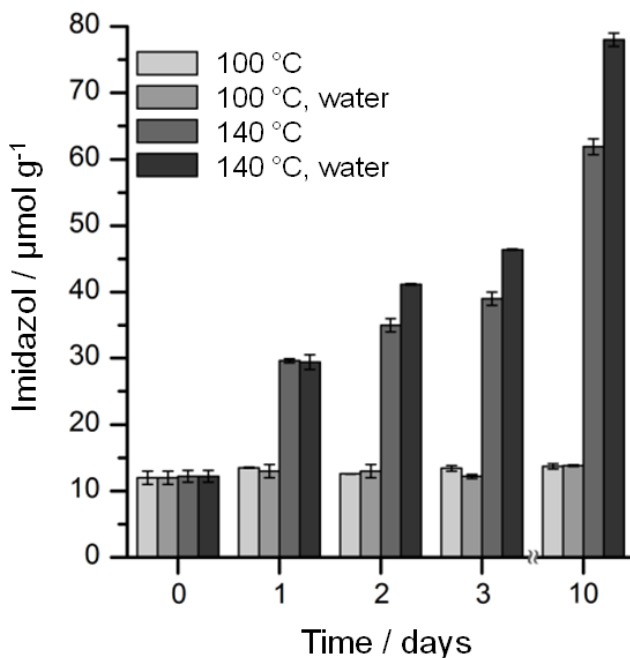


Figure 13.6: Effect of water (2 wt%) on long-term stability of [BMIM]Cl samples heated at 100 and 140 °C [27]

Recently, solvent systems comprising IL and molecular solvents were reported [29]. They circumvented some of the most difficult hurdles faced when using neat ILs. For instance, cellulose clumps are not formed, the dissolution takes place quickly, and the amount of ILs required for the process can be markedly reduced [29].

Figure 13.7 shows the effect of the concentration of [BMIM]Cl on the dissolution of microcrystalline cellulose (Avicel, 10 wt%) dispersed in 1,3-dimethyl-2-imidazolidinone (DMI). The dissolution process starts upon the addition of [BMIM]Cl into the suspension. A white paste is obtained in the system containing 10 wt% IL. The increase of IL concentration from 20 to 40 wt% makes the mixture gradually more transparent. Cellulose dissolves completely in a 50 wt% solution of [BMIM]Cl in DMI after only 3 minutes [29]. For the sake of comparison, the regular dissolution of cellulose in neat [BMIM]Cl typically takes more than 10 hours to complete [22].

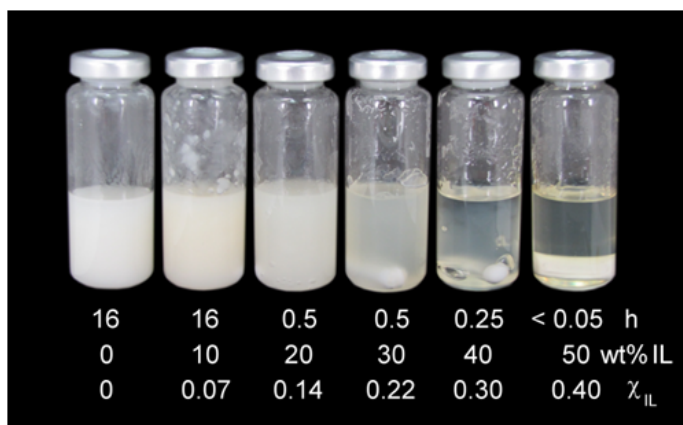


Figure 13.7: Appearance of the mixtures comprising microcrystalline cellulose (Avicell), DMI and [BMIM]Cl (0-50 wt%) after stirring at 100 °C for the time indicated in the figure [29]

Instantaneous dissolution of cellulose at 100 °C is achieved when [BMIM]Cl is replaced by 1-ethyl-3-methylimidazolium acetate, [EMIM][AcO]. Figure 13.8 shows some examples of IL-based electrolyte solutions capable of dissolving cellulose instantaneously at 100 °C [29].

The mole fraction of [EMIM][AcO], $\chi_{[EMIM][AcO]}$, required for the dissolution of cellulose depends on the molecular solvent used in the electrolyte solution. For several of the reported amide-containing solvents, the dissolution takes place even when $\chi_{[EMIM][AcO]}$ is lower than 0.30. The DMSO/[EMIM][AcO] system requires the smallest $\chi_{[EMIM][AcO]}$ (0.09). On the other hand, the dissolution of cellulose in acetylacetone, *tert*-butanol and *tert*-pentanol happens only when an equimolar amount of IL is present in the mixture. Surprisingly, *N,N,N,N*-tetramethylurea,

an analogue of DMI, requires the largest $\chi_{[\text{EMIM}][\text{AcO}]}$ (0.59) for the dissolution of cellulose [29].

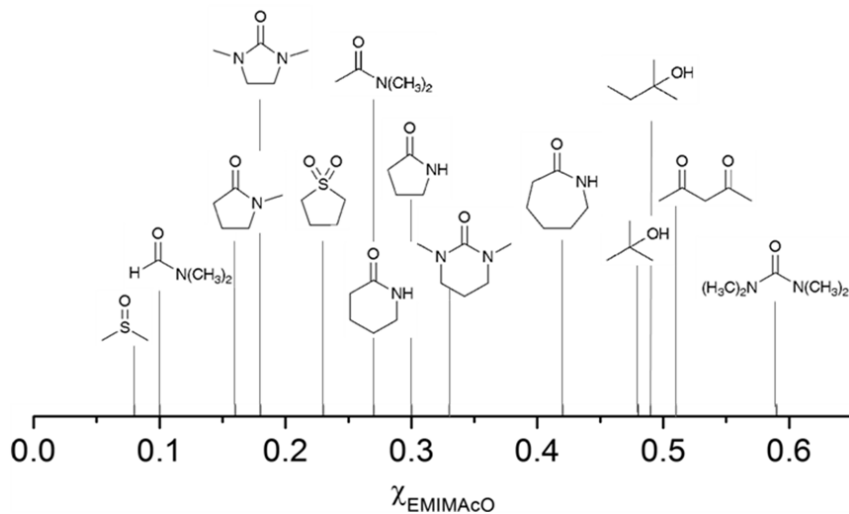


Figure 13.8: The mole fraction of $[\text{EMIM}][\text{AcO}]$ required for the dissolution of microcrystalline cellulose (10 wt%) in several molecular solvents at 100 °C. Adapted from [29].

The concept of distillable acid-base conjugate ILs was recently introduced [30]. Cellulose (10 wt%) is soluble in $[\text{TMGH}^+][\text{RCOO}^-]$, where $[\text{TMGH}^+]$ stands for 1,1,3,3-tetramethylguanidinium and R is -H, -CH₃ and -C₂H₅. These guanidinium-based ionic liquids can be distilled in a K \ddot{u} gelrohr short-path distillation apparatus (3 g, 100 to 200 °C over 30 minutes, 1 mmHg) [27]. This is possible because of the equilibrium: $[\text{TMGH}^+][\text{RCOO}^-] \rightleftharpoons \text{TMG} + \text{RCOOH}$, where TMG stands for 1,1,3,3-tetramethylguanidine. Above 100 °C and under vacuum, the equilibrium shifts towards the molecular compounds enabling the distillation. At room temperature, the molecular compounds recombine regenerating the IL.

13.4 Homogeneous Hydrolysis of Cellulose

Hydrolysis of cellulose is typically performed under heterogeneous reaction conditions, i.e., the substrate is not dissolved in the reaction medium [5]. However,

the solvent does not function merely as a dispersant. Cellulose can also be swollen in the solvent. This activates the substrate. In heterogeneous reactions, the chemical transformation of cellulose occurs first on its surface [5]. Soluble intermediates, formed by the attack of the surface, undergo further reactions in solution, yet the complete conversion of cellulose is often not achieved in heterogeneous reactions. Hence, very recalcitrant cellulose accumulates in the process raising difficulties for catalyst recovery [2, 5]. In the homogeneous hydrolysis of cellulose, the substrate is soluble in the reaction medium. Under this condition, the physical barriers to efficient hydrolysis are no longer present (e.g., crystallinity, morphology, surface area and other physical features) [5]. In this manner, the hydrolysis rate is several orders of magnitude higher than that found for the heterogeneous hydrolysis. Moreover, the integral utilization of cellulose can be achieved with ease [5]. As described in the previous section, several solvents for cellulose are available, but the choices become scarce when one envisages carrying out catalytic reactions in these media. In this section, the experience gained in the hydrolysis of cellulose in solutions of concentrated mineral acids [11, 31–34], melt salt hydrates [35, 36], and ionic liquids [5, 23] is briefly described.

Hydrolysis of cellulose in concentrated mineral acids was one of the first methods used in the investigation of the composition of plant tissues. Anselme Payen in the 1830s discovered that the extracts, obtained from acid hydrolysis of oak and beech wood, have an elemental composition similar to that of starch [5]. Currently, the composition of lignocellulosic material is determined by the quantitative saccharification in sulfuric acid [37]. In the first stage, this method employs the dissolution and hydrolysis of cellulose (and hemicelluloses) in 72 wt % sulfuric acid at room temperature. In the second stage, the complete saccharification is achieved in dilute acid solution (3 wt%) at 130 °C. Monosaccharides are obtained as main products. Despite efficacy, this method is not feasible on large scale due to problems with corrosion and acid recycling.

The saccharification of wood in fuming hydrochloric acid (40 wt%), known as Bergius process, is the only process employing concentrated mineral acid that so far has been applied on a large scale [31]. Cellulose is soluble in fuming hydrochloric acid at room temperature. Under these conditions, the biopolymer hydrolyses to oligosaccharides within a few hours without considerable formation of dehydration products (e.g., furfural and 5-hydroxymethylfurfural [5-HMF]) [31]. In practice, after the removal of hydrochloric acid, about 1 wt% of the acidic content still remains in the raw hydrolyzate. The residual acidic content catalyzes the hydrolysis of the oligosaccharides to fermentable sugars, which is performed in a second stage at 120 °C for 0.5 hours. By the Bergius process, a ton of dry wood was claimed to yield 320 L of 95% ethanol [31]. Fuming hydrochloric acid shows two major advantages over sulfuric acid. First, hydrochloric acid permeates bet-

ter than sulfuric acid into the wood fibers. Second, up to 99% of the hydrochloric acid can be recycled. However, the main economical drawbacks of this technology are the requirement of corrosion-resistant plants, and the expensive recovery of hydrochloric acid [38].

Concentrated phosphoric (85%) acid dissolves considerable amounts of cellulose (e.g., 20 wt% cotton linter) [34]. Moreover, cellulose controllably depolymerizes in this solvent. This method was first explored to produce low crystallinity, low DP celluloses for pharmaceutical purposes. The decay rate of DP is enhanced from $4.79 \times 10^{-3} \text{ h}^{-1}$ at 25 °C to 0.314 h^{-1} at 50 °C. The activation energy of the reaction corresponds to a value of 106 kJ mol^{-1} ; this value is, for example, 20 to 40 kJ mol^{-1} lower than those found for the heterogeneous hydrolysis of cellulose [5, 34]. Recently, mixtures comprising 70% phosphoric acid and 30% sulfuric acid were employed as reaction media for hydrolysis of cellulose [32]. The load of substrate (corn cob) was 30 wt%. This was slowly mixed in a blender at 30 °C. The initial thick mixture was left to decrystallize for 16 hours. Finally, water was added and the mixture was heated at 80 °C. The process led to about 90% sugar yield after 4 hours [32].

Several molten salt hydrates (Table 13.2) are good solvents for cellulose. Homogeneous hydrolysis of cellulose is reported to take place at 85 °C in zinc chloride tetrahydrate (using 0.4 molal of hydrochloric acid as catalyst) [35, 36]. The reaction achieves a 70% yield of glucose after 0.5 hours [36]. Interestingly, salts cannot only dissolve cellulose, but they can also swell it [33]. In the heterogeneous hydrolysis of cellulose, the presence of CaCl_2 (1.6 mol L^{-1}) or LiCl (6 mol L^{-1}) was shown to be beneficial in the hydrolysis of cellulose in hydrochloric acid ($6\text{--}7 \text{ mol L}^{-1}$, 7 wt%) at 90 °C. Yields up to 85% glucose are claimed [33]. The swelling effect of the salts in the cellulosic fibers is pointed out as a factor accounting for the enhancement of the hydrolysis rate [33].

Ionic liquids are the most explored solvents for the hydrolysis of cellulose. Recent reviews outline in detail the progress in the field [5, 18, 23, 39]. The first report on hydrolysis of cellulose dissolved in [BMIM]Cl was given by Li and Zhao in 2007 [40]. They demonstrated that cellulose dissolved in [BMIM]Cl hydrolyzes in the presence of catalytic amounts of sulfuric acid or other mineral acids at 100 °C. A typical problem found in this reaction is the degradation of glucose into several products (Figure 13.9). Recently, a solution for this problem was given [41]. The selective production of glucose can be achieved upon controllably adding small amounts of water into the mixture over the course of the reaction [41]. Nonetheless, the separation of the highly polar products from the IL is still a problem without a practical solution.

The activation of cellulose toward hydrolysis requires a strong acid [5, 42]. This prohibits the utilization of acetate- or phosphonate-based ionic liquids—or

any other kind of ionic liquid comprising a weakly basic anion. These anions capture the H_3O^+ species preventing the activation of the glycosidic bonds. Additionally, the presence of *N*-methylimidazole, often found at different concentration levels as an impurity in $[\text{BMIM}]\text{Cl}$, decreases proportionally the catalytic performance of this system [42].

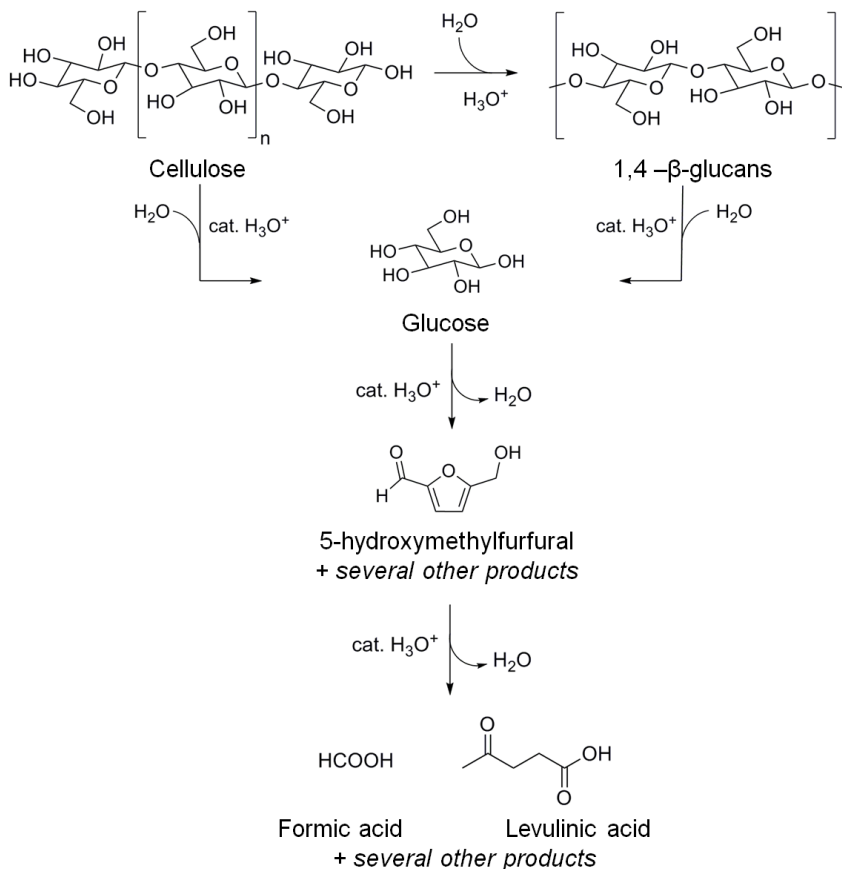


Figure 13.9: Selected products formed by acid-catalyzed reactions starting from cellulose. As hemicelluloses are typical impurities of commercial celluloses, xylose and other monosaccharides as well as their degradation products (furfural, furoic acid, and others) may be also present in the reaction mixture [42].

The addition of H_3O^+ species into a solution of cellulose in $[\text{BMIM}]\text{Cl}$ initiates a complex reaction chain, as illustrated in Figure 13.9 [42]. In the first step, cellulose undergoes depolymerization via hydrolysis of 1,4- β -glycosidic bonds. Either smaller 1,4- β -glucans (cellooligomers) or glucose can be formed at this stage. Glucose is likely to be dehydrated under acidic conditions yielding several compounds (e.g., 5-HMF, levulinic acid, formic acid and several others) [42]. These products are prone to recombine with sugars or oligosaccharides via aldol-condensation, resulting in polymers with undefined structure and stoichiometry called humins [42].

Performing the acid-catalyzed depolymerization of cellulose using Amberlyst 15DRY, instead of molecular acids, enables the direct control of the reaction progress [42, 43]. The initial rate of depolymerization is controlled by the slow release of H_3O^+ species into the reaction medium. As the reaction proceeds at a slow rate, a preferential cleavage of large polymeric molecules is detected in the beginning of the reaction. Hence, cellooligomers with a tunable DP can be conveniently produced. Furthermore, the reaction can be also conducted to quantitatively produce water-soluble products. In practice, however, it is much more interesting to stop the process at the stage in which cellooligomers are the main products because the work-up for the extraction of sugar and dehydration products is commonly very difficult—or even unachievable—due to the high solubility of these products in ILs [5, 43]. Cellooligomers can be separated as main products by adding water (Figure 13.10), methanol, dichloromethane or liquid ammonia into the reaction mixture [5].

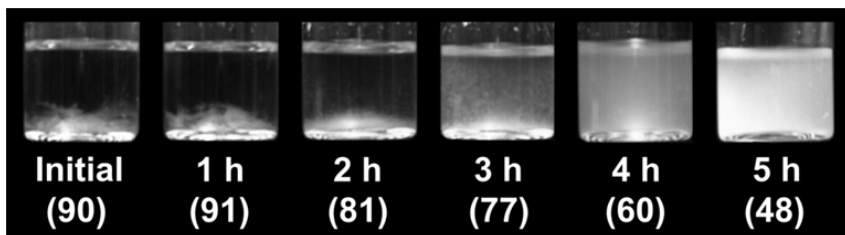


Figure 13.10: Hydrolysis of microcrystalline cellulose. Appearance of the cellulose recovered from $[\text{BMIM}]\text{Cl}$ by addition of water. The values between parentheses represent the percentage of isolated cellulose [43].

Cellooligomers regenerated from IL comprises up to 95 wt% water. The high degree of swelling suggests that the cellulosic chains are highly accessible (Figure

13.11). Indeed, starting from the cellooligomers almost quantitative conversion of cellulose into fermentable sugars is achieved in the enzymatic catalysis in aqueous medium, as shown in Figure 13.12 [44].

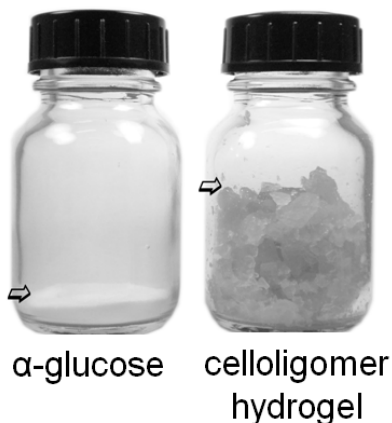


Figure 13.11: Making cellulose accessible. Both flasks contain the equivalent to 1 g of dry cellulose [44].

Figure 13.12 shows the performance of a commercial cellulase preparation (Celluclast®, T. reesei) in the enzymatic hydrolysis of several cellulosic materials. The untreated α -cellulose and cellulose regenerated from ILs show substrate conversions of 46 and 79%, respectively. In contrast, the cellooligomers obtained from the acid-catalyzed depolymerization are, in the best cases, nearly quantitatively hydrolyzed (94%) by cellulases within 4 hours.

Furthermore, this reaction produces exclusively cellobiose and glucose, maintaining the enzymatic selectivity [44]. Surprisingly, no marked effect of the DP on the enzymatic performance is observed in the reactions carried out with cellooligomers smaller than 800 anhydroglucose units (AGU). This finding has important implications for process development. Starting from native cellulose (DP between 2,000 and 10,000 AGU), suitable cellooligomers for the enzymatic hydrolysis would be already produced after 3 to 16 scissions of the cellulosic chains, which is reached in less than 1 hour through the acid-catalyzed depolymerization in IL. As cellooligomers are preferably produced in the earlier stages of acid-catalyzed depolymerization, losses of glucose, due to its dehydration, are completely suppressed. Consequently, the integration of acid- and enzyme-catalyzed

conversion unites the advantages of both “worlds” bringing rapid and quantitative conversion of cellulose to fermentable sugars [44].

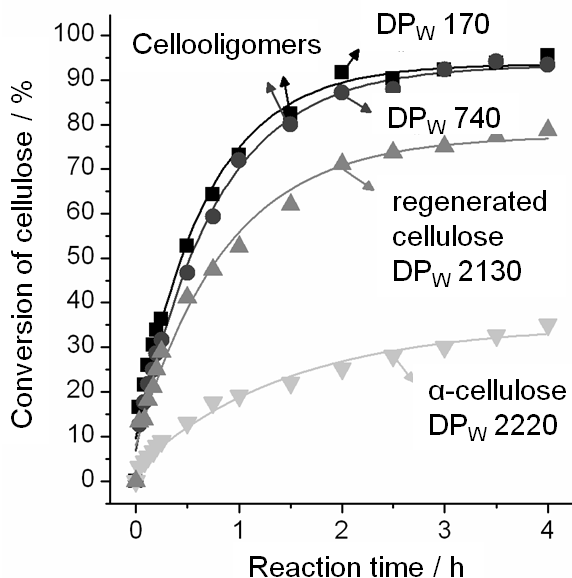


Figure 13.12: Enzymatic hydrolysis of α -cellulose, cellulose regenerated from IL and cellulooligomers. Conditions: substrate (equals 1 g of dry cellulose), cellulase (Celluclast®, 350 U/g substrate), pH 4.5 (acetate buffer), 45 °C [44]

13.5 Final remarks

The biorefining of lignocellulose to produce bio-based chemical assets, and ultimately biofuels, requires solvents. This is the main feature that distinguishes biorefinery processes from the ones currently in practice in oil refineries and petrochemical industries. In the crude oil based industries commonly no solvent is required, because the raw materials and the products are often liquids.

The experience gained in the heterogeneous hydrolysis of cellulose, such as in the two-stage dilute sulfuric acid process [11], shows that a considerable volume of solvent is necessary. For instance, processing 1 kg of dried oven wood uses about 3 L of water. Moreover, for each liter of ethanol, 32 L of industrial wastewater is generated in its production from wood. In a large industrial plant with

a capacity to process 10,000 tons of lignocellulosic material a day (wood, straw and others), producing 870 tons of ethanol, the amount of industrial wastewater generated would reach 32,070,000 liters! This large volume of water is enough to supply a town with, for example, 300,000 inhabitants in an industrialized area daily.

Although water is the most environmentally friendly solvent known, this statement is only valid when water is returned clean to the environment. In the case of the dilute acid process, several dehydration products, such as 5-HMF, furfural, formic acid and even some phenols are formed [2]. The concentration of some of these impurities has to be at the ppm level for the proper reuse of water. Accordingly, high-cost advanced oxidation processes for the industrial wastewater cleaning are mandatory.

Looking at the present technologies in development, avoiding the use of solvents in the biorefinery process chains appears to be unfeasible. Accordingly, the use of solvents should be rationally applied. For instance, in the two-stage dilute sulfuric acid process, water functions merely as a dispersant of the substrate in the medium. Replacing water with a solvent that at least swells the lignocellulosic matrix could already improve markedly the performance of the acid-catalyzed hydrolysis of cellulose (and hemicellulose) at lower temperatures than currently in use. However, the best solution would be to perform the process under homogeneous conditions. This would then take advantage of carrying out the hydrolytic process at room temperature, making the overall energetic demands lower.

Although the dissolution of cellulose is a process still not fully comprehended, it is clear from the thermodynamic prediction models that solvents for cellulose are liquids (or solutions) that possess high cohesion energy densities, i.e., are commonly compounds that have high boiling points. Hence, research on advanced processes for solvent reclamation is necessary to avoid energy intensive processes in their reuse.

The use of solvents is a central, but often neglected problem in lignocellulosic biorefining. This most urgently needs to change in order to place cellulosic ethanol, and ultimately the third generation biofuels, as a cost competitive and more sustainable alternative to fossil fuels.

Bibliography

- [1] D. Klemm, B. Heublein, H.-P. Fink, and A. Bohn. Cellulose: Fascinating Biopolymer and Sustainable Raw Material. *Angewandte Chemie International Edition* 44(22) (2007):76–81.
- [2] R. Rinaldi and F. Schüth. Acid Hydrolysis of Cellulose as the Entry Point into Biorefinery Schemes. *ChemSusChem* 2(12) (2009):1096–1107.
- [3] Y. Nishiyama, J. Sugiyama, H. Chanzy, and P. Langan. Crystal Structure and Hydrogen Bonding System in Cellulose Ia from Synchrotron X-Ray and Neutron Fiber Diffraction. *Journal of the American Chemical Society* 125(47) (2003):14300–14306.
- [4] A.C. O’Sullivan. Cellulose: The Structure Slowly Unravels. *Cellulose* 4(3) (1997):173–207.
- [5] R. Rinaldi and F. Schüth. Design of Solid Catalysts for the Conversion of Biomass. *Energy & Environmental Science* 2 (2009):610–626.
- [6] R. Wolfenden and M.J. Snider. The Depth of Chemical Time and the Power of Enzymes as Catalysts. *Accounts of Chemical Research* 34(12) (2001):938–945.
- [7] H. Zhao, J.H. Kwak, Y. Wang, J.A. Franz, J.M. White, and J.E. Holladay. Effects of Crystallinity on Dilute Acid Hydrolysis of Cellulose by Cellulose Ball-Milling Study. *Energy and Fuels* 20(2) (2006):807–811.
- [8] P. Kumar, D.M. Barrett, M.J. Delwiche, and P. Stroeve. Methods for Pretreatment of Lignocellulosic Biomass for Efficient Hydrolysis and Biofuel Production. *Industrial and Engineering Chemistry Research* 48(8) (2009):3713–3729.
- [9] B. Yang and C.E. Wyman. Pretreatment: The Key to Unlocking Low-Cost Cellulosic Ethanol. *Biofuels, Bioproducts and Biorefining* 2(1) (2008): 26–40.
- [10] T. Liebert. *Cellulose Solvents—Remarkable History, Bright Future*. 1033. ACS Symposium Series, 2010. 3–54.

- [11] J.F. Harris, A.J. Baker, A.H. Conner, T.W. Jeffries, J.L. Minor, R.C. Petersen, R.W. Scott, E.L. Springer, T.H. Wegner, and J.I. Zerbe. *Two-Stage, Dilute Sulfuric Acid Hydrolysis of Wood: An Investigation of Fundamentals*. General Technical Report FPL-45. Madison, WI: U.S. Department of Agriculture, Forest Service, Forest Products Laboratory, 1985.
- [12] T. Shen, P. Langan, A.D. French, G.P. Johnson, and S. Gnanakaran. Conformational Flexibility of Soluble Cellulose Oligomers: Chain Length and Temperature Dependence. *Journal of the American Chemical Society* 131 (41) (2009):14786–14794.
- [13] N. Huu-Phuoc, H. Nam-Tran, M. Buchmann, and U.W. Kesselring. Experimentally Optimized Determination of the Partial and Total Cohesion Parameters of an Insoluble Polymer (Microcrystalline Cellulose) by Gas-Solid Chromatography. *International Journal of Pharmaceutics* 34 (3) (1987):217–223.
- [14] R.J. Roberts and R.C. Rowe. The Solubility Parameter and Fractional Polarity of Microcrystalline Cellulose as Determined by Mechanical Measurement. *International Journal of Pharmaceutics* 99(2-3) (1993):157–164.
- [15] C.M. Hansen and A. Bjoerkman. The Ultrastructure of Wood from a Solubility Parameter Point of View. *Holzforschung* 52(4) (1998):335–344.
- [16] A.F.M. Barton. *Handbook of Solubility Parameters*. CRC Press, 1983, pp. 153–157.
- [17] C.M. Hansen. *Hansen Solubility Parameters*. URL: <http://hansen-solubility.com/>.
- [18] M. Mora-Pale, L. Meli, T.V. Doherty, R.J. Linhardt, and J.S. Dordick. Room Temperature Ionic Liquids as Emerging Solvents for the Pretreatment of Lignocellulosic Biomass. *Biotechnology and Bioengineering* 108 (6) (2011):1229–1245.
- [19] S. Fischer, H. Leipner, K. Thümmel, E. Brendler, and J. Peters. Inorganic Molten Salts as Solvents for Cellulose. *Cellulose* 10(3) (2003):227–236.
- [20] T. Heinze and A. Koschella. Solvents Applied in the Field of Cellulose Chemistry: A Mini Review. *Polimeros* 15(2) (2005):84–90.
- [21] A.F. Turbak, R.B. Hammer, R.E. Davies, and H.L. Hergert. Cellulose Solvents. *Chemtech* 10(1) (1980):51–57.
- [22] A. Pinkert, K.N. Marsh, S. Pang, and M.P. Staiger. Ionic Liquids and Their Interaction with Cellulose. *Chemical Reviews* 109 (2009):6712–6728.

- [23] N. Sun, H. Rodriguez, M. Rahman, and R.D. Rogers. Where are Ionic Liquid Strategies most Suited in the Pursuit of Chemicals and Energy from Lignocellulosic Biomass? *Chemical Communications* 47 (2011):1405–1421.
- [24] M. Zavrel, D. Bross, M. Funke, J. Büchs, and A. Spieß. High-Throughput Screening for Ionic Liquids Dissolving (Ligno-)Cellulose. *Bioresource Technology* 9(100) (2009):2580–2587.
- [25] J. Kahlen, K. Masuch, and K. Leonhard. Modelling cellulose solubilities in ionic liquids using COSMO-RS. *Green Chemistry* 12 (2010):2172–2181.
- [26] R.P. Swatloski, S.K. Spear, J.D. Holbrey, and R.D. Rogers. Dissolution of Cellulose with Ionic Liquids. *Journal of the American Chemical Society* 124(18) (2002):4974–4975.
- [27] N. Meine, F. Benedito, and R. Rinaldi. Thermal Stability of Ionic Liquids Assessed by Potentiometric Titration. *Green Chemistry* 12 (2010):1711–1714.
- [28] P.J. Scammells, J.L. Scott, and R.D. Singer. Ionic Liquids: The Neglected Issues. *Australian Journal of Chemistry*, 58(3) (2005):155–169.
- [29] R. Rinaldi. Instantaneous Dissolution of Cellulose in Organic Electrolyte Solutions. *Chemical Communications* 47 (2011):511–513.
- [30] A.W.T. King, J. Asikkala, I. Mutikainen, P. Jaervi, and I. Kilpelaeinen. Distillable Acid-Base Conjugate Ionic Liquids for Cellulose Dissolution and Processing. *Angewandte Chemie International Edition* 50(28) (2011): 76–81.
- [31] F. Bergius. Conversion of Wood to Carbohydrates. *Industrial and Engineering Chemistry* 29(3) (1937):247–253.
- [32] M.A. Harmer, A. Fan, A. Liauw, and R.K. Kumar. A New Route to High Yield Sugars from Biomass: Phosphoric-Sulfuric Acid. *Chemical Communications* (2009):6610–6612.
- [33] P.L. Ragg, P.R. Fields, and P.B. Tinker. The Development of a Process for the Hydrolysis of Lignocellulosic Waste. *Philosophical Transactions of the Royal Society* 321 (1987):537–547.
- [34] S. Wei, V. Kumar, and G.S. Bankerb. Phosphoric Acid Mediated Depolymerization and Decrystallization of Cellulose: Preparation of Low Crystallinity Cellulose - A New Pharmaceutical Excipient. *International Journal of Pharmaceutics* 142(2) (1996):175–181.

- [35] R.M. de Almeida, J. Li, C. Nederlof, P. O'Connor, M. Makkee, and J.A. Moulijn. Cellulose Conversion to Isosorbide in Molten Salt Hydrate Media. *ChemSusChem* 3(3) (2010):325–328.
- [36] N.J. Cao, Q. Xu, and L.F. Chen. Acid Hydrolysis of Cellulose in Zinc Chloride Solution. *Applied Biochemistry and Biotechnology* 51(1) (1995): 21–28.
- [37] J.F. Saeman, J.L. Bubl, and E.E. Harris. Quantitative Saccharification of Wood and Cellulose. *Industrial Engineering Chemistry, Analytical Edition* 17(1) (1945):35–37.
- [38] M.R. Ladisch. Fermentable Sugars from Cellulosic Residues. *Process Biochemistry* 14(1) (1979):21–25.
- [39] S.V. de Vyver, J. Geboers, P.A. Jacobs, and B.F. Sels. Recent Advances in the Catalytic Conversion of Cellulose. *ChemCatChem* 3(1) (2011):82–94.
- [40] C. Li and Z.K. Zhao. Efficient Acid-Catalyzed Hydrolysis of Cellulose in Ionic Liquid. *Advanced Synthesis Catalysis* 349(11-12) (2007):1847–1850.
- [41] J.B. Binder and R.T. Raines. Fermentable Sugars by Chemical Hydrolysis of Biomass. *Proceedings of the National Academy of Sciences of the United States of America* 107(10) (2010):4516–4521.
- [42] R. Rinaldi, N. Meine, J. vom Stein, R. Palkovits, and F. Schüth. Which Controls the Depolymerization of Cellulose in Ionic Liquids: The Solid Acid Catalyst or Cellulose? *ChemSusChem* 3(2) (2010):266–276.
- [43] R. Rinaldi, R. Palkovits, and F. Schüth. Depolymerization of Cellulose Using Solid Catalysts in Ionic Liquids. *Angewandte Chemie International Edition* 47(42) (2008):8047–8050.
- [44] R. Rinaldi, P. Engel, J. Buechs, A.C. Spiess, and F. Schüth. An Integrated Catalytic Approach to Fermentable Sugars from Cellulose. *ChemSusChem* 3(10) (2010):1151–1153.